ABSTRACT COLLECTION

Shenzhen, CHINA
11~13 March, 2023

ACF2023_ETSL

4th Asian Concrete Federation Symposium on Emerging Technologies for Structural Longevity

Keynote Sessions

Green and Low-Carbon Construction Materials

Chang-Wen MIAO

Southeast University

Abstract

Under the background of implementing the dual-carbon strategy, carbon emission in the construction field takes up significant portion of the total emission and is continuously rising year by year, which brings new challenges to the construction industry. In this presentation, the current situation and trend of carbon emission in global and Chinese construction industry, as well as energy consumption and carbon emission in the whole process of construction are analyzed. On basis of above content，the latest key technologies relevant to green and low-carbon building materials, along with the leading technologies of carbon capture, utilization and storage are introduced for coping with the challenges of carbon emission reduction and carbon neutralization in the construction industry.

Stochastic Damage Mechanics ： Developments and recent progress

Jie LI

Tongji University

Abstract

Concrete is one of the most widely used materials in civil engineering. Concrete structures subjected to extreme loading conditions will probably exhibit evident random and nonlinear behaviours. However, the lack of the general formulation for constructing refined stochastic numerical models that adequately represent the prototype structures has long been a major challenge in analysis and design of complicated concrete structures.

Starting from the material randomness and nonlinear performance of concrete, the stochastic damage mechanics of concrete has been systematically investigated in recent years in Tongji University. Within the framework of stochastic damage mechanics, the spatial variability of concrete is modelled as a two-scale stationary random fields, and on which a stochastic constitutive of concrete materials is established. Taking advantage of the probability density evolution theory, both the microscopic random damage evolution of concrete and the fluctuation of macroscopic structural responses can be numerically represented. Numerical investigation in terms of a prototype reinforced concrete structure is carried out. It is indicated that the randomness from concrete may dramatically affect the collapse behaviour of the structure, and even lead to entirely different failure modes.

It is believed that the stochastic damage mechanics of concrete laid a solid foundation for the reliability based design and control of concrete structures.

Ultra-high toughness cementitious composites (UHTCC) for resilient and sustainable infrastructures

Shilang Xu [*, #]

Institute of Advanced Engineering Structures, Zhejiang University
[*]*Presenter:* slxu@zju.edu.cn, [#]*Corresponding author:* slxu@zju.edu.cn

Abstract

In the past two decades, one of the major advances in modern concrete technology is the design and development of concrete materials with high tensile ductility (e.g., over 3%), which pushed the performance envelop of cement-based materials and attracted increasing attentions of the research community. Ultra-High Toughness Cementitious Composites (UHTCC) are typical fiber-reinforced cement-based materials featured with high/ultra-high tensile ductility and multiple-cracking behaviors (**Fig. 1** and **Fig. 2**). UHTCC are designed based on fracture mechanics, micromechanical theory, and nano technologies, and this advanced material is also known as bendable concrete, strain-hardening cementitious composite (SHCC), or engineered cementitious composite (ECC) in the research community.

In this study, the recent advances in UHTCC technology contributed by the author's research group are introduced. Emphasis is placed on several aspects, including nano- and micro-scale material design, dynamic mechanical properties, advanced construction technologies, and novel structural applications. To be specific, green UHTCC with ultra-high-volume industrial by-product were successfully designed and developed, and the carbon emission is only half that of the conventional strain-hardening cementitious composites. In addition, high/ultra-high-strength UHTCC were developed with a tensile strain capacity ranging from 3%–10%, which is 300–1000 times that of ordinary concrete materials (**Fig. 3** and **Fig. 4**). Compared to conventional (fiber-reinforced) concrete, UHTCC showed significantly higher mechanical performance under monotonic, fatigue, and impact loadings. Furthermore, sprayable UHTCC technology and UHTCC permanent formwork were proposed to enhance the crack resistance and mechanical performance of reinforced concrete structures. Owing to the superior mechanical and durability performance, UHTCC have great potential in strengthening and repair of existing structures or in new construction of building, transportation, underground, hydraulic, and marine structures subjected to complex loading conditions and under severe service environments.

It is worth mentioning that in the past decade, the UHTCC technology has been successfully applied in many critical infrastructures in mainland China, and notable examples include Wusong Military Port in Shanghai, Zhejiang Xinling Tunnel (**Fig. 5**), Changshangang Super-Large Bridge, and Zhoushan Yushan Sea Bridge (**Fig. 6**). In summary, UHTCC technology is attractive in the construction industry for achieving a safer, more durable, and more sustainable built environment, and the recent development of UHTCC laid important groundwork for the construction of resilient and sustainable infrastructures in the future.

Keywords: Ultra-high toughness cementitious composites (UHTCC); Strain-hardening; Nano and micro technologies; Resilient infrastructures; Sustainability

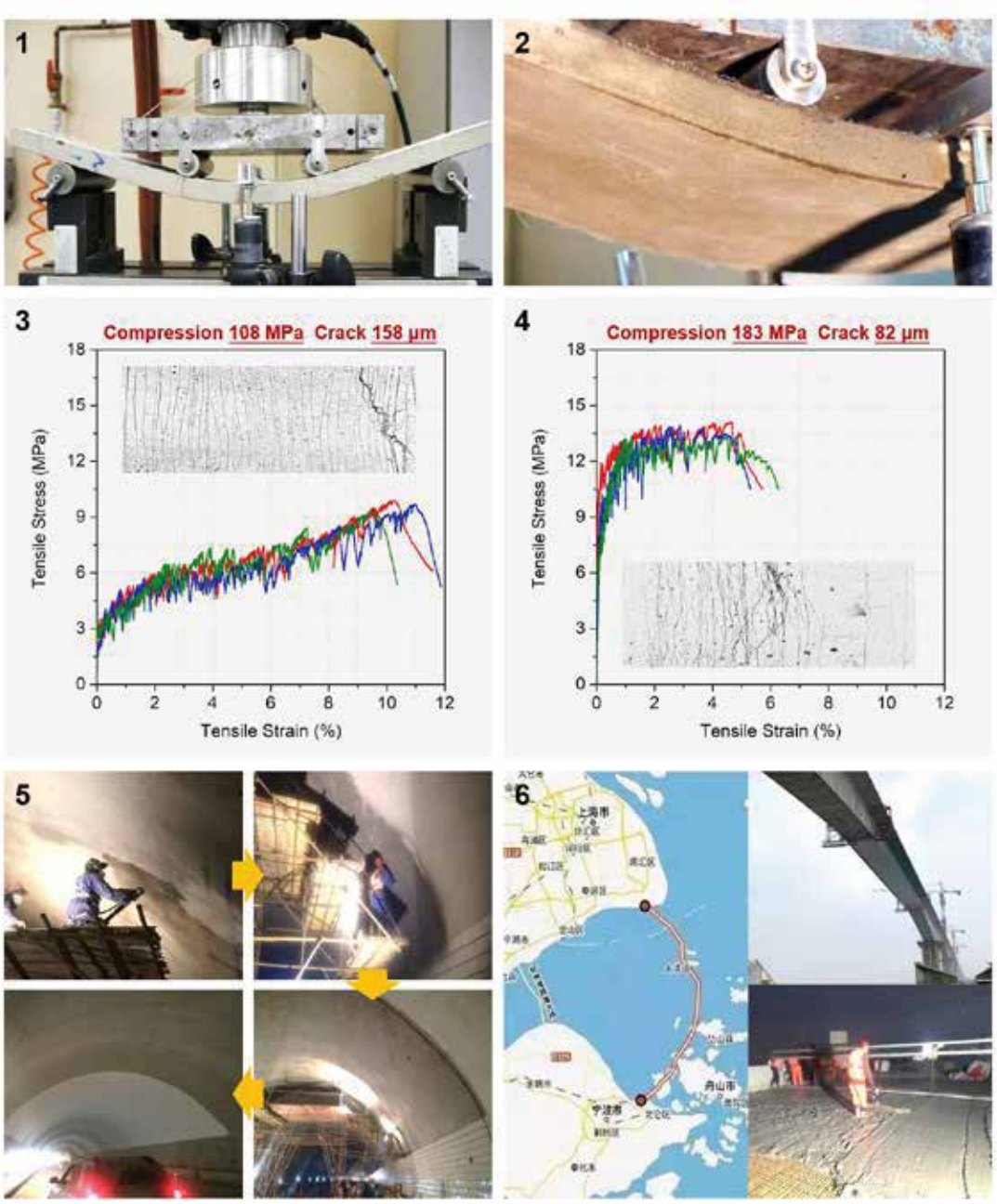

Fig. 1 Four-point bending test of UHTCC; **Fig. 2** UHTCC in bending (no visible crack); **Fig. 3** Tensile performance of UHTCC with ultra-high ductility (over 1000 times that of ordinary concrete); **Fig. 4** Tensile performance of ultra-high strength UHTCC (over 180 MPa); **Fig. 5** Application of UHTCC technology in Zhejiang Xinling Tunnel; and **Fig. 6** Application of UHTCC technology in Zhoushan Yushan Sea Bridge.

Acknowledgment

The author would like to acknowledge the support from the National Natural Science Foundation of China (51878601).

Self-healing Materials and Technology for Marine Concrete

Feng Xing[1,2*, #]

[1] Guangdong Province Key Laboratory of Durability for Marine Civil Engineering,
[2] College of Civil and Transportation Engineering, Shenzhen University, Shenzhen, Guangdong 518060, People's Republic of China
[*]*Presenter:* xingf@szu.edu.cn, [#]*Corresponding author:* xingf@szu.edu.cn

Abstract

Marine deteriorates in service safety and durability due to the accelerated damage and structural failure, as it is exposed to largely fluctuating temperature, strong radiation or/and severely corrosive environments in complex marine environment, leading to the concrete cracking, ion erosion and steel corrosion. It is vital to repair the degraded parts in time to maintain the performance and the long-term safety of marine concrete structure. Up to now, several materials and techniques have been conducted to repair and strengthen the degraded area in concrete, such as grout repair method, reinforced rust inhibitor and fiber-reinforced composited materials. These methods belong to the passive protection method, it is difficult to regulate under different degraded situation and achieve the sustainable protection. Self-healing materials and technology are utilized to achieve the active repair of degraded area, which can be designed according to different degraded situation and healing purposes.

In this study, the recent advances in self-healing materials and technology contributed by the author's research team are introduced. Emphasis is placed on the new concrete structure and the existing concrete structure. For the new concrete, a new type of self-healing materials called microcapsules based self-healing concrete was established by the author's research group in 2008 to achieve the intelligent self-healing of concrete. To be specific, the crack-sensitive microcapsules based self-healing concrete was successfully designed and developed, and the crack-healing ratio of concrete can reach over 80%. In addition, the corrosive ion sensitive microcapsules self-healing concrete was proposed and development to bind the chlorine ions and adjust the pH value of concrete. It is demonstrated that the microcapsules design above can help to delayed the starting time of steel corrosion by 2-10 times, and the rust-induced cracking time by 1.8-3 times. What's more, an embedded 3D printed micro pipeline was designed to achieve the long-term continuous protections for marine concrete.

For the existing concrete structure, typic methods for the corrosion prevention of existing concrete structures are cathodic protection and structural strengthening (SS). However, structural strengthening can improve the load-carrying capacity but not able to prevent long-term degradation. On the other hand, cathodic protection can prevent steel corrosion but not able to recover the mechanical properties. As early as 2009, the author took the lead to study the electrochemical and mechanical dual characteristics of carbon fiber reinforced polymer (CFRP), based on which a composite intervention technology for reinforced concrete durability combining impressed current cathodic protection (ICCP) and SS. Using CFRP as the auxiliary anode material of ICCP and SS reinforcement material realizes the dual protection of corrosion and mechanical properties of reinforced concrete structure, thus forming an effective solution to the durability and safety of reinforced concrete structure in the whole life cycle through system innovation.

Keywords: Self-healing materials; microcapsules; crack-healing; corrosion inhibitation; ICCP-SS system.

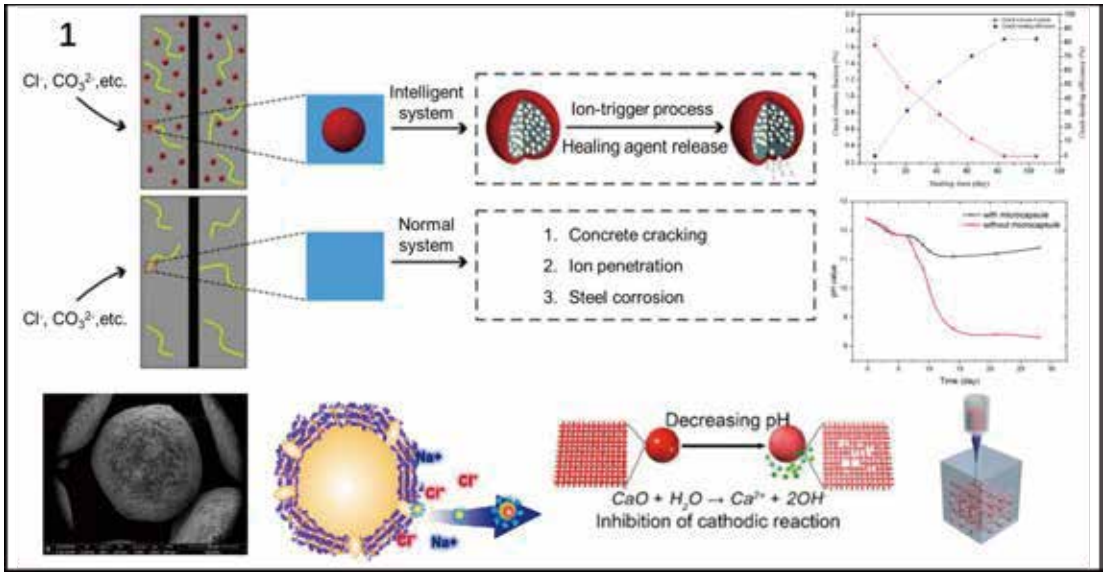

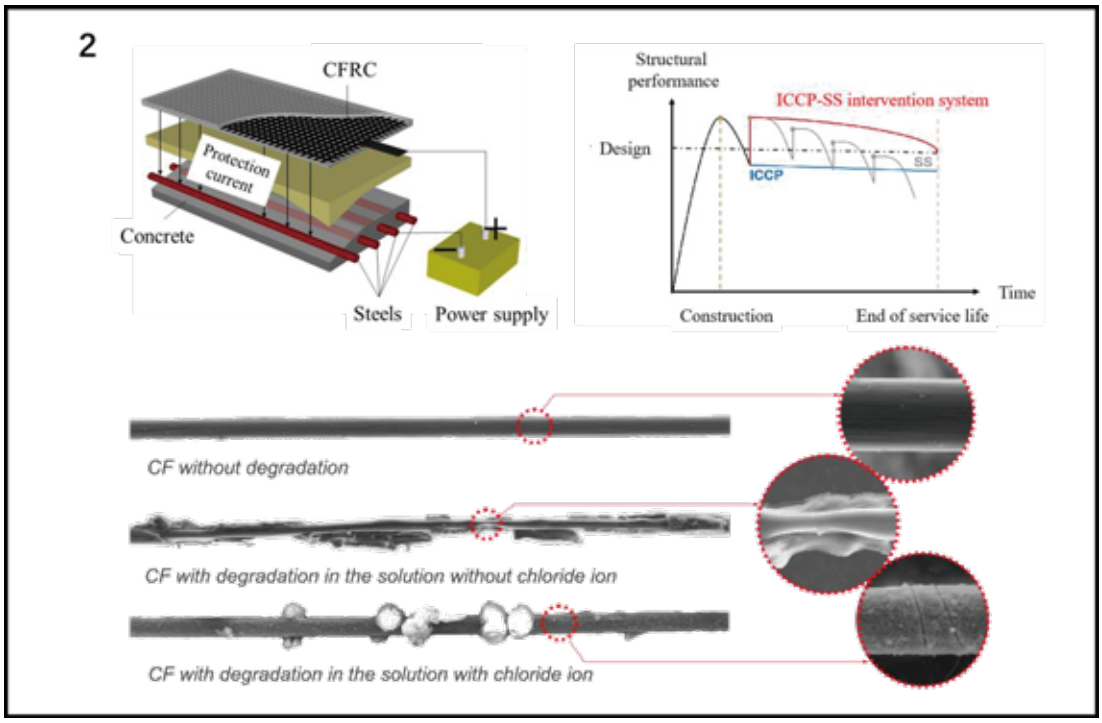

Fig. 1 Microcapsules based self-healing materials; Fig.2 ICCP-SS system.

Acknowledgment

The author would like to acknowledge the support from the National Natural Science Foundation of China (51538007), the Key-Area Research and Development Program of Guangdong Province (2019B111107002) and the National Key Research and Development Program of China (2018YFE0124900).

Evolution of fib Model Code 2020

Akio Kasuga

fib President, Sumitomo Mitsui Construction, Japan
Presenter: akasuga@smcon.co.jp

Abstract

MC2020, with sustainability and performance-based design at its core, is the Model Code for future thinking. It is designed so that both new construction and interventions can be completed based on this Model Code, bringing together the world's most advanced technologies. In this paper, the basic stance of fib toward sustainability is firstly described. Then, as the future envisioned by MC2020, examples of low-carbon concrete structures will be presented. The paper also discusses the form and uses of conceptual design that MC2020 emphasizes and presents examples of new construction and the extension of service life / adaptation / upgrading of existing structures. Sustainability has economic, social, and environmental aspects, and the optimization of each will eventually lead to carbon neutrality. It can be said that MC2020 will help us to arrive at solutions to those complex challenges.

Keywords: performance-based design, sustainability, conceptual design, *fib* Model Code

1. *fib*'s basic stance on sustainability

fib has incorporated sustainability into the Model Code since MC2010, earlier than anywhere else. *fib*'s work on sustainability began in 1999 with the creation of a sustainability committee, Commission 3. This was followed by the creation of the Special Activity Group in 2010, which straddled the entire fib and addressed sustainability as a common issue for all committees. It was then reorganised into Commission7 in 2015 and continues to the present day. In 2021, an official statement was published summarising *fib*'s sustainability activities to date and informing the world of the achievements in structural concrete [1]. After this statement, fib vision including fib Platform (Fig. 1) was approved.

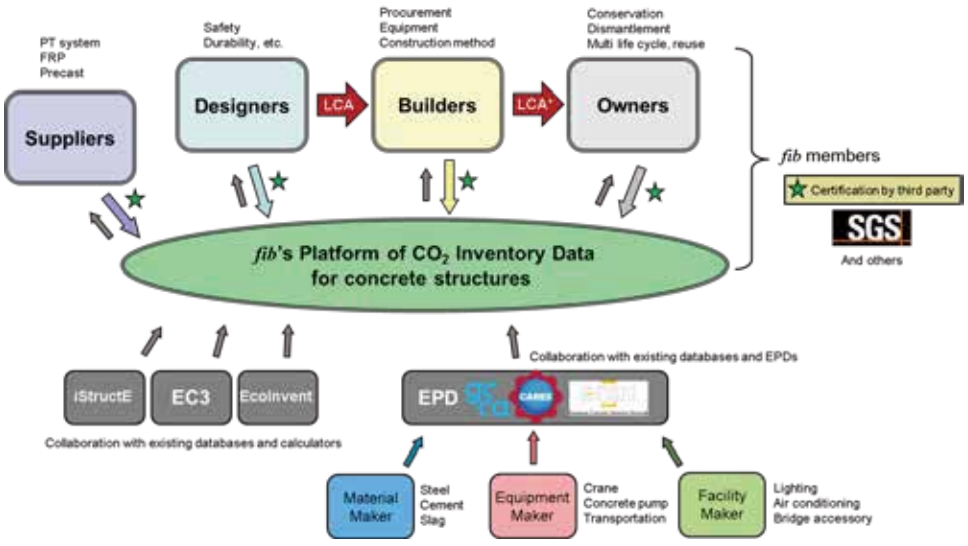

Fig. 1 Concept of fib Platform

Regarding CO_2 emissions, EN15978 distinguishes between impacts arising in the product stage (materials) (A1 to A3), in the construction stage (A4 and A5), and in the post-construction use stage (B1 to B5). As far as concrete structures are concerned, they are characterised by the fact that CO_2

emissions in A1 to A3 and B1 to B5 account for most of the emissions, with the latter being a particularly large proportion of the overall amount. For the product stage, the Environmental Product Declarations (EPD) database for steel and concrete can be used. However, for the use stage, the relationship between durability and maintenance CO_2 emissions is not clear and there is very little data. In order to build a platform for CO_2 inventory data of all stage in EN15978, *fib* has formed a SAG across all committees, and the main theme of the vision is action to support the realisation of concrete structures in accordance with MC2020. In particular, data from the use stage will require further research. And it takes time. The *fib* vision in response to the new MC2020 shows the action of *fib* to

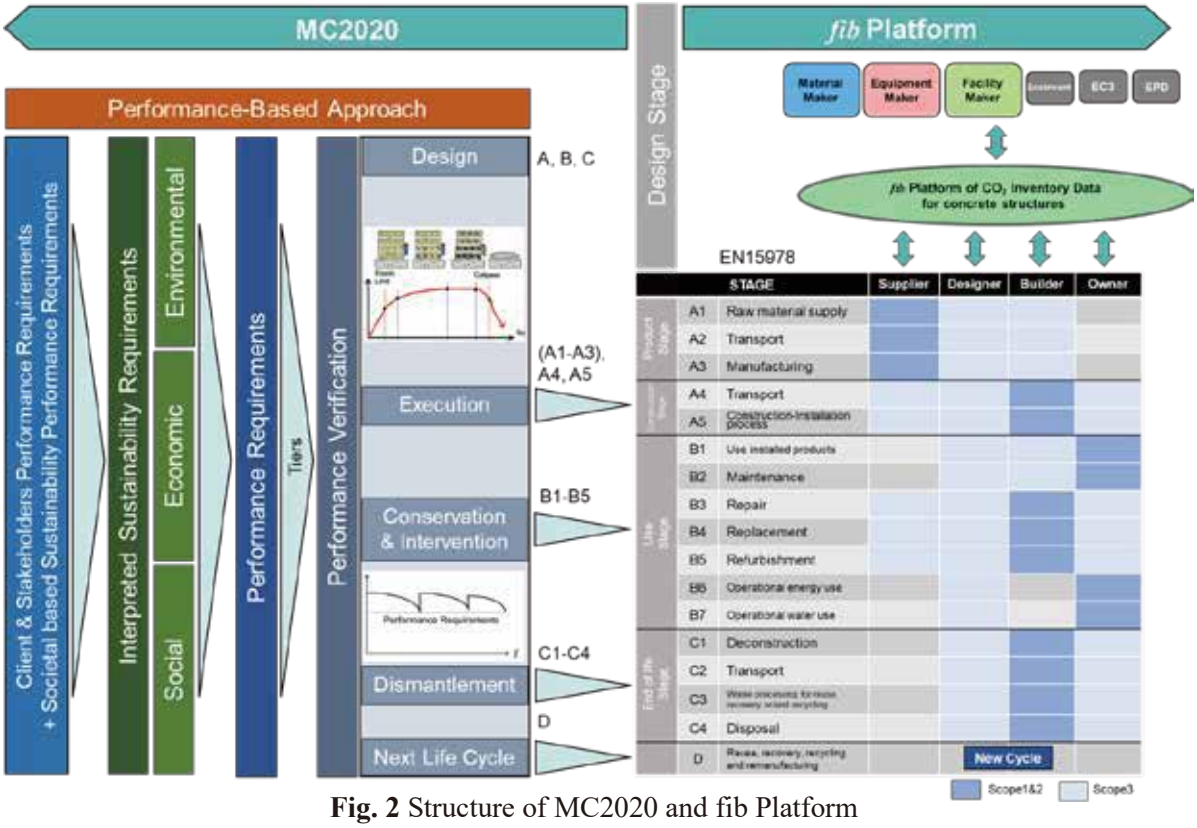

Fig. 2 Structure of MC2020 and fib Platform

realise sustainable concrete structures. (Fig. 2)

2. Future envisioned by Model Code 2020

Conceptual design optimises the three pillars of sustainability. Conceptual design is a very important process for realising the MC2020 philosophy. As shown in Fig. 3, conceptual design is tackled in the early stages of the design flow. It does not require elaborate software and thick standards and can be done with paper and pencil in the extreme. This has been proven by the feats of great engineers of the past, such as Freyssinet. In conceptual design, materials, structures, construction methods and rough estimated costs are considered to minimise the impact on social, economic, and environmental aspects.

3. Conceptual design for sustainability

An important aspect of the design flow is that conceptual design is employed not only for new construction, but also for interventions upon of existing structures as well. This is a key feature of the MC2020. In every case, it always comes back to conceptual design and the search for the optimum solution that contributes to sustainability.

3.1 The extension of service life / adaptation / upgrading of existing structures

A good example of conceptual design achieving sustainability in the upgrading of an existing structure is shown in the widening of the Los Santos bridge in Spain, built in 1986. The biggest challenge was how to share the dead and live loads of the newly added lanes between the existing structure and the

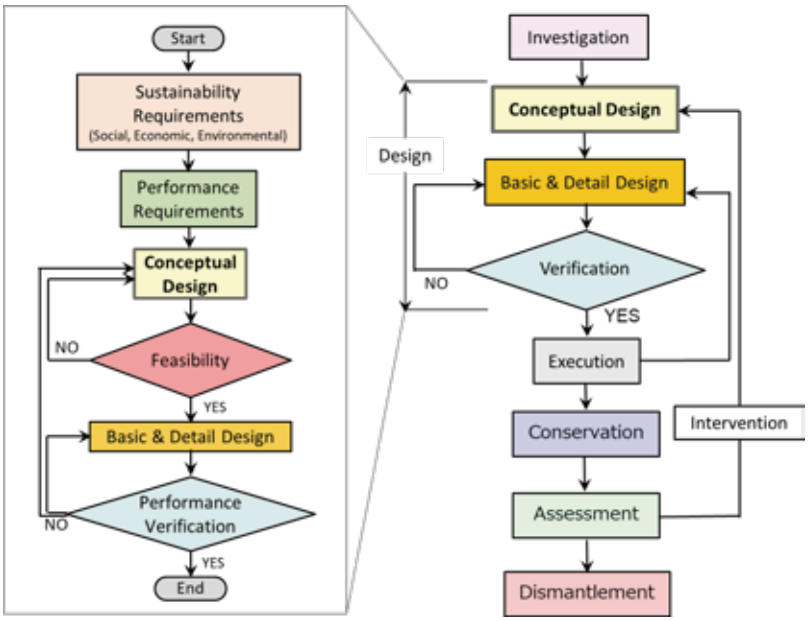

Fig. 3 Design Flowchart of Life Cycle Management

new structure, the MC2020 can accommodate such an intervention. Once the assessment of the existing structure is completed, the process returns to conceptual design at the beginning of the design flow to find the optimum solution.

Fig. 4 shows the solution. The dead loads of the additional overhanging slab and the live loads it bears are transferred through the struts to the transverse beams placed under the girders. The transverse beams are then connected just below the web in the new girder, from where the new loads are transferred to the girder. This is a conceptual design in which the load transfer paths are clearly divided between the existing structure and the new structure. Clear force flows are the basis of good conceptual design. And this solution had minimal impact on the surrounding social activities.

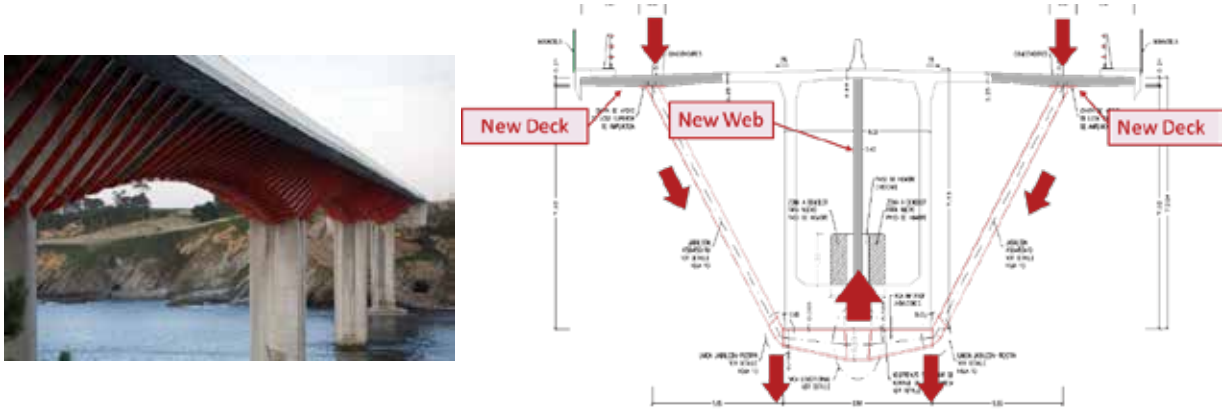

Fig. 4 Conceptual Design of Los Santos Bridge (by FHECOR)

4. Back to Roman concrete?

The Roman Pantheon is still a functioning structure after 2000 years. This is because it is unreinforced concrete with no reinforcing steel, which can cause deterioration due to corrosion. The invention of reinforced concrete 150 years ago greatly expanded the forms of concrete structures which can be employed or adopted, which until then had been limited to domes and arches utilising the comprehensive strength of concrete. At the same time, however, it also introduced an inherent deterioration factor associated with the potential for corrosion of steel reinforcement. Research into the corrosion of steel has been ongoing for a long time but has yet to completely solve the problem. So, what can be done? The steel reinforcement can be replaced by FRP, which does not rust. Although

plastic is a much newer material compared to concrete, at least the deterioration factor of rust can be removed. Also, the main material of Roman concrete is volcanic ash, a local material with no CO_2 emissions. Creating ultra-durable structures with rust-free FRP can significantly reduce the CO_2 emissions of the B1 to B5 Stages mentioned earlier. Zero-clinker concrete made with by-products can also significantly reduce CO_2 emissions from Stages A1 to A3.

4.1 Non-metallic reinforcements in non-clinker concrete

Concrete girders employed low-carbon technology for the future are presented here. The structure is made of zero-clinker concrete reinforced with FRP tendons shown in Fig. 5 [2]. The concrete is fibre-reinforced concrete made of blast furnace slag, fly ash and silica fume, and its strength exceeds 100 MPa. Aramid FRP is used as the tensioning material. Factors responsible for deterioration have been removed, which makes this material ultra-durable. According to estimates, CO_2 emissions can be reduced by 85% to 90% compared to conventional concrete. If the cement and steel eventually achieve zero carbon, the CO_2 emissions of the A1 to A3 product stages will be significantly reduced. However, the reduction of CO_2 emissions in the B1 to B5 use stages can only be achieved by making the structure ultra-durable.

Fig. 5 Non-clinker and non-metallic concrete girder

5. Conclusions

The MC2020 can accommodate new materials and structures shown in this paper. And sound conceptual design is required not only for new construction but also for interventions. It is the next generation that will benefit from the advanced nature of the MC2020.

References

1. Kasuga, A., (2021) The fib official statement on sustainability, *Structural Concrete*, Vol 22, Issue 4, 1909 -1910
2. Shinozaki, H., Matsuda, T., Kasuga, A. (2022) Construction of non-metallic bridge using zero cement concrete, *fib Oslo Congress*

Performance-Based Earthquake Design of Building Structure in Korea

Hong-Gun Park[1*]

[1] Department of Architecture & Architectural Engineering, Seoul National University, Korea
E-mail: parkhg@snu.ac.kr

ABSTRACT

Non-linear analysis is required for performance-based seismic design and evaluation of structures, and a rational non-linear analysis model should be presented to improve the accuracy of non-linear analysis. The joint committee in Architectural Institute of Korea and Korea Concrete Institute developed a new nonlinear analysis model and a guideline, based on many existing experimental results and theoretical studies at home and abroad. The model contained in this guideline is one of the most advanced models based on theory and experiment, reflecting the opinions of experts and the results of the practical feasibility review of field practitioners. In addition, commentary was added to help engineers understand the modeling method of nonlinear structural analysis, and examples for determining design variables and values of nonlinear analysis models were included in the appendix for user convenience.

Keywords: Performance, nonlinear analysis, building, structure, earthquake design

1. INTRODUCTION

Performance-based seismic design of building structures is an alternative design method for designing structures that are difficult to apply conventional elastic design based on response modification factors (ductility factors) or for designing important structures that require multiple performance goals. In Korea, Performance-based seismic design was first introduced in the Building Structure Design Code (KBC 2016)[1], and related regulations were revised in 2019 in accordance with the enactment of the Building Seismic Design Code[2]. In order to apply performance-based design, a detailed modeling technique for nonlinear analysis is required. For the purpose, the Guidelines for Performance-Based Seismic Design of Reinforced Concrete Buildings (2021)[3] and Nonlinear Analysis Models for Performance-Based Seismic Design of Reinforced Concrete Buildings (2021)[4] were published by the Architectural Institute of Korea and Korea Concrete Institute (Fig. 1). The Guidelines provide detailed explanations for the methods, examples, and theoretical basis, based on nonlinear analysis models newly presented by domestic researchers for performance-based design.

Fig. 1 Guidelines for Performance-Based Seismic Design of Reinforced Concrete Buildings[3] and Nonlinear Analysis Models for Performance-Based Seismic Design of Reinforced Concrete Buildings[4]

2. PROCEDURE OF PERFORMANCE-BASED DESIGN

Performance-based design is performed in the procedure of basic design – analysis modeling/execution – verification of analysis results. In the basic design, elastic analysis-based conventional design is performed according to the Building Seismic Design Code [2]. Generally, linear dynamic analysis (response spectrum analysis) is performed for elastic analysis. The design coefficient of the response modification factor is determined corresponding

to the seismic resistance system intended for performance-based seismic design. For nonlinear static and dynamic analysis (Fig. 2), a behavior model including hysteresis behavior of each member should be established, and the material stress-strain curve and member hysteresis curve should be defined and applied to the member model. In the verification of analysis results, the interstory drift ratio, the deformation and material strain of the deformation-controlled behavior, and the force of the force-controlled behavior should not exceed the allowable values.

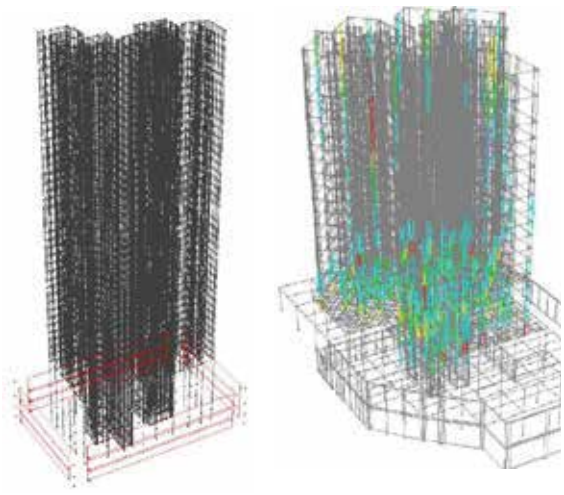

Fig. 2 Structure models for nonlinear numerical analysis of high-rise residential buildings

3. NONLINEAR ANALYSIS MODELING

The initial damping ratio of reinforced concrete structures is defined to be not more than 2.5%. The behavior of all members is classified into deformation-controlled behavior and force-controlled behavior (Fig. 3). Deformation-controlled behavior refers to the behavior of a member with ductile performance during seismic resistance, and flexural behavior is the representative one (Table 1). Force-controlled behavior refers to the behavior of a member with brittleness characteristics, which reaches its maximum strength with limited inelastic deformation during seismic resistance, and cannot provide resistance thereafter. In general, force-controlled behavior includes the shear behavior of beams, columns, and walls, or the compression behavior of columns (Table 1).

Table.1 Classification of behavior model : deformation-controlled and force-controlled behavior

Member type	Deformation-controlled behavior	force-controlled behavior
beam	flexure	shear
column	flexure	compression, shear
wall	flexure	compression, shear
coupling beam	flexure	shear

As for the structural model, nonlinear finite element model, inelastic distributed model, and concentrated plastic hinge model can be used depending on the type of member and the accuracy of numerical analysis. The models are defined with the stress-strain curves or moment-plastic rotation curves that take into account the material characteristics of concrete and reinforcement and the associated reinforcement details. In order to use new structural details, materials, or high-strength concrete that are not defined in current design codes, the results of structural experiments and nonlinear finite element analysis conducted by experts can be used for the material and member modeling.

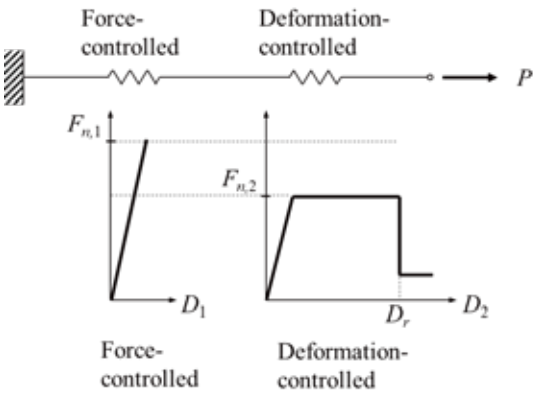

Fig. 3 Force-controlled behavior and Deformation-controlled behavior

4. FIBER MODEL

Nonlinear FE analysis is the most advanced and detailed method of structural analysis. However, the modeling and interpretation require elaborate effort and time, making it difficult to apply to analysis of the entire structure. Therefore, for structural analysis, simplied macro models are used. In the case of slender columns and walls, the inelastic distributed model (i.e., fiber model)

that can efficiently simulate flexural behavior can be used. When a member is modeled with fiber models, the stress and strain of fiber elements of concrete and reinforcing bars are determined from the Bernoulli planar assumption and uniaxial material models. The stiffness, cross-sectional force, and deformation of the member are calculated by integrating the stress, strain, and curvature of each fiber element. For slender walls, a simplified fiber model can be used for each story, assuming uniform stress and strain distributions in the story without integrating stress and strain(Fig. 4).

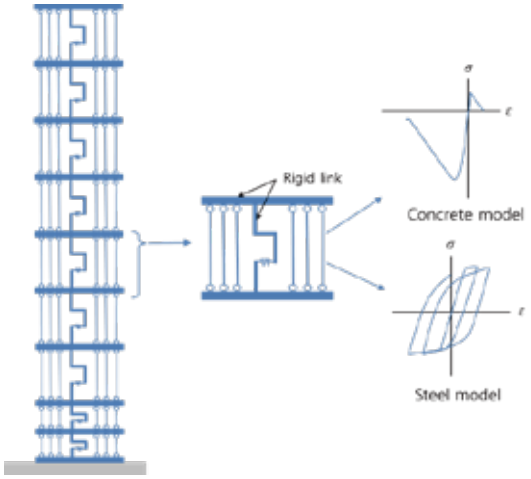

Fig. 4 Simplified fiber model for slender wall

5. CONCENTRATED PLASTIC HINGE MODEL

The concentrated plastic hinge model consists of two plastic hinge elements at the ends of the member and an elastic element in the middle to simulate inelastic flexural behavior. Shear elements may be inserted in the middle or end of the member to simulate inelastic shear deformation if necessary. The plastic hinge element is defined with a moment-rotation relationship representing inelastic flexural behavior of the member ends. The elastic element is defined with the effective stiffness addressing the effect of concrete cracking.

The Guidelines[3,4] provides plastic hinge models for columns, beams, beam-to-column joints, connections, and walls as well as fiber models. In this paper, due to the paper length limitation, the plastic hinge model only for column is briefly explained in Chapter 6.

6. PLASTIC HINGE MODEL FOR COLUMNS

Compared to existing guidelines including ASCE 41-17[5], the proposed modeling method of the columns (Guidelines[3,4]) has the following characteristics. First, the force-deformation relationship of column and related modeling variables were proposed based on the failure modes rather than the regression analysis of the experimental data. Second, the effective stiffness and yield deformation were defined to be more consistent with existing experimental results. Third, the definition of energy dissipation ratio and an energy-based cyclic model were introduced to define the cyclic moment-rotation relationship. Major revisions for each item are as follows [8].

6.1 Effective stiffness and yield deformation

The effective flexural stiffness of column is usually defined as a function of the compression force ratio, but such predictions do not follow the trend of existing test results. In the Guidelines[3,4], in addition to the compression force ratio, the shear span ratio is considered to enhance the accuracy of the effective stiffness prediction (Eq. (1)). The effective stiffness and yield deformation of column (Eq. (2)) are defined as follows.

$$EI_e = (0.2 + n)\left(\frac{l_s}{4.5h}\right)E_c I_g \quad (1)$$

$$\theta_y = \frac{M_n l_s}{3EI_e} \quad (2)$$

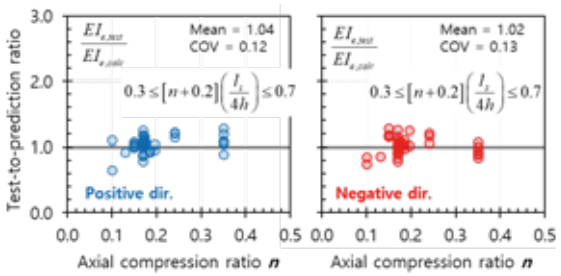

(a) Guidelines (Eq. (1))

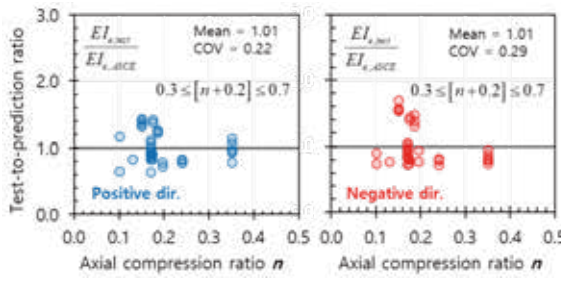

(b) ASCE 41-17

Fig.5 Effective stiffness of columns

where n = compression force ratio of the column, l_s = shear span of the column, h = depth of the column cross-section, E_c= elastic modulus of concrete, I_g= second moment of inertia of the uncracked section, and M_n= nominal flexural strength of the column ($0.3E_cI_g \le EI_e \le 0.7E_cI_g$). Fig. 5 compares the tested effective stiffness values and predicted values for 40 column specimens tested in Korea. It can be seen that the coefficient of variation by the Guidelines[3,4] (Fig. 5(a)) was significantly improved, compared to that of ASCE 41-17 (Fig. 5(b)).

6.2 Force-Deformation Relationship of Plastic Hinge

The failure modes of the columns observed in existing tests can be generally classified into four categories (See Fig. 6.). Failure modes (1) – (3) is related to the shear strength degradation, and occur when the shear resistance capacity (V_{nS}) decreases as deformation increases, as indicated by the dotted line in Fig. 6. Unlike this, Failure mode (4) is a compressive failure mode that occurs after column shear damage, and failure deformation can be predicted using the compressive shear failure theory proposed by Elwood and Moehle (2005)[7].

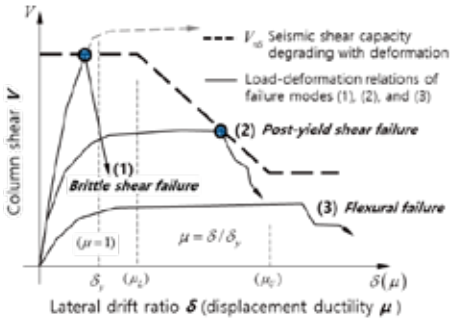

Fig.6 Failure modes in columns [8]

Table.2 Ductility ratio μ (=θ_u/θ_y) at point C

Condition	Seismic details	Non-seismic details
$V_s < V_M$	$5-3\left(\frac{V_M-V_s}{V_c}\right)\le 5$	$4-2\left(\frac{V_M-V_s}{V_c}\right)\le 4$
$V_s > V_M$	5	4

V_M = flexural strength, V_c = shear strength resisted by concrete, V_s = shear strength resisted by transverse reinforcement

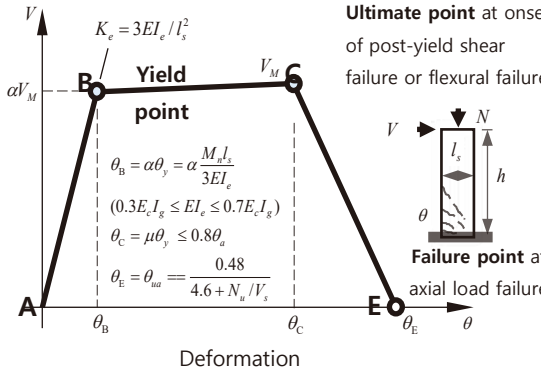

Fig.7 Force-deformation relationship of column model [8]

In the Guidelines[3,4], the force-deformation relationship of a plastic hinge (Fig. 7) is defined based on the four failure modes mentioned above. In Fig. 7, the yield point B is defined by the effective stiffness (Eq. (1)) and the yield rotation (Eq. (2)). The limit point C (Fig. 7) at which the degradation of lateral loading capacity begins is defined as a function of displacement ductility (μ), based on the shear strength degradation model of Kim et al. (2019) [8]. The failure point corresponding to compression failure is determined from Elwood and Moehle (2005)'s theory of compression shear fracture. The strength degradation behavior is simplied as a straight line connecting point C and failure point E.

The deformation of points C and E are determined as follows.

$$\theta_C = \mu\theta_y \le 0.8\theta_E \quad (3)$$

$$\theta_E = \frac{0.48}{4.6+N/V_s} \quad (4)$$

where N = compression force of column, V_s = shear resistance of lateral reinforcement.

Displacement ductility (μ) is defined in Table 2. In plastic hinge elements, only plastic rotation excluding elastic deformation is used. Thus, the plastic rotations corresponding to points C and E are defined as follows.

$$a = \theta_C - \theta_y \quad (5)$$
$$b = \theta_E - \theta_y \quad (6)$$

6.3 Energy dissipation ratio and hysteresis model

As illustrated in Fig. 8, the energy dissipation capacity of a column during cyclic loading is defined by a ratio κ of actual energy dissipation (shaded part, E_D) to the energy dissipation (E_{ep}) corresponding to the idealized elastic-plastic unloading/reloading behavior. In the Guidelines[3,4], the energy dissipation ratio κ for columns with rectangular and circular cross-section is calculated as follows.

For rectangular section column

$$\kappa = \frac{3}{2}\frac{f_{yl}A_{sl}h_l}{M_P+M_N}\lambda \geq 0.15 \quad (7)$$

For circular section column

$$\kappa = \frac{3}{8}\frac{f_{yl}\rho_l D_l D^2}{M_P+M_N}\lambda \geq 0.15 \quad (8)$$

where f_{yl} = rebar yield strength, A_{sl} = cross-sectional area of the end tensile reinforcement in a rectangular section, ρ_l= rebar ratio to the gross area in a circular cross-section, M_P and M_N = the positive and negative flexural strength, respectively (Figures 9 and 10). In Equation (7) and (8), λ indicates a reduction in energy dissipation due to shear pinching occurring during the cyclic behavior, and is approximately defined as the shape ratio (i.e., l_s/h or l_s/D) divided by 3.

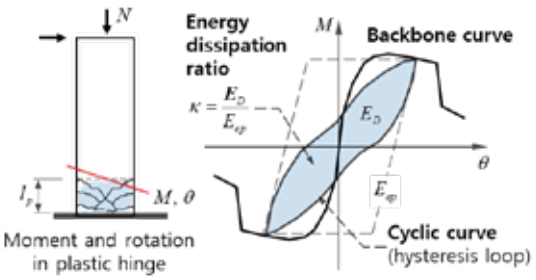

Fig. 8 Cyclic curve and energy dissipation ratio [8]

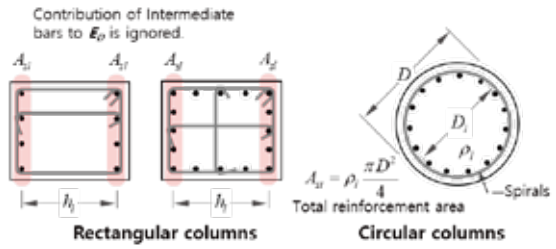

Fig. 9 Definition of symbols for energy dissipation ratio [8]

In the plastic hinge modelling, first, the area of the hysteresis loop is determined by the energy dissipation ratio κ in Equations (7) and (8), and the unloading/reloading stiffness and the pinching effect are determined such that the area of the hysteresis loop is satisfied. This energy-based hysteresis modeling is being used in commercial programs such as Perform 3D and Midas-Gen. Thus, using the proposed energy dissipation ratio κ, the cyclic moment-rotation relationship can be conveniently defined.

Figure 10 shows how the proposed modeling method is applied to column. A column is modeled with an elastic column element (elastic deformation) and moment hinges (plastic deformation) at both ends. The effective stiffness (EI_e) in Eq. (1) is applied to the elastic element. The force-deformation relationship and variables a, b (Equations (5) and (6)), the energy dissipation ratio (Equations (7) and (8)) and hysteresis modeling of (Fig. 10(b)) are applied to the moment hinge elements.

Figure 11 compares the modeling of the Guidelines[3,4] with existing test results of column specimens. As shown in the figure, the modeling method of the Guidelines[3,4] rationally predicts the force-deformation envelope and cyclic behavior of columns with various conditions.

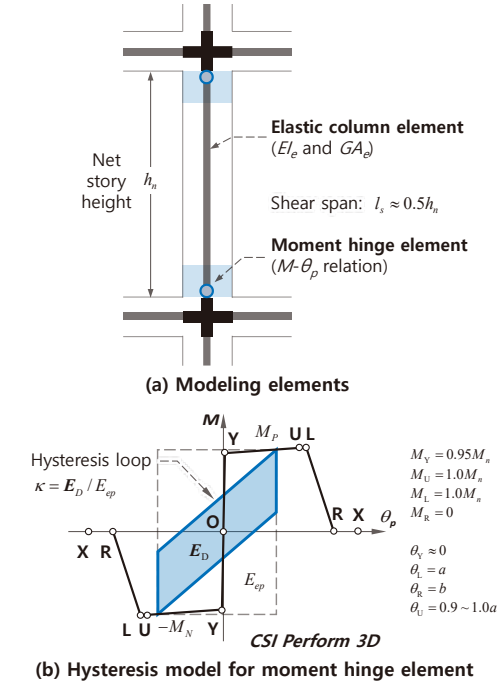

Fig. 10 Practical application of proposed nonlinear modeling for columns [8]

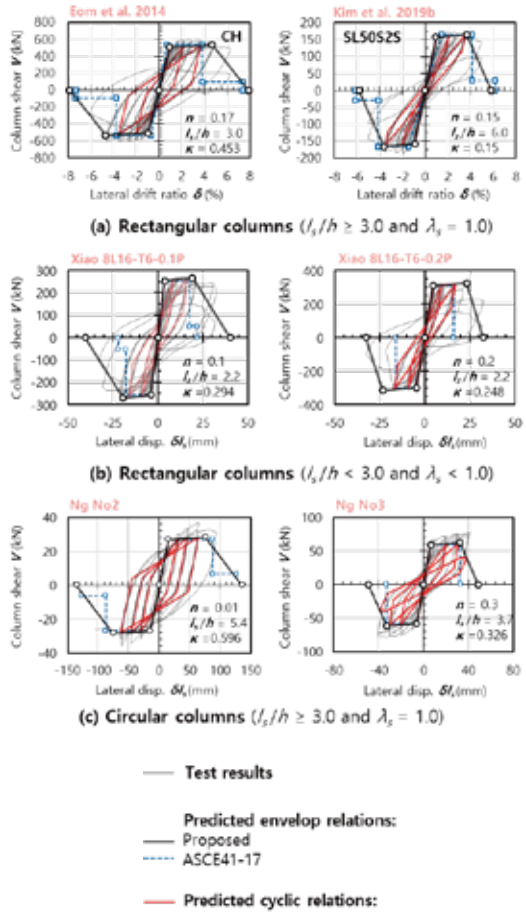

Fig. 11 Verification of proposed nonlinear modeling for columns

7. CONCLUSIONS

In near future, the use of performance-based earthquake design using nonlinear structural analysis will be increased because of the uncertainty of inelastic dynamic response of structures under earthquake. For nonlinear analysis, the Nonlinear Analysis Models for Performance-Based Seismic Design of Reinforced Concrete Buildings(2021) is expected to be useful as a rational modeling guidelines.

REFERENCES

[1] Ministry of Land and Transportation in Korea, *Building Structure Design Code*, 2016.
[2] Ministry of Land and Transportation in Korea, *Building Seismic Design Code*, 2019.
[3] Architectural Institute of Korea, The Guidelines for Performance-Based Seismic Design of Reinforced Concrete Buildings, AIK, 2021.
[4] Architectural Institute of Korea and Korea Concrete Institute, Nonlinear Analysis Models for Performance-Based Seismic Design of Reinforced Concrete Buildings, AIK and KCI, 2021
[5] ASCE, Seismic evaluation and retrofit of existing buildings, ASCE/SEI 41-17, 2017
[6] Tae-Sung Eom, Seung-Jae Lee, Chul-Goo Kim, and Hong-Gun Park, "Nonlinear Modeling of Reinforced Concrete Colum ns under Cyclic Loading", *ACI Structural Journal*, Vol. 119, 2, March 2022, pp. 159-208.
[7] Elwood, K. J., and Moehle, J. P. (2005). "Axial capacity model for shear-damaged columns." ACI Structural Journal, 102(4), 578-587
[8] Kim, C.-G., Park, H.-G., and Eom, T.-S. (2019a). "Cyclic Load Test and Shear Strength Degradation Model for Column with Limited Ductility Tie Details," Journal of Structural Engineering, 145(2), 1-17

Reliability assessment of NDT in Civil Engineering

Sylvia Keßler[1,* #]

[1] Chair of Engineering Materials and Building Preservation,
Helmut-Schmidt-University/ University of the Federal Armed Forces Hamburg, Germany

[*]*Presenter:* sylvia.kessler@hsu-hh.de, [#]*Corresponding author:* sylvia.kessler@hsu-hh.de

Abstract

Our aging infrastructure requires frequent condition survey in order to maintain it properly and to ensure the design service life. The basic tool for condition survey is the application of preferably non-destructive testing (NDT) to get the necessary information about the structure. Firstly, NDT data supports the comparison if the structure complies with the design. Secondly, NDT data provides the information about the identification and the localization of different kind of defects and allows the supervision of the defect evolution over time. All these information are essential for the performance of condition assessment and enables the structural engineer to judge whether the structures is still safe or not. Even though, the safety of our infrastructure relies on data, information about the reliability of the applied NDT methods in civil engineering is scarce. This situation leads to the following questions – (i) can we trust our NDT data and in consequence (ii) can we rely our condition assessment?

No measurement system is perfect, so we need to be aware that the indication of a defect does not prove the existence of a flaw. Even more concerning, if there is no indication of a defect, can we trust that there is really no defect? The reliability of NDT systems is the result of several factors affecting the whole NDT process. Major factors are (i) the Intrinsic Capability, which unites the physical principle and their limits to detect defects; (ii) the Application Parameters, which considers boundary condition during the time of measurement, (iii) the Human Factors describing the influence of any person involved in the process and (iv) the Organizational Context, which takes into account the complete process of the in-service inspection. This so-called modular model leads to a holistic description of the quality of a testing system. The neglect of one factor might affect the reliability evaluation.

At reinforced concrete structures, multiple inspection tasks are of importance such as the detection of cracks, honeycombs, spalling, delamination, reinforcement corrosion and so on. Several NDT techniques enable the detection of these kind of defects using different physical or electrochemical principles. In the last years, many techniques, e. i. ultrasonic techniques, impact-echo, RADAR or half-cell potential measurement are no longer expert techniques and their application in civil engineering is very common. Even though, the capability of these NDT systems for a certain inspection task remains unknown. The challenge is that there is no standardization nor specification on how to assess the reliability of NDT in civil engineering.

In Germany, we want to overcome this issue and currently, we are preparing a standard on ‘Evaluation of Testing Data – Guideline to Estimate the Reliability of Nondestructive Testing Applications’. This standard is the major outcome of the joint research project ‘Standardization for probabilistic evaluation of the reliability of non-destructive testing systems’. The standard covers all major steps in the NDT reliability evaluation procedure including (i) the definition of the application, (ii) development and production of test specimens, (iii) statistical evaluation test results, (iv) the consideration of human factors and much more. The overall objective of the standard is to ensure comparability of reliability assessments and to increase the acceptability of NDT in civil engineering. This standard

provides the basic requirements on what to consider, how to perform and how to evaluate measurement reliability with respect to qualitative test methods. The outcome is the Probability of Detection (POD), which is the generally accepted parameter to quantify measurement reliability for a defined test situation. Among others, the suitable stochastic approach can rely on binary or signal response methods depending on the type of NDT outcome. NDT techniques producing qualitative outcome in terms of the binary responses such as the "1 or HIT" (defect detected) or "0 or MISS" (defect undetected) HIT-MISS methods are used. NDT techniques providing a signal response, â (signal response) vs. a (defect size) approaches are applicable. Both approaches like hit-miss or signal response methods aim to estimate POD curves and the outcome of a POD curve is the $a_{90/95}$ (reliably detectable defect size with 90% probability and 95% confidence) value. This $a_{90/95}$ value helps in taking right decisions for approving components during inspection, identifying maintenance schedules, etc. Figure 1 summarizes the overall procedure in general (left) and for the specific case of detection of reinforcement corrosion (right).

Keywords: Non-destructive Testing (NDT); Reliability; Probability of Detection (POD); Condition Assessment, Reinforced Concrete

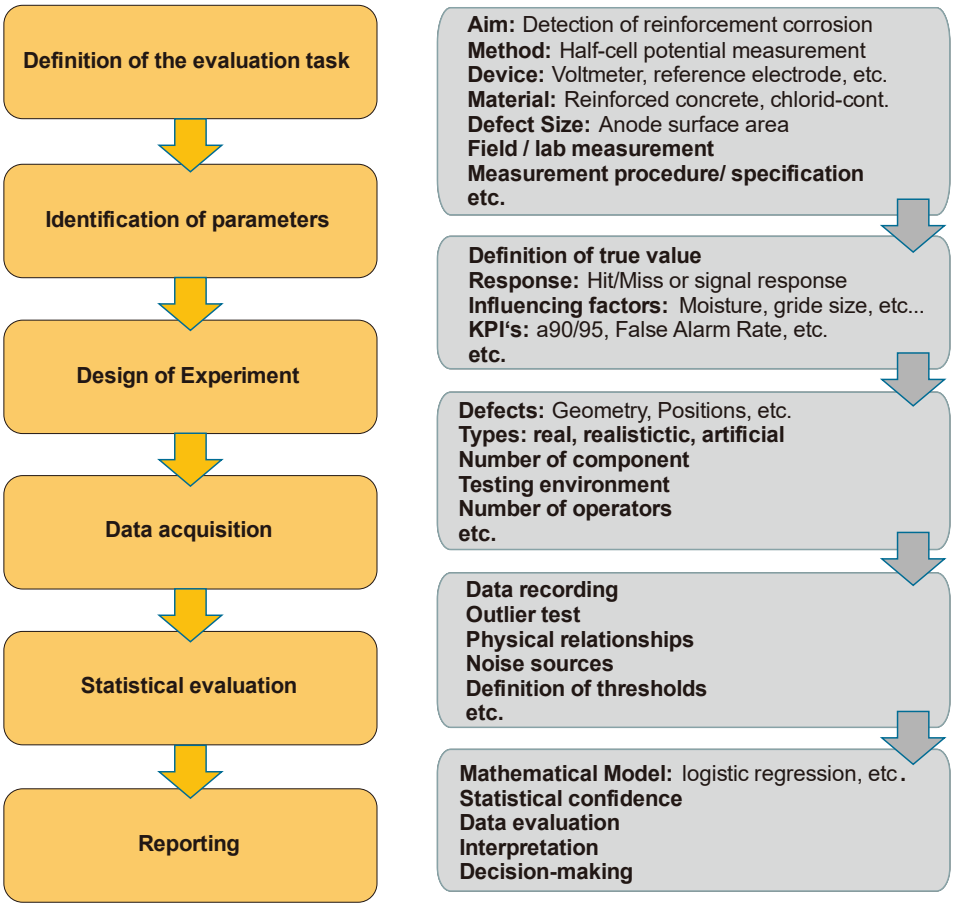

Fig. 1 Flow-chart for NDT reliability assessment in Civil Engineering: in general (left), exemplarily for detection of reinforcement corrosion (right)

Acknowledgment

The author would like to acknowledge funding of the WIPANO project "Standardization for probabilistic evaluation of the reliability of non-destructive testing systems (normPOD)" by the German Federal Ministry for Economic Affairs and Climate Action under the signature 03TN0006A.

Concrete durability and the corresponding test methods

Zongjin Li
Faculty of Innovation Engineering
Macau University of Science and Technology

Abstract

Concrete is the most versatile and the most widely produced materials in the world. It has been predicted that concrete will continue to be the most popular industrial material in the 21st century. Except for strength, durability is another important property of concrete. Durability of concrete can be defined as its ability to resist weathering action, chemical attack, abrasion, or any other process of deterioration to remain its original shape, dimension, quality and serviceability.

Durability plays an important role in determining the long-term performance of reinforced concrete structures, especially for those exposed to aggressive environments. Although it is rare for concrete structures to fail due to lack of intrinsic strength, gradual deterioration which is caused by lack of durability makes concrete structures fail to survive their specified service lives in ever increasing numbers. The extent of the problem is such that concrete durability has been recently described as a “multimillion dollar opportunity”.

The understanding of the mechanism of deterioration caused by poor durability is limited. There are even no effective methods for detecting deterioration. Thus, it is difficult to make a right decision for maintenance and repairing. It is clear that research on concrete durability is an urgent issue for Civil Engineering and construction industry, both academically and practically.

This talk will focus on the discussions of causes of deterioration of concrete structure, major concrete durability problems and their corresponding evaluation methods. The recently developed techniques in durability research such as using change of electromagnetic field to detect the steel corrosion and smart soft sensor to detect the surface crack will also be introduced.

Keywords: Concrete; Durability; Corrosion; Deterioration; Evaluation

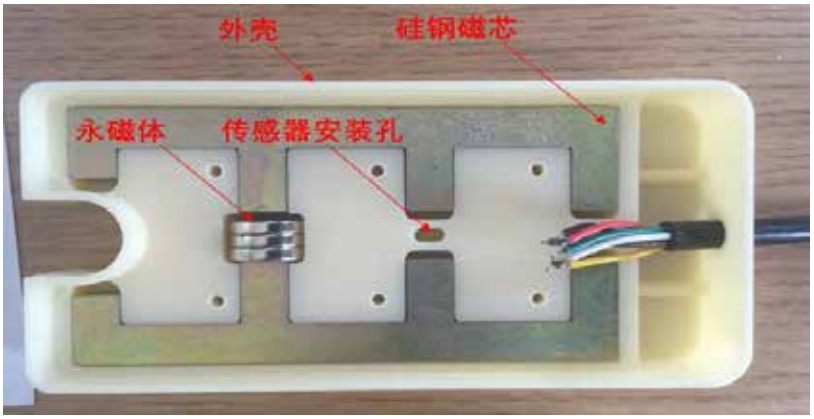

Fig. 1 Newly developed magnetic sensor

Parallel Sessions-1

Ionic Transport and Electrochemical Rehabilitation: Mechanisms & Techniques

Effect of conductive coating on the cathodic protection and prevention of steel reinforcement in concrete

Arezou Ahmadi[1], Shunfeng Wang[1,2] and Luping Tang[1*#]

[1] Dept. of Architecture and Civil Engineering, Chalmers University of Technology
[2] Key Laboratory of Advanced Civil Engineering Materials of Ministry of Education, School of Materials Science and Engineering, Tongji University, Shanghai, 201804, China
Presenter: tang.luping@chalmers.se, #Corresponding author: tang.luping@chalmers.se

Abstract

In this study, different conductive coatings based on a micro-graphite and a mix with graphene were investigated for their effect on the cathodic protection and prevention of steel reinforcement in concrete. A simple method has been developed to quickly measure the conductivity of the coatings. A layer of micro-cement-based coating was covered on the black conductive coating for protection of the conductive coating as well as ethics of concrete surface. A pull-out test was carried out to evaluate the bonding strength between different coating layers and concrete. An accelerated test was carried out to evaluate the durability of conductive coatings as anode for the cathodic protection and prevention of steel reinforcement in concrete. The testing results will be presented and discussed with respect to the cathodic protection and prevention, mechanical bonding, ands the durability of coatings.

Healing of concrete cracks by in-situ synthesis of ettringite induced by electric field

Abstract: Cracking is inevitable in concrete and can seriously threaten the durability of the structures. This paper proposed electric-induced in-situ synthesis of ettringite as a crack healing strategy for concrete structure. Composite solutions of aluminum sulfate and calcium acetate with four different molar ratios of Ca to Al (1, 3, 5, 7) were used as electrolyte solutions. The effectiveness of healing was evaluated by crack closure ratio, permeability, and coverage ratio of the crack section, while the composition and microstructure of products were also investigated. From the results, when the Ca-Al ratio is 3 or 5, the crack closure time shortened to 1 day, and the permeability coefficient reduced by nearly 4 orders of magnitude compared to the unrepaired specimen after healing for 7 days. Of all the groups, the products penetrated the entire crack, and the coverage ratio of crack section can reach more than 60% when the Ca-Al ratio is 5. Additionally, ettringite was detected as the main phase of products by X-ray diffraction and thermogravimetric analysis (TGA). Needle-shaped ettringite can be observed during the whole healing period through scanning electron microscopy (SEM). In-situ synthesized ettringite crystals evolved from small and short prismatic shapes to long and acicular shapes. These crystals overlapped with each other and formed a dense network structure.

Keywords: in-situ synthesize ettringite, crack healing, electric field, concrete.

Chloride Penetration into Steam Cured Concrete at Tidal Zone

Penggang Wang [1*#], Xiaofeng Han [1], Zuquan Jin [1], Li Tian [1], Xiaomeng Sui [1]

[1] School of Civil Engineering, Qingdao University of Technology, Qingdao 266033, P. R. China
E-mail: wangpenggang007@163.com, h1449001076@163.com, jinzuquan@126.com, tlsxf@163.com, 1269519496@qq.com

Abstract
Steam curing as a main technical means to produce precast concrete elements is widely used in practical engineering. Chloride penetration is an important factor affecting the durability and safety of reinforced concrete structures in marine environments, especially in marine tidal zone where more severe corrosion occurs. The chloride penetration behavior and transport method based on experimental and theoretical analysis of steam curing concrete in the tidal zone were researched. The different types of steam curing concrete were exposed in real marine environments for 3-, 6- or 24-months, the chloride concentration distribution include free chloride and total chloride were obtained. The influences of types and dosages of mineral admixtures and exposure times for chloride ion diffusion coefficient and chloride ion binding capacity of steam curing and standard curing concrete were researched, and based on XRD, TGA, LF-NMR, ^{29}Si NMR and ^{27}Al NMR for future studies and observe. A theoretical prediction model about the time-dependence of chloride penetration and chloride ion binding capacity of concrete was established. It provides a theoretical reference for the long-life and long-life prediction of steam curing concrete structures in marine environment.

Keywords: steam cured concrete, chloride, tidal zone, real marine environments

[*] *Penggang Wang: Presenter;* [#] *Penggang Wang: Corresponding author*

Reactive-transport numerical model in reinforced concrete structures with chloride attack and the active electric field corrosion control

Bingbing Guo[a], Ditao Niu[a], Guofu Qiao[b], Jinping Ou[b]

[a]School of Civil Engineering, Xi'an University of Architecture and Technology, Xi'an, 710055, China
[b]School of Civil Engineering, Harbin Institute of Technology, Harbin 150090, China

Chloride-induced steel corrosion is one of the primary factors to cause the deterioration of those RC structures located in the coastal environment. The prediction of chloride attack in concrete using a numerical model can provide some effective strategies in designing the durability of new RC structures, and forecasting and prolonging the service life of existing RCSs. In the previous investigations, the empirical linear, Langmuir, or Freundlich binding isotherms have been generally used to express the relationship between free and bound chlorides in the numerical transport models of chloride transport in concrete. Essentially, the chloride binding is the result of the physical and chemical reactions between pore solution and hydration products. Herein, the reactive transport model has been established to investigate the chloride attack in concrete, in which the thermodynamic modeling has been developed to describe the chloride binding behaviors in concrete.

Considering that electrochemical protection technologies, i.e., cathodic protection (CP), electrochemical chlorine removal (ECR), electrochemical realkalization (ERA), are considered to be the most direct and effective ways to control the corrosion of RC structures, the active electric field corrosion control method for RC structures that integrates CP, ECR and ERA is proposed. The ionic migration in concrete determines the efficiency of its corrosion control for RC structures, and hence, the reactive transport numerical have been applied to the active electric field corrosion control. In this model, the ionic transport, thermodynamic equilibrium and electrode reactions are included. Additionally, the effects of cracking of concrete and variation of saturation degree on the corrosion control have been investigated.

Correspondence should be addressed to Bingbing Guo at the following address, phone number and email:

Address: 13 Yanta Road, Xi'an 710055, P.R.China

Phone number: +86 18846083995

Email: guobingbing212@163.com; guobingbing212@xauat.edu.cn

A novel method for assessing C-S-H chloride adsorption in cement pastes

Xiaolong Wang[1], Chencong Li[1] and Honglei Chang[1*#]

[1] School of Qilu Transportation, Shandong University, Jinan, China
E-mail: wangxl923@mail.sdu.edu.cn，lcc125@mail.sdu.edu.cn，hlchang@sdu.edu.cn

Abstract

The binding of chloride can retard the penetration process and is of important significance for the durability of concrete structures. The previous researches calculated the content of C-S-H absorbed chloride mainly through chemical synthesized C-S-H and thermodynamic modeling, rather than in real cement pastes. This study proposed a feasible method for assessing C-S-H adsorbed chloride in real cement pastes by utilizing the order of decomposition of Friedel's salt, Kuzel's salt and C-S-H gel during carbonation and the significant content difference between them. All the parameters used for analysis were obtained experimentally, and thus have high reliability. The content of bound chloride adsorbed on C-S-H and combined in Friedel's salt was determined with this novel method in pastes under two different exposure conditions.
Keywords: Bound chloride, Cement paste, C-S-H gel, Friedel's salt

: Presenter; #: Corresponding author

Numerical simulation of the effect of crack dynamic self-healing process on chloride ion transport and reinforcement corrosion in concrete

Jun Xu[*] [#], Chen Peng, Tao Wang, Dagang Du and Chuanye Su

College of Civil Engineering and Architecture, Jiangsu University of Science and Technology, Zhenjiang, China
E-mail: xujun@just.edu.cn, 2973321850@qq.com, 1339986351@qq.com, 3272473365@qq.com, 1692647842@qq.com

Abstract

Concrete cracks have the characteristics of self-healing. Studying the effects of crack self-healing on chloride ion transmission, reinforcement corrosion and electrochemical chlorine removal has engineering value and significance for studying and improving the service life of reinforced concrete structures. Based on the finite element software COMSOL multiphysics, this paper simulates the dynamic process of crack self-healing from the perspective of chloride ion "entering and discharging" concrete, and reveals the influence of crack self-healing on chloride ion concentration distribution, reinforcement corrosion and chloride ion distribution in the process of electrochemical dechlorination. The results show that the chloride concentration in concrete with crack self-healing is gradually lower than that without crack self-healing; The self-healing of transverse cracks will not only reduce the corrosion rate and the surface potential of reinforcement, but also reduce the diffusion rate of chloride ions in concrete; The effect of single crack with different self-healing rate on electrochemical chlorine removal is not obvious.

Keywords: Self-healing of cracks, Chloride ion transport, Steel corrosion, Electrochemical dichlorination, Numerical simulation

[*]: *Jun Xu;* [#]: *Jun Xu*

Effect of Stress on Corrosion Behavior of Steel Bars Embedded in Concrete

In this research, the electrochemical tests, including the open circuit potential (OCP) test, electrochemical impedance spectroscopy (EIS) test, and polarization resistance (LPR) test, were performed to determine the critical chloride threshold of carbon steel after treatment in cementitious environments at different tensile stress levels (0, 100, 200, 300 MPa). Meanwhile, scanning electron microscopy (SEM) and X-ray photoelectron spectroscopy (XPS) were used to conduct qualitative and quantitative analyses on the degradation of the passive film. Also, a de-passivisation process model was proposed to describe the relationship between the critical chloride threshold the degradation of the passive film under tensile stress.

For the multi-field coupling model, an empirical model was used to describe the effect of stress on the mass transmission. Based on the existing theory that the degradation degree of concrete stiffness was used to characterize concrete damage, an empirical relationship between stress correction coefficient and scalar damage was established to characterize the effect of stress on chloride ion transport in concrete.

Mechanochemistry effects (MCE) are mainly considered for the corrosion process of steel bars in concrete. MCE is a phenomenon in which mechanics affects chemical reactions. Mechanochemical effect and chemical mechanical effect are two coexisting and interacting phenomena under the coupling of force field and chemical field. This research mainly discusses the mechanochemical effect of steel bar corrosion. Overall, considering the stress effect on mass transmission and steel bar corrosion, a multi-physical field coupling of mechanics-mass transfer-electrochemistry in the electrochemical model is realized based on the quantitative relationship among the mass transport parameters of the concrete, the electrochemical parameters of the steel bars, and the structural mechanical characteristic parameters.

Main References

[1] X. Feng, Y. Zuo, Y. Tang, X. Zhao, X. Lu. The degradation of passive film on carbon steel in concrete pore solution under compressive and tensile stresses[J]. Electrochim Acta. 2011, 58: 258-263.

[2] Z. Song, Y. Zhang, L. Liu, Q. Pu, L. Jiang, H. Chu, Y. Luo, Q. Liu, H. Cai. Use of XPS for quantitative evaluation of tensile-stress-induced degradation of passive film on carbon steel in simulated concrete pore solution. Construction and Building Materials[J]. 2021, 274: 121779.
[3] G. Liu, Y. Zhang, M. Wu, R. Huang. Study of depassivation of carbon steel in simulated concrete pore solution using different equivalent circuits[J]. Construction and Building Materials. 2017,157: 357-362.
[4] J. Xia, T. Li, J. Fang, W. Jin. Numerical simulation of steel corrosion in chloride contaminated concrete[J]. Construction and Building Materials. 2019, 228: 116745.
[5] J. Ožbolt, G. Balabanić, E. Sola. Determination of critical anodic and cathodic areas in corrosion processes of steel reinforcement in concrete[J]. Materials and Corrosion. 2017, 68: 622-631.
[6] B. Yu, L. Yang, M. Wu, B. Li. Practical model for predicting corrosion rate of steel reinforcement in concrete structures[J]. Construction and Building Materials. 2014, 54: 385-401.
[7] Li Y Z, Wang X, Zhang G A. Corrosion behaviour of 13Cr stainless steel under stress and crevice in 3.5 wt.% NaCl solution[J]. Corrosion Science, 2020, 163: 108290.
[8] Boddy A, Bentz E, Thomas M D A, et al. An overview and sensitivity study of a multimechanistic chloride transport model[J]. Cement and Concrete Research, 1999, 29(6): 827-837.
[9] Wang J, Basheer P A M, Nanukuttan S V, et al. Influence of service loading and the resulting micro-cracks on chloride resistance of concrete[J]. Construction and Building Materials, 2016, 108: 56-66.
[10] Jiang L, Li C, Zhu C, et al. The effect of tensile fatigue on chloride ion diffusion in concrete[J]. Construction and Building Materials, 2017, 151: 119-126.
[11] Du X, Jin L, Zhang R. Chloride diffusivity in saturated cement paste subjected to external mechanical loadings[J]. Ocean Engineering, 2015, 95: 1-10.
[12] Zhang S, Pang X, Wang Y, et al. Corrosion behavior of steel with different microstructures under various elastic loading conditions[J]. Corrosion Science, 2013, 75: 293-299.
[13] Gao Y, Zheng Y, Zhang J, et al. Time-dependent corrosion process and non-uniform corrosion of reinforcement in RC flexural members in a tidal environment[J]. Construction and Building Materials, 2019, 213: 79-90.

Numerical study on electrochemical rehabilitation methods for reinforced concrete damaged by various factors

Zhaozheng Meng[1,2*], Qing-feng Liu[1,2#]

[1] State Key Laboratory of Ocean Engineering, School of Naval Architecture, Ocean and Civil Engineering, Shanghai Jiao Tong University, Shanghai, China
[2] Shanghai Key Laboratory for Digital Maintenance of Buildings and Infrastructure, Shanghai, China
[*]*Presenter: mengzhaozheng@sjtu.edu.cn,* [#]*Corresponding author: liuqf@sjtu.edu.cn*

Abstract

Reinforced concrete (RC) structures have been widely constructed in harsh environments where the resultant durability problems can lead to serious deterioration in carrying capacity and thus limiting the designed service life. In recent years, various electrochemical rehabilitation methods for RC structures have been proposed including electrochemical chloride removal (ECR) and electrochemical realkalization (ER) which have been proved to be effective in rehabilitating RC structures damaged by chloride induced corrosion. However, RC structures are commonly exposed in the combined attack of various durability problems, and the previously mentioned rehabilitation methods with single targeted durability issues cannot prevent multiple deterioration factors at the same time. Therefore, it is necessary to find comprehensive electrochemical rehabilitation methods with multiple advantages in mitigating various durability issues and healing cracks so as to better prolong the service life.

In this study, a mesoscopic numerical model has been developed for promising electrochemical rehabilitation methods of electrochemical deposition method (EDM) as shown in Fig. 1, and improved electrochemical chloride removal method as shown in Fig. 2. In addition to traditional functions such as chloride removal and realkalization, advantages including alkali silica reaction (ASR) mitigation and cracking repairing can also be achieved by migrating lithium and magnesium ions respectively into the damaged concrete. The entire process involved in the life cycle of reinforced concrete structures was represented by three sub-models: concrete mechanical damage model, multi-ionic transport model, and electrochemical rehabilitation model. The local mechanical variations of multiphase concrete have been considered in the mechanical damage model. The interaction among various ionic species was also quantitively expressed by the multi-ionic transport model. In addition, mitigation effectiveness on ASR affected concrete and dynamic crack closure status were also successfully reproduced by the proposed electrochemical rehabilitation model.

After validation against the third-party experimental data, a detailed parametric analysis has also been conduced to explore and discuss the potential influence factors on the efficiency of electrochemical rehabilitation treatment. Results showed that although large current density can facilitate the migration of lithium ions and removal of chloride ions, the crack closure rate is negatively affected because the previously formed deposition products will block the subsequent supply of magnesium ions (Fig. 3). Increasing ambient temperature is beneficial to the overall improvement of electrochemical rehabilitation efficiency. Meanwhile, crack distribution pattern has an obvious influence on the crack closure status, and for ASR induced more discrete cracks distribution, it is recommended to arrange all exposure surface as working anodes to ensure a better repairing effect (Fig. 4).

Keywords: Electrochemical rehabilitation; Reinforced concrete structures; Mechanical cracking; Multi-species transport; Crack repair; Numerical model

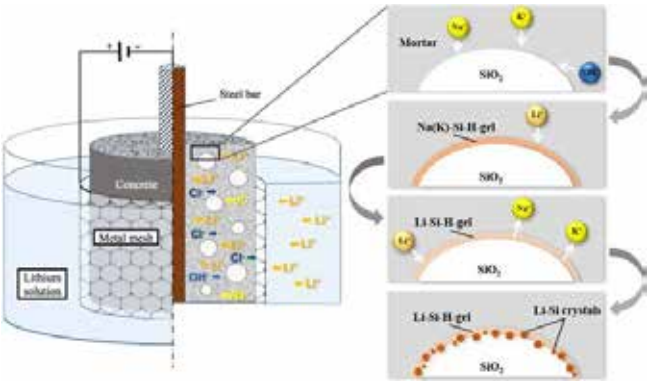

Fig. 1 Schematic diagram of improved electrochemcial chlrode removal method with additional advantages in ASR mitigating.

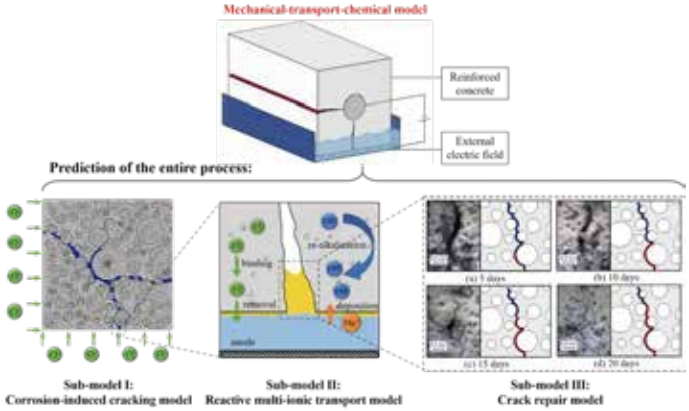

Fig. 2 Schematic diagram of the electrochemical deposition method with additional advantages in crack closure.

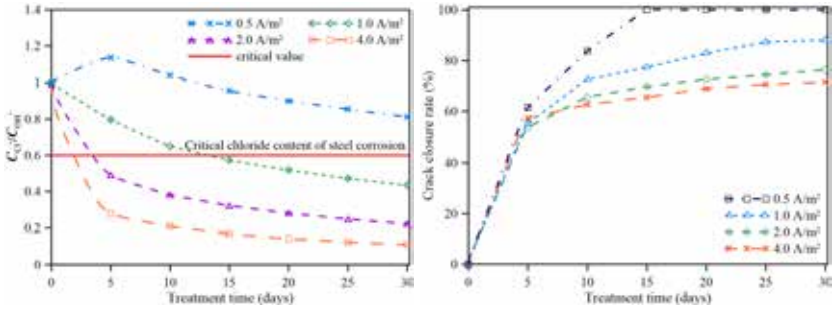

Fig. 3 Influence of current density on chlroide removal and crack closure.

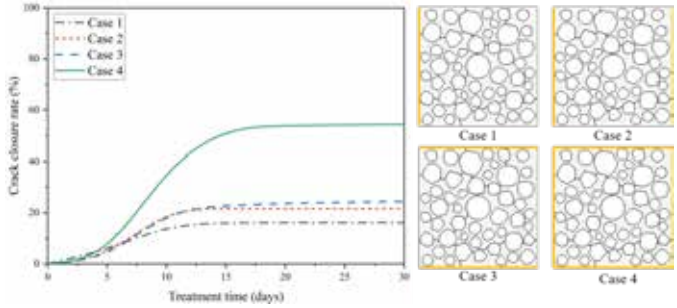

Fig. 4 Influence of anode arrangement on crack closure rate.

Acknowledgment

This work was funded by the National Natural Science Foundation of China [51978396], the Natural Science Foundation of Shanghai, China [22ZR1431400], and the Oceanic Interdisciplinary Program of Shanghai Jiao Tong University, China [SL2021MS016].

Oxygen transportation into non-saturated concrete and induced corrosion of steel bar

Zuquan Jin [1*], Yuan Gao[1], Guangyan Feng[2]

[1] *Engineering Research Center of Concrete technology in marine environment, Ministry of Education, Qingdao University of Technology, Qingdao 266033, China*
E-mail: jinzuquan@126.com

[2] Key Laboratory for Green & Advanced Civil Engineering Materials and Application Technology of Hunan Province, College of Civil Engineering, Hunan University, Changsha 410082, China

Abstract

This paper aims to study the oxygen transportation into concrete with 5-85%RH, and induced corrosion propagation behavior of reinforced bar. A novel custom-designed wire beam electrode (WBE) covered by mortar was applied to record the evolution of the corrosion current distribution and electrochemical impedance spectrum (EIS) results. The corrosion expansion stress was calculated based on the evolution of strain on inner surface of reinforcement. And the corrosion production of reinforcement in different oxygen concentration was detected by SEM. The results showed the oxygen diffusion coefficient of mortar increased with its W/B and RH. The WBE technique can effectively monitor the entire process of passivation and pitting corrosion, especially for the propagation behaviour of corrosion. The corrosion expansion stress increased with corrosion time and decreased due to crack of concrete. Pitting corrosion is the main form of initial corrosion that then propagates to surrounding positions and eventually evolves to the uniform corrosion of steel. Corrosion propagation of wire electrodes mainly determined by the chloride distribution, which changes with increasing crack width and prolonged erosion time.

Keywords: Corrosion, crack, wire beam electrode (WBE), concrete, oxygen.

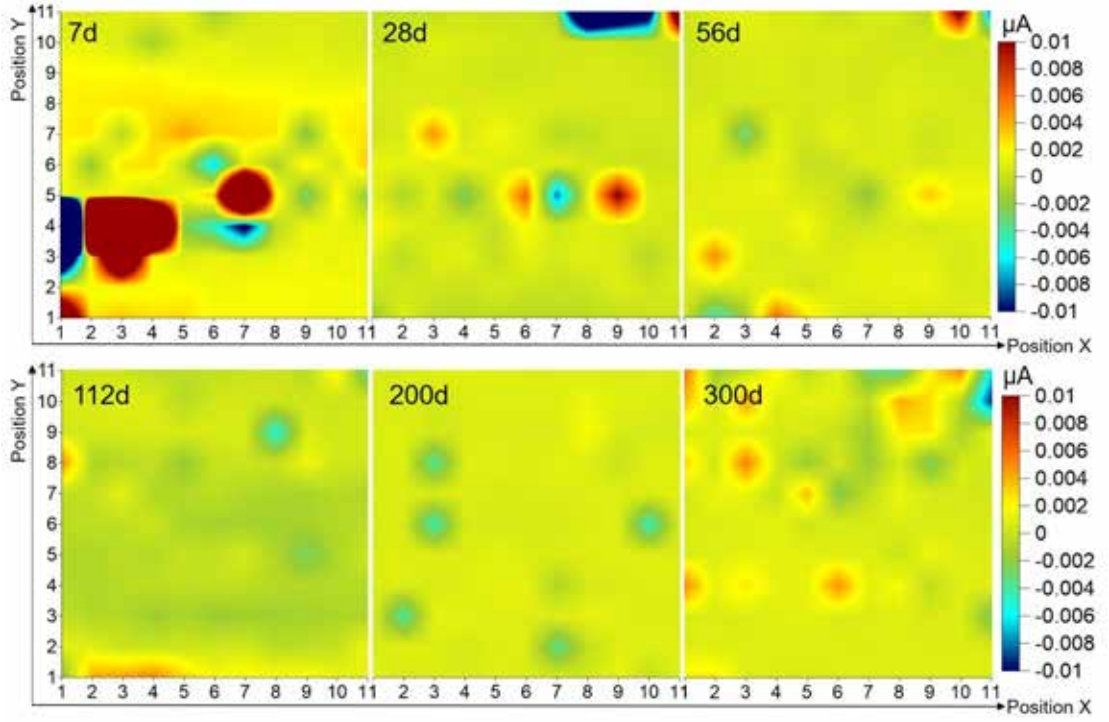

Fig. 1 Evolution of the corrosion current of WBE covered by uncracked mortar with seawater erosion time

*: *Presenter*; #: *Corresponding author*

“锈蚀钢筋混凝土电化学除氯与加固一体化技术”摘要

李 悦

北京工业大学

氯盐侵蚀引起的钢筋锈蚀会造成钢筋混凝土结构性能失效。因此，对已被氯盐污染的钢筋混凝土进行电化学除氯和修补加固具有重要的理论价值和实际工程意义。本研究采用磷酸镁（MPC）作为粘结和导电材料，粘结碳纤维布 CFRP 形成 MPC-CFRP 复合材料，对已经锈蚀的钢筋混凝土进行除氯和加固一体化。介绍了 MPC 材料的基本性能和改性技术，MPC-CFRP 阳极参数设计方法，电化学除氯对钢筋混凝土微观结构、宏观力学性能和抗震性能的影响，提出了保证钢筋混凝土综合性能较优的除氯条件。

英文：

Integrated technology of electrochemical chloride extraction and reinforcement of corroded reinforced concrete

Li Yue

Beijing University of Technology

Abstract: The corrosion of steel bars caused by chloride corrosion leads to the failure of reinforced concrete structure. Therefore, carrying out electrochemical dechlorination and repair reinforcement of reinforced concrete polluted by chloride has important theoretical value and practical engineering significance. This study applies magnesium phosphate cement (MPC) as the conductive bonding material, connecting Carbon Fibre Reinforced Plastics (CFRP) to form MPC-CFRP composite material, which integrates dechlorination and reinforcement of corroded concrete. The basic properties and modification technology of MPC materials, the method to design anode parameters of MPC-CFRP, the effect of electrochemical chlorine removal on the microstructure, macroscopic and mechanical properties, as well as the seismic performance of reinforced concrete have been introduced. The dechlorination conditions to ensure the better comprehensive performance of reinforced concrete are proposed.

Mechanical performance of concrete structure component after Electrochemical Rehabilitation

Jianghong Mao[a,b], Xianglin Wang[c], Jiangxing Long[d], Weiliang Jin[d], Jun Zhang[d]

[a] *College of Architecture & Environment, Sichuan University, Chengdu 610065, China;*

[b] *State key laboratory of hydraulics and mountain river engineering, Sichuan University, Chengdu 610065, China;*

[c] *School of Civil Engineering, Kunming University of Science and Technology, Kunming 650031,China;*

[d] *College of Civil Engineering and Architecture, Ningbo Tech University, Ningbo 315100, China;*

Abstract: The electrochemical repair technology drives the harmful substances in the protective layer of concrete structures through the action of an electric field to improve durability. Unreasonable electrochemical repair parameters have adverse effects on material properties, such as reducing the strength of the bond between steel and concrete, increasing the hydrogen embrittlement of steel, declining plasticity, changing the pore structure of concrete, and varying the strength of concrete. The degradation of material performance will further affect the static, fatigue, and seismic performance of the components of structures. To study the influence of the degradation caused by electrochemical repair on the mechanical performance of structures, reinforced concrete beams and columns were set up at different current densities for electrochemical hydrogen charging. Considering the time effect, components was distinguished into EHC components with static standing and EHC components without static standing. The static loading and low-cycle reciprocating test determined the failure mode, crack characteristics, hysteresis curves, skeleton curve, stiffness degradation curves, and ductility performance of the reinforced concrete components. The experimental results show that the crack characteristics of the components remarkably differ based on the influence of the strength of concrete and bond-slip performance degradation of the reinforced concrete; however, the differences disappear with increasing the static standing time. The failure mode, bearing capacity, and energy dissipation capacity of the components do not change significantly under the different parameters used herein. The test results are discussed, and the degradation and recovery mechanism for the structural performance of reinforced concrete component undergoing electrochemical repair are expounded. The research conclusions provide a scientific basis for applying electrochemical repair technology.

Keywords: Reinforced concrete structure; electrochemical repair; low-cycle reciprocating loading; bond slip; seismic performance; time effect

Case studies of cathodic prevention and cathodic protection for reinforced concrete structures and steel-framed masonry structures

Yu-You Wu

School of Transportation, Civil Engineering & Architecture, Foshan University, China

Abstract

Corrosion of steel is one of the major factors affecting the durability of reinforced concrete infrastructure and steel-framed masonry structures such as bridges, buildings, parking structures, harbors and jetties, cooling towers due to the carbonation of concrete or mortar, ingress of chlorides from either marine environments or deicing salts, resulting in the serious loss of steel section, the cracking, delamination, and spalling of concrete or masonry.

Cathodic prevention (CPre) is widely employed on newly constructed structures while cathodic protection (CPro) is generally used on existing structures, both are exposed to aggressive environments. This presentation reports an update on the application of CPre and CPro systems on bridges, buildings, nuclear cooling towers, jetties, etc. In the meantime, the design, installation, and performance monitoring of these systems are also included.

Keywords: reinforced concrete structures, steel-framed masonry structures, corrosion, cathodic protection, cathodic prevention.

Bio: Yu-You Wu, Ph.D., FICorr, is currently a full professor of civil engineering in the School of Transportation, Civil Engineering & Architecture at Foshan University, China. He obtained his Ph.D. in Structural Materials and Corrosion from Sheffield Hallam University, UK. His areas of research are mainly concerned with the corrosion of steel in concrete and masonry environments, cathodic protection and electrochemical remediation, nanomaterials reinforced cement-based composites and polymer composites, etc. He also has extensive industrial experience and has played key technical roles in a wide range of projects in structural design, structural inspection and materials testing, and structural rehabilitation and electrochemical remediation including bridges, buildings, docks, jetties, and industrial facilities in China, the UK, and the USA.

He is a Fellow of the Institute of Corrosion, UK.

Chloride transport in fiber reinforced mortars under unsaturated and saturated conditions

Cao Zhudi[1,2,*], Lin Yang[2,#]

[1] School of Water Conservancy and Civil Engineering, Zhengzhou University, Zhengzhou 450001, China.
[2] Yellow River Laboratory, Zhengzhou University, Zhengzhou 450001, China.
[*]Presenter: 202012222014258@gs.zzu.edu.cn , [#]Corresponding author: yanglin06142@zzu.edu.cn

Abstract

Ordinary concrete has high brittleness and low fatigue resistance, which cracks easily under the action of internal and external factors, such as load, temperature and humidity changes, shrinkage, and so on. The addition of fibers to ordinary concrete can effectively improve the tensile strength, flexural strength and toughness. Specifically, the randomly distributed fibers in concrete limit the expansion and cracking of concrete and improve its crack resistance. The addition of fibers inevitably affects the transmission of external hazardous substances in concrete while improving its mechanical properties and crack resistance, however, it is insufficient and not matured in this area.

This study focused on the effect steel fibers (0-1.5% by volume) and polypropylene fibers (0-0.5% by volume) on chloride transport in mortars under unsaturated and saturated conditions. Moreover, the micromorphology of fiber-mortar interface and the pore structure of fiber reinforced mortars were detected using scanning electron microscope (SEM) and mercury intrusion porosimetry (MIP), respectively. The results show that both of the steel fibers and polypropylene fibers have insignificant effect on the chloride diffusion coefficient of mortars, no matter under unsaturated and saturated conditions. The incorporation of steel fibers has no obvious action on the pore structure of mortars, and the interfacial zone around the steel fibers is not a preferential path for chloride transport. However, the addition of 0.1-0.5% polypropylene fibers refines the pore size of mortars, and yet slightly increases the total porosity. The polypropylene fiber-mortar interface is insignificant, while the agglomerate of polypropylene fibers exists.

Keywords: Steel fiber reinforced concrete; durability; chloride; microstructure

Electrochemical performance and functionalization application of carbon fiber under chloride environment

Ji-Hua Zhu[1,2*], Chun Pei[1,2], Hong-Tao Yu[1,2], Feng Xing[1,2#]

[1] Guangdong Province Key Laboratory of Durability for Marine Civil Engineering,
[2] College of Civil and Transportation Engineering, Shenzhen University, Shenzhen, Guangdong 518060, People's Republic of China
Presenter: zhujh@szu.edu.cn, #Corresponding author: xingf@szu.edu.cn

Abstract

Composite materials with carbon fiber (CF) as reinforcement, such as carbon fiber reinforced polymer (CFRP) and carbon fiber reinforced cementitious material (CFRCM) have been utilized in the structural reinforcement and enhancement in civil engineering. Meanwhile, CF can be exploited as electrode material due to its excellent electrical conductivity and stable electrochemical properties. In this paper, the electrochemical performance of CF under the coupled effect of polarization and chloride ion was revealed. It was found that the chloride solution had splendid infiltration effect on the surface of CFRP. Meanwhile, the chloride ion could promote the electrochemical activity of CF, thus enhancing the stability of CF under anodic polarization. Therefore, CF can withstand higher anode current density, load more charge (Fig. 1), and maintain better mechanical properties (Fig. 2) in the chloride environment. The research results can guide the functional applications of CF.

Based on the revealed excellent anodic polarization stability of CF in chloride, a dual-functional intervention method for concrete durability 'Impressed Current Cathodic Protection - Structural Strengthening (ICCP-SS)' was established, in which carbon fiber composite was functionalized as both auxiliary anode and structural reinforcement material. ICCP-SS can effectively inhibit steel corrosion in chlorinated concrete (Fig. 3) and improve the load-carrying capacity simultaneously. Moreover, ICCP-SS can be adopted as a novel composite structure of seawater sea-sand reinforced concrete.

Based on the composite effect of penetration and activation of chloride to CFRP, a nondestructive recycle technology of CFRP waste was invented. The electrochemical behavior of CF was regulated by optimal design of polarization conditions. The recycling of CF was realized through the rapid infiltration and oxidative degradation of the substrate by the derivative products of the anode reaction. The recovery rate of carbon fiber can reach 99% at room temperature and pressure. The tensile strength and the interfacial shear strength of recycled carbon fiber (rCF) can retain 90% and 120% of the original CF (Fig. 4). The premium rCF can be reutilized in concrete (Fig. 5), which is expected to break the cost bottleneck of large-scale application of CF in civil engineering and promote sustainable development in multiple fields.

By adjusting the anodic polarization conditions, swelling and exfoliation of the carbon layers occur on the surface of CF, resulting in a great increase of the specific surface area, oxygen-containing functional group contents and electrochemical activities. The obtained CF with enhanced capacitive properties (Fig. 6) can be used as electrode materials for cement-based energy storage devices. This research may further lead to the diversified and integrated application of high-performance energy-storage fiber reinforced concrete structures.

Keywords: Carbon Fiber; CFRP Waste Recycle; Electrochemical Performance; Functionalization Application; ICCP-SS

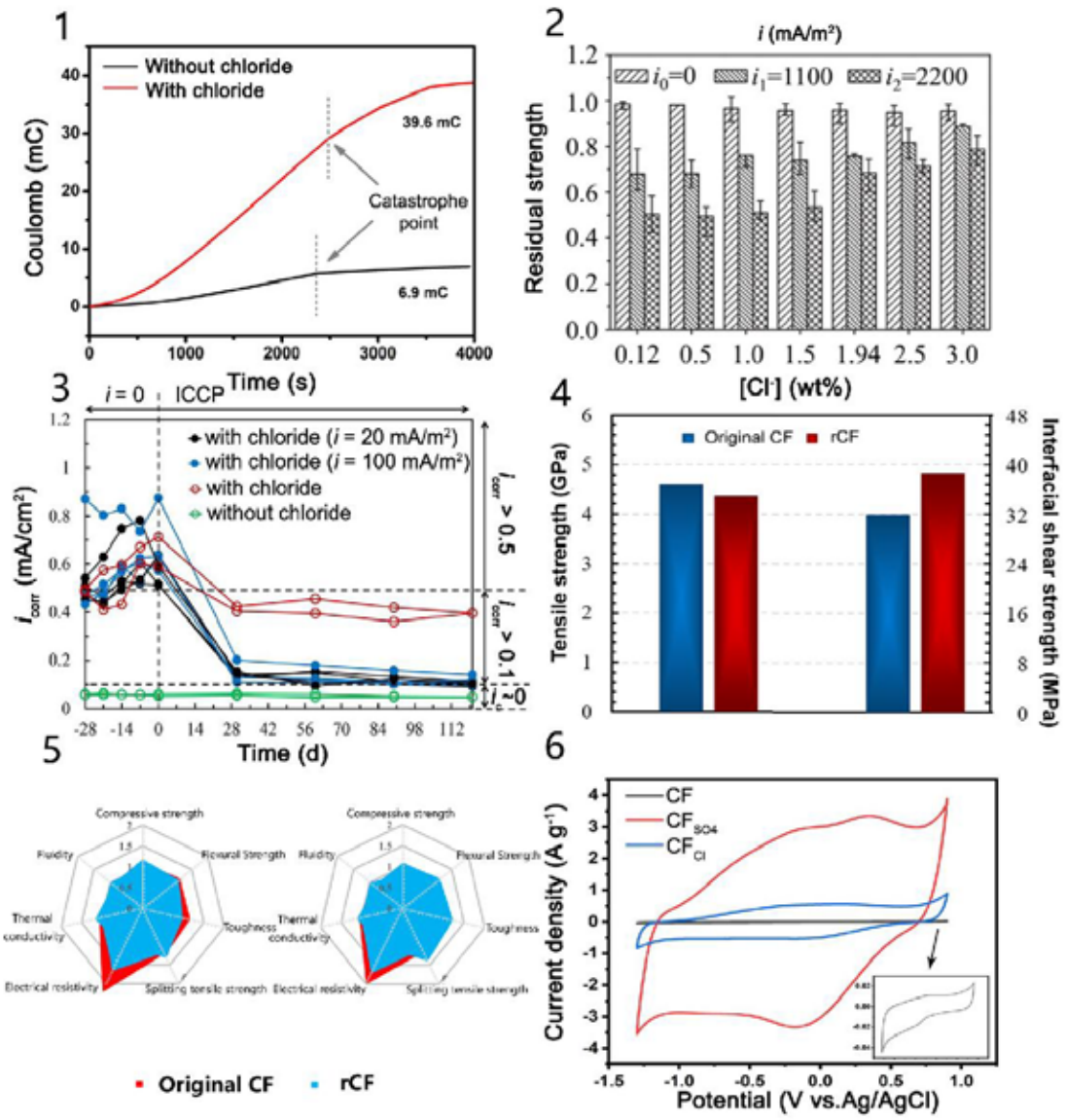

Fig. 1 Charge load on CF surface; **Fig. 2** Effect of polarization current density and chloride ion concentration on tensile properties of CF after polarization; **Fig. 3** Corrosion protection effect of ICCP-SS on chlorinated concrete; **Fig. 4** Comparison of tensile strength and interfacial shear strength between rCF and original CF; **Fig. 5** Comparison of the properties of carbon fiber reinforced concretes made from original CF and rCF; **Fig. 6** Cyclic voltammetry curves of CF before and after electrochemical treatment in different electrolytic salt solutions

Acknowledgment

The authors would like to acknowledge the funding support from the Key-Area Research and Development Program of Guangdong Province (2019B111107002) and the National Key Research and Development Program of China (2018YFE0124900).

The influence of lightweight functional aggregates on the acidification damage in the external anode mortar during cathodic protection for reinforced concrete

Wenhao Guo[1,2], Jie Hu[1*#], Jiangxiong Wei[1] and Qijun Yu[1]

(1) School of Materials Science and Engineering, South China University of Technology, Guangzhou 510640, Guangdong, China

(2) School of Transportation, Civil Engineering & Architecture, Foshan University, Foshan 528225, Guangdong, China

[*]*Presenter:* msjiehu@scut.edu.cn, [#]*Corresponding author:* msjiehu@scut.edu.cn

Abstract

Impressed current cathodic protection (ICCP) is an effective corrosion protection and prevention technique for reinforced concrete structures served in chloride-contaminated environment [1]. However, the anodic reactions occurred during ICCP treatment will both reduce the catalytic activity of the primary anode and result in dissolution of hydration products in the secondary anode mortar (leading to more porous microstructure and reduced adhesion at the primary anode/secondary mortar interface) [2, 3]. Therefore, improving the acidification resistance of the external anode mortar is of great importance for the long term application of ICCP treatment. In this study, a novel type of lightweight functional aggregates (LFA) was proposed to mitigate the acidification damage in the external anode system (Fig.1). The influence of the prepared LFAs both on the electrochemical performance (Fig.2 and Fig.3) of the primary anode and morphology, mineral compositions and microstructure of the secondary mortar were investigated.

In this study, severe acidification damage happened in the mortar matrix within a distance of 300 μm from the primary anode; beyond this region, the acidification damage was mainly propagated along the interfacial transition zone around the aggregates and resulted in cracks in the mortar matrix (Fig.4). Because the lightweight functional aggregates maintained the high alkalinity in the secondary mortar by releasing OH^- from the aggregates (Fig.1), the acidification damage both in the vicinity of the primary anode and ITZ around aggregates was significantly halted (Fig.4). Meanwhile, LFAs efficiently mitigated the damage of MMO coating on the primary anode surface, thus maintaining the high stability and catalytic activity of the primary anode, e.g. lower anodic polarization potential (Fig.2) and charge transfer resistance of the primary anode. Therefore, the prepared LFAs can be potentially used for preparing the high performance external anode mortar, further improving the stability and efficiency of ICCP treatment and durability of reinforced concrete structures.

Key words: Corrosion of reinforced concrete; Impressed current cathodic protection; Anode system; acidification mitigation.

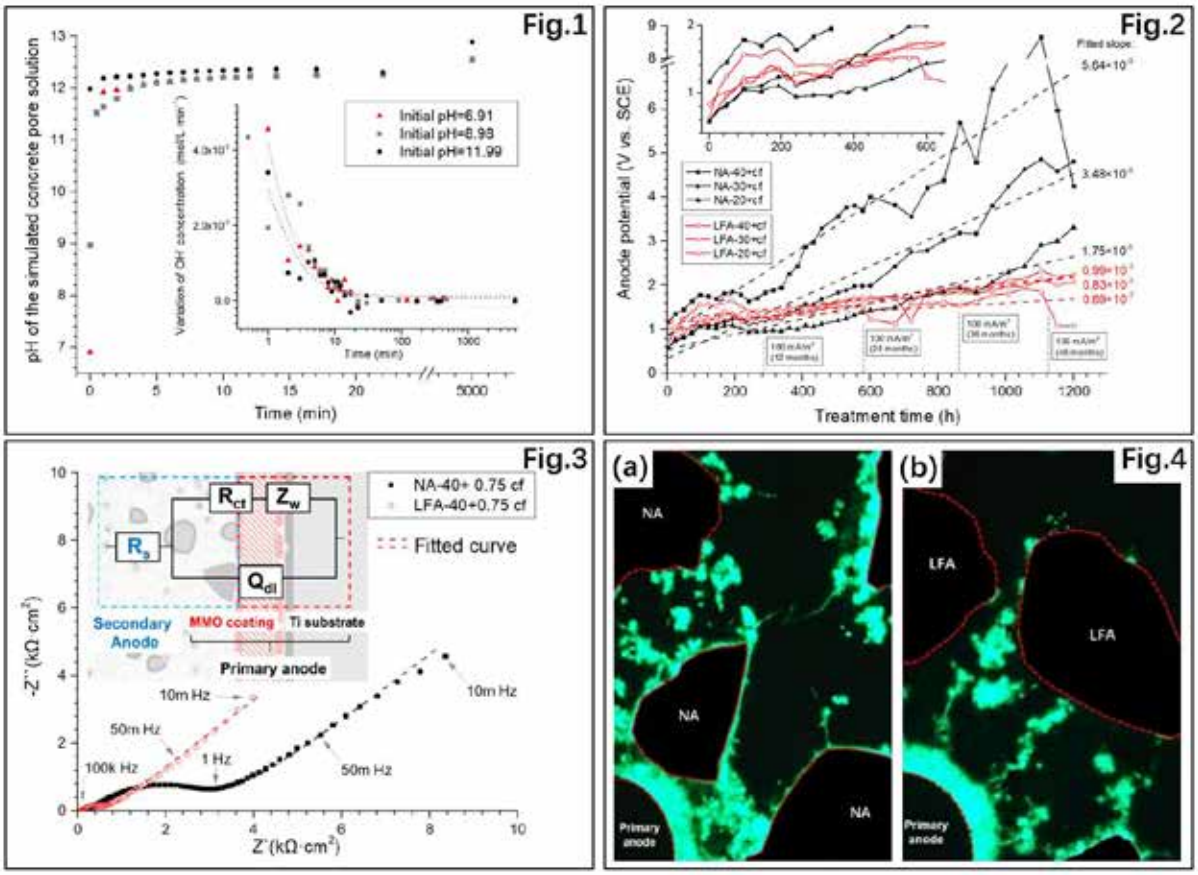

Fig. 1 The influence of LFA on the pH value of simulated concrete pore solution; **Fig. 2** Monitored anode potential of samples with varied aggregate volume fraction; **Fig. 3** Typical experimental EIS response from anode specimens with different types of aggregates and fitted curves with the designed equivalent circuit; **Fig. 4** Comparison of fluorescence microscopy images from anode specimens with normed aggregates (NA) (a) and LFAs (b) after the accelerated acidification test;

Acknowledgment

The authors would like to acknowledge the funding support from ( ) and the ( ).

[1] P. Pedeferri, Cathodic protection and cathodic prevention, Construction and Building Materials, 10 (1996) 391-402.
[2] K. Wilson, M. Jawed, V. Ngala, The selection and use of cathodic protection systems for the repair of reinforced concrete structures, Construction and Building Materials, 39 (2013) 19-25.
[3] S.D. Cramer, B.S. Covino, G.R. Holcomb, S.J. Bullard, W.K. Collins, R.D. Govier, R.D. Wilson, H.M. Laylor, Thermal sprayed titanium anode for cathodic protection of reinforced concrete bridges, Journal of Thermal Spray Technology, 8 (1999) 133-145.

Abstract

Electrodeposition of Cu_2O on the concrete surface was applied to protect the concrete sewers from microbially induced corrosion. The effect of deposition time, current density, solution type and concentration on the antimicrobial properties was investigated. XRD and SEM-EDS were used to analyze the morphology and chemical compositions of the depositions. The results indicated that the main compositions of the depositions were Cu_2O and Cu, and the copper content of the depositions increased with increasing the deposition time and current density. However, high current density (over 1.5mA/cm_2) caused a decrease in the permeability resistance of mortar specimens due to the thermal expansion of steels inside. Taking into consideration the copper content, bactericidal property, permeability and adhesion between depositions and substrate, optimum parameters of electrodeposition were determined. This preliminary study provided a basis for further investigating the antimicrobial performance of the developed concrete sewers in the real sewer situation.

Keywords: Microbially induced corrosion; concrete; SRB; Cu_2O; Electrodeposition

Parallel Sessions-2

High/Ultra-High Performance Fiber-Reinforced Cementitious Composites

Characterization and modification of interface transition zone in high performance fiber-reinforced concrete

Shan He[1], En-Hua Yang[1*#]

[1] School of Civil and Environmental Engineering, Nanyang Technological University, Singapore 639798
[*]*Presenter: ehyang@ntu.edu.sg,* [#]*Corresponding author: ehyang@ntu.edu.sg*

Abstract

The interfacial transition zone (ITZ) governs the mechanical properties and durability of fiber-reinforced cement-based composites. A new approach to characterize ITZ between microfiber and cement matrix is reported. Results show that microstructure of hydrated cement paste is highly modified in the vicinity of microfibers, with higher porosity and less anhydrous cement. ITZ can extend up to 100 μm from the interface into the matrix. The larger extent of ITZ suggests that perturbation due to inclusion of microfibers to packing of cement grains is severer than that due to inclusion of aggregates. Furthermore, ITZ between microfiber and cement matrix is highly heterogeneous along its axial direction. Existing ITZ analysis methods performed on 2-D cross-sectional plane intersecting with fiber axis thus can lead to errors and uncertainties. Mechanical properties of ITZ between microfiber and cement matrix are anisotropic. Stiffness and ductility of ITZ in the radial direction are 31% and 28% higher than that in the tangential direction, respectively.

A novel idea of using carbon nanofibers (CNFs) to strengthen the ITZ and to enhance the interface frictional bond strength between polyethylene (PE) fibers and cement-based matrix was proposed and realized by coating CNFs on surface of PE fibers through hydrophobic interactions. Such strategic strengthening of the ITZ by simple coating of CNFs on microfibers resulted in a 22% enhancement of the fiber/matrix bond. Results show that strategic application of CNFs greatly densified the ITZ with much reduced voids and defects. A distinctive hairy microstructure, resembling the setae on the toes of geckos, and less portlandite were found in the CNF-ITZ. The indentation hardness and indentation modulus were enhanced in both the radial and the tangential directions. The resulting CNF-reinforced ITZ is tougher and stronger with improved mechanical properties against deformation and cracking, which leads to enhanced fiber/matrix bond and elevated load transfer efficiency between fiber and matrix. As a result, a strain hardening ultra-high performance concrete (SHUHPC) incorporating such CNF-coated PE fibers was developed. The resulting CNF-SHUHPC has a compressive strength over 150 MPa and exhibits 15% enhancement in tensile strength, 20% improvement in tensile strain capacity, and reduced cracking spacing.

Keywords: Interfacial transition zone (ITZ); fiber/matrix interface; carbon nanofibers (CNFs); microstructure; ultra-high performance concrete (UHPC); strain hardening cementitious composites (SHCC)

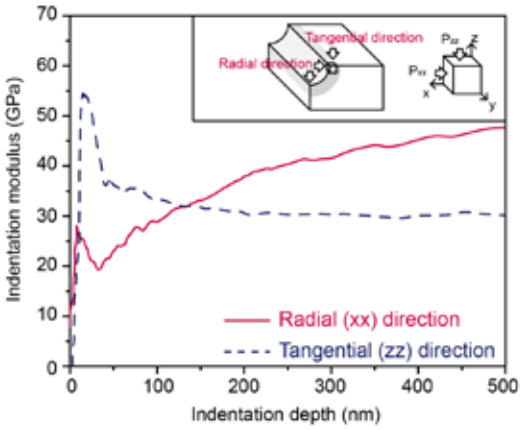

Fig. 1

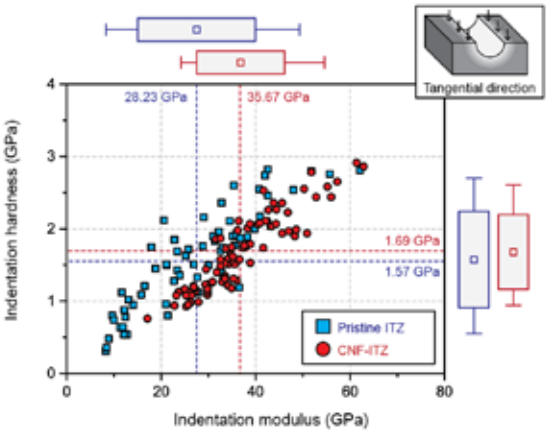

Fig. 2

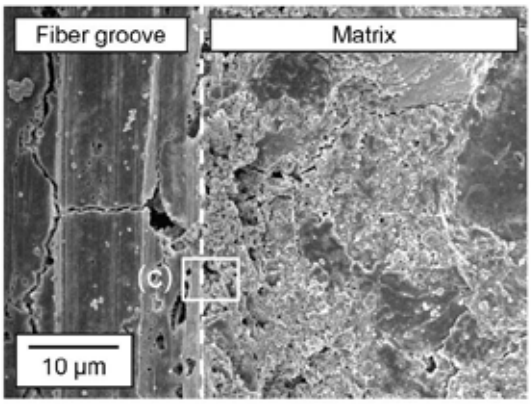

Fig. 3

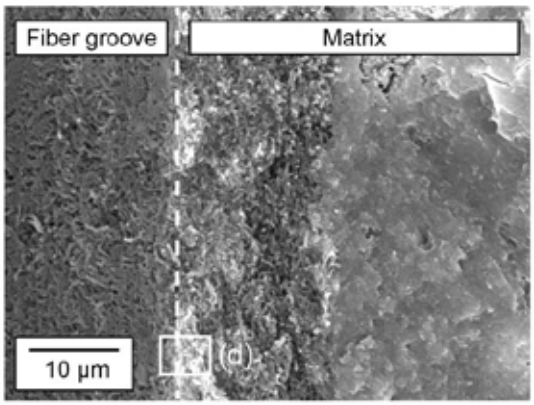

Fig. 4

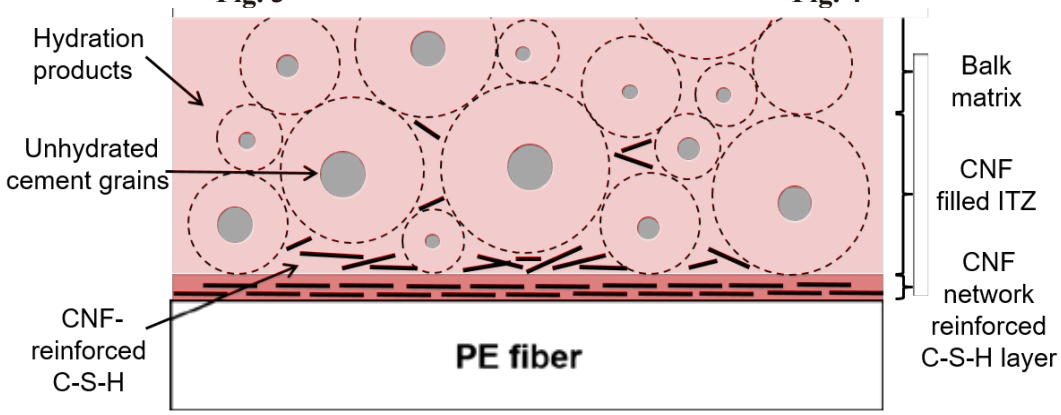

Fig. 5

Fig. 1 Anisotropic properties of the ITZ; **Fig. 2** CNF-reinforced ITZ with enhanced modulus and hardness; **Fig. 3** Microstructure of fiber/matrix ITZ; **Fig. 4** Microstructure of CNF-reinforced fiber/matrix ITZ; **Fig. 5** Schematic illustration of strategic strengthening of fiber/matrix ITZ with CNFs.

Acknowledgment

The authors would like to acknowledge the funding support from Ministry of National Development (L2NICCFP2-2015-4), Economic Development Board (EDB IPP-JACOB LIM), and ceEntek Pte Ltd (RCA-11/164).

Strain-Hardening Behavior of Ultra-High Performance Concrete Based on Silane Modification of Polyethylene (PE) Fiber

Gai-Fei Peng [1*], Gui Zhang [1#], Zehao Lei [2], Hong Ding [3], Yuheng Jiang [4], Xujing Niu [5], Pengju Wang [1]

[1] Faculty of Civil Engineering, Beijing Jiaotong University, Beijing 100044, China
[2] Department of Civil, Structural & Environmental Engineering, Trinity College Dublin, The University of Dublin, Dublin D02 PN40, Ireland
[3] Beijing Construction Engineering Group, Advanced Construction Materials Limited Liability Company, Beijing 100015, China
[4] Chinese Academy of Science (CAS) Key Laboratory of Nanosystem and Hierarchy Fabrication, CAS Center for Excellence in Nanoscience, National Center for Nanoscience and Technology and University of Chinese Academy of Sciences, Beijing 100190, China
[5] School of Mechanics and Civil Engineering, China University of Mining and Technology (Beijing), Beijing 100083, China
*Presenter: gfpeng@bjtu.edu.cn, #Corresponding author: guizhang@bjtu.edu.cn

Abstract

Generally ultra-high performance concrete (UHPC) possesses excellent mechanical properties and durability, in which fiber constitutes an indispensable raw material for toughening UHPC. Polyethylene (PE) fiber has been used for preparation of UHPC with obvious strain-hardening behavior. Although silane coupling agent (SCA) has an effective modification effect on the PE Fiber and hence on mechanical properties of UHPC, the mechanism for interaction between SCA-modified fiber and the matrix remains to be a controversial issue. In this research, SCA solutions at various concentrations from 1 % to 5 % were used to modify the surface of PE fiber to verify the mechanism for the interaction between SCA-modified PE fiber and the matrix of UHPC with strain-hardening behavior.

The stress-strain curves of UHPC containing PE fiber modified by SCA (Fig. 1) manifest that the modification of fiber surface significantly affected the strain-hardening behavior of UHPC. Compared with the ultimate tensile stress (6.11 MPa) of reference group (SCA18-0), the ultimate tensile stress of UHPC incorporating PE fiber modified by 1%, 3% and 5% concentrations of SCA solution reached to 7.39 MPa, 8.01 MPa and 7.04 MPa. The direct-tensile specimens containing original pristine PE fiber failed at a typical main-crack failure mode, while the specimens incorporating SCA-modified PE fiber exhibited a multi-cracking failure mode (Fig. 2), among which the UHPC incorporating PE fiber modified by 3% concentration of SCA solution obtained the optimum multi-cracking behavior.

The contact angle between SCA-modified PE film and water was 43 °, which was approximately half of that between the unmodified PE film and water (Fig. 3), which proved the improvement of hydrophilic feature of PE fiber. In the XRD diagrams of inorganic C–S–H (I–C–S–H), SCA solution modified C–S–H (M–C–S–H) and organic C–S–H (O–C–S–H) (Fig. 4), within the range of 0 °-10 °, the peak of M–C–S–H was broadened and interlamellar distance d001 (1.34 nm) of M–C–S–H was greater than that of I–C–S–H (1.31 nm), reveals that a chemical reaction might happen between the hydrolysate of SCA and I–C–S–H. The FTIR spectra of inorganic C–S–H (I–C–S–H), SCA solution modified C–S–H (M–C–S–H) and dried SCA solution (D–SCA) (Fig. 5) reveals that M–C–S–H contained Si-CH_3 groups at 802 cm^{-1} and 1261 cm^{-1}, while no Si-CH_3 group was detected in the unmodified I–C–S–H, and –OH groups in hydrolysate of SCA might participate in chemical reaction. The FTIR spectrum of M–C–S–H also suggests that hydroxyl groups of I–C–S–H condensed with hydroxyl groups of SCA's hydrolysate.

Based on the above results, the mechanism for the effect of SCA modification of PE fiber on the strain-hardening behavior of UHPC should be a combination of both physical and chemical interactions between fiber and matrix, and a modification layer formed on the surface of PE fiber (Fig. 6). Nevertheless, too thick a modification layer is undesirable for improving strain hardening behavior of UHPC.

Keywords: Ultra-high performance concrete; Strain-hardening; Polyethylene fiber; Surface modification; Mechanism

1

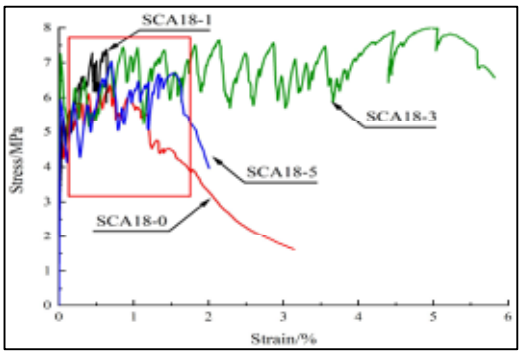

2

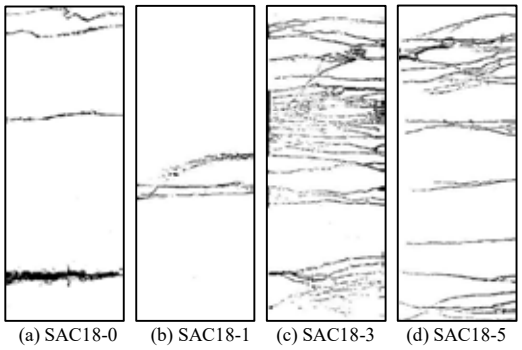

3

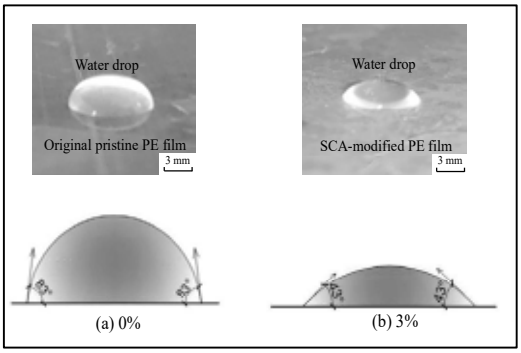

4

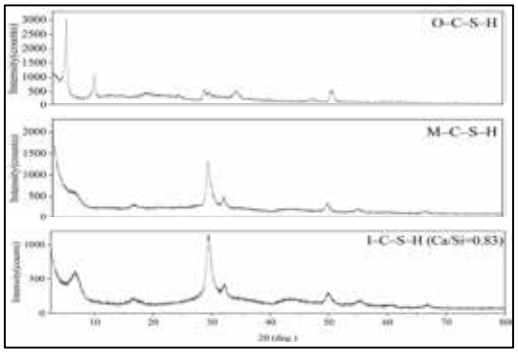

5

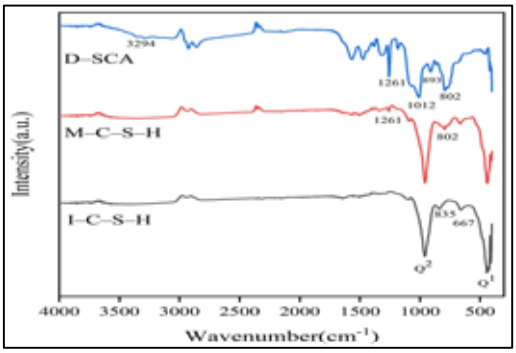

6

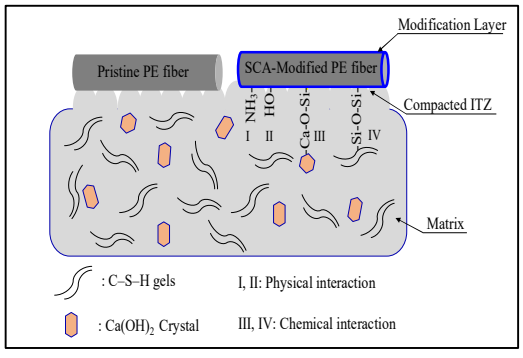

Fig. 1 Stress-strain curves of UHPC incorporating PE fiber modified by different concentrations of SCA solution; **Fig. 2** Crack development of UHPC incorporating PE fiber modified by different concentrations of SCA solution; **Fig. 3** Contact angle of original pristine PE film and SCA-modified PE film; **Fig. 4** XRD patterns of synthesized I–C–S–H, M–C–S–H and O–C–S–H; **Fig. 5** FTIR spectra of I–C–S–H, M–C–S–H and D–SCA; **Fig. 6** Schematic diagram of physicochemical interactions between SCA-modified PE fiber and UHPC matrix

Acknowledgment

The authors would like to express their gratitude to the National Science Foundation of China (Grant Nos. 51878032 and 52008230) and the Natural Science Foundation of Beijing (Grant No. 8212013 and 8172036), for their financial support.

Study on mechanism of basic tensile creep of recycled fine aggregate ultra-high performance concrete

Tao Ji[1*#], Qiang-Shun Sun[1], Yong-Ning Liang[1]

[1] College of Civil Engineering, Fuzhou University, Fuzhou, Fujina 350108, People's Republic of China

Presenter: jt72@163.com, #Corresponding author: jt72@163.com

Abstract

The traditional UHPC has excellent mechanical properties and durability, but its preparation cost is high and its autogenous shrinkage is large. Recycled fine aggregate (RFA) is a kind of fine aggregate obtained by crushing waste concrete, which has high water absorption and can play an internal curing role in concrete. In this paper, a saturated surface-dried RFA was used to replace natural river sand to prepare UHPC, so as to reduce the cost and autogenous shrinkage of UHPC.

RFA content is air-dried RFA/ (air-dried RFA+ river sand) (mass ratio). Air-dried (initial moisture content of 5%, AD) RFA was weighed and changed to saturated surface-dried (initial moisture content 11%, SSD). Saturated surface-dried state RFA was used in all groups. The effect of RFA content (0, 25, 50, 75 and 100%) on the mechanical properties, internal relative humidity, autogenous shrinkage and basic tensile creep of UHPC was studied. The microstructure, interfacial transition zone and pore structure of UHPC were studied by BSE, microhardness and MIP to reveal the mechanism of basic tensile creep of UHPC.

The results show that with the increase of RFA content, the autogenous shrinkage and basic tensile creep of UHPC first decrease and then increase (Fig. 1 and 2), respectively. In Figs.1-4, SSD25 means a UHPC with RFA content of 25%, and so on. When RFA content is 25%, the autogenous shrinkage and basic tensile creep of UHPC are the minimum. There are three main influencing factors of autogenous shrinkage (Fig. 3): (1) static elastic modulus; (2) mesoporous (<50 nm); (3) internal relative humidity. When the RFA content increases from 0 to 25%, the static elastic modulus of UHPC decreases, and the mesoporous increases, the internal relative humidity increases; the internal relative humidity plays a leading role in UHPC autogenous shrinkage, therefore the autogenous shrinkage of UHPC decreases. When the RFA content increases from 25 to 100%, the static elastic modulus of UHPC decreases, the mesoporous increases, and the internal relative humidity increases; the static elastic modulus and the mesoporous play a leading role, hence the autogenous shrinkage of UHPC increases.

There are three main influencing factors of basic tensile creep (Fig. 4): (1) autogenous shrinkage; (2) microhardness of ITZ3 (interface transition zone between old cement paste and UHPC matrix); (3) ink bottle pore volume. Autogenous shrinkage is the macroscopic driving force of basic tensile creep. Therefore, with the increase of autogenous shrinkage, the basic tensile creep of UHPC increases. The water filled in ink bottle pore, which is benefit for the slippage of hydration products. The larger ink bottle pore volume, the higher the basic tensile creep With the increase of RFA content from 0 to 25%, the autogenous shrinkage and ink bottle pore volume of UHPC decreases, so the basic tensile creep of UHPC decreases. With the increase of RFA content from 25 to 100%, the autogenous shrinkage and ink bottle pore volume of UHPC increase, and the microhardness of ITZ3 decreases, and the basic tensile creep of UHPC increases.

Keywords: Ultra-high performance concrete; recycled fine aggregate content; saturated surface dry; autogenous shrinkage; basic tensile creep

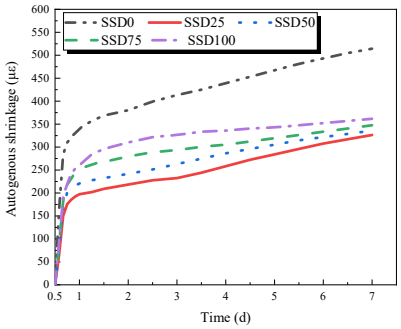

Fig.1

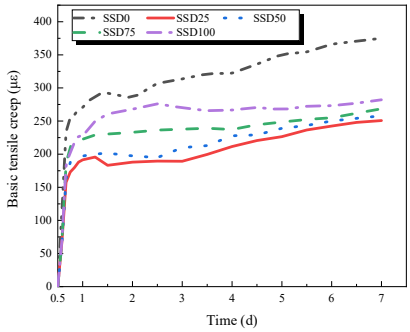

Fig.2

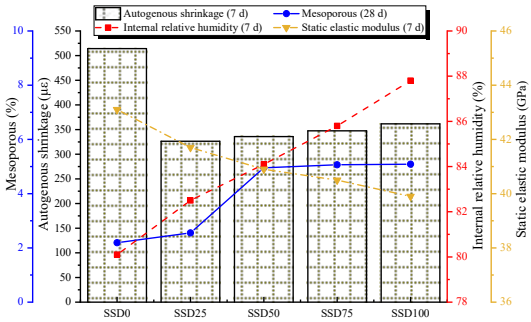

Fig.3

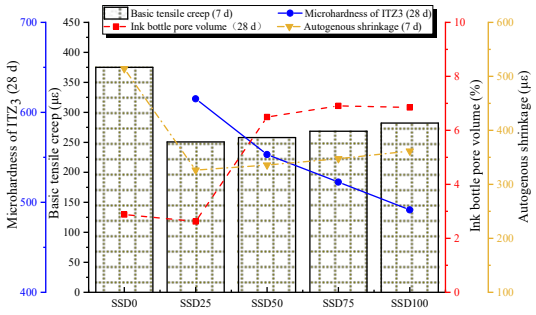

Fig.4

Fig. 1 Influence of RFA (SSD) content on UHPC autogenous shrinkage； **Fig. 2** Influence of RFA (SSD) content on UHPC basic tensile creep; **Fig. 3** Influencing factors of UHPC autogenous shrinkage; **Fig. 4** Influencing factors of UHPC basic tensile creep

Acknowledgment

The authors would like to acknowledge the funding support from the National Nature Science Foundation of China (51878179).

Flow-induced steel fiber alignment for improving mechanical performance of UHPC

Xiaojian Gao[1*], Huanghuang Huang[2, 3]

[1] School of Civil Engineering, Harbin Institute of Technology, Harbin, 150090, China,
[2] School of Materials Science and Engineering, Wuhan University of Technology, Wuhan, 430070, China
[3] State Key Laboratory of Silicate Materials for Architectures, Wuhan University of Technology, Wuhan, 430070, China
[*]*Corresponding author:* gaoxj@hit.edu.cn

Abstract

Steel fibers in UHPC cast by conventional method showed random orientation, and the orientation of a large number of fibers does not match the direction of principal tensile stress of samples, resulting in fiber underutilization. Considering the highly flow-dependent characteristics of fiber orientation, this paper developed a flow-induced casting method using a L-shape device to favor fiber alignment during UHPC placement. The alignment of fibers during flow of UHPC mixture was simulated using the Smoothed Particle Hydrodynamics (SPH) and visualization methods. The results showed that the fiber has a tendency to rotate to the streamline direction with the flow of UHPC (Fig. 1 and Fig. 2). The spread of fiber orientation coefficient obtained from image analysis and SPH simulation was limited to 15%.

The influence of fiber length, volume, and outlet height of L-shape device on flexural properties of fiber-aligned UHPC was investigated. The results showed that, compared to UHPC with random fiber orientation, fiber alignment can secure a 35% greater fiber orientation coefficient. Such improvement in fiber orientation led to 60% and 80% higher flexural strength and toughness, respectively (Fig. 3). This can enable 50% reduction in fiber volume, given the similar flexural properties. When the ratio of fiber length to outlet height (l_f/H) was 1.0-1.3, a better fiber alignment can be obtained (Fig. 4). A l_f/H value greater than 1.3 can lead to blockage.

The impact resistance of UHPC with fiber alignment under strain rates 160-290 s^{-1} was studied using the Spilt Hopkinson Pressure Bar (SHPB). The results showed that, given a similar strain rate, UHPC has a greater impact resistance when fiber orientation was predominantly aligned to be perpendicular, relative to the direction of impact loading. Dynamic compressive strength, peak strain, and energy absorption capacity were enhanced by 20%, 55%, and 95%, respectively, compared to those with random fiber orientation (Fig.5 and Fig. 6).

Keywords: UHPC; Flow-induced casting; Fiber alignment; Flexural properties; Dynamic properties

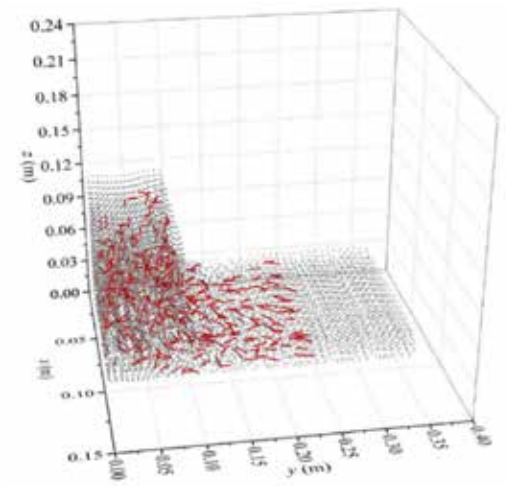

Fig. 1 SPH simulation of fiber alignment during flow-induced casting of UHPC

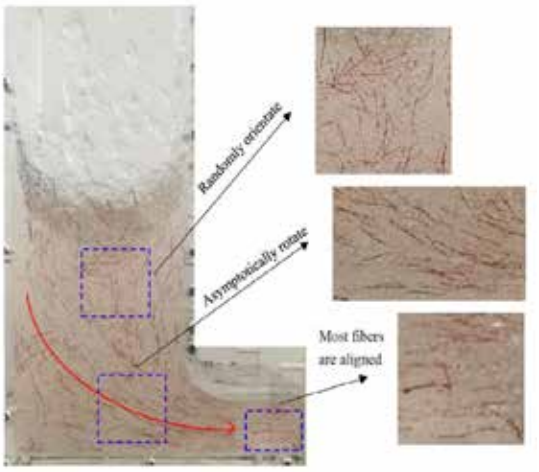

Fig .2 Visualization analysis of fiber alignment during flow-induced casting of UHPC

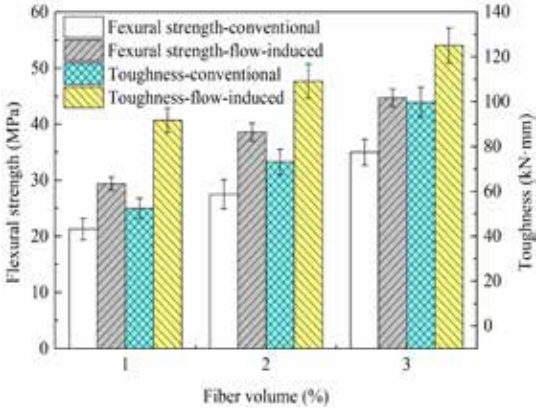

Fig. 3 Flexural strength and toughness of UHPC with random orientation and fiber alignment

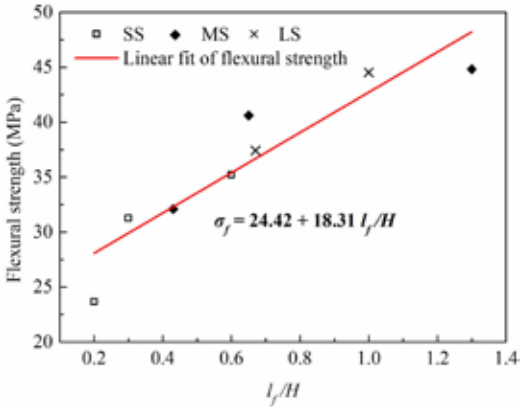

Fig. 4 Effect of l_f/H values on flexural strength of UHPC cast by flow-induced method

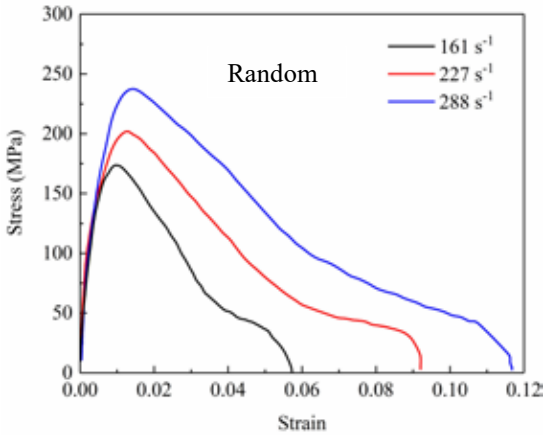

Fig. 5 Dynamic compressive strength-strain curves of UHPC with random fiber orientation

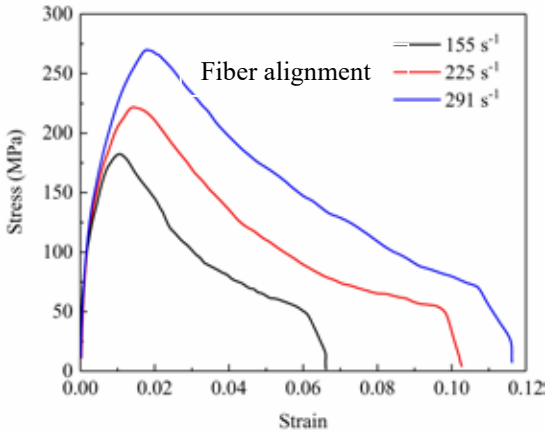

Fig. 6 Dynamic compressive strength-strain curves of UHPC with fiber alignment

Acknowledgment

The authors would like to acknowledge the funding support from the National Natural Science Foundation of China (grant number: U2106220).

Multifunctional stainless steel wires reinforced ultra-high performance concrete for upgrading structural longevity

Su-Fen Dong[1], Xin-Yue Wang[2], Bao-Guo Han[2, *, #]

[1] School of Transportation and Logistics, Dalian University of Technology, Dalian, 116024 China,
[2] School of Civil Engineering, Dalian University of Technology, Dalian, 116024 China

[*]*Presenter:* hanbaoguo@dlut.edu.cn, [#]*Corresponding author:* hanbaoguo@dlut.edu.cn

Abstract

As the main structural material for structures, concrete is in an important stage of transition to sustainable development due to its significant impact on the resilience of resources and energy as well as environment. Upgrading the performance of concrete (i.e., improving the mechanical properties and endowing multifunctional properties) to enhance structural longevity is an effective approach to indirectly reduce carbon emissions caused by the concrete production and usage. For example, if the service life of concrete structures is increased from 50 years to 100 years, the carbon emission will be reduced by half. Despite its remarkable fresh and hardened properties, the performance of ultra-high performance concrete (UHPC) needs to be continuously modified due to the complexity of service environments and the demand for structural performance improvement and expansion. Owing to the microscale diameter, high aspects, large specific surface area, similar thermal expansion coefficient to concrete matrix, high strength and modulus, resistance to corrosion, and good electrically/thermally conductive properties, stainless steel wires (SSWs) can not only modify the interface transition zone and microstructures of concrete but can also form a widely distributed enhancing, toughening, conductive and thermal network in UHPC at a low content level, thus endowing UHPC with multifunctional properties including enhanced mechanical performances and durability as well as smart property. Especially, the stainless profile of wires is beneficial to maintain the long-term stability of properties of UHPC, thus avoiding the adverse effects of steel fiber corrosion on the long-term properties of concrete structures.

In our study, the static/dynamic mechanical behaviors as well as electrically conductive, self-sensing, and thermally conductive characteristics of SSWs reinforced UHPC are investigated, and the modification mechanisms of SSWs on UHPC are revealed through microstructure, intrinsic electrical and thermal conductivity analysis. The experimental results demonstrate that the flexural strength, flexural toughness of UHPC unnotched beams and equivalent flexural strength of UHPC notched beams can be increased by 103.2%, 146.5% and 80.0%, respectively, due to the addition of 1.5 vol. % of SSWs with diameter of 20 μm (Fig.1). The average flexural fatigue life of UHPC is enhanced by 636.6%, 558.3% and 1010.7% at the maximum stress levels of 0.7, 0.8 and 0.9, and the calculated ratio of flexural fatigue endurance limit to static flexural strength for SSWs reinforced UHPC reaches up to 0.64. In addition, incorporating only 0.5 vol.% SSWs into UHPC enables the uniaxial compressive fatigue life and energy dissipation capacity to increase by 252.0% and 262.3%. The strain sensitivity of 0.5 vol.% SSWs (with diameter of 8 μm) reinforced UHPC is 22.5, 94.9 and 43.6 under cyclic compression, monotonic compression and flexure, respectively, much higher than the gauge factor of commercial strain gauge. Meanwhile, the cracking opening process of composites under flexural loading can be real-timely monitoring (Fig. 1). The results of finite element simulations indicate that the temperature gradients for UHPC pavement slab with a size of 4.5 m×5 m×0.4 m is dropped by 6.9 ℃, and the maximum thermal stress is reduced by 0.90 MPa as 1.5 vol% of SSWs with diameter of 20 μm are added (Fig. 2). Microstructure analyses reveal that the modification mechanisms of SSWs on UHPC mainly come from the microstructure refinement effect, the widely connecting network, the

restraining effect on initiation and convergence of microcracks, and the pull-out and stripping of SSWs under loading.

The developed multifunctional SSWs reinforced UHPC has great potential to enhance the structure safety, durability, multifunctionality/intelligence, resilience and sustainability, as well as update structural longevity to reduce the life cycle cost of structures. Under the same bearing capacity, the employment of multifunctional SSWs reinforced UHPC can also decrease section size of structural elements and optimize structural design to reduce the relative demand for concrete materials. This is an effective approach to address the ecological issues of concrete materials and structures and reduce environmental footprint (especially carbon emission) caused by the extensive use of concrete.

Keywords: Ultra-high Performance Concrete (UHPC); Stainless Steel Wires; Mechanical Properties; Multifunctional Performance; Structural Longevity

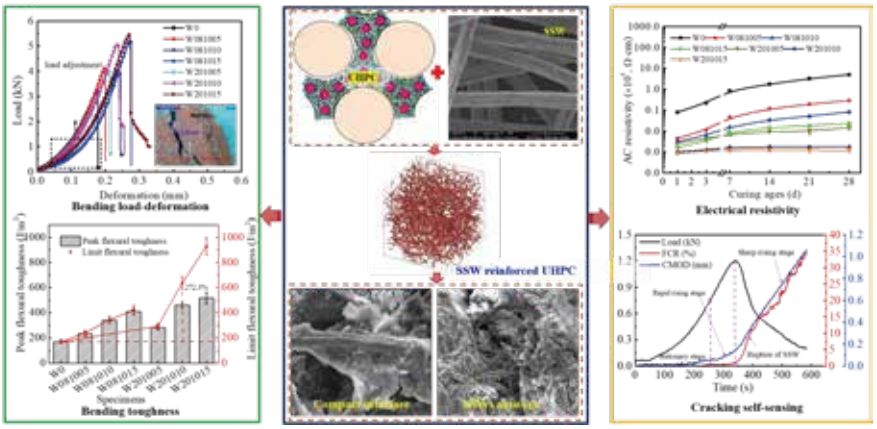

Fig. 1 Toughness, electrical resistivity and cracking self-sensing of SSWs reinforced UHPC

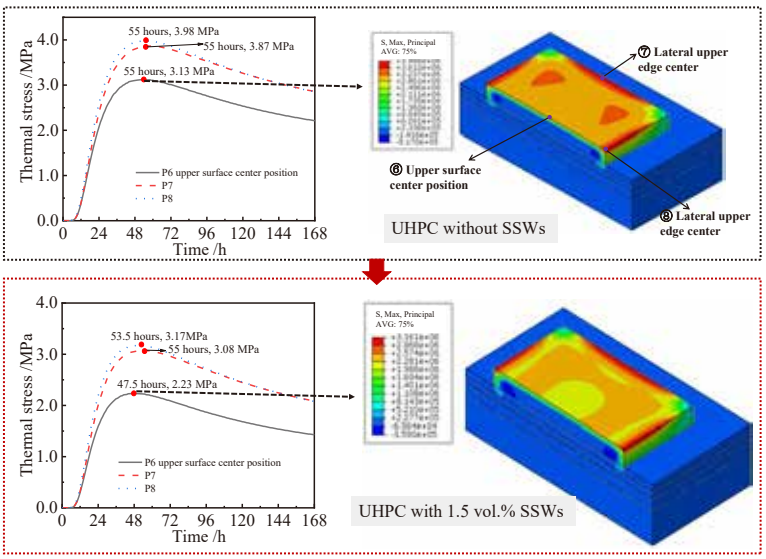

Fig. 2 Thermal stress and hydration time relationships in pavement slabs fabricated by using UHPC without and with 1.5 vol.% SSWs

Acknowledgment

The authors would like to thank the National Science Foundation of China (52178188, 51908103 and 51978127), the Fundamental Research Funds for the Central Universities (DUT21RC(3)039) for providing funding to carry out this investigation.

Shear Failure Mechanism and Loading-Capacity Model of Reinforced ECC Beams

Dawei Gu[1], Jinlong Pan[1*]

[1] School of Civil Engineering, Southeast University, Nanjing, China

Presenter: cejlpan@seu.edu.cn, #Corresponding author: cejlpanf@seu.edu.cn

Abstract

To enhance the structural and seismic resistance, as well as durability of concrete structures, an ultra ductile fiber reinforced cementitious composites called Engineered Cementitious Composite (ECC), also known as Strain Hardening Cementitious Composite (SHCC), was developed. ECC has a similar compressive and tensile strength to conventional concrete, but it exhibits a pseudo-strain-hardening behaviour under uniaxial tension with excellent crack control ability. The ultimate tensile strain of ECC can reach 3-12%, which is 300-1200 times higher than that of concrete. It is reported that ECC can also exhibit at least twice as high shear carrying capacity compared to traditional concrete, signifying a potential to use ECC material in shear-resistance elements. However, the shear resisting mechanism of reinforced ECC (R/ECC) members is still not clear.

In most existing codes and models, the shear strength of reinforced structural members (V_u) is divided into two parts, i.e., shear resistance coming from the matrix (V_c) and from the transverse reinforcement (V_s). To quantify accurately V_c and V_s and also their development throughout the loading, a well-designed testing method consisting of continuous strain quantification along the stirrups, was used in this research. That is, cutting the stirrup leg into two halves, and installing strain gauges continuously inside a small cavity at the center of the bar. With such a full record of strain, the V_s can be determined by the stirrup strain where shear crack crossed, and V_c can be calculated by subtracting V_s from the total shear force. Six steel reinforced beams incorporating different matrix (ECC, concrete and mortar) were tested under four-point bending.

Shear compression failure was found for all tested beam specimens with crushing of matrix in compression zone. Unlike sudden and rapid shear crack propagation in reinforced concrete and mortar beams, steady and multi-cracking behavior was observed in ECC beams. For all samples, R/ECC, RC or R/mortar, V_c was found not constant after first shear cracking. Besides, stirrups crossed by shear crack did not always yield when ultimate shear strength was reached. Therefore, assuming yielding for all the stirrups along shear cracking path would lead to overestimation on V_s. The shear strength of R/ECC without stirrups was found to be 170% that of the reference concrete beam. However, when reinforced with stirrups ($\rho_t = 0.38\%$), the shear strength of R/ECC beam was found only 13% higher than that of concrete ones, which resulted from incomplete yielding of stirrups at ultimate shear failure. Finally, a simplified truss-strut model for predicting shear carrying capacity of reinforced ECC beams is proposed, and a good agreement is achieved with the experimental results.

Keywords: Engineered Cementitious Composite (ECC), Shear strength components, Stirrup

Fig. 1 Cavity inside stirrup legs and steel cage

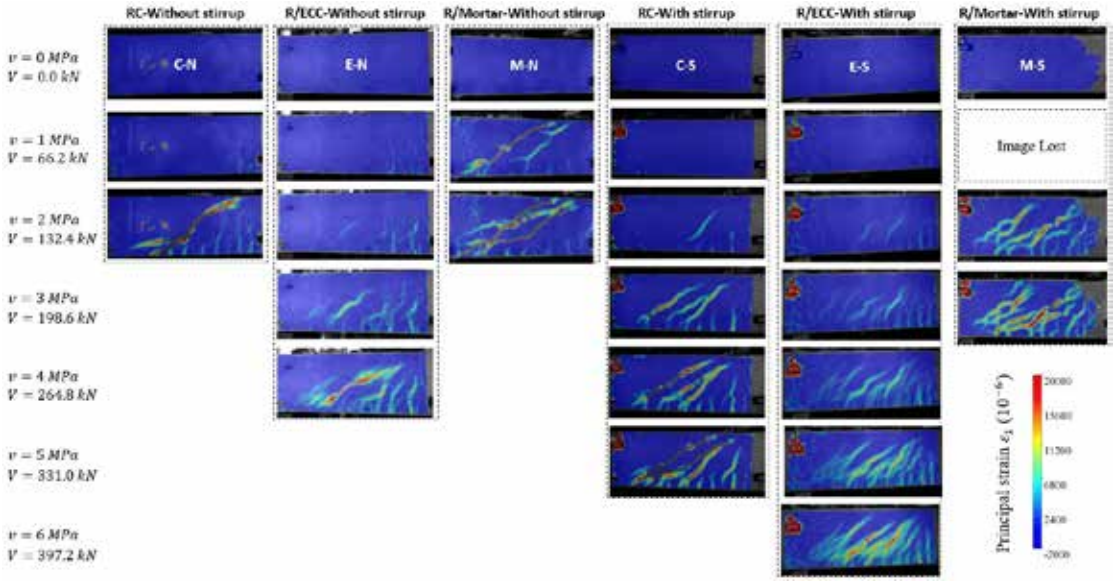

Fig. 2 Principal strain distribution in RC, R/ECC and R/mortar beams at different load stage

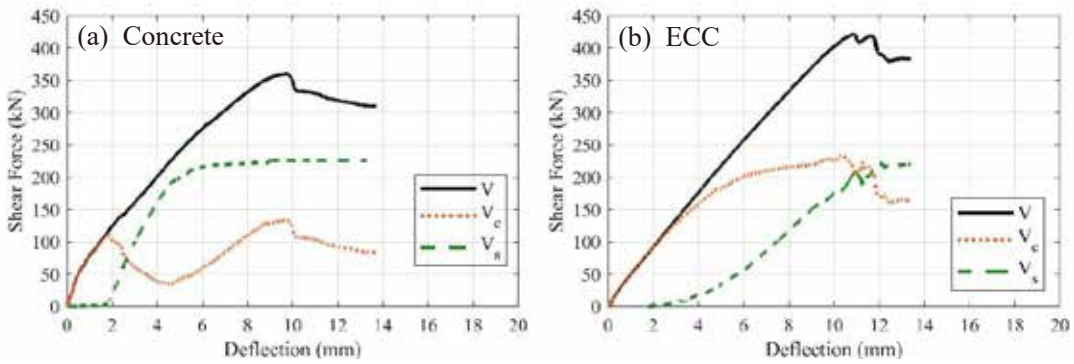

Fig. 3 Variation in V_s and V_c against deflection for: (a) RC beam; (b) R/ECC beam

Acknowledgment

The authors would like to acknowledge the funding support from the Key Project of National Natural Science Foundation of China (52130210) and the General Project of National Natural Science Foundation of China (51778131).

Sustainable Engineering Cementitious Composites (ECC) with granite fine as fine filler

Abstract. In this research, an industrial waste material-granite fine (GF) has been used to replace silica sand (SS) with ratios 50% and 100% to develop sustainable ECC. Mechanical properties (compressive strength and tensile strength) tests were conducted to evaluate the feasibility of GF in ECC. It turned out that the tensile performance was significantly improved. Scanning electron microscope (SEM) was used to analyze the morphology and microstructure of hydration products. An enhancement of strain-hardening performance by the incorporation of GF is indicated in the results. As the consequence, GF could be used as the fine filler in ECC to replace SS to improve the performance and reduce the detrimental environmental impact due to waste disposal.

Keywords: Engineering Cementitious Composites (ECC), Recycled granite fine, Mechanical properties, Sustainability

Effect of waste clay brick powder on key performance of UHS-UHDCC

Li-Ping Guo [a, b, *], Jian-Dong Wu [a], Yao-Yi Qin [a]

[a] *School of Materials Science and Engineering, Southeast University, Nanjing 211189, P.R. China*
[b] *Collaborative Innovation Center for Advanced Civil Engineering Materials, Jiangsu Key Laboratory of Construction Materials, Nanjing 211189, P.R. China*
[*] *Presenter and corresponding author:* guoliping691@163.com

Abstract

Large quantities of waste clay bricks from construction and demolition (C&D) waste are currently stockpiled in landfills, which is an environmentally, technically, and economically detrimental procedure. It is considered that grinding waste clay brick into the waste clay brick powder (WCBP) with sufficient fineness, aiming to exhibit the pozzolanic activity, as an additive for the production of cement or concrete initiates a promising new opportunity for the treatment of waste clay brick. In this work, WCBP was assessed to determine its feasibility as an alternative to cement for ultra-high-strength and ultra-high ductility cementitious composites (UHS-UHDCCs). The influences of WCBP on the fluidity, hydration, mechanical properties, fiber/matrix interface performances, autogenous shrinkage, and ecological overload capacity of UHS-UHDCC with different replacement levels ranging from 0-50% were investigated. The results indicate that WCBPs reduce the fluidity of the UHS-UHDCC matrix (Fig. 1). WCBP content of 20% slightly accelerates the hydration process and exhibits the highest compressive and flexural strength in the specimens (Fig. 2).

The incorporation of WCBP in UHS-UHDCC mixtures causes the first cracking stress and tensile stress to increase at first and then decrease, of which WCBP20 shows the best performance. All UHS-UHDCCs exhibited an apparent tensile strain hardening characteristic (Fig. 3). Moreover, the addition of WCBP tends to produce more cracks in UHS-UHDCC specimens meanwhile narrows the crack width.

The performance of the interface frictional bond (τ) with different WCBP content was obtained through single-fiber pullout tests, which reasonably explained the macroscopic tensile properties of UHS-UHDCC. The average interface frictional bond (τ) between the fiber and matrix of UHS-UHDCC reaches the maximum 1.72 MPa in the WCBP20 specimen. The average slip hardening coefficient (β) of UHS-UHDCC is distributed between 0.0031 and 0.0075 and tends to be excellent in the WCBP20 specimen (Fig. 4).

The theoretical fiber bridging stress *vs* crack displacement relationship of UHS-UHDCC was calculated through the limitation of interface parameters, which had an excellent correlation with the experimental results. Furthermore, the introduction of WCBP remarkably reduces the autogenous shrinkage of UHS-UHDCC (Fig. 5). The ecological overload capacity of UHS-UHDCC is decreased by the introduction of WCBP, which provides an environmentally friendly solution for the C&D and cement industries.

Keywords: ultra-high-strength and ultra-high ductility cementitious composites; waste clay bricks powder; mechanical properties; tensile strain capability; single-fiber pullout; ecological evaluation

1

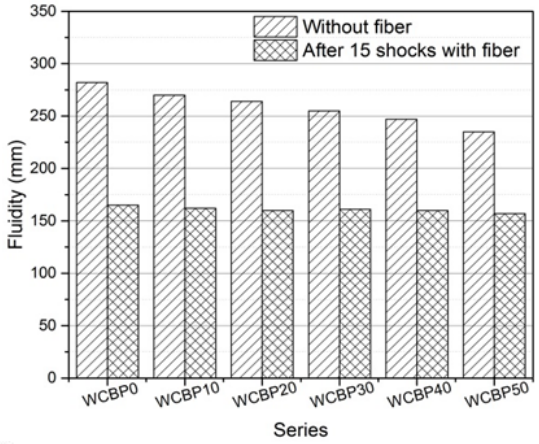
Without fiber
After 15 shocks with fiber
Fluidity (mm)
350
300
250
200
150
100
50
0
WCBP0
WCBP10
WCBP20
WCBP30
WCBP40
WCBP50
Series

2

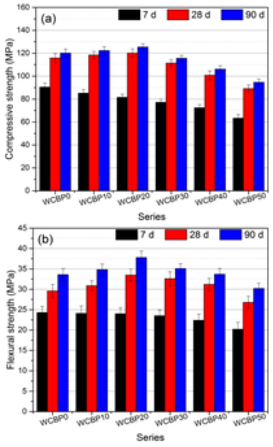
(a)
7 d
28 d
90 d
Compressive strength (MPa)
(b)
Flexural strength (MPa)
Series

3

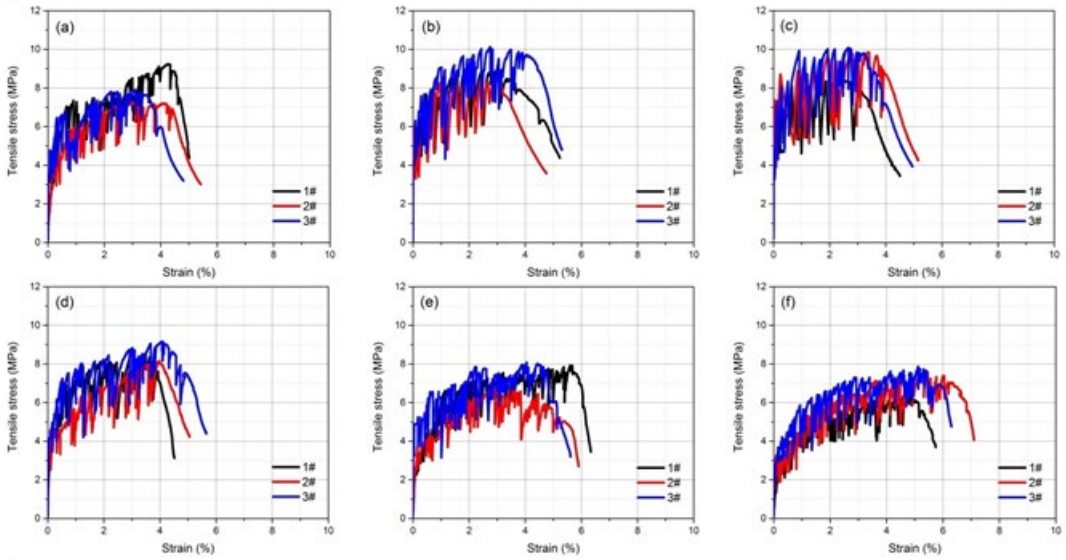
(a)
(b)
(c)
(d)
(e)
(f)
Tensile stress (MPa)
Strain (%)
1#
2#
3#

4

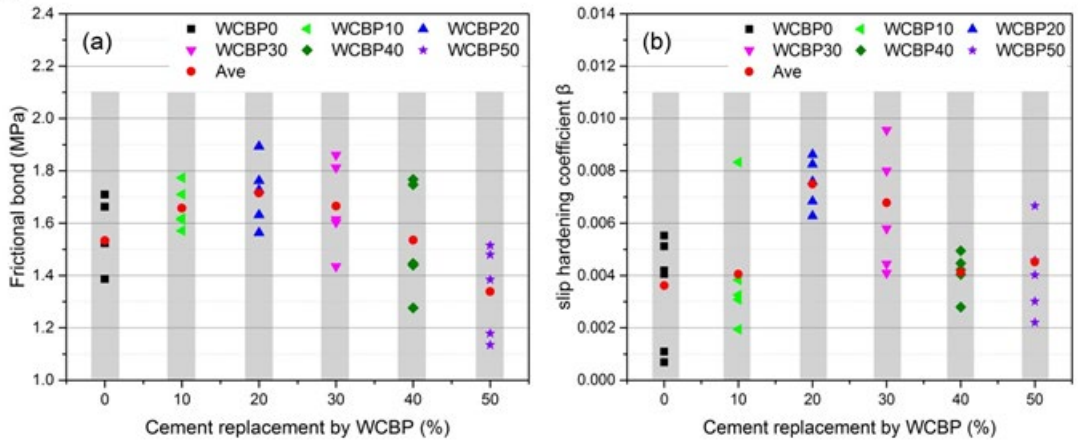
(a)
(b)
WCBP0
WCBP10
WCBP20
WCBP30
WCBP40
WCBP50
Ave
Frictional bond (MPa)
slip hardening coefficient β
Cement replacement by WCBP (%)

5

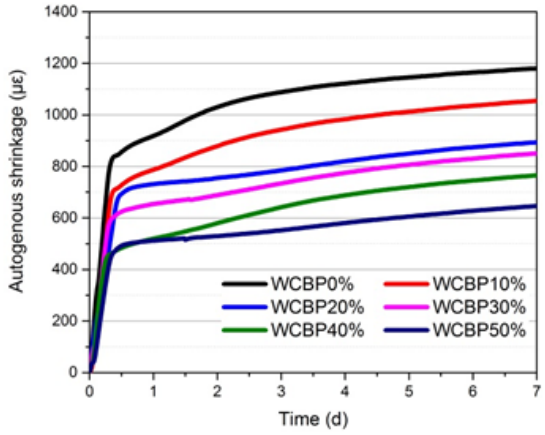

Fig. 1 The effect of WCBP replacement level on UHS-UHDCC fluidity; **Fig. 2** (a) The compressive strength and (b) flexural strength of UHS-UHDCCs at 7 d, 28 d, and 90 d; **Fig. 3** Tensile stress vs strain curves of UHS-UHDCCs with different content of WCBP: (a) 0%, (b) 10%, (c) 20%, (d) 30%, (e) 40%, and (f) 50%; **Fig. 4** Fiber/matrix interface parameters (a): frictional bond; (b) slip hardening coefficient; **Fig. 5** Autogenous shrinkage of UHS-UHDCCs with different content of WCBP

Acknowledgment

The authors would like to acknowledge the funding support from the National Natural Science Foundation of China (Grant No. 52178191; 51778133).

Effect of uniform and non-uniform corrosion on cracking propagation and bonding performance of mortar and ECC specimens

Chuan-qing Fu[1,2*], Rui He[3], Ke-jin Wang[2#]

[1]College of Civil Engineering, Zhejiang University of Technology, Hangzhou, 310023, People's Republic of China
[2]Department of Civil, Construction and Environmental Engineering, Iowa State University, Ames, IA, 50010, USA
[3]College of Civil Engineering and Architecture, Zhejiang University, Hangzhou 310027, People's Republic of China
Presenter: chqfu@zjut.edu.cn, #corresponding author: kejinw@iastate.edu

Abstract

Engineered Cementitious Composite (ECC), which has a strain-hardening behavior under tension, has been widely used for repairing and retrofitting the reinforced concrete structures. In such applications, the performance of the bonding between the ECC and corroded rebar is critical for the service life prediction of the repaired structures.

In this work, a new experimental method was firstly proposed to rapidly induce non-uniform distribution of rust layers around steel bars. The proposed method is based on the impressed current method with short testing duration, but capable of inducing morphologies of rust distribution closer to those observed in natural corrosion environments than other existing methods. X-ray microto mography with image analysis techniques was implemented to quantify the rust formation and propagation in the proposed setups. A finite element model to systematically and semi-quantitatively investigate several experimental parameters (e.g., the distance between anode and cathode, the anode to-cathode area ratio) was established and verified by a series of independent experimental programs. The corrosion current density distributions of uniform and non-uniform corrosion simulation are presented in Fig. 1. It can be seen that in non-uniform corrosion simulation, the corrosion current was mostly concentrated around the steel rebar on the side near the cathode (i.e., steel wire), while on the side facing away from the cathode, the corrosion current density was low. The corrosion current density was uniformly distributed in uniform corrosion simulation model.

The uniform corrosion induced cracks evenly distributed around the steel rebar while the non-uniform corrosion induced cracks concentrated in a line perpendicular to the rebar -steel wire line which can be attributed to the rust accumulation.Pull-out induced cracks developed along with the corrosion induced cracks. The pull-out cracks of uniform corroded specimens uniformly distributed around the specimen surface while the non-uniform corrosion specimens showed concentrated pull-out cracks on one side with more rust, which can be attributed to the corrosion pits which increased the friction and mechanical forces on the side close to the steel wire (Fig. 2).

The bond strength of ECC and mortar specimens is independent with corrosion method. Both ECC and mortar specimens showed a trend of increasing first and then decreasing with the development of corrosion rate. The threshold corrosion rate for mortar specimen is 0.125% while the ECC specimen has the threshold corrosion rate value of 0.922% (Fig. 3).

Keywords: Uniform corrosion; Non-uniform corrosion; Engineered Cementitious Composite (ECC); Cracking pattern; Bond strength

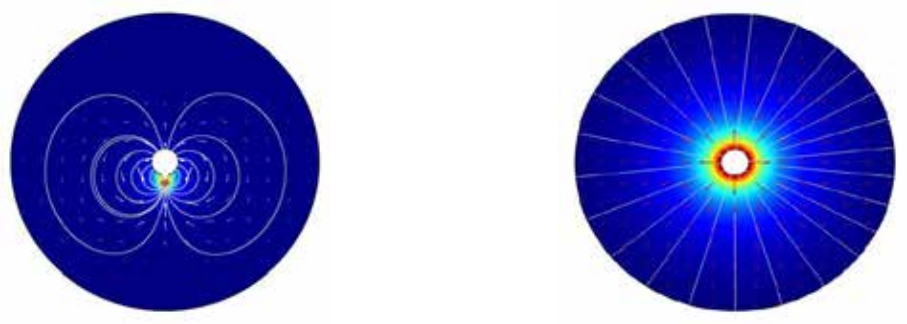

(a) Non-uniform corrosion (b) Uniform corrosion

Fig. 1. Corrosion current density distribution simulation results.

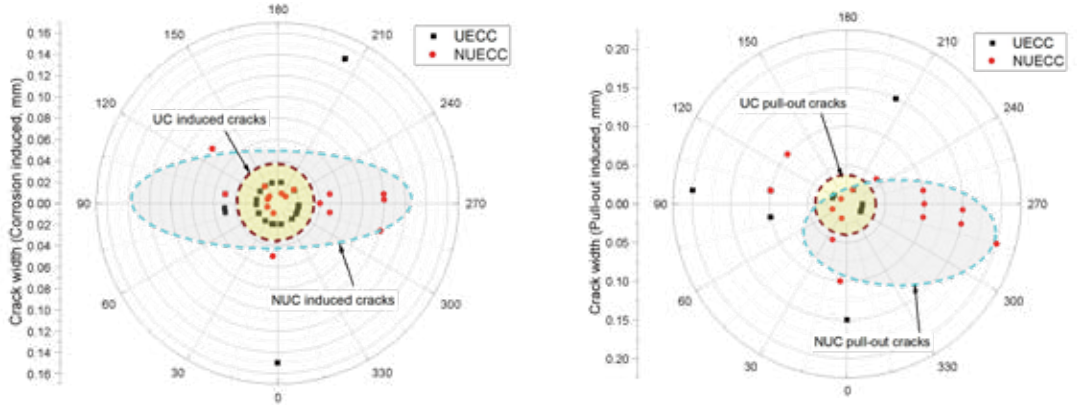

(a) Corrosion induced cracking patterns of ECC specimens. (b) Pull-out induced cracking patterns of ECC specimens.

Fig. 2. Cracking patterns of mortar and ECC specimens.

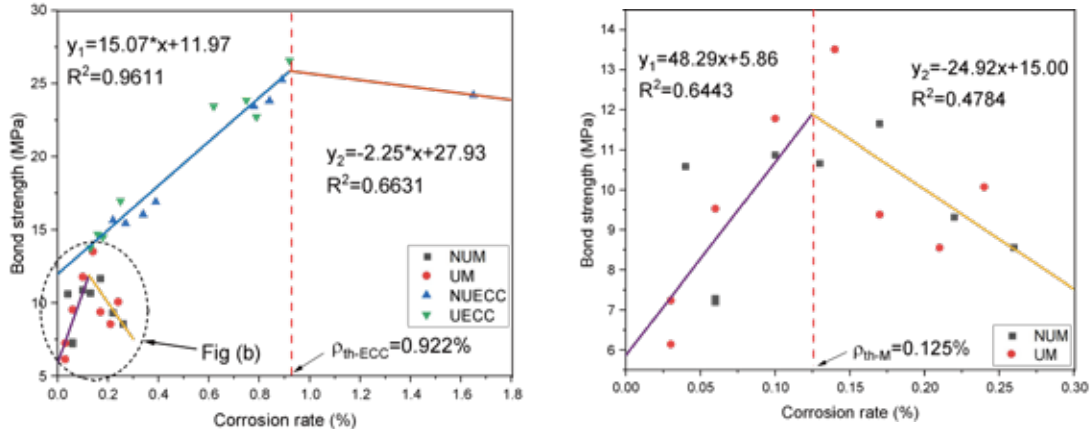

(a) ECC specimens (b) Mortar specimens

Fig. 3. Bond strength of corroded specimens in terms of corrosion rate.

Acknowledgment

Authors would like to acknowledge the financial support from the Natural Science Foundation of Zhejiang Province (Grant No. LR21E080002, LZ20E080003), and the National Natural Science Foundation (Grant Nos. 51678529 and 51978620).

Development of Basalt-fiber ECC

Mingfeng Xu [1], Jian Zhou [1*#], Hui Li [1]

[1] School of Civil and Transportation Engineering, Hebei University of Technology, Tianjin, 300401, China

*Presenter: zhoujian@hebut.edu.cn, #Corresponding author: zhoujian@hebut.edu.cn

Abstract

Fiber plays a key role in the mechanical properties of Engineered Cementitious Composites (ECC), a new generation of fiber-reinforced concrete with excellent ductility and exceptional crack control capability. However, ECC loses its high ductility when exposed to fire, as the synthetic fibers typically used in ECC melt resulting in a loss of crack-bridging ability in elevated temperatures. In this study, the feasibility of using basalt fiber, an inorganic fiber with high-temperature resistance, to develop ECC is investigated experimentally. the Basalt Fiber Engineered Cementitious Composites (BF-ECC) with different amounts of basalt fiber and matrix ingredients were designed. Compressive and uniaxial tensile tests were conducted to characterize the macro-scale mechanical properties. The underlying mechanisms of the crack pattern are investigated from the perspective of meso-scale relationship of fiber bridging and crack opening displacement.

The results show that basalt fiber reinforced ECC (BF-ECC) exhibits a very unique strain-hardening and multiple-cracking behavior when compared with typical ECCs. Extremely tight and densely distributed cracks are exhibited on BF-ECC specimens after tensioning into the strain-hardening regime. The average crack width is less than 8 μm, about one order of magnitude smaller than typical ECCs prepared with PVA, PP or PE fibers. The tensile stress-strain curve of BF-ECC is uniquely smooth. Stress drops during strain-hardening in ECC is found to scale linearly with crack width. The almost imperceptible stress drops in BF-ECC is due to its extremely tight crack width. Increasing cement content (from 10% to 20%) in the studied BF-ECC leads to an increase in the first cracking strength of (from 1.86 MPa to 2.44 MPa) and the ultimate tensile strength (from 3.29 MPa to 3.51 MPa), but a decrease in the tensile strain capacity. As expected, the ultimate tensile strength and tensile strain capacity of BF-ECC both increase with fiber content.

This work paves the way for further developing ECC with high-temperature resistance.

Keywords: Basalt fiber; Engineered Cementitious Composites; Mechanical properties; Crack pattern.

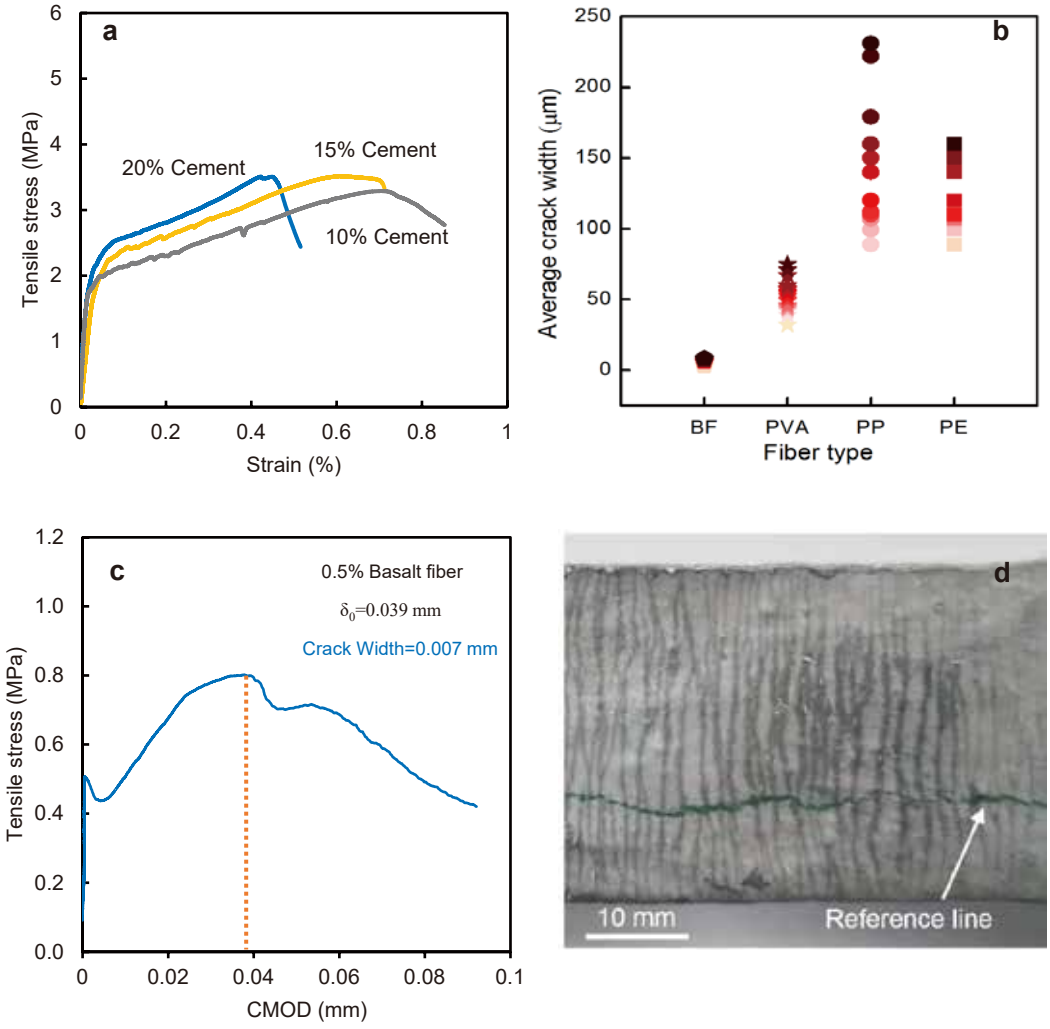

Fig. 1 Tensile stress-strain curves of BF-ECCs at the age of 28days; **Fig. 2** Comparison on the average crack with of BF-ECC, PVA-ECC, PP-ECC and PE-ECC; **Fig. 3** Experiment stress-CMOD curves obtained from notched tensile specimens of BF-ECC; **Fig. 4** saturated multiple-cracking of BF-ECC with 15% cement and 3.0% fiber after uniaxial tension test under optical microscopy.

Acknowledgment
The authors gratefully acknowledge the financial support of Natural Science Foundation of China (No. 51878238, 51702082).

Experimental and numerical investigation on the long-term performance of Engineered Cementitious Composites (ECC) with high-volume fly ash

Cong Lu[1,*], Zhi-Ming Pang[2], Han Chu[3], Christopher K.Y. Leung[4]

[1, 2, 3] School of Civil Engineering, Southeast University, Nanjing211189, China
E-mail: conglu@seu.edu.cn, zhimingpang@seu.edu.cn, chuhan@seu.edu.cn
[4] Department of Civil and Environmental Engineering, The Hong Kong University of Science and Technology, Hong Kong, China
E-mail: ckleung@ust.hk

Abstract

High-volume fly ash (FA) has been widely adopted in the material design of engineered cementitious composites (ECCs) to improve the mechanical properties of the material, and to develop a green approach for preparing ECCs. Previous studies have mainly focused on the mechanical performance of ECCs cured for 28 days. The secondary hydration of fly ash leads to delayed strength gain after 28 days, which may cause the composites to violate the long-term strain hardening criterion. In this study, multiple-scale experiments were conducted on ECC with high-volume FA at curing ages of 28, 90, 180, and 365 days, to investigate the long-term performance of ECC with evolving micromechanical properties. The results showed that after 28 days, the fiber/matrix interfacial bonding, matrix compressive strength, and fracture toughness gradually increased with curing time and plateaued at a certain value after 180 days, while the tensile strain capacity of the specimens continued to decrease with age. Based on the micromechanical parameters tested at different ages, a physical model was developed to simulate and predict the tensile performance of ECCs as it evolves with time. The simulation results were in agreement with those of the experimental tests. Therefore, design guidelines were proposed based on the predictions to enhance the robustness of the ECC's long-term performance.

Keywords: ECC; Fly Ash; Long-Term Performance; Micromechanics; Tensile Properties

Advances of ECC micromechanics

Junxia Li [1, *]

[1]Institute of Materials Research and Engineering, A*STAR (Agency for Science Technology and Research), 2 Fusionopolis Way, #08-03, Innovis, Singapore 138634, Republic of Singapore

[*]*Presenter:* li_junxia@imre.a-star.edu.sg

Abstract

Engineered Cementitious Composite (ECC) micromechanics relates material microstructures to the composite tensile behavior, which enables backward component tailoring to achieve targeted tensile performance at the minimum fiber dosage. Progressive advances have been made for ECC micromechanics towards forward prediction/modelling of ECC tensile behavior. Specifically, the heterogeneity of the microstructure of ECC has been observed and considered in qualitatively predicting its potential of strain-hardening behavior and quantitatively predicting the composite tensile behavior involving the tensile capacity, the crack width and the crack spacing.

Strain hardening criteria of ECC as Eqns. 1 and 2 is the main tool to qualitatively predict the strain-hardening potential, which is deterministic with constant values of each micromechanical parameter. To consider the heterogeneity and to ensure robust tensile strain-hardening, one approach is to propose large margins between J_b' and J_{tip} and between σ_0 and σ_c. A probabilistic approach is proposed and realized by taking all micromechanical parameters in the strain hardening criteria as random variables to capture sources of randomness. As such, J_b', J_{tip}, σ_0, and σ_c would also become random variables, and thus the boundary separating the safe and failure domain is the limit state surface (performance function) which can be defined as Eqns. 3 and 4.

$$J_b' \geq J_{tip} \quad (1)$$

$$\sigma_0 \geq \sigma_c \quad (2)$$

where J_b' is the complementary energy of fiber bridging behavior; J_{tip} is the crack tip toughness; σ_0 is the fiber-bridging strength; σ_c is the composite tensile cracking strength.

$$G(x) = J_b' - J_{tip} = 0 \quad (3)$$

$$F(x) = \sigma_0 - \sigma_c = 0 \quad (4)$$

where x denotes each micromechanical parameter as random variable. $G(x) > 0$ and $F(x) > 0$ denote the 'safe' (i.e., tensile strain-hardening) domain, while $G(x) < 0$ and $F(x) < 0$ denote the 'failure' (i.e., tensile strain-softening) domain as shown in Fig. 1.

The quantitatively prediction of the composite tensile behavior is realized by the analysis and modelling of multiple cracking sequence and termination at a random crack plane as Fig. 2. In sequential cracking analysis, the critical transfer distance x_d, the minimal distance necessary for the fiber-bridging stress transferring back to the matrix, is the key to analyze the cracking sequence. Considering the microstructure heterogeneity, the calculation of x_d has been involved from constant values to random variables by taking all micromechanical parameters as random variables. While the strain hardening criteria as Eqns. 1 and 2 become the constraint conditions to assess the termination crack plane of multiple cracking. Consequently, the variability of properties at each scale can be considered and stochastic model of ECC tensile behavior is achieved.

Keywords: engineered cementitious composites; ECC; micromechanics; probabilistic; strain-hardening; stochastic

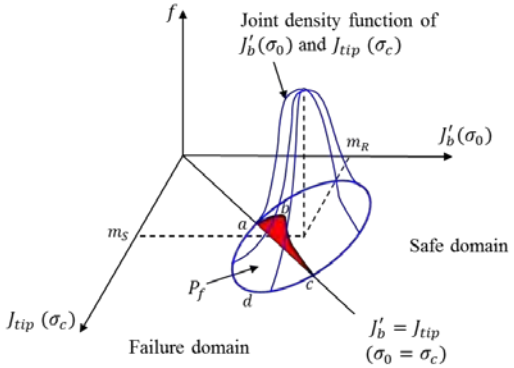

Fig. 1 The probabilistic-based strain hardening evaluation method of ECC

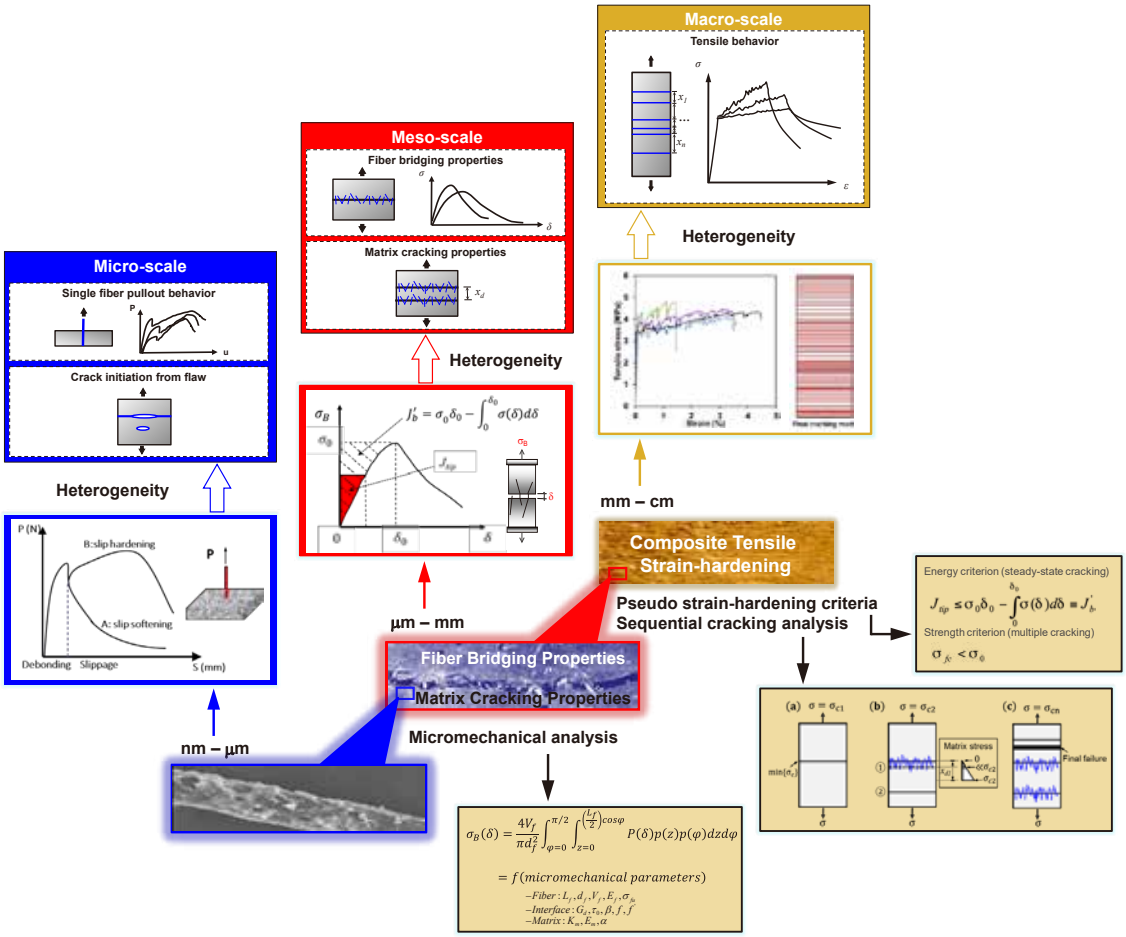

Fig. 2 Illustration of scale-linking approach of ECC micromechanics

Acknowledgment

The authors would like to acknowledge the support by the Singapore National Research Foundation under its Environmental & Water Technologies Strategic Research Programme and administered by the Environment & Water Industry Programme Office (EWI) of the PUB.

Effect of post-fire curing on strength recovery of thermally damaged ultra-high performance concrete

Ye Li, Haodong Wang, Tiejun liu*

School of Civil and Environmental Engineering, Harbin Institute of Technology, Shenzhen 518055, PR China

*Corresponding author.

Email adresses : liye@hit.edu.cn (Ye Li), 15818602282@163.com (Haodong Wang), liutiejun@hit.edu.cn (Tiejun Liu)

Abstract

Post-fire curing is a promising approach for recovering the properties of fire-damaged concrete. This study investigates the effects of post-fire water and CO_2 (40-90% cycled relative humidity and 20% CO_2) on the strength recovery and physicochemical changes of thermally damaged ultra-high performance concrete (UHPC). The UHPC samples were subjected to elevated temperatures up to 1000 °C and experienced recuring for 30 days. Multiple characterization methods, including X-ray diffraction (XRD), thermogravimetric analysis (TGA), scanning electron microscopy (SEM), mercury intrusion porosimetry (MIP), and energy-dispersive X-ray spectrometry (EDX), were utilized to identify the phase change, microstructure, and porosity of the UHPC samples. The results show that the recovered compressive strength can even surpass their original compressive strength after 600 and 800 °C exposure and recuring. A high silica content is unfavorable for strength recovery because the calcium silicates formed have low reactivity. After 1000 °C exposure, carbonation is needed for strength recovery. The reactivity of the products after heat exposure determines the degree of healing and the strength recovery primarily depends on filling of the microcracks.

Keywords: Post-fire curing, Ultra-high performance concrete, Physicochemical changes

Numerical simulation of the tensile strain hardening and multiple cracking behavior of ECC/SHCC

Chang WU[1,2*#], Chenhua JIN[1,3], Yanli SU[1,2], Mingwen XU[1,2], Xinru WANG[1,2]

[1] Key Laboratory of Concrete and Pre-stressed Concrete Structures of Ministry of Education,
[2] School of Civil Engineering, Southeast University, Nanjing,
Jiangsu 211189 People's Republic of China;
[3] School of Architectural Engineering, Jinling Institute of Technology, Nanjing
Jiangsu 211169 People's Republic of China.

[*]*Presenter:* changwu@seu.edu.cn, [#]*Corresponding author:* changwu@seu.edu.cn

Abstract

Engineered Cementitious Composites (ECC), or so-called Strain Hardening Cementitious Composites (SHCC), have ultra-high tensile ductility and crack control ability, which can effectively solve the structural and durability problems caused by the tensile brittleness of traditional concrete. In this paper, different from frictional pulley model (Fig.1), a modified equivalent elastic foundation beam model describing the single fiber pullout behavior in ECC is proposed, and a multi-scale numerical model of uniaxial tensile strain hardening and multiple cracking behavior of ECC is established.

Based on the elastic foundation beam theory, the matrix under the fibers was considered as an elastic foundation with variable stiffness; while the embedded fiber segment was equivalent to an "elastic foundation beam" and the fiber segment between the crack surfaces was equivalent to the "cantilever beam with elastic constraint" (Fig.1), to establish a micromechanics-based model for the explanation of the pullout process of fibers from the wrapped matrix. The fibers embedded in the matrix were further assumed to be discrete equivalent continuous beams, while the matrix was equated to a linear spring constraint (Fig.2). By introducing the flexibility of the matrix, the embedded fiber segment-matrix interaction system was equated to a rotating spring and a linear spring as the end constraint of the fiber extraction segment (Fig.3). Under the action of the axial force P_d, the fibers were pulled out along the axial direction; then the axially pulled-out fibers were bent under the action of the lateral force P_b, and the corresponding forces and displacements were calculated by the small deformation bending theory. Through the plane strain finite element analysis of the cutting plane of the fiber-matrix system (Fig.4), an explicit calculation method of the spring constrained stiffness of the equivalent continuous beam was proposed, and a modified equivalent foundation beam model was established to further improve the calculation efficiency. The model was applied to the numerical simulation of ECC tensile strain hardening and multiple cracking behavior, and the ECC stress-strain relationship curves were calculated based on the frictional pulley model and the equivalent elastic foundation beam model, respectively, and compared with the experimental stress-strain curves for verification.

The peak bridging stress σ_{bmax} of a single-crack and its corresponding crack opening width obtained from the equivalent elastic foundation beam model are larger than those from the friction pulley model (Fig.5), mainly because the frictional pulley model underestimates the bridging capacity of inclined fibers due to the ignoring of the fiber bending stiffness, which leads to the underestimation of the fiber bridging performance of a single fiber. The ultimate tensile strength and ultimate tensile strain of ECC calculated by the equivalent foundation beam model considering the fiber bending effect are higher; in general, the calculation results based on the equivalent foundation beam model are in better agreement with most of the experimental results for PE-ECC (Polyethylene fiber reinforced ECC) (Fig.6).

Keywords: Engineered Cementitious Composites (ECC); Strain Hardening Cementitious Composites (SHCC); equivalent elastic foundation beam model; tensile behavior; multiple cracking; multi-scale modeling

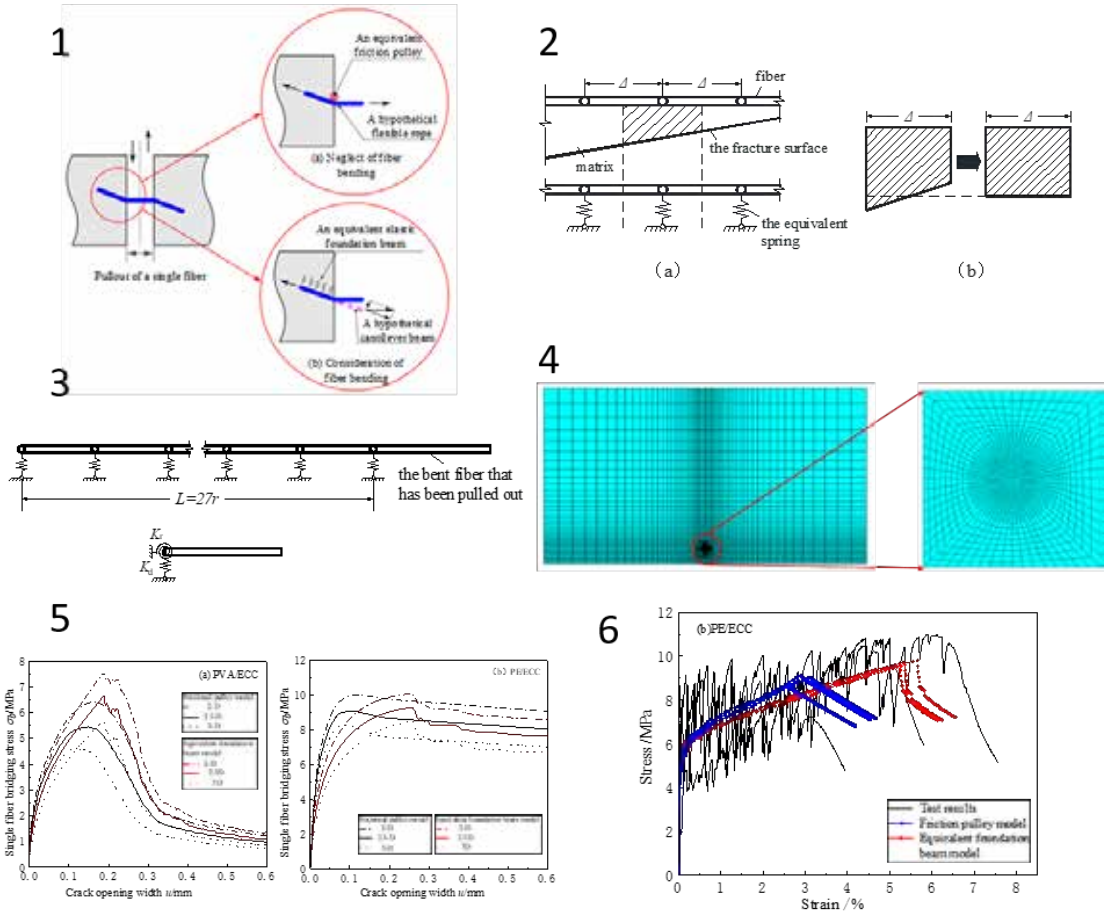

Fig. 1 Two types of single fiber pullout models; **Fig. 2** Discretization of fiber-matrix equivalent foundation beam model; **Fig. 3** Equivalent spring at the restrained end of the extracted fiber; **Fig. 4** Plane strain finite element model of the fiber-matrix system; **Fig. 5** Fiber bridging stress-crack opening width（σ_b-u) curve of a single crack of ECC: (a)PVA/ECC; (b)PE/ECC; **Fig. 6** Comparison between test results and numerical results of PE/ECC

Acknowledgment

The authors would like to acknowledge the funding support from the National Natural Science Foundation of China (Grants Number: 52108119) and the Natural Science Foundation of Jiangsu Province (Grants Number: BK20200376).

Mechanical Performance of Geopolymer Aggregate Engineered Cementitious Composites: Influence of Aggregate Sizes

Xu L. Y.*, Huang B. T. and Dai J. G.

Department of Civil and Environmental Engineering, The Hong Kong Polytechnic University, Hong Kong, CHINA
E-mail: ling-yu.xu@connect.polyu.hk, botaohuang@zju.edu.cn, cejgdai@polyu.edu.hk

Abstract

In this study, Engineered Cementitious Composites (ECC) with ultra-high strength and ductility were developed using artificial geopolymer aggregates (GPA), and the influence of GPA size (i.e., 0.3-0.6 mm, 0.6-1.18 mm, and 1.18-2.36 mm) on the mechanical performance of ECC was investigated. From the calorimetry test, it was found that GPA could react with the cementitious pastes, and the hydration heat became higher with the decrease of the GPA size. In addition, although the increase of GPA size resulted in a reduction of the compressive strength of GPA-ECC, the obtained values of all the mixes were above 145 MPa, which guaranteed the ultra-high strength nature of the produced ECC. Moreover, from direct tensile tests, GPA-ECC with the aggregate size of 0.3-0.6 mm showed the best performance with the highest tensile strength (over 15 MPa), tensile strain capacity (over 8%) and strain energy density (over 850 kJ/m^3), and the increase of the aggregate size resulted in a reduction of the tensile performance of GPA-ECC. Furthermore, X-ray computed tomography (X-CT) demonstrated the flaw effect of the GPA in ECC. The findings in this study provided a fundamental database for the future application of GPA-ECC in civil infrastructure.

Keywords: Engineered Cementitious Composites (ECC), Flaw effect, Geopolymer aggregates (GPA), Particle size, Ultra-high strength.

Bond-Slip Behaviors of BFRP Bar Embedded in Ecological High Ductility Concrete Using the Beam Test

Li-Juan Chai[a*], Li-Ping Guo[b]

[a] College of Civil Engineering, Taiyuan University of Technology, Taiyuan 030024, China (E-mail: 572068470@qq.com)

[b] School of Materials Science and Engineering, Southeast University, Nanjing 211189, China (*Corresponding Author*, E-mail: guoliping691@163.com)

Abstract: To better understand the design parameters of bridge deck link slabs prepared with basalt fiber reinforced polymer (BFRP) bar and ecological high ductility concrete (Eco-HDC), the bond performance of BFRP bar embedded in Eco-HDC using beam test based on RILEM standard was studied. The beam specimens had variable factors namely the diameter, embedment length and cover thickness of BFRP bar. Results indicate that most beam specimens display a failure mode of BFRP bar pulling out with Eco-HDC splitting. Besides, with the increasing diameter or embedment length of bar, the bond strength will be smaller. As the cover thickness is larger, the bond strength and first cracking bond stress show an increasing trend. The free end slip increases with the increasing value of embedment length or cover thickness. In addition, the value of loaded end strain is larger than the value of free end strain as the load increases. Moreover, the equations of bond strength and peak slip are obtained combined with the test data. At last, the embedment length and cover thickness of BFRP bar embedded in the bridge deck link slabs are recommended.

Strain-hardening cementitious composites with high volume fly ash and non-oiled PVA fibers

Chang Lin*, Zhi-Gao Yao, Shu-Ying Xu, Li-Sha Pan

School of Chemical Engineering and Technology, Hainan University, Haikou, Hainan 570228, People's Republic of China
*Presenter and Corresponding author: clin@hainanu.edu.cn

Abstract

Strain-hardening cementitious composite (SHCC) displays high ductility and toughness due to its multiple-cracking and strain-hardening behavior under direct tension. Polyvinyl alcohol (PVA) fibers have been widely used to manufacture ultra-ductile SHCC, such as Engineered Cementitious Composite (ECC). Because of its hydrophilic nature, PVA fiber has such a strong bond with cementitious matrix that leads to premature rupture of PVA fibers and relatively low value in ultimate strain for SHCC with PVA fibers (PVA-SHCC). Hence, the PVA fiber commonly used in PVA-SHCC is coated with about 1.2% by mass oiling agent. The cost for this oil-coated PVA fiber is generally 8 times higher than that of non-oiled PVA fiber at Chinese market.

In this paper, SHCCs were produced with cement pastes containing high volume fly ash as matrices and using low cost non-oiled PVA fibers as reinforcement. A part of fly ash acts as a supplementary cementitious material. Besides, the large amount of unreacted fly ash particles plays the role of fine aggregate. With the increase in fly ash content, the 28 d compressive strength of the matrix declined within the range of 93~18 MPa. The strength range is consistent with that of most existing PVA-SHCCs. The results for uniaxial tensile tests are shown in Fig. 1, indicating that the influence of fly ash at 20% and 50% dosages by mass fraction is insignificant. With the fly ash dosage increasing to 67% and 80%, the multiple-cracking and strain-hardening characteristics of SHCC tend to be enhanced. Especially, the composite with 80% fly ash and non-oiled PVA fibers exhibits ultra-high ductility with an ultimate strain up to 7.2%. Also, the SHCCs have a light weight, and the density is as low as 1 490 kg/m^3 for the case with 80% fly ash. SEM observation on tensile specimens confirms that PVA fibers were mostly pulled out without rupture with the presence of high volume fly ash.

The results of fiber pullout tests are shown in Fig. 2. It can be seen from Fig. 2 that there is a sudden load drop at the limit of proportionality of the fiber pullout load-displacement curve for the case without fly ash. This sudden load drop is caused by the debonding between PVA fiber and the matrix, and its intensity indicates the scale of chemical bond. With the presence of fly ash, the load gradually declines after the peak without sudden load drop. This implies that high volume fly ash reduces the chemical bond between PVA fibers and the matrix. Furthermore, the results from fiber pullout tests indicate that high volume fly ash also weakens the interfacial friction. Therefore, high volume fly ash effectively inhibits the premature rupture of PVA fibers during the pull-out process, and enhances the ductility of SHCC with non-oiled PVA fibers. It can also be seen from Fig. 2 that the maximum pullout load increases with the age increasing from 7 to 28 d, which indicates that the interfacial interactions increase with age.

Keywords: Polyvinyl Alcohol Fiber; Uniaxial Tensile; Fiber Pullout; Strain-Hardening; Multiple-Cracking

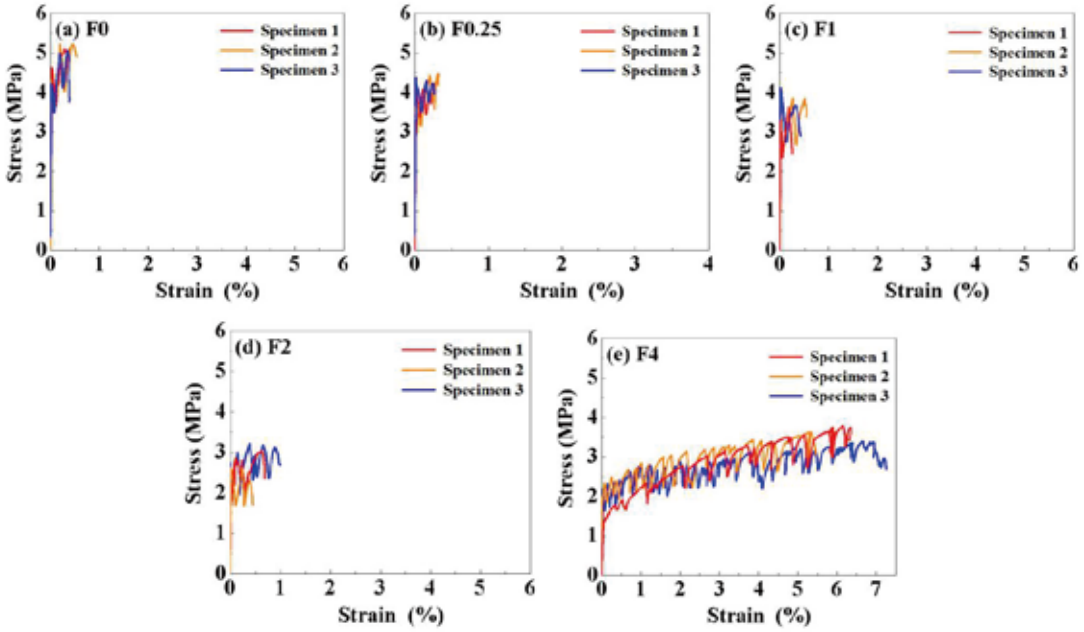

Fig. 1 Stress-strain curves from uniaxial tensile tests

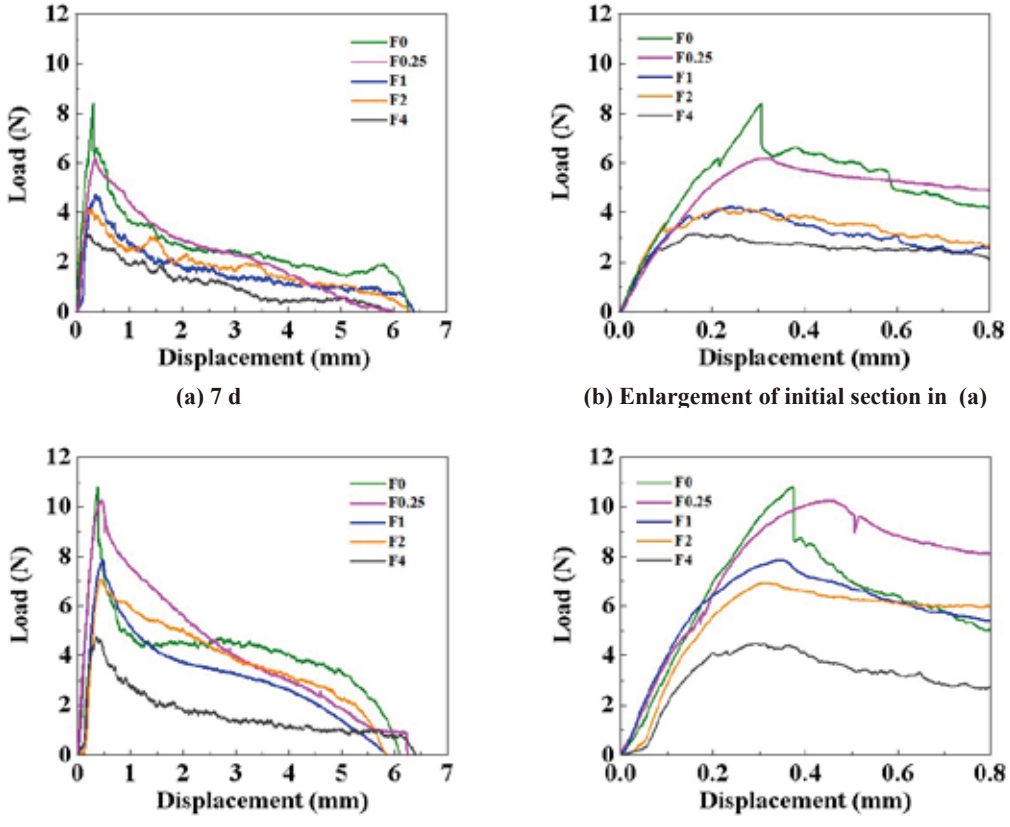

(a) 7 d **(b) Enlargement of initial section in (a)**

(c) 28 d **(d) Enlargement of initial section in (c)**

Fig. 2 Fiber pullout load-displacement curves for 7 d and 28 d

Acknowledgment

The authors would like to acknowledge the funding support from Natural Science Foundation of Hainan Province (Grant Number: 520RC550), National Natural Science Foundation of China (Grant Number: 51608157)

Shenzhen, China

Deep learning potential for predicting C-S-H/PVA/graphene interfaces

Xiao-Ye Zhou[1], Chun Pei[1], Ji-Hua Zhu[1*]

Guangdong Province Key Laboratory of Durability for Marine Civil Engineering, College of Civil and

Transportation Engineering, Shenzhen University, Shenzhen, 518060, Guangdong, China

*Presenter: xiaoye_zhou@szu.edu.cn, #Corresponding author: zhujh@szu.edu.cn

Abstract

A deep learning potential with high precision was developed for predicting the interfaces between C-S-H, PVA and graphene with large scale molecular dynamics (MD) simulations. MD simulations can generate atomic scale details of deformation mechanisms, failure mode and interfacial structures of cementitious materials modified by PVA and graphene. However, accurate MD potential for describing the interactions at the interfaces is lacking, and owing to the complexity of the C-S-H/PVA/graphene interfaces, it is difficult for empirical potentials to predict the interactions between different materials with high precision. Recent development of machine learning potentials such as deep learning potential provide a plausible way for developing MD potential for complicated systems with high accuracy. Herein, we developed a deep learning potential for the C-S-H/PVA/graphene system using the DeePMD package.The deep learning potential was fitted with its prediction error in energy and force respectively being 12.1 meV/atom and 352 meV/Å, in comparison with first-principles calculations. The interfacial structures between C-S-H, PVA and graphene were than predicted by large scale MD simulations. The developed MD potential allows for further studies on the reinforcing mechanisms of graphene on cementitious materials. The deep learning potential can be easily extended to be used in other systems because of the great scalability of deep neutral network.

Keywords: Machine learning potential; Deep neutral network; Graphene; Cementitious materials; Molecular dynamics simulations.

Acknowledgment

The authors would like to acknowledge the funding support from the Key-Area Research and Development Program of Guangdong Province (2019B111107002) and the National Key Research and Development Program of China (2018YFE0124900).

Optimal Design of Precast UHPC Utility Tunnel based on Life Cycle Cost Analysis

Xia Zhanghua1，Xu Yousheng[2]，Wu Zelin[1]，Ding Sipan[1]

[1] Fuzhou University Fuzhou, Fuzhou, Fujian 350108, China,
[2] Shenzhen Municipal Engineering Design Institute Lt. Co Shenzhen 518035, China
[*]Presenter: xiatian@fzu.edu.cn, [#]Corresponding author: xiatian@fzu.edu.cn

Abstract

Conventional underground utility tunnels are generally made by reinforced concrete. As a quasi-brittle material, ordinary concrete is easy to crack under tensile loadings and has durability problems of external parts exposed to complex underground environments. With the development of Ultra High-Performance Concrete (UHPC), the UHPC utility tunnel has gradually come out. UHPC utility tunnel has the characteristics of light weight and good durability, which can solve the problems of heavy self-weight and durability in the conventional utility tunnels. However, the costs of this material are significantly higher than that of ordinary concrete. Hence, a cost-effective utilization of UHPC is critical for the widespread practical applications. In this paper, a trial design of UHPC utility tunnel is carried out, and the wall thickness is analyzed. The optimal structure of UHPC utility tunnel with stiffeners is proposed. Also, a cost analysis comparing with ordinary concrete utility tunnel is presented.

Based on a practical project, the utility tunnel (see Fig.1) is used as a prototype to carry out trial design research for UHPC utility tunnel and the designed UHPC utility tunnel is shown in Fig.2. The UHPC utility tunnel is optimized by setting stiffeners and mediastinal plates (see Fig.3). According to the ABAQUS finite element simulation results of the optimized structure, the maximum deflection and damage are in the mid span area of the top and bottom plates. Moreover, the deflection and stress are similar to the structure before optimization.

According to the analysis based on the economic indexes, the optimized UHPC utility tunnel reduces the concrete consumption by nearly 56%, the steel consumption by nearly 58% and the overall weight by 56% compared with the prototype utility tunnel. The overall material cost of the project is only about 40% higher than that of the prototype utility tunnel. Due to the use of stiffeners the deflection is reduced, the use of a thinner cross-section can meet the stress requirements and fully improve the material utilization rate.

Based on the analysis of the life-cycle cost of the optimized utility tunnel, the life-cycle cost of the optimized prefabricated UHPC utility tunnel is only 63% of the prototype structure, and the construction period is about 48% of the prototype utility tunnel. It can greatly save the life-cycle cost and speed up the construction process. Compared with the concrete utility tunnel, the prefabricated UHPC utility tunnel has better development prospects.

Keywords： UHPC; utility tunnel; life cycle; optimized structure

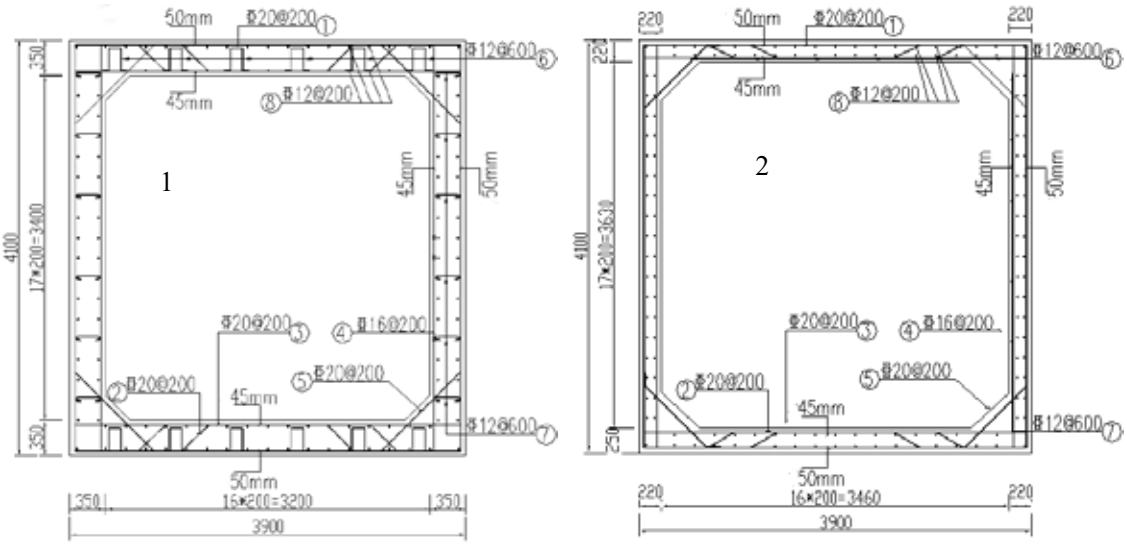

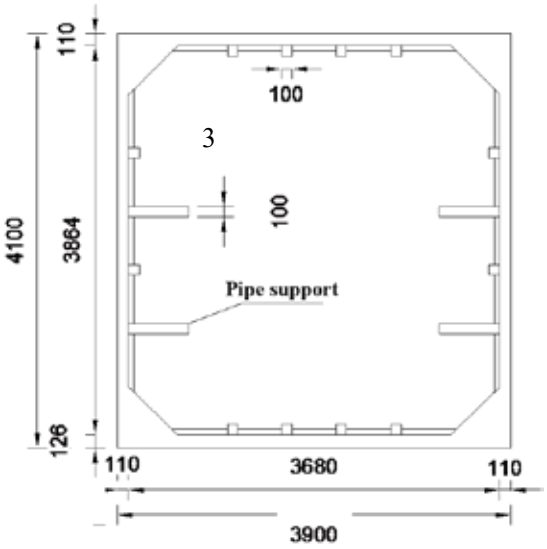

Fig.1 Standard section size and reinforcement drawing of utility tunnel; **Fig.2** Standard section size and reinforcement drawing of UHPC utility tunnel; **Fig. 3** Optimal structure diagram of utility tunnel

Acknowledgment

The authors would like to acknowledge the funding support from the National Natural Science Foundation of China (Grant No. 51408360), the Natural Science Foundation of Fujian Province（Grant No. 2020J01477，2016J01231）and the Transfer and transformation project of scientific and technological achievements in Fuzhou（2020-GX-18）.

Recent Advances in self-healing performance of Engineered/Strain-Hardening Cementitious Composite (ECC/SHCC)

Feng Hu [1*], Jing Yu [1#]

[1] School of Civil Engineering, Sun Yat-Sen University, Guangzhou 510275, PR China
[*]*Presenter:* hufeng9@mail2.sysu.edu.cn
[#]*Corresponding author:* yujing63@mail.sysu.edu.cn

Abstract

Concrete is the most widely used construction material in modern engineering. Its durability and long-term performance are of great significance to the safety and longevity of infrastructures. However, concrete is a type of brittle material with very low tensile strength, and cracks may occur at any stage during the life cycle of a structure. Therefore, it is urgent to find a cementitious material with reliable crack control ability and self-healing potential. Engineered/Strain-Hardening Cementitious Composites (ECC/SHCC) are a class of advanced fiber-reinforced cementitious materials that can enhance the safety and longevity of structures. Benefiting from its excellent crack control ability and low water/binder ratio, the autogenous self-healing potential of ECC has attracted extensive attention. Many scholars have investigated the self-healing performance of ECC with different binder compositions, pre-load levels and curing conditions.

The main self-healing mechanism of ECC is the continuous hydration of un-hydrated cementing materials and the formation of calcium carbonate (**Fig.1**). The short random fibers in ECC can provide nucleation sites for healing products, which can promote the crystal deposition and recovery of fiber-bridging capacities (**Fig.2**). The tight crack width is conducive to self-healing progress, and the abundant un-hydrated components in the matrix provide the material basis.

The self-healing properties of ECC under different service conditions are mainly affected by the moisture condition as well as the concentration of calcium and carbonate ions. The condition with wet-dry cycles shows the best healing effects (**Fig.3**), followed by the water curing and air curing conditions. Likewise, ECC also show reliable self-healing performance under a natural environment (**Fig.4**). Moreover, ECC can maintain satisfactory self-healing performance under harsh ionic environments (**Fig.5**) and extreme temperatures. In addition, different supplementary cementitious materials have their own contributions to the self-healing capacity (**Fig.6**), while the curing age and loading conditions also affect the self-healing performance.

This article tries to summarize some recent advances in the self-healing performance of ECC, with particular focus on the self-healing mechanism and some key affecting factors (i.e., crack width, humidity, temperature, ionic environment, binder composition and curing age). We try to provide a reference for the material design and practical application of high-performance fiber-reinforced cementitious composites with self-healing properties.

Keywords: Engineered Cementitious Composites (ECC); Strain-Hardening Cementitious Composites (SHCC); Self-healing properties; Self-healing mechanism

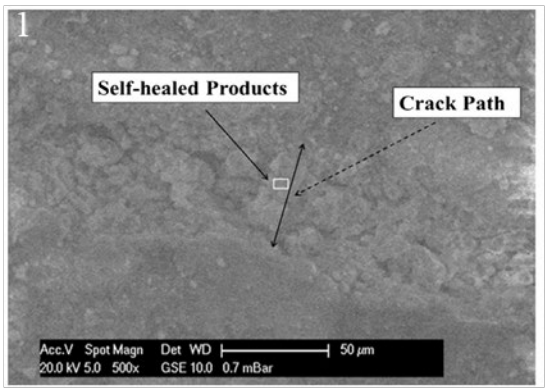

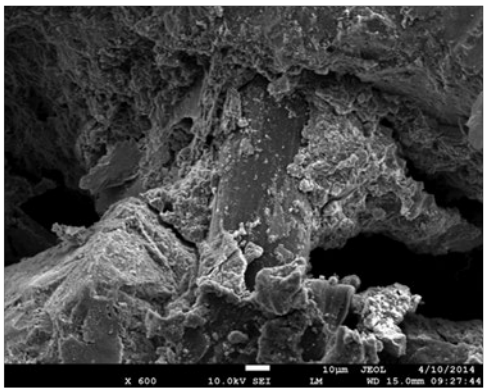

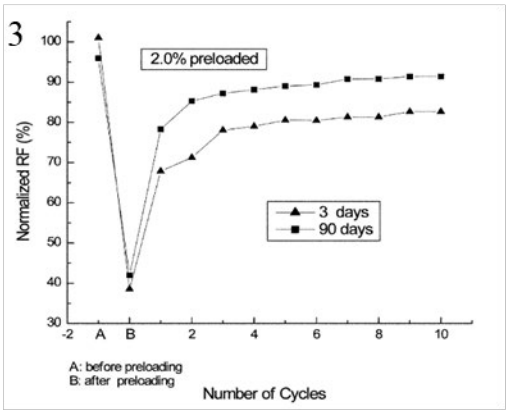

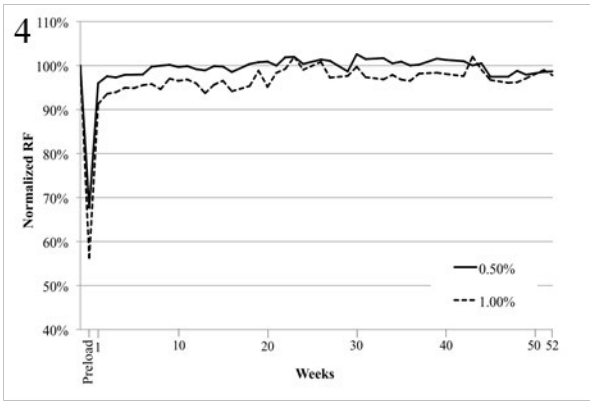

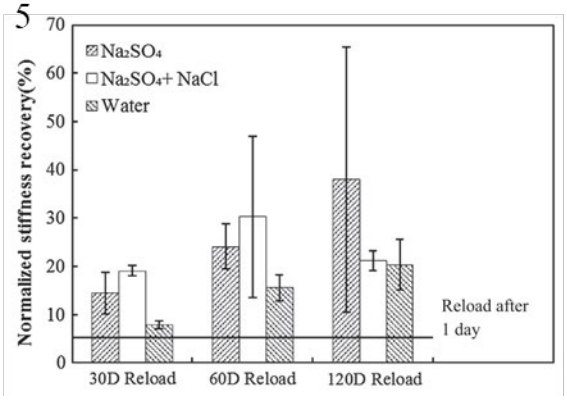

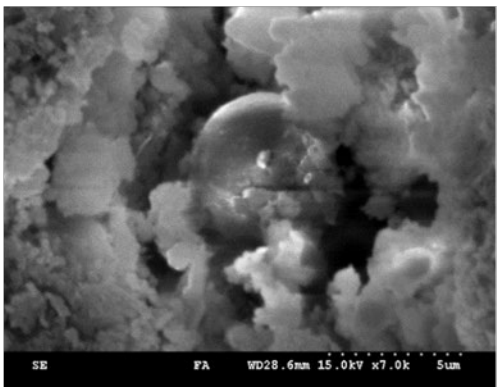

Fig.1 ESEM micrograph of self-healing products in ECC; **Fig.2** Self-healing products precipitated on PVA fiber; **Fig.3** Resonant frequency recovery of ECC under wet-dry cycles for 2% preload strain; **Fig.4** Effect of natural environment exposure time on the recovery of resonant frequency ; **Fig.5** Effect of harsh ionic environment on the recovery of stiffness; **Fig.6** Unreacted fly ash particles in a crack

Acknowledgments

The authors would like to acknowledge the funding support from the National Natural Science Foundation of China (52108264) and the Natural Science Foundation of Guangdong Province (2022A1515010808).

Finite element analysis of heavily-corroded reinforced concrete beam strengthened by high-strength Engineered Cementitious Composites

Zi-Hao Song [1*], Jing Yu [1#]

[1] School of Civil Engineering, Sun Yat-sen University, Guangzhou 510275, PR China
[*]*Presenter:* songzh25@mail2.sysu.edu.cn
[#]*Corresponding author:* yujing63@mail.sysu.edu.cn

Abstract

Reinforced concrete (RC) structures are widely used in civil engineering, while the severe corrosion of steel rebars can greatly affect their load-carrying capacity. Existing methods for dealing with heavily-corroded rebars (such as rebar-planting) are time-consuming and labor-intensive. Therefore, researchers are seeking other alternative methods. Exhibiting excellent crack resistance ability and high toughness, high-strength Engineered Cementitious Composites (HS-ECC) have been used in repairing pavements and dams. Recently, (Chen et al. 2018) reported that HS-ECC have the potential to fully recover the load-carrying capacity of RC beams with heavily-corroded steel rebars. Based on the test results from the literature, this study aims to use a finite element approach to explore the key parameters affecting the repair effectiveness of the HS-ECC patch for RC beams with heavily-corroded steel rebars.

Finite element models (**Fig.1**) were established to explore the effectiveness of HS-ECC patch on heavily-corroded RC beams under four-point bending. The specimens REF-F and REF-R represent two types of reference beams (without patching) with full and reduced rebar sections, respectively; while B40 and B55 represent two different bond lengths (4.0D and 5.5D) of the patch (**Fig.2**). The steel rebar with reduced section is a continuous Y20 rebar with a 50 mm-long reduced area with a diameter of 17.3 mm (**Fig.1**), which represents a 25% nominal area loss. Generally speaking, the simulation results have good agreement with the test results, especially in terms of the peak load (**Fig.3, Fig.4, Fig.5**). Additionally, some key parameters affecting the repair effectiveness of HS-ECC patch were systematically discussed, including the tensile strength of ECC, the ultimate tensile strain of ECC, as well as the bonding length between ECC and steel rebar.

Results showed that the heavy corrosion of steel rebars can significantly affect the load-carrying capacity of RC beams, while the proposed HS-ECC patching approach has satisfactory repair effectiveness when the nominal area loss for steel rebars is no more than 25%. To ensure the repair effectiveness, the tensile properties of HS-ECC material and the bond length have to fall within the suggested ranges. Overall considering the cost and time, the repair method mentioned in this paper is superior to the existing method. The findings of this study can support future repair applications using HS-ECC in practical engineering.

Keywords: Engineered Cementitious Composites (ECC); Strain-Hardening Cementitious Composites (SHCC); Finite element analysis; Flexural strengthening; Reinforced concrete beam

1

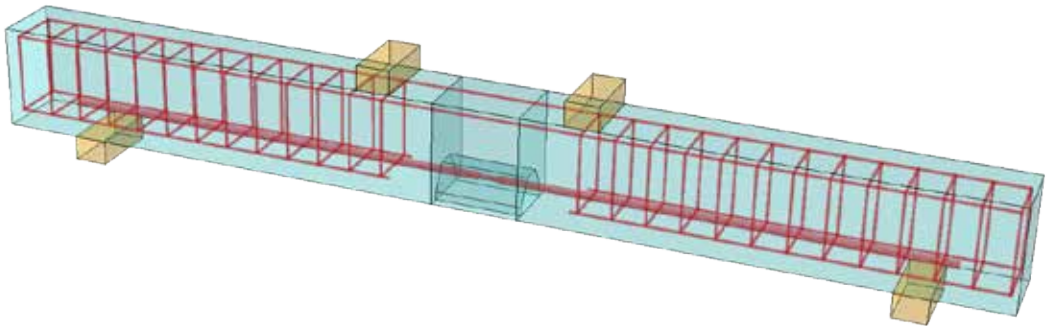

2

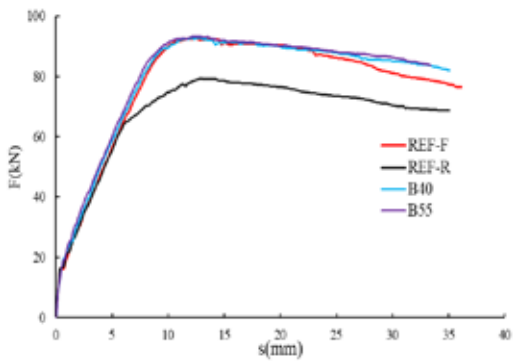

3

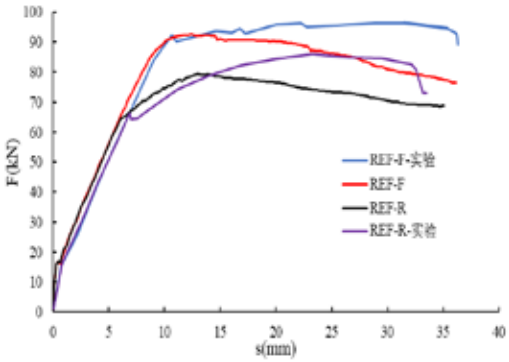

4

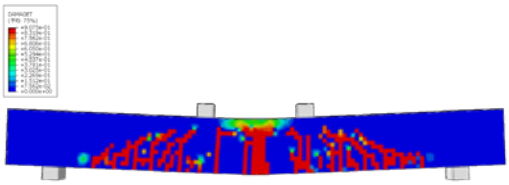

5

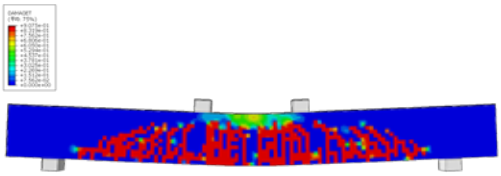

Fig.1 The FE model for heavily-corroded RC beam in ABAQUS; **Fig.2** Simulation results of load vs. displacement curves for four RC beams; **Fig.3** Comparison of load vs. displacement curves between test and simulation results; **Fig.4** Stress diagram of the damaged RC beam; **Fig.5** Stress diagram of the repaired RC beam.

Acknowledgment

The authors would like to acknowledge the funding support from the National Natural Science Foundation of China (52211530099).

Development of low-carbon concrete for improving durability of composite foundation with plain concrete piles under marine environment

Weipeng Chen[1*] and Jing Yu[1#]

[1] School of Civil Engineering, Sun Yat-sen University, Guangzhou 510275, PR China
[*]*Presenter:* chenwp23@mail2.sysu.edu.cn
[#]*Corresponding author:* yujing63@mail.sysu.edu.cn

Abstract

Low-grade concrete is commonly applied in composite foundations with plain concrete piles. Fly ash (FA) has been widely used in low-grade concrete, but the content is typically no more than 40% of the binder. In coastal areas, concrete can be attacked by ions in seawater, which can react with the hydration products, resulting in the dissolution and formation of expansive products that can lead to cracking. Moreover, service conditions of alternate drying-wetting and sudden changes in groundwater levels can accelerate the deterioration of concrete. To improve the durability of composite foundations with plain concrete piles, increasing the content of supplementary cementing material (SCM), such as fly ash and ground granulated blast-furnace slag (GGBS), can be an effective approach. Additionally, the use of SCM helps lower the embodied carbon in concrete, which is beneficial for achieving carbon neutrality.

This study aims to explore the feasibility of using high-volume SCM to improve the durability of C15 concrete in the marine environment. First, the cementing efficiency factors (k) of both FA and GGBS at various dosages were ascertained, and mortar with 40-80% SCM was designed based on the relationship between the equivalent water/cement ratio and compressive strength (Fig. 1). Then, the compressive strength and marine erosion resistance of mortar were tested, and an optimized binder composition was obtained. Finally, based on the aforementioned results, a new mix proportion of C15 concrete was designed, and it was compared with commercially available concrete (with 40% FA) in terms of mechanical properties, material cost, environmental impacts, and durability in the marine environment.

The results showed a linear relationship between the k value and the dosage of SCM (Fig. 2 and Fig. 3). Concrete with 60% FA or 40-80% GGBS reaches or even slightly exceeds the 28-day compressive strength of the control group (concrete with 40% FA) (Fig.4). As for the environmental impacts, concrete with 60-80% SCM was eco-friendly in terms of low embodied carbon and embodied energy (Fig.5). The durability of concrete in the marine environment can be compared by the anti-erosion coefficients, and the results will be obtained soon. The findings from this study can shed light on the design of low-carbon and durable low-grade concrete.

Keywords: Low-carbon concrete, Cementing efficiency factor, Fly ash, Ground granulated blast-furnace slag, Marine environment.

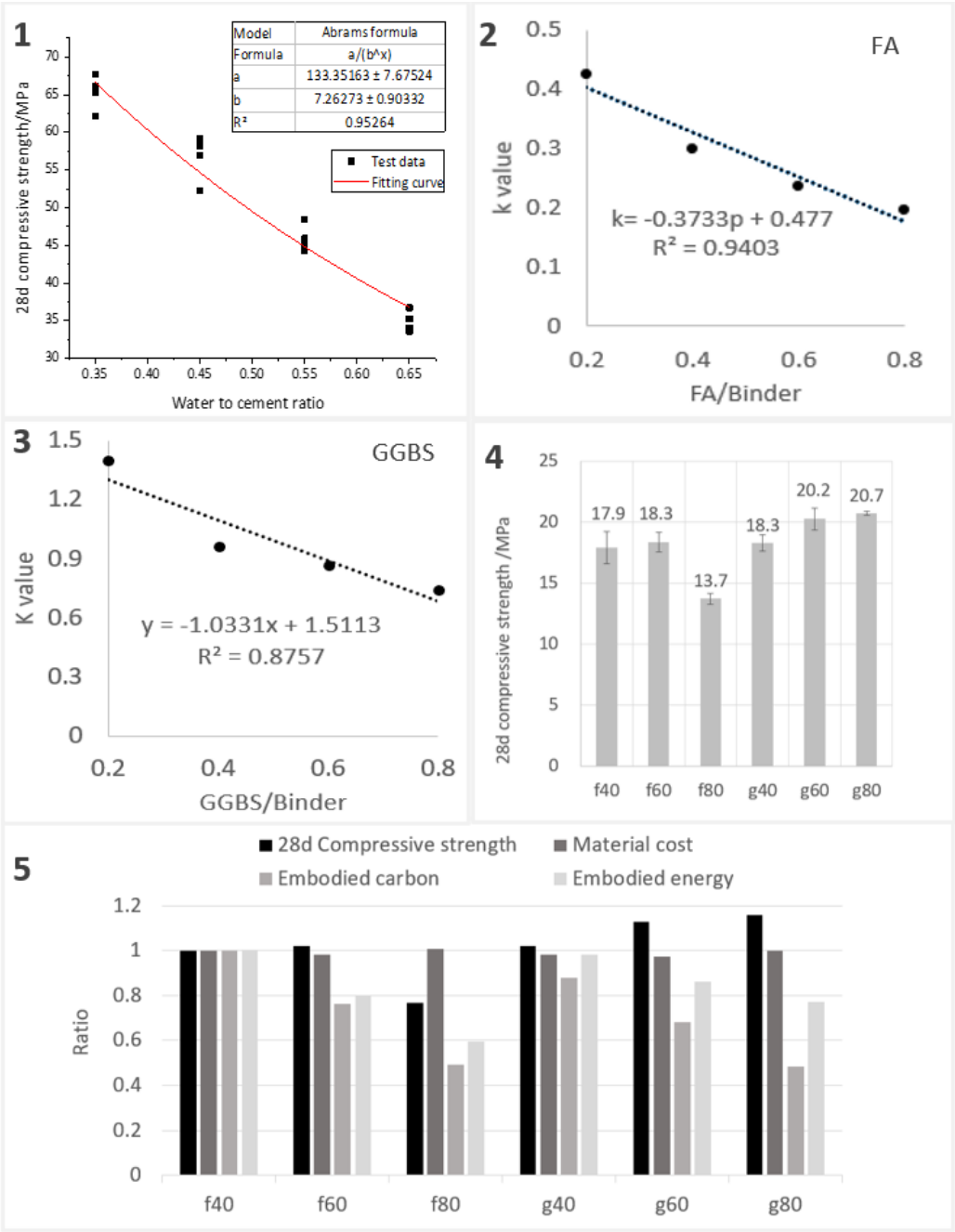

Fig. 1 Fitting curve of compressive strength and water to cement ratio, and formula 1; **Fig. 2** Fitting curve of k value and the proportion of FA, and formula 2; **Fig. 3** Fitting curve of k value and the proportion of GGBS, and formula 3; **Fig. 4** 28-day compressive strength of 6 groups; **Fig. 5** Comparison of mechanical property, economy and environment benefits of 6 groups, the ordinate value is the ratio of the corresponding data of each group to f40 (control group, commonly used as C15 concrete mix).

Acknowledgment

The authors would like to acknowledge the funding support from the Natural Science Foundation of Guangdong Province (2022A1515010808), and the Zhuhai Science and Technology Innovation Bureau (ZH22017001200149PWC).

Parallel Sessions-3

Improvement on The Strengthening Efficiency of Concrete Structures with Advanced Composite Materials

Hybrid strengthening of concrete beams with shape memory alloy and carbon fiber reinforced polymer plates

Miaochang Zhu[1], Jun Deng[1*#]

[1] School of civil engineering, Guangzhou University, Guangzhou 510006, China
E-mail: zhumiaochang@gzhu.edu.cn, dengjun@gzhu.edu.cn

Abstract

A novel hybrid strengthening approach that incorporates near-surface mounted shape memory alloys (SMAs) and externally bonded carbon fiber reinforced polymer (CFRP) has been proposed to strengthen concrete beams. Prestressing forces can be introduced to concrete because of the recovery stress of SMAs generated during heating activation, representing a quicker and more expedient prestressing technique compared to conventional prestressing techniques that usually necessitate hydraulic jacks. Three-point bending tests were performed to investigate the efficiency of this hybrid strengthening approach. The results show that the cracking, yielding, and ultimate moments can be considerably enhanced for the strengthened beam compared to the control beam. Furthermore, significant improvement in the displacement ductility can also be observed for the strengthened beam, which surmounts the issues associated with the compromised ductility for near-surface mounted or externally bonding CFRP. Therefore, this hybrid strengthening approach appears attractive for strengthening concrete structures, especially when the need for large ductility is valued.

Keywords: CFRP, Concrete beams, Ductility, Hybrid strengthening, SMA

*: *Presenter;* #: *Corresponding author*

Bond behavior of UHPC-based TRC plate under freeze-thaw cycles

Lina Wang [1], Chaoyang Zhou[1], Kohei Nagai[2] and Yi Wang[1*]

[1] School of Civil Engineering, Central South University, Changsha, CHINA
E-mail: 204811030@csu.cn, cyzhou@csu.edu.cn, wangyi.ce@csu.edu.cn
[2] Institute of Industrial Science, The University of Tokyo, Tokyo, JAPAN
E-mail: nagai325@iis.u-tokyo.ac.jp

Abstract

This study proposes an ultra-high performance concrete (UHPC) based textile-reinforced concrete (TRC) plate for hybrid strengthening of frost-damaged concrete structures. The TRC plate is made of fiber reinforced polymer (FRP) grid and UHPC, which act as the reinforcement and matrix, respectively. In this new strengthening system, long and short fibers can improve the mechanical behavior of TRC plates due to the enhanced crack bridging effect. However, the bond properties of the FRP grid and UHPC will deteriorate under freeze-thaw cycles (FTCs), which will affect the cooperative work, and thus decrease the reinforcement effect. To study the bond property degradation of TRC plates under FTCs, the bond behavior of fully saturated TRC plates under FTCs is examined. First of all, the crack bridging effect of hybrid fibers under FTCs is studied by carrying out the bending and compressive tests on UHPC specimens. Then the pull-out and axial tension tests on TRC plates are conducted, from which the interaction mechanism of hybrid fibers and FRP grid with the cement-based matrix of UHPC will be investigated. Moreover, the effect of FTCs on bond property degradation of the FRP-UHPC interface could be clarified. Finally, the damaging and enhancing mechanism of FTCs and the hybrid strengthening will be revealed respectively. The results will be significant to the development and design of the new efficient and durable hybrid strengthening methodology.

Keywords: Bond behavior, Crack bridging effect, Freeze-thaw cycles, Textile reinforced concrete (TRC), UHPC.

ChatGPT in Structural Engineering Research

Cheng Jiang[1*#], Wenzhai Bi[1], ChatGPT[2]

[1] Centre for Infrastructure Engineering, Western Sydney University, Penrith, NSW 2751, Australia
[2] OpenAI L.L.C., 3180 18th Street, San Francisco, CA 94110, USA
[*]*Presenter:* cheng.jiang@westernsydney.edu.au,
[#]*Corresponding author:* cheng.jiang@westernsydney.edu.au

Abstract

ChatGPT is a conversational language model developed by OpenAI, based on the transformer architecture. It was trained on a massive dataset of diverse conversations to generate human-like text on a wide range of topics. It has created significant impacts on various fields. This presentation aims to discuss the impact of ChatGP on research work in structural engineering and summarize its advantages and disadvantages. It is found that ChatGPT can well solve structural engineering problems in design. Meanwhile, ChatGPT has powerful information retrieval capabilities, which can be applied to discover research gaps. However, it also has some disadvantages that should be considered. Due to a lack of creativity to a dependency on data quality, these disadvantages can impact the quality and reliability of the work produced.

In this work, ChatGPT was tested for its ability to solve structural engineering problems by some questions. For instance, ChatGPT was asked about how to design reinforced concrete beams. It can provide accurate and detailed design methods. On this basis, ChatGPT can solve the design examples given in ACI code. Even if some data in the question is changed, ChatGPT can still calculate the result. This means that in addition to a certain information retrieval ability, ChatGPT also has a certain degree of self-learning ability, which is beyond the traditional search engine, such as Google and Baidu. ChatGPT can be used by engineers to generate quick design sketches and prototypes for their products, reducing the time required for design iteration.

Besides, ChatGPT was evaluated for its ability to discover and solve research gaps in this study. In the case of the area of fiber reinforced polymer (FRP) structures, it can summarize its research gaps and divide them into three areas: material science, structural behavior, and durability and sustainability. However, when queried regarding methods to resolve these difficulties, ChatGPT can provide only generalized and inapplicable information, and is unable to furnish specific and efficacious strategies to address them. In addition, when presented with inquiries such as assessing the contributions of a particular academic or identifying the preeminent scholars in a specific discipline, ChatGPT frequently delivers unsatisfactory responses and may even be unable to supply a reply.

The cause of these outcomes can be attributed to the absence of creativity in ChatGPT and its reliability on the caliber of the data it was trained on. This implies that it is unable to generate innovative concepts or produce truly novel content. ChatGPT's responses are derived from the training data and are limited to the information contained therein. If the training data is prejudiced, obsolete, or of subpar quality, the responses generated by ChatGPT will embody these biases. This can lead to erroneous or unsuitable responses. Thus, ChatGPT can be used to retrieve existing information and assist engineers and researchers to solve problems with fixed answers or solutions. However, it is currently incapable of substituting for researchers in executing innovative work, and it lacks the cognitive capability to assess an individual or entity by taking into account a multitude of factors in a comprehensive manner. Therefore,

there is a long way to be developed for effective uses of ChatGPT in structural engineering research.

Keywords: ChatGPT; Structural Engineering; Research; Structural Design; FRP

Acknowledgment

The authors would like to acknowledge the funding support from the Australian Research Council (DE210101662).

Factors Affecting the Ductility of CFRP-to-concrete Bonded Joints with End Anchors: A Theoretical Study

Kai Liu, Tian-li Huang, Yi Wang, Hao Zhou[*,#]

[1]School of Civil Engineering, Central South University, Changsha, China
[*]*Presenter and corresponding author: hao.zhou@csu.edu.cn*

Abstract

Strengthening of reinforced concrete (RC) structures by using externally bonded (EB) carbon fiber reinforced polymers (CFRP) laminates has gained increasing popularity within last few decades due to the high strength-to-weight ratio and excellent durability performance of CFRP. However, as the concrete substrate is often the weak layer in the bonding interface, an abrupt premature debonding happening within the concrete substrate is the predominant failure mode. As such, the load-carrying capacity of the CFRP-to-concrete bonded joints is much less than the strength of the CFRP laminate, which results in a very low material efficiency. To tackle this problem, researchers have proposed different mechanical anchors, such as FRP spike anchors, self-anchorage buckles and hybrid anchors etc. to constrain the slip of the bonding interface, thus improving the ultimate load-carrying capacity. However, existing experimental research have shown that bonded joints with end anchorages could still exhibit brittle failure mode. Through an analytical study, the anchorage stiffness and strength were identified as two factors affecting the ductility of the bonded joints. However, as the interfacial bond behavior, such as the ultimate deformation of the bonded joints is governed by the local bond-slip relation, the interaction between the anchorage and the bonded interface, as well as the maximum deformation of the bonded joints with end anchorage will be also affected. Unfortunately, the effect of the bond-slip model on the ductility hasn't been thoroughly investigated.

Against this background, this study conducted a theoretical study to reveal the factors affecting the bond behavior of CFRP-to-concrete bonded joints with end anchorage. The anchor was simplified as a spring with non-linear force-displacement behavior. As such, the classical interfacial fracture mechanics can be employed to derive closed-form solutions for the interfacial bond behavior. Then a finite element analysis was conducted to validate the accuracy of the presented analytical solution. Results show that the obtained analytical solutions are valid in predicting the bond behavior of CFRP-to-concrete bonded joints with end anchorages, given the force-displacement behavior of the anchorage is known (**Figs. 1-3**). It is also found that though the stiffness and force of plastic plateau in force-displacement relation of the anchor are important in determining the ductility (**Figs. 4-5**), the relation between the ultimate interfacial slip and anchorage deformation also shows significant influence. When the ultimate interfacial slip is less than the maximum anchorage deformation, the anchor will fail before the full debonding of the bonded joints. As such, the anchorage performance is not sufficient, and a brittle failure will occur (**Fig. 6**). Therefore, while designing the anchor, factors, such as the anchor stiffness, force of plastic plateau in the anchor's force-displacement relation, the local bond-slip relation of CFRP-to-concrete bonded joints and CFRP strengthen should be considered to get a ductile failure mode of the bonded joints.

Keywords: CFRP-concrete, end anchorage, analytical solution, ductile failure

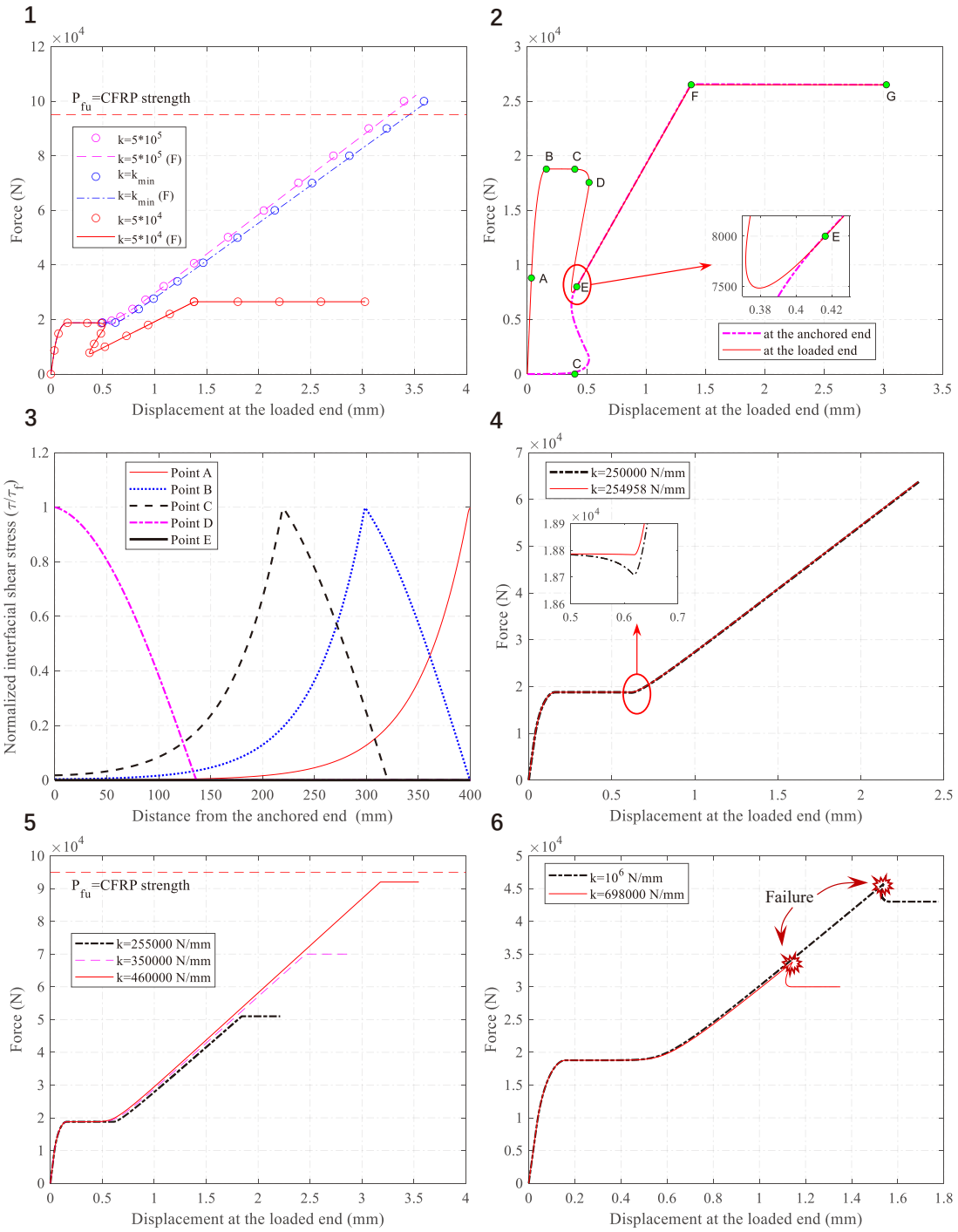

Fig. 1 Comparison between the analytical solution and FEA results; **Fig. 2** Load-displacement curve at the anchored end and loaded end; **Fig. 3** Interfacial shear stress distribution at different loading stage; **Fig. 4** The minimum stiffness required to achieve a ductile failure mode; **Fig. 5** The load displacement curves when the ultimate interfacial slip is less than the maximum anchor deformation; **Fig. 6**. The load displacement curves when the ultimate interfacial slip is greater than the maximum anchor deformation.

Acknowledgment

The authors would like to acknowledge the funding support from the Natural Science Foundation of Hunan Province, China (2021JJ40777).

Axial Compressive Performance of Rectangular Short Concrete Column Strengthened with CFRP Grid Reinforced ECC Matrix

Hailong Wang, Kangjian Lin, Zhiwei Chen, Xiaoyan Sun
(College of Civil Engineering and Architecture, Zhejiang University, Hangzhou 310058 China)

Abstract: Based on the relevant research on analytical models of confined concrete, the key factors affecting the compressive performance of passive confined concrete columns were discussed. Then, rectangular short concrete columns strengthened with carbon-fibre-reinforced-plastics (CFRP) grid reinforced engineering cementitious composite (ECC) matrix were prepared, and the compressive performances of short columns were experimentally studied. The effect of different lateral constraints on the improvement of compressive performance were clarified. The test results show that the brittle failure characteristics of concrete is improved for concrete columns strengthened with CFRP grid reinforced ECC matrix, which exhibits a smaller slope in downward section. The failure of concrete columns strengthened with CFRP grid reinforced ECC matrix is characterized as the peeling of CFRP grid and ECC matrix at the corner. With the increase of reinforcing layers, higher values of compressive strength and peak strain can be achieved for confined concrete while the transverse effective strain of constraint layer declines. A model for predicting the compressive strength of confined concrete strengthened with CFRP grid reinforced ECC matrix is obtained on the basis of the comparative analysis between analytical models of confined concrete and relevant experimental results.

Keyword: confined concrete; CFRP grid; ECC matrix; analytical model; lateral constraint stiffness; transverse effective strain

Fatigue Performance of Superimposed T-girders under Cyclic Overloading: an Experimental Study

Zhi-yu Xie, Da-wei Zhang*, Jian-Guo Dai, Yu-xi Zhao and Wei-liang Jin

Institute of Structural Engineering, College of Civil Engineering and Architecture, Zhejiang University, Hangzhou, China

School of Civil Engineering & Architecture, Ningbo Institute of Technology, Ningbo, China.

Department of Civil and Environmental Engineering, The Hong Kong Polytechnic University, Hung Hom, Hong Kong.

Corresponding author Email: dwzhang@zju.edu.cn

Abstract

The wet connection method is widely used in construction of superimposed prefabricated concrete structures. Existing studies have proved that interfaces between the prefabricated layer and the cast-in-place layer significantly affect the static structural performance of superimposed reinforced concrete (RC) girders, while little has bene known about the fatigue performance. The objective of this study is to investigate the low cycle fatigue behavior of superimposed T-shape prefabricated RC girders under hogging moment induced by high-stress level cyclic load. In total 15 superimposed T-girders with three different interface connection configurations were tested. The failure mode, cracking and deflection behavior, steel strain development and the new-old concrete interfacial deformation were recorded and analyzed. It was found that the fatigue life of the superimposed T-girders is significantly reduced by the debonding of interface between the cast-in-layer and pre-cast layer concrete, although the eventual failure is still governed by the fracturing of tension reinforcement. As a result, the interfacial connection configuration plays a critical role in preventing such debonding failure. The corresponding debonding mechanisms were clarified through analyzing the histories of measured interfacial slips and steel strains.

Keywords: superimposed T-girders, fatigue, new-old concrete interface, interface debonding, shear key

Bond properties of deformed steel bar with geopolymer incorporating multi-walled carbon nanotubes under monotonic load.

Weitao Li[1*], Yiyan Lu[2], Zhenzhen Liu[3], Shan Li[4#]

[1]School of Civil Engineering, Wuhan University, Wuhan, China
E-mail: liweitaowhu@163.com
[2]School of Civil Engineering, Wuhan University, Wuhan, China
E-mail: yylu901@163.com
[3]School of Civil Engineering, Wuhan University, Wuhan, China
E-mail: zzliu_1988@163.com
[4]School of Civil Engineering, Wuhan University, Wuhan, China
E-mail: lishan@whu.edu.cn

Abstract

Geopolymer is a kind of green and environment-friendly cementing material. The bond between steel bar and geopolymer is an important factor to determine the mechanical properties of geopolymer structure under static and dynamic loads. In this paper, the local bonding properties of steel bars in geological polymers were studied experimentally. The monotonic loading tests of 120 specimens were carried out by using the central tensile test method. The main variables include the volume content of PVA fiber, the diameter of special-shaped steel bar and the Anchorage length of steel bar. The results show that compared with the specimens without PVA fiber, the bonding property between geopolymer and steel bar is significantly improved by the addition of PVA fiber. Among the specimens mixed with PVA fiber, the bond strength of the specimen with 2% volume fraction of PVA fiber is the lowest, but these specimens have the best energy dissipation performance under large slip. In addition, the increase of special-shaped steel bar diameter and Anchorage length is not conducive to the improvement of peak bond strength and energy dissipation capacity in the process of steel bar pull-out. Finally, a mathematical model of bond stress-slip relationship is proposed, which is suitable for the bond-slip curve of geopolymer and steel bar.

Keywords: Bond properties, Bond stress-slip model, Deformed steel bars, Engineering Geopolymers Composites

[*]: Presenter; [#]: Corresponding author

Detection of CFRP-concrete bond defects by using electrical measurements

Jianyan He[1], Shaohua He[1*], Tamon Ueda[2], Yi Wang[3#]

[1] School of Civil and Transportation Engineering, Guangdong University of Technology, Guangzhou, Guangdong 510006, China,
[2] Guangdong Province Key Laboratory of Durability for Marine Civil Engineering, College of Civil and Transportation Engineering, Shenzhen University, Shenzhen, Guangdong 518060, China,
[3] School of Civil Engineering, Central South University, Changsha, Hunan 410075, China (corresponding author)

Presenter: 2112009030@mail2.gdut.edu.cn, #Corresponding author: wangyi.ce@csu.edu.cn

Abstract

To extend the service life of a reinforced concrete (RC) structure, carbon fiber reinforced polymer (CFRP) laminates with a high strength to weight ratio and excellent corrosion resistance are extensively used to strengthen deficient structures. However, due to the poor construction, overloading or harsh environments, a series of defects at the CFRP-concrete interface may cause serious structural safety problems. In this study, a detecting protocol based on the electrical measurement is proposed to effectively locate defects at the CFRP-concrete interface. Since the electrical conductivity of bonding defects is significantly different from the intact region in the CFRP-concrete interface, the electrical measurement could be used to detect the bonding defects. It was found that the current pathway in the interfacial defects could be equivalent to a parallel circuit (Fig. 1), which can help to assess detailed information about the defects.

Based on the equivalent circuit, an analytical model (Fig. 2) was established to assess the number, location and size of defects by analyzing the resistance distribution curves (Fig. 3). The length of defects had been quantified by determining a reliable defect edge coefficient mathematically and statistically (Fig. 4). The investigation of high-efficiency electrode arrangement was also carried out. Using comparatively small electrode intervals and distances between electrodes and the bonding interface could improve the detection precision. To reduce the interference effect from the steel reinforcement, the electrodes should be arranged as far as possible from the stirrups. Additionally, it was also found that the defect severities could be assessed by the comparison of minimal resistances. The outcomes of this study can be served as a possible methodology for evaluating the bond defects between CFRP and concrete.

Meanwhile, to apply the proposed method in practice, steel reinforcement's quantified effects on detecting accuracy were determined. Since the reinforcement cage in concrete would change electrical field distribution in concrete, the variation of the electrical field leads to the unexpected current pathway that flowed from defects to electrodes, which may change the resistance distribution curves. Experimental results indicated that the number and location of longitudinal reinforcement had less impact on detecting the number and location of defects (Fig. 5). In the contrast, the stirrups would result in the misidentified defect locations. Because of this, the analytical model was modified to assess the detailed information of defects and showed satisfactory accuracy.

The detection methodology based on the electrical measurement is promising to continuously monitor the bond performance of the CFRP-concrete interface under the hygrothermal environment. However, there are some limitations that remain and further studies are needed for the practical implementation of this proposed method. For example, the relationship between mechanical properties and electrical responses of adhesive under hygrothermal aging is not developed yet. Meanwhile, to achieve non-destructive detection, the embedded depth of electrodes in concrete should be investigated so that the use of external-paste electrodes on the surface of the concrete can be realized. Also, it is important to visualize the electrical results in the future, which is necessary to achieve the resistivity tomography of the bond layer.

Keywords: CFRP-concrete; Interface; Defect Detection; Electrical Measurement; Parallel Circuit

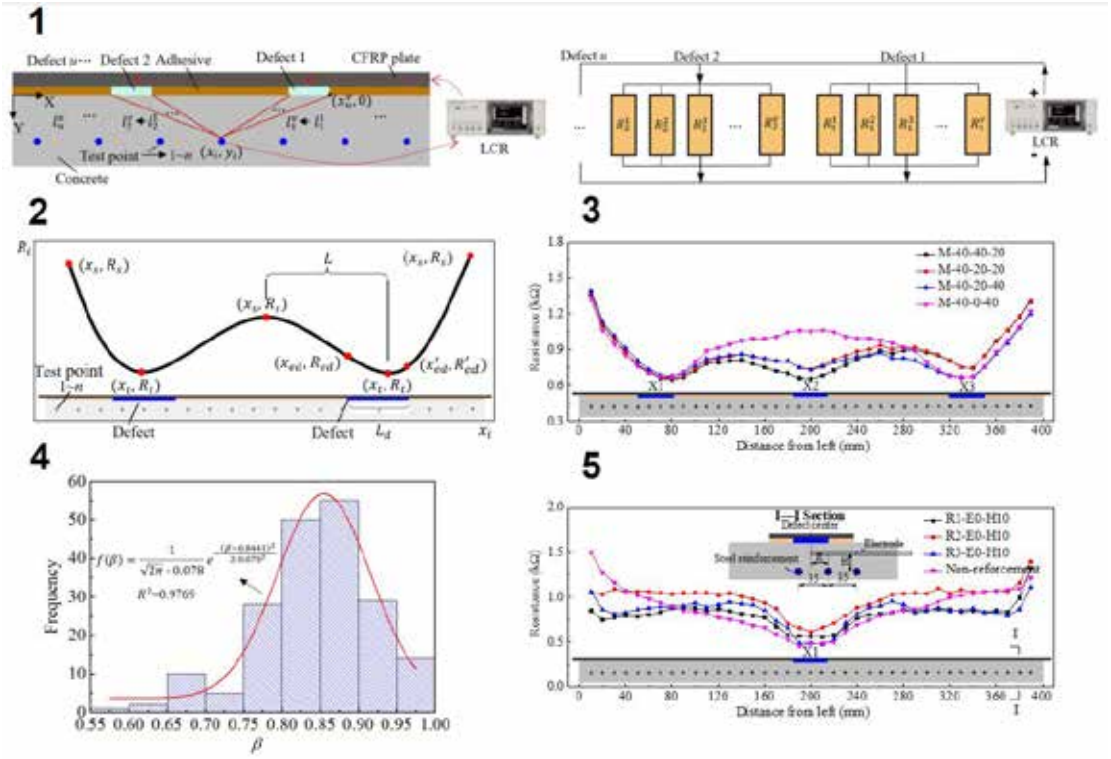

Fig. 1 Equivalent circuit for the bond defects; **Fig. 2** The analytical model to assess the detail information of defects; **Fig. 3** Successful detection of the number and location of defects; **Fig. 4** Mathematically and statistically determine the reliable defect edge coefficient; **Fig. 5** The effects of longitudinal reinforcement on detecting accuracy

Acknowledgment

The authors are grateful for the financial support received from the National Natural Science Foundation of China (Grant No. 52178308, 51708133).

Electrochemical Realization of High-Performance Carbon Fiber as Electrode Materials for Cement-Based Systems

Hongtao Yu[1,2*], Jihua Zhu[1,2#] and Feng Xing[1,2]

[1] School of Civil and Transportation Engineering, Shenzhen University, Shenzhen, Guangdong 518061, China
[2] Guangdong Provincial Key Laboratory of Durability in Coastal Civil Engineering, Shenzhen, Guangdong 518061, China
E-mail: iamhtyu@szu.edu.cn, zhujh@szu.edu.cn, xingf@szu.edu.cn

Abstract

Carbon Fiber (CF) is a remarkable material composed of graphite wire, typically with a diameter ranging from 5 to 10 μm. It possesses several desirable characteristics, including high strength, a large modulus, lightweight nature, strong alkaline corrosion resistance, and non-toxicity. As the field of construction undergoes intelligent development, CF has gained significant attention and found extensive applications in the construction sector. However, the effective utilization of CF as an electrode material in construction processes, such as cement-based batteries and cathodic protection, heavily relies on its electrochemical properties.

Presently, the majority (more than 90%) of CF materials available on the market are produced from polyacrylonitrile (PAN). Nevertheless, these initial CF variants often exhibit poor electrochemical activity and possess a low specific surface area. To address this limitation, this study focuses on investigating the evolution of PAN-based CF's surface states under electrochemical oxidation conditions in ordinary electrolytes. Moreover, a straightforward, cost-effective, and environmentally friendly modification strategy is proposed to enhance the surface electrochemical properties of CF on a large scale.

Experimental investigations conducted during this study reveal distinctive variations in the surface oxidation process and morphology of CF under different ionic conditions, as depicted in Figure 1a. In strongly alkaline chloride (Cl-) solutions, the content of oxygen-containing functional groups on the CF surface substantially increases. This augmentation results in a remarkable enhancement of CF's electrochemical activity, as illustrated in Figure 1b. Consequently, the modified CF can serve as an excellent anode material for cathodic protection systems in reinforced concrete structures exposed to high-chlorine environments.

Furthermore, when subjected to a highly alkaline sulfate (SO42-) solution, CF experiences swelling and spalling of the carbon layers on its surface. These transformations lead to a significant increase in the specific surface area, as illustrated in Figure 1c. The resulting CF with enhanced capacitive properties can be effectively utilized as electrode materials for cement-based battery devices.

Keywords: Carbon fiber, Oxidation treatment, Cl^-, SO_4^{2-}, Electrode materials

[*]:Presenter; [#]:Corresponding author

The findings of this study offer a straightforward and practical method to enhance the electrochemical properties of CF, thereby enabling its efficient utilization as electrode materials in strongly alkaline cement matrices. This research contributes to the ongoing efforts in the construction industry to develop sustainable and high-performance materials for intelligent building applications. The proposed modification strategy not only provides a cost-effective solution but also ensures compatibility with large-scale production processes. With further research and development, the modified CF can find wider applications, offering significant advantages in terms of electrochemical performance and environmental impact.

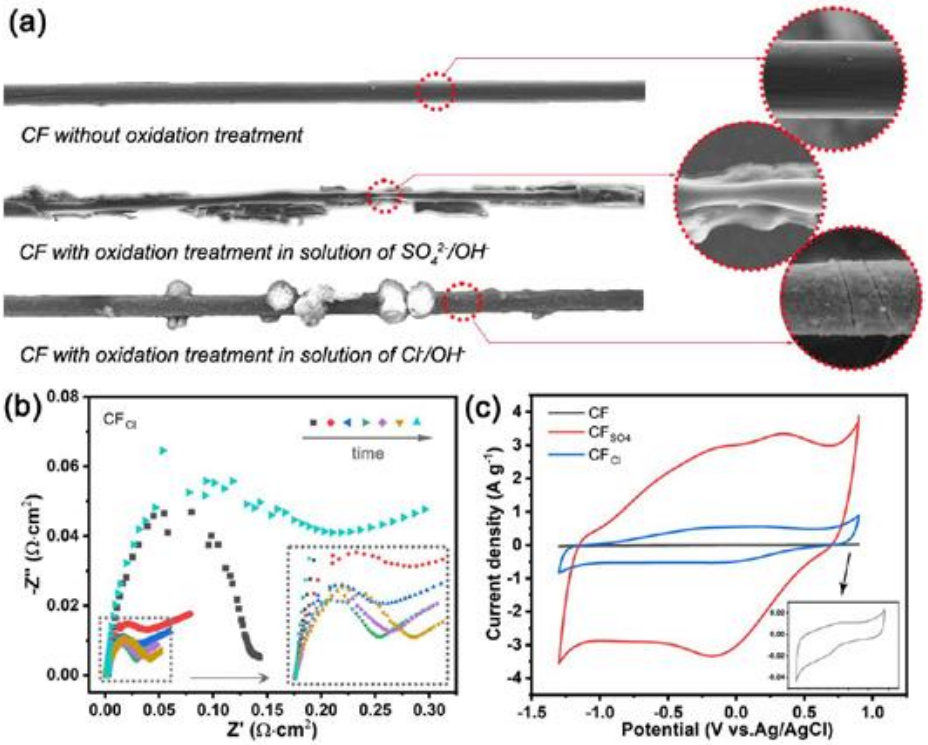

Fig.1 (a) Morphological changes of CF before and after electrochemical oxidation treatment in different electrolytes; (b) Impedance spectra of CF after electrochemical treatment in alkaline solutions containing chloride ions; (c) Cyclic voltammetry curves of CF before and after electrochemical treatment in different electrolytic salt solutions.

Acknowledgment

This work was supported by the National Key Research and Development Program of China (2018YFE0124900), the Key-Area Research and Development Program of Guangdong Province (2019B111107002), the National Natural Science Foundation of China (51538007/51778370/52108231), and the Shenzhen Science and Technology Project (GJHZ20180928155819738).

A study on HyFRCC consisting of PE and carbon fiber: Investigation of electrical and fracture properties based on orthogonal design

Zhu Ji-Hua[a], Shen Haowei[a], Wei Liangliang[b*]

[a] Guangdong Province Key Laboratory of Durability for Marine Civil Engineering, College of Civil and Transportation Engineering, Shenzhen University, Shenzhen, Guangdong 518060, China

[b] School of Environment and Civil Engineering, Dongguan University of Technology, Dongguan, Guangdong 523808, China

[*] Corresponding author: liangwei@dgut.edu.cn (L.L. WEI)

E-mail address: zhujh@szu.edu.cn (J.H. ZHU), shenhaowei2021@email.szu.edu.cn (H.W. SHEN)

Abstract

A hybrid fiber reinforced cementitious composites (HyFRCC) consisting of polyethylene (PE) and carbon fiber has a potential on new composite materials integrating high mechanical properties with smart functions based on electrical properties. However, an evaluation of electrical and fracture properties of HyFRCC has not yet reported. An orthogonal experimental design method was used to investigate the significance sequence of four influencing factors on electrical and fracture properties of HyFRCC in this paper. The influencing factors included the length (two levels) and volume fraction (five levels) of PE fiber, the volume fraction of carbon fiber (five levels) and water-to-cement ratio (four levels). A total of 25 groups were tested based on the mixed orthogonal design. Results showed that the water-to-cement ratio plays a major role in controlling the electric properties of HyFRCC in the case of adding PE and carbon fiber. Further orthogonal analysis showed that the optimal mix proportion regarding electrical properties is adding 0.75 vol% carbon fiber and 0.5 vol% PE fiber in the water-to-cement ratio of 0.4. Carbon fiber has a significant effect on the initial fracture toughness of HyFRCC, while PE fiber determines the unstable fracture toughness. Considering both electrical and fracture properties, 1.0 vol% - 1.5 vol% PE fiber and 0.75 vol% carbon fiber can be adopted in the hybrid fiber system.

Keywords: Carbon fiber, PE fiber, HyFRCC, Orthogonal design.

Effect of Anodic Polarization on Mechanical Behavior of Carbon Fabric Reinforced PE/CF Hybrid Fiber Cementitious Composites

Wei Liangliang*, Zhu Ji-Hua and Shen Haowei

Guangdong Provincial Key Laboratory of Durability for Marine Civil Engineering, College of Civil and Transportation Engineering, Shenzhen University, Shenzhen City, China
E-mail: liangwei@szu.edu.cn, zhujh@szu.edu.cn, shenhaowei2021@email.szu.edu.cn

Abstract

An integration of impressed current cathodic protection (ICCP) and structural strengthening (SS) as ICCP - SS technology has emerged which aims at improving the structural longevity of corroded reinforced concrete structures. The carbon fabric reinforced cementitious matrix (C-FRCM) has been adopted as a dual-functional material for transferring protection current and enhancing loading capacity simultaneously. However, the brittle property of cementitious matrix and poor bond performance between carbon fabric and matrix limited the efficiency of carbon fabric. Moreover, the degradation of C-FRCM resulted by anodic polarization in ICCP process further constricted the efficiency of carbon fabric. In the present paper, a hybrid fiber reinforced cementitious composites (HyFRCC) was prepared as the matrix. The mechanical behavior and degradation of carbon fabric mesh reinforced HyFRCC (CFM-HyFRCC) was studied and discussed.

HyFRCC was composed of polyethylene (PE) fiber and carbon fiber as well as mortar matrix. The volume fraction and length of carbon fiber were considered in the preparation of HyFRCC. The mechanical behavior of CFM-HyFRCC was studied by uniaxial tensile tests and digital image correlation (DIC) measuring. In addition, an anodic polarization test was performed at different anodic current densities on CFM-HyFRCC. The degradation of mechanical behavior of CFM-HyFRCC was evaluated.

The results show that the mechanical strength of CFM can be released and activated completely in the case of the synergistic effect of CFM reinforcement and HyFRCC matrix. An excellent tensile performance of CFM-HyFRCC was obtained by using HyFRCC at hybridizing 1.5 vol% PE fiber and 1.0 vol% carbon fiber with 3 mm length. A trilinear tensile constitutive model of CFM-HyFRCC was proposed based on the cracking strength and debonding strength as well as ultimate strength. The tensile strength of CFM-HyFRCC was decreased as increasing charge densities, resulting in the reduction of the utilization efficiency of CFM. However, the deterioration of mechanical behavior and the feeding voltage of ICCP system were decelerated by hybridizing carbon fiber in the single-doped PE fiber reinforced cementitious matrix. The tensile constitutive model of CFM-HyFRCC was also transformed from trilinear to bilinear relation after anodic polarization.

Keywords: Cathodic protection, HyFRCC, PE fiber, Mechanical behavior, Carbon fiber

Numerical Evaluation of Space Averaging of Electric Field, Macro-cell Corrosion of Reinforcement and Anti-corrosion with Verification

Zhao Wang[1*], Koichi Maekawa[1#]

[1] Institute of Urban Innovation, Yokohama National University, Yokohama, Kanagawa 240-8501, Japan
[*]*Presenter:* wangzhaoousyo@gmail.com, [#]*Corresponding author:* maekawa-koichi-tn@ynu.ac.jp

Abstract

Steel corrosion is one of the deterioration factors for reinforced concrete structures, where macro-cell corrosion type is detrimental due to the fast corroding speed associated with external circuit. The macro-cell corrosion is induced by the natural potential gap due to chloride penetration/carbonation or impressed electric field such as stray current, which may happen in different scales from kilometer to centimeter level. It requires us to capture the features of macro-cell corrosion with global viewpoint instead of only corroding spot, so that the effective anti-corrosion methods can be applied. This paper aims to validate a space-averaged electric filed simulation, where the whole surfaces of reinforcing bars are blended into the 3D extent of finite volume, for identifying the electric potential to drive the macro-cell corrosion of structural concrete. The overlaid scheme of electro-chemical analysis can not only tackle with the wide scale span, but also integrate with the smeared scheme of non-linear mechanics. Experiment is also conducted with transparent pseudo concrete materials, which has chemical pore-solutions similar to those of concrete, to validate the integrated simulation platform qualitatively. Satisfied agreement is found and the possible anti-corrosion methodologies are proposed.

Keywords: Space averaging, Macro-cell corrosion, Anti-corrosion method, Numerical simulation, Experiment, Pseudo concrete material.

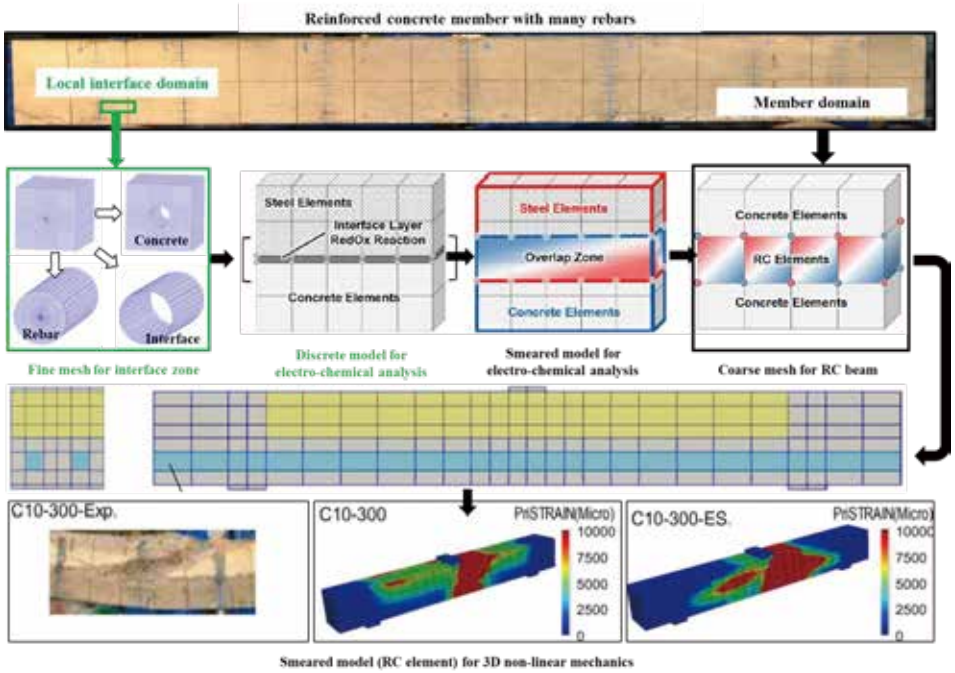

Fig. 1 Space-averaged modeling of reinforcement originated from exact discrete idealization

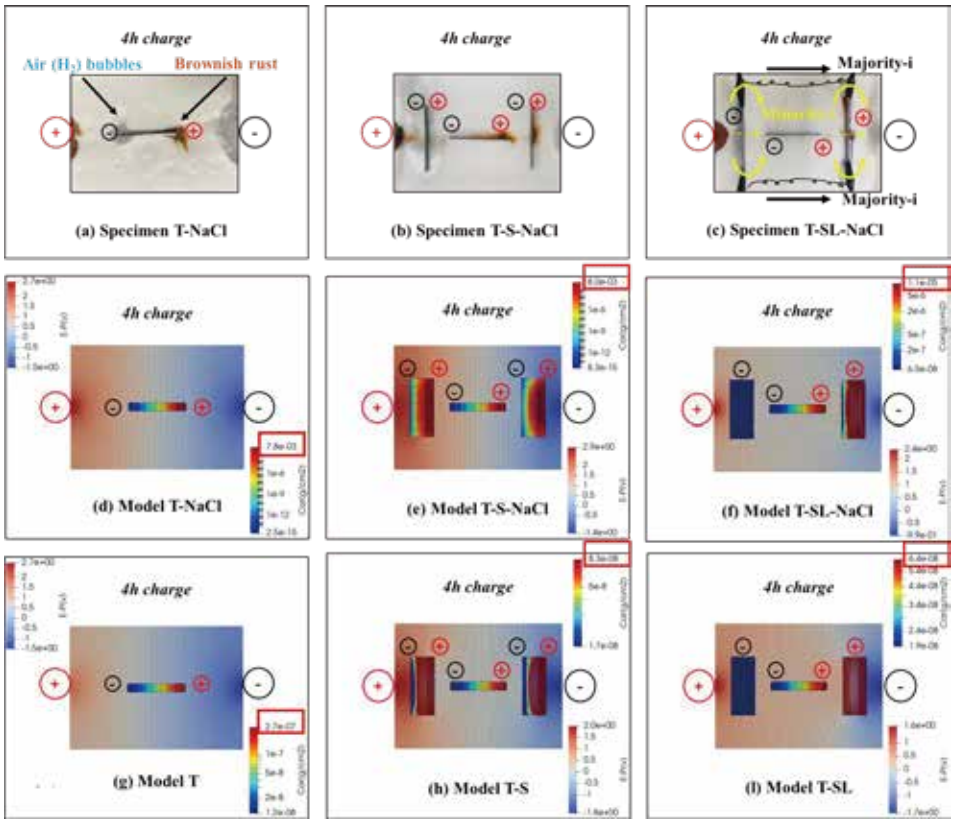

Fig. 2 Simulation and experiment on large scale macro-cell corrosion

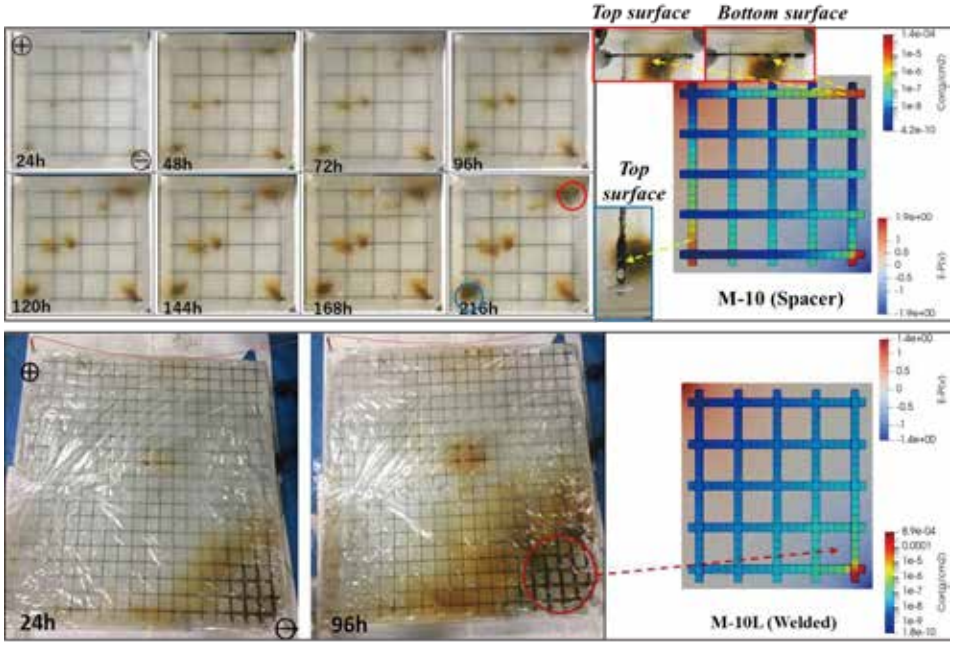

Fig. 3 Simulation and experiment on small scale macro-cell corrosion

Acknowledgment

The authors would like to acknowledge the funding support from Grant-in-Aid for JSPS Fellows of Japan Society for the Promotion of Science (20F20367) and Grant-in-Aid for Scientific Research (A) of Japan Society for the Promotion of Science (20H00260).

Study of the anode degradation behavior of various CFRP materials in ICCP system

Bao Zhong[1, 2], Hongtao Yu[1, 2*], Ji-Hua Zhu[1, 2], Feng Xing[1, 2]

1. School of Civil and Transportation Engineering, Shenzhen University, Shenzhen, Guangdong 518061, China

2. Guangdong Provincial Key Laboratory of Durability in Coastal Civil Engineering, Shenzhen, Guangdong 518061, China

Abstract: Carbon Fiber Reinforced Polymer (CFRP) consists of carbon fibers and a resin matrix. Due to its good mechanical properties, electrical conductivity and electrochemical stability, CFRP can be used not only as a reinforcing material for structures, but also as an anode material for impressed current cathodic protection (ICCP) of buildings. In this work, the anodic degradation behavior of CFRP materials with different profile in simulated hole solution of cement and the development process of their mechanical properties were investigated to show the regular variation of resion content with the amount of charges for effective polarization, thus establishing the relevant criteria for the application of different CFRP materials in the ICCP system. The preliminary test results are shown below: first, all CFRP materials with different profiles can show good working stability in the simulated ICCP system, and the drive voltage remains stable under different current densities (in **Figure 1a, b, c**); secondly, with the prolongation of polarization time and the increase of current density, the degradation behavior of different CFRP materials gradually strengthened, resulting in the color deepening of the electrolyte, which was the result of the dissolution of the surface carbon fibers; thirdly, different structural shapes and resin contents have a significant influence on the mechanical properties of CFRP materials for polarization. For example: the residual tensile strength of the CFRP grid with 3% resin content is 69.01% when the electric charge density for polarization is ~0.7×10^7 C/m^2 (in **Figure 1d**), while the residual tensile strength of the CFRP plate with 25% resin content under the same conditions is 82.43% (in **Figure 1e**). In summary, the structural shape and resin content of CFRP are key factors for its highly efficient application in the ICCP system as an anode material.

Key words: CFRP; ICCP; Anodic degradation; Structural shape; Resin content

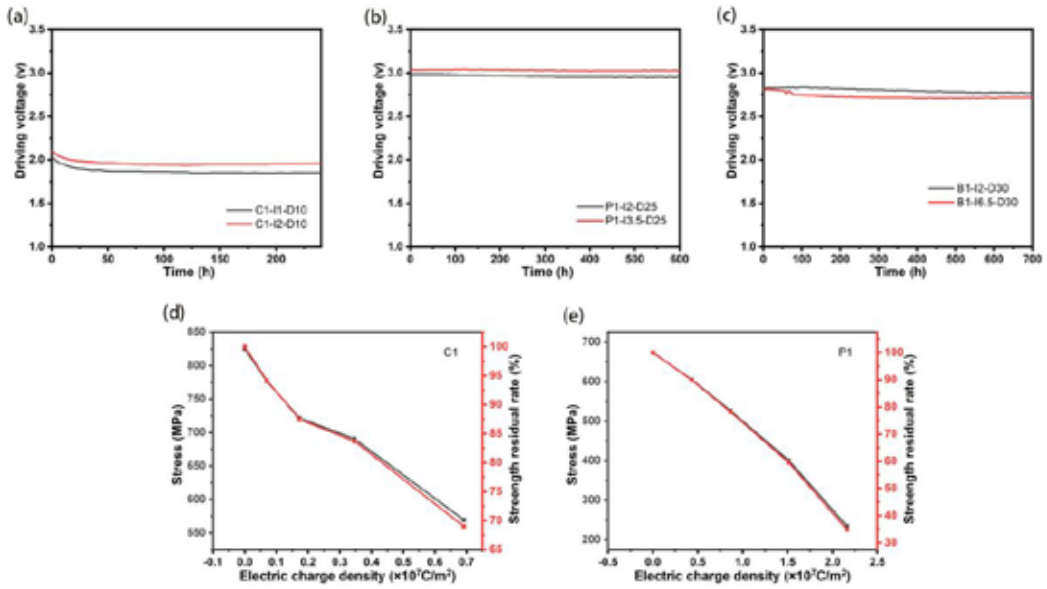

Figure 1 (a), (b), and (c) are the drive voltage and polarization time curves for CFRP-C1 (grid), CFRP-P1 (plate), and CFRP-B1 (bar); (d) and (e) are the relationship curve of mechanical properties and electric charge density for polarization of CFRP-C1 (grid) and CFRP-P1 (plate).

*** Foundation items:**

Guangdong Provincial Key Research and Development Program(no.2019B111107002); National Key Research and Development Program of China, No.2018YFE0124900;

National Natural Science Foundation of China, No.51861165204/51778370;Shenzhen Science and Technology Project (GJHZ20180928155819738)

Corresponding author:
Hongtao Yu, E-mail: iamhtyu@szu.edu.cn

Thermo-hydro-mechanical Analysis of Saturation-dependent Creep Behavior for RC Beam under Sustained Load and Wet-dry Cycles

Yiping Yang[1*], Fuyuan Gong[1#], Yuxi Zhao[1], Koichi Maekawa[2]

[1] College of Civil Engineering and Architecture, Zhejiang University, Zhejiang, Hangzhou 310058, People's Republic of China
[2] Department of Civil Engineering, Yokohama National University, Japan.
[*]*Presenter:* yangyp_zju@zju.edu.cn, [#]*Corresponding author:* gongfy@zju.edu.cn

Abstract

The alternating wet and dry environment is one of the complex service environments and mostly acts on coastal structures and cross-sea bridges. For cross-sea bridges, the phenomenon of increasing creep deflection year by year has attracted the attention of scholars and research. In order to study the deflection variation law of concrete beams under dry and wet varying environments, this paper uses a combination of experiments and numerical calculations to reveal the development mechanism of creep under wet-dry environments. Based on hydro-thermal analysis combined with the effect of cracks on moisture transport to calculate the internal pore saturation of concrete, the local creep coefficient is influenced by the local saturation. And combined with the structural inhomogeneous drying shrinkage to obtain the deformation law of the beam during the wet-dry cycles. The study shows that in general, the creep deformation increases as the period of the cycle increases and increases as the drying humidity decreases, but the uneven shrinkage of the beam during drying caused by the bottom crack will lead to a certain degree of upwarping of the beam.

For more details of the creep development in wet-dry environment, the study finds out that when the drying RH is a fixed value, the creep deflection increases with continuous drying time. As shown in Fig.1, When wet-dry cycle period is the 1 day or 90 days, the creep deflection increases as drying RH decreasing. Nevertheless, when wet-dry cycle period is the 7 days or 30 days, the inhomogeneity of the RH of the cross section will cause the inhomogeneity of the drying shrinkage and cause the upwarping of the beam.

As for the upwarping of the beam when experiences drying process, Fig.2 shows upwarping by inhomogeneity of the drying shrinkage should be considered. Upwarping by drying is the result of the cracks, crack is able to cause different permeation rate of the moisture. In drying time, the tension zone of the beam dry faster than the compressive zone and the final saturation is lower also, which makes inhomogeneity of the RH and then causes the inhomogeneity of the drying shrinkage. Besides the inhomogeneity of the drying shrinkage, the lower drying RH is also an indispensable condition to generate the upwarping.

Besides, the creep is developing rapid in early time, so the environment of the early time is important to analysis the creep of the reinforcement concrete. As the same wet-dry cycle period (90d), if the drying process is front of wetting process, then the creep deflection is larger as shown in Fig.3.

Keywords: Creep development; Wet-dry cycles; Moisture transmission; Inhomogeneous shrinkage; Crack

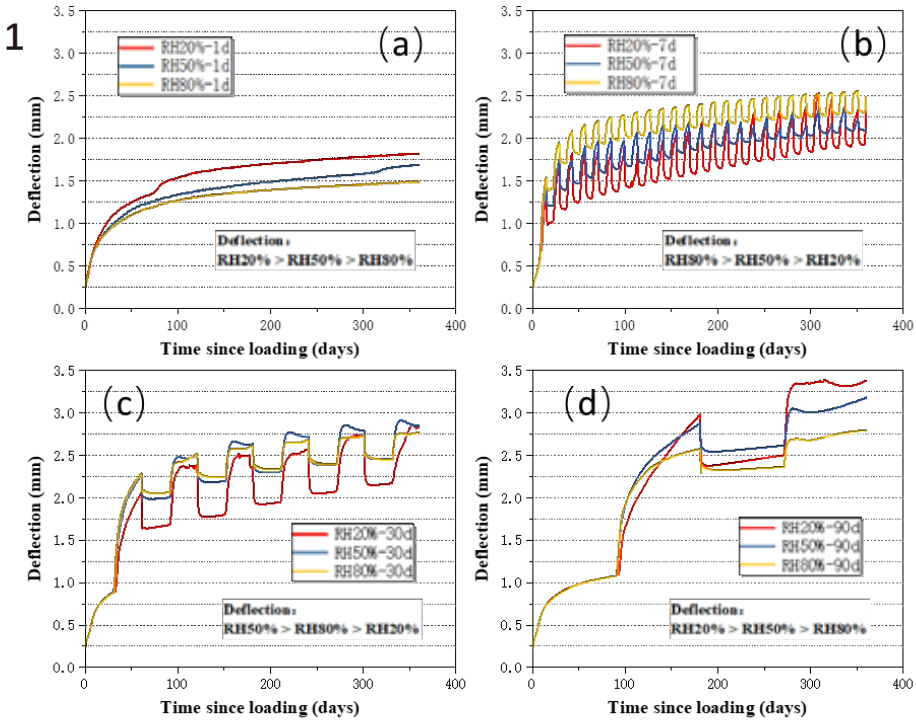

* RH x-y: x is the drying RH and y is the wetting(drying) time in a wet-dry cycle

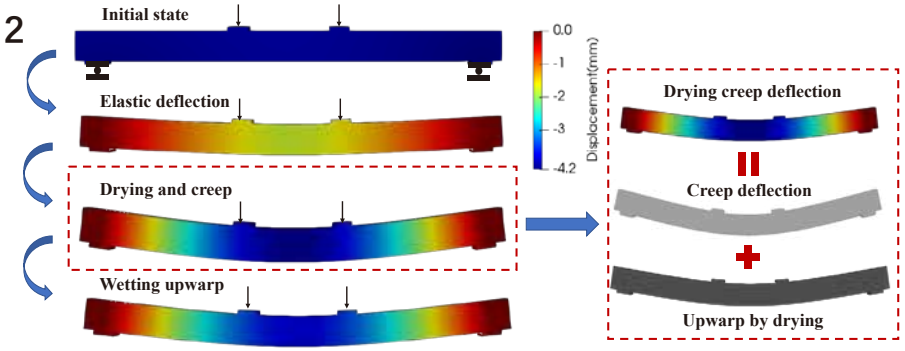

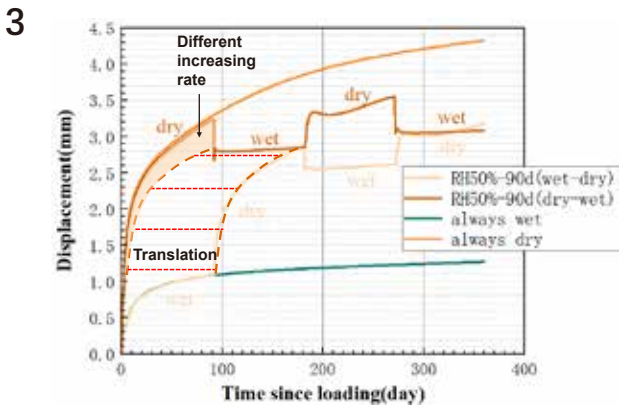

Fig. 1 Creep deflection of beams in wet-dry cycle; **Fig. 2** Composition of deflection of beams in wet-dry environments; **Fig. 3** Differences in creep caused by different early humidity

Acknowledgment

The authors would like to acknowledge the funding support from National Natural Science Foundation of China (51820105012, 52038010).

Piezoresistive Effect of Carbon Fabric Reinforced Cement Matrix (CFRCM) under Cyclic Loading

Bo Yi[1*],Jihua Zhu[2] and Dawei Zhang[3]

[1,2] Guangdong Province Key Laboratory of Durability for Marine Civil Engineering, College of Civil and Transportation Engineering,ShenZhen University, ShenZhen, CHINA
E-mail: yibo2021@email.szu.edu.cn
E-mail: zhujh@szu.edu.cn
[3] College of Civil Engineering and Architecture, Zhejiang University, Hangzhou, CHINA
E-mail: dwzhang@zju.edu.cn

Abstract

Fabric Reinforced Cementitious Matrix (FRCM) have been gradually applied in the repairing and strengthening of reinforced concrete (RC) structures. The necessity of monitoring and assessment of stress and damage state of FRCM during its service life is also increasing. However, traditional technique of strain measurement cannot accurately reflect the real stress state of carbon fabric and FRCM. To fully utilize the piezoresistive effect of Carbon Fabric Reinforced Cement Matrix (CFRCM) to self-monitor its stress state and damage, this paper studied the piezoresistive effect of CFRCM under cyclic loading. Before cyclic loading, the CFRCM plates were firstly subjected to monotonic tensile load to determine the magnitude of the load and static piezoresistive effect. Five sets of cyclic loading tests with different loading levels were then performed to evaluate the influence of cyclic loading on the piezoresistive effect of CFRCM plate. The crack pattern, the resistance, the stress state and the failure mode of CFRCM plate were recorded. Based on the test results, the evolution of piezoresistive effect of CFRCM plate under cyclic loading was investigated and the relative mechanism was discussed based on the SEM image analysis of failure sections.

Keywords: FRCM, CFRCM ,monitoring, piezoresistive effect, cyclic loading.

[*]: Presenter; [#]: Corresponding author

Parallel Sessions-4

Limestone Calcined Clay Cement Concrete: Material Development, Physical Properties, Structural Implementation and Durability

Limestone calcined clay cement (LC^3) concrete and LC^3 concrete structure: research status in Shenzhen University

Yingwu Zhou[1,2*#], Zhenyu Huang[1,2], Biao Hu[1,2], Menghuan Guo[1,2]

[1] Guangdong Province Key Laboratory of Durability for Marine Civil Engineering,
[2] College of Civil and Transportation Engineering, Shenzhen University, Shenzhen, Guangdong 518060, People's Republic of China
[*] *Presenter and corresponding author: ywzhou@szu.edu.cn*

Abstract

To address the inadequacy of traditional supplementary cementitious materials (SCMs), limestone calcined clay cement (LC^3) appears to be an excellent alternative. Both kaolinite clay and limestone are abundant worldwide, which ensures an adequate supply. The production of both materials consumes low amounts of energy, and the resulting CO_2 emission is largely reduced compared to conventional cement clinkers. Extensive studies concerning the hydration mechanism and microstructural characteristics of LC^3 and the macrostructural mechanical performance of LC^3 concrete have been carried out in Shenzhen University. Various LC^3 concrete types including natural aggregate concrete, recycled aggregate concrete, seawater sea sand concrete, engineered cementitious composites, and ultra-high performance concrete have been investigated. The flexural behaviors of LC^3 (recycled) concrete beams reinforced by CFRP, steel or their hybrid were studied, and the bond behavior between LC^3 concrete and CFRP/steel has been investigated. Besides, the stress-strain modelling of LC^3 concrete has been performed, and the life cycle design and energy saving analysis of LC^3 concrete structure has been conducted.

Keywords: Limestone Calcined Clay Cement (LC^3); LC^3 Concrete; Mechanical Performance; Flexural Behavior; Bond Behavior; Energy Saving

Acknowledgment

The authors would like to acknowledge the funding support from the National Natural Science Foundation of China (Grants No. 51878414) and the Ministry of Science and Technology of China (Grant No. 2018YFE0125000).

Development and structural implementation of LC^3 concrete using raw materials in South China

Zhenyu Huang[1,2*], Xiaolong Zhao[1,2], Weixiong Deng[1,2], Yingwu Zhou[1,2], Feng Xing[1,2]

[1] Guangdong Province Key Laboratory of Durability for Marine Civil Engineering,
[2] College of Civil and Transportation Engineering, Shenzhen University, Shenzhen, Guangdong 518060, People's Republic of China
[*]*Presenter:* huangzhenyu@szu.edu.cn, [#]*Corresponding author:* huangzhenyu@szu.edu.cn

Abstract

Limestone calcined clay cement (LC3), consisting of ordinary Portland cement (OPC) clinker, calcined clay, limestone powder, and gypsum, has been considered a promising solution to current challenges in the cement and concrete industry, such as high carbon emissions, high energy consumption, and resource shortages. The first part of this study presents a series of experimental investigations of LC3-based paste, mortar, and concrete, including microstructural analyses and macro-scale testing, using raw materials from south China. The results show that, in LC3 paste, the replacement of clinker by calcined clay and limestone leads to an increased volume of small pores but decreased total volume of pores. The workability of LC3 mortar and concrete can be readily tailored using conventional superplasticizers. When designed for comparable 28-d compressive strength, the LC3 concrete tend to have lower early-age compressive strength, but comparable compressive strength and higher flexural strength than those of the OPC counterparts at late ages.

To further evaluate the reliability and short-term structural performance of reinforced LC3 concrete members, the second part of the present study focuses on flexural and shear behavior of reinforced concrete (RC) beams using the new developed ecologically green cement consist of limestone, calcined clay and cement clinker (LC3). Full-scale flexural and shear tests were conducted on RC beams with varying reinforcement ratio, concrete strength, shear-span-to-depth ratios and stirrup reinforcement ratios. The test results showed that the crack development and failure modes of LC3 concrete beams were similar to those of OPC beams, both of which exhibited typical flexural and shear failure. The flexural and shear resistance of LC3 concrete beams was evaluated by Chinese, American and Eurocode codes, and the Chinese code had the closest predictions. These findings on LC3 concrete provide fundamental information and guidance for furthering the application of LC3 binder in structural concrete in the near future.

Keywords: Limestone calcined clay cement (LC3); Hydration; Bond-slip; Shear resistance; Reinforced concrete.

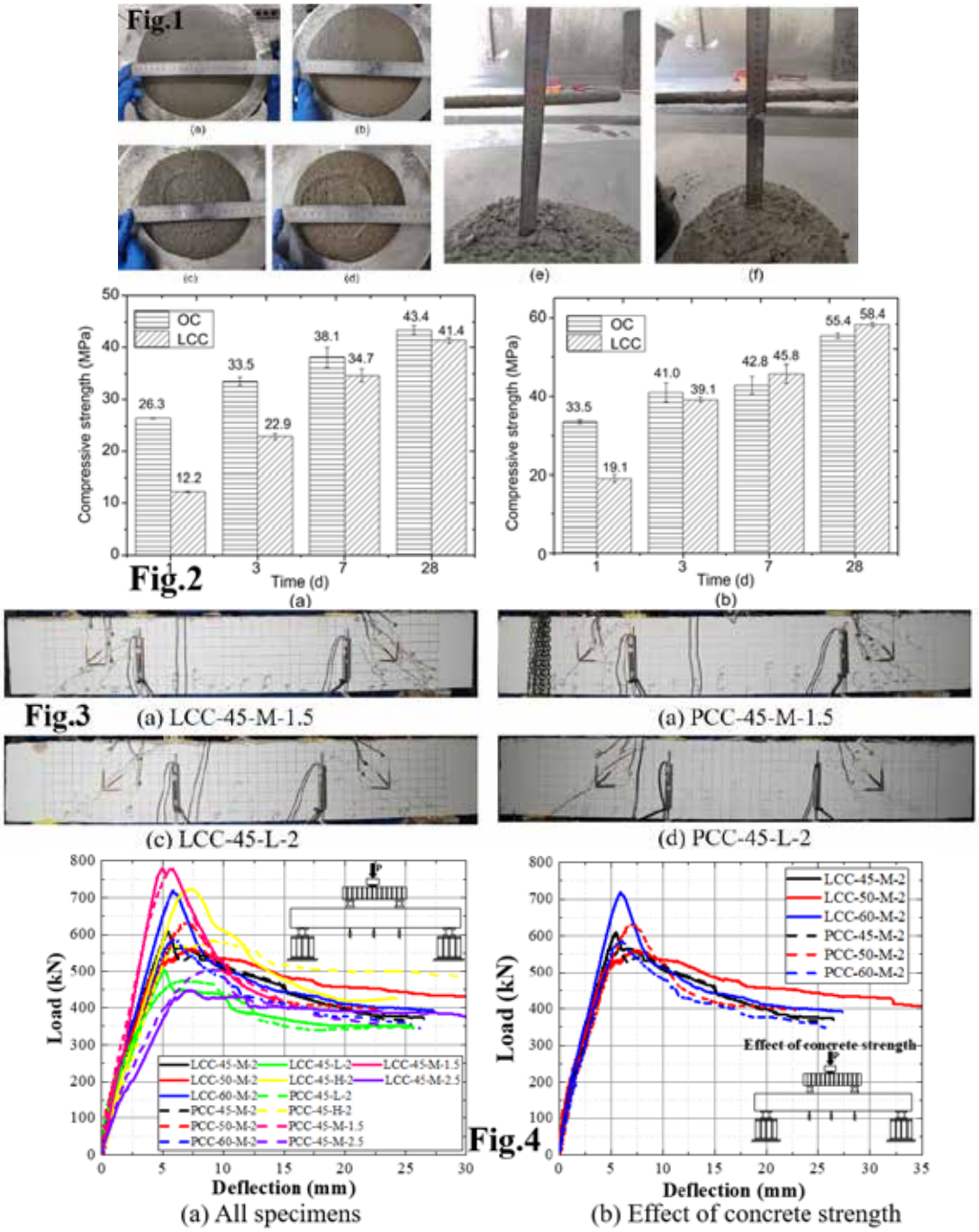

Fig. 1 Workability of OPC and LC3 mortar and concrete; **Fig.2** Compressive strengths of LC3 concrete; **Fig.3** Failure modes of tested beams; **Fig.4** Load-deflection curves of tested beams

Acknowledgment

The authors would like to acknowledge the funding support from the National Natural Science Foundation of China (No. 51978407), Guangdong Provincial Outstanding Youth Fund (No. 2022B1515020037), Shenzhen International Science and Technology Cooperation Project (No. GJHZ20200731095802008) and Natural Science Foundation of Guangdong Province (No. 2021A1515010932), Key Projects for International Cooperation in Science, Technology and Innovation of China (No. 2018YFE0125000) and Guangdong Provincial Key Laboratory of Durability for Marine Civil Engineering (No. 2020B1212060074).

Multiscale modelling of LC3 concrete performance

Tiao Wang[1*#], Medepalli Satya Chai [1], Yuqian Zheng[1], Chunhe Li[2]

[1] The University of Tokyo, 7-3-1 Hongo, Bunkyo-ku, Tokyo 113-8656, Japan,
[2] The University of Miyazaki, 1-1 Gakuenkibanadainishi, The University of University of Miyazaki, 889-2155, Japan
Presenter: wangtiao@g.ecc.u-tokyo.ac.jp, #Corresponding author: wangtiao@g.ecc.u-tokyo.ac.jp

Abstract

Supplementary cementing materials (SCMs) have been widely used to improve the performance of reinforced concrete (RC) structures. Limestone calcined clay cement (LC3) is a recently developed material that is popular in the construction industry due to its low CO_2 emissions. However, the pozzolanic reaction of clay and its contribution to concrete performance is still poorly understood. Therefore, this study develops a multiscale modelling system to simulate the performance of LC3 concrete.

The material properties of calcined clay are first characterized by SEM-EDS mapping method (**Fig.1**). Experimental result shows that the reactive phase of calcined clay is metakaolin. The unified multiphase reaction model is extended to simulate the pozzolanic reaction of metakaolin in cement systems (**Fig.2**). A microstructure model is also developed based on the latest characterization of C-(A)-S-H gel. A multiscale modelling system that incorporates the unified multiphase reaction model and the microstructure model of C-(A)-S-H gel is subsequently developed. This modelling system provides satisfied predictions on the performance of metakaolin concrete, such as compression strength and water loss (**Fig.3**).

This study also develops a reliability analysis system that incorporates the coupled degradation effects of crack development and corrosion progression into the assessment of the corrosion failure probability of RC structures (**Fig. 4**). Coupling with the performance prediction of LC3 concrete by the multiscale modelling system, this reliability system can be used to assess the corrosion failure probability of RC beam using LC3 under chloride attack. Analysis result shows that SCMs significantly improve the durability of RCs under chloride ingress. Our analyses also show that the performance of LC3 RC is similar to that of slag RC (**Fig.5**); this is significant, as LC3 concrete is a promising green cementitious material.

Keywords: LC3; Metakaolin; Pozzolanic reaction; Multiscale modelling; Reliability analysis.

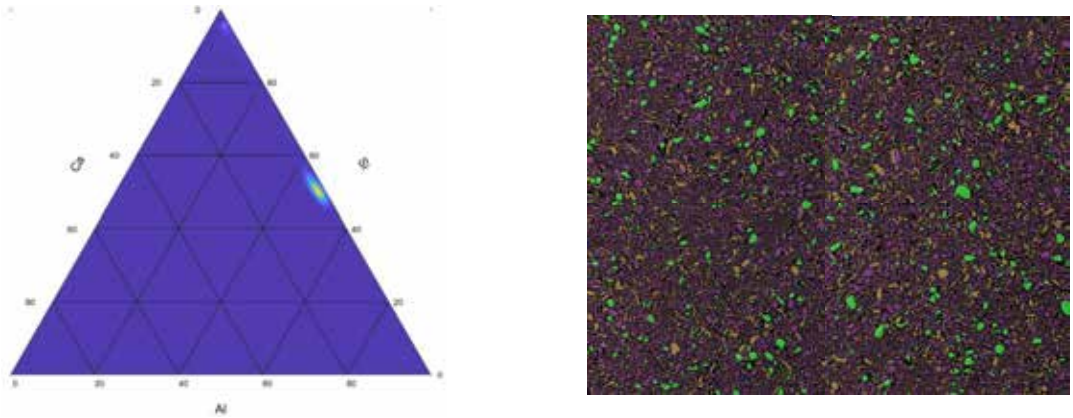

(a) Ca-Si-Al element distribution (b) Mineralogical mapping based on SEM-EDS

Fig.1 Material characterization of calcined clay

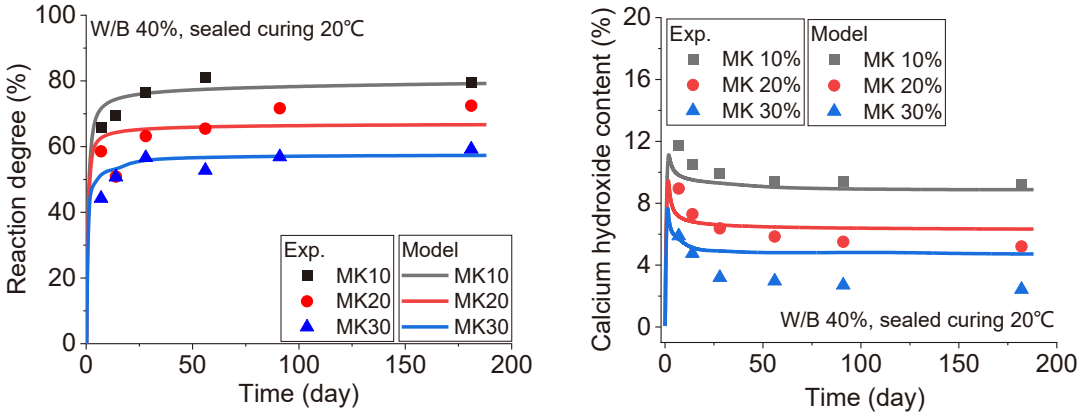

(a) Reaction degree of metakaolin (b) Calcium hydroxide content

Fig. 2 Modeling pozzolanic reaction of metakaolin in cement systems

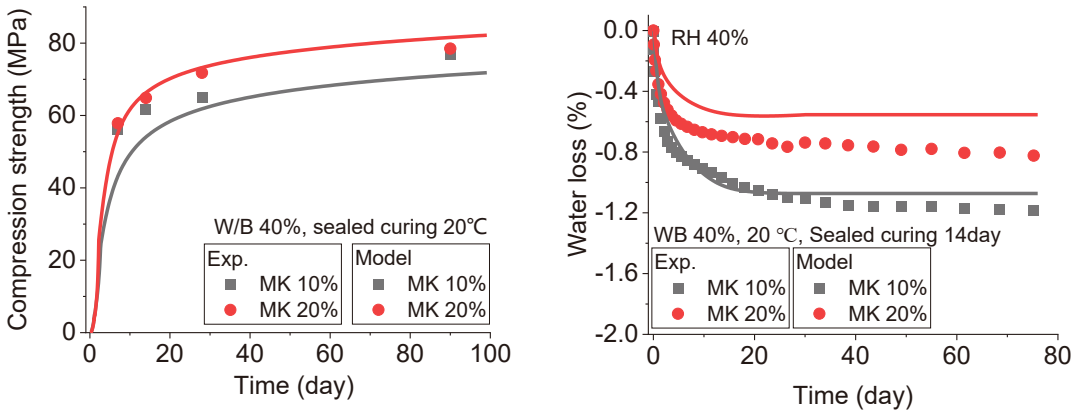

(a) Compression strength (b) Water loss

Fig. 3 Performance modelling of metakaolin concrete

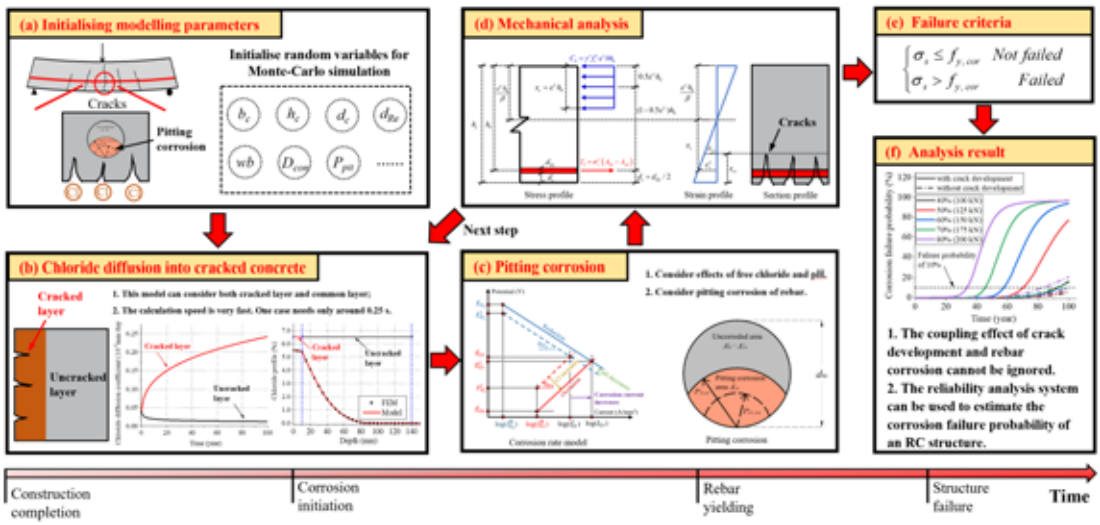

Fig.4 Reliability assessment system for RC structures subjected to chloride ingress.

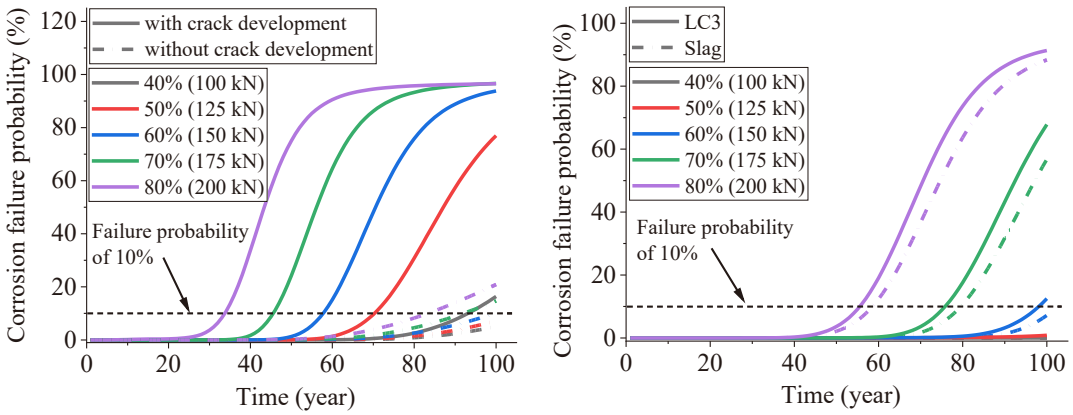

(a) RC beam using OPC (b) RC beam using LC3 or slag

Fig.5 Corrosion failure probability of reinforced concrete beam.

Acknowledgment
The authors are grateful for financial support from The Taisei Foundation (2020), the Japan Cement Association (Grant project in 2020 and 2022), the Japan Concrete Institute (Grant project in 2022), the National Key Research and Development Project of China (Grant No. 2018YFE0125000).

Performance assessment of LC3 concrete structures considering life-cycle cost and environmental impacts

Xiao-Xu Huang[1,2*], Zhen-Xiao Jiao[1,2], Ying-Wu Zhou[1,2#]

[1] Guangdong Province Key Laboratory of Durability for Marine Civil Engineering,
[2] College of Civil and Transportation Engineering, Shenzhen University, Shenzhen, Guangdong 518060, People's Republic of China
[*]*Presenter:* xxhruby@szu.edu.cn, [#]*Corresponding author:* ywzhou@szu.edu.cn

Abstract

Traditional concrete, composed of cement, aggregate, fresh water, and river sand, has caused huge damage to the natural ecological environment. Developing green materials in infrastructure construction is of vital importance for sustainable development. Limestone calcined clay cement (LC3) is a suitable alternative for the reduction of CO_2 emission and resource consumption in the cement industry. Recycle concrete aggregate (RCA), seawater and sea sand are potentially advantageous from a sustainability perspective, especial in coastal regions. Fiber-reinforced polymer (FRP) bars with excellent corrosion resistance are ideal alternative materials for steel bars in a corrosive environment to minimize maintenance. In this paper, a type of green concrete structure combining LC3, seawater, sea sand, RCA, and FRP bar has been focused on, and the structural performance considering life cycle cost and environmental impacts have been assessed to verify the considerable sustainable advantages.

Compared with traditional concrete, the green concrete developed has lower cost and environmental impact (Fig.1, Fig. 2): the global warming potential (GWP) and energy consumption have reduced by 40.9% and 25.6%, respectively. In addition, the effects of the substitution rate level of LC3, the production process of calcined clay and cement, and the transportation distance of RAC on the environmental impacts and cost have been identified quantitatively. The results show that the GWP and energy consumption for the green concrete with a 50% substitution rate of LC3 was 14.6% and 6.1% lower than that of the 35% substitution rate. Compared with the remaining two production processes, the environmental impacts of the high investment best available technology (BAT) level have been reduced by 26%~33.7% (CO_2 emissions) and 17%~40.2% (energy consumption) (Fig.3, Fig. 4). With the decrease in the distance from demolished buildings to the recycling process plant, the environmental impacts of the green concrete were reduced gradually, indicating that the utilization of RCA in a more sustainable form depends on the continuous optimization of recycling planning in urban (Fig.5, Fig. 6).

Keywords: LC3; Seawater Sea sand; RCA; FRP; Environmental impacts; CO_2 emissions; Energy consumption.

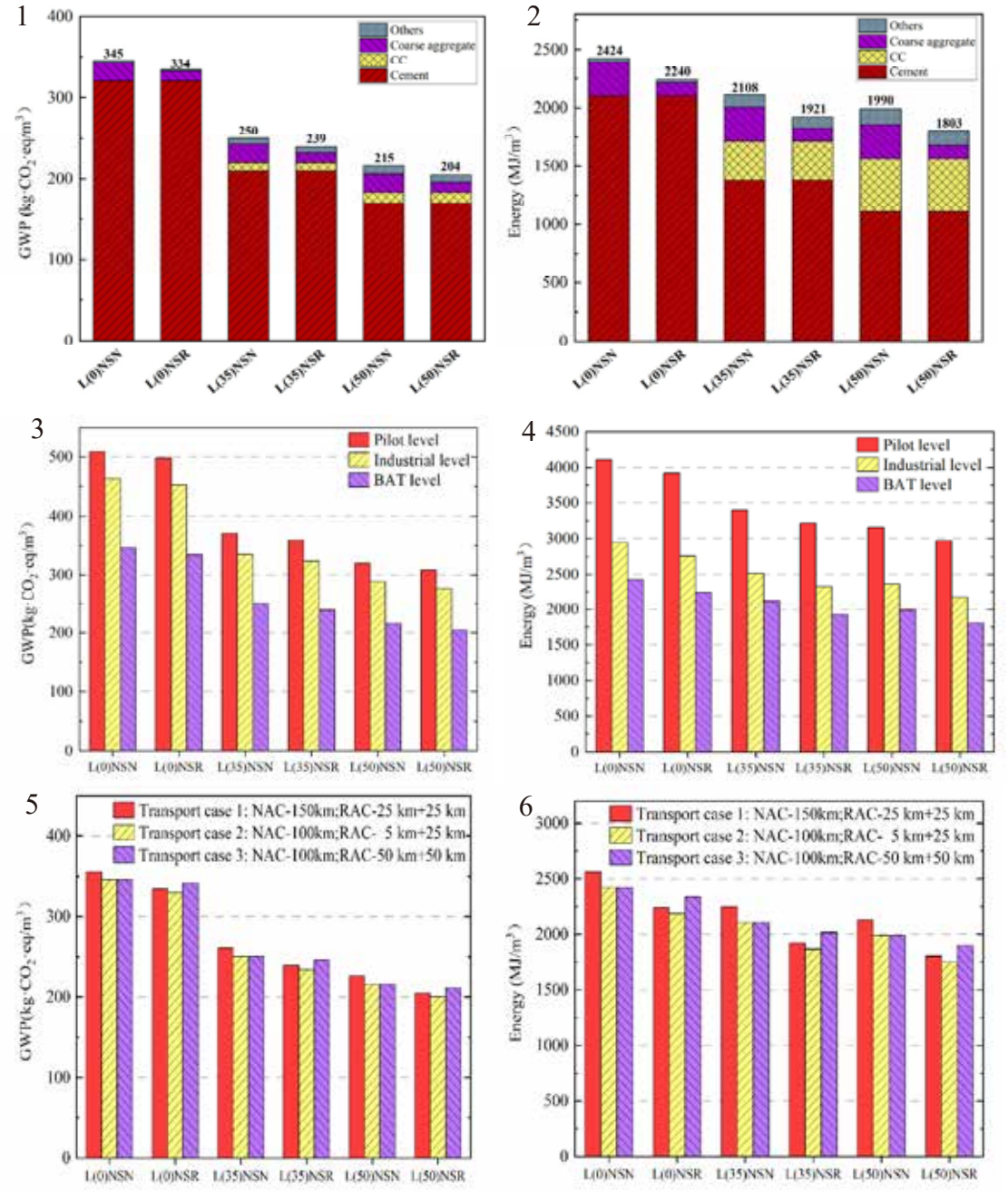

Fig. 1 Carbon emissions of concrete with different LC^3 substitution rates; **Fig. 2** Energy consumption of concrete with different LC^3 substitution rates; **Fig. 3** Carbon emissions of concrete with different processes; **Fig. 4** Energy consumption of concrete with different processes; **Fig. 5** Carbon emissions of concrete with different aggregate transport distances; **Fig. 6** Energy consumption of concrete with different aggregate transport distances.

Acknowledgment

The authors would like to acknowledge the funding support from the National Key Research and Development Program of China (2018YFE0125000).

Development of ultra-lightweight low-carbon LC^3 cement composites (ULLC-LC3): mechanical performances, chloride resistance, carbonation resistance and life cycle assessment

Zhenyu Huang[a], Lijie Chen[b]* and Tingting Liang[a]

[a]Guangdong Provincial Key Laboratory of Durability for Marine Civil Engineering, Shenzhen University, Shenzhen, China

[b]Department of Civil Engineering, The University of Hong Kong, Pokfulam Road, Hong Kong, China

Abstract

Ultra-lightweight cement composites (ULCC) are characterized by low density and high specific strength. However, the wide application of ULCC has been limited by a large amount of Portland cement content. Limestone and calcined clay cement (LC3) are a promising eco-friendly cementitious material, in which limestone and calcined clay (LC2) are used to partially replace Portland cement for reducing carbon footprint. This paper introduces the development of a novel cement composite, namely ultra-lightweight low-carbon LC3 cement composites (ULCC-LC3) by partially replacing Portland cement in ULCC with LC2. Experiments were conducted to investigate the effects of mix design on mechanical performances, resistances towards chloride ion penetration and CO2 ingression, and the carbon footprint of the composites. The experimental results indicate that ULCC-LC3 has favorable mechanical performances and better chloride resistance and sustainability performance as compared with its ULCC counterpart.

Experimental study on the effect of sea water on the hydration behavior and compressive strength of LC3 cement

Satya Medepalli[1*], Yuqian Zheng[1], Tiao Wang[1#], Chunhe Li[2]

[1] The University of Tokyo, 7-3-1 Hongo, Bunkyo-ku, Tokyo 113-8656 Japan,
[2] The University of Miyazaki, 1-1 Gakuenkibanadainishi, Miyazaki, 889-2155,Japan
[*]*Presenter:* satya@g.ecc.u-tokyo.ac.jp, [#]*Corresponding author:* satya@g.ecc.u-tokyo.ac.jp

Abstract

The use of sea water and LC3 cement has been gaining attention in recent years as a potential solution to address the environmental impact of conventional cement production. LC3 stands for Limestone Calcined Clay Cement, a type of cement made by blending calcined clay and limestone. One of the benefits of using LC3 cement is that it has a lower carbon footprint than traditional Portland cement due to its reduced reliance on clinker, which is a major contributor to carbon dioxide emissions in cement production. Additionally, the use of sea water as a mixing water for LC3 cement has shown promising results in reducing the amount of freshwater consumption and improving the durability of the concrete. This study therefore focusses on hydration behavior, pozzolanic reaction degree of calcined clay and compressive strength performance of LC3 cement with sea water in comparison to common/fresh water.

The material properties of calcined clay, limestone and cement clinker were initially determined using XRF. Two types of mixing water were used in this study. One is common water that uses deionized water and the other is artificial sea water prepared according to ASTM D1141-98. Standard LC3 cement blends were prepared by blending limestone, calcined clay and cement in the proportion of 15%, 30% and 50%. An additional 5% gypsum was added to cement for sulphate optimization and to avoid false set due to high proportion of calcined clay. Cement paste blends were prepared using a fixed water to binder ratio of 40%. Around 1% high range water reducer was used to achieve the required workability in the mix. Hydration stoppage using isopropanol was carried out at respective ages and the samples were vacuum dried for pozzolanic reaction test. The pozzolanic reaction degree of calcined clay was determined using selective dissolution method based on NaOH and EDTA as a solvent (**Fig. 1**). Cement hydration behavior was studied using isothermal calorimetry on cement paste specimens. The compression strength was determined on 40mm size cube specimens prepared using mortar with a sand to binder ratio of 2.5 and water to binder ratio of 40%. The samples for reaction degree and compression strength were sealed cured at 20 °C until testing.

Compared to common water, sea water has shown a significant increase in the rate of hydration as seen from the isothermal calorimetry plot (**Fig. 1** (a)). The presence of salts in sea water could have accelerated the reaction of cement and calcined clay in LC3 mixes. This could be corroborated with **Fig.1** (b) that shows a higher reaction of calcined clay in LC3 mixes with sea water. The compressive performance of LC3 with sea water (**Fig. 3**) has also shown an increase with sea water due to the probable higher reaction of calcined clay in LC3 mixes. Overall, the use of sea water has shown a positive performance on the hydration behavior, pozzolanic reaction degree as well as on the compressive strength of LC3 cement. This innovative approach has the potential to not only reduce the environmental impact of cement production with the use of low clinker cement such as LC3 alongside provide a sustainable solution by reducing the demand on fresh water consumption in the construction industry.

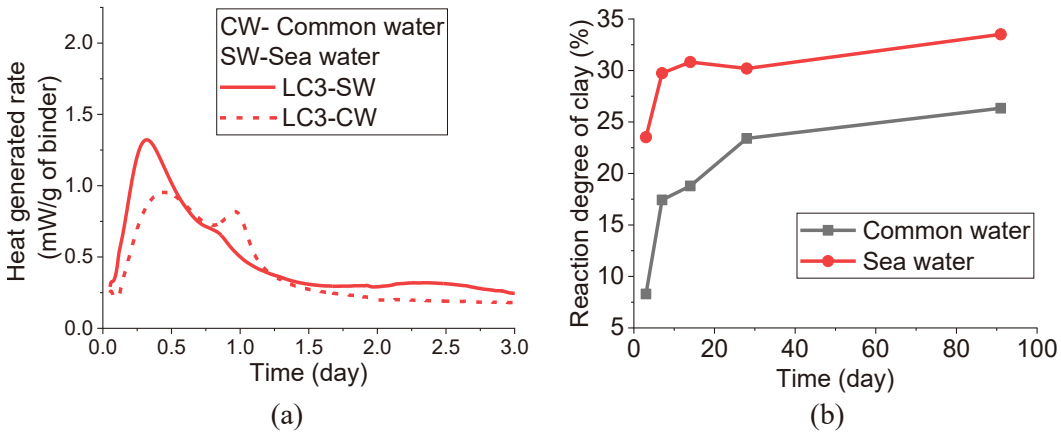

(a) (b)

Fig. 1 (a) Effect of sea water on the rate of heat evolution for LC3 cement mixes; **(b)** Effect of sea water on the reaction degree of calcined clay in LC3 cement mixes;

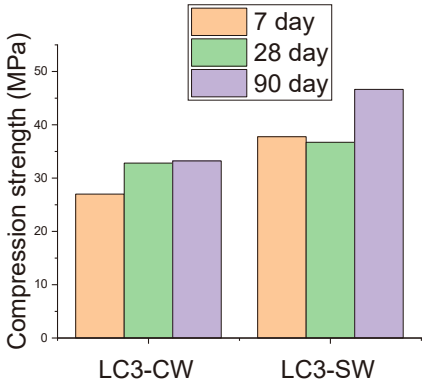

Fig. 3 Effect of sea water on the compressive strength of LC3 cement with sea water

Keywords: Limestone calcined clay (LC3) cement; compressive strength; sea water; pozzolanic reaction; heat of hydration;

Acknowledgment

The authors are grateful for financial support fromThe Taisei Foundation (2020),the Japan Cement Association (Grant projectin 2020and 2022),the Japan Concrete Institute (Grant projectin 2022), the National Key Research and Development Project ofChina (Grant No.2018YFE0125000).

The Rheological Characteristics and mechanism of the Limestone Calcined Clay Cement

Pengkun Hou, Xin Cheng
University of Jinan, pkhou@163.com/mse_houpk@ujn.edu.cn

Abstract: This report can be divided into two parts, firstly, the rheological properties of pastes made from ordinary Portland cement blended with different amounts of calcined clay and limestone were reported in order to understand the combined and independent effects of limestone and calcined clay on the rheological properties of limestone calcined clay cement (LC3). The results showed that calcined clay leads to increased static and dynamic yield stress, initial thixotropic index, plastic viscosity and cohesion, while limestone has an opposite effect (Table 1). It is believed that these results will aid in understanding the viscoelasticity of this blended cement.

Table 1. The discrepancy between SYS and DYS and the thixotropic index.

Sample	Resting time	Static yield stress (Pa)	Dynamic yield stress (Pa)	Thixotropy index [(SYS-DYS)/DYS]
REF	2 min	27.0	21.6	0.25
	30 min	181.6	21.6	7.41
	60 min	559.4	35.1	14.94
C80/Cc10/L5	2 min	102.1	53.1	0.92
	30 min	255.8	59.2	3.32
	60 min	443.7	75.8	4.85
C65/Cc20/L10	2 min	191.8	108.4	0.77
	30 min	296.8	120.7	1.46
	60 min	893.5	138.8	5.44
C50/Cc30/L15	2 min	448.4	222.8	1.01
	30 min	772.3	258.1	1.99
	60 min	1120	274.5	3.08

Secondly, the thixotropy of LC3 was deeply investigated by using focused beam reflectance measurement, zeta potential, ^{1}H nuclear magnetic resonance relaxometry and micro X-ray computed tomography to track the colloidal interaction and hydration extent within LC3. Results showed that flocculation due to the negative surface charge (Fig. 1) and water affinity of calcined clay introduced by its physiochemical features appears to be the dominating factor. This leads to a reduction of the water available to contribute to the fluidity of paste and, in turn, governing the development of thixotropy over time (Fig.2 and Table 2). In addition, the dilution effect due to high clinker substitution diminishes thixotropy growth with time.

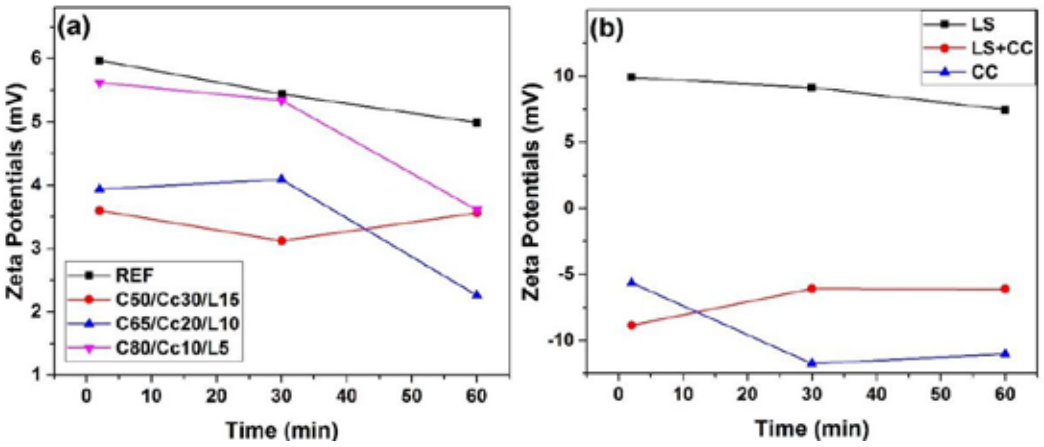

Fig. 1. Variation of zeta potential with resting time for (a) binder samples, and (b) SCMs.

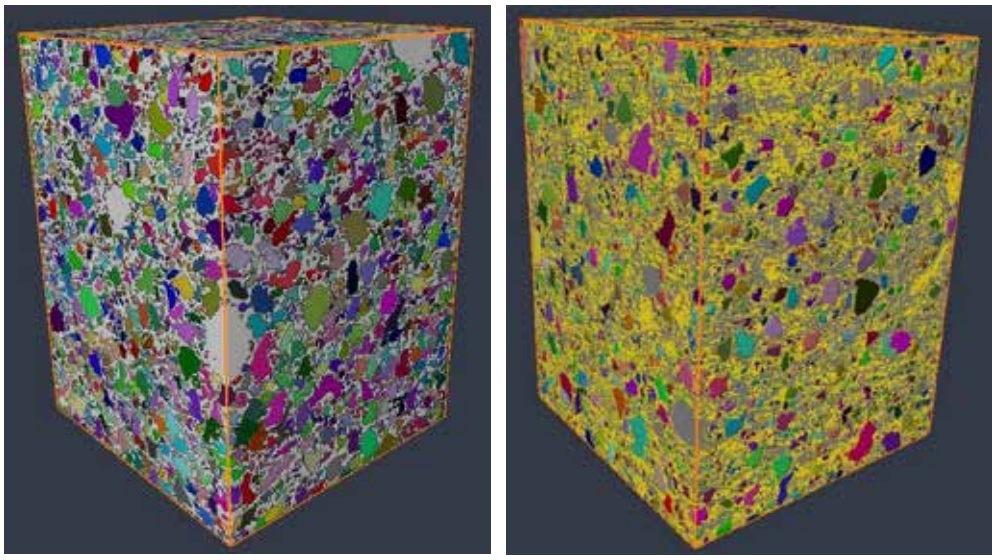

Fig. 2. 3D imaging of REF (right) and C50Cc30L15 (left).

Table 2. Volume fraction, mean length and mean diameter according μCT.

	Volume fraction (solids) (%)	Volume fraction (liquid)/filling and bleeding water (%)	Gel and adsorpted water (%)	Mean Diameter (μm)	Mean length (μm)
REF	53.9	46.1	13.5	11.4	18.4
C50Cc30L15	Clinker: 31.6 LC2: 36.4	32.0	25.5	7.1	11.2

Use of LC3 for Sustainable Urban Development

Hongjian Du*

Department of Civil and Environmental Engineering, National University of Singapore

**Presenter:* ceedhj@nus.edu.sg,

Abstract

Marine clay, a low-grade kaolinitic clay widely existing in coastal areas, can be used to partially replace cement in concrete after calcination to reduce construction waste and embodied carbon in concrete. This research project investigated the sulfate resistance of mortars with 10 wt% and 20 wt% marine clay replacement ratios and varying kaolin contents. These mixes were exposed to 50 g/L Na_2SO4 solution after 28-day curing in saturated lime water. Marine clay from the construction sites was calcinated at 700 ℃ to ensure pozzolanic reactivity during hydration. Thermogravimetric analysis and X-ray diffraction were conducted to calculate the content of kaolinite and components of clay minerals in marine clay, respectively. The progressive deterioration of compressive strength and the relative length change of mortars were evaluated through compressive strength tests and length change apparatus. Results from this study could estimate the effects of marine clay on sulfate resistance and obtain an optimal cement replacement level with no significant strength reduction and length change.

The paper will also report the use of low-grade calcined clay (LCC), to produce low-carbon and lightweight strain-hardening cement composites (SHCC). The influence of LCC content (20, 40 and 60% by mass) on the hydration, microstructure, strength, ductility, shrinkage and embodied carbon of SHCC has been investigated. Pozzolanic reaction between LCC and cement hydration products has been observed, which results in significant pore refinement at 20% and 40% cement replacement. The density of SHCC containing LCC was only around 1600 kg/m3. The compressive strength, tensile strain, and tensile strength of SHCC mixtures containing 20% LCC were improved by 3.21%, 22.10%, and 32.28%, respectively. A continued increase in LCC substitution caused a decrease in the strength by the agglomeration of LCC and insufficient calcium hydroxide supply. Furthermore, a significant reduction in embodied carbon was achieved by replacing cement with LCC. Overall, this study shows that low-grade calcined clay has a high potential in producing low-carbon and lightweight SHCC.

Keywords: Marine clay; Microstructures; Durability; Sustainability

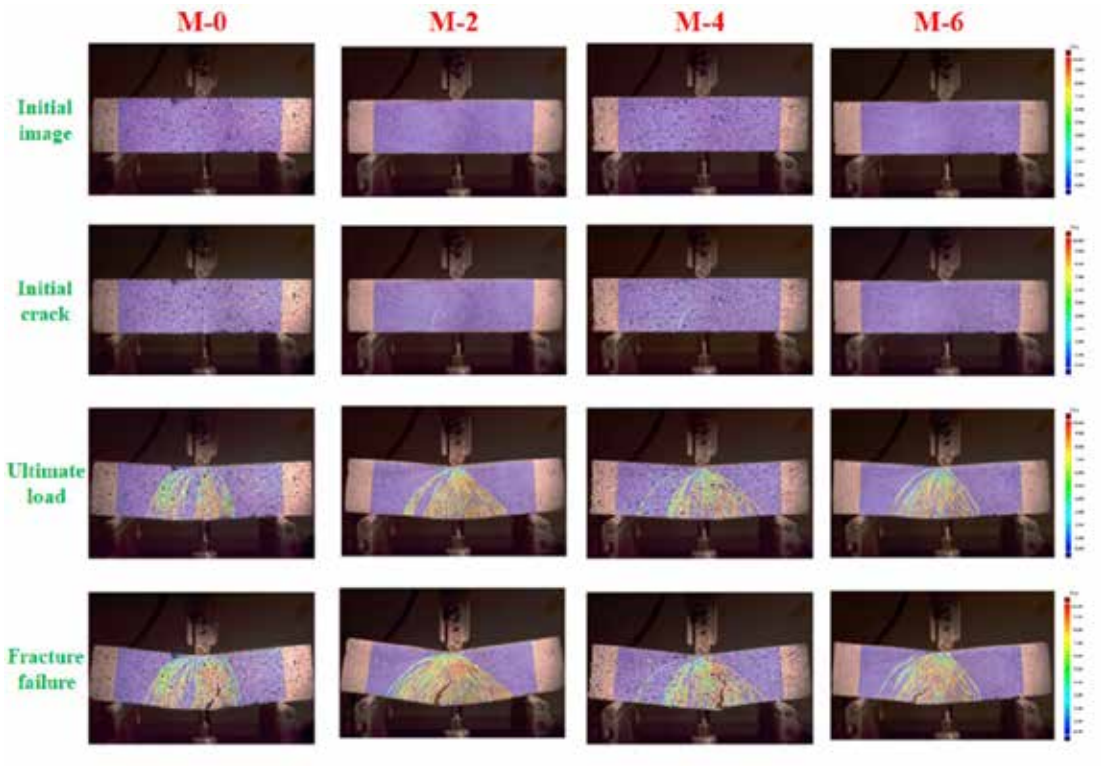

Fig. 1 Crack propagation under the bending action of the mixtures (M0: reference group; M-2: 20% cement replacement; M-1: 40% cement replacement; M-6: 60% cement replacement).

Acknowledgment

The authors would like to acknowledge the funding support from Singapore MOE ACRF Tier 1 Research Grant (A-0009301-01-00).

Investigation on the Performance of Engineered Cementitious Composites Incorporating PE Fiber and Limestone Calcined Clay Cement (LC^3)

Guoqiang Gong[1], Menghuan Guo[1,2,3], Yingwu Zhou[1,2,3,*], Shuyue Zheng[1], Biao Hu[1,2,3], Zhongfeng Zhu[1,2,3] and Zhenyu Huang[1,2,3]

[1] Guangdong Province Key Laboratory of Durability for Marine Civil Engineering,
[2] College of Civil and Transportation Engineering, Shenzhen University, Shenzhen, Guangdong 518060, People's Republic of China
[1] College of Civil and Transportation Engineering, Shenzhen University, Shenzhen 518060, China; ggq13501559741@126.com (G.G.); menghuan.guo@szu.edu.cn (M.G.); 1810332085@email.szu.edu.cn (S.Z.); biaohu3-c@szu.edu.cn (B.H.); zhongfeng.zhu@szu.edu.cn (Z.Z.); huangzhenyu@szu.edu.cn (Z.H.)
[2] Guangdong Provincial Key Laboratory of Durability for Marine Civil Engineering, Shenzhen University, Shenzhen 518060, China
[3] Key Laboratory for Resilient Infrastructures of Coastal Cities, Shenzhen University, Ministry of Education, Shenzhen 518060, China
[*]*Presenter: ywzhou@szu.edu.cn,* [#]*Corresponding author: ywzhou@szu.edu.cn.*

Abstract

Engineered cementitious composites (ECC) exhibits obvious strain hardening behavior overcomes the inherent drawback of brittleness in normal concrete. Nevertheless, the fabrication of ECC that consumes a high content of cement not only increases the initial material cost but also compromises the carbon and energy footprints of the composites. To promote the broader application of ECC and enhance the sustainability of ECC-made infrastructure, the usage of environmentally friendly ingredients is highly needed. Limestone calcined clay cement (LC^3) promises to be one of the suitable alternatives. The embodied energy and carbon for producing calcined clay and limestone powder are much lower than those for cement production. In this paper, the mechanical performance of ECC incorporating three dosages of LC^3 (0, 35%, and 50%) was investigated. The cubic compression test and uniaxial tensile test of dog-bone-shaped specimens were performed. The fiber dispersion state was studied by fluorescence technique, and the digital image analysis was carried out. The single fiber pullout test was performed to quantitatively analyze the fiber/matrix interfacial properties. Mercury intrusion porosimeter (MIP) test was used to study the influence of LC^3 on the pore structure of ECC. X-ray diffraction (XRD) and thermogravimetric analysis (TGA) tests were conducted to analyze the phase assemblage of ECC matrix incorporating LC. Through performing the life cycle assessment, the environmental advantages of using LC^3 in ECC are also discussed.

The micropore structure of the cementitious matrix is one of the key factors influencing the macroscopic mechanical performance of ECC. Fig 1 demonstrates the pore size distribution of the three kinds of binder systems. It is remarked that the distribution peak shifts towards the smaller pore size regions with the incorporation of LC^3. Fig 2 shows that the total porosity is significantly reduced owing to the incorporation of LC^3. The substitution of OPC by 35% LC^3 demonstrates a more significant influence on the micropore structure of ECC. The chemical phase compositions of the three kinds of ECC are presented in Fig 3. For LC^3-based blends, hemi-carboaluminates (Hc) are observed, which are generated due to the reaction between the aluminates, in both calcined clay and cement, and $CaCO_3$ from limestone. For the LC^3-based paste matrix, the peaks of $Ca(OH)_2$ are remarkably reduced with the usage of calcined clay and limestone, which could be attributed to the pozzolanic reaction between

$Ca(OH)_2$ and the reactive silica and alumina phases in calcined clay. Fig 4 presents the TGA and different thermal gravimetric (DTG) curves of the three kinds of specimens. For the LC^3-based matrix, the magnitude of the second peak of mass loss around 170 °C is quite modest, which corresponds to the loss of water from carboaluminates. The peak of mass loss around 460 °C is related to the dehydroxylation of Ca(OH). It is remarked that the $Ca(OH)_2$ is largely consumed by the pozzolanic reaction and that its content is significantly reduced with the increase of LC^3 dosage.

The compressive strength of the three studied ECC types is illustrated in Fig 5. At 3 days, the strength increases with the incorporation of LC^3, and the increasing ratios attain 21.74% and 10.23%, respectively, for ECC-LC^3-35 and ECC- LC^3-50 similar trend was observed at 7 days. While at 28 days, for ECC-LC^3-35, the increasing ratio is 10.28%, and for ECC-LC^3-50, the reduction ratio is 8.89%. The tensile stress-strain curves of the three kinds of ECC are presented in Fig 6. It is noted that LC^3-based ECCs exhibit strain hardening behavior. The ultimate tensile strength σ_{tu} of ECC-LC^3-35 attains 9.55 ± 0.59 MPa, and the ultimate tensile strain ε_{tu} of ECC-LC^3-50 reaches 8.53 ± 0.30%. The results imply that the combination of calcined clay and limestone could be successfully used to fabricate ECC exhibiting both high strength and high ductility. For the three studied ECC matrix types, the force-displacement curves of the single fiber pullout test are depicted in Fig 7. The slight slip-hardening behavior was observed after the debonding between fiber and matrix. The applied external fiber load is dominantly resisted by the interfacial frictional stress between fiber and matrix. It is remarked that the frictional bond strength τ_0 demonstrated firstly an increasing and then a decreasing tendency with the incorporation of LC^3, which is consistent with the trend of the tensile strength at the composite scale. The fiber dispersion homogeneity is found to rise with the substitution of OPC by LC^3 through the increase ratio does not show a linear relationship with the replacement ratio of OPC. The results of fluorescence analysis indicate that the combined action of calcined clay and HRDR positively alters the flocculated structure formed by cement paste and that the flowability, as well as the rheology properties of the composites are improved.

The life cycle inventories were adopted from the database of GaBi software. Two environmental impact criteria, energy, and global warming potential (GWP) were calculated. The obtained results are presented in Fig 8 and Fig 9. It is noted that the environmental impact of cement among all the components of ECC is the highest. PE fiber ranks only second to cement although its dosage is quite low. When OPC is partly replaced by LC^3, the two studied environmental impact criteria descend, especially the GWP with the reduction ratio attaining 40.31%.

Keywords: Engineered cementitious composites; Limestone calcined clay cement; Strength; strain; Fiber dispersion.

1

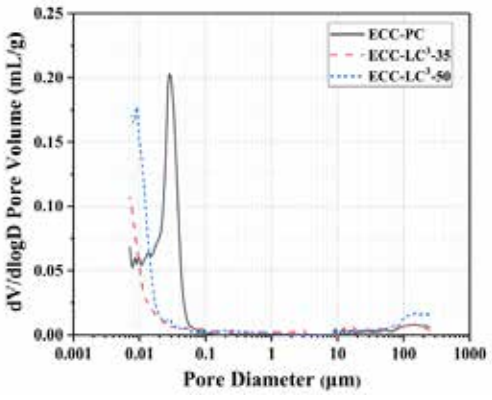

2

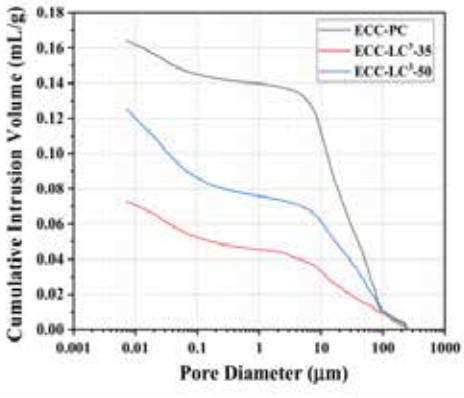

3

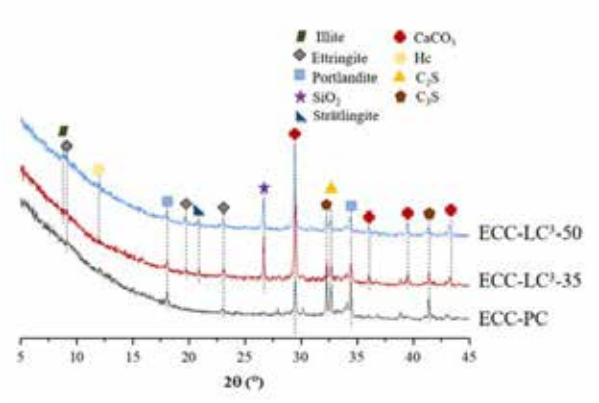
Illite
Ettringite
Portlandite
SiO_2
Strätlingite
$CaCO_3$
Hc
C_2S
C_3S
ECC-LC³-50
ECC-LC³-35
ECC-PC
2θ (°)

4

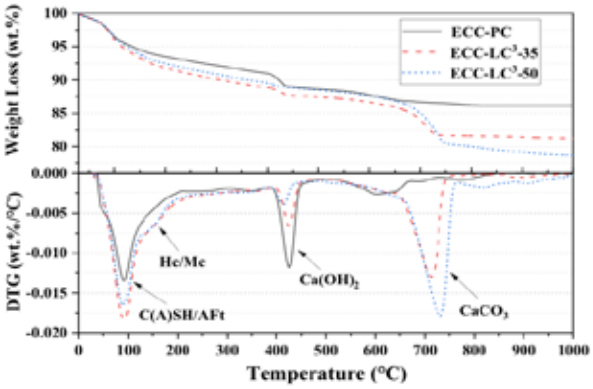
Weight Loss (wt.%)
DTG (wt.%/°C)
ECC-PC
ECC-LC³-35
ECC-LC³-50
Hc/Mc
C(A)SH/AFt
$Ca(OH)_2$
$CaCO_3$
Temperature (°C)

5

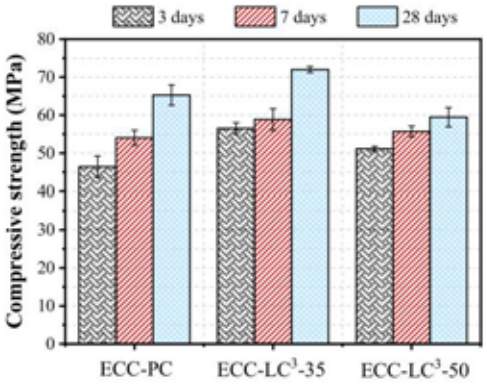
3 days
7 days
28 days
Compressive strength (MPa)
ECC-PC
ECC-LC³-35
ECC-LC³-50

6

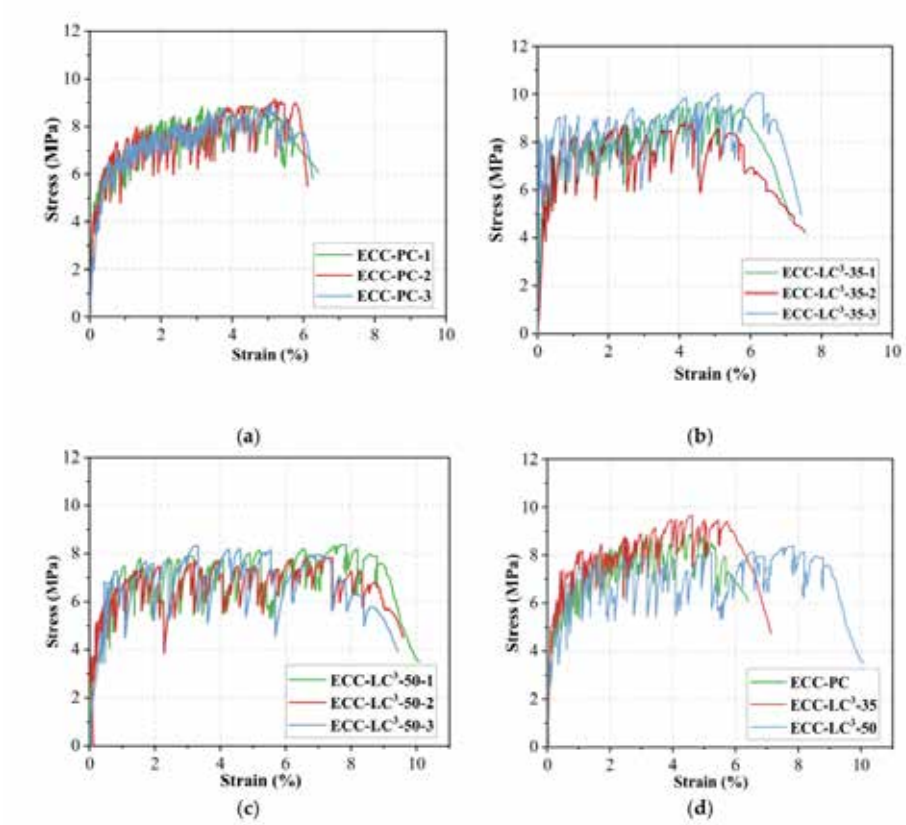
Stress (MPa)
Strain (%)
ECC-PC-1
ECC-PC-2
ECC-PC-3
(a)
ECC-LC³-35-1
ECC-LC³-35-2
ECC-LC³-35-3
(b)
ECC-LC³-50-1
ECC-LC³-50-2
ECC-LC³-50-3
(c)
ECC-PC
ECC-LC³-35
ECC-LC³-50
(d)

7

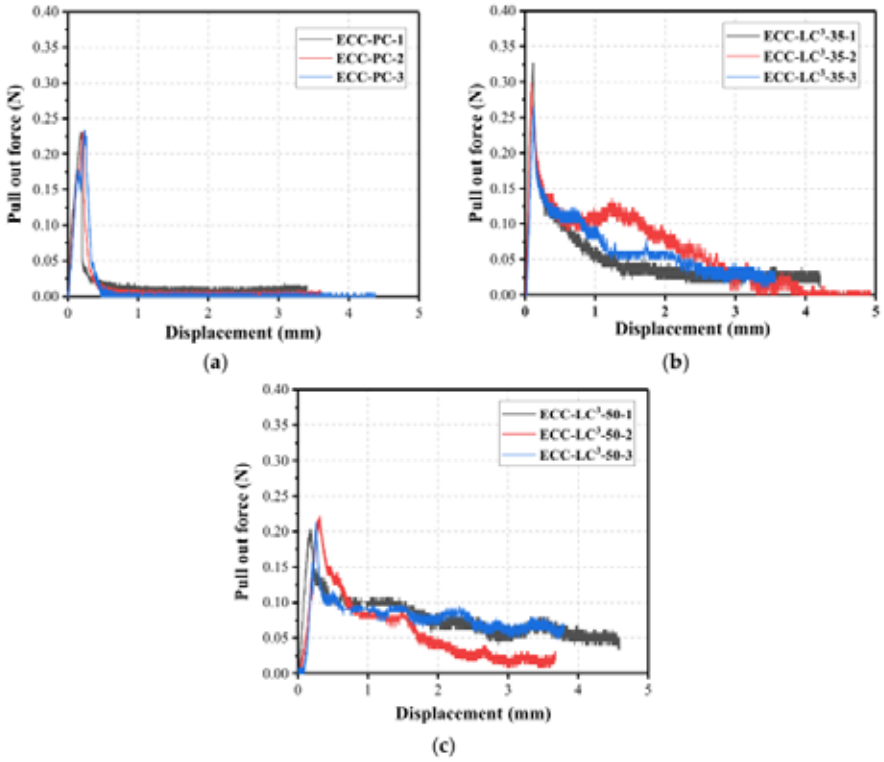

8

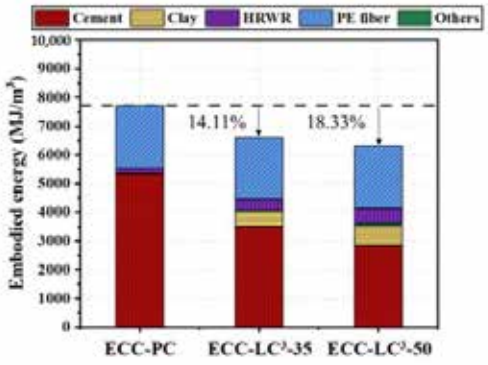

9

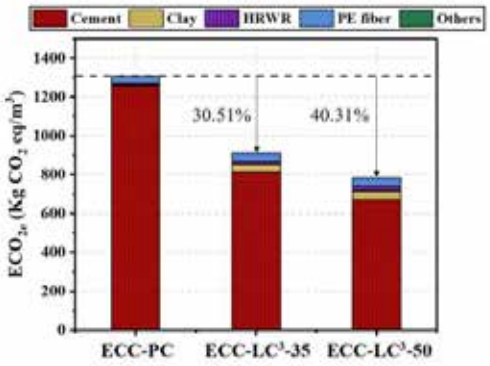

Fig. 1 Pore distribution; **Fig. 2** Cumulative pore volume; **Fig. 3** XRD patterns; **Fig. 4** TGA and DTG curves; **Fig. 5** Compressive; **Fig. 6** Tensile stress-strain curves of the three types of ECC: (a) ECC-PC; (b) ECC- LC^3-35; (c) ECC-LC^3-50; (d) representative curve; **Fig. 7** Single fiber pullout curves: (a) ECC-PC; (b) ECC- LC^3-35; (c) ECC-LC^3-50; **Fig. 8** Summarization of the consumed energy by each component of ECC; **Fig. 9** Summary of the GWP by each component of ECC.

Acknowledgment

This research was funded by the Ministry of Science and Technology of China (Grant No. 2018YFE0125000); the National Natural Science Foundation of China (NSFC) (Grants No. 51908369 and 52178236); NSFC and Guangdong province (Grants No. U2001226); Guangdong Provincial Key Laboratory of Durability for Marine Civil Engineering (Grants No. 2020B1212060074).

Using limestone calcined clay cement and recycle fine aggregate to make eco-friend ultra-high performance concrete: properties and environmental impact

Dingcong Guo[1,2*#], Menghuan Guo[1,2], Yingwu Zhou[1,2]

[1] Guangdong Province Key Laboratory of Durability for Marine Civil Engineering,
[2] College of Civil and Transportation Engineering, Shenzhen University, Shenzhen, Guangdong 518060, People's Republic of China
[*]*Presenter:* 1950471001@email.szu.edu.cn, [#]*Corresponding author:* 1950471001@email.szu.edu.cn

Abstract

Limestone calcined clay cement has been used in concrete as a new type of low-carbon and environmentally friendly cement in many examples. Recycled fine aggregate is also widely used in concrete as a green aggregate. This paper uses Limestone calcined clay cement and Recycled fine aggregate to produce eco-ultra-high performance concrete with comparable mechanical properties to traditional ultra-high performance concrete. The experimental results show that the compressive strength of eco-ultra-high performance concrete made with Limestone calcined clay cement and Recycled fine aggregate is comparable to that of traditional ultra-high performance concrete (Fig. 1), while the tensile strength is slightly lower than that of traditional ultra-high performance concrete, and the ultimate tensile strain is increased (Fig. 2).
In this paper, seven days of Heat of hydration analysis with different mix-IDs were studied. The experimental results showed that due to the addition of Limestone calcined clay, in the induction period of 1–3 h heat flow increased. At 7th hour, LC315 and LC330 simultaneously appeared the first exothermic peak, while the second exothermic peak decreased, indicating that the early calcined clay had participated in the hydration reaction (Fig. 3).

The pore structure distribution of different mix-IDs was tested by MIP experiments (Fig. 4), and the experimental results showed that Limestone calcined clay cement can effectively reduce the proportion of macropores in the total pore volume and optimize the pore results. And the total pore volume of LC330 was smaller than that of the control group (Fig. 5).

The impact of different mix-IDs on the environment was analyzed through life cycle analysis (Fig. 6). The results show that Limestone calcined clay cement and Recycled fine aggregate can effectively reduce the impact on the environment, indicating that Limestone calcined clay cement and Recycled fine aggregate are feasible to make eco-ultra-high performance concrete.

Keywords: Limestone calcined clay cement; Recycled fine aggregate; Ultra-high performance concrete; Mechanical properties; Microstructure; Eco-friendly.

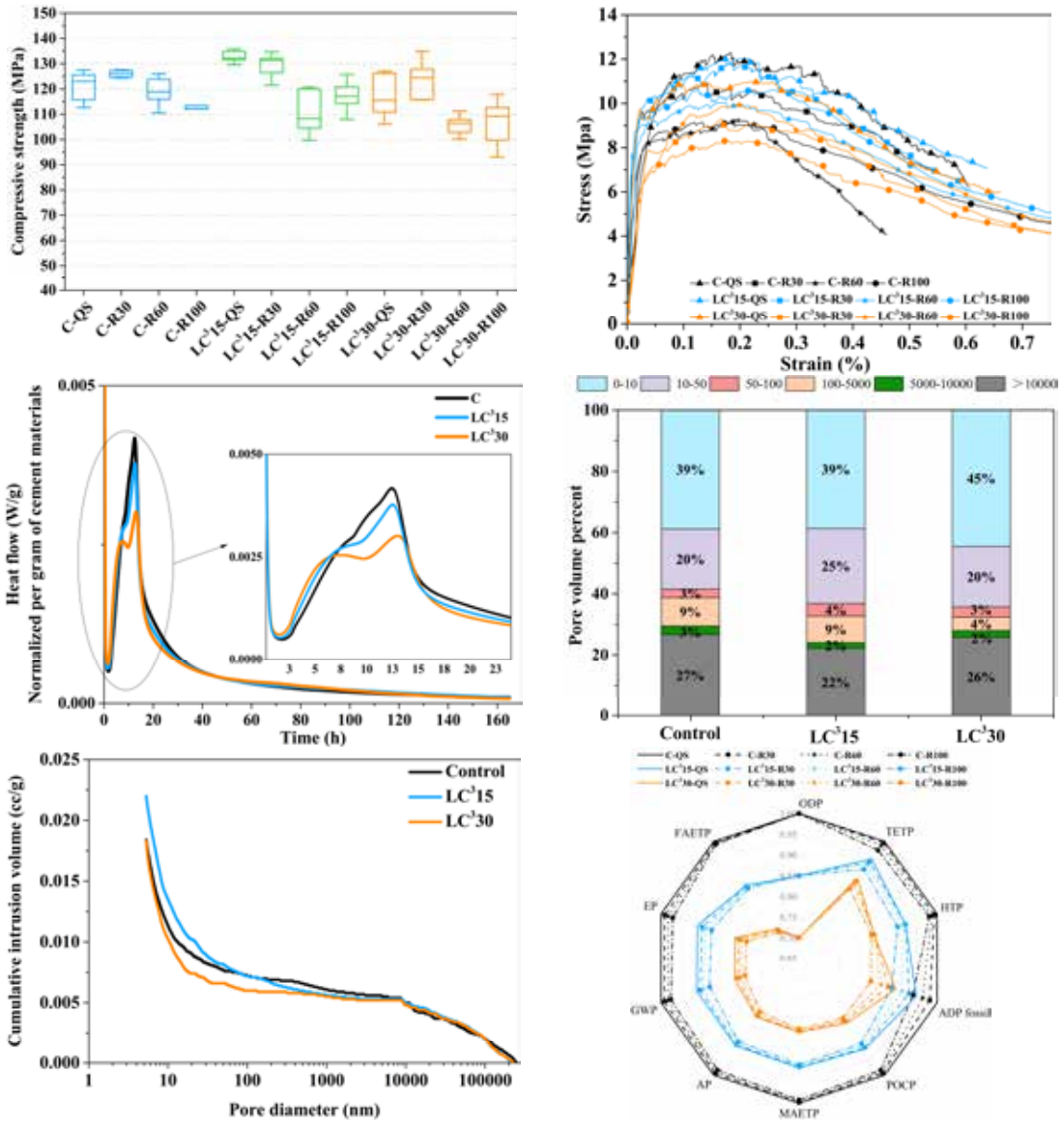

Fig. 1 Compressive strength in 28 days after 2 days 90℃ curing; **Fig. 2** Average stress-strain curves of different mix-IDs; **Fig. 3** Heat flow of per gram cementitious materials; **Fig. 4** Pore volume percent distribution; **Fig. 5** Cumulative distribution; **Fig. 6** Summary of environmental impact: (GWP: Global Warming Potential; AP: Acidification Potential; EP: Eutrophication Potential; ODP: Ozone Layer Depletion Potential; ADP: Abiotic Depletion fossi; FAEP: Freshwater Aquatic Ecotoxicity Potential; HTP: Human Toxicity Potential; MAEP: Marine Aquatic Ecotoxicity Potential; POCP: Photochem. Ozone Creation potential; TETP: Terrestric Ecotoxicity Potential)

Investigation on hydration mechanism of limestone calcined clay cement (LC^3) with seawater and sea sand

Ruyin Zhang[1,2], Yingwu Zhou[1,2], Menghuan Guo[1,2#]

[1] Guangdong Province Key Laboratory of Durability for Marine Civil Engineering,
[2] College of Civil and Transportation Engineering, Shenzhen University, Shenzhen, China
[#]*Corresponding author: menghuan.guo@szu.edu.cn*

Abstract

Limestone-calcined clay cement (LC^3) is a new type of green cement with less environmental impact than ordinary OPC . The use of seawater for concrete production further contributes to the economic and environmental benefits. This paper aims to investigate the hydration mechanism of limestone-calcined clay cement in pure water and seawater.

It is found that limestone-calcined clay cement and seawater can simultaneously promote the early-age hydration process. The second hydration peak observed in the LC^3 system corresponds to the precipitation of hemicarboaluminate and monocarboaluminate owing to the reaction between aluminates, from cement clinker and calcined clay, and calcium carbonate, from limestone. Dissolved ions in seawater have a non-negligible effect on hydrated phase composition. Monocarboaluminates react with chloride ions in seawater to form the stable phase of Friedel's salts.

In the presence of LC^3 and seawater, the reactivity of cement clinker decreases, and the increase in chloride ion content can promote the hydration of aluminates and ferrites, generating other phases such as C-A-S-H, strätlingite and carboaluminate. In both pure water and seawater systems, the amount of CH decreases over time as it is consumed by the pozzolanic reaction of metakaolin. At a given cement content, these phases can improve the engineering properties of the material.

With the addition of LC^3 and seawater, the hydrate phase composition and microstructure of the cementitious material changed, which did not cause deteriorating effect on the physical and mechanical properties of the cementitious material. The samples with limestone calcined clay content of 35% obtained higher compressive strength than other content, and the comprehensive strength activation index had the best effect. The research results can provide a reference for the application of green seawater sea sand concrete in marine infrastructure, which can promote the sustainable development of civil engineering.

Keywords: Limestone-calcined clay cement; hydration; hydration products; Friedel's salt; Mechanical properties

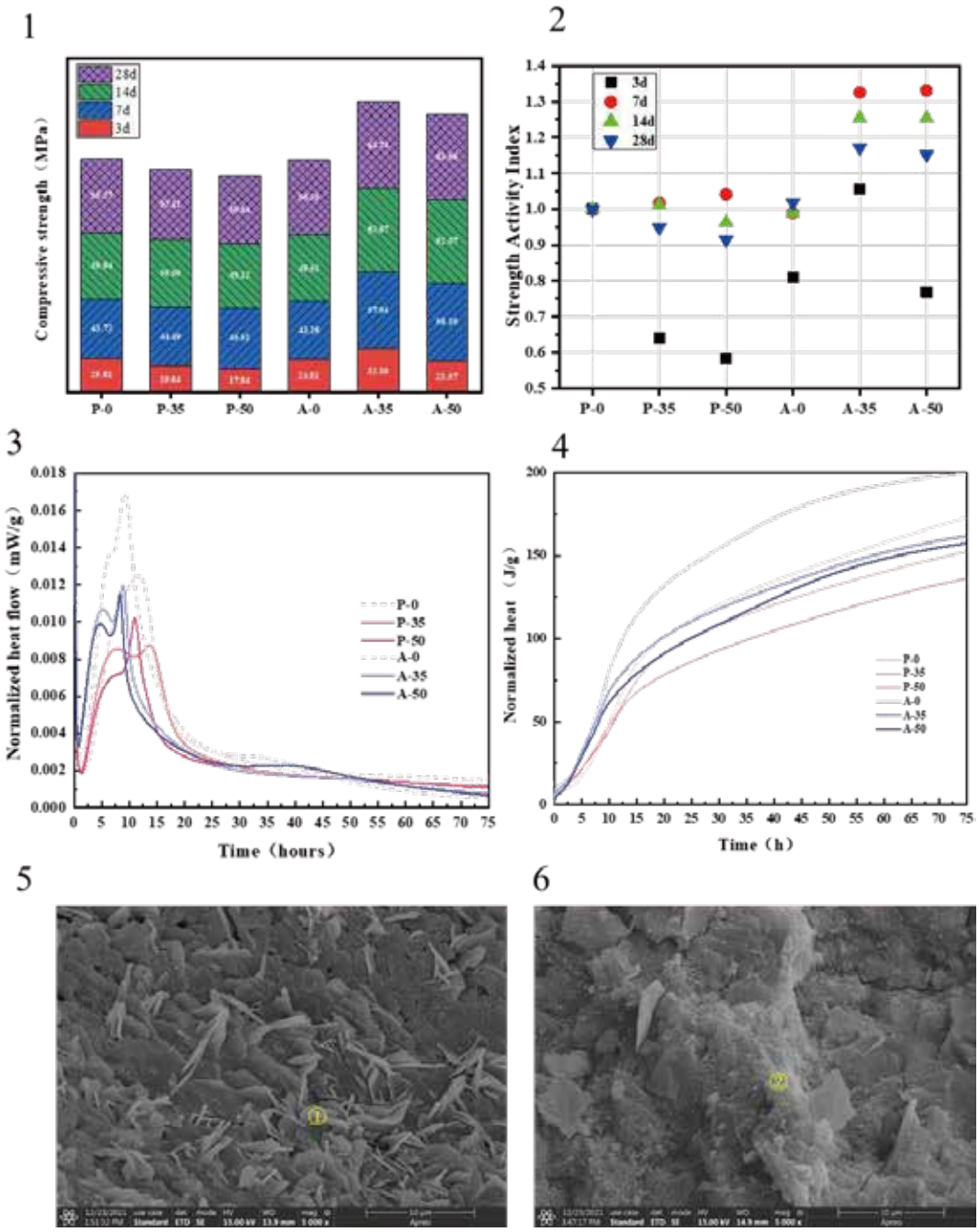

Fig. 1 Compressive strength of cement mortar with different types of water; **Fig. 2** Strength Activity Index; **Fig. 3**& **Fig. 4** Heat evolution of hydrated in pure water and sea water; **Fig. 5** &**Fig. 6** Microstructure of paste hydrated in LC^3 and sea water in 28 days.

Acknowledgment

The authors would like to acknowledge the funding support from the National Key Research and Development Program of China (2018YFE0125000).

Quantification Assessment on Chemicals and Pore Structures of Limestone Calcined Clay Cement under Carbonation

Wei-Wen Li[1,2], Zu-Hua Xu[2*], Jian-Sheng Huang[2], Kai-Feng Yu[2], Yao-Cheng Wang[1,2#]

[1] Guangdong Province Key Laboratory of Durability for Marine Civil Engineering,
[2] College of Civil and Transportation Engineering, Shenzhen University, Shenzhen, Guangdong 518060, People's Republic of China
Presenter: 1910472078@email.szu.edu.cn, #Corresponding author: wangyc@szu.edu.cn

Abstract

Limestone Calcined Clay Cement (LC3) has been utilized in civil engineering industry in some coastal regions and nations not only because it is a category of low-carbon cement, but also due to its brilliant capacity of blocking and binding Cl^-. On the other aspect, carbonation of cementitious materials has been a well-known issue for several decades due to problems like alkalinity neutralization, hydrates decomposition and swelling products formation ($CaCO_3$, CC), damaging durability performance severely. In this paper, the carbonation performance of LC3 cement was investigated, especially regarding its quantification and distribution of essential chemicals like gel products, Al-Fe-mono phases (AFm), Ca $(OH)_2$ (CH) and CC; and its development of pore structure, which is significantly crucial for service life. It was found that LC3 cement demonstrated much higher phenolphthalein carbonation depth compared to Portland Cement (PC), with a carbonation rate k = 3.04, shown in Fig.1, indicating that LC3 cement is possibly carbonated more easily than PC. The XRD results revealed that in case of slight carbonation (sample from deep position), there was higher amount of AFm phases (X = OH^-, CO_3^{2-}, etc.) but obvious lower content of CH in LC3 paste, compared to PC, Fig.2.

Under intensive carbonation, it was quantitively disclosed that CH was nearly depleted (Fig.3) and enormous of gel products and AFm phases were decomposed to yield CC (Fig.2 & 4), compared to PC sample. As can be seen in Fig.5, the contribution of CH and other hydrates (gel products and AFm, etc.) on CC yield in PC and LC3 is completely different. Around 70% of CC in PC sample was mainly yielded from CH reaction while in LC3, around 60-70% of CC was formed by hydrates reaction with CO_2. Based on the phase quantification, the fully carbonated, partially carbonated and non-carbonated areas were defined. LC3 demonstrated evidently wider carbonation area (X_f) than PC, with apparent fully carbonated width (X_b).

With respect to the changes of pore structure, as is shown in Fig.6, the pores diameter became larger (from 0.01 to 0.1 microns) when LC3 was severely carbonated. On the contrary, in PC, the pore structure became rather denser after carbonation.

Keywords: LC3; Carbonation performance; Chemicals quantification; Pore structure

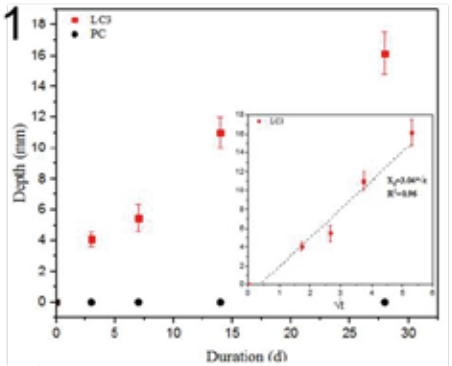
1
LC3
PC
Depth (mm)
Duration (d)

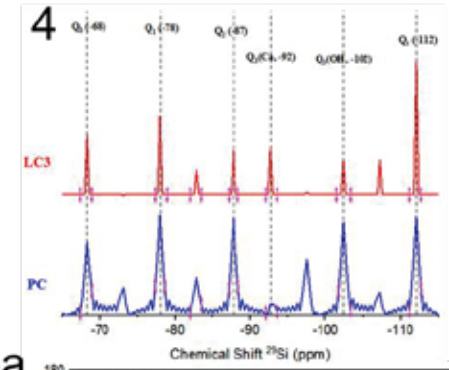
4
LC3
PC
Chemical Shift ^{29}Si (ppm)

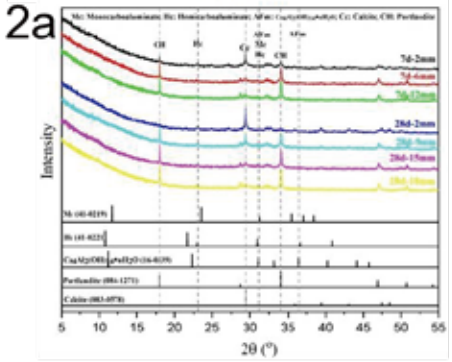
2a
Intensity
2θ (°)

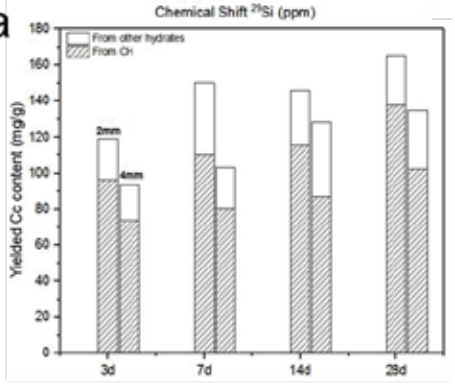
5a
From other hydrates
From CH
Yielded Cc content (mg/g)
2mm
4mm
3d
7d
14d
28d

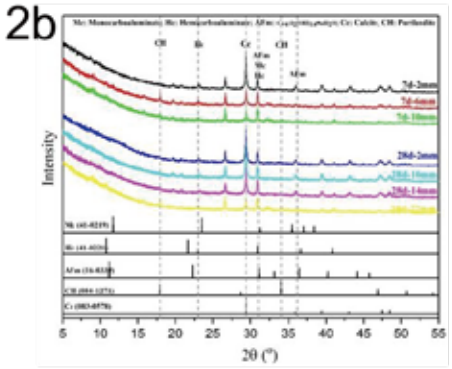
2b
Intensity
2θ (°)

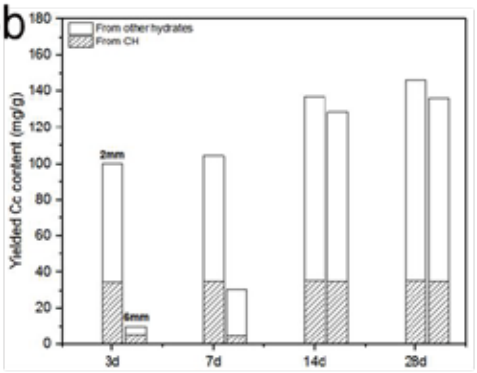
5b
From other hydrates
From CH
Yielded Cc content (mg/g)
2mm
6mm
3d
7d
14d
28d

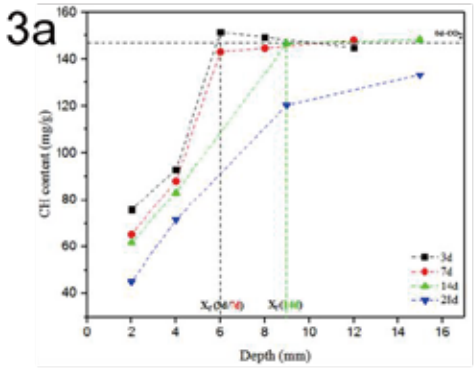
3a
CH content (mg/g)
Depth (mm)
3d
7d
14d
28d

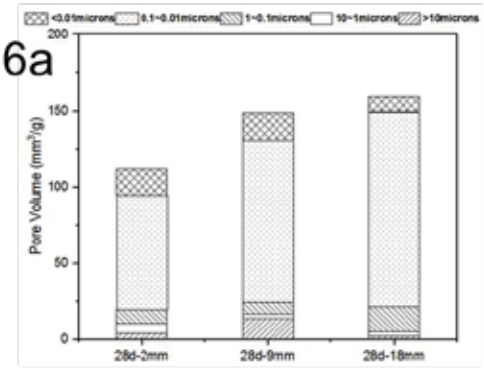
6a
<0.01microns
0.1~0.01microns
1~0.1microns
10~1microns
>10microns
Pore Volume (mm³/g)
28d-2mm
28d-9mm
28d-18mm

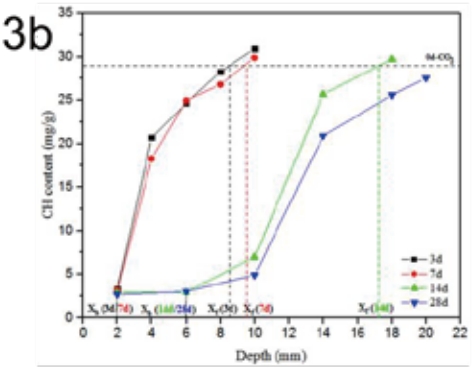
3b
CH content (mg/g)
Depth (mm)
3d
7d
14d
28d

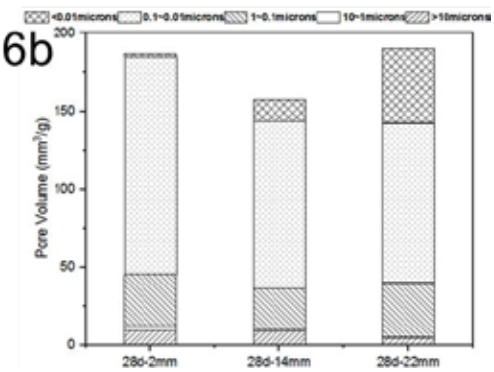
6b
<0.01microns
0.1~0.01microns
1~0.1microns
10~1microns
>10microns
Pore Volume (mm³/g)
28d-2mm
28d-14mm
28d-22mm

Fig. 1 Phenolphthalein carbonation depth; **Fig. 2** XRD pattern of (a) PC and (b) LC3 pastes under various durations; **Fig. 3** CH content of (a) PC and (b) LC3 pastes under different carbonation durations; **Fig. 4** 29Si NMR of PC and LC3 pastes at 8 mm depth; **Fig. 5** Yielded CC of (a) PC and (b) LC3 from CH and other hydrates; **Fig. 6** Pore size distribution in (a) PC and (b) LC3

Acknowledgment

The authors gratefully acknowledge the funding support from the National Natural Science Foundation of China (grant number 51878415 and 52078301) and the platform provided by Guangdong Provincial Key Laboratory of Durability for Marine Civil Engineering, SZU (grant number 2020B1212060074).

Hydration Accelerating Effect and Strength Characteristics of Mixed Cement by C-S-H Based Hydration Core

Jeong-Min Ra[1*], Jun-Hyung PARK[1], Gi-Hun BAE[1], Jin-Man KIM[1#]

[1] Kongju National University, Cheonan, Korea

[*]Presenter: jmra1417@kongju.ac.kr, [#]Corresponding author: jmkim@kongju.ac.kr

Abstract

When an admixture such as blast furnace slag and fly ash used as a substitute for cement is used, there is a problem in that initial hydration and strength are lowed. In this study, it was concluded that the problem of hydration and strength degradation could be improved using C-S-H(Calcium silicate hydrate) nucleation seeding, which plays a core role in cement hydrate formation, and the resulting hydration performance and strength characteristics could ne analyzed to compensate for the shortcomings of mixed cement.

Keywords: Nucleation effect, Calcium silicate hydrate, Blast furnace slag, Fly ash, Mixed cement

1. Introduction

The South Korean government also declared carbon neutrality by 2050 to reduce domestic CO_2 emissions after the announcement of the EU Green Deal. The cement industry plans to expand the use of blended cement to reduce the usage of clinker, which is the main cause of CO_2 emissions in response to the carbon-neutral policy. Blended cement using supplementary cementitious materials (SCMs), such as fly ash and blast furnace slag, can reduce the amount of cement usage drastically. However, as the amount of SCMs usage increases, delay in setting time and securing initial strength become issues. Accelerating admixtures, which promote setting and hardening, are used to improve these issues. However, there are limitations such as a decrease in long-term strength, low activity compared to the amount of usage, and the content of chloride.

Various studies have been conducted in diverse ways to synthesize calcium silicate hydrate (C-S-H), a cement hydration product, in nano-particle size and use it as a material for promoting the initial hydration reaction of cement to overcome the shortfalls of these existing accelerating admixtures.

Based on this background, this study aimed to evaluate the possibility of applying a C-S-H-based nano seed as an accelerating admixture to increase the use of blended cement by analyzing its hydration promoting effects and strength characteristics after applying the C-S-H-based nano seed to blended cement.

2. Materials and Methods

2.1 Materials

This study used ordinary Portland cement (OPC) with a specific gravity of 3.15 and a fineness of 4,088cm^2/g, ground granulated blast furnace slag (GGBS) with a specific gravity of 2.9 and a fineness of 4,058cm^2/g, and fly ash (FA) with a specific gravity of 2.15 and a fineness of 3,651cm^2/g. The C-S-H nano seed was synthesized by using calcium-based reagents and silica-based reagents and a polycarboxylate dispersing agent was used to suppress the aggregation of

C-S-H nanoparticles. The prepared C-S-H nano-seed was used for mixing with water in a suspension state with a solid content of 12.8%. Standard sand meeting the ISO standard was used for the fine aggregate.

2.2 Experimental Design

Table 1 shows the experimental design and measurement items for analyzing the hydration characteristics of blended cement using C-S-H based nano seeds. A paste satisfying KS L ISO 9597 and a mortar mixture satisfying KS L ISO 679 were selected for setting and compressive strength tests. blast furnace slag and fly ash were chosen as admixtures used as cement substitutes. The amount of cement substitute usage was fixed at 50% of the weight of cement. The water to binder ratio was set at 50% to secure fluidity and induce sufficient hydration.
The amount of C-S-H nano-seed addition was set to 1%, 2%, or 3% of the weight of the binder. This study carried out setting, compressive strength, and differential thermal (TG/DTG) analyses to understand the hydration promoting effect and strength characteristics of C-S-H-based nano seeds.

Table 1. Experimental Plan

Experiment Variables	Experiment Levels	Measurement Items
Binder Types	Cement, blast furnace slag, fly ash	- Setting time - Compressive strength - TG-DTA
Amount of CSH-based Nano Seed Addition	0, 1, 2, and 3 %	

2.3 Experimental Methods

The setting time was tested according to the KS L ISO 9597 test method. This study measured it at intervals of 5 to 10 minutes until the Vicat needle no longer penetrated into the specimen. The compressive strength specimen was prepared with mortar as shown in the mixture table according to the KS L ISO 679 test method. It was cured in water at 20±2°C. This study prepared specimens of 1, 3, 7, and 28 days of age for analyzing specimens according to the curing age.
For accurate analysis by age, this study stopped hydration by immersing specimens in acetone after curing them for 3, 7, and 28 days. The specimens were ground into fine powders and analyzed with TG-DTA. TG/DTG increased the temperature from 20 to 1000°C at a temperature increase rate of 20°C/min to analyze hydration products.

3. Results and Discussion

3.1 Setting Time

Fig. 1 shows the results of measuring setting by adding CSH nano seeds 0-3% to OPC. The final setting time of the P-CSH0 specimen using only OPC was 285 minutes, and it was confirmed that the setting time was shortened to 180, 155, and 115 minutes as the amount of CSH nano seeds increased.
Moreover, in the case of the blended cement specimen using blast furnace slag and fly ash, the final setting times of the GGBS-CSH0 and GGBS-CSH3 specimens were 370 minutes and 125 minutes, respectively, which shortened the setting 4 hours or more. The fly ash specimen also showed the same tendency as the blast furnace slag specimen.

The results of the setting test showed that the setting time (both initial and final setting times) was the shortest in the order of P-CSH3, GGBS-CSH3, and FA-CSH3 specimens, which contained 3% CSH nano seeds. It was believed that the setting was accelerated because the core of cement hydrate was formed actively as CSH nano seeds, which had a large specific surface area, acted as a core.

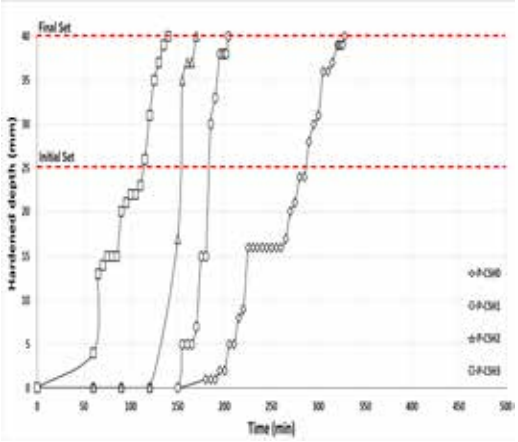

Figure 1. Setting time of Cement paste

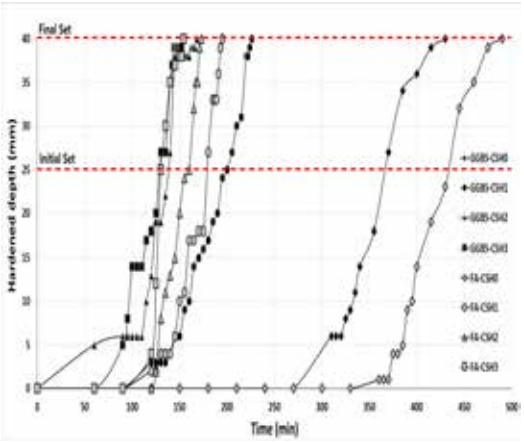

Figure 2. Setting time of Blended cement paste

3.2 Compressive Strength

Figs. 3-5 show mortar compressive strength measurements by age (1, 3, 7, and 28 days) according to the amount of added CSH nano seeds. This study analyzed the effects of compressive strength according to the amount of added CSH nano seeds for each binder. The compressive strength of all specimens, except for the specimens using fly ash, tended to increase as the content of CSH nano seeds increased. In the case of OPC, the strength expression rate of the P-CSH3 specimen was about 160% higher compared to the P-CSH0 specimen at 1 day of age. and the strength expression rate at 28 days of age was about 110%.

The specimen with 50% blast furnace slag substitution showed a subtle difference in compressive strength expression at the initial age. However, the compressive strength of the GGBS-CSH3 specimen at 28 days of age was 63.4 MPa, which was about 170% higher than that of the GGBS-CSH0 specimen. The compressive strength increased as specimens aged longer. It is believed that CSH nano seeds not only promote the hydration of cement but also affect the latent hydraulic reaction of blast furnace slag.

Contrary to the results of the setting test, in the case of fly ash, CSH nano seeds did not influence compressive strength greatly. It is considered to be a phenomenon caused by an insufficient amount of $Ca(OH)_2$ produced for the pozzolan reaction due to insufficient hydration of cement as a result of excessive mixing of fly ash.

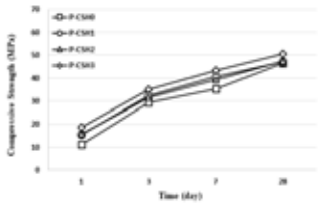

Figure 3. Compressive strength of ordinary Portland cement mortar by age

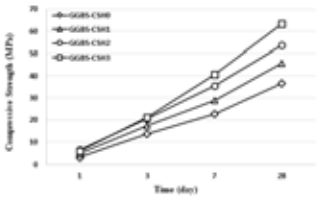

Figure 4. Compressive strength of blast furnace slag mixed mortar by age

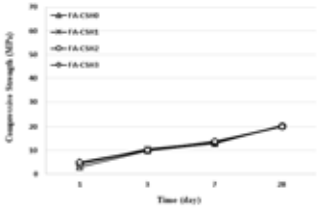

Figure 5. Compressive strength of fly ash mixed mortar by age

3.3 TG-DTA

Fig. 6 presents weight reduction for each specimen at 28 days of age in a certain temperature range on a TG curve. Water, the interlayer water of CSH hydrate, is lost and CSH gel hydrate is decomposed between 100 and 300℃. Portlandite is thermally decomposed between 400 and 520℃. The section between 550 and 950℃ is due to the decarboxylation of carbon dioxide from calcium carbonate, and calcium carbonate is decomposed into calcium oxide and carbon dioxide. It is possible to quantify CSH and $Ca(OH)_2$ due to this weight reduction. Table 2 shows the results of the quantitative analysis of CSH and $Ca(OH)_2$ for each specimen. The results of 3 days of age, when the hydration reaction was most active, revealed that the production of CSH and $Ca(OH)_2$ tended to increase as the amount of added CSH nano seeds increased, and the CSH production of specimens using blast furnace slag showed the largest difference 21.22 and 23.00%, respectively. Specimens using fly ash showed a tendency of increasing the amount of CSH production drastically after 7 days of age. It is thought to be because fly ash does not affect the initial hydration reaction and generates a pozzolan reaction after 7 days of age.

Table 2. Quantitative analysis of calcium hydroxide and CSH

	3day		7day		28day	
	CH (%)	CSH (%)	CH (%)	CSH (%)	CH (%)	CSH (%)
P-CSH1	11.72	20.79	12.87	23.27	13.2	26.9
P-CSH3	11.26	21.61	11.92	23.49	12.8	27.4
GGBS-CSH1	6.6	21.22	7.01	22.07	7.3	25
GGBS-CSH3	5.9	23.00	6.60	24.07	7	24.7
FA-CSH1	5.8	14.83	6.32	17.92	6.8	23.3
FA-CSH3	5.3	15.33	5.91	18.31	6.1	22.4

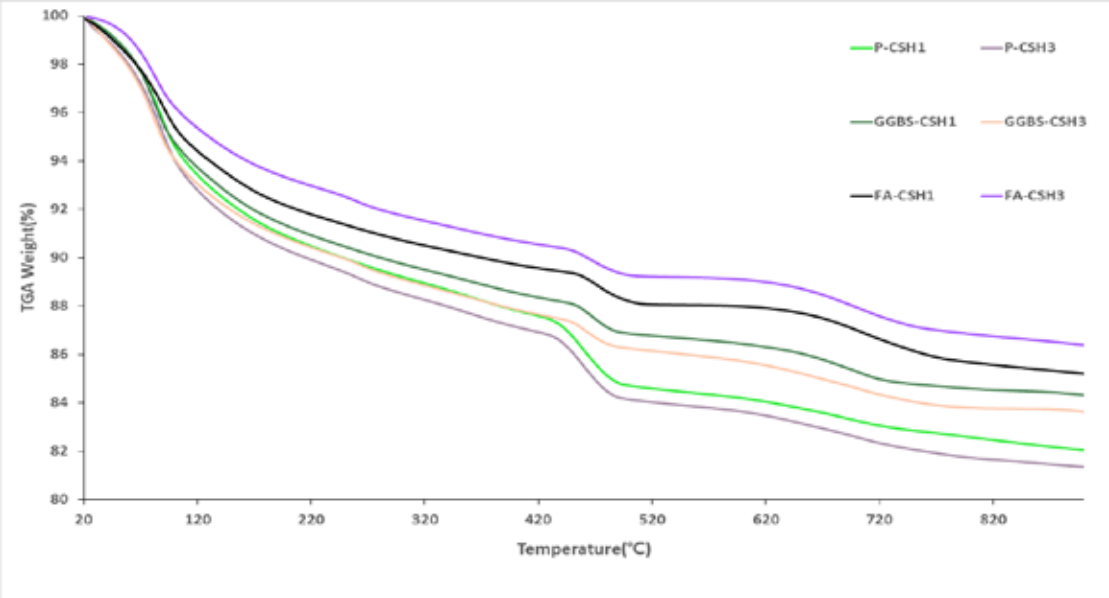

Figure 6. TG weight loss curve

4. Conclusions

This study analyzed and evaluated the hydration promoting effects and strength characteristics by applying an accelerating admixture prepared by using synthesized C-S-H nano seeds to blended cement. The following conclusions were withdrawn.

1) The results of the setting test showed that the setting of blended cement using OPC, blast furnace slag, and fly ash was promoted as the amount of added CSH nano seeds increased. The results implied that CSH nano seeds could solve the problem of delay in the setting of blended cement and could be used in low temperatures such as winter.

2) The results of the compressive strength test confirmed that the larger amount of added CSH nano seeds increased the compressive strength of all specimens except the fly ash specimens. It was also confirmed that CSH nano seeds influenced not only cement hydration but also the latent hydraulic reaction of blast furnace slag. In the case of fly ash, it showed low strength expression due to the pozzolanic reaction. Therefore, it will be necessary to analyze the strength characteristics at long-term age.

3) The results of the hydration product analysis based on weight change confirmed that the production of hydrate increased as the amount of added CSH nano seeds increased. In the case of the fly ash specimen, the CSH production tended to increase drastically after 7 days of age. Therefore, it will be needed to analyze strength characteristics and weight at long-term age.

4) It is judged that CSH nano seeds can be applied as an accelerating admixture to solve the problems of the delayed setting of blended cement and lowered initial strength expression. Additional studies such as durability evaluation will be needed by applying it to concrete.

Acknowledgment

This work was supported by the National Research Foundation of Korea(NRF) grant funded by the Korea government(MSIT) (No. 2020R1A2C2013161)

References

L. Falchi, E. Zendri, P. Fontana, The influence of water-repellent admixtures on the behaviors and the effectiveness of Portland limestone cement mortars, Cem. Conr. Compos. 59(2015) 107-118

M. Wu, Y. Zhang, Y. ji, G. Liu, C. Liu, W. She, W. Sun, Reducing environmental impacts and carbon emissions : study of effects of superfine cement particles on blended cement containing high volume mineral admixtures, J. Clean. Prod. 196(2018) 358-389

C. Naber, F. Bellmann, T. Sowoidich, F.Goetz-Neunhoeffer, J. Neubauer, Alite dissolution and C-S-H precipitation rates during hydration, Cem. Conr. Res. 115 (2019) 283-293

M.C.G. Juenger, R. Siddique, Recent advances in understanding the role of supplementary cementitious materials in concrete, Cem. Conr. Res. 78 (2015) 71-80

V. Kanchanason, J. Plank, Effectiveness of a calcium silicate hydrate – Polycarboxylate ether (C-S-H-PCE) nanocomposite on eartly strength development of fly ash cement, Constr. Build. Mater. 169 (2018) 20-27

Parallel Sessions-5

Sustainable Construction Materials Towards Carbon Neutrality

Use of luminescent-glass aggregates and CO_2 curing treatment for the production of decorative concrete products

Tung-Chai Ling*, Yujia Xiao, Yingting Wang

College of Civil Engineering, Hunan University, Changsha 410082, Hunan, China

* *Corresponding author: tcling@hnu.edu.cn*

Abstract

This project was first aimed to utilize the transparent characteristic of recycled glass (RG) and glow light ability of luminescent powder (LP) to trap light on the daytime and emit back during the nigh time. As shown in Fig. 1, transparent adhesive was successfully used to adhere the LP on the RG for the preparation of luminescent-glass (LG). The different particle sizes (2.36~5mm and 5~10mm) of LG was then used as 100% aggregates in the production of white cement based architectural luminescent-glass mortar, and the glow light performance and mechanical properties of the mortar were assessed accordingly. The results show that the produced luminescent-glass mortar can attain ~30 MPa compressive strength and ~7 MPa flexural strength, meeting most of the building construction and paving application. Moreover, the luminescent-glass mortar can maintain its yellowish-green light (glow) for about 8 h, and the larger particle size of LG is found to perform better glow light than that of smaller size of LG. This is mainly due to the fact that larger LG had more even deposition of LP across the glass surface and able to accumulate more lights in one place.

However, the major concern of incorporating RG in concrete is known to be the risk of alkali-silica reaction (ASR). This is because the amorphous SiO_2 of glass aggregate is very reactive and prone for the precipitation of ASR gels formation in the alkaline environment of concrete. Moreover, due to the crushing process of glass from discarded soda-lime bottles, the ASR is more easily initiated at the residual internal cracks (>2.5 μm) in the glass. For this reason, this project was further investigated the influence of CO_2 curing treatment on the ASR mitigation for mortar containing 100% of RG. Compared with standard curing (0.04% CO_2, 95% relative humidity, RH), a short period (3 h) of CO_2 curing (20% CO_2 and 65% RH) could fully suppress the 14-day ASR expansion according to ASTM C1260 results (see Fig. 2). With the reduction of calcium hydroxide in the cement matrix upon CO_2 curing treatment, silica could dissolve from the RG surface and induced ASR at the RG-cement interface with less expansive expansion compared to that of gels formed at the internal cracks of RG. Furthermore, the pressure from the surface ASR gel and strength enhancement due to $CaCO_3$ precipitation lead to higher cracking resistance in RG and matrix.

Keywords: Recycled glass; CO_2 curing treatment; Alkali-silica reaction; Glow light; Decorative concrete

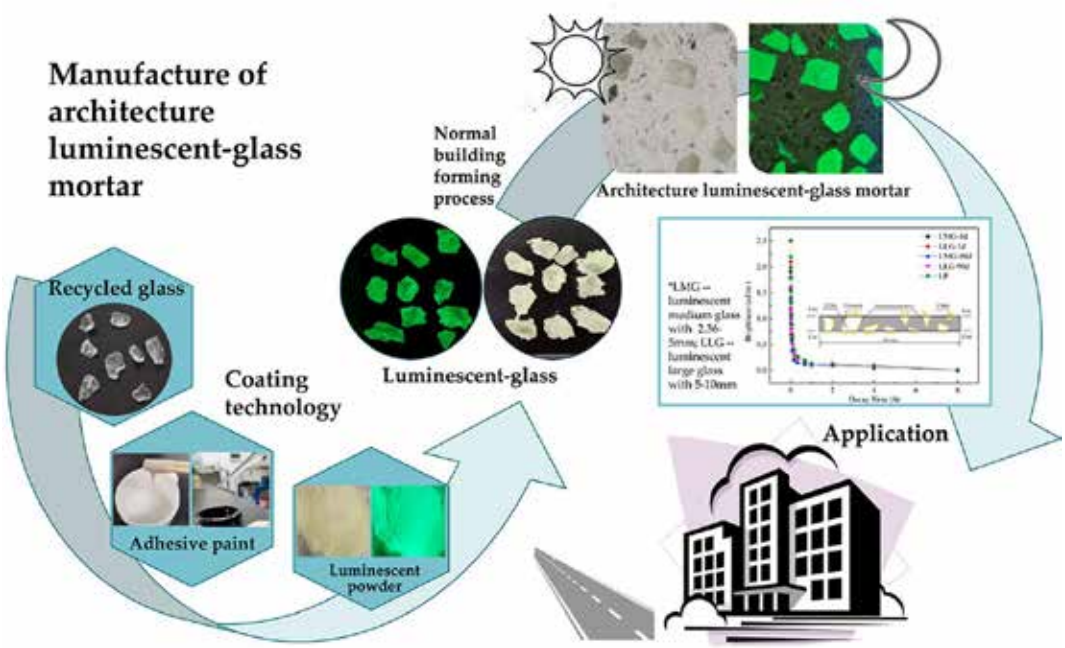

Fig. 1 Manufacture and application of luminescent-glass concrete with glow light function [1]

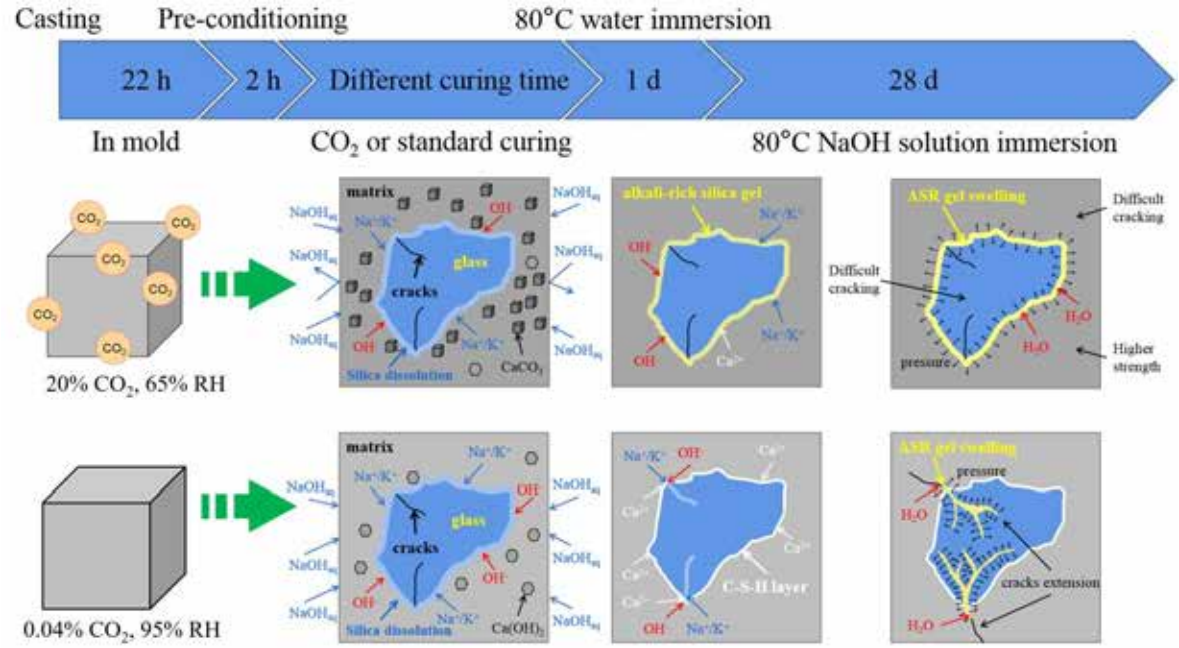

Fig. 2 CO_2 curing treatment and its underlying mechanism in suppressing the ASR [2]

Acknowledgment
This work was supported by the National Natural Science Foundation of China (NSFC) and the State Administration of Foreign Experts Affairs (SAFEA).

References

[1] Xiao, Y.J., Pham, B.T., Guo, M.Z., Ling, T.C. (2022). Use of luminescent-glass aggregates for the production of decorative architectural mortar. Journal of Building Engineering, 50: 104233.

[2] Wang, Y.T., Mo, K.H., Du, H.J., Ling, T.C. (2022). Effects of CO_2 curing treatment on alkali-silica reaction of mortars containing glass aggregate. Construction and Building Materials, 323: 126637.

Surface treatment of cement-based materials by anti-ultraviolet aging hybrid nanoparticles

Yue Gu[1*#], Kai-Lun Xia[1], Ming-Zhi Guo[1], Kai Lyu [2]

[1] College of Mechanics and Materials, Hohai University, Nanjing 210098, PR China
[2] College of Civil and Transportation Engineering, Hohai University, Nanjing, 210098, PR China
[*]*Presenter: gubetter@hhu.edu.cn,* [#]*Corresponding author:gubetter@hhu.edu.cn*

Abstract

Improving the durability of concrete through surface treatment is a crucial step toward low carbonization of building materials. In recent years, the superhydrophobicization of concrete surfaces has been achieved through the binary synergy of hybrid nanoparticles. However, the coatings formed by ordinary hybrid nanoparticles (HN-N) are prone to deteriorate under UV irradation.

Herein, a novel UV-resistant fluorinated hybrid nanocomposite, HN-F was synthesized and used for coating hardened cement-based materials. The penetration resistance of the NS-U coating was evaluated and compared to the HN-N coating. The experimental results showed that the HN-F treated samples possess enhanced water and gas impermeability after 336 hours of exposure to UV rays. Moreover, a hierarchical microstructure hypothesis (Fig.1) was proposed and the mechanism of HN-F was further explored.

This research indicates a higher quality application for hybrid nanoparticles to optimize concrete under harsh UV irradiation.

Keywords: cement ; concrete ; nanocomposite; coating

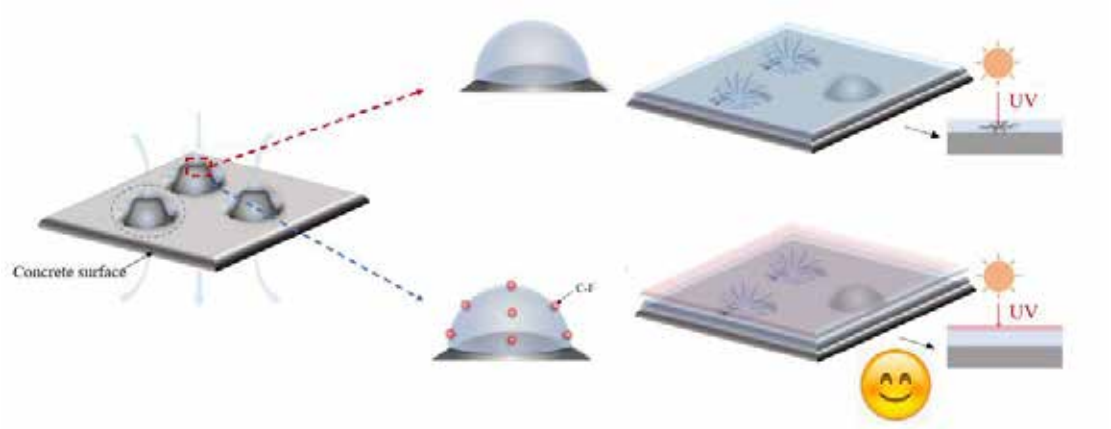

Fig. 1 A hierarchical microstructure hypothesis of HN-F treated samples

Acknowledgment
The authors would like to acknowledge the funding support from the National Natural Science Foundation of China (Grant Nos.51808188, 52178202 and 52108206)

Utilization of dredged sediment in magnesium oxychloride cement to improve water resistance

Zijian Song[1#], Wenhao Xu[1], Ming-Zhi Guo[1], Linhua Jiang[1]

[1] College of Mechanics and Materials, Hohai University, Nanjing, 211100, China.
[*]*Presenter: songzijian@hhu.edu.cn*

Abstract

Dredged sediment (DS) derived from dredging operations poses a potential threat to the ecological environment. Proper disposal and utilization of DS remain a challenge. In this study, magnesium oxychloride cement (MOC) was adopted as an eco-friendly carrier for effective recycling of DS.

Multiscale characterizations were applied to MOC pastes incorporated with DS or calcined dredged sediment (CDS) to investigate the feasibility of combining MOC with DS. Despite the negative influence on mechanical properties induced by the dilution effect, DS/CDS ameliorated the water resistance of MOC pastes. Strength retention test revealed that the compressive strength retention rate of MOC pastes blended with 10-40% DS was positively correlated to DS content, and the modification effect of DS was better than that of CDS.

X-ray Diffraction, Fourier Transform Infrared spectroscopy, Thermogravimetry -Differential Thermogravimetry, Mercury Intrusion Porosimetry and Scanning Electron Microscope with Energy Dispersive Spectrometer were conducted to further decipher the modification mechanism of DS/CDS on MOC system. The results revealed that the addition of DS increased the porosity of the modified MOC pastes, providing more channels for water intrusion. Interestingly, the improvement of water resistance of MOC paste was still enhanced with the increasing content of DS. Insoluble gel-like phases was speculated to widely exist on MOC substrate and acicular Phase 5 crystals, impeding the intrusion of water and thereby improving the stability of MOC pastes in water.

All the results pointed to the formation of amorphous Mg-Al-Si-Cl-H gel that improved the water resistance of the modified MOC paste. The developed MOC paste presents a promising strategy to improve the water resistance of MOC products and alleviate the burden of DS on the environment.

The work in this report is part of our recent published work.

Keywords: Dredged sediment; Magnesium oxychloride cement; Water resistance; Solid waste

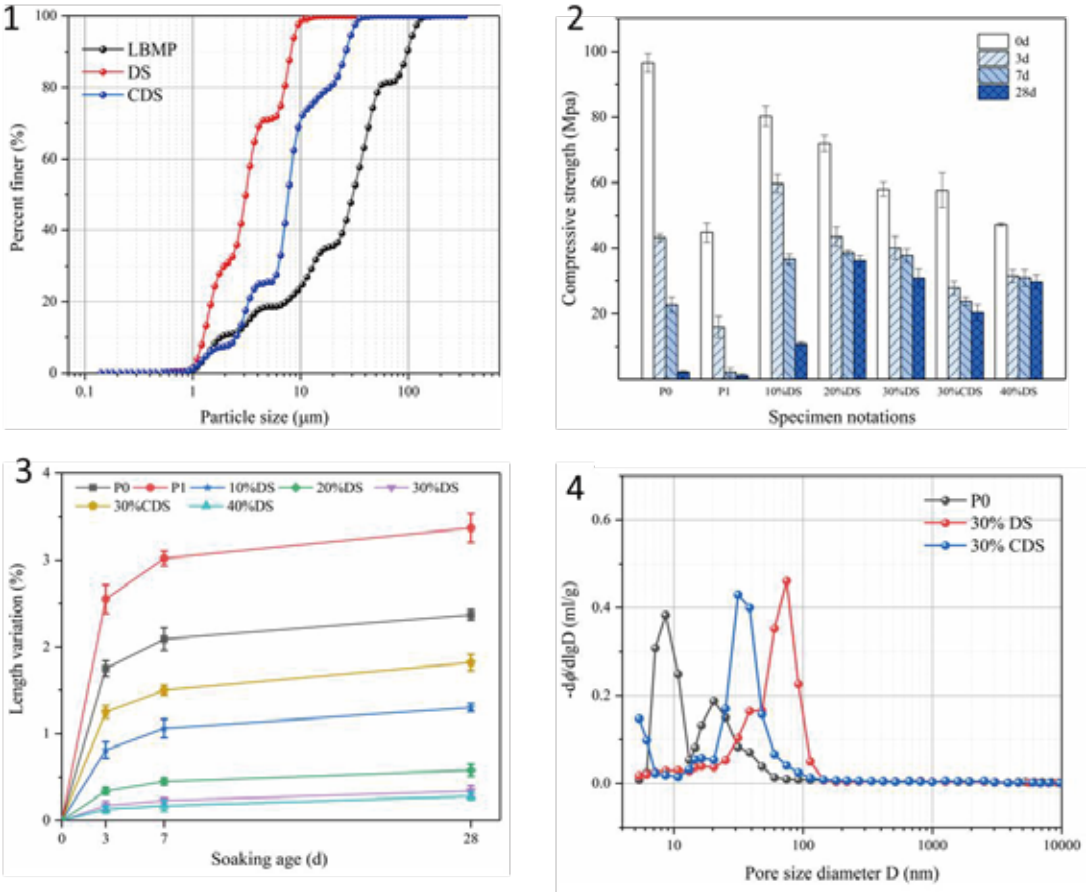

Fig. 1 Particle size distributions of LBMP, DS, and CDS; **Fig. 2** Compressive strength of MOC pastes immersed in water for 0, 3, 7, and 28 d; **Fig. 3** Increase in length of MOC pastes after soaking in water for 3, 7, and 28 days; **Fig. 4** Pore size distributions of MOC pastes with and without DS/CDS

Acknowledgment
This work was supported by the National Natural Science Foundation of China (52071130), the Fundamental Research Funds for the Central Universities under grant (B200202123), the Open Research Fund of Key Laboratory of Construction and Safety of Water Engineering of the Ministry of Water Resources, China Institute of Water Resources and Hydropower Research, (202008), and the Nantong Science and Technology Project (JC2020093).

High-temperature performance of SCMs blended cementitious materials subject to CO_2 curing

Ming-Zhi Guo[1*#], Qifeng Song[1,2], Tung-Chai Ling[2]

[1] College of Mechanics and Materials, Hohai University, Nanjing, Jinagsu 211100, People's Republic of China
[2] College of Civil Engineering, Hunan University, Changsha, Hunan 410082, People's Republic of China
*Presenter: mzguo@hhu.edu.cn, #Corresponding author: mzguo@hhu.edu.cn

Abstract

Supplementary cementitious materials (SCMs) are increasingly used to partially replace cement in the construction industry due to the expected reduction in CO_2 emissions and improvement in the mechanical and durability performance. Meanwhile, the application of CO_2 curing in cement-based materials is garnering growing attention against a backdrop of current green and sustainable development trends However, the influence of CO_2 curing on the high-temperature properties of the SCMs blended cementitious materials remains largely unknown. This study seeks to understand the influence of CO_2 curing on the high-temperature performance of cement paste incorporated with different types of common SCMs (Fig. 1).

The results showed that for the cement paste containing SCMs, pure CO_2 curing reduced the 28-day compressive strength by approximately 10% compared with standard curing. Further standard curing of 2 days promoted the hydration of the unreacted cement and SCMs in the CO_2 cured specimens, compensating for the reduced compressive strength of the pure carbonated SCMs cement paste (Fig. 2).

Due to the simultaneous generation of $CaCO_3$ and hydration products, the samples carbonated for 2 days and then standard cured for 26 days (CS curing) had the best high-temperature resistance, which was reflected by higher compressive strength, lower water absorption and decreased water sorptivity (Fig. 3). BSE imaged revealed that the porosity of the CS cured ground granulated blast furnace slag (GGBS)-incorporated cement paste decreased by 7.93% after exposure to 600 ℃, corresponding to a 57% decrease in water sorptivity due to the transformation of large loose pores into more compact small pores (Fig. 4).

The DTG and XRD analysis demonstrated that Glass powder (GP) was inert in the cement matrix with no obvious pozzolanic reaction and negligible improvement of carbonation degree, leading to the lowest high-temperature performance; whereas, GGBS and fly as (FA) increased the generation of $CaCO_3$ by 19.05% and 15.08%, respectively (Fig. 5). Samples after two days of carbonation were completely carbonated, and subsequent standard curing further promoted the formation of $CaCO_3$, which was present as calcite and remained stable after exposure to 600 ℃.

Findings from this study well demonstrate that the combined use of early CO_2 curing and subsequent standard curing to treat the SCMs blended binders has great potential to reduce carbon footprint and improve elevated temperature resistance.

Keywords: Supplementary Cementitious Materials; CO_2 Curing; Steel Slag; High-temperature Performance; Microstructure

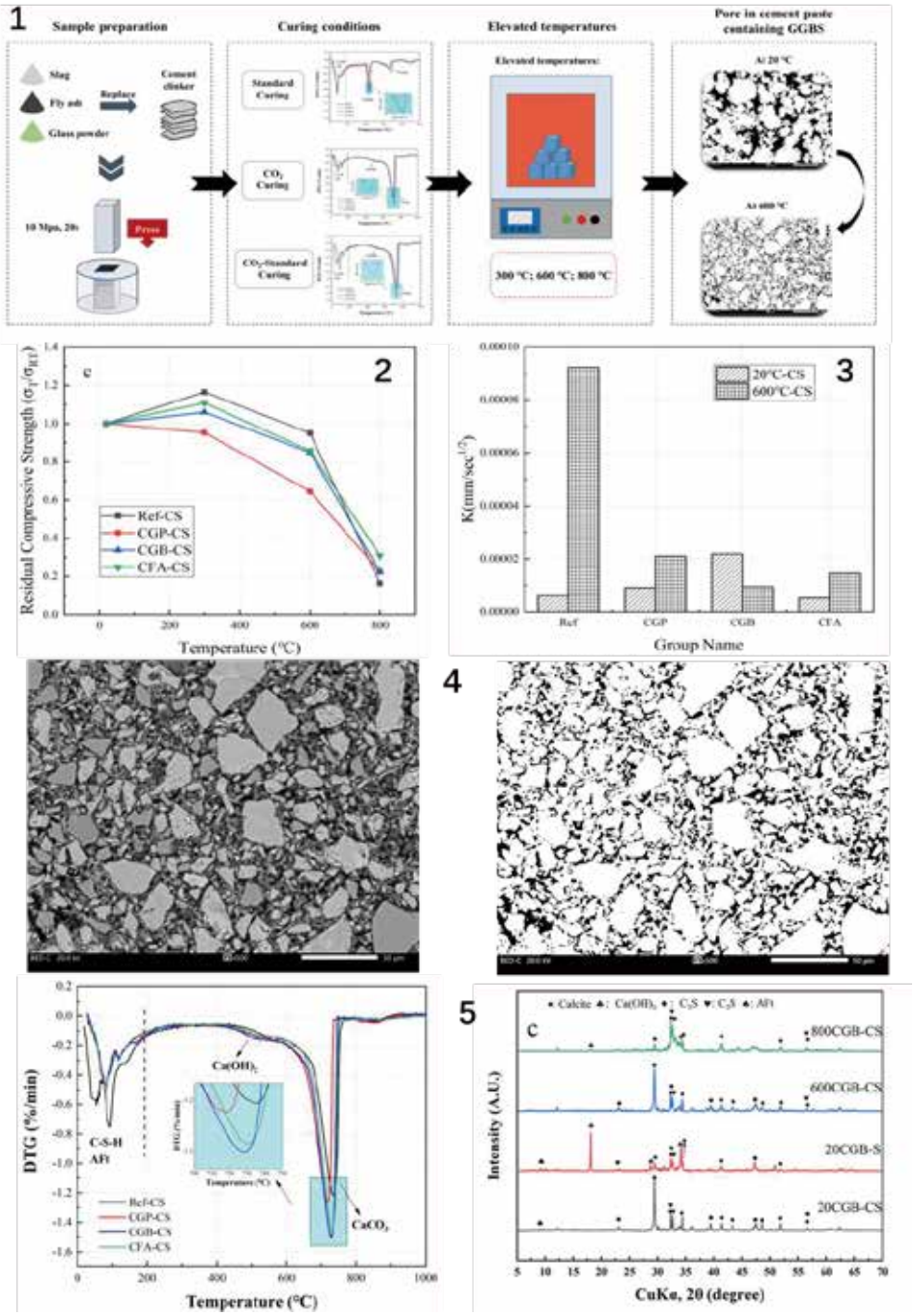

Fig. 1 Overview of the experimental design; **Fig. 2** Residual compressive ratio of the SCMs blended samples with CS curing; **Fig. 3** Comparison of water sorptivity of CS cured SCMs cement pastes at 20 and 600 °C; **Fig. 4** BSE images of CS cured CGB samples; **Fig. 5** DTG curves and XRD patterns of CS cured GGB groups

Acknowledgment

The authors would like to acknowledge the funding support from the China Postdoctoral Science Foundation (2018M632219), the National Natural Science Foundation of China (52078202) and Opening Project of State Key Laboratory of Geomechanics and Geotechnical Engineering (Z020012), Institute of Rock and Soil Mechanics, Chinese Academy of Sciences.

Carbon Footprint Analysis of Graphene Nanofluid Additive Modified Cement Materials Based on LCA Evaluation

Zhijian Yao[1*], Chun Pei[2] and Ji-Hua Zhu[3#]

[1,2,3]College of Civil and Transportation Engineering, Shenzhen University, Shenzhen, CHINA
E-mail: yaozhijian2021@email.szu.edu.cn, ccpei@szu.edu.cn,zhujh@szu.edu.cn

Abstract

The production of concrete is a significant contributor to global carbon emissions, accounting for approximately 5-7% of the total. However, recent advancements in concrete technology have shown promising results in terms of mitigating the environmental impact of this widely used construction material. One such innovation is the incorporation of graphene into concrete, which has demonstrated enhanced mechanical strengths and extended service life compared to conventional concrete.

Graphene-modified concrete offers several advantages over traditional concrete. Its application in structural engineering can lead to stronger and more durable constructions. By utilizing graphene-modified concrete, the same level of structural strength can be achieved with less concrete, resulting in a reduced need for building materials. This reduction in material usage has the potential to significantly decrease the carbon footprint associated with concrete production, thereby contributing to more sustainable construction practices.

In assessing the environmental impact of graphene nanofluidic additives (GNAs) modified cement materials, life cycle assessment (LCA) is a commonly employed method. LCA provides a comprehensive and representative evaluation by considering the entire life cycle of a product, from material acquisition and processing to use and disposal. Accordingly, this study aims to quantitatively analyze the carbon emissions and other environmental impacts, such as global warming potential and acidification potential, associated with modified cement materials prepared using three different GNAs, in comparison to conventional cement.

To achieve this objective, a mathematical model for LCA of GNAs modified cement was developed. This model encompasses the complete "from cradle to grave" process, taking into account material acquisition, processing, use, and waste. To ensure the accuracy and reliability of the LCA, well-established databases such as GaBi and other software were utilized to perform a comprehensive assessment of GNAs modified cement materials.

In addition to the environmental assessment, the strength of the GNAs modified cement materials was tested. Material strength and carbon emissions were considered as key factors for conducting a comparative analysis with conventional cement. The evaluation results demonstrated that GNAs modified cement materials offer an optimized combination of material strength and carbon emission, outperforming conventional cement. Specifically, the GNAs modified cement material prepared with poly-carboxylate superplasticizer (PCE) surfactant exhibited the most favorable comprehensive evaluation.

Keywords: Graphene, LCA, Low carbon concrete, Modified cement, Surfactant

[*]:Presenter; [#]:Corresponding author

concrete production technology while minimizing negative environmental impacts. By incorporating graphene and employing suitable surfactants like PCE, the construction industry can achieve greener production practices. This advancement not only enhances the mechanical properties and service life of concrete structures but also reduces their carbon footprint, contributing to a more sustainable built environment.

In conclusion, the utilization of GNAs modified cement materials represents a viable approach to reducing the environmental impact associated with concrete production. The comprehensive LCA analysis conducted in this study demonstrates the superiority of graphene-modified concrete in terms of material strength and carbon emissions. The findings underscore the potential of incorporating graphene technology into the construction industry to achieve more sustainable and environmentally friendly concrete production practices. Further research and development efforts should continue to explore and optimize the application of GNAs in concrete materials to foster greener construction methods on a global scale.

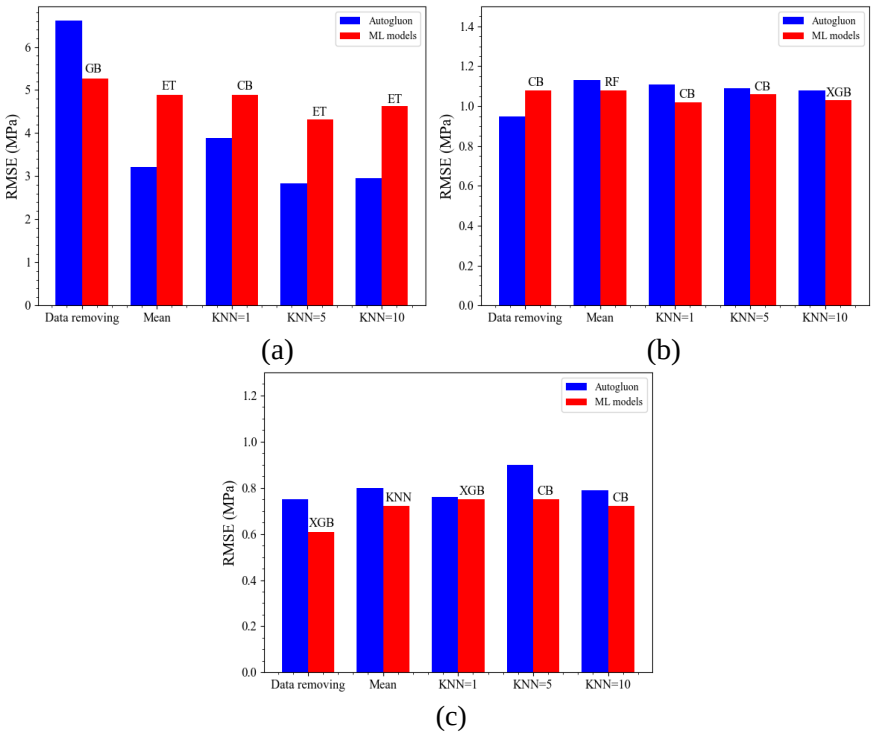

Fig.1. Comparison of imputation performance on different datasets with RMSE value as the indicator : (a) CD; (b) FD; (c) TD.

Acknowledgment

This work was supported by the National Key Research and Development Program of China (2018YFE0124900), the Key-Area Research and Development Program of Guangdong Province (2019B111107002), the National Natural Science Foundation of China (51538007/51778370/52108231), and the Shenzhen Science and Technology Project (GJHZ20180928155819738).

Application of Cement-based Inorganic Cementitious Coating Modified by Graphene-titanium dioxide Composite Fibers

Xiang-Fei Wang*，Chun Pei，Ji-Hua Zhu#

Guangdong Province Key Laboratory of Durability for Marine Civil Engineering, College of Civil and Transportation Engineering, Shenzhen University, Shenzhen, Guangdong, CHINA.
E-mail: *wangxiangfei1993@outlook.com*

Abstract

Titanium dioxide (TiO_2) is a kind of semiconductor photocatalyst, which could directly absorb solar energy to catalyze and degrade environmental pollutants, has great application potential in improving environmental pollution. However, TiO_2 can only utilize ultraviolet light (UV) accounts for 5% of sunlight due to its wide band gap and high electron-hole recombination ratio. To improve photocatalytic efficiency and utilization of visible light, graphene-modified TiO_2 composite nanofibers were prepared by electrospinning ways and characterized by a variety of instrumental analysis methods. Inorganic cementitious coating with photocatalytic property were prepared by the incorporation of cement and as-prepared graphene-modified TiO_2 composite nanofiber. The air purification capacity of coating was evaluated by the catalysis of nitric oxide (NO). As expected, the coating with modified TiO_2 fiber showed high photocatalytic efficiency for NO, the absorption and utilization of visible light and photocatalytic efficiency have been significantly improved. Besides，considering the fiber could improve ductility of materials effectively, the tensile tests of structures coated with fiber modified cement-based inorganic cementitious were also carried out. The test results show that the coating with fiber improves the tensile properties of the structures. In addition, the existence form and integrity of composite nanofibers in coating were also studied and as desired, the fiber has good stability. Therefore, graphene-modified TiO_2 composite nanofiber in cement-based inorganic cementitious coating could effectively purify air and improve the tensile performance of structures.

Keywords: Graphene, Titanium dioxide fiber, Inorganic Cementitious Coating, Photocatalysis, Tensile property.

Mitigating shrinkage of alkali-activated slag pastes by cellulose fibre

Xinyan Liu[1,*], Bo Li[1,#] , Yung-Tsang Chen[1]

[1] Department of Civil Engineering, University of Nottingham Ningbo China, Taikang Road, Ningbo, China.
[*]*Presenter: xinyan.liu@nottingham.edu.cn*
[#]*Corresponding author: bo.li@nottingham.edu.cn*

Abstract

Alkali-activated slag (AAS) has been recognized as a green binder to replace the ordinary Portland cement (OPC). As compared to the OPC, it can considerably reduce the embodied carbon of construction material. However, AAS material exhibits large shrinkage, which subsequently increases the cracking tendency of components made by AAS. In this study, cellulose fibres are adopted as internal curing agents to mitigate the shrinkage of AAS paste. The liquid released from the cellulose fibres can achieve internal curing, while the fibres can also reinforce the AAS paste against the shrinkage. The influences of cellulose fibre dosage and length on the properties of the AAS pastes are investigated.

The results indicate that the autogenous shrinkage of the AAS paste is mainly affected by the cellulose fibre dosage, and increasing the fibre dosage can reduce the autogenous shrinkage of the AAS paste by up to 33%. Increasing the fibre length can slightly reduce the autogenous shrinkage of the AAS pastes due to the fibre reinforcement effect. Moreover, adding 5% fibres can decrease the drying shrinkage of the AAS paste due to their reinforcement effect. However, the drying shrinkage of AAS pastes increases with the cellulose fibre dosage, resulting from the accelerated moisture loss through the paths created by the fibres. Additionally, the compressive strengths of the AAS pastes decrease as the cellulose fibre dosage increases, which is mainly caused by larger pores left by the fibres and the weak bonding between the fibre and paste.

Keywords: Alkali-activated slag; internal curing; cellulose fibre; shrinkage; compressive strength

Development of lightweight engineered geopolymer composite with fly ash cenospheres

Jia-Qi Wu[1,*], Bo Li[1,#] , Yung-Tsang Chen[1]

[1] Department of Civil Engineering, University of Nottingham Ningbo China, Taikang Road, Ningbo, China.
[*]*Presenter: slxjw2@nottingham.edu.cn*
[#]*Corresponding author: bo.li@nottingham.edu.cn*

Abstract
Engineered geopolymer composite (EGC) has attracted great attention due to its superior tensile performance and crack control capacity. For its application in structural repair, reducing the weight of EGC can facilitate the installation of EGC and limit additional load. Therefore, lightweight EGC has been recognized as an innovative and effective composite for structural repair. Fly ash cenospheres (FACs), with hollow sphere structure, have been proved as a successful lightweight filler in cementitious materials. The FACs may react with alkaline activator, which alters the properties of EGC containing FACs. This study proposes a lightweight EGC with a high tensile strain capacity. The FACs are incorporated into EGC as the lightweight fillers. Increasing the FACs content gradually decreases the density and compressive strength of EGC due to their hollow structure. All the EGCs incorporating FAC present strain-hardening and multiple cracking behaviour. Using FAC to replace silica sand results in similar tensile strengths of EGCs around 6 MPa. Increasing the FAC/binder ratio from 0.3 to 0.7 slightly decreases the tensile strength of EGCs to around 4.6 MPa, which is mainly due to the reduced the fibre/matrix frictional bond. Besides, increasing the FAC content has a marginal impact on the ultimate tensile strain capacity of EGCs, which is around 9%. In addition, a higher content of FAC introduces more flaws to the matrix, and consequently increases the crack numbers and reduces the average crack width of EGCs. The scanning electron microscopic image demonstrates FACs partially react with the alkaline activator, which is beneficial to the properties of lightweight EGCs. Overall, the FACs can be utilised as effective fillers to produce lightweight EGC with acceptable strength and ultra-high tensile strain capacity.

Keywords: Engineered Geopolymer Composite; fly ash cenospheres; tensile-strain capacity; lightweight.

Investigation on the recycled aggregate from worn ballast in heavy haul railways

Wenjun Zhu[1*], Chengyue Yang[1], Zhongxu YU[1], Yude XU[2]

[1] College of Transportation 7 Engineering, Tongji University, Shanghai 201804, China,
[2] Shanghai Key Laboratory of Rail Infrastructure Durability and System Safety, Tongji University, Shanghai 201804, China
[*]*Presenter:* wjzhu@tongji.edu.cn, [#]*Corresponding author:* wjzhu@tongji.edu.cn

Abstract

The dirty worn ballast was produced during the ballast cleaning process, which would result in a seriously environmental problem, not only the air pollution but also the waste of a huge amount of the field, which challenges the railway engineering significantly. In China, the transportation capacity of the cargoes is increased more and more rapidly in order to meet the requirement of the economic, which induces the deterioration of the ballast bed in a shorter period subsequently. To make sure of the safety of the transportation, the maintenance of the heavy haul railway was necessary and the frequency of ballast cleaning is enlarged significantly. Moreover, as the "Strong transportation" has pointed out that a sustainable way should be realized in the railway engineering in China, the dirty worn ballast should be recycled in a suitable way in the future.

The investigation of the heavy haul railway in China was conducted, including five main rail net in the north of China. The cleaning distance of the relative lines was cumulated, the cumulated waste from the cleaning process was evaluated based on the daily records. As a result, the total quality of the dirty worn ballast was assessed. The challenge of these worn ballast would be analyzed based on the statistical results.

The compositions of the worn ballast were analyzed. It was found that the worn ballast was polluted due to the coal powder which come from the transportation of the cargos inevitably. According to the seizing of the worn ballast, it was found that it could meet the requirement of both the fine aggregate and coarse aggregate. Some other properties of the worn ballast, such as the composition of the coal was tested, and the crushing strength of the worn ballast was about 2.6.

The recycled aggregate of the worn ballast was conducted. The mechanical properties of the concrete based on the recycled aggregate was compared with the normal materials, as well as crushed aggregate. The slump of the specimens was also conducted. it could be found that the worn ballast could be a suitable choice for the recycled aggregate.

Keywords: Mechanical properties; recycled aggregate; worn ballast; railway engineering

Fig. 1 Worn ballast during the cleaning process

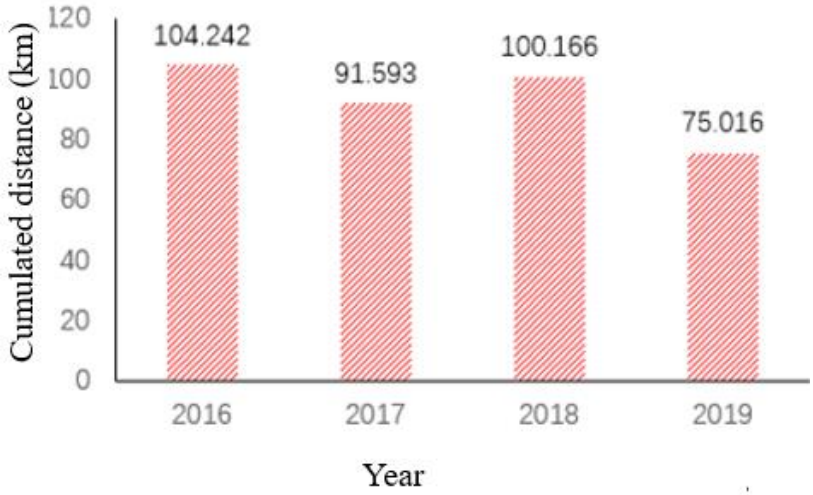

Fig. 2 Cummulated cleaning distances of some heavy haul railway;

Table 1 Evaluation of the worn ballast produced by the cleaning process of some railway

Frequency	Cleaning distances		Evaluation of the worn ballast	
	（km）	（%）	Volume（m^3）	Quality（t）
0	269.042	44.84%	0	0
1	297.052	49.51%	121156.26	151445.32
2	28.688	4.78%	23401.50	29251.87
3	4.527	0.75%	5539.18	6923.97
4	0.452	0.08%	737.42	921.77
5	0.240	0.04%	489.44	611.79

Preparation of reactive urchin-like recycled concrete aggregate by wet carbonation: towards improving the bonding capability

Peiliang Shen[1*], Yi Jiang[1], Chi Sun Poon [1#]

[1] Department of Civil and Environmental Engineering, The Hong Kong Polytechnic University, Hung Hom, Kowloon, Hong Kong
[*]Presenter: peiliang.shen@polyu.edu.hk, [#]Corresponding author: cecspoon@polyu.edu.hk

Abstract

To enhance the bonding capability between recycled concrete aggregate (RCA) and paste, an innovative carbonation method was developed to modify the surface characteristic of RCA by promoting the formation of needle-like aragonite using accelerated carbonation in $Mg(NO_3)_2$ solution under an elevated temperature (75 ℃). The evolution of surface microstructure, phases and reaction kinetics was investigated using multiple testing methods including scanning electron microscopy, nanoindentation, X-ray diffraction, etc. The results revealed that reactive urchin-like RCA could be prepared within less than an hour after exposing to CO_2. The urchin-like wrapping with a thickness of about 100 μm was seen rapidly grown on the surface of RCA, consisting of an outermost layer of aragonite coating, a thin layer of brucite and a silica-rich layer. The mineral wrapping induced by carbonation significantly modified the roughness, topography and geochemistry of RCA's surface entirely, contributing to enhanced bonding strength between RCA and new mortar (33.54%).

Keywords: Carbonation, recycled concrete aggregate, urchin-like aragonite, bonding strength, kinetics

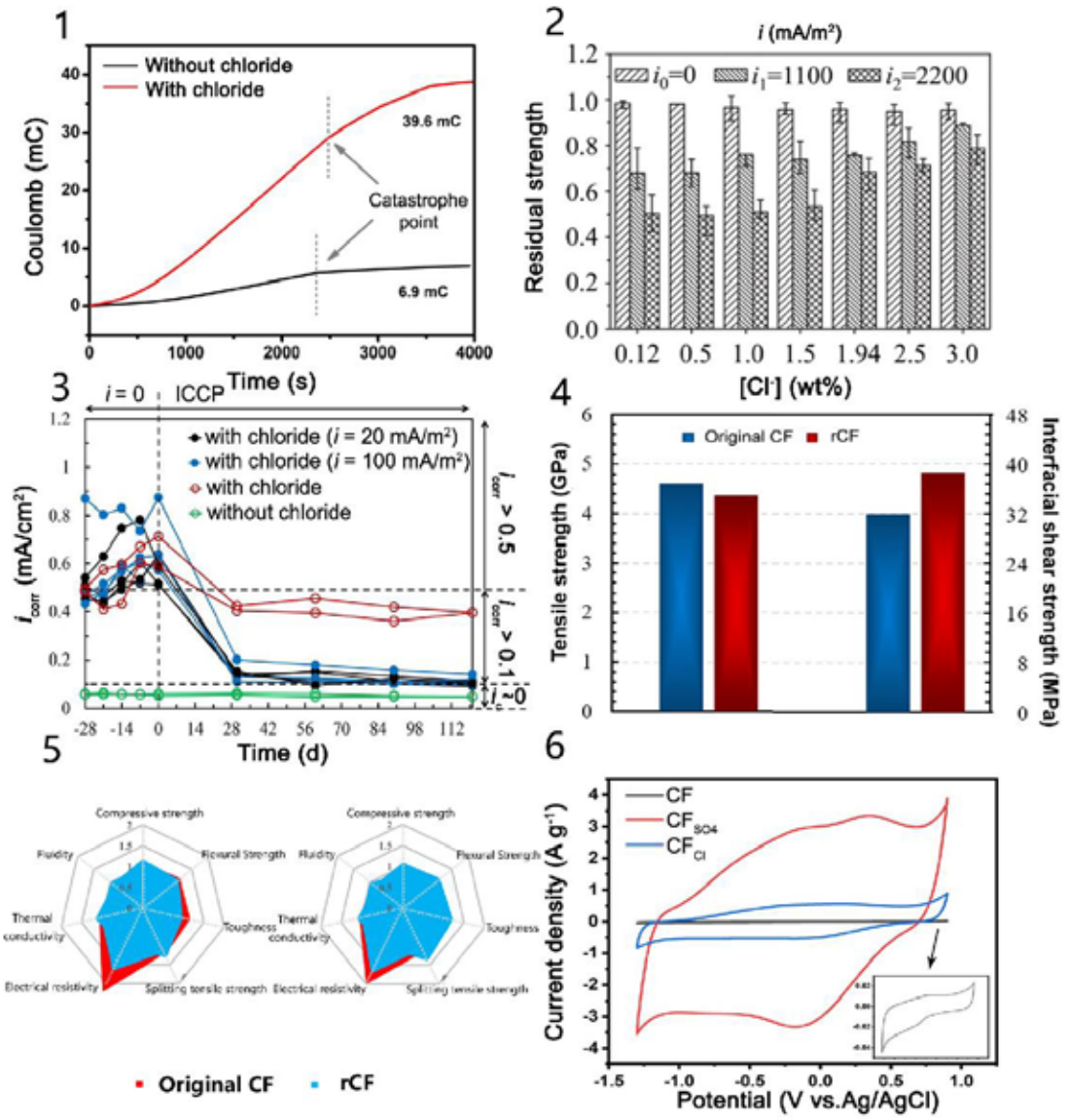

Fig. 1 Charge load on CF surface; **Fig. 2** Effect of polarization current density and chloride ion concentration on tensile properties of CF after polarization; **Fig. 3** Corrosion protection effect of ICCP-SS on chlorinated concrete; **Fig. 4** Comparison of tensile strength and interfacial shear strength between rCF and original CF; **Fig. 5** Comparison of the properties of carbon fiber reinforced concretes made from original CF and rCF; **Fig. 6** Cyclic voltammetry curves of CF before and after electrochemical treatment in different electrolytic salt solutions

Acknowledgment

The authors would like to acknowledge the funding support from the Key-Area Research and Development Program of Guangdong Province (2019B111107002) and the National Key Research and Development Program of China (2018YFE0124900).

Valorization of waste glass in low carbon products

Jian-Xin LU*#, Ligang PENG, Ziwei CHEN, Weiyi JI, Chi Sun POON#

Department of Civil and Environmental Engineering & Research Centre for Resources Engineering Towards Carbon Neutrality (RCRE), The Hong Kong Polytechnic University, Hung Hom, Hong Kong, China
*Presenter: jxinlu@polyu.edu.hk, #Corresponding author: cecspoon@polyu.edu.hk

Abstract

In Hong Kong, the waste glass is a nonnegligible component among municipal solid wastes, but the recycling rate of waste glass is usually lower than 20% due to the lack of recycling outlets. Glass is a silica-rich solid waste with high strength and low permeability, which provides advantages in the application in cement-based materials. This paper reviews the research outcomes on the development of low-carbon building materials incorporating waste glass in Hong Kong, with a view to creating new approaches on the use of waste glass in the cement-based materials. The waste glass in the forms of glass powder, glass aggregates and glass-based alkali activator was used for the development of architectural mortar, dry-mixed concrete and alkali activated materials. Furthermore, the waste glass was combined with other solid wastes to produce lightweight aggregates for lightweight concrete.

Keywords: Waste glass; Cement-based materials; Glass powder; Low carbon; Lightweight aggregates

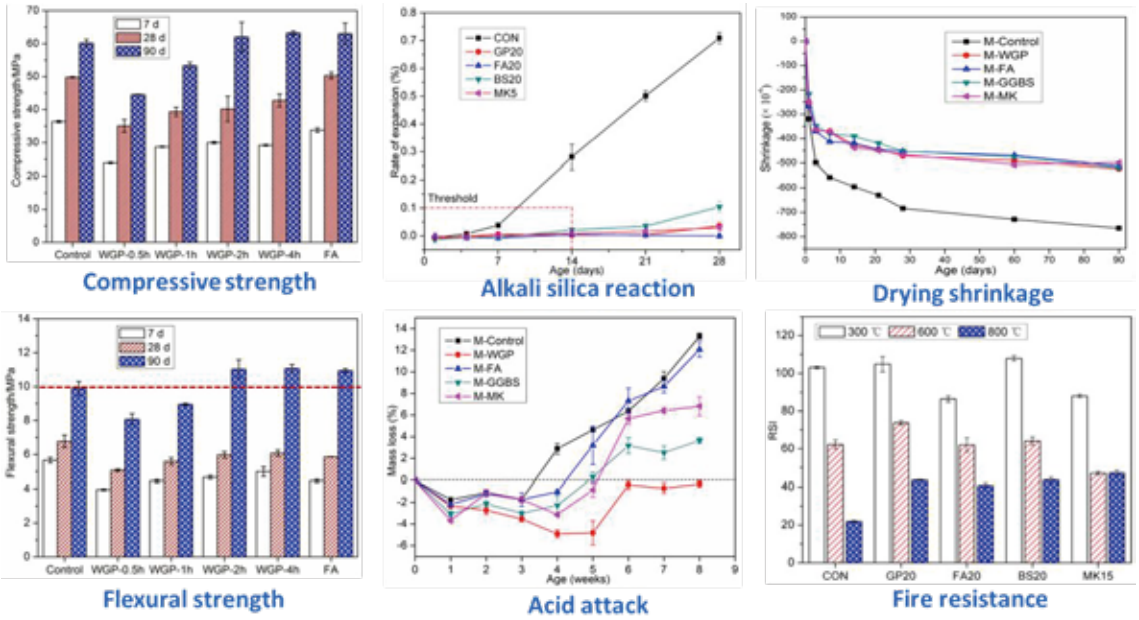

Fig. 1 Use of glass powder enhanced the strength, reduced alkali silica reaction expansion, lower drying shrinkage, and improved resistance to acid attack and high temperature.

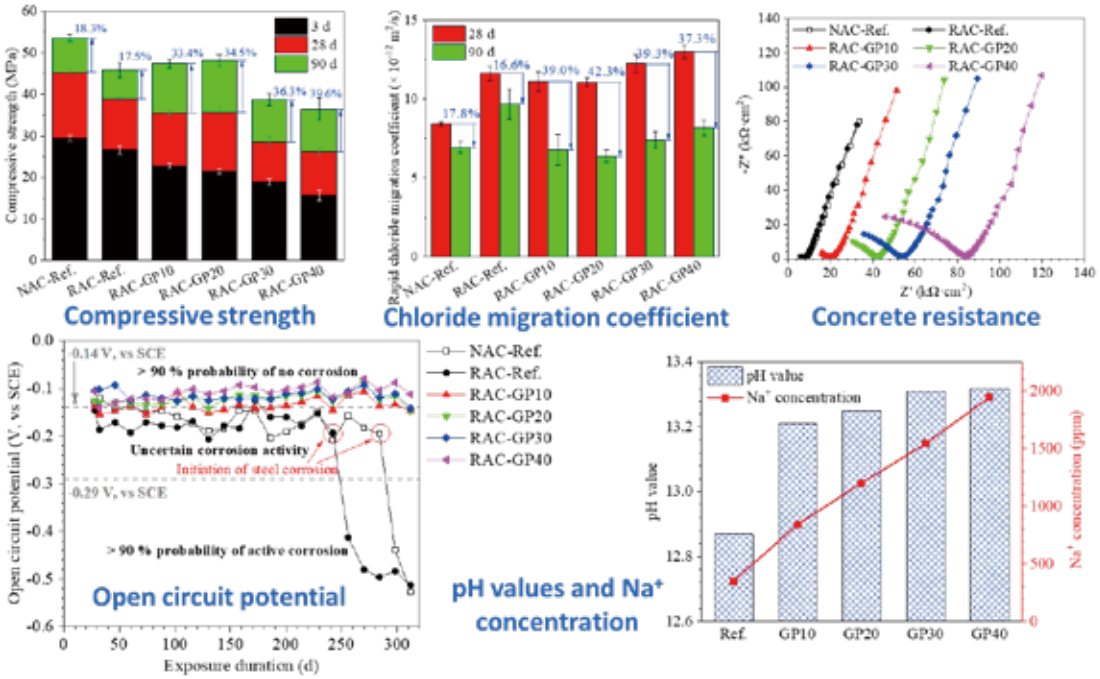

Fig. 2 Use of glass powder enhanced the chloride penetration resistance, increased alkalinity of the matrix and lower corrosion risk of concrete.

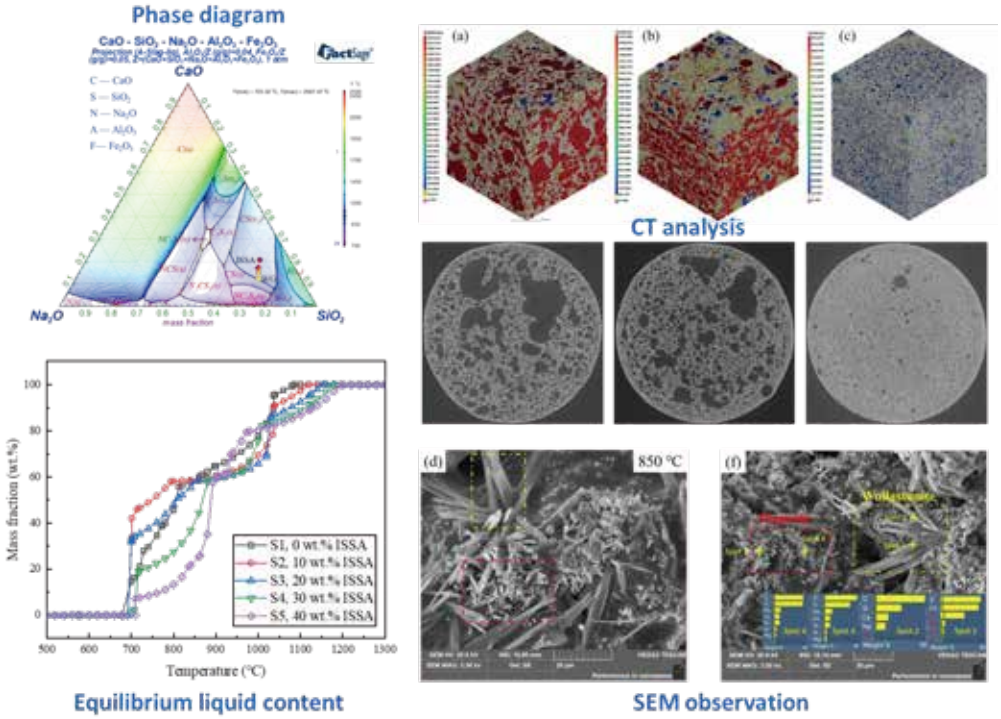

Fig. 3 Production of glass-ceramic with waste glass and microstructure analyses by CT and SEM.

Acknowledgment

The authors would like to acknowledge the funding support from the Hong Kong Innovation and Technology Fund (ZM3H, ZS1H), the General Research Fund from the Hong Kong Research Grants Council (Q80K) and Collaborative Research with World-leading Research Groups Fund (SAC3).

Comparative study on the effect of fiber type on the abrasion resistance of recycled aggregate concrete

Qi Deng[1], Zhen-Hua Duan[1*#]

[1] College of Civil Engineering, Tongji University, Shanghai 200092, China
[*]*Presenter:* zhduan@tongji.edu.cn, [#]*Corresponding author:* zhduan@tongji.edu.cn

Abstract

The application of recycled aggregate in concrete mixture is an effective method to solve the disposal of construction and demolition (C&D) waste, which has become the current research hotspot. In some special application scenarios susceptible to erosion by mobile media and solid (such as road and hydraulic structure), besides mechanical properties, abrasion resistance is also a significant factor affecting the service life of concrete structure. In order to realize the wide application of recycled aggregate concrete (RAC), it is necessary to study the abrasion resistance of RAC. The objective of this study is to investigate the effects of length, volume fraction, types and hybridization of fibers on the mechanical properties and abrasion resistance of RAC. At the same time, time-varying law of abrasion behavior of fiber reinforced RAC exposed to solid impact is studied. And the relationship between the mechanical properties and abrasion resistance of fiber reinforced RAC is analyzed in this research.

Volume fraction, length, type and hybridization of fiber were considered as the influencing factors and the test procedure was designed. To evaluate the basic mechanical properties of fiber reinforced RAC, tests of compressive strength, flexural strength and elastic modulus were carried out. According to Fig. 1, the flexural strength and elastic modulus of RAC with PE fiber content of 0.3% by volume increased by 22.47% and 12.63% respectively. However, the enhancement of PE fiber to compressive strength is not obvious.

Fig. 2 presents the typical time-varying curves of abrasion rate of RAC with different fiber contents and lengths. It is shown that the curves fluctuated during the first 200 revolutions. After 500 revolutions, as the specimens gradually became spherical, the growth rate of specimen abrasion decreased slightly. As shown in Fig. 3, the influence of fiber content on abrasion rates of RAC at 500,700 and 1000 revolutions is consistent. When the fiber content reached 0.3% by volume, the abrasion rate of mixture C3 decreased by 32.98%, 32.19% and 31.18% respectively after the above three revolutions. The fitting relationship between velocity and revolution times appeared to be a power function (Fig. 4).

In order to predict the abrasion performance of fiber reinforced RAC without test, the correlation between abrasion rate after 1000 revolutions and mechanical properties was analyzed. The range of R^2 values of fitting curves in Figure 15 were 0.80-0.90, indicating that flexural strength showed the greatest correlation with abrasion resistance (Fig. 5).

This investigation attempts to establish an empirical model of abrasion resistance of RAC using the available test results as a basis for predicting long-term abrasion performance. Logarithmic models seem to be the most suitable for the experimental data (Fig. 6).

Keywords: Recycled aggregate concrete (RAC); Abrasion resistance; Fiber; Time-varying characteristics

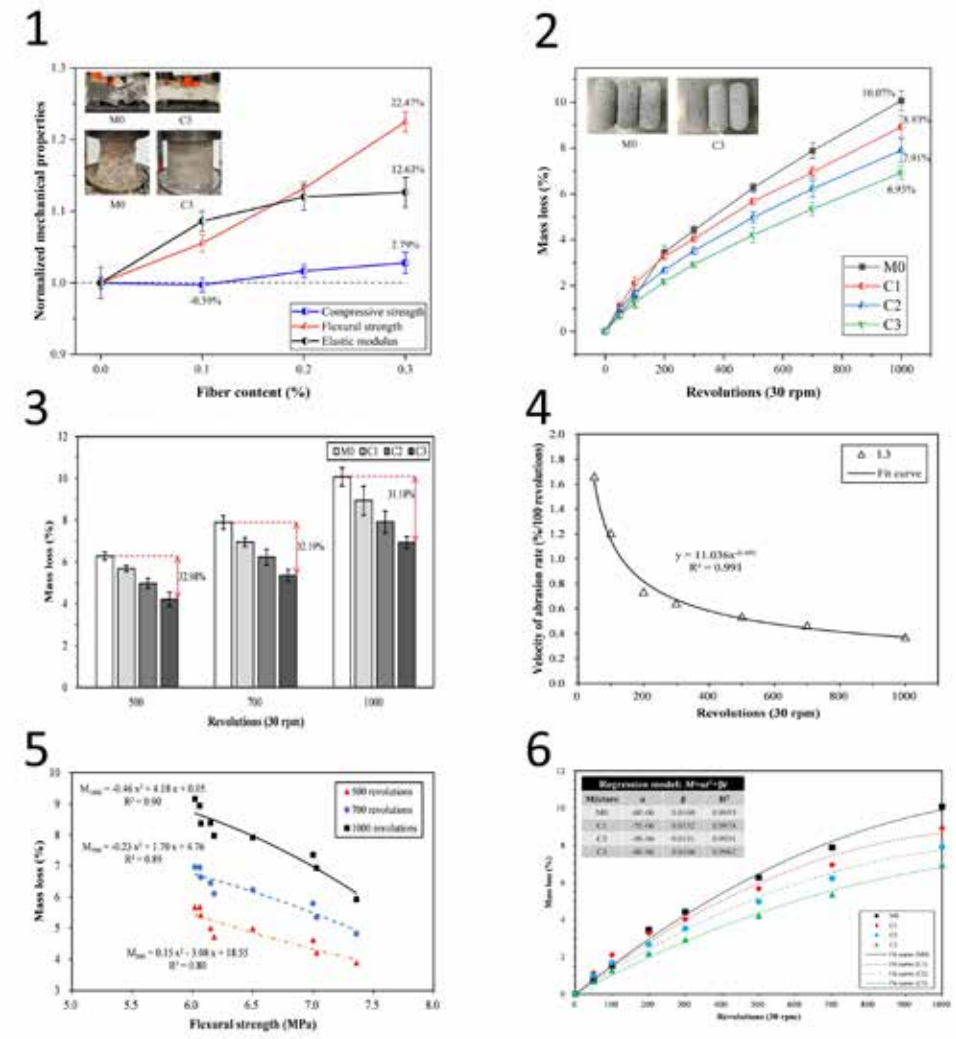

Fig. 1 Influence of fiber content on the mechanical properties of RAC; **Fig. 2** Time-varying curves of abrasion rate influenced by fiber contents; **Fig. 3** Mass loss after 500, 700 and 1000 revolutions of mixtures influenced by fiber contents; **Fig. 4** Typical abrasion velocity of RAC; **Fig. 5** Correlation between abrasion rate and flexural strength; **Fig. 6** Fitting results of abrasion time-varying curves.

Acknowledgment

The authors would like to acknowledge the funding support from the Natural Science Fund Project of Shanghai 2021 "scientific and technological innovation action plan" (21ZR1465000).

Life Cycle Assessment of Upcycling CO_2 Pre-treated Waste Slags in Cement Paste: Comparative Study between Yellow Phosphorus Slag and Basic Oxygen Furnace Slag

Xin Shao[1,*], Hamideh Mehdizadeh[1], Lufan Li[1,2], Tung-Chai Ling[1,#]

[1] College of Civil Engineering, Hunan University, 410082 Changsha, China,
[2] Department of Civil Engineering, Hangzhou City University, 310015 Hangzhou, China
[*]*Presenter:* shaoxin@hnu.edu.cn, [#]*Corresponding author:* tcling@hnu.edu.cn

Abstract

Mineral carbonation is considered to be an effective method to convert solid wastes, such as yellow phosphorus slag (YPS) and basic oxygen furnace slag (BOFS), into valuable products for the construction industry. The mineralization process can be conducted directly under dry (DC) or aqueous (AC) conditions. However, the slow reaction and low CO_2 fixation efficiency of DC and high water consumption required for AC are the key challenges for large-scale applications. In this study, we evaluated the environmental impact of carbonation of YPS and BOFS via dry and aqueous routes, and the upcycling of these CO_2 pre-treated waste slags in cement paste production.

The environmental impacts from materials preparation to blended cement paste manufacturing (cradle-to-gate) were quantified by life cycle assessment (LCA), which consists of the following two system boundaries (Fig. 1):
System boundary 1: DC and AC of YPS and BOFS;
System boundary 2: Using carbonated YPS/BOFS and raw YPS (raw-YPS) to replace cement at ratios of 10% and 20%.

According to the midpoint assessment results (Fig. 2), the GWP value of AC was 11% and 214% lower than that of DC for YPS and BOFS, respectively. This is mainly due to the long duration and significantly lower CO_2 uptake of DC. As seen, the emissions from the operation process can nearly be offset by the positive impact of BOFS due to the considerable amount of CO_2 that can be captured and avoided disposal of the waste in landfill (BOFS recovery). This reduced CO_2 emission is particularly obvious in the case of AC, which reaches ~187 kg of negative CO_2 emissions. In terms of human carcinogenic toxic (HCT), no significant difference can be observed in the DC and AC of YPS, as it is a non-toxic substance. While the recycling of BOFS is of great significance to reduce HCT, due to metal precipitation and other problems in the landfilling process, which remains the main reason for the huge difference between YPS and BOFS in mineral resource scarcity. The higher liquid-to-solid (L/S) ratio of AC for YPS leads to a higher water consumption which is 3 times of BOFS.

Results of endpoint assessment (Fig. 3) showed that carbonation of BOFS causes lower impacts compared to YPS in all three categories, mainly associated with the recovery of BOFS leading to the avoidance of a large amount of metal ion precipitation in the landfill process. The fine particulate matter formation potential of carbonation of YPS is significantly higher than that of BOFS, since the longer carbonation duration the higher consumption of additional electricity, which has a large impact on human health.

Cement production has the highest contribution (over 90%) for GWP in the manufacturing process of blended cement paste (Fig. 4). However, as carbonated slags contribute less than 10% of total emissions, only 6-14% of carbon emissions can be reduced even if the replacement rate increases from 10% to 20%. Replacing cement with 20% aqueous

carbonated YPS (AC-YPS) shows no effect on strength, but can reduce GWP by 11%. As for BOFS, the addition of dry carbonated (DC-BOFS) and aqueous carbonated BOFS (AC-BOFS) showed a quite similar effect on the compressive strength of cement paste, while 20% of AC-BOFS cement paste exhibited the lowest carbon footprint, approximately 24% reduction compared to OPC paste.

Keywords: yellow phosphorus slag; basic oxygen furnace slag; dry carbonation; aqueous carbonation; life cycle assessment; sensitivity analysis

(1)

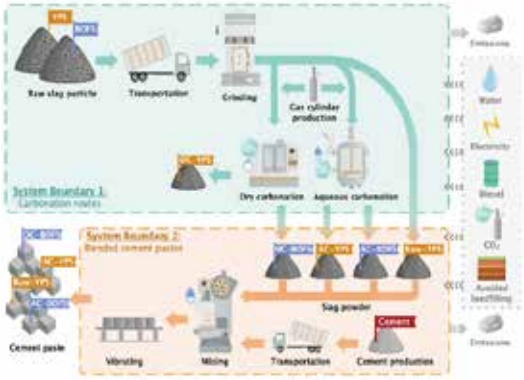

(2)

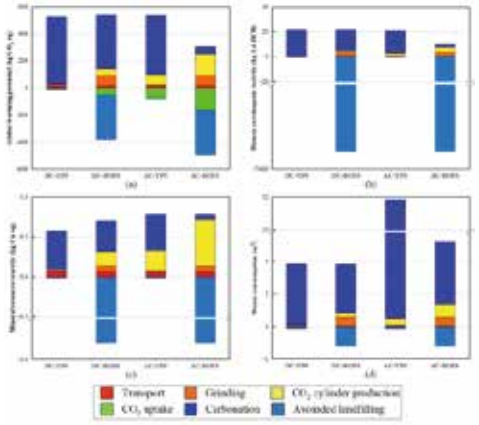

(3)

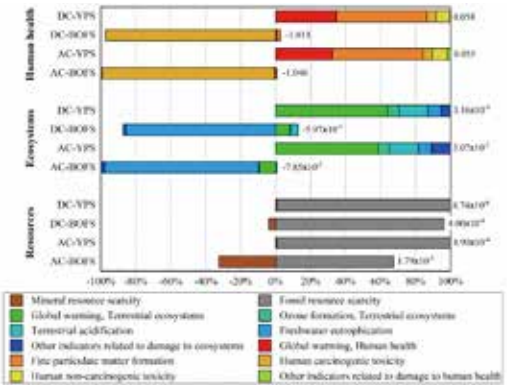

(4)

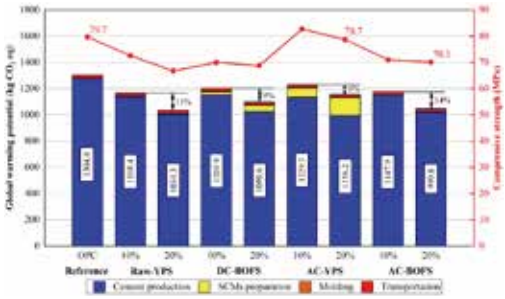

Fig. 1 System boundaries of this study; **Fig. 2** Midpoint assessment of DC and AC of YPS and BOFS; **Fig. 3** Comparison of normalized endpoint assessment results related to DC and AC of YPS and BOFS; **Fig. 4** GWP and 28-day compressive strengths for blended cement pastes.

Acknowledgment

This work was supported by National Natural Science Foundation of China (NSFC) (Research Fund for International Senior Scientists) [Grant number: 52250710158].

Reference

Shao, X., Mehdizadeh, H., Li, L., Ling, T.-C., 2022. Life cycle assessment of upcycling waste slag via CO_2 pre-treatment: Comparative study of carbonation routes. J. Clean. Prod. 378, 134115. https://doi.org/https://doi.org/10.1016/j.jclepro.2022.134115

Recovery of vaterite $CaCO_3$ from recycled concrete fines for use in profiting the cementitious properties of cement pastes

Hamideh Mehdizadeh[1*], Tung Chai Ling[1#]

[1] College of Civil Engineering, Hunan University, Changsha 410082, Hunan, China

[*]*Presenter: hamideh.mehdizadeh@gmail.com,* [#]*Corresponding author: tcling@hnu.edu.cn*

Abstract

In recent decades, rapid urbanization in China has increased the need to demolish and replace old buildings. As a result, a considerable amount of construction and demolition (C&D) waste is generated, accounting for more than one-third of global C&D waste generation. Currently, annual C&D waste production in China is about 1.8 billion tones with a recycling rate of <10%. Concrete waste is the major constituent (approximately 65%) of C&D waste, and techniques have been developed to recycle concrete waste into recycled concrete aggregates. However, high amount of very fine particles (<150 μm) was produced during the recycling process. Hence, this study proposes a two-stage leaching-carbonation process to recover high-purity of vaterite $CaCO_3$ from recycled concrete fines (RCF) (Fig. 1), and utilize in the cement paste at different water-to-cement ratios (w/c ranging from 0.4 to 0.6) so as to explore their performance at fresh and hardened stages.

The experimental results showed that the maximum Ca^{2+} leaching rate of 65.7% can be achieved under the optimal leaching conditions (2 mol/L NH_4Cl solution, liquid to solid ratio of 10 mL/g, 85 °C, and for 60 min). Also, 615 g of spherical vaterite $CaCO_3$ (1-10 μm) with a purity of 97.8% (Fig. 2) can be successfully synthesized from 1 kg of RCF by injecting CO_2 into the leachate containing 1 mol/L NH_4OH at 25 °C and 0.025 MPa for 30 min. Meanwhile, the high-purity vaterite $CaCO_3$ could be used as an additive in accelerating the hydration rate of cement paste and improving the mechanical strength. The addition of vaterite $CaCO_3$ in cement paste can shorten the setting time (Table 1) by about 2 hours, but revealed a different impact on the flowability of cement (Fig. 3). The acceleration of cement hydration could be related to the increase in the nucleation sites provided by vaterite particles and the synergetic effect of Cl^- ions existed in the vaterite $CaCO_3$. The decrease in the flowability of the cement mixture could be related to a significant increase in the wetting surface associated with the porous vaterite particles with a large specific surface area, resulting in the increase of water demand and subsequent decrease of the amount of excess water. Moreover, mechanical test results (Fig. 4) demonstrated that the compressive strengths of cement paste increased with the addition of vaterite $CaCO_3$, regardless of the w/c. Increase of w/c slightly enhanced the later age strength of cement paste, reflecting that vaterite particles are more effective in densifying the pore structure of cement paste with 0.6 w/c. The thermal analysis results (Fig. 5) revealed that vaterite $CaCO_3$ promotes the hydration process of cement paste, i.e. more hydration products, such as C-S-H gel, ettringite (Ett) and monocarboaluminate (Mc), were formed owing to the nucleation effect of $CaCO_3$, which made the denser cement paste with better mechanical properties. The proposed approach provides a green solution for CO_2 fixing and RCF recycling in the construction industry and offers a promising method for improving the hydration and mechanical properties of cement paste.

Keywords: Recycled concrete fines; Vaterite $CaCO_3$; Leaching-carbonation process; Fresh and hardened properties; Cement paste; Water-to-cement ratio (w/c).

Fig. 1

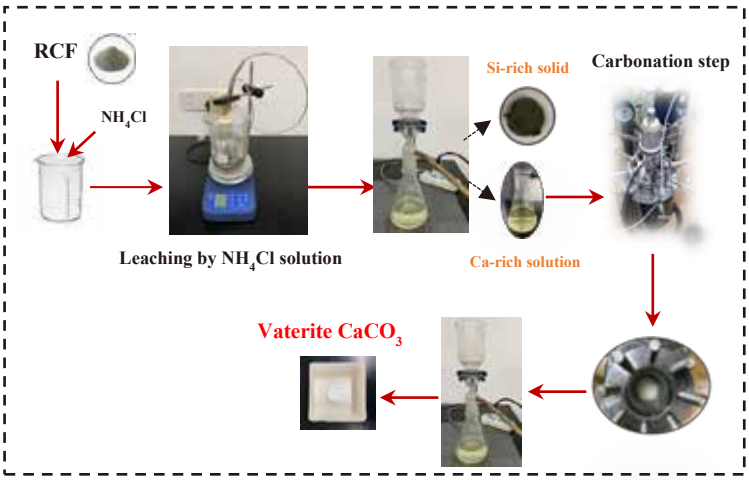

Fig. 2

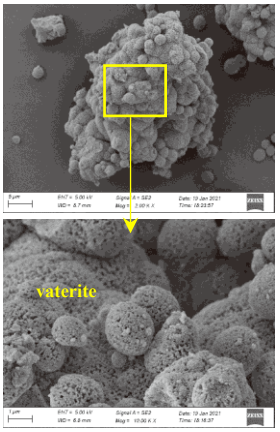

Table 1.

Sample	w/c	Initial setting time (hr)	Final setting time (hr)
Pure OPC	0.4	4.45	5:34
OPC + 3% vaterite		3:13	4:02
Pure OPC	0.5	6:19	7:33
OPC + 3% vaterite		4:13	5:02
Pure OPC	0.6	7:18	8:24
OPC + 3% vaterite		5:32	7:07

Fig. 3

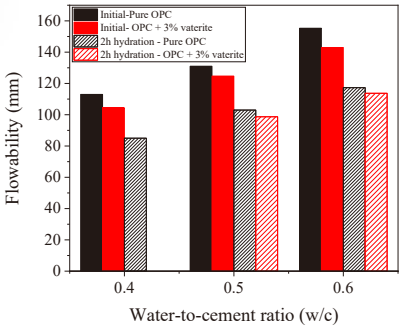

Fig. 4

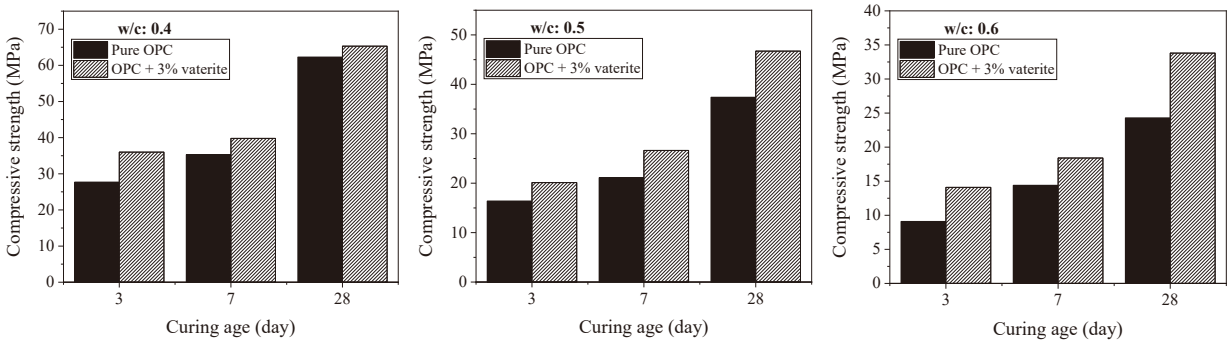

Fig. 5

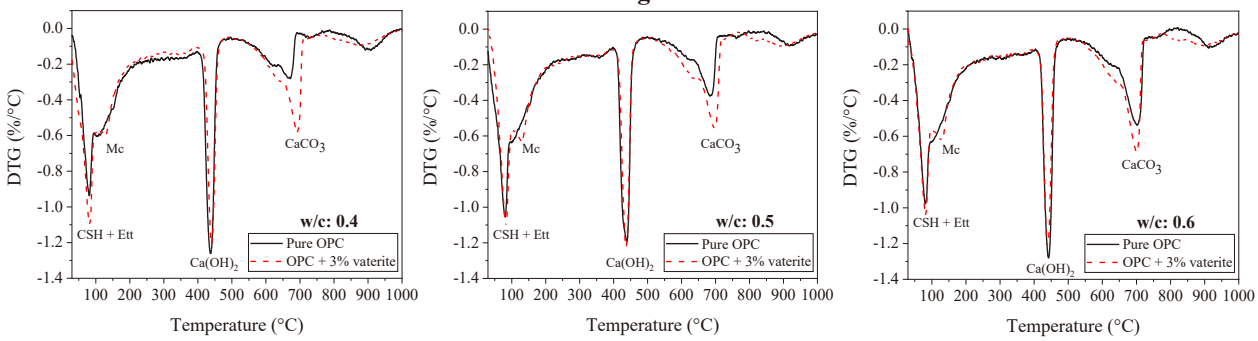

Fig. 1 Illustration of leaching-carbonation process; **Fig. 2** Polymorph and morphology of synthesized vaterite $CaCO_3$ [1]; **Fig. 3** Effect of vaterite $CaCO_3$ on the flowability of fresh and 2-h hydrated cement paste; **Fig. 4** Effect of w/c and vaterite $CaCO_3$ on 3-, 7- and 28-day compressive strength of cement paste; **Fig. 5** DTG curves of 28-day cement paste samples; **Table 1** Setting time of cement paste samples.

Acknowledgment

The authors would like to acknowledge the funding support from the National Natural Science Foundation of China (NSFC) (grant No. 51950410584 & 52250710158).

References

[1] Mehdizadeh, H., Mo, K.H., Ling, T.C., 2023. CO_2 fixing and recovery of high-purity vaterite $CaCO_3$ from recycled concrete fines. Resour. Conserv. Recycl., 188, 106695.

Carbonation characteristics of BOFS aggregate and properties analysis of carbonated pure BOFS blocks

Qifeng Song[1*], Tung-Chai Ling[1#], Ming-Zhi Guo[2]

[1] College of Civil Engineering, Hunan University, Changsha, Hunan, China.

[2] College of Mechanics and Materials, Hohai University, Nanjing, Jiangsu, China.

**Presenter:* qfsong@hnu.edu.cn, #*Corresponding author:* tcling@hnu.edu.cn

Abstract

To increase the use of basic oxygen furnace slag (BOFS), this study aims to prepare pure BOFS blocks using BOFS powder (<75 μm) and aggregate (<5 mm) as raw materials. BOFS aggregates were first subjected to carbonation through two distinct methods (dry carbonation and slurry carbonation). Then, three types of BOFS aggregates (two carbonated aggregates and fresh aggregates) mixed with BOFS powders were pressed into blocks and have a dry carbonation. (Fig.1).

Characterization of the carbonated aggregate revealed that the dry carbonated aggregates contained less $CaCO_3$ than the slurry carbonated specimens, but had more $Mg(OH)_2$ and residual $Ca(OH)_2$ (Fig.2). This was caused by the difference in solubility of Ca and Mg under different moisture contents.

Subsequently, the properties of pure BOFS blocks prepared with different BOFS aggregates were investigated. Compared with blocks prepared from fresh BOFS aggregate (SAB), blocks prepared with two types of carbonated BOFS aggregates exhibited higher CO_2 absorption and displayed continued strength growth during the subsequent standard curing process (Fig.3). This was because the $CaCO_3$ produced from BOFS powder carbonation in SAB obstructed the contact between the aggregates and the diffused CO_2, and a denser microstructure also reduced the residual CO_3^{2-}/HCO_3^- in the pore solution. Despite a lower level of carbonate formation, the SAB still exhibited the highest compressive strength (Fig.4). This was attributed to the co-carbonation of the powder and aggregate, which effectively reinforced the ITZ. The bonding between the carbonated aggregate and the paste was hindered by the carbonate layer formed on the surface of the aggregate, resulting in a porous structure (Fig.5). Conversely, the presence of larger pores was conducive to CO_2 absorption and thereby increase the potential of subsequent improvements in mechanical properties. Findings from this study have the potential to facilitate the utilization of BOFS as an eco-friendly material in the field of construction, paving the way for its wider adoption and integration into the construction industry.

Keywords: BOFS aggregate; Carbonation; Block; CO_2 absorption; ITZ

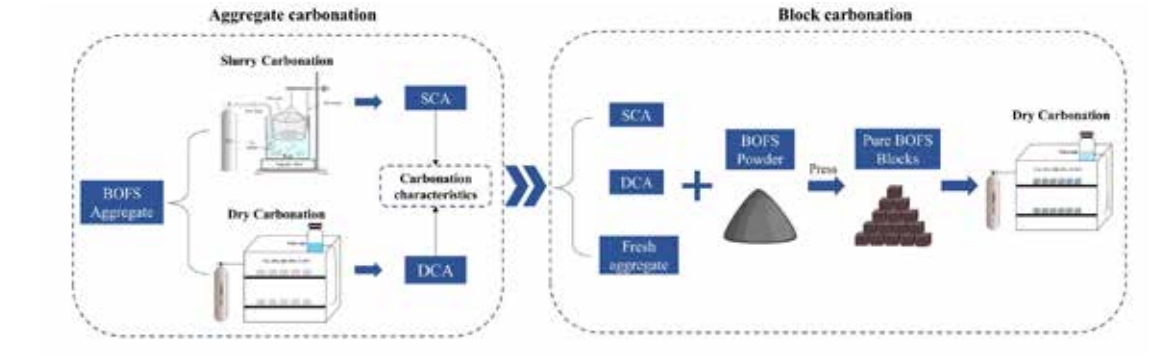

(1)

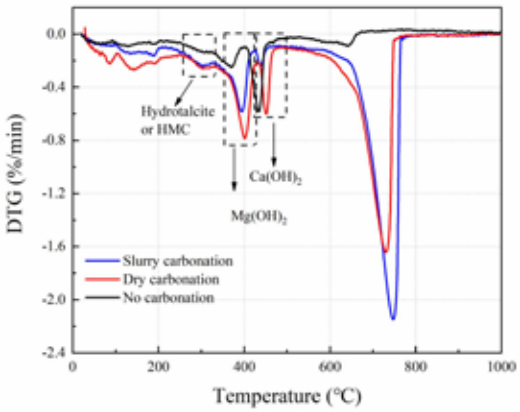

(2)

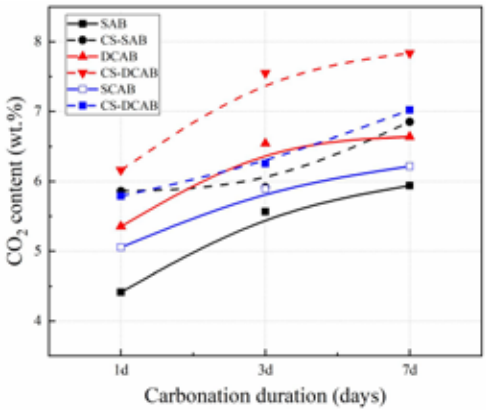

(3)

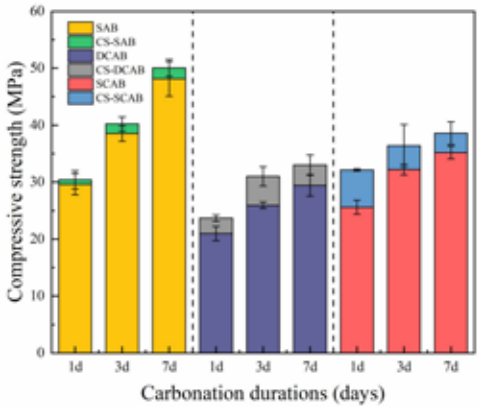

(4)

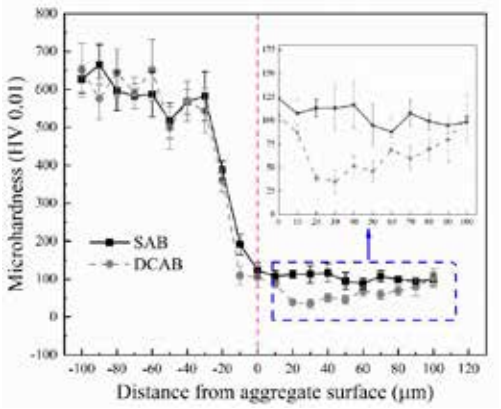

(5)

Fig.1 Process schematic diagram of this study. (SCA presents slurry carbonated BOFS aggregate; DCA presents dry carbonated BOFS aggregate) **Fig.2** Differential thermogravimetry of the raw and carbonated BOFS aggregate; **Fig.3** CO_2 content of carbonated BOFS blocks (SAB presents blocks prepared from fresh BOFS aggregate, DCAB presents blocks prepared from dry carbonated aggregate, SCAB presents blocks prepared from slurry carbonated aggregate, CS presents subsequent standard curing to 28 days); **Fig.4** Compressive strength of BOFS blocks; **Fig.5** Microhardness of the SAB and DCAB.

Acknowledgment
This work was supported by National Natural Science Foundation of China (NSFC) (Research Fund for International Senior Scientists) [Grant number: 52250710158].

Effect of early carbonation and hydration on high temperature performance of cement blocks

Zhe Yu[1*], Ming-Zhi Guo[2], Tung-Chai Ling[1#]

[1] College of Civil Engineering, Hunan University, Changsha 410082, Hunan, China
[2] College of Mechanics and Materials, Hohai University, Nanjing 210098, Jiangsu Province, China.

[*]Presenter: yuzhe@hnu.edu.cn, [#]Corresponding author: tcling@hnu.edu.cn

Abstract

Early-age carbonation can accelerate the curing process of cement-based materials. This technology holds several benefits, such as improved engineering properties and CO_2 capture, and thereby garners increasing attention from academics and industry experts with an aim to further develop low-carbon construction materials. Previous studies well demonstrate that proper and complete hydration after early-age carbonation curing is crucial for the development of mechanical properties at a later age and beneficial for the recovery of pH in maintaining the long-term durability of concrete.

In this study, the effect of early carbonation coupled with further standard curing (CS) on the performance of cement blocks subjected to different high temperatures was investigated. The change in mechanical properties was investigated in terms of residual compressive strength and microhardness. The impact of elevated temperatures on microstructure evolution was also analyzed using backscattered electron microscopy and thermogravimetric analysis.

The experimental results showed that the strength of all samples increased after exposure to 200 and 400°C (Fig. 1), owing to the fact that heating temperature can accelerate the hydration of unreacted clinker (Fig. 2). In addition, the micro-hardness continuously increased before 400°C, which was associated with the dehydration of calcium silicate hydrate (C-S-H) (Fig. 3). However, compared to those cured with single carbonation (C) or standard curing (S), the cement pastes with CS curing showed a higher residual compressive strength and thermal stability with a lower apparent cracking at 600°C. The microstructure results revealed that the $CaCO_3$ skeleton prevented matrix cracking by restricting the range of volume shrinkage of the C-S-H gels. Meanwhile, the C-S-H formed after carbonation adhered to the $CaCO_3$ skeleton after dehydration, which further enhanced the skeleton system (Fig. 4). However, the carbonated layer was transformed to a weaker layer when $CaCO_3$ was decomposed into lime at 800°C, resulting in a 70% loss (e.g., CS curing samples) in compressive strength. This study successfully develops a novel method for simultaneously ensuring good residual mechanical properties and maintaining the integrity of cement-based materials at elevated temperatures.

Keywords: Early-age carbonation; Further hydration; Elevated temperature; Cement paste; Calcium Carbonates

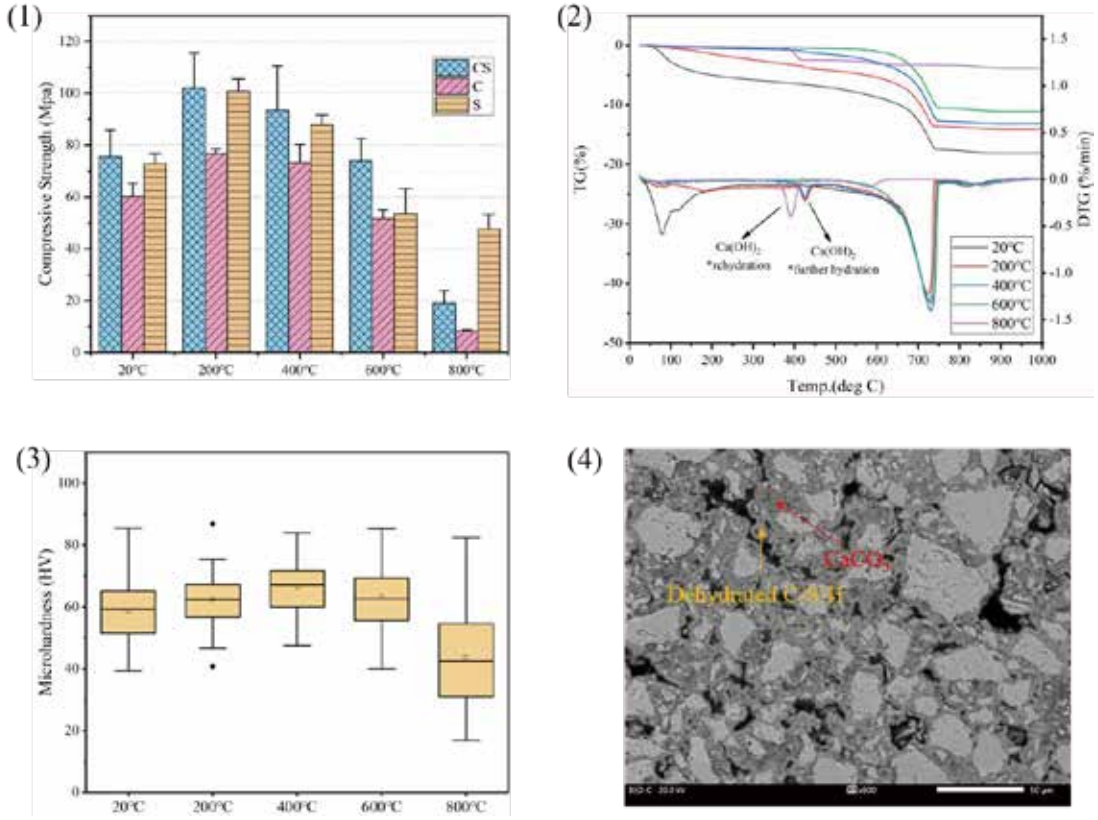

Fig. 1 Relative strength of cement blocks before and after being subjected to high temperatures; **Fig. 2** TG and DTG curves of CS sample before and after exposed to elevated temperatures; **Fig. 3** Micro-hardness values of CS sample across the depth of the sample before and after being subjected to high temperatures; **Fig. 4** BSE images of CS sample after exposed to elevated temperatures of 600°C.

Acknowledgment

The authors would like to acknowledge the funding support from the National Natural Science Foundation of China (NSFC) (grants no. 52078202), the Natural Science Foundation of Jiangsu Province (BK20221503), and Jiangsu Province Department of Science and Technology (BE2022605).

Parallel Sessions-6

FRP/Fibre Textile-Reinforced Cementitious Composites

Development of 3D printable ECC and its bio-mimetic flexural members

Jiangtao Yu[1*], Junhong Ye[2] and Kequan Yu[3]

[1, 2] Department of Disaster Mitigation for structures, Tongji University, Shanghai, China
E-mail: yujiangtao@tongji.edu.cn, 1710745@tongji.edu.cn, 12kequanyu@tongji.edu.cn

Abstract

3D concrete printing (3DCP) is gaining more and more attentions due its easy operation, quick construction, and low labour cost. However, there still remains challenges to embed longitudinal reinforcement into printed concrete during the printing process. This study aims to develop a self-reinforced concrete (i.e., engineered cementitious composites, ECC) with appropriate printability and superior tensile strain capacity for 3DCP.

To obtain the mix proportion of printable ECC, the printability and mechanical properties of ECC were tailored by changing the dosage of water reducer and replacing silica sand with different volume fractions of crumb rubber, respectively. Based on the developed proportion, the workability of the ECC was quantitatively evaluated by jumping table tests and consistency tests at different open times. As shown in Fig.1, the optimal open time interval was determined as 5~35 min, the corresponding spreading diameter and penetration depth were 49~162 mm and 53~80 mm, respectively.

A series of tensile tests and compressive tests under different loading directions were carried out to explore the hardened propertyies of printed ECC. The tensile and compressive stress-strain curves are plotted in Fig. 2 and Fig.3, respectively. It was found that the printing process showed negative effect on the fiber orientations of printed ECC, resulting in decreased tensile properties. The average tensile strength and strain capacity of printed ECC were 5.75 MPa and 7.54%, respectively. The printed ECC exhibited enhanced compressive strength than the mold-cast ECC. The compressive strength of printable ECC ranged from 36.7 MPa to 44.6 MPa.

Based on the developed printable ECC, a series of bio-mimetic flexural members with no reinforcement were designed for four-point bending tests, including nacre-inspired beams, hollow-assembling beams, and hollow-assembling slabs. The results indicated that all the printed members exhibit multiple cracking, flexural hardening, and ductile failure mode despite the absence of longitudinal reinforcement, as shown in Figs. 4~6. The deflection-span ratio of all printed beams and slabs exceeded 1/50 at the ultimate state. This article preliminarily confirmed the feasibility of using ECC to achieve 3D printed structure without longitudinal reinforcement.

Keywords: 3D concrete pinting, Bio-memitic, Engineered cementitious composites, Four-point bending test.

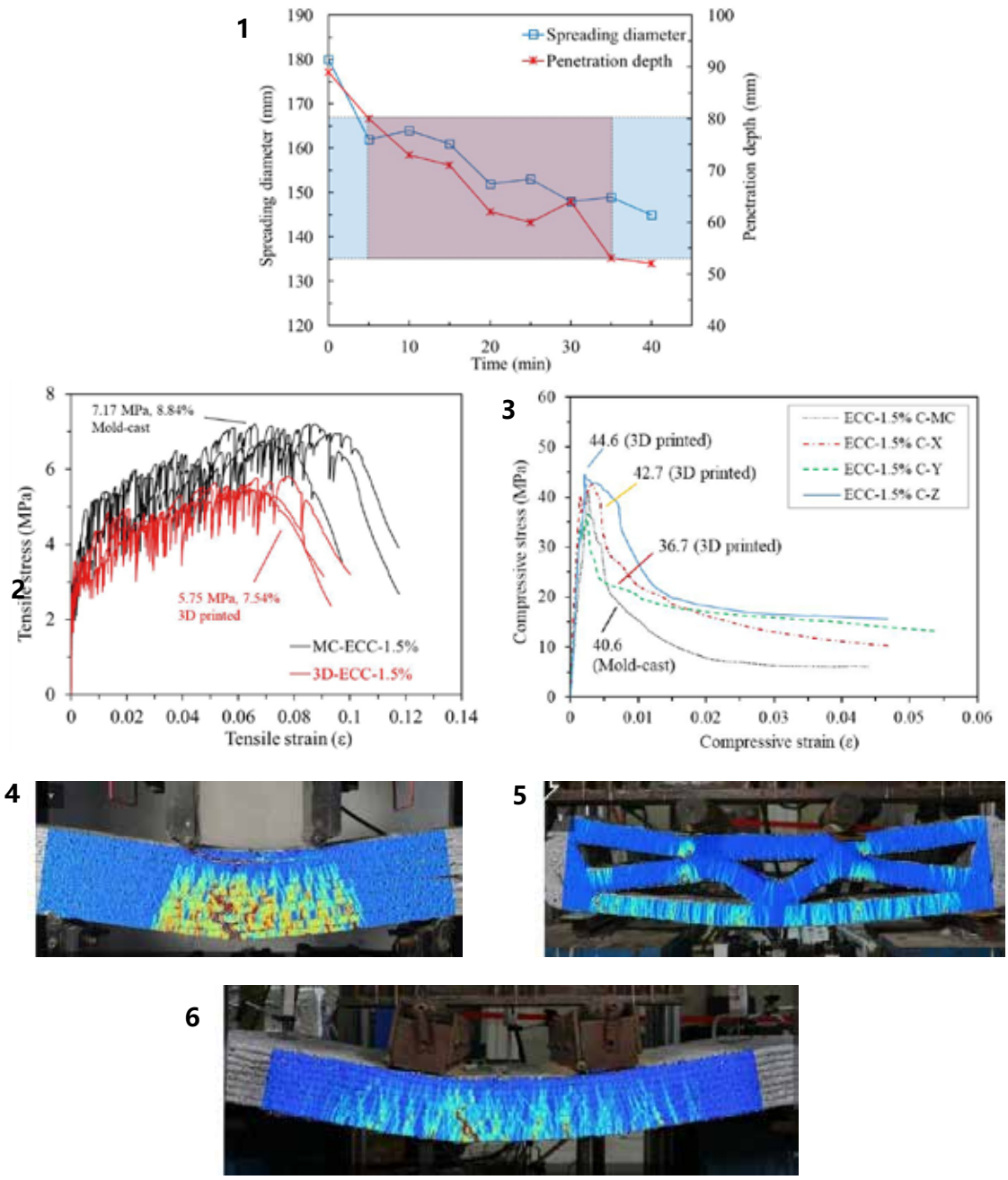

Fig. 1 Spreading diameter and penetration depth of printable ECC under different open times, **Fig. 2** Tensile stress-strain curves of mold-cast and printed ECC, **Fig. 3** Compressive stress-strain curves of mold-cast ECC and printed ECC under different loading directions, **Fig. 4** Crack pattern of nacre-inspired beam, **Fig. 5** Crack pattern of hollow-assembling beam, **Fig.6** Crack pattern of and hollow-assembling slab.

Acknowledgment

The authors gratefully acknowledge to the National Natural Science Foundation of China (No. 51778461 and 51978504) and Shanghai Municipal Science and Technology Commission (No. 19DZ1202500).

Axial Behavior of CFRP Grid Confined Concrete

Yi Tao[1,2*], Dan Wang[1]

[1] School of Civil Engineering, Xi'an University of Architecture and Technology, Xi'an, China
[2] State Key Laboratory of Green Building in Western China, Xian University of Architecture and Technology, Xi'an, China

E-mail: y.tao@xauat.edu.cn

Abstract

This paper introduces an experimentally study on the axial behaviour of CFRP grids confined concrete cylinders. Total of thirty concrete cylinders were received different CFRP confinement configurations and tested under a monotonic compression loading. The test variables include the CFRP grids layers, concrete strengths and CFRP confinement configurations. The preferred confinement configuration was eventually determined and the effects from the main variables were investigated.

The test results showed that CFRP grids confinement can provide a superior ductility performance to the ordinary concrete. However, the grid structure leads to a moderate increase in the axial compressive strength of confined cylinder. Excellent results on both strength and ductility improvements can be achieved by providing the combination confinement of CFRP grid and CFRP strips. It is also found that the results from the CFRP grid-CFRP strips configuration was better than the CFRP strips-CFRP grid configuration.

The existing stress-strain model were reviewed in order to determine one rational and accurate model for the confinement behaviour with softening. A stress-strain model for moderate confinement, such as CFRP grid confinement, was proposed. The performance of the proposed model were evaluated by comparing to the test data.

Keywords: CFRP grid, CFRP strips, Confinement, Concrete, Constitutive model.

Fig.1

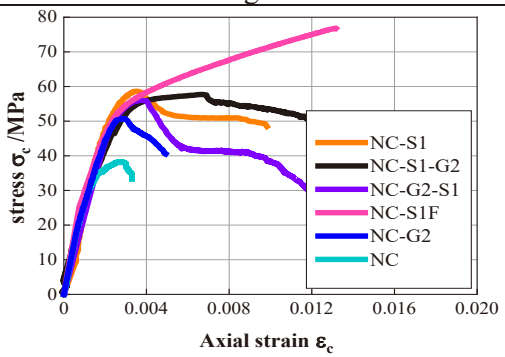

Fig.2

Fig.1 The failure modes of different confinement configurations

Fig.2 Axial stress-strain behaviour of different confinement configurations

Acknowledgment

The authors gratefully acknowledge to the National Natural Science Foundation of China (No. 51978567) and Collaborative Innovation Center Project of ShaanXi Provincial Department of Education (21JY025).

Bending Tests of Corroded RC Continuous Beams Strengthened with ICCP-SS Dual-Function Retrofitting System

Feng R[1*], Tang JP[2], Liu PP[3] and Zhu JH[4]

[1, 2, 3] School of Civil and Environmental Engineering, Harbin Institute of Technology, Shenzhen, CHINA
E-mail: fengran@hit.edu.cn, tangjingpu629@outlook.com, 19b954016@stu.hit.edu.cn
[4] College of Civil and Transportation Engineering, Shenzhen University, Shenzhen, CHINA
E-mail: zhujh@szu.edu.cn

Abstract

This paper presents an experimental study on the flexural behavior of reinforced concrete (RC) continuous beams strengthened by carbon-fabric reinforced cementitious matrix (C-FRCM) in impressed current cathodic protection-structural strengthening (ICCP-SS) system. A total of five continuous beams were subjected to in-plane asymmetric loading. The influences of the layers of carbon fiber mesh in the C-FRCM plates and further use of U-shaped wrapping as end anchorage were carefully investigated. The failure modes, flexural bearing capacities, load-deflection curves and ductilities of the specimens were fully discussed. In addition, the influence of electrification on the fiber deterioration in C-FRCM plates under the ICCP-SS system was observed by scanning electron microscope (SEM). The complete crack development patterns, the crack widths and the deflections of the beams were obtained by digital image correlation (DIC) system, which are evaluated according to the existing concrete design criteria. The experimental results show that ICCP-SS dual-function retrofitting system can effectively improve the yield and ultimate loads of continuous beams, but there is still a debonding problem at the interface between C-FRCM and concrete. Adding U-shaped wrapping as end anchorage of C-FRCM plates can effectively avoid this problem and give full play to the reinforcing effect of C-FRCM, thus further enhance the flexural behavior of continuous beams. It is worth mentioning that the maximum crack widths of the strengthened beams are significantly lower than the calculated values, which proves that ICCP-SS dual-function retrofitting system provides good crack width control.

Keywords: Asymmetric loading, C-FRCM, Continuous beam, Corroded, ICCP-SS.

Local compressive behavior and seismic performance of ECC ring beam connection

Dong Bingqing[1]*, Xu Li[2] and Pan Jinlong[2#]

[1] Key Laboratory of Building Structural Retrofitting and Underground Space Engineering, Shandong Jianzhu University, Ministry of Education, Jinan, China.
[2] Key Laboratory of Concrete and Prestressed Concrete Structures of Ministry of Education, Southeast University, Nanjing, China.
*Presenter: dongbingqing21@sdjzu.edu.cn, #Corresponding author: cejlpan@seu.edu.cn

Abstract

Concrete filled steel tube (CFST) composite columns have been extensively investigated and employed because of their high ultimate bearing capacity and ductility. The design of the beam-to-column connections have significant effect on the mechanical performance and safety of a CFST composite frame structure. However, limited research can be found on the connection between a CFST composite column and a reinforced concrete (RC) beam. Recently, a new type of RC ring beam connection has been recently proposed linking the CFST composite column and RC beam. The RC ring beam connection has a definite force transfer mechanism and greatly simplifies the construction process. However, due to the disconnection of the steel tube, the compressive behaviour of the ring beam connection is one of the most important factors that affect the mechanical performance, and the load carrying capacity inevitably decreases for this kind of connection.

To reduce the damage degree and ensure the connection zone have a sufficient strength for safely transferring the load from the CFST composite column, a novel through-beam ECC ring beam connection, which is designed for linking an CFST composite column (ECC-encased CFST column) and RC beam, is proposed (Fig. 1). The steel tube in the ECC-encased CFST column is completely interrupted and the RC ring beam connection is replaced by an ECC ring beam connection. The ECC ring beam connection consisted of a core region and a ring beam encircling it. Several stirrups and circumferential steel reinforcements were used inside the encircling ring beams. Due to the superior high ductility of ECC ring beam which can provide persistent lateral restraint to the joint core region, introducing ECC in the ring beam connection region is effective to improve the load carry capacity under local compressive loading, as well as control the crack width of the ring beam connection. Meanwhile, additional longitudinal bars in the connection anchored into the outer ECC layer of the column are designed to transfer the axial force and bending moment from the column. Both the enhanced ring beam connection and the additional longitudinal bars make the connection zone have sufficient strength for safely transferring the load from the CFST composite column. More importantly, due to the interruption of the steel tube, ECC is cast continuously in the frame beam end and the ring beam connection zones, and the longitudinal steel bars in the frame beam can pass through the connection zone directly. The force transfer mechanism of the bending moment and shear force from the frame beam is definite, similar to that of the normal RC structures. It is well known that the connection region is subjected to high shear stress. Stirrups arranged in the core region are useful to restrain the ECC and participate in joint shear resistance. Also, the shear capacity of the proposed connection is expected to be improved by the excellent shear resistance of the ECC ring beam under reversed cyclic loading.

To investigate the compressive behaviours of ECC ring beam connections, local compressive tests on 15 ring beam connections with various matrix type, width ratio, height-to-width ratio and reinforcement ratio are reported. According to the test results, ECC connections showed a higher load carrying capacity and more ductile behaviour than regular concrete connections. Compared with concrete ring beam connections, the displacement

ductility of the ECC ring beam connections was improved by 25.7% to 62.2%. The energy dissipation of the ECC connection specimens was 1.5 and 1.7 times larger than that of the concrete connections, respectively. The test results also indicated that the width ratio had the greatest impact on delaying cracking in the ECC connection. Increasing the reinforcement ratio can efficiently increase the peak load. Increasing the width ratio resulted in an obvious increase in the energy dissipation of the ECC ring beam connections.

To investigate the seismic behaviours of ECC ring beam connections, seven ring beam connection specimens, including two concrete specimens and five ECC specimens, with different reinforcement ratios, ring beam sizes and axial compression ratios, were tested under reversed cyclic loading. The seismic performance of the proposed connection was evaluated in terms of failure mode, hysteresis characteristics, stiffness degradation, ductility and energy dissipation. Based on the test results, introducing ECC in ring beam region resulted in a higher load bearing capacity, ductility and energy dissipation than those observed for concrete specimens. The relative reinforcement ratio had a significant effect on the failure modes of the ECC connections. Additionally, the increase in the circumferential reinforcement ratio and joint size have favourable influences on the seismic behaviours of ECC connections. These test results verified the potential applications of ECC material in ring beam connections for ECC-encased CFST columns.

Keywords: ECC; ECC-encased CFST column; Beam-column connection; Local compression; Seismic resistance.

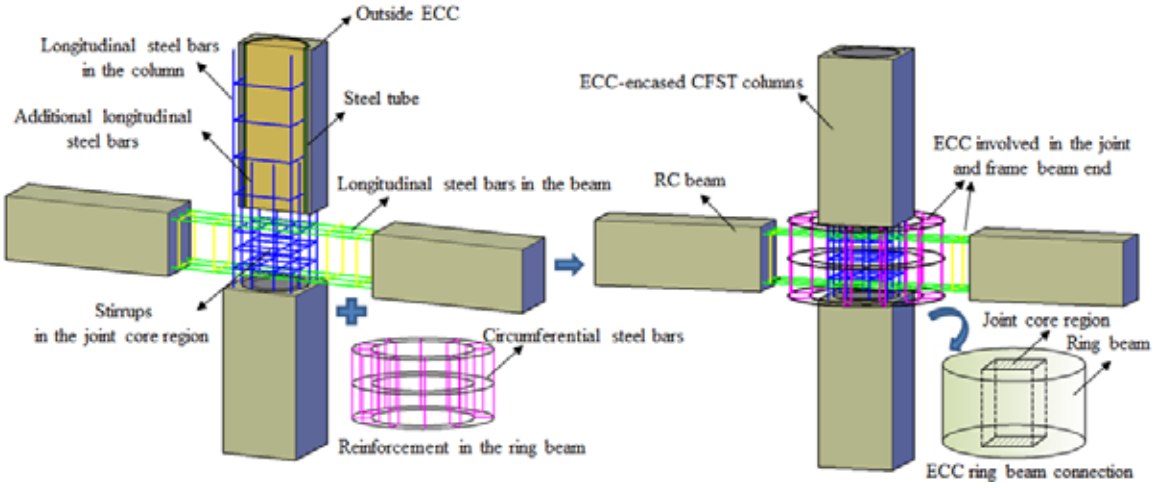

Fig. 1. The proposed ECC ring beam connection.

Acknowledgment

This work was supported by National Natural Science Foundation of China (NO.51778131), and Shandong Provincial Natural Science Foundation (NO.ZR2021QE052).

Fire resistance performance of concrete-filled steel tubular column protected by FRCR-ECC

Yan Xiong [1*], Lin Kairen[2] and Shuai Fang [3]

[1] State Key Laboratory of Subtropical Building Science, South China University of Technology , Guangzhou, China
E-mail: xyan@scut.edu.cn
[2,3] School of Civil Engineering and Transportation, South China University of Technology, Guangzhou, China
E-mail: 942612501@qq.com, 251069160@qq.com

Subjected to environmental impact, or seismic load even service load, the traditional fire insulation material will be easy to cracking or even drop off from protected substrate, due to low tensile strength, limited ductility and poor bonding with anti-corrosion primers. Deteriorated protection is supposed to an impair or even totally loss of fire insulation capacity.

In this paper, a lightweight, high ductility (Fig. 1) fire-resistive and corrosion-resistive engineered cementitious composites (FRCR-ECC) suitable for spraying (Fig. 2) was developed for the protection of concrete filled steel tubular (CFST) columns. Lightweight fly ash cenosphere (FAC) was added to the matrix as artificial defect. FAC reduces the matrix density and thermal conductivity (Fig. 3), and also activates the development of fine multi-cracks in the ECC and makes the cracks width less than 50 μm (Figure 4). These help to prevent the transfer of high external temperature to the interior of the structure and effectively resists the ingress of corrosive media. According to the requirements of the GB14907-2018 Fireproof Coatings for Steel Structures, the bond strength of FRCR-ECC to steel substrate was tested. The results show that FRCR-ECC has good bonding performance with steel (Fig. 5).

In this paper, the finite element software ABAQUS was used to analyse and simulate the fire test of CFST columns without fire coating and with FRCR-ECC protection. The temperature field distribution of CFST columns with the protection of different thickness FRCR-ECC subjected to four-side fire (Fig. 6) and vertical deformation-time curve (Fig. 7) were obtained. When the CFST column with axial compression ratio of 0.51 suffered fire for 240 minutes, temperature of steel tube wall without fire coating is 1142℃, temperature of steel tube wall with 30 mm thick FRCR-ECC protection is 607℃, and the case of 40 mm thick FRCR-ECC protection is 512℃. With a certain axial compression ratio, the section temperature of CFST column decreases significantly with the increase of FRCR-ECC layer thickness. Fire resistance of CFST column without fire coating is only 29 minutes, that of the column with 30 mm thick FRCR-ECC protection is 246 minutes, and that of the column with 40 mm thick FRCR-ECC protection is more than 250 minutes. The fire resistance of CFST columns with FRCR-ECC protection is significantly improved, which is more than 240 min, and fully meets the 1-Class fire resistance requirement.

The fire test of CFST column with FRCR-ECC protection under constant load heating condition would be carried out to investigate the effect of protective coating thickness and load ratio on fire resistance of the column, and the results would be compared with those of finite element analysis.

Keywords: concrete filled steel tubular, engineered cementitious composites, fireproof and anti-corrosion integrated protective performance, high ductility.

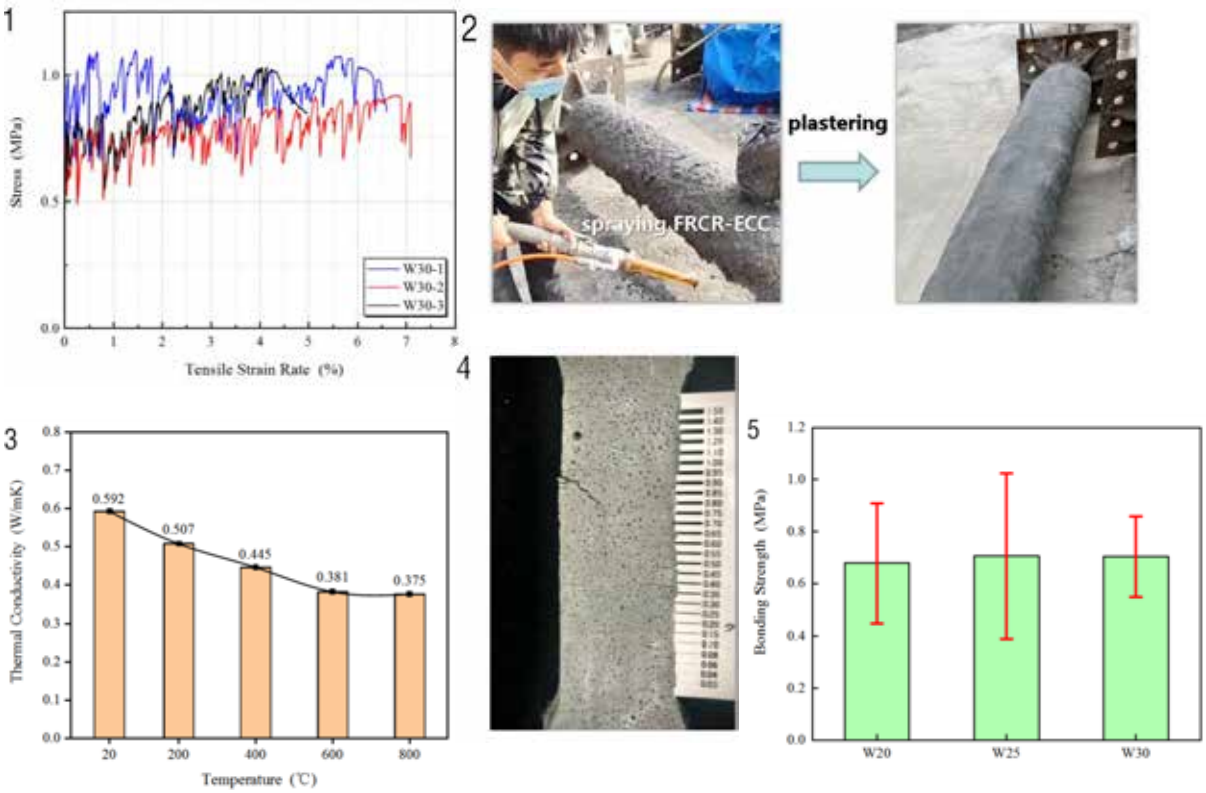
1
Stress (MPa)
Tensile Strain Rate (%)
W30-1
W30-2
W30-3
2
spraying FRCR-ECC
plastering
3
Thermal Conductivity (W/mK)
0.592
0.507
0.445
0.381
0.375
Temperature (℃)
4
5
Bonding Strength (MPa)
W20
W25
W30

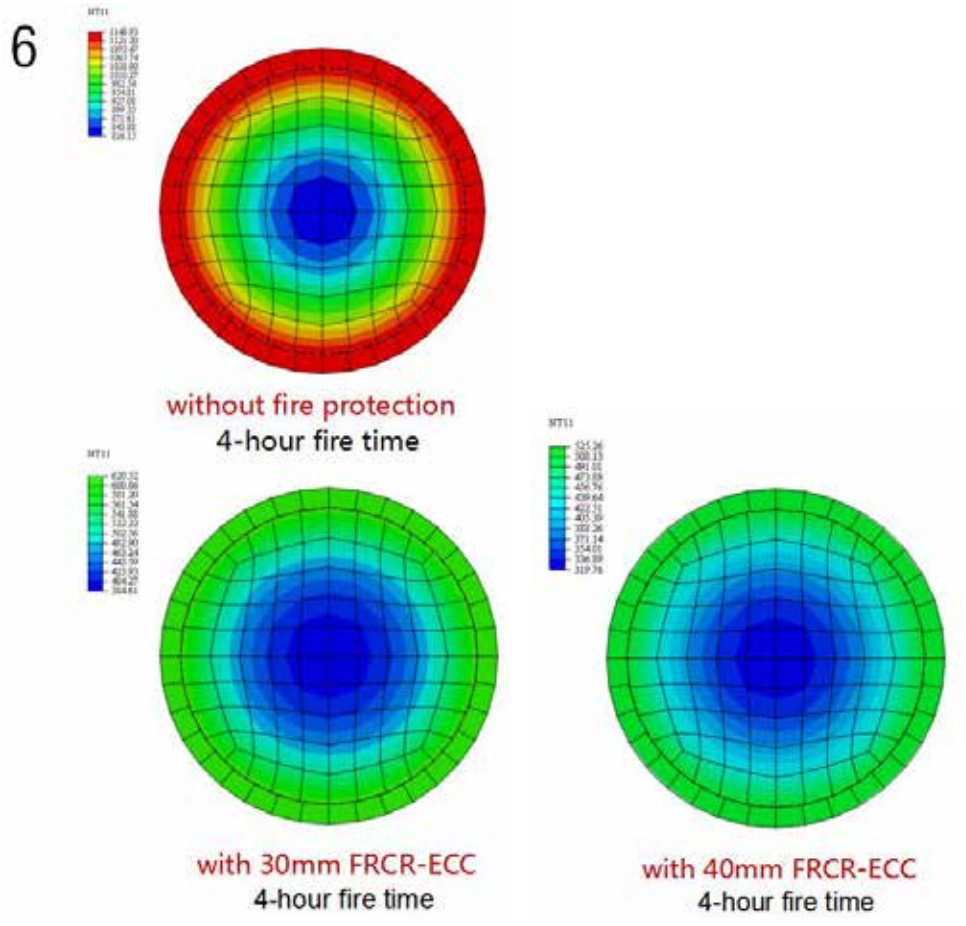
6
without fire protection
4-hour fire time
with 30mm FRCR-ECC
4-hour fire time
with 40mm FRCR-ECC
4-hour fire time

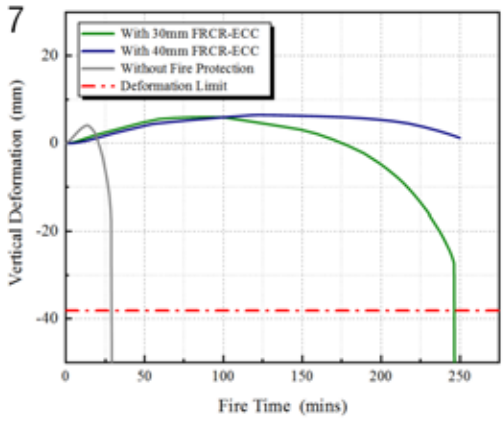

Fig. 1 Stress-ultimate tensile strain rate curve of dog bone specimens; **Fig. 2** Spraying and plastering of FRCR-ECC; **Fig. 3** Thermal conductivity test results of FRCR-ECC; **Fig. 4** Development of fine multi-cracks of FRCR-ECC; **Fig. 5** Bond strength test results of FRCR-ECC; **Fig. 6** Temperature field distribution of CFST columns with the protection of different thickness FRCR-ECC in fire environment; **Fig. 7** Vertical deformation-time curve of CFST columns with the protection of different thickness FRCR-ECC in fire environment.

Bonding mechanism between FRP rebar and self-compacting concrete: a multiscale investigation

Renyuan QIN[#], Bo DI, Yu ZHENG*

School of Environment and Civil Engineering, Dongguan University of Technology, Dongguan, CHINA
E-mail: qinry@dgut.edu.cn, dibo@dgut.edu.cn, zhengy@dgut.edu.cn

Abstract
The bonding performance between fiber reinforced polymer (FRP) rebar and concrete is one of the critical issues that affect the structural performance of FRP reinforced concrete elements. Self-compacting concrete (SCC) has been demonstrated as an alternative material to native to enhance the bonding with FRP rebar with refined interfacial transition zone (ITZ) between FRP rebar and matrix. Owing to the different material morphology, the bonding mechanism between FRP rebar and SCC could be different from that of normal concrete, which has not been understood comprehensively. In this study, the bonding performance between FRP rebar and SCC is investigated through direct pull-out tests coupled with acoustic emission techniques. The AE signal strength exhibited a good correlation with the bond-slip relationship measured in each specimen. Based on the AE location technique, the invisible non-uniform distribution of bonding stress along the bar was further revealed. Moreover, the mesoscale finite element analysis (FEA) has been conducted to illustrate the damage initiation and development between FRP rebar and SCC. The contribution of chemical adhesion, friction, and mechanical interlocking toward the bonding performance between FRP rebar and concrete is revealed through acoustic emission analysis and FEA. The findings from current study provide fundamental understanding on the bonding mechanism between FRP and concrete materials, which can be further adopted in the material design of FRP reinforced concrete structures for better bonding performance.

Keywords: FRP rebar; SCC; bonding performance; multiscale analysis

*: *Presenter*; #: *Corresponding author*

Bending behaviour of corroded RC continuous beams with C-FRCM strengthening system

Ran Feng[1], Panpan Liu[2*], Jingzhou Zhang[3], Fangying Wang[4], Yin Xu[5], Ji-Hua Zhu[6#]

[1, 2, 5] School of Civil and Environmental Engineering, Harbin Institute of Technology, Shenzhen, Guangdong 518055, People's Republic of China
[3] School of Civil Engineering, Guangzhou University, Guangzhou,Guangdong 510006, People's Republic of China
[4] Department of Civil Engineering, University of Nottingham, Nottingham, England NG7 2RD, United Kingdom
[6] College of Civil and Transportation Engineering, Shenzhen University, Shenzhen, Guangdong 518060, People's Republic of China
[*]*Presenter: 19b954016@stu.hit.edu.cn*, [#]*Corresponding author: zhujh@szu.edu.cn*

Abstract

The durability of reinforced concrete (RC) has always been one of the major concerns in construction, especially for offshore or coastal engineering where the RC structures are prone to long-term erosion of chloride salts. Fiber reinforced cementitious material (FRCM) strengthening technology can effectively solve the durability problem of corroded RC structures. This paper presents a numerical investigation into the bending behaviour of strengthened RC continuous beams, considering interface performance (Fig. 1). The numerical load-displacement curves (Fig. 2), failure modes (Fig. 3) and moment redistribution values of the RC beams in the loading process are validated against those obtained from experiments. After parametric study and evaluation of flexural capacity according to codes, it can be concluded that the carbon-fabric reinforced cementitious matrix (C-FRCM) strengthening system as a strengthening method is feasible for RC beams and finite element analysis (FEA) can effectively predict the failure mode and strengthening performance of specimens.

In view of the member ductility discussion, the ductility of RC beam retained well with one or two layers of carbon-fabric (CF) mesh (Fig. 4), yet the combination of the C-FRCM plate and the U-shaped wrapping as the end anchorage is more effective than the C-FRCM plate only. The increase of the layer of CF mesh in the C-FRCM plate or U-shaped wrapping will enhance the strengthening effect (Fig. 5).

Given the parametric study on 35 supplemented FEA models of RC beams, the effectiveness of C-FRCM strengthening system is verified and demonstrated. The theoretical flexural capacities of RC beams with C-FRCM strengthening system are assessed according to the existing codes and compared with those obtained from numerical analyses.

By evaluating the flexural capacity of RC beam with C-FRCM strengthening system, the design formula for flexural capacity of RC beam is proposed by introducing the correction factors that considered the layer of CF mesh and U-shaped wrapping as well as degree of corrosion of steel bar. The modified calculation method for Bulletin 14 can provide more accurate estimation on RC beams considering the effects of the layer of CF mesh and U-shaped wrapping, and the degree of corrosion of steel bar.

Keywords: Carbon-Fabric Reinforced Cementitious Matrix (C-FRCM), Continuous Beam, Finite Element Analysis (FEA), Interface Performance, U-Shaped Wrapping.

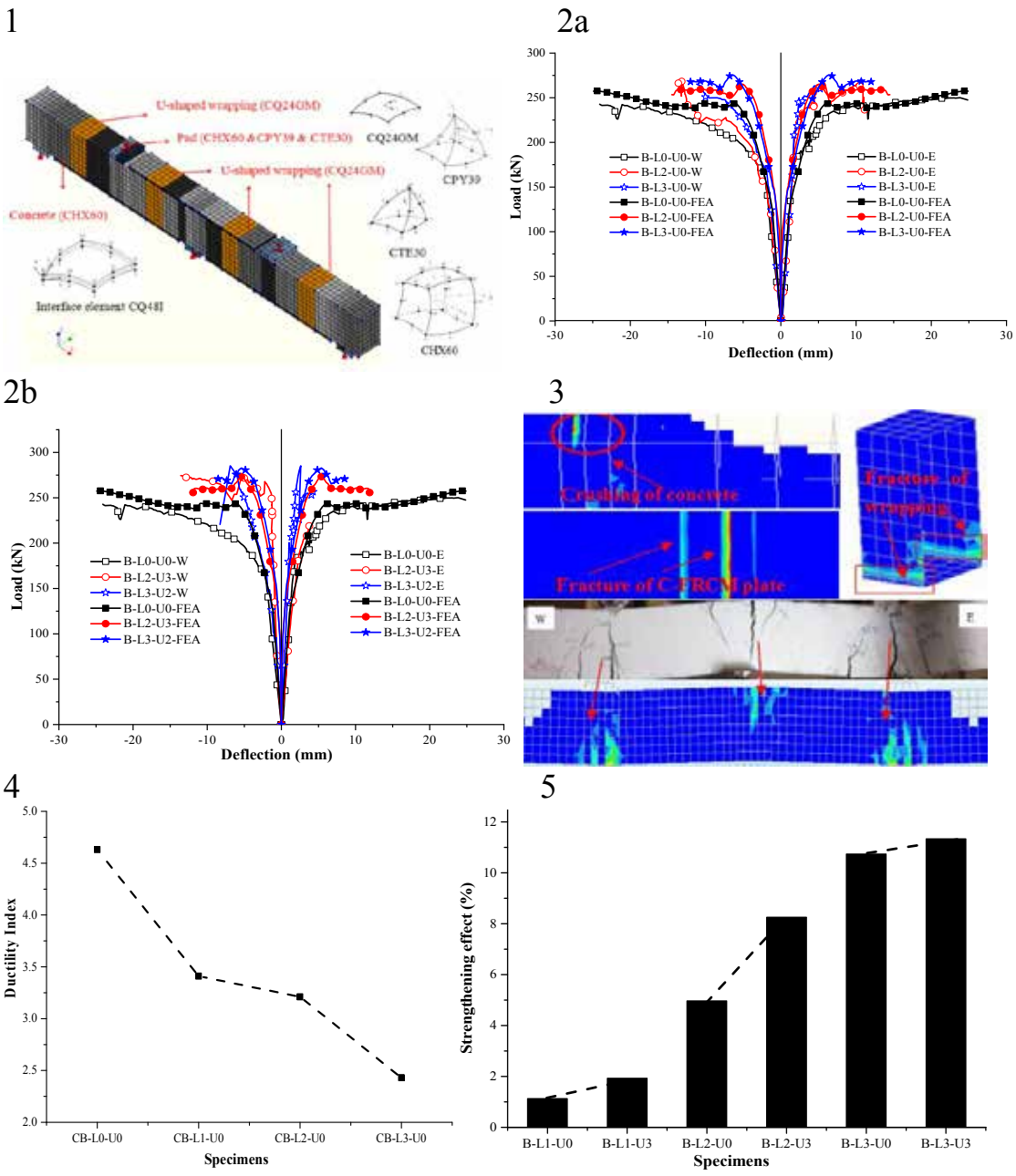

Fig. 1 Finite element model of RC continuous beam; **Fig. 2** Comparison and validation of load-deflection curves of the specimens; **Fig. 3** Failure modes of numerical simulation; **Fig. 4** Comparison of specimen ductility under different layers of CF mesh; **Fig. 5** Influence of U-shaped wrapping on the strengthening effect

Acknowledgment

The authors are grateful for the financial support from Key-Area Research and Development Program of Guangdong Province (Grant No. 2019B111107002), National Key Research and Development Program of China (Grant No. 2018YFE0124900), National Natural Science Foundation of China (Grant Nos. 52178131/51538007/51778370/51861165204), Shenzhen Science and Technology Program (Grant No. GXWD20201230155427003-20200804174353001).

Seismic behavior of engineered cementitious composites coupling beams with low aspect ratio

Zuan-Feng Pan[1*], Yong Li[2], Dong Cao[1]

[1] *State Key Lab of Disaster Reduction in Civil Engineering, Tongji University, Shanghai 200092, China;*
[2] *School of Civil Engineering, Hebei University of Science and Technology, Shijiazhuang 050018, China*
[*]*Presenter: zfpan@tongji.edu.cn*

Abstract

Diagonally reinforced concrete coupling beams have good ductility due to the shear resistance of diagonal bars, however, substantial reinforcement detailing is required in the beam, which may lead to bars congestion problems and construction difficulties. In order to improve the seismic performance of coupling beam with small span-to-depth ratio, engineered cementitious composites (ECC), which is a high toughness composite material with pseudo strain hardening behavior and multiple cracking characteristics, can be used to replace conventional concrete. Compared with ordinary concrete, ECC has a higher shear capacity, which can reduce the amount of diagonal bars. The end of the diagonal bars can be bent horizontally and extended into the wall pier, which is beneficial to assembly construction.

The pseudo-static tests of diagonally reinforced ECC beams, one ordinary reinforced ECC beams and one diagonal reinforced concrete coupling beams were carried out. The variable parameters were stirrup ratio, diagonal reinforcement ratio, types of layout of reinforcement, material of matrix, types of fibers and connection mode between the coupling beam and the wall pier. The seismic performance of the coupling beam, such as failure mode, hysteresis curve, displacement ductility, stiffness degradation and energy dissipation capacity were analyzed. Results showed that with the increase of stirrup ratio and diagonal reinforcement ratio, the shear capacity and ductility of the coupling beam increase gradually. Compared with the concrete coupling beam, the use of ECC in the matrix can improve the shear capacity and ductility of the beam, reduce the damage to the beam, which is easy to repair after earthquake. Compared with PVA fibers, using PE fibers as matrix materials can improve the strength, stiffness, ductility and energy dissipation capacity of coupling beam, reduce the amount of diagonal bars, and facilitate assembly construction. Diagonally reinforced ECC beams have higher shear capacity, ductility and energy dissipation capacity compared with conventionally reinforced ECC beams. The seismic performance of the coupling beam, which is connected to the wall piers with grouting sleeves, is excellent. It should be pointed out that the U-shaped reinforcement is needed to be added at the interface of the beam and the wall pier to improve the connection performance.

The averaged principal stress-strain relationships in the MCFT and local stress conditions at crack locations for ECC were modified based on the characteristics of ECC. When the coupling beam cracks, the fiber bridging action on the crack plane is considered. Considering the arch effect and the compatibility deformation between the truss model and the arch model, the formula for calculating the shear capacity of conventionally reinforced ECC coupling beam is proposed. Then, a formula for calculating the shear capacity of the diagonally reinforced ECC coupling beam was proposed. Based on the calculation results, the variation of the shear forces of diagonal ECC strut-and-tie, diagonal reinforcement and sub-struts with the span-to-depth ratio of the coupling beeam is given.

Keywords: Engineered Cementitious Composite; coupling beam; low aspect ratio; seismic performance; shear strength

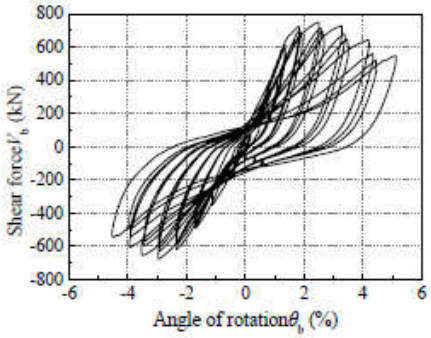

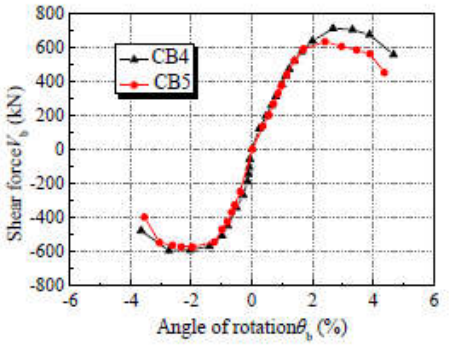

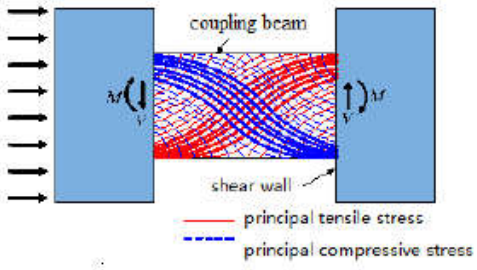

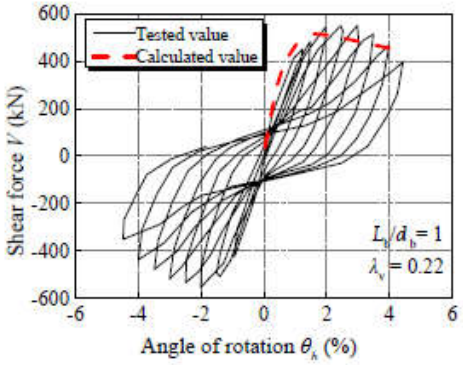

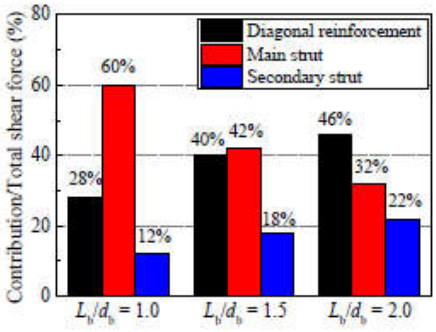

Fig. 1 Hysteretic responses of typical ECC specimen; **Fig. 2** Skeleton hysteresis curve of Specimen CB4 and CB5; **Fig. 3** Principal stress trace distribution of coupling beam; **Fig. 4** Comparison of calculated and tested values; **Fig. 5** Contribution to shear versus aspect ratio

Acknowledgment

The authors acknowledge the funding supports of the National Natural Science Foundation of China (Grant No. 52078368).

Experimental and numerical investigation on the dynamic behavior of RC bridge columns confined with CFRP/ECC subjected to truck collision

Wen-Wei Wang, Chang Zhou
Department of Bridge engineering, School of Transportation, Southeast University, Nanjing, Jiangsu 210089, People's Republic of China
**Presenter: wenweiwang@seu.edu.cn, #Corresponding author: wenweiwang@seu.edu.cn*

Abstract

Reinforced concrete (RC) bridge columns are susceptible to vehicle collisions. To enhance the impact resistance of RC bridge piers, a composite material composed by Carbon Fiber Reinforced Polymer (CFRP) grid and Engineered Cementitious Composites (ECC) is employed to strengthen RC column. Laboratory tests on cantilever RC column and CFRP/ECC confined RC column subjected to lateral horizontal impact are carried out. Test results showed that CFRP/ECC has a significant effect in limiting the development of shear cracks and improving the shear capacity of RC column (Fig. 1).

Detailed finite element (FE) model of the laboratory tests is established and the response CFRP/ECC confined column under impact loading is predicted with the FE model. Numerical results indicated that the impact force, displacement and failure mode of CFRP/ECC confined column could be well predicted by the finite element model (Fig. 2). Furthermore, ECC confined columns were prone to shear failure, while CFRP/ECC confined columns are more likely to suffer an overall failure at the footing of the column.

With the validated FE method, high-resolution FE model of truck-bridge collision scenarios are established. Numerical analysis is carried out to compare post-impact damage of RC column and column confined with CFRP/ECC. The results demonstrate that CFRP/ECC has a significant effect on decreasing the tension stress of longitudinal reinforcements (Fig. 3) and reduce the damage level caused by flexural and shear cracks (Fig. 4). Moreover, CFRP grid and ECC has a significant influence on the dynamic shear capacity of columns, while weight of engine and impact velocity of truck are the key factors that affecting the dynamic shear demand. Finally, empirical equations for calculating dynamic shear capacity and shear demand of CFRP/ECC confined RC piers subjected to truck collision are proposed and the shear mechanism of confined piers is also clarified.

Keywords: Reinforced Concrete Column; CFRP grid; ECC; Impact Response; Truck-bridge Collision

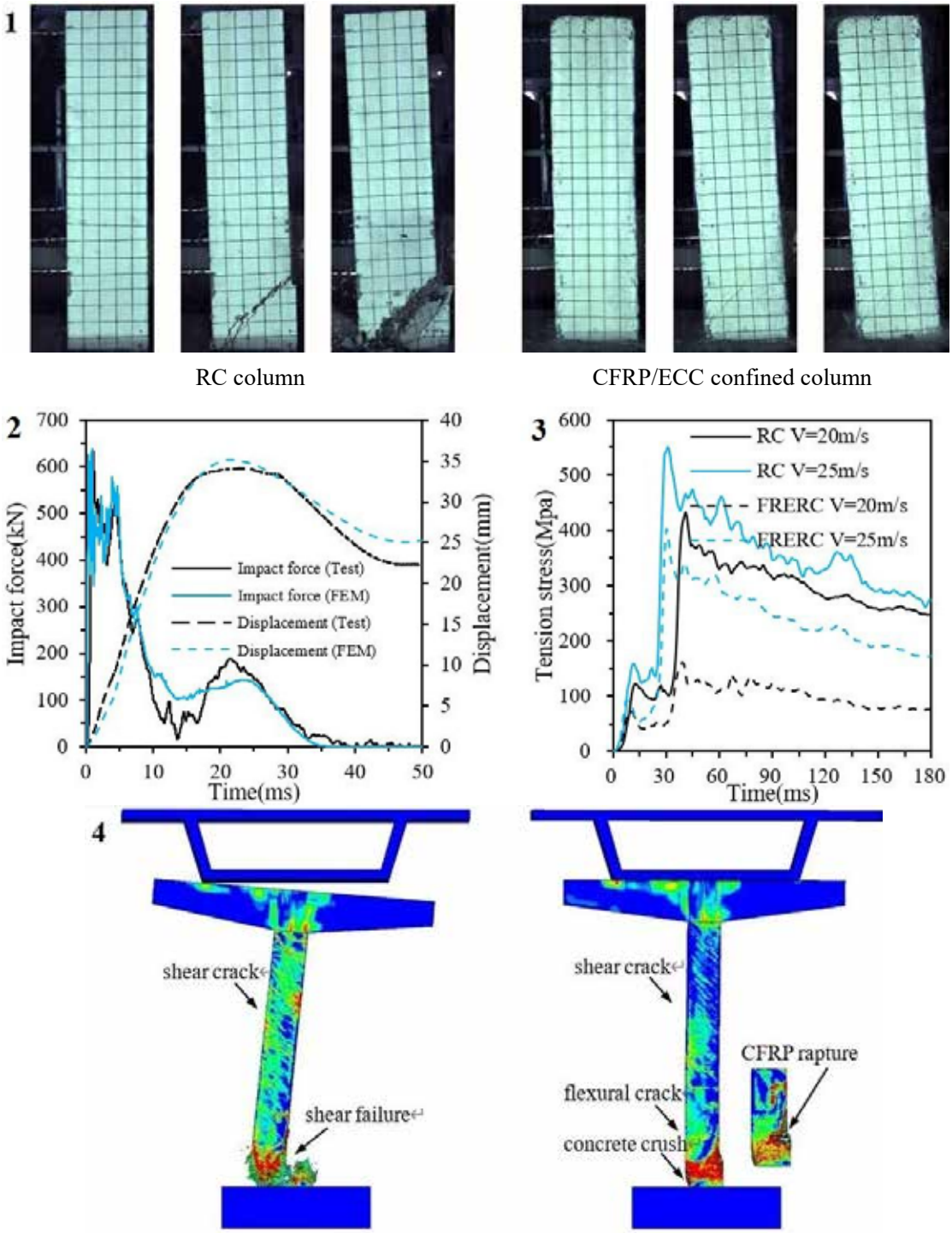

Fig. 1 Failure process of RC column and CFRP/ECC confined column; **Fig. 2** Comparison of experimental and numerical impact force and displacement; **Fig. 3** Comparison of longitudinal reinforcement tension stress belonging to RC column and CFRP/ECC confined column; **Fig. 4** Comparison of post-impact damage of RC column and CFRP/ECC confined column;

Acknowledgments

The authors would like to acknowledge the funding support from the National Natural Science Foundation of China (Grant No:51578135, 51878156) and Postdoctoral Fund of

Jiangsu Province (No. 2018K087B)

Creep behavior of hybrid FRP-concrete-steel double-skin tubular columns under sustained loading

Guangming Chen[1*], Cheng Zhao[1] and Pan Xie[2]

[1] School of Civil Engineering and Transportation, South China University of Technology, Guangzhou, China
[2] College of Water Conservancy and Civil Engineering, South China Agricultural University, Guangzhou, China

E-mail: guangmingchen@scut.edu.cn

Abstract

Hybrid FRP-concrete-steel double-skin tubular member (FCS DSTM) is a new type of composite structural member consisting of outer FRP tube, inner steel tube and concrete filled in between. The DSTM is featured by a number of salient characteristics, such high load-carrying capacity, easy construction and excellent corrosion resistance. Although the short-term behavior of DSTMs has been extensively investigated and based on which design/analysis methods have been developed, their long-term behavior, especially the creep behavior under sustained loading, has not yet been studied by the research community. In recent years, the authors' research group has successfully implemented the application of DSTMs in bridge piers, bridge girders and arch bridges. Under this background, the research into the long-term behavior of DSTMs has become an urgent need in terms of both research significance and engineering applications. This lecture introduces a recent study carried out on the creep behavior of the FCS double-skin tubular columns (FCS DSTCs) under sustained loading. Effects of a number of parameters, including concrete type (normal concrete and self-compacting concrete), loading time, thickness of GFRP tubes and steel tubes, loading methods, as well as shear studs and internal steel reinforcements, have been investigated.

The test results showed that compared with plain concrete column and concrete-filled FRP tubes (CFFT), the creep strain of DSTCs is appreciably smaller. It was found that the creep coefficient is much less than1.0 for most of the specimens when the axial compression ratio is between 0.3 to 0.4. It was also found that deployment of shear studs and/or internal steel reinforcements has a favorable effect on reducing the creep strain. The DSTCs, after being subjected to sustained loading for about 230 days, were then tested under axial compression load, and it was found that the compression behavior, including failure mode, load-carrying capacity and deformation capacity, as well as the initial axial stiffness and GFRP cracking load, remains nearly unchanged. The test results suggest that when the axial compression ratio is low (0.3-0.4), the effects of creep on the compressive behavior of DSTCs are marginal.

Keywords: DSTC, Creep behavior, Self-compacting concrete, Compressive behavior, GFRP tube.

Fig.1 The test set-up for studying creep behavior of DSTCs

Acknowledgment

The authors gratefully acknowledge to the National Natural Science Foundation of China (No. 51978281).

Structural behavior of ECC link slabs strengthened with GFRP reinforcement

Lifei Zhang[1,2], Yu Zheng[1,*], Lipeng Xia[1]

[1] School of Environment and Civil Engineering, Dongguan University of Technology, Dongguan 523808, China, People's Republic of China
[2] The College of Mechanics and Materials, Hohai University, Nanjing 211100, People's Republic of China
Presenter: zhengy@dgut.edu.cn, #Corresponding author: zhengy@dgut.edu.cn

Abstract

A majority of high-way bridges are composed of multiple-span steel or prestressed concrete girder simply supported at piers. those expansion joints are designed to protect the substructure from exposure to corroding substances by provided watertight seal between the adjacent bridge decks over piers and abutments. However, it is well reported that the mechanical joints are expensive to install and maintain. Deterioration of traditional mechanical expansion joints significantly affects the durability of bridge structures (Fig. 1).

A possible approach to solve the durability problem and reduce the high cost of maintenance in expansion joints is the elimination of mechanical deck joints in multi-span bridges. One type of jointless bridge design proposed by a number of researchers is the application of link slab elements within bridge decks (Fig. 2). Engineered cementitious composites (ECC) have been proposed as an expansion joint material that can eliminate the joints in bridge decks. The ECC link slab concept was developed based on the high ductility and tight crack-width in ECC materials for structural application. ECC link slab was designed to resist an expected moment due to end rotations of the adjacent decks. As a result of the moment demand and restrictions on the working stress of the reinforcement, which was limited to 40% of the yield strength, the link slab was heavily reinforced and consequently did not behave as a joint. Due to this high reinforcement percentage generally used, the resulting large bending stiffness of the link slab and consequently the negative moment generated in the joint are undesirable effects and deserve additional consideration.

Glass fiber reinforced polymer (GFRP) has been utilized in the ECC link slabs for joint-less bridge due to the light weight, high tensile strength, non-corrosive and nonmagnetic properties. According to correct researches, GFRP bars reinforced ECC link slab has greater deformation capacity and smaller stiffness. In this paper, six full-scale ECC link slabs (Fig. 3) reinforced with GFRP bars were cast and tested under monotonic cyclic loading (Fig. 4). The parameters included reinforcement diameter and ECC fiber volume.

The proposed link slabs demonstrated sufficient flexibility to meet the current design protocols (Fig. 5). The diameter of GFRP bar has a significant influence on the deformation stiffness of the link slab. It is due to the link slab are mainly subjected to tensile deformation. The volume of ECC fibers has limited effect on the deformation stiffness at the initial stage of deformation. The link slab has small crack width, which can meet the limitation of the crack width of 0.1mm (Fig. 6). Simultaneously, it is beneficial to improve the deformability of link slab.

The sensitivity analysis of parameters based on linear finite element models were constructed (Fig. 7). ECC fiber volume, depth-span ratio and reinforcement ratio of such link slabs should not exceed 2.4%, 8% and 1.2%. Link slab debonding length should be larger than 4% of span

length of bridge to obtain low bending stiffness. This research may further lead to the diversified and integrated application of GFRP reinforced ECC link slab for jointless bridge.

Keywords: Link slabs; Engineered cementitious composites; Glass fibre reinforced polymer; Structural behavior; Nonlinear finite element; Sensitivity analysis

1

2

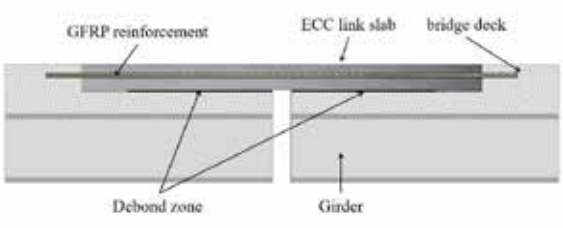

3

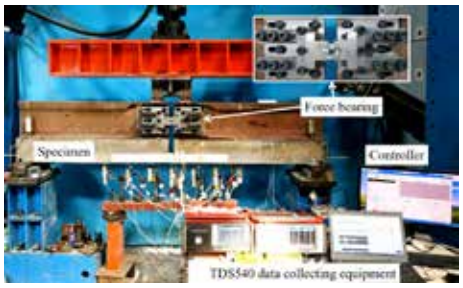

4

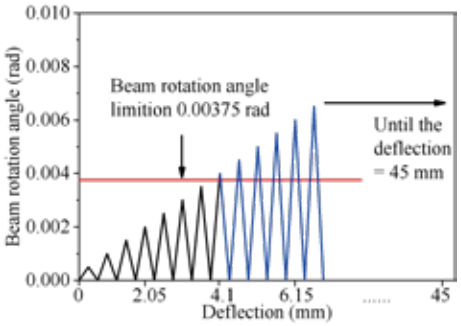

5

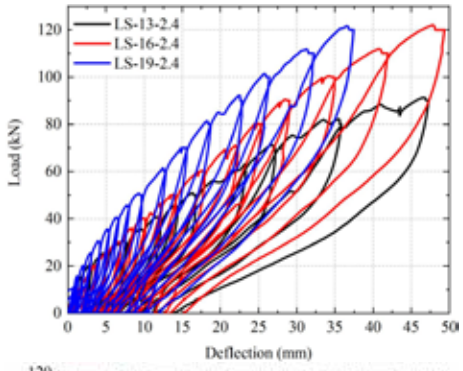

6

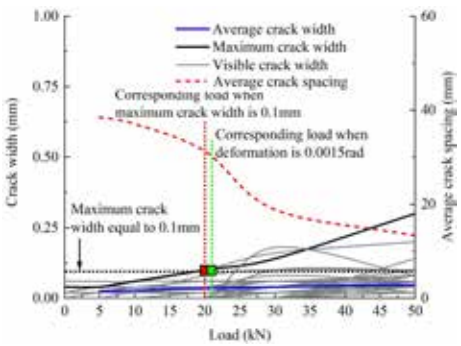

7

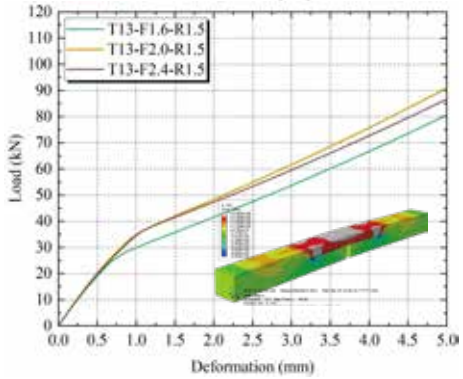

8

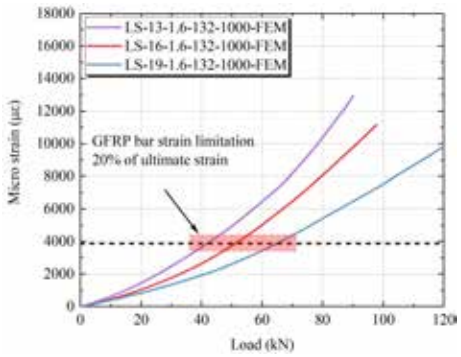

Fig. 1 Traditional expansion joint damage; **Fig. 2** GFRP reinforced ECC link slab for jointless bridge; **Fig. 3** Experimental equipment of link slab; **Fig. 4** Loading sequence used in this study; **Fig. 5** Response of load vs. deflection at midspan under monotonic load; **Fig. 6** Crack development of link slab; **Fig. 7** Sensitivity analysis of link slab; **Fig. 8** The micro-strain development process of link slab;

Acknowledgment
The authors would like to acknowledge the funding support from the Guangdong Science and Technology Planning (2021A0505110016).

Compressive behavior of UHPC under active confinement

S.S. Zhang[1*], J.J. Wang[1], Guan Lin[2], T. Yu[2], D. Fernando[3]

[1] School of Civil and Hydraulic Engineering, Huazhong University of Science and Technology, Wuhan, China.
[2] Department of Civil and Environmental Engineering, The Hong Kong Polytechnic University, Hung Hom, Kowloon, Hong Kong, China.
[3] School of Engineering, University of Edinburgh, Scotland, EH9 3FG, United Kingdom.

[*]*Presenter:* shishun@hust.edu.cn, [#]*Corresponding author:* shishun@hust.edu.cn

Abstract

As promising cementitious composite materials with excellent mechanical properties and durability, Ultra-high performance concrete (UHPC) and ultra-high performance fiber reinforced concrete (UHPFRC) have attracted worldwide attentions in both research and practice. While the uniaxial compressive and tensile properties of UHPC/UHPFRC has been investigated by a large number of research groups, their behavior under multiaxial stresses has not been well exposed and has been in an urgent necessity to meet the large potential engineering demand of UHPC/UHPFRC.

Against the above background, an experimental study on the triaxial compressive behavior of UHPC and UHPFRC under active confinement (i.e., under a combined axial compression and lateral hydraulic pressure) was conducted by the authors, with investigated variables including the level of lateral hydraulic pressures, steel fiber volume fraction, and uniaxial compressive strength of UHPC/UHPFRC. It was observed in the tests that a sharp diagonal major crack occurred in all UHPC and UHPFRC specimens during the loading process (as shown in Fig. 1). It was also found that an increase in the lateral hydraulic pressure led to a smaller inclined angle (with respect to horizon) of the diagonal crack and a smaller diagonal crack width.

The obtained typical axial stress-axial strain curves and lateral-to-axial strain curves are shown in Figs. 2 and 3 respectively. The stress-strain curves of UHPC and UHPFRC specimens generally have three branches: an ascending first branch up to the peak stress point (ε_{cc}, f_{cc}); a descending branch after the peak stress; and a third branch which is much flatter (i.e., the stresses reduced much more gradually) than the second branch or even with a residual stress plateau. The UHPFRC specimens generally possess a more gradual stress reduction for the second branch compared with the UHPC specimens, indicating the beneficial effects of steel fibers on the ductility of concrete. In addition, it can be seen that the steep descending second branch of UHPC specimens is little affected by the pressure; however, the increase in pressure evidently reduces the slope of the descending second branch of UHPFRC specimens.

Existing models developed for normal strength concrete failed to predict the axial stress-strain behavior of UHPC and UHPFRC subjected to triaxial compression; new axial stress-strain models were therefore proposed in the present study. In addition, a new equation was proposed for the prediction of the lateral-to-axial strain relationship of UHPC and UHPFRC specimens.

Keywords: Ultra-high performance concrete (UHPC); ultra-high performance fiber reinforced concrete (UHPFRC); active confinement; compressive behavior

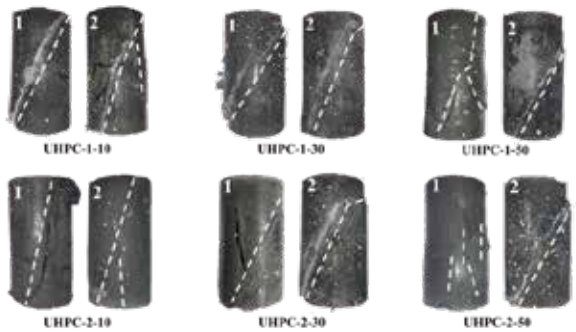

Fig. 1 Failure modes of UHPC specimens under triaxial compression

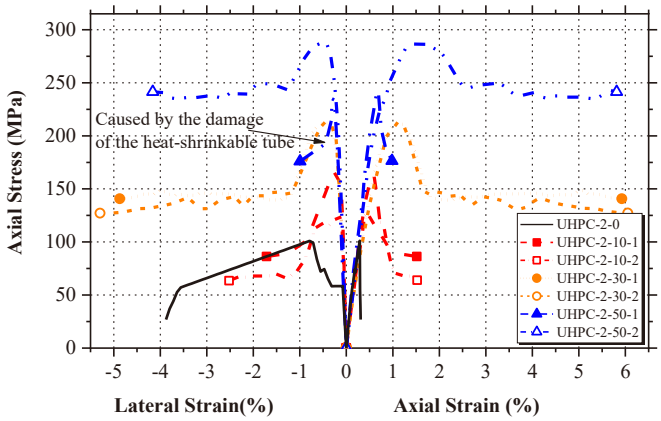

Fig. 2 Stress-strain curves of UHPC under different confining pressures

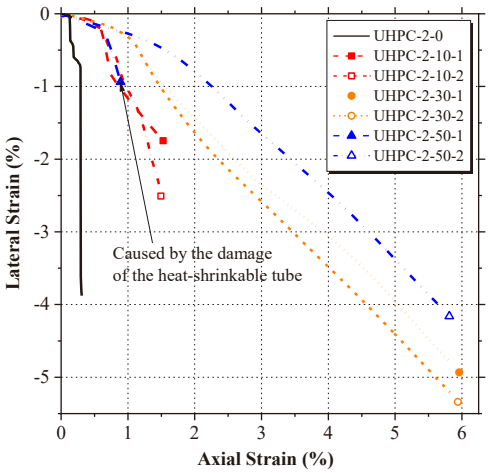

Fig. 3 lateral-to-axial strain curves of UHPC specimens under different confining pressures

Acknowledgment

The authors are grateful for the financial support received from the National Natural Science Foundation of China (Project No. 52078231), the Key Research and Development Program of Hubei Province of China (Project No. 2021BCA150), and the Hong Kong Research Grants Council (Project No.: T22-502/18-R).

Experimental and Numerical Investigation of SCC Beams Reinforced with Internal CFRP Meshes in Shear

Di Bo*, **Zheng Yu#** **and Chen Taigu**

School of Environment and Civil Engineering, Dongguan University of Technology, Dongguan, People's Republic of China
Presenter: dibo@dgut.edu.cn, #Corresponding author: zhengy@dgut.edu.cn

Abstract
This study aims to develop a new method for shear reinforcing concrete beams by using the CFRP meshes as a replacement for conventional stirrups inside concrete cover. Seven self-compacting concrete (SCC) beams shear reinforced with CFRP meshes were tested along with one conventional SCC beam for reference to investigate their performance improvement, particularly in shear capacity. The experimental results highlighted that the failure modes of the tested beams were dominated with shear-compression failure in the shear/bending moment regions. In addition, the shear capacity and the shear carried by CFRP meshes significantly improved with a higher number of the internal mesh layers. However, the increasing ratio of shear capacity was not proportional to the shear reinforcing ratio. Furthermore, finite element analyses (FEA) based on ABAQUS/Standard software were conducted to provide analytical estimations of the shear behavior of the proposed SCC beams. It was observed that the average tensile strain of the internal CFRP meshes varies between 5000 and 9000με at ultimate state, which further clarified the efficiency of the proposed shear reinforcing method. Finally, an explicit calculation formula is developed based on nonlinear regression analysis (NRA). The analytical results revealed that the predicted values agree very well with the test data, which can effectively predict the shear capacity of SCC beams reinforced with internal CFRP meshes in shear.

The test specimens include eight large-scale, simply supported concrete beams shear reinforced with CFRP meshes and one without shear reinforcement, GFRP bars were used for flexural reinforcement. The beams were constructed and tested until failure under four-point bending. The geometric properties and reinforcement layouts of the beams are shown in Fig. 1. The crack patterns of tested specimens under ultimate limit state are shown in Fig. 2. The relationship between applied load and mid-span deflection is shown in Fig. 3. Finite analysis model and stain distribution of concrete under ultimate limit state of the tested specimens are shown in Fig. 4. and Fig. 5., respectively.

Keywords: CFRP mesh, Stirrup, SCC, Shear Capacity, Average Tensile Strain.

Acknowledgment
The authors would like to acknowledge the research grant received from the National Key R&D Program of China (Grant No. 2019YFC1511000), National Natural Science Foundation of China (Grant No. 52178192), Guangdong Basic and Applied Basic Research Foundation (Grant No. 2020A1515110573), and Research Start-up Funds of DGUT (Grant No. GC300502-31).

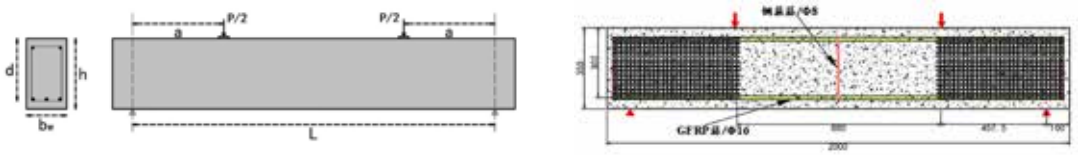

Fig. 1. Details of specimens.

(a) B0 (b) B1

Fig. 2. Photos of crack patterns of tested specimens.

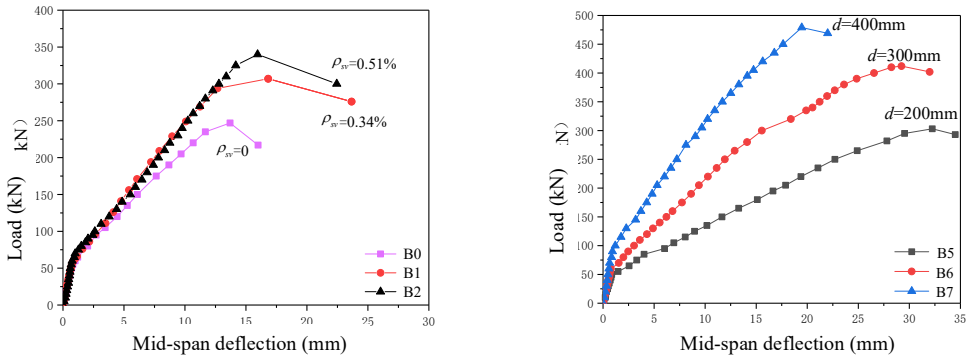

(a) B0-B1 (b) B5-B6

Fig. 3. Load versus mid-span deflection for tested specimens.

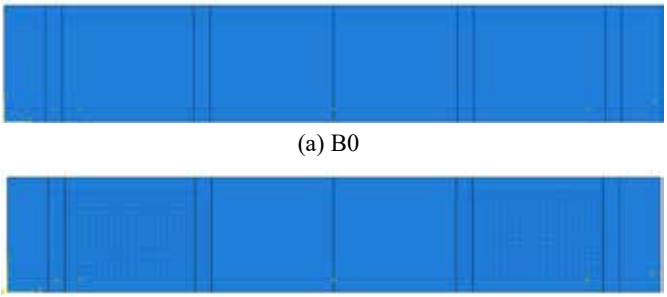

(a) B0

(b) B1

Fig. 4. Finite element analysis model for tested specimens.

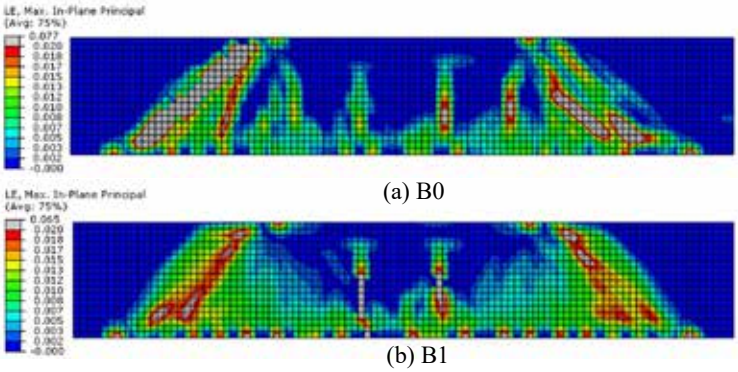

(a) B0

(b) B1

Fig. 5. Strain distribution diagram of concrete beams under ultimate limit state.

Interfacial approaches for toughness enhancement in fiber reinforced cementitious composite from nano to macroscale

Huinan Wei*, Ao Zhou, Tiejun Liu#

School of Civil and Environmental Engineering, Harbin Institute of Technology, Shenzhen, Shenzhen 518055, People's Republic of China
*Presenter: huinanw@yeah.net, #Corresponding author: liutiejun@hit.edu.cn

Abstract

The significant advances in innovative cementitious material lead to the generation of steel fiber reinforced cementitious composite (SFRCC). SFRCC is characterized by excellent compressive strength and durability, which exhibits great potential application in innovative and specialized structures. However, the brittle failure mode of SFRCC is still observed under tension and extreme loads due to the weak interfacial performance between steel fiber and cementitious matrix, resulting in a high risk of catastrophic failure. Therefore, a lot of approaches have been proposed and applied to enhance the interfacial performance of SFRCC from the perspectives of cementitious matrix and steel fiber. In this paper, advanced interfacial approaches for SFRCC, i.e. mechanical enhancement of cementitious matrix, physical arrangement and chemical modification of steel fiber, are systematically presented and summarized. To estimate the effect of these approaches on the global mechanical performance of SFRCC, the structural performance of SFRCC with interfacial modulation is reviewed, and the underlying mechanisms behind these approaches are illustrated through macroscale characterizations. Furthermore, the key challenges and future prospects of the enhancement approaches are also discussed, which is expected to provide insightful viewpoints on interfacial performance enhancement and accelerate the application of SFRCC in practical engineering.

Keywords: Interfacial enhancement; nanomaterials reinforcement; physical treatment; chemical modification; fiber reinforced cementitious composite; multi-scale mechanisms

Acknowledgment

The authors would like to acknowledge the funding support from the National Science Fund for Distinguished Young Scholars (52025081) and the Key Research and Development Program of Guangdong Province (2019B111107001).

Parallel Sessions-7

High-Performance Hybrid/Composite Structures Combining Concrete with Various Constructional Materials

Load Distribution Factors in Curved Composite Multi-Box Girder Bridges with Corrugated Steel Web

Yiyao Zhang[1], Liyan Xu[2*]

[1, 2] Department of Transportation Science and Engineering, Beihang University, Beijing, CHINA
E-mail: yiyaozhang@buaa.edu.cn, xuliyan@buaa.edu.cn

Abstract

Steel-concrete composite multi-box girder bridges with corrugated steel web have been widely used in curved bridge structures due to their advantages such as high bearing capacity, light self-weight, and convenient construction. The curve layout and live load distribution significantly affect the magnitude of stress developed in the composite girders and have not been fully addressed in design codes. In this study, to evaluate the force distribution of multi-girder composite bridges with corrugated steel web under live loads, an experimentally calibrated parametric investigation is employed with the finite element method. First, scaled model experiments on both simply-supported curved single- and double-box girder bridges are carried out, with setting the curvature as the main test variable. A series of live load conditions with different loading positions are applied to the bridge girders, and the distributions of the stress, deflection, and reaction force in key sections are intensively analyzed. In addition, a three-dimension finite element modeling is conducted to determine the moment distribution factor of curved composite girder bridges with corrugated steel web by considering different configuration parameters, including the curvature, span length, girder spacing, cross bracing layout, and the number of girders. Finally, the design formula of the transverse load-distributing influence line for curved composite multi-box girder bridges is developed by the rigid-jointed girder (RJG) method. The validity of the proposed equations is verified by comparing their theoretical prediction with the test responses and numerical results.

Keywords: Curved composite bridges, Load distribution factor, Corrugated steel web, Rigid-jointed girder method, Finite element method.

Comparison of Two Wind Turbine Hybrid Tower Transition Pieces: Reinforced Concrete Configuration, and Concrete-Filled Steel Tube Configuration

Xiaogang Huang [1], Yuhang Wang [2*]

[1] School of Civil Engineering, Chongqing University, Chongqing, China
E-mail: xghuang@cqu.edu.cn
[2] School of Civil Engineering, Chongqing University, Chongqing, China
E-mail: wangyuhang@cqu.edu.cn

Abstract

In recent years, the steel–concrete hybrid tower (SCHT) has attracted great interest in the wind energy industry. While most wind turbine manufacturers have agreed on the advantages of the SCHT, their approach to constructing the transition piece between the concrete and steel portions has varied. To date, two types of transition pieces have emerged in China to reduce their steel cost: (1) reinforced concrete configuration involving traditional mould cast and dense bar groups, and (2) concrete filled steel tube configuration using the inner and outer steel tubes to serve as the concrete formwork and using the core concrete to prolong the steel local buckling. This paper examines these two configurations and presents the hysteretic behaviors, damage and failure mechanisms of each when subjected to the complex loads. The results will form a theoretical basis for the application of these transition pieces in practice and the efficient use of wind resources in low wind speed regions.

Keywords: Transition Pieces; Wind turbine supporting system; Nonlinear analysis; Finite element simulation; Ultimate responses.

Experimental study on seismic performance of composite beam with laminated slabs using comprehensive anti-cracking technology

CHEN Juan[1*], LI Bingnan[2] and CHEN Ju[3#]

[1]College of Civil Aviation, Nanjing University of Aeronautics and Astronautics, Nanjing, Jiangsu 211106, People's Republic of China
2Architectural Design & Research Institute Co., Ltd. of Southeast University, Nanjing, Jiangsu 210096, People's Republic of China
3College of Civil Engineering and Architecture, Zhejiang University, Hangzhou,Zhejiang 310058, People's Republic of China
[*]*Presenter:* chenjuan@nuaa.edu.cn, [#]*Corresponding author:* cecj@zju.edu.cn

Abstract

Composite beam with laminated slabs is a kind of composite beam which is suitable for long-span, heavy-load and assembly construction, but the concrete slabs are easy to crack in tension under negative moment.

In order to improve the anti-cracking performance of concrete slabs, comprehensive anti-crack technology was adopted, including uplift-restricted and slip-permitted (URSP) connectors and cast-in-situ layer of fiber anti-cracking high performance concrete (HPC). A new URSP perfobond leiste (PBL) connector was introduced, which include a steel plate with obround holes and rebars penetrating the obround hole, and both sides of the penetrating rebars in the obround hole are filled with low elastic modulus materials (Fig. 1). The URSP PBL connector has the following characteristics: (1) the slip distance can be adjusted by the size of the obround holes, which can adapt to the large longitudinal slip demand; (2) the steel plate is only provided with obround holes, which does not need special processing, and the steel plate are welded on the beam without special welding equipment; (3) the transverse rebars penetrate through the obround holes, which improves the constructability of rebar layout; (4) the perforated steel plate is arranged longitudinally along the flange, which can improve the shear and bending stiffness of the beam.

Five composite beam-steel column joints were tested by quasi-static test (Fig. 2), the connector types of the specimens include URSP PBL connectors and traditional URSP STUD connectors, the cast-in-situ concrete include HPC concrete and normal concrete, and rebar strength include HRB400 and HRB500.

The test results indicate that: (1) the anti-cracking performance of the specimens can be improved by adopting URSP PBL connectors and fiber anti-cracking HPC in cast-in-situ layer, the initial crack load and displacement are increased by about 50%, while the strength of rebars in cast-in-situ layer has less influence on it; (2) the ultimate bending capacity of composite beams under negative moment is less affected by the concrete material of cast-in-situ layer and the strength of rebars; (3) the bending stiffness of composite beams can be improved by using URSP PBL connectors (Fig. 3); (4) the ductility and seismic performance of specimens with URSP PBL connectors are better than that with URSP STUD connectors, and can be further improved when fiber anti-cracking HPC is adopted in the cast-in-situ layer (Fig. 4~8), but are less affected by the strength of rebars.

Keywords: Composite beam with laminated slabs; Uplift-restricted and slip-permitted connectors; Experimental investigation; Seismic performance; Anti-cracking performance

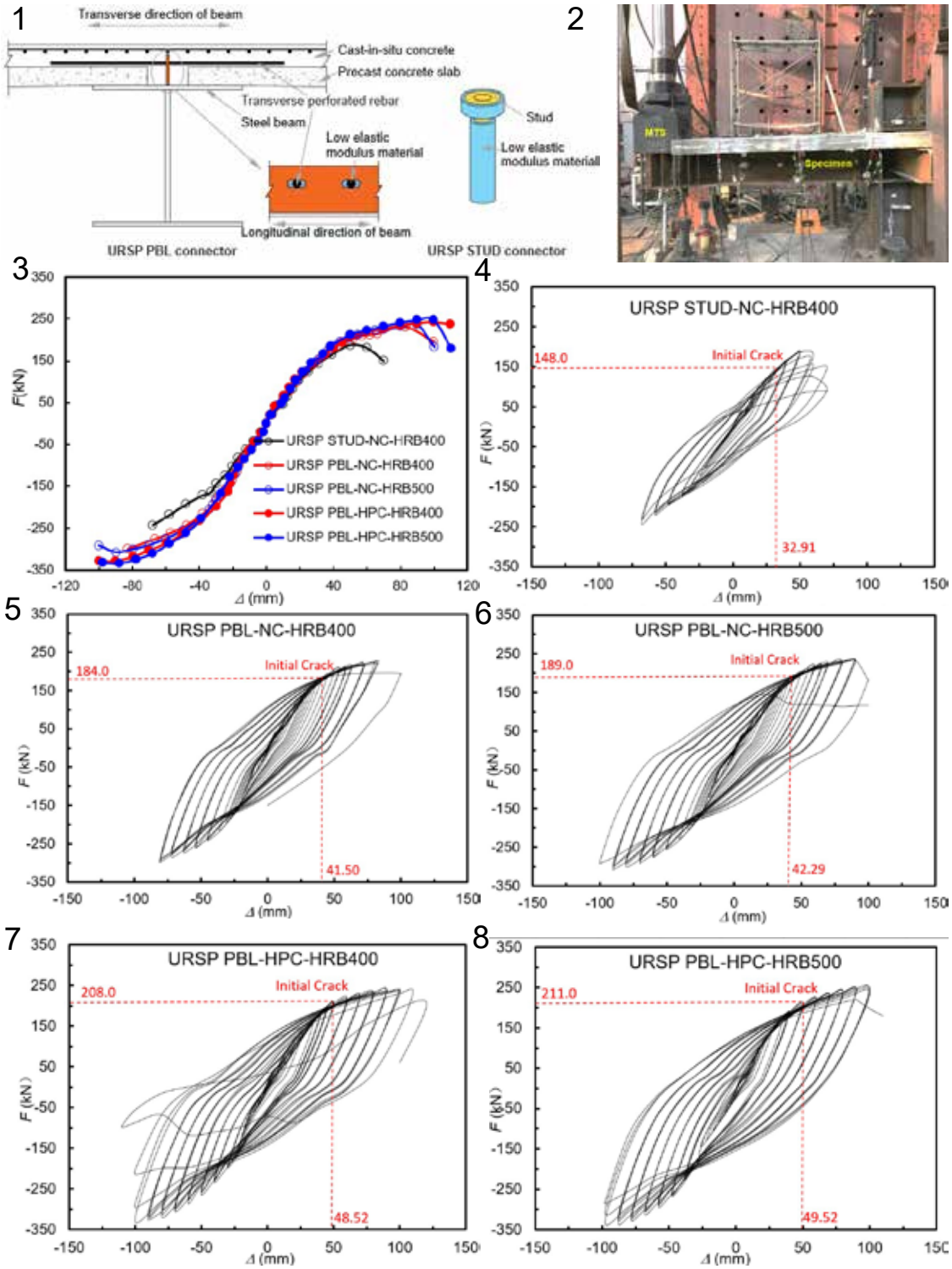

Fig. 1 URSP PBL connector; **Fig. 2** Test setup; **Fig. 3** Skeleton curves of specimens; **Fig.4~ Fig.8** Hysteretic curve of specimens

Acknowledgment

The authors would like to acknowledge the funding support from the National Natural Science Foundation of China (51778291), Six Talents Peaks Program of Jiangsu Province (JZ-009), and Jiangsu Transportation Science and Technology Project (2021Y17-2).

Lateral cyclic loading tests of precast recycled fine aggregate concrete shear wall with pressed sleeve connections

Chang-Min Yuan[1,2], Jian Cai[1,2], An He[1,2,*,#], Bing-Quan He[3]

[1] State Key Laboratory of Subtropical Building Science, South China University of Technology, Guangzhou
[2] School of Civil Engineering & Transportation, South China University of Technology, Guangzhou
[3] Guangzhou Jishi Construction Group Co. Ltd, Guangzhou
Guangdong 518060, People's Republic of China
[*]*Presenter:* hean@scut.edu.cn, [#]*Corresponding author:* hean@scut.edu.cn

Abstract

Resource and carbon dioxide emission constraints have prompted the implementation of precast structures and recycled aggregate concrete (RAC) in buildings to achieve high-efficiency construction and environmental benefit. An innovative type of precast recycled fine aggregate (RFA) concrete shear walls with pressed sleeve connections was proposed. The detail of the pressed sleeve connection is displayed in Fig. 1, in which the reinforcements are connected by the pressed sleeves. Hydraulic moulds were applied to produce plastic deformation in the sleeve, forming a tight contact between the bar splice and the sleeve. The assembly process of the specimens is indicated in Fig. 2. The wall panel with a loading girder and the foundation were prefabricated in the factory. Then they were assembled through pressed sleeves and lap-splice connections. Finally, the boundary members and the connection region were cast with RAC.

To study the seismic behaviour of the proposed shear walls, seven precast shear wall specimens with the pressed sleeve connections, as well as one reference cast-in-situ specimen, were fabricated and tested under lateral cyclic loading. The effects of the aspect ratio, the axial compression ratio, and the replacement ratio of RFA in concrete of the member were considered in the experiments. Tensile tests on the pressed sleeve connections and the reinforcements confirmed that the sleeve connections had similar strengths with better deformation capacity when compared to the reinforcements (See Fig. 3). The wall specimens were subjected to constant axial load and cyclic horizontal loads, with the test setup displayed in Fig. 4. The typical crack patterns of the precast and cast-in-situ specimens are displayed in Figs. 5 and 6, respectively. The lateral force–drift angle hysteresis curves of the precast and cast-in-situ specimens are shown in Figs. 7 and 8, with their skeleton curves shown in Fig. 9.

The test results demonstrated that the pressed sleeve connections were capable of transmitting both tensile and compressive force between reinforcements, and the precast shear walls with pressed sleeve connections had almost the same hysteresis behaviour, strengths, ductility coefficient and energy dissipation capacity as the cast-in-situ ones. Moreover, the seismic behaviour of the precast specimens with the RFA replacement ratio of 30% was almost identical to that of the precast specimens with natural aggregate concrete. The drift angles at the yield loads of the precast specimens ranged from 1/463 to 1/267, with their ultimate loads in the range between 1/195 and 1/81. The equivalent viscous damping factor varied from 0.05 to 0.15 prior to severe damage of the specimens. This indicated a favourable deformation and energy consumption capacity of the proposed precast shear walls.

Keywords: Precast concrete structure; Shear wall; Recycled aggregate concrete (RAC); Pressed sleeve; Seismic performance

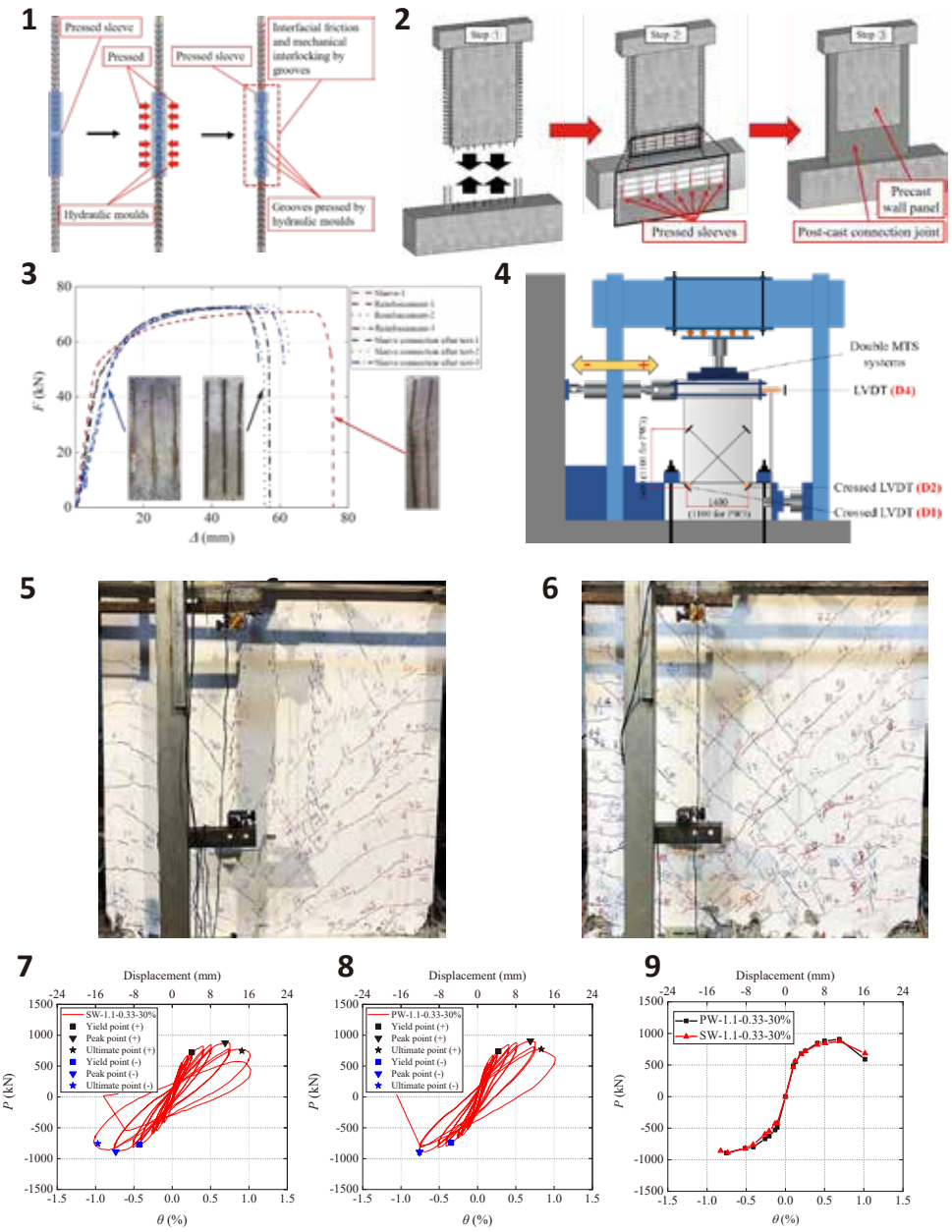

Fig. 1. Details of pressed sleeve connection system. **Fig. 2.** The assembly process of precast specimens. **Fig. 3**. Force–displacement curves of the sleeve connections and the reinforcements. **Fig. 4**. Lateral cyclic loading test setup. **Fig. 5**. Crack pattern of precast specimen. **Fig. 6**. Crack pattern of cast-in-situ specimen. **Fig. 7**. Hysteresis curve of precast specimen. **Fig. 8**. Hysteresis curve of cast-in-situ specimen. **Fig. 9**. Skeleton curves of precast and cast-in-situ specimens.

Acknowledgment

This work was supported by National Natural Science Foundation of China (52178139), and Science and Technology Planning Project of Guangzhou Municipal Construction ([2021]-KJ004; [2021]-KJ021; [2021]-KJ036; [2021]-KJ037).

Eccentric Compressive Behavior of Circular Concrete-filled Steel Tubes with Internal Latticed Steel Angles

Ju Chen[1], Liang Hu[1,2], Jun Wang[3]*, Sha-Sha Song[1]

1. Institute of Structural Engineering, Zhejiang University, Hangzhou, 310058, Zhejiang, China
2. DongFang Boiler Group Co. LTD, Chengdu, 610097, Sichuan, China
3. Guangdong Province Key Laboratory of Durability for Marine Civil Engineering, College of Civil and Transportation Engineering, Shenzhen University, Shenzhen, 518060, Guangdong, China

Abstract: The eccentric compressive behaviour of the CFSTs with inner latticed steel angles was experimentally investigated, and test results such as the load-displacement curves, load-strain curves, distributions of the lateral deflection and ultimate load were obtained and analyzed. Test results showed that the influence of steel angles on the ultimate load was not obvious when the steel consumption was relatively small, and there was no obvious lateral deformation when the compressive load was smaller than 80% of the ultimate load. Corresponding finite element (FE) models were established and validated with the test results, and parametric analysis was conducted after the validation. Analysis results showed that the contribution of steel angles to the ultimate load would be reduced when the eccentric distance increases. Moreover, design equations for the ultimate load were proposed based on the FE results, and calculation results showed that the proposed design equations could conservatively and safely predict the ultimate load.

Keywords: Eccentric compressive behaviour; Latticed steel angles; Ultimate load; Parametric analysis; Design equations.

* Corresponding author. Tel.: +86-151 5808 1657

E-mail address: wangjun123@szu.edu.cn

Compound Concrete Filled FRP Tubular Columns Containing Recycled Concrete Lumps

Guan Lin[1*#] and Junjie Zhang[2]

[1] Department of Ocean Science and Engineering, Southern University of Science and Technology, Shenzhen, Guangdong 518055, China
[2] Department of Civil and Environmental Engineering, The Hong Kong Polytechnic University, Hong Kong, China
Presenter; #Corresponding author: guanlin@polyu.edu.hk

Abstract

A recently proposed technique of recycling waste/old concrete is to directly mix large pieces of recycled concrete lumps (RCLs) and fresh concrete to form the so-called "compound concrete". Compared with conventional recycling techniques (e.g., recycled aggregates), this novel technique has many advantages, including: (1) a much more simple, cost-effective, and energy-saving recycling process; (2) a much larger recycling ratio; and (3) a capability of alleviating the problems of hydration heat and shrinkage in casting mass concrete structural members. To date, a large number of studies have been carried out to explore the properties of compound concrete, including its axial compressive, tensile, flexural, freeze-thaw, fatigue, and fire resistance properties and size effect [1-6]. However, due to the low strength and internal weaknesses of RCLs, compound concrete generally exhibits inferior performance with large scatters compared with normal concrete, especially when the strength of RCLs is lower than that of fresh concrete, which is common in practice. Confining compound concrete through a steel tube has been explored by researchers to improve the behavior of compound concrete. However, it was found that the detrimental effects of RCLs can be minimized or eliminated only when a thick steel tube (i.e., one with a small diameter/width-to-thickness ratio) is used [7].

Against the above background, Teng et al. [8] explored the use of an external fiber-reinforced polymer (FRP) confining tube to confine compound concrete, to form the so-called compound concrete filled FRP tubular (CCFFT) columns. It has been showed that the compressive strength and the ductility of FRP-confined compound concrete was comparable to that of FRP-confined normal concrete, indicating that the detrimental effects associated with the use of RCLs can be significantly reduced or eliminated when the compound concrete is provided with a substantial amount of FRP confinement (Fig. 1). The authors' group have also conducted systematic investigations on the behavior of CCFFT columns under different loading conditions (e.g., monotonic compression, cyclic compression) [10, 11]. It was found that the presence of RCLs had marginal effects on the cyclic behavior of FRP-confined compound concrete provided that the FRP confinement was sufficiently large. More recently, the authors' group conducted an experimental study on the size effect of square CCFFT columns under axial compression by testing such columns of three different sizes [12]. It was found that the column size effect was obvious in such columns and the presence of RCLs may aggravate the column size effect. In fact, compared with FRP-confined normal concrete columns, the size effect in CCFFT columns is much more complex as the size of the column as well as the size of the RCLs play significant roles in the behavior of CCFFT columns. The results presented in [12] indicate that more experimental studies should be carried out in the future for a better understanding of the size effect in CCFFT columns.

Keywords: Fiber reinforced polymer (FRP), Recycled concrete lumps (RCLs), Compound concrete, FRP tubes, Size effect.

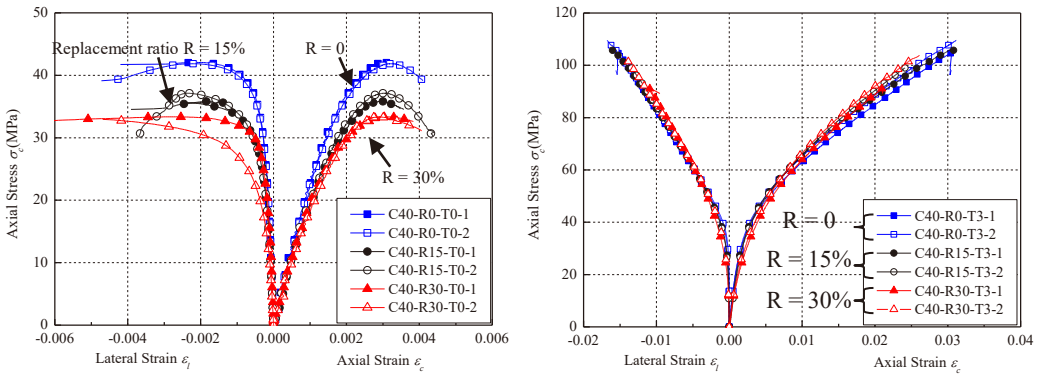

(a) Unconfined concrete (b) FRP-confined concrete

Fig. 1 Effect of FRP confinement on the stress-strain behavior of compound concrete

Acknowledgment

The authors would like to acknowledge the funding support received from the National Natural Science Foundation of China (Project No.: 52008361).

References:

[1] Wu B, Liu CH, Wu YP. (2014). Compressive behaviors of cylindrical concrete specimens made of demolished concrete blocks and fresh concrete. *Construction and Building Materials*, 53, 118-130.

[2] Wu B, Li Z, Chen ZP, Zhao XL. (2018). Tensile-splitting behaviors of compound concrete containing demolished concrete lumps. *Journal of Materials in Civil Engineering,* ASCE, 30(3), 04018014.

[3] Wu B, Xu Z, Ma ZJ, Liu QX, Liu W. (2011). Behavior of reinforced concrete beams filled with demolished concrete lumps. *Structural Engineering and Mechanics*, 40(3), 411-429.

[4] Wu B, Li Z. (2017). Mechanical properties of compound concrete containing demolished concrete lumps after freeze-thaw cycles. *Construction and Building Materials*, 155, 187-199.

[5] Wu B, Jin HM. (2019). Compressive fatigue behavior of compound concrete containing demolished concrete lumps. *Construction and Building Materials*, 210, 140-156.

[6] Wu B, Yu Y, Zhao XY. (2019). Residual mechanical properties of compound concrete containing demolished concrete lumps after exposure to high temperatures. *Fire Safety Journal*, 105, 62-78.

[7] Wu B, Liu W, Liu QX, Xu Z (2010). Experimental study on the behavior of recycled-concrete-segment/lump filled steel tubular stub columns subjected to concentrically axial load. *China Civil Engineering Journal*, 43(2), 32-38.

[8] Teng JG, Zhao JL, Yu T, Li LJ, Guo YC (2016). Behavior of FRP-confined compound concrete containing recycled concrete lumps. *Journal of Composites for Construction*, ASCE, 20(1), 04015038.

[9] Zhao JL, Xu CH, Sun LZ, Wu DY (2020). Behaviour of FRP-confined compound concrete-filled circular thin steel tubes under axial compression. *Advances in Structural Engineering*, 23(9), 1772-1784.

[10] Zhou JK, Lin G, Teng JG (2021). Stress-strain behavior of FRP-confined concrete containing recycled concrete lumps. *Construction and Building Materials*, 267, 120915.

[11] Zhou JK, Lin G, Teng JG (2021). Compound concrete-filled FRP tubular columns under cyclic axial compression. *Composite Structures*, 275, 114329.

[12] Chen GM, Zhang JJ, Lin G, Wu YF, Jiang T (2022). Behavior of different-sized FRP-confined square compound concrete columns containing recycled concrete lumps. *Journal of Composites for Construction*, ASCE, 26(2), 04022003.

Behavior of Infilled RC Frames under Out-of-Plane Lateral Loads using Digital Image Correlation Techniques

Syed Humayun Basha[1*#], Zi-Xiong Guo[2]

[1] Associate professor, College of Civil Engineering, Huaqiao University, Xiamen 361021, China.
[2] Professor, College of Civil Engineering, Huaqiao University, Xiamen 361021, China. Email: guozxcy@hqu.edu.cn
[*]*Presenter:* syedhbasha@hqu.edu.cn, [#]*Corresponding author:* syedhbasha@hqu.edu.cn

Abstract

Recent seismic events showed that a crucial issue for life-safety and loss reduction in existing reinforced concrete (RC) frame buildings with internal partition or external cladding masonry wall panels is related to the mitigation of the out-of-plane collapse of wall panels. Most of the previous research studies mainly focused on frame-infill interaction subjected to in-plane lateral loads, but a few studies were carried out on to evaluate the out-of-plane (OOP) behavior. In the current research, a comprehensive experimental investigation was carried to evaluate the out-of-plane behavior of full-scale, single-bay, single-storey RC frame specimens with burnt clay brick masonry infill wall panels. The influence of frame-infill interaction, connection details between individual wall panel elements and surrounding frame members, slenderness ratio of wall panels, and arching effect on the seismic performance and failure mechanisms were evaluated. The out-of-plane load was applied on the infill wall by means of two MTS servo-controlled hydraulic actuators of 250 kN load capacity with a stroke length of ± 250 mm. Linearly varying displacement transducers (LVDTs) were used at different locations on the columns, infill walls and base beam to record the deformations. Non-contact optical GOM ARAMIS 3D measuring system was used to capture the full field out-of-plane deformation and strain concentration analysis of the masonry infill wall panel and frame members. The post-processing analysis of the images was carried out using GOM Correlate Professional analysis software to evaluate the development of cracks and its propagation, final failure mechanisms of the specimens.

The OOP behavior of masonry infilled RC frames were evaluated in terms of failure mode, force-displacement response, strength, and stiffness degradation were analyzed. 3D DIC provided a better characterization of the initiation and development of cracks in the infills (Fig. 1). The typical infill failure mechanism was characterized by predominant horizontal and vertical crack at mid-height of the infills and the stepwise crack pattern, initiating from the mid-height and propagating diagonally towards the corners of the infill. Under the action of monotonic out-of-plane lateral load, two-way arch resisting mechanism was clearly formed. The OOP displacement of the infill wall was found to be larger in the center of infill and smaller in the surrounding frame members indicating frame-infill interaction. The out-of-plane capacity of masonry wall was predominantly affected by the slenderness ratio. Tie bars played an important role in sustaining the out-of-plane overall stability of infills. Using the full-field strain data and crack patterns obtained from 3d-DIC analysis, the early damage locations were found and the strengthening measures to contain the out-of-plane failure in the future earthquakes were suggested. The research is of high theoretical and social importance as the seismic design principles of RC frame buildings with internal and external cladding wall panels were improved considering the vulnerability of out-of-plane collapse mechanism, which can ensure public life-safety and reduce high socio-economic losses in future earthquakes.

Keywords: RC frames; Out-of-plane behavior; Digital image correlation techniques; Monotonic loading.

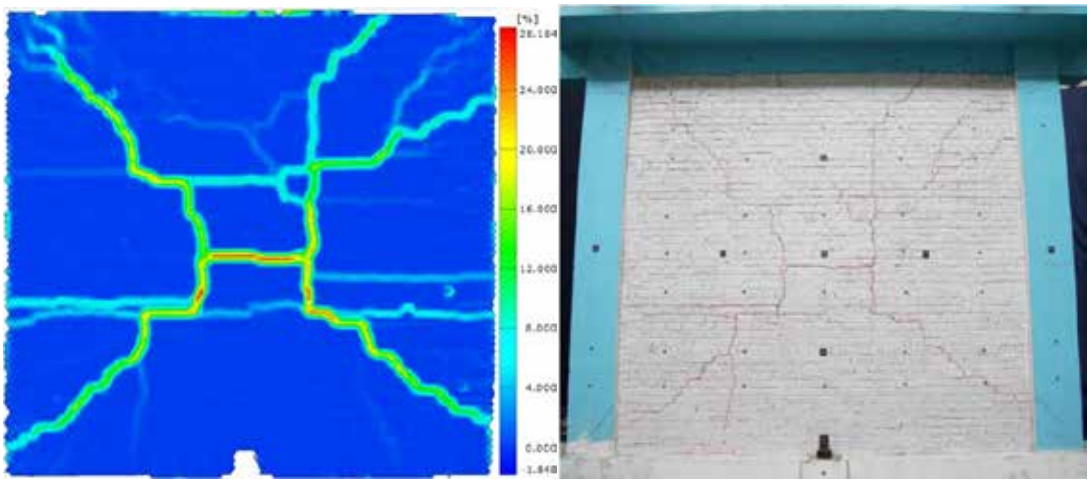

Fig. 1. Failure mode and damage pattern of full-scale infilled frame under out-of-plane loads.

Acknowledgment

The authors would like to acknowledge the financial assistance provided by Department of Science and Technology, Huaqiao University, China [Grant No. 605-50X19032].

Parallel Sessions-8

The First Greater Bay Area Forum on Low Carbon Construction Materials and Technologies (LCCMT)

Application of molecular dynamics simulation in green building materials

Dong-Shuai Hou[1*#], Wei Zhang[1]

[1] Department of Civil Engineering, Qingdao University of Technology, Qingdao, 266520, People's Republic of China
Presenter: dshou@outlook.com, #Corresponding author: dshou@outlook.com

Abstract

To achieve low-energy consumption and environmentally friendly green design of building materials, the aluminum-rich mineral admixtures (fly ash, mineral powder, metakaolin, and etc.) were introduced into cementitious materials, resulting in the formation of calcium aluminosilicate hydrate (C-A-S-H) gel. In this paper, the molecular dynamics (MD) simulation method was utilized to investigate the nanostructure, mechanical and transport properties of C-A-S-H gel. The results show that at molecular scale, Al[4] in C-A-S-H structure can bridge the defective silicate chains to form longer aluminosilicate chains. As compared with bridging silicate tetrahedra, the presence of bridging aluminate species shows the same influence on the mean chain length of aluminosilicate chains but increase the basal spacing of C-A-S-H gel. Compared with C-S-H, the water molecules in the vicinity of the C-A-S-H interface exhibit characteristics: Larger bulk density and dipole moment, water molecules are arranged in order, and the inclination angle is consistent. The surface of C-A-S-H is fixed with more Na^+ and Cl^-, and the reasons for adsorption of anion and cation are different (Fig. 1). The transport behavior of water and ions in C-S-H/C-A-S-H nanopore was explored and the microscopic mechanism was revealed. The unsaturated transport curve of NaCl solution in C-S-H/C-A-S-H nanopore meets the classical capillary adsorption theory Lucas-Washburn equation. The migration of water molecules and ions in the C-A-S-H gel pores is slower than that of C-S-H. The introduction of aluminum in C-S-H resists the intrusion of water and ions (Fig. 2). Furthermore, Al incorporation shows little effect on the mechanical properties along *x* and *z* directions while increases its mechanical properties in *y* direction (Fig. 3). The research results of this paper can provide theoretical basis for the design and preparation of sustainable and environmentally friendly cement-based materials.

Keywords: Al incorporated cementitious materials; C-A-S-H; Molecular dynamics; Mechanical properties; Transport behavior

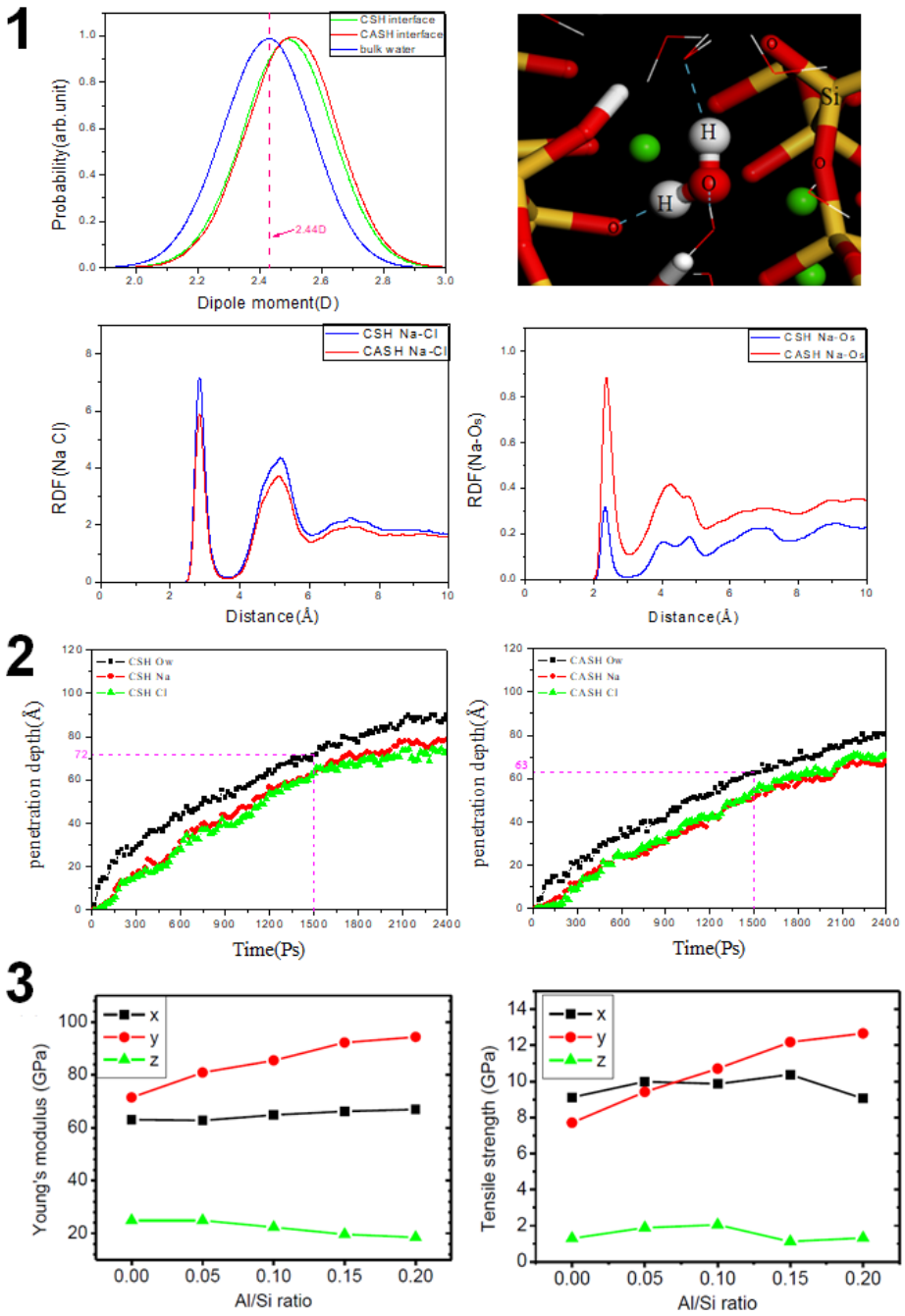

Fig. 1 Local structure of C-A-S-H; **Fig. 2** Variation of water and ion intrusion depth with time under C-S-H and C-A-S-H models; **Fig. 3** Young's modulus and tensile strength of C-A-S-H structure along *x*, *y* and *z* directions.

Acknowledgment

Financial support from National Natural science foundation of China under Grant U2006224, 51978352, Natural science foundation of Shandong Province under Grant ZR2020JQ25, Qingdao Science and Technology Leading Talent 19-3-2-13-zhc are gratefully acknowledged.

Use of Biochar and Dioxide Curing for Production of Low-Carbon Cement-Based Composites

Lei Wang[1*]

[1]State Key Laboratory of Clean Energy Utilization, Institute for Thermal Power Engineering, Zhejiang University, Hangzhou, 310027, China.
[*]*Presenter:* wanglei.leo@zju.edu.cn, [#]*Corresponding author:* wanglei.leo@zju.edu.cn

Abstract

Biochar is a green material obtained from the thermochemical conversion of biomass under an oxygen-limited condition. This study demonstrated a novel and sustainable method for incorporating wood biochar in cement-based composites with carbon dioxide curing. The X-ray diffraction (XRD) and thermogravimetric analyses (TGA) illustrated that the incorporation of biochar in an ordinary Portland cement system promoted the generation of additional hydration products due to moisture regulation effects, but did not accelerate or delay the hydration process, as indicated by the isothermal calorimetry results. Specifically, the addition of 1 wt% biochar increased the compressive strength of the composites by 8.9%. However, the incorporation of 5 wt% biochar reduced the compressive strength due to the porous and brittle structure of biochar. CO_2 curing was employed to mitigate these adverse effects. The CO_2 curing (for blocks) approach more effectively accelerated carbonation than the method without CO_2 curing. After carbonation, the additional hydrates enhanced the bonding strength and the carbonates densified the microstructure, which substantially enhanced the mechanical strength and carbon sequestration. Therefore, the synergistic utilisation of waste biochar and CO_2 curing could be a green technology for enhancing the properties of cement-based composites and would also promote waste recycling and CO_2 sequestration.

Biochar also could be recycled into the magnesia cement (MC) and magnesia-Portland binary cement (MP)-based composites. The TGA and XRD showed that the incorporation of biochar, especially CO_2 gasification biochar, promoted the generation of hydration products. The use of CO_2 curing effectively accelerated the carbonation of composites. Hydrated magnesium carbonates were preferentially formed in CO_2-cured MC composites, whereas $CaCO_3$ was preferentially generated in CO_2-cured MP composites. Moreover, the incorporation of porous biochar could further facilitate CO_2 diffusion and promote carbonation. As a result, the synchronous use of biochar and CO_2 curing significantly enhanced the mechanical strength of composites. Therefore, biochar-augmented and CO_2-enhanced composites could be a novel and low-carbon construction material for sustainable engineering applications.

Keywords: Wood waste biochar; Accelerated carbonation; Carbon neutral; Biomass recycling; Sustainable construction materials.

Acknowledgement

The authors would like to acknowledge the funding support from the State Key Laboratory of Clean Energy Utilization (ZJUCEU2022001).

Extrusion-based 3D printing of Ultra-High Performance Strain-Hardening Cementitious Composites (UHP-SHCC)

Yan Sun, Ye Qian#

Department of Civil Engineering, The University of Hong Kong, Pokfulam Road, Hong Kong
Presenter: suny@connect.hku.hk #Corresponding author: yjqian@hku.hk

Abstract

3D printing (3DP) technology is gaining interest in building and construction industry. However, the development of 3D concrete printing (3DCP) technique is not compatible with the conventional reinforcing strategies such as adding steel rebars. Therefore, fiber reinforced cementitious materials, especially strain hardening cementitious composites (SHCC) with strain hardening and multicracking behavior, are promising in 3D concrete printing.

However, the high volume fraction of fibers in SHCC makes the continuous pumping and extrusion process during 3D printing very challenging. Clogs during pumping and discontinuity during extrusion occur often. In this study, various materials parameters are probed to evaluate the pumpability and extrudability of SHCC. A SHCC mixture with high fiber dosage (2.0 vol%) are pumped and 3D printed continuously and smoothly. Direct tensile tests are conducted on the 3D printed filaments along the printing direction, after 28-day water curing. The tensile strength and ultimate strain are found to be significantly affected by the fiber dosage, etc.

Keywords: 3D concrete printing; Direct tensile properties; Ultra-High Performance Strain-Hardening Cementitious Composites (UHP-SHCC).

Acknowledgment

The authors would like to acknowledge the financial support received from Hong Kong RGC General Research Fund (Project No. 27209020 and 17204322).

Development of artificial geopolymer aggregates with thermal energy storage capacity

Yi Fang[1,2], Jian-Cong Lao[2*], Jian-Guo Dai[2#]

[1] College of Mechanics and Materials, Hohai University, Nanjing, Jiangsu 211100, People's Republic of China
[2] Department of Civil and Environmental Engineering, The Hong Kong Polytechnic University, Kowloon, Hong Kong
[*]*Presenter:* attic.lao@connect.polyu.hk, [#]*Corresponding author:* cejgdai@polyu.edu.hk

Abstract

Integrating phase change materials (PCMs) into building materials has been widely used to improve the energy efficiency of buildings, for which microencapsulation and shape stabilization are considered as two most effective solutions. Various types of porous materials, including expanded graphite, expanded perlite, expanded shale, mesoporous zeolite, ceramic foam, and recycled expanded glass aggregate have been reported for such purpose. However, the cost of these porous supporting materials is usually relatively high and the mechanical properties are generally poor and their porosity is non-tunable.

In this study, artificial geopolymer aggregate (GPA) was employed as a novel PCM carrier for energy storage purpose using a vacuum impregnation technique (Fig. 1). Detailed investigations were conducted into the physical, mechanical, and thermal properties of GPA-PCM, which can be engineered through different raw material selections (e.g., slag content, water/binder ratio, and incineration bottom ash (IBA) content). It was demonstrated that increasing the IBA content is an efficient means to increase the porosity of GPA (Fig. 3), an index of the capacity to accommodate PCM. Up to 16 wt.% PCM could be absorbed into the GPA through vacuum suction (Fig. 3), resulting in a significant melting enthalpy of 24.74 J/g (Fig. 4). Besides, GPA-PCM could achieve an excellent mechanical strength greater than 53.2 MPa (Fig. 2) and a thermal conductivity of 0.510 – 0.589 W/mK (Fig. 5). The time-temperature history curves of GPA revealed that up to 10.5°C of thermal regulation was achieved due to PCM impregnation (Fig. 6). The developed GPA-PCM composites facilitate an innovative and low-carbon solution for utilizing PCMs in construction for temperature-regulating and energy-saving purpose.

Keywords: Phase change materials; Artificial geopolymer aggregates; Energy storage; Thermal performance; Mechanical properties

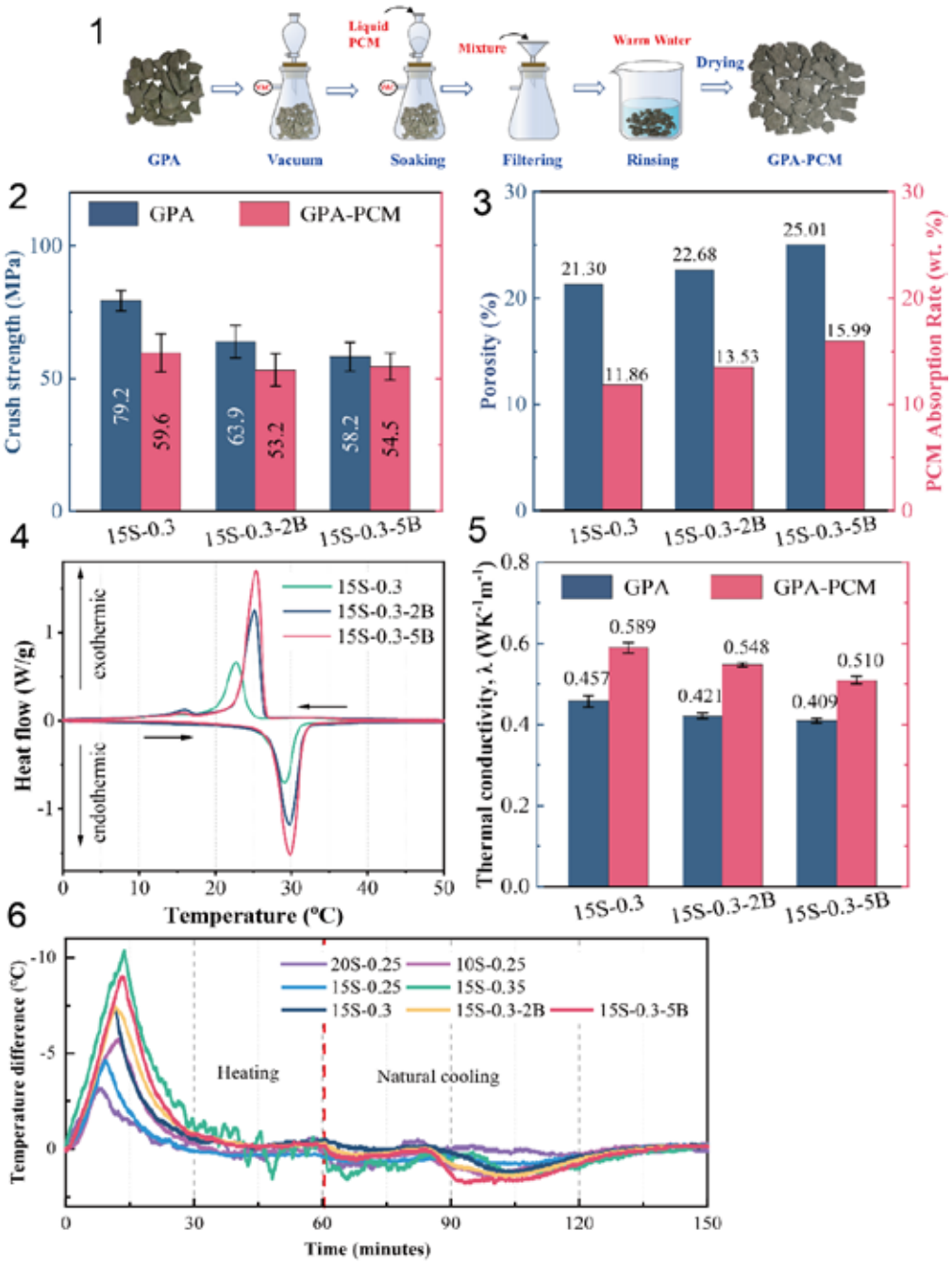

Fig. 1 Preparation process for GPA-PCM; **Fig. 2** Crushing strength of aggregates with the regular size of 20 mm × 20 mm × 20 mm before and after being filled with PCM; **Fig. 3** Porosity of GPA and absorption rate of PCM in GPA-PCM; **Fig. 4** DSC curves of GPA-PCM; **Fig. 5** Thermal conductivity of GPA and GPA-PCM; **Fig. 6** Temperature difference achieved by PCM according to time-temperature curve tests.

Acknowledgment

The authors would like to acknowledge the financial support received from NSFC/RGC Joint Research Scheme (N_PolyU542/20), Hong Kong RGC General Research Fund (No. 15223120), and Research Centre for Resources Engineering towards Carbon Neutrality (No. BBC7).

Geopolymer-based sub-ambient daytime radiative cooling coating

Ning Yang[1*], Jian-Guo Dai[1#]

[1] Department of Civil and Environmental Engineering, The Hong Kong Polytechnic University, Hung Hom, Hong Kong, China
[*]Presenter: ning20033281r.yang@connect.polyu.hk, [#]Corresponding author: cejgdai@polyu.edu.hk

Abstract

Sub-ambient daytime radiative cooling coating (SDRCC) is an appealing thermal management technology that has great potential for alleviating the global warming and urban heat island effect. The radiative cooling effect can be achieved by engineering a surface with a high solar reflectance as well as a high emittance in the sky transparent window (infrared atmospheric window). Over the past few years, various types of polymeric SDRCCs have been developed. However, they may face problems of environmental ageing under UV, moist and fire due to their organic nature. In this study, an ambient-cured inorganic alkali-activated geopolymer (AAGP)-based daytime radiative cooling coating was synthesized with the modification of barium sulphate ($BaSO_4$) and nano-silica (SiO_2) particles (Fig. 1). The optical and physicochemical properties were systematically investigated. The chemical composition, functional groups as well as surface morphologies of the raw materials and the formed geopolymer coating were characterized by XRD, FTIR and EDS. The microstructural of the section of the AAGP cooling coating was presented by false-colored SEM (Fig. 3). The developed AAGP coating exhibited a high infrared emissivity of 0.9491 and solar reflectance of 97.6%. When exposed to direct sunlight and based on a self-made field test setup (Fig. 5), the coating's surface was found to be able to cool down up to 8.9 ℃ below the ambient air temperature under Hong Kong's climate (Fig. 4). Due to the inherit advantages of an inorganic coating over its organic counterpart, the developed AAGP coating is expected to be able to broaden the applicability of the SDRCC technology for efficient thermal management and energy saving purpose.

Keywords: Geopolymer; daytime radiative cooling; sub-ambient; alkali activation

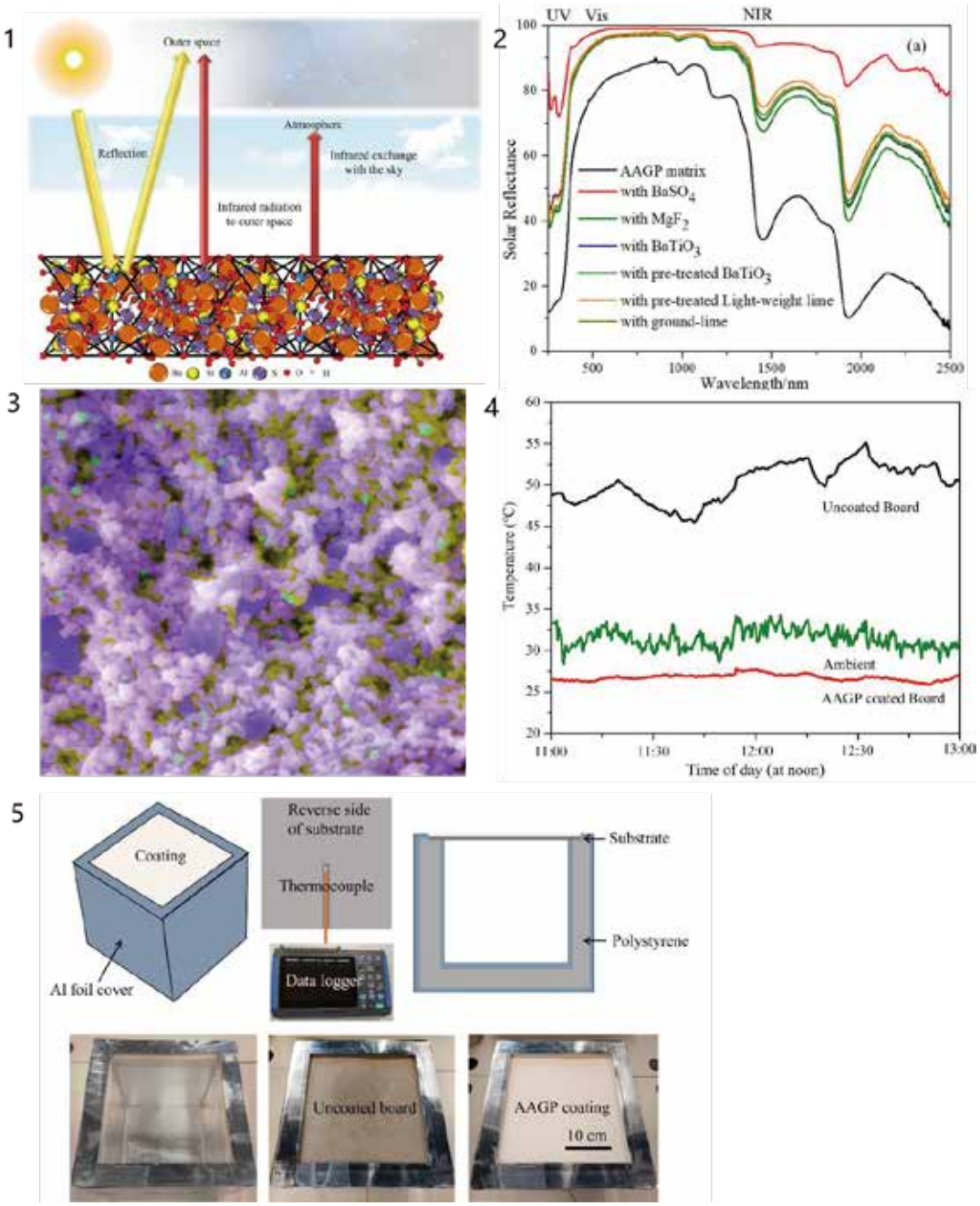

Fig. 1 Schematic cooling mechanism of the geopolymer cooling coating; **Fig. 2** Solar reflectance of AAGP matrix and AAGP coatings with different fillers; **Fig. 3** False-colored SEM image of section of the AAGP cooling coating (purple for Ba, green for Si, yellow for Al); **Fig. 4** Cooling performance of an AAGP-coated board in comparison to an uncoated board and the ambient temperature; **Fig. 5** Schematics and photos of the field test setup for AAGP coating

Acknowledgment

The authors would like to acknowledge the funding support from RGC General Research Fund (Project No. 15223120), Research Institute for Sustainable Urban Development (Project No. 1-BBWX) and Research Institute for Smart Energy (Project No. CDBL) of The Hong Kong Polytechnic University. The first author would like to thank the PhD studentship provided the Hong Kong Polytechnic University.

Alkali-activated Artificial Aggregates Made from Red mud

Kaige Tian[1, 2*], Yanshuai Wang[2], Biqin Dong[2], Feng Xing[1, 2#]

[1] Key Laboratory of Earthquake Engineering and Engineering Vibration, Institute of Engineering Mechanics, China Earthquake Administration, Harbin 150080, China
[2] College of Civil and Transportation Engineering, Shenzhen University, Shenzhen 518060, China
[*]*Presenter:* tiankaige@outlook.com, [#]*Corresponding author:* xingf@szu.edu.cn

Abstract

Shortage of aggregates is becoming a prominent issue in the construction industry due to rapid urbanization. Meanwhile, recycling of various solid wastes has called for ecological sustainability. Preparing artificial aggregates with solid wastes is expected to address the above engineering and environmental problems synchronously. In this research, red mud was adopted as the raw material for alkali-activated aggregates preparation considering its high alkalinity, huge reserves and low utilization ratio.

Currently, there are generally two methods for the preparation of alkali-activated artificial aggregates: sintering and cold-bonding pelletization. Sintering aggregates usually behavior the high strength, low density, and high performance of aggregates, but its production leads to high energy consumption and a large CO_2 footprint, which is harmful to the environment and limits the further application of this manufacturing technique. To avoid environmental burden, cold-bonding aggregates have been proposed and studied by many researchers. In the present work, artificial aggregates were produced using an alkali-activated cold-bonding pelletization process with a high-volume of red mud (RM) as the precursor, fly ash (FA)/ granulated blast furnace slag (GGBS) as the silico-calcium additive, and a mixture of sodium silicate and sodium hydroxide as the activator (Fig. 1).

The mechanical properties, densities, and internal structures of the fabricated artificial aggregates were characterized, as well as the microstructure analysis and product identification (Fig. 2 and Fig. 3). The average single particle crushing strengths of the RM-FA aggregates were in the range of 1.46–6.18 MPa and the mechanical properties of the R80F20 aggregates were optimal (6.18 MPa). Based on the results of the 1-h water absorption tests and the densities, all the RM-FA aggregates can be classified as lightweight aggregates. The internal structural characteristics of the aggregates were porous in the center but dense near the surfaces. The polymerization and hydration products of ettringite (AFt) and C-N-A-S-H gel were found through the analysis of microstructure and chemical composition of the aggregates. For RM-GGBS aggregates, the single particle crushing strengths and cylinder compressive strengths were characterized and the crushing strength of the optimal RM-GGBS aggregates was 10.61 MPa and the compressive strength was 21.17 MPa. The bulk densities and 1-h water absorption results show that the RM-GGBS aggregates are also lightweight aggregates. The morphology and microstructure analysis and chemical composition analysis results show that the internal structures of RM-GGBS aggregates are similar to that of RM-FA ash aggregates and the polymerization and hydration products of RM-GGBS aggregates are more.

The results showed that the optimal artificial aggregates could be possible candidates for mortar and concrete preparation.
Keywords: Alkali-activated Artificial Aggregates; Red Mud; Fly Ash; Granulated Blast Furnace Slag

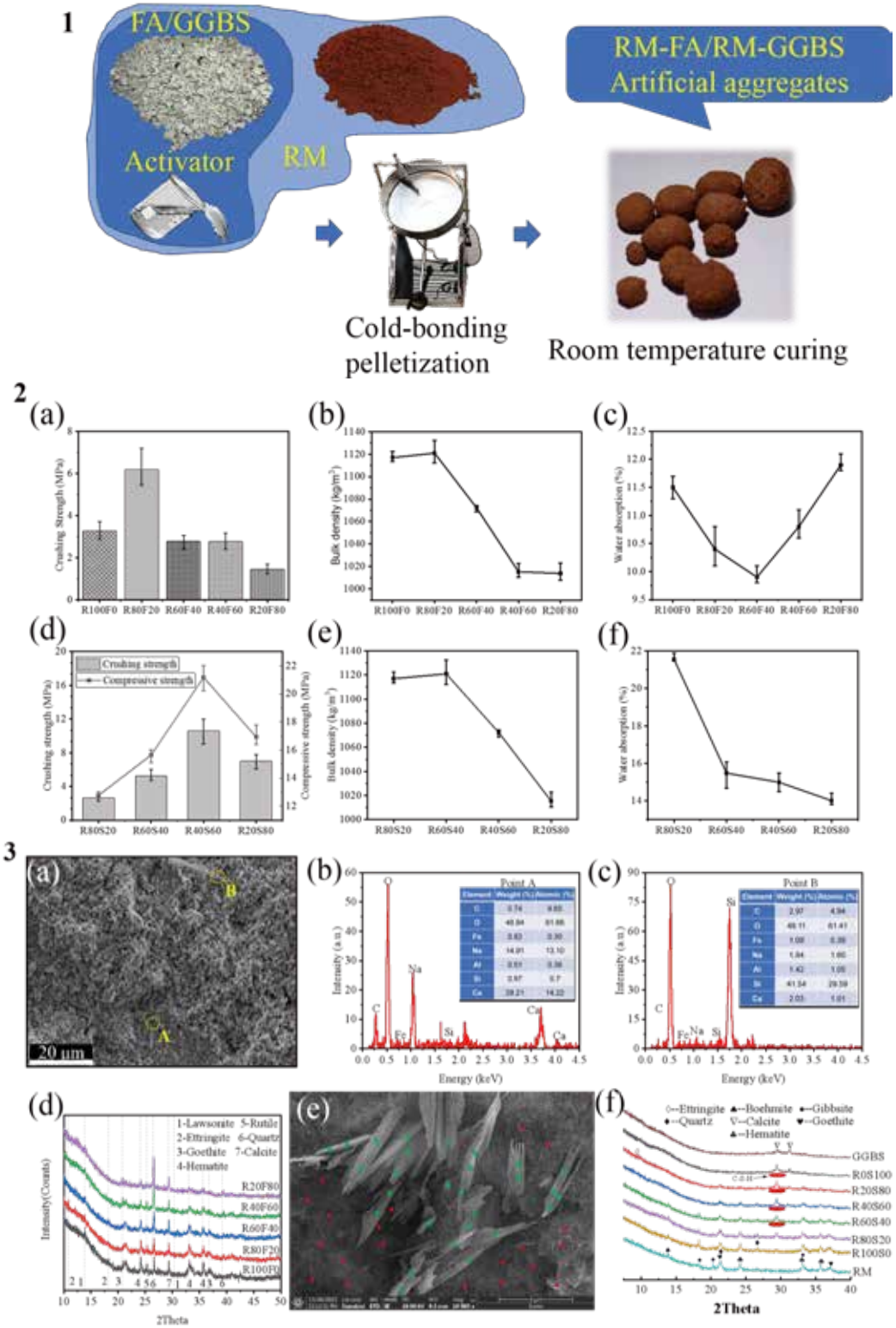

Fig. 1 Cold-bonding palletization process of artificial aggregates; **Fig. 2** The mechanical properties, bulk densities, and water absorption of RM-fly ash aggregates (a, b, c) and RM-slag aggregates (d, e, f); **Fig. 3** Microstructure analysis and product identification of RM-fly ash aggregates (a, b, c, d) and RM-slag aggregates (e, f).

Acknowledgment

The authors would like to appreciate the financial support from the National Natural Science Foundation of China (No. 52061160481 and 52108228), Project of Department of Education of Guangdong Province, China (No. 2018KZDXM060), and Guangdong Provincial Key Laboratory of Durability for Marine Civil Engineering (SZU) (No. 2020B1212060074).

Parallel Sessions-9

Properties of Seawater and Sea-Sand Concrete (SSC)

Development of low-alkalinity seawater sea sand concrete for BFRP bar reinforced marine infrastructure

Yong Yi[1], Deju Zhu[1,2*#], Guo Shuaicheng[1,2], Zhijian Liu[1], Caijun Shi[1, 2]

1Key Laboratory for Green & Advanced Civil Engineering Materials and Application Technology of Hunan Province, College of Civil Engineering, Hunan University, Changsha, 410082, PR China
2International Science Innovation Collaboration Base for Green & Advanced Civil Engineering Materials of Hunan Province, Hunan University, Changsha, 410082, PR China
Guangdong 518060, People's Republic of China
*Presenter: dzhu@hnu.edu.cn, #Corresponding author: dzhu@hnu.edu.cn

Abstract

During the recent decade, the use of FRP bar reinforced seawater sea sand concrete (SWSSC) as alternative to traditional steel bar reinforced concrete for the construction of marine infrastructures has been increasingly investigated and promoted. Compared to normal RC, FRP-SWSSC are believed more durable under the seawater invasion because FRP bar is highly resistant to chloride attack. The use of seawater and sea sand for concrete production avoids the consumption of river sand fresh water, which are two resources in shortage. Seawater and sea sand are also easily available for coastal and island construction. However, the durability problem of FRP bars in strong alkaline environment of concrete is still open to be addressed, especially for the newly developed BFRP bar. It has been demonstrated that the degradation rate of BFRP bars can be significantly mitigated as the alkalinity of the pore solution decreases (Fig. 1).

According to the improved durability of BFRP bar in low-alkalinity environment, low-alkalinity binder comprising of cement, silica fume and fly ash was been designed. The heat output during hydration (Fig. 2) of the low-alkalinity binder is lower than ordinary Portland cement and the hydration product, portlandite, is completely depleted (Fig. 3 and 4).

Based on the formulation of the above low-alkalinity binder, low-alkalinity SWSSCs were developed. The measured pH of low-alkalinity SWSSCs (11.6-11.7) was one unit lower than that of normal SWSSC (~12.5). After 180 days accelerated aging in 55°C artificial seawater, the tensile strength degradation of BFRP bars embedded in the low-alkalinity SWSSCs was significantly reduced compared to their counterparts in normal SWSSC. The respective retentions of specimens wrapped by SWSSC with high (H) and low (L) compressive strength (C100SF0FA0-H and C100SF0FA0-L) were 16.66 % and 23.56 % (Fig. 5). In contrast, BFRP bars embedded in the two low-alkalinity SWSSCs (C65SF35FA0-H/L and C35SF15FA50 H/L) retained about 70% or more of their tensile strength regardless of the compressive strength grade of the concrete.

The recorded internal relative humidity of the two low-alkalinity SWSSCs are always lower than normal SWSSC, especially during early exposure period (Fig. 6). The reduced alkalinity and humidity in low-alkalinity SWSSC contributed to the mitigated the deterioration of BFRP bars. Low-alkalinity SWSSC was recommended to construct BFRP bar reinforced concrete structures with better durability in marine environment.

Keywords: Alkalinity; BFRP bar; SWSSC; Durability; Marine

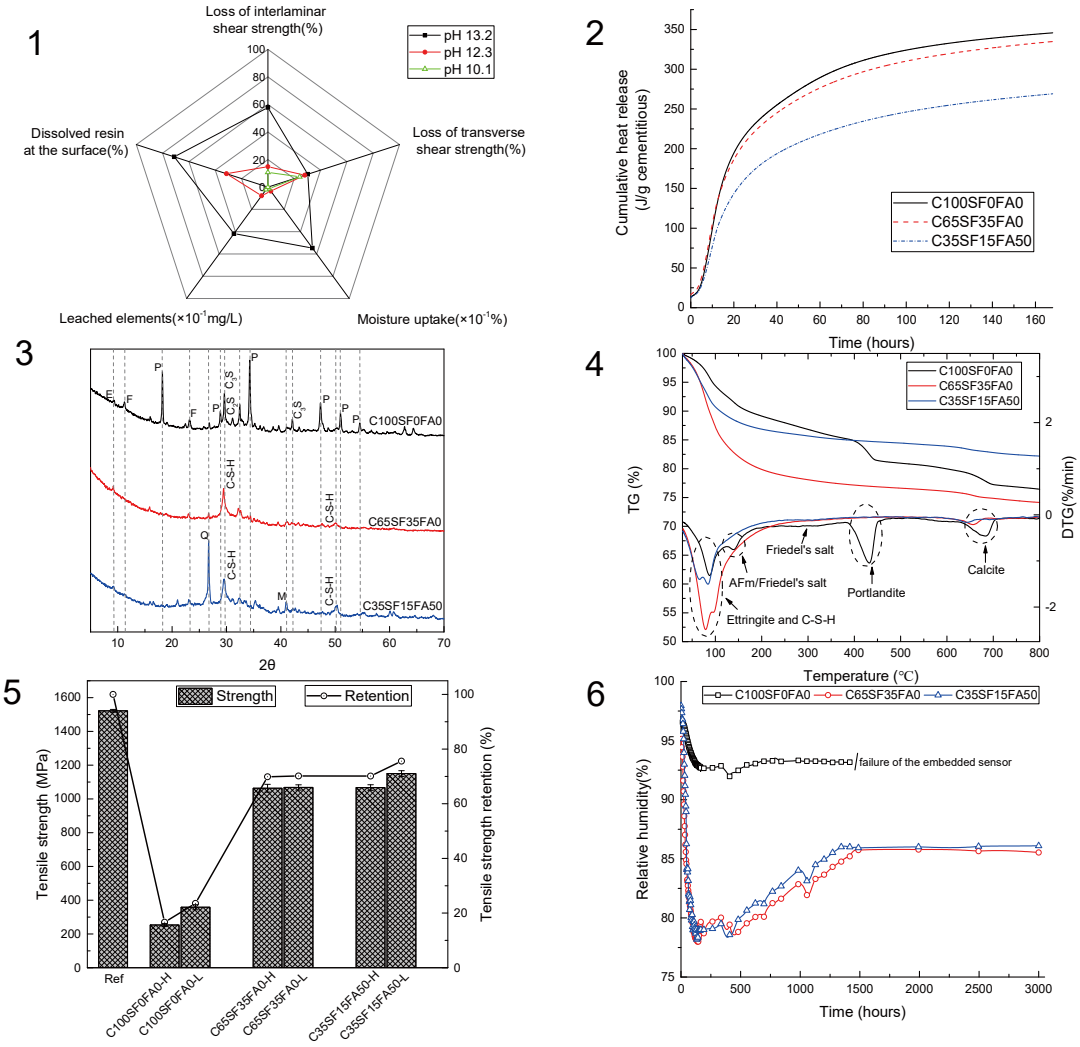

Fig. 1 effect of alkalinity on the degradation of BFRP bar; **Fig. 2** Hydration heat of different seawater pastes; **Fig. 3** XRD patterns of the normal and low-alkalinity pastes at 180 days; **Fig. 4** TGA/DTG of the normal and low-alkalinity pastes at 180 days; **Fig. 5** Tensile strength of BFRP bars embedded in normal and low-alkalinity SWSSCs after 180 days exposure to seawater at 55℃; **Fig. 6** Evolution of internal relative humidity for normal and low-alkalinity SWSSCs during aging process

Acknowledgment

The experiments conducted in this study were financially supported by the National Natural Science Foundation of China (U1806225) and High-Tech Industry Science and Technology Innovation Leading Plan of Hunan Province (2020GK2079).

Effect of seawater sea-sand concrete on tensile strength reduction of GFRP rebars and corresponding degradation mechanism

Peng Wang*, Linyuwen Ke, Haoliang Wu, Christopher K. Y. Leung#

Department of Civil and Environmental Engineering, Hong Kong University of Science and Technology, Hong Kong, China
*Presenter: pwangal@connect.ust.hk, #Corresponding author: ckleung@ust.hk

Abstract

Steel corrosion could not only result in severe structural damage and huge economic loss but also threaten the safety of structures over their lifetimes. In contrast, glass fiber reinforced polymer (GFRP) presents advantages in high strength-to-weight ratio and good chemical resistance. With these merits, GFRP rebar is considered a substitute for steel reinforcement in concrete structures to address the steel corrosion issue. Particularly, Recently, GFRP rebars have been considered for the construction of major reinforced concrete structures. However, many researchers found that the tensile strength of GFRP rebars inside concrete might gradually decrease with time, i.e., the durability of GFRP rebars is still under the threat of aggressive environmental conditions.

Seawater sea-sand concrete (SWSSC) has also attracted the attention of worldwide researchers because it can make use of seawater and sea sand which are enormously reserved in nature. GFRP-SWSSC structure is believed to be highly promising since salt-induced steel corrosion can be effectively avoided. However, as there are a lot of cations (e.g., Na^+, K^+ and Ca^{2+}) and anions (e.g., Cl^- and SO_4^{2-}) in seawater and sea sand, research on the durability of GFRP rebars in SWSSC is complex and challenging.

The purpose of this paper is to investigate the effects of SSC on the durability of GFRP rebars and reveal the potential degradation mechanisms. Firstly, the GFRP rebars are immersed in the simulated pore solution (pH = 13.6) of normal concrete (NC) and SWSSC at 23, 40 and 60 °C for up to 12 months. The tensile strength reduction is found to be similar for GFRP rebars exposed to NC and SWSSC solutions (**Fig. 1**), indicating that the salt content in SWSSC has no significant effect on the tensile performance of GFRP rebars. To confirm this finding, the microstructure morphology and chemical compositions of SWSSC-GFRP samples are observed by conducting scanning electron microscopy (SEM) and energy-dispersive X-ray spectroscopy (EDS) tests, respectively. As a result, strong chemical reactions between ions and the glass fibers and matrix mostly occur on the rebar's exterior, while the rebar's core basically remains unchanged (**Fig. 2**). Further, the compared GFRP rebars are immersed in distilled water (pH = 7) and sodium hydroxide solutions (pH = 11, 12 and 13) at 23, 40 and 60 °C for up to 12 months, which is conducted to illustrate the effect of exposure pH level on GFRP's degradation. Experimental results show smaller tensile strength retention in a high-pH exposure (**Fig. 3**), implying that a higher pH level could result in more severe corrosion. In addition, the residual tensile strength retention of GFRP rebars is found to follow an exponential function with the ambient pH level (**Fig. 4**). Lastly, the activation energy (E_a) corresponding to the GFRP corrosion at different pH levels is obtained based on Arrhenius equation, and the relationship between E_a and pH level is found to reveal the degradation mechanism behind the GFRP corrosion. As E_a linearly decreases with increasing pH level and both NC- and SWSSC- GFRP samples obey the same function (**Fig. 4**), the GFRP corrosion of rebars in NC and SWSSC is believed to be attributed to the cementitious alkalinity.

Based on the bench-scaled investigation, this study reveals that GFRP corrosion is mainly attributed to the exposure pH level, but the seawater sea-sand slightly affects the durability of GFRP. This study yields useful information to engineers regarding the degradation mechanism of GFRP corrosion. The measurement of ambient pH is believed to be an effective method to rapidly estimate the potential GFRP corrosion.

Keywords: GFRP rebar; NC; SWSSC; pH level; tensile strength retention; activation energy

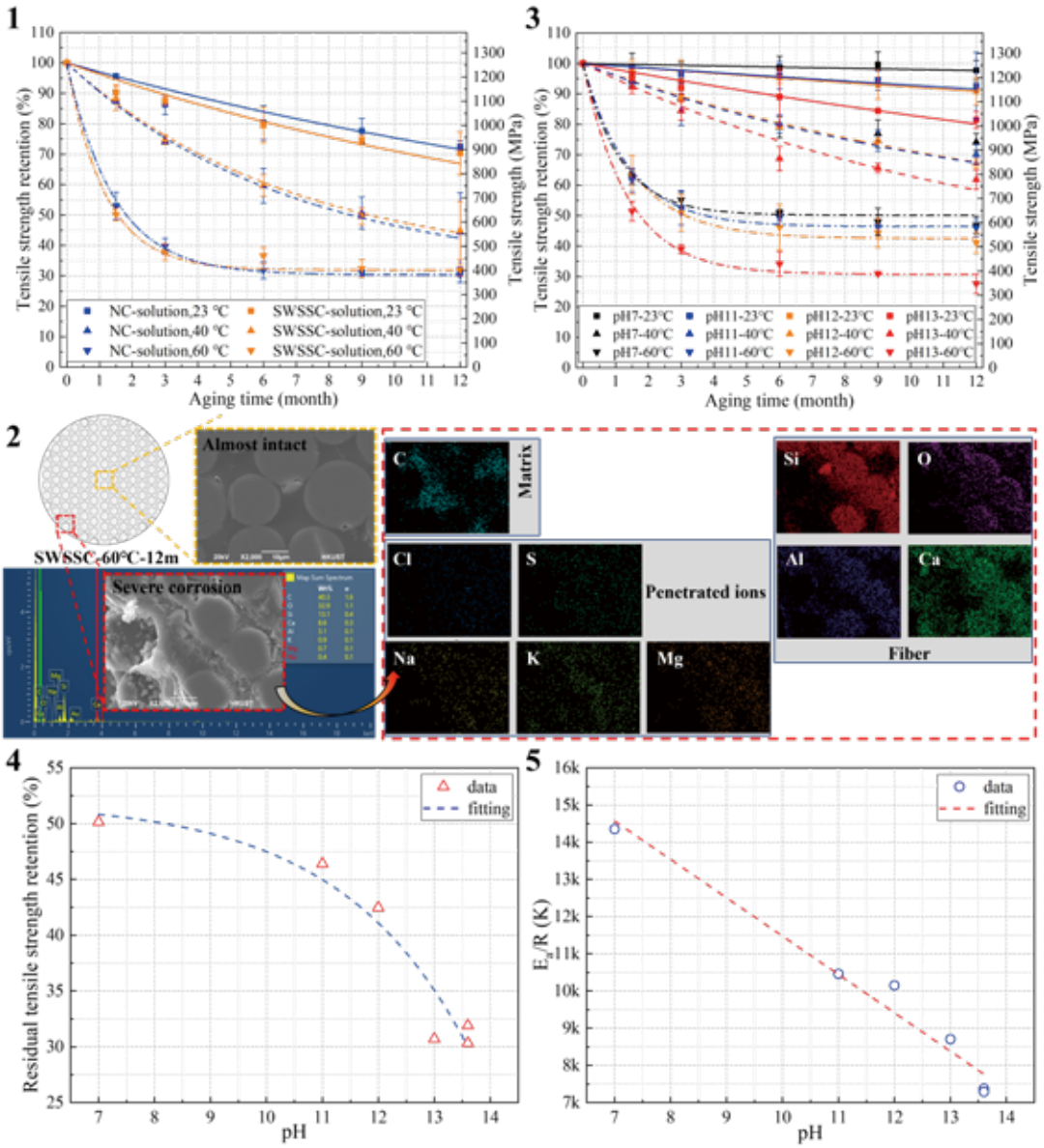

Fig. 1 Tensile strength retention of GFRP rebars exposed to simulated NC and SWSSC solutions; **Fig. 2** SEM and EDS images of conditioned GFRP rebar; **Fig. 3** Tensile strength retention of GFRP rebars exposed to distilled water and alkaline solutions; **Fig. 4** Relationship between residual tensile strength retention of GFRP rebar and ambient pH level; **Fig. 5** Relationship between activation energy of GFRP corrosion and ambient pH level

Acknowledgment

The authors gratefully acknowledge the financial support provided by the Hong Kong Research Grants Council (T22-502/18-R and HKUST VPRDO19EG01). The second author would also acknowledge her support from the Hong Kong PhD Fellowship Program.

Chloride-binding capacity of cement-GGBFS-nanosilica composites under seawater chloride-rich environments

Fulin Qu[1,2*], Yipu Guo[1], Wengui Li[1#]

[1] School of Civil and Environmental Engineering, University of Technology Sydney, NSW 2007, Australia

2 Department of Civil and Environmental Engineering, The Hong Kong Polytechnic University, Hong Kong, China

[*]*Presenter:* Fulin.qu@polyu.edu.hk , [#]*Corresponding author:* Wengui.li@uts.edu.au

Abstract

Increasing chloride-binding capacity of cementitious composites is considered as a controlling property of the reinforced concrete in the marine environment. In this paper, there were three specific objectives: firstly, to evaluate the effect of ground granulated blast furnace slag (GGBFS) on the chloride-binding capacity of cementitious composites; secondly, to examine the effect of nano-silica (NS) content on the chloride-binding capacity of GGBFS-based cementitious composites; and thirdly, to investigate the effect of different concentrations of chloride solutions (e.g. NaCl, $MgCl_2$, and NaCl + $MgCl_2$ solutions) on the chloride-binding capacity of cementitious composites.

It was found that the GGBFS replacement for cement significantly improved the chemical and physical chloride-binding capacity of cementitious composites and decreased the pH of exposure solutions (Fig. 1). Due to the pozzolanic reaction consuming Portlandite (CH) (Fig. 3), large amounts of C-S-H/C-A-S-H gels are generated, further increasing the physical chloride binding. The higher aluminum content in GGBFS increased the formation of chloroaluminate (Friedel's salts), which enhanced the chemical chloride binding (Fig. 2).

The results also illustrated that the addition of NS decreased the pH of exposure solutions, and the addition of 1.0 wt.% NS further enhanced the total chloride-binding capacity of GGBFS-based cementitious composites. However, when the content of NS is higher than 1.0 wt.%, the total chloride-binding capacity (especially, the chemical chloride-binding capacity) of GGBFS-based cementitious composites was decreased. The addition of NS increased physical chloride-binding capacity due to the formation of more C-S-H/C-A-S-H gels, while leaving less aluminum phase available for the formation of Friedel's salts (Fig. 4).

Compared to exposure to salt solutions with sodium ions, more chlorides of cementitious composites were found to be bound when exposed to salt solutions with magnesium ions. The magnesium ions increased the amount of physically bounded chloride in the gels' diffuse layer due to the decreasing pH of the $MgCl_2$ solutions. Except for Friedel's salts' formation, the hydrotalcite with high element proportions of Cl confirmed by EDX results is expected to be generated, further increasing the chloride binding.

The thermodynamic model (Fig. 5) could display relatively accurately in predicting most of the phase assemblage of the cement-GGBFS-NS composites exposed to different chloride-ride environments. The cementitious composite with 30 % GGBFS and 1.0% NS having the highest value of chloride-binding ratio provide a prospective way to enhance the long-term chloride-binding capacity (Fig. 6). Therefore, the utilization of GGBFS and NS in chloride binding is supposed to guide the improvement of marine constructions.

Keywords: Cementitious composite; Chloride-binding ratio; Corrosion; Nano-silica; Thermodynamic modeling

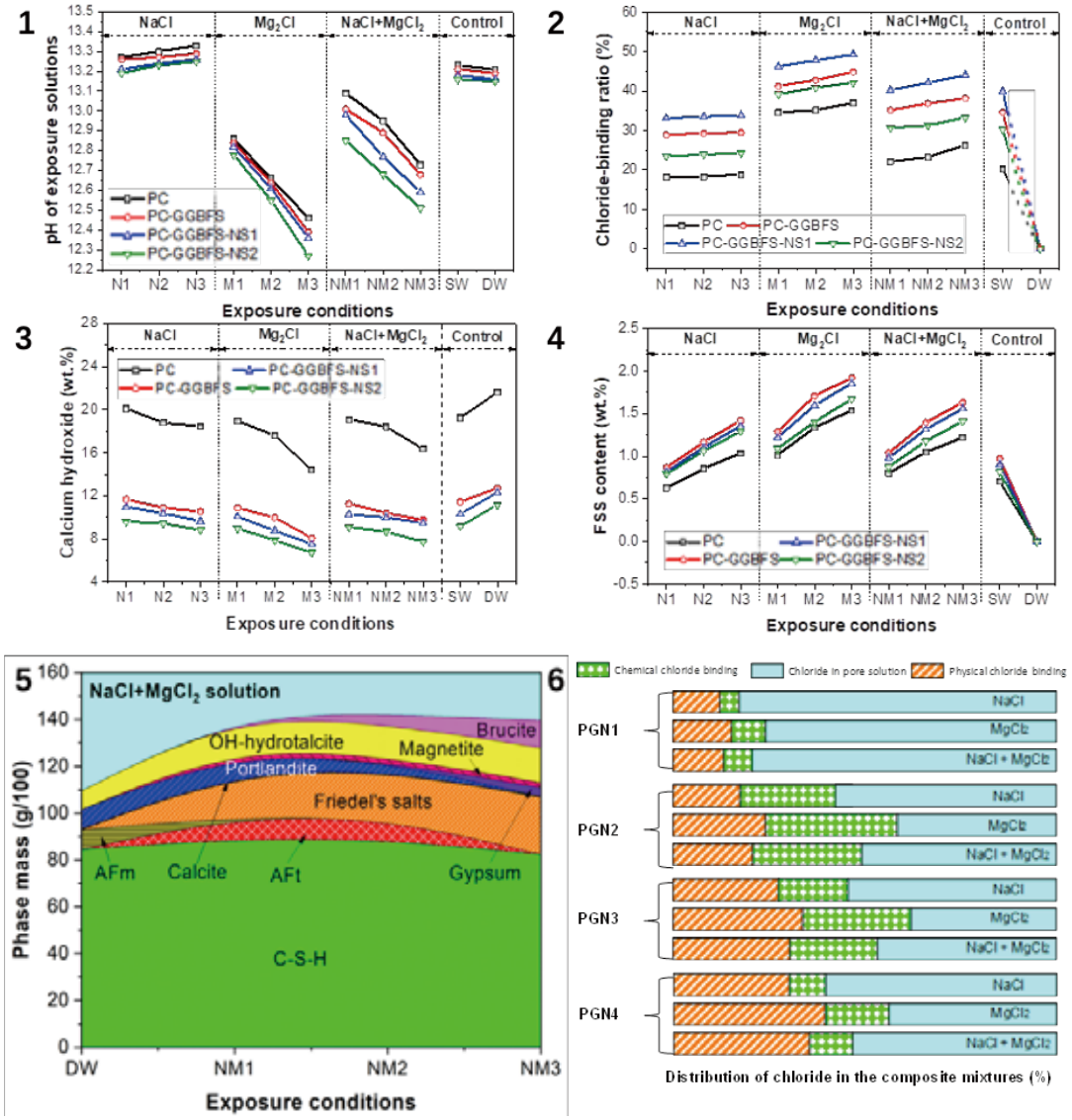

Fig. 1 pH of the supernatants; **Fig. 2** Chloride-binding ratio of well-hydrated cementitious pastes; **Fig. 3** Calcium hydroxide contents (wt.%) of the well-hydrated cementitious pastes; **Fig. 4** FSS contents of the well-hydrated cementitious pastes; **Fig. 5** Phase assemblages for well-hydrated Portland cement-GGBFS-NS composites; **Fig. 6** The chloride distribution in Portland cement-GGBFS-NS composites.

Acknowledgment

The authors appreciate the Australian Research Council (FT220100177, DP220101051; DP220100036) and University of Technology Sydney Research Academic Program at Tech Lab (UTS RAPT).

The Mechanism of Performance Difference Between Seawater Sea-sand and Freshwater River-sand Ultra High Performance Concrete Based on X-CT Technology

Fang-ying Shi[1*], Tian-yu Li[2#], Xiao-yan Liu[3], Xinyu-Wang[3], YangTao-Li[2], Teng-fei Bao[2], Surendra P. Shah[3,4]

[1] College of the Environment, Hohai University, Nanjing 210098, China
[2] College of Water Conservancy and Hydropower Engineering, Hohai University, Nanjing 210098, China
[3] College of Mechanics and Materials, Hohai University, Nanjing 210098, China
[4] Center for Advanced Cement-Based Materials (ACBM), Northwestern University, Evanston, Illinois 60208, USA

Presenter: 1439760037@qq.con, #Corresponding author: 20220916@hhu.edu.cn

Abstract

At present, river sand was the main source of sand for construction. But the supply of river sand was limited by resources and environmental impact, and cannot fully met the demand for construction. China's coastal areas were rich in sea sand resources, and the total amount of sea sand resources in China's offshore was about 67.96×10^{10} ~ 68.49×10^{10} m^3. The mining of sand for construction has gradually shifted to the marine environment. The orderly development, research and utilization of abundant sea sand resources as construction aggregates has become an inevitable development trend. How to use sea sand to prepare innovative water conservancy construction materials with excellent mechanical and durable properties is an intense and urgent task.

Based on the preparation principle of UHPC, sea sand and artificial sea water were used to replace river sand and fresh water to prepare seawater sea-sand ultra high performance concrete (SSUHPC), and freshwater river-sand ultra high performance concrete (FRUHPC) was prepared for comparative study. The compressive strength of SSUHPC and FRUHPC is 162.1 MPa and 173.3 MPa, respectively. Both SSUHPC and FRUHPC have high fatigue resistance characteristics, and SSUHPC takes the lead in stress failure in high stress fatigue test. Both SSUHPC and FRUHPC show excellent durability characteristics, while SSUHPC performs better. The microstructure characteristics of SSUHPC and FRUHPC were studied by SEM, XRD and MIP technology. The continuous section data were obtained by μ X-CT technology, and the fibre and pore structure were reconstructed and established, so as to study the performance difference mechanism between SSUHPC and FRUHPC.

Hydration degree of mortar, characteristics of pore structure and dispersion of steel fibre were important factors on mechanical properties and durability of concrete materials. Excellent mechanics and durability of UHPC were guaranteed by uniformly dispersed steel fibre, hydrated cement mortar with mature structure and reasonable pore structure. Compared with FRUHPC, the mortar in SSUHPC has a higher degree of hydration, and the mortar with mature hydration structure and dense structure make the concrete material have higher corrosion resistance. Due to the uneven distribution of pore and steel fibre, the compressive strength and fatigue resistance of SSUHPC were inferior to that of UHPC prepared with freshwater river-sand. Firstly, this paper verifies the possibility of using seawater seasand to produce concrete with ultra high mechanical properties and durability. SSUHPC was slightly inferior to UHPC prepared from freshwater river-sand in mechanical properties, but it has more excellent durability characteristics. In view of these problems, the performance of SSUHPC can be further improved by improving the pore structure and fibre distribution.

The performance difference of mechanic properties and durability between SSUHPC and FRUHPC was systematically studied, and the mechanism of performance difference between the two kinds of concrete materials were revealed, which lay a solid theoretical foundation for the utilization of sea sand resources and the promotion of seawater seasand concrete.

Keywords: Sea Sand; UHPC; Pore Structure; Steel Fibre Structure; Mechanism Analysis

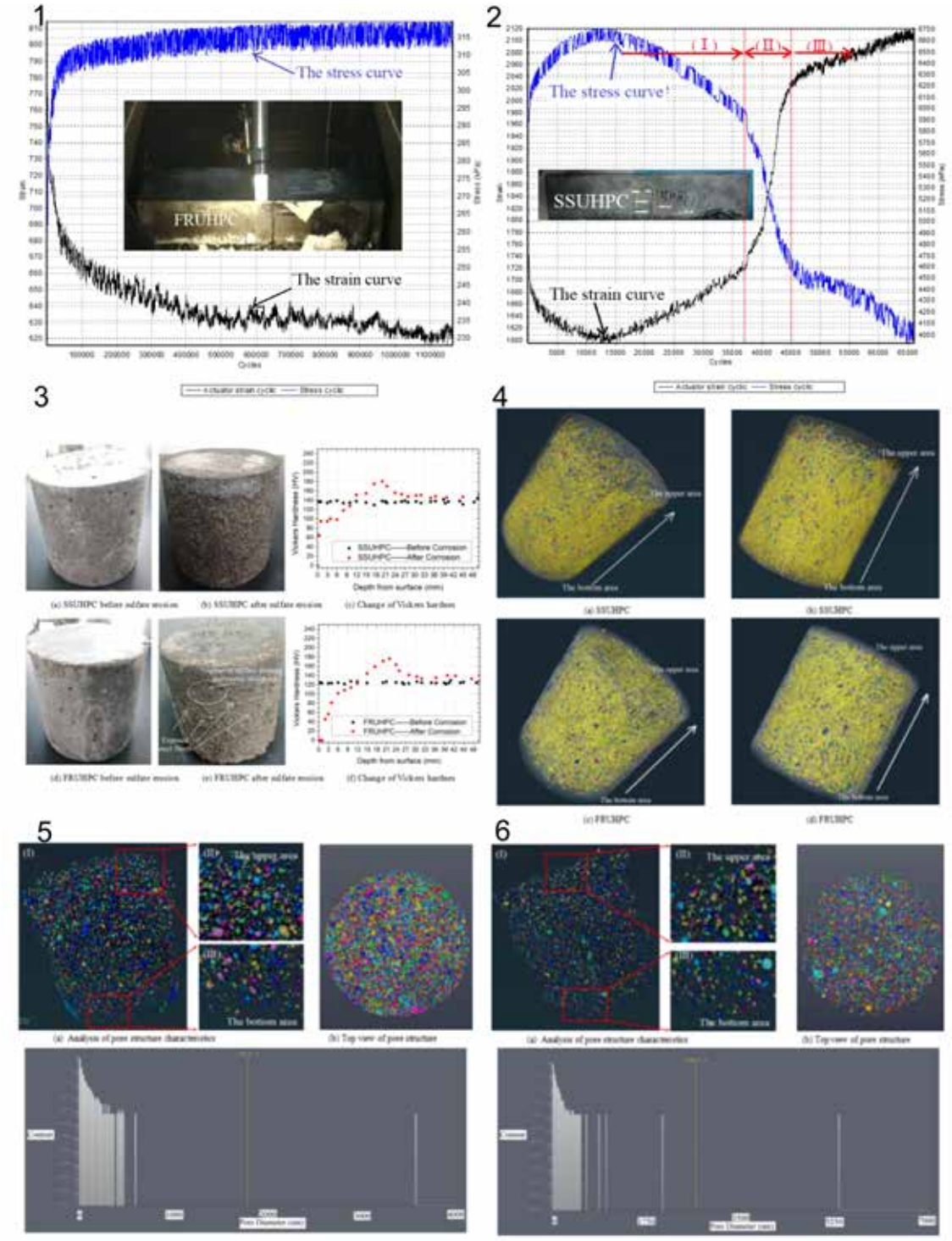

Fig. 1 500000 loading times of FRUHPC when the loading value was 10 kN; **Fig. 2** 500000 loading times of SSUHPC when the loading value was 10 kN; **Fig. 3** Comparison of SSUHPC/FEUHPC before and after sulfate erosion; **Fig. 4** Difference of UHPC prepared with seawater seasand and freshwater river-sand; **Fig. 5** Reconstruction pore structure model of SSUHPC (above 200 μm); **Fig. 6** Reconstruction pore structure model of FRUHPC (above 200 μm)

Acknowledgment

The authors would like to acknowledge the funding support from Shandong Key Laboratory of Corrosion Science, China, and the National Natural Science Foundation of China (Grant No. 41827805 and 51879093).

Experimental study on mechanical properties of seawater sea-sand concrete with sea-sands from different regions

GENG Jianzhi, ZHU Deju, GUO Shuaicheng, YI Yong, ZHOU Linlin

(Key Laboratory for Green & Advanced Civil Engineering Materials and Application Technology of Hunan Province, Hunan University, Changsha 410082, China)

This study selected the undisturbed sea sands from Shandong Province, Fujian Province and Guangxi Province as the research objects, and studied the influence mechanism of the sea sands from different regions on the mechanical properties of concrete. The physical and chemical properties of the sea sands were first characterized with the optical microscope, element titration, XRD and SEM. And the results were further compared to those of the river sand from Changsha. It is indicated that the mineral composition, fineness modulus and crushing value of sea sands are consistent with those of river sand. Meanwhile, the sea sands from different regions possess different chloride and shell contents. Then the seawater sea-sand concretes (SWSSCs) with three different strength grades (C30, C40 and C50) were prepared with the sea sands from different regions and the artificial seawater. The mechanical tests were conducted to examine the cubic and axial compressive strengths, static elastic modulus and splitting tensile strength of the prepared SWSSC. Then the evolution mechanism was examined with the combined XRD and SEM study. And the results were also compared with those of the OC. The results showed that the early-age (3 d and 7 d curing age) compressive strength of the SWSSC was higher than these of the ordinary concrete (OC), while its late-age (After 28 d curing age) compressive strength is lower than that of OC. The tensile strength gap between SWSSC and OC gradually decreased with the curing age, and the long-term (360 d curing age) tensile strength of SWSSC was still higher than that of OC. Finally, the pore structures of SWSSC and OC at different ages were compared through the low field ^{1}H NMR test. It was found that the pore structure development of SWSSC and OC were consistent with their strength development. This study can provide a solid basis for the mix design and engineering application of SWSSC.

Keywords: sea sand, concrete, mechanical property, pore structure

Durability study of sea-sand concrete under the combined effects of carbonation and chloride redistribution

Yongqiang Li [1*], Wei Liu [1], Feng Xing [1#]

[1] Guangdong Provincial Key Laboratory of Durability for Marine Civil Engineering, Key Laboratory for Resilient Infrastructures of Coastal Cities (Ministry of Education), College of Civil and Transportation Engineering, Shenzhen University, Shenzhen, 518060, Guangdong, PR China

Presenter: liyo@chalmers.se, #Corresponding author: xingf@szu.edu.cn

Abstract

For the sea-sand concrete, the chloride ions should be uniformly distributed after casting. However, the chlorides are redistributed after being exposed to the carbonation environment, which can significantly reduce the effective service life of sea-sand concrete. In this study, a new mathematical model, coupling several parameters, including the changes in carbonation degree, moisture transport and release of bound chlorides under the carbonation, were firstly proposed to accurately predict the phenomenon of chloride redistribution in chloride blended and carbonated concrete. It was found that experimental results of chloride redistribution were fitted well with the proposed model. The rebar corrosion in this case was initiated by the excess of chloride ions rather than carbonation or oxygen diffusion. The ratio of $[Cl^-]/[OH^-]$ is a key parameter in prediction of corrosion initiation. Next, the model was extended to predict the effective service time of newly-built and existed sea-sand concrete structures in practical engineering. The relationships between affecting parameters, e.g., chloride and moisture diffusion coefficient, carbonation rate and initial chlorides, on the effective service time exposed to carbonation effect were analyzed. Some practical suggestions were put forward for extending the service time of new-built sea-sand concrete structures to the designed time. It is expected the results of this study can be used for the basis of understanding the durability performance of sea-sand concrete subjected to carbonation environment.

Key Words

Sea-sand concrete; Chloride redistribution; Carbonation; Durability; Service life

Acknowledgment

We want to thank the financial support from the National Natural Science Foundation of China (51978408) and the Guangdong Provincial Key Laboratory of Durability for Marine Civil Engineering (SZU) (2020B1212060074)

Flexural behaviour of seawater sea-sand coral aggregate concrete beams reinforced with FRP bars

Fang Yuan

Associate Professor, Guangdong Provincial Key Laboratory of Durability for Marine Civil Engineering, Shenzhen University, Shenzhen 518060, China, E-mail: fyuan@szu.edu.cn

Abstract: The use of locally available raw materials, such as seawater, sea sand, and coral reefs, for construction on remote islands saves transportation costs and guarantees the construction period. These raw materials contain high amounts of corrosive substances such as chloride ions, which increases the corrosion risk of steel reinforcement. The corrosion problem can be addressed by combining chloride ion-carrying raw materials with non-corrosive fibre-reinforced polymer (FRP) reinforcement. In contrast to natural aggregate concrete (NAC), coral aggregate concrete (CAC) is rather brittle in compression, and the applicability of the design formula of FRP-reinforced NAC members to FRP-reinforced CAC members is questionable. This study investigated the flexural behaviours of FRP-reinforced seawater sea-sand CAC beams, where all the raw materials for concrete were collected directly from local islands. First, a group of beams was loaded under four-point bending to evaluate the influence of concrete type and reinforcement ratio on the flexural behaviour of the beams. It is found that the ultimate moment capacity and ductility of FRP-reinforced CAC beams were lower than those of the corresponding FRP-reinforced NAC beams. Subsequently, flexural theorems were applied to derive a model of equivalent rectangular stress block parameters for FRP-reinforced CAC beams. Finally, the flexural strengths calculated using the proposed model were compared with the measured test results, as well as predictions using existing design codes. The proposed model not only reduces the prediction error of the flexural strengths but is also safer and more conservative compared with existing design codes, which is critical for non-ductile FRP-reinforced concrete beams.

Keywords: Fibre-reinforced polymer (FRP); coral aggregate concrete (CAC); reinforced concrete beam; flexural behaviour; experiments; stress block parameter

Workability, mechanical properties, drying shrinkage behavior and micro-structural characteristics of seawater and sea-sand concrete

Zhi-Lu Jiang[1*], Ran An[1,2], Jun Liu[1,2#], Ji-Hua Zhu[1,2], Feng Xing[1,2]

[1] College of Civil Engineering and Architecture, Zhejiang University of Technology, Hangzhou, 310014, China
[2] Guangdong Province Key Laboratory of Durability for Marine Civil Engineering,
[3] College of Civil and Transportation Engineering, Shenzhen University, Shenzhen, Guangdong 518060, People's Republic of China
Presenter: zljiang@zjut.edu.cn, #Corresponding author: liujun@szu.edu.cn

Abstract

Adopting greener and lower carbon materials in cement industry, such as limestone calcined clay (LC2), fly ash (FA) and slag as supplementary materials, is the key breakthrough of energy saving and emission reduction. Additionally, a large amount of concrete in the construction industry every year leads to the consumption of fresh water and river sand increasing. The shortage of fresh water and river sand may lead to the destruction of river ecosystem, especially for coastal regions. Therefore, it is an important approach to study the replacement of fresh water and river sand by seawater and sea sand to improve resources shortage and achieve sustainable development. Based on the concept of global resource depletion and sustainable development, seawater and/or sea sand (mainly seawater) have interesting application values in the fields of unreinforced concrete, FRP reinforced concrete, ICCP-SS (Impressed Current Cathodic Protection-Structural Strengthening) and so on. In this study, eight kinds of concrete were designed by using three different water-binder ratios, two supplementary cementitious materials (SCMs). This study reports the comprehensive results of workability, mechanical strength, drying shrinkage behavior and microstructures of seawater and sea sand concrete (SSC). At the same time, to fully analyze mechanical properties and deformation properties, SSC hydration products and the characteristics of the SSC microstructures is explored by XRD, TGA, SEM-EDS and MIP.

The results show that adding seawater and sea sand can lead to the increase of early compressive strength and the declining of concrete workability, while the utilization of seawater and sea sand can result in the decrease of later strength (Fig. 1). With the rising of curing age, SSC with adding SCMs (FA/LC2) has similar or better comprehensive performance than OPC-SSC. The MIP results (Fig. 2) show that the pore structure of SSC can be refined by using seawater and sea sand, reducing water-binder ratio and replacing OPC with FA/LC2. The pore structure of SSC is closely related to its drying shrinkage behavior (Fig. 3). Scanning electron microscope (SEM) analysis (Fig. 4) also confirmed that the SSC with mineral admixtures has a more uniform and compact microstructure after long-term curing, and the SSC with 25% LC2 content has the best microstructural property. X-ray diffraction (XRD) and thermogravimetry analysis (TGA) also proved that LC2 system had better reaction performance and higher early activity than FA system (Figs. 5 and 6). This study can provide an insight into the utilization of seawater and sea sand in concrete and the impact of SCMs on SSC.

Keywords: Seawater and sea sand concrete; Fly ash; Limestone calcined clay; Mechanical strength; Drying shrinkage behavior

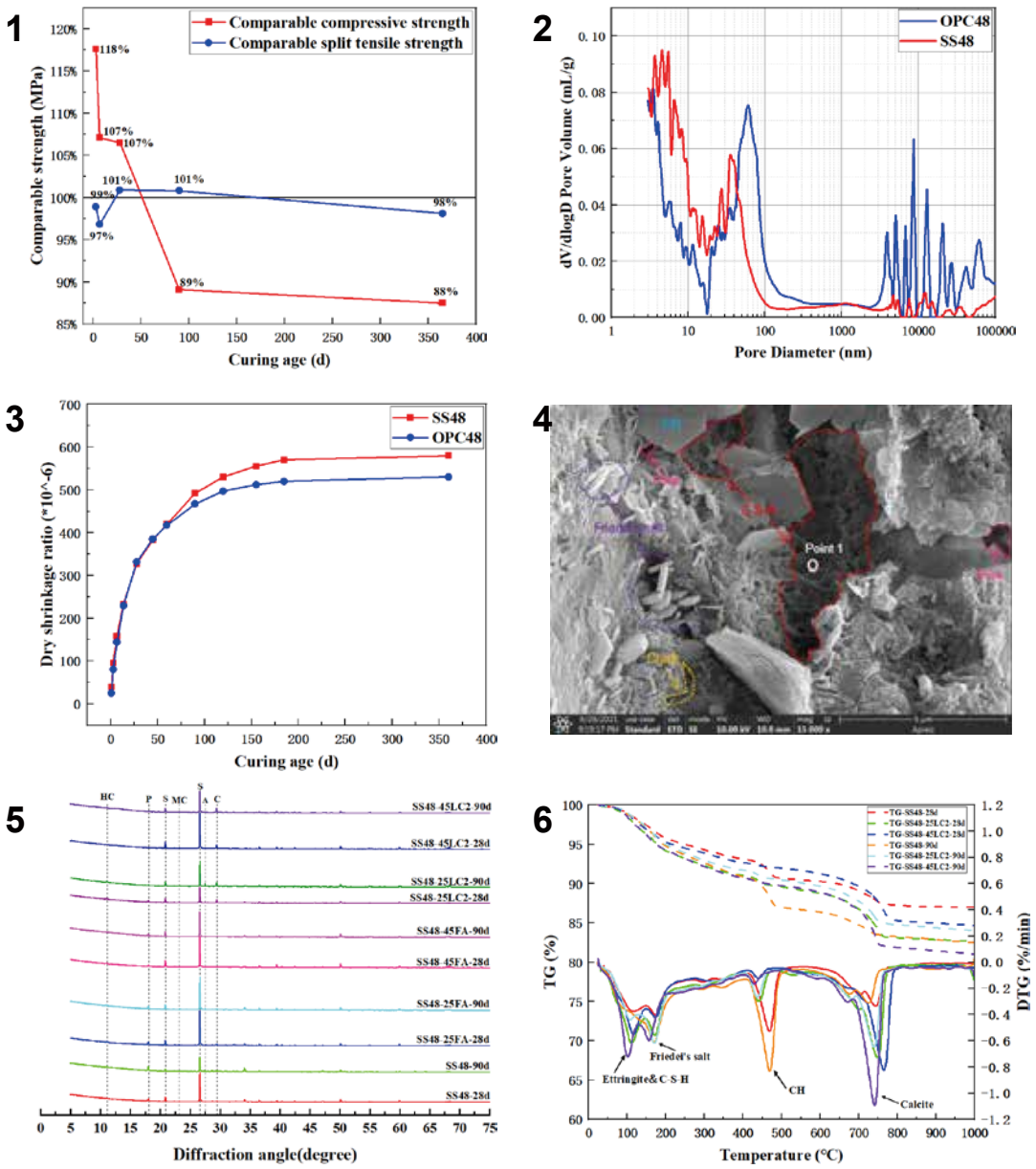

Fig. 1 Effect of seawater and sea sand on comparable strength; **Fig. 2** Pore size distribution by MIP; **Fig. 3** Effect of seawater and sea sand on dry shrinkage; **Fig. 4** SEM graph of SSC specimen SS48 at 28 d; **Fig. 5** Effect of SCMs on XRD patterns of concrete (F-Friedel's salt; P-CH; S-Quartz; A-Calcium silicate hydrate; C-$CaCO_3$; G-Gypsum; M-$Mg(OH)_2$; HC-Hemicarboaluminate; MC-Monocarboaluminate); **Fig. 6** Effect of LC2 content change on TG/DTG curves of concrete

Acknowledgment

The authors would like to acknowledge the funding support from the Key-Area Research and Development Program of Guangdong Province (2019B111107002).

Performance and characterization of seawater blended cement-based material incorporated with polycarboxylate superplasticizer

Shengye Xu[1,2*], Xianfeng Wang[1,2#], Jun Ren[3,#], Yunhui Fang[4], Jihua Zhu[1,2]

[1] Guangdong Provincial Key Laboratory of Durability for Marine Civil Engineering,
[2] College of Civil and Transportation Engineering, Shenzhen University, Shenzhen, Guangdong 518060, People's Republic of China
[3]School of Architecture and Planning, Yunnan University, Kunming 650500, China
[4]KZJ New Materials Group Co., Ltd, Xiamen 361199, China
[*]*Presenter: shixiao5561@163.com,* [#]*Corresponding authors: xfw@szu.edu.cn, renjunking@aliyun.com*

Abstract

Manufacturing concrete with seawater could mitigate the freshwater shortage with both economic and environmental benefits. However, the effect of superplasticizers in seawater blended cementitious materials on the performance and characterization, such as fresh properties and hydration, and hardened characteristics has not been systematically explored. In this study, the effects of two typical polycarboxylate superplasticizers (PCEs, including water-reducing and slump-retaining PCEs) on the rheological properties (plastic viscosity, yield stress, thixotropic area), hydration heat, hardened properties, and microstructure of the hydration products of the seawater blended cementitious materials, were investigated, and compared with those of conventional OPC. Experimental results indicate that the addition of PCEs has changed the rheological behavior of both the tap water and seawater mixed cement paste in terms of shearing-thinning and shear-thickening. Moreover, although the seawater increased the hydration heat of the specimen with both PCEs, the components of hydration products were not affected. Furthermore, in the presence of both PCEs, the compressive strength of the seawater cementitious material increased, and the microstructures were densified after blending with seawater.

Keywords: Seawater; Superplasticizer; Rheological properties; Hydration; Microstructure

Acknowledgments

The authors would like to acknowledge the funding support from the Key-Area Research and Development Program of Guangdong Province (2019B111107002), the National Natural Science Foundation of China (51978409, 52168038, 51908526), Guangdong Provincial Key Laboratory of Durability for Marine Civil Engineering (2020B1212060074), and Miss Lina Zhong from KZJ New Materials Group Co., Ltd is also gratefully acknowledged for her help in this work.

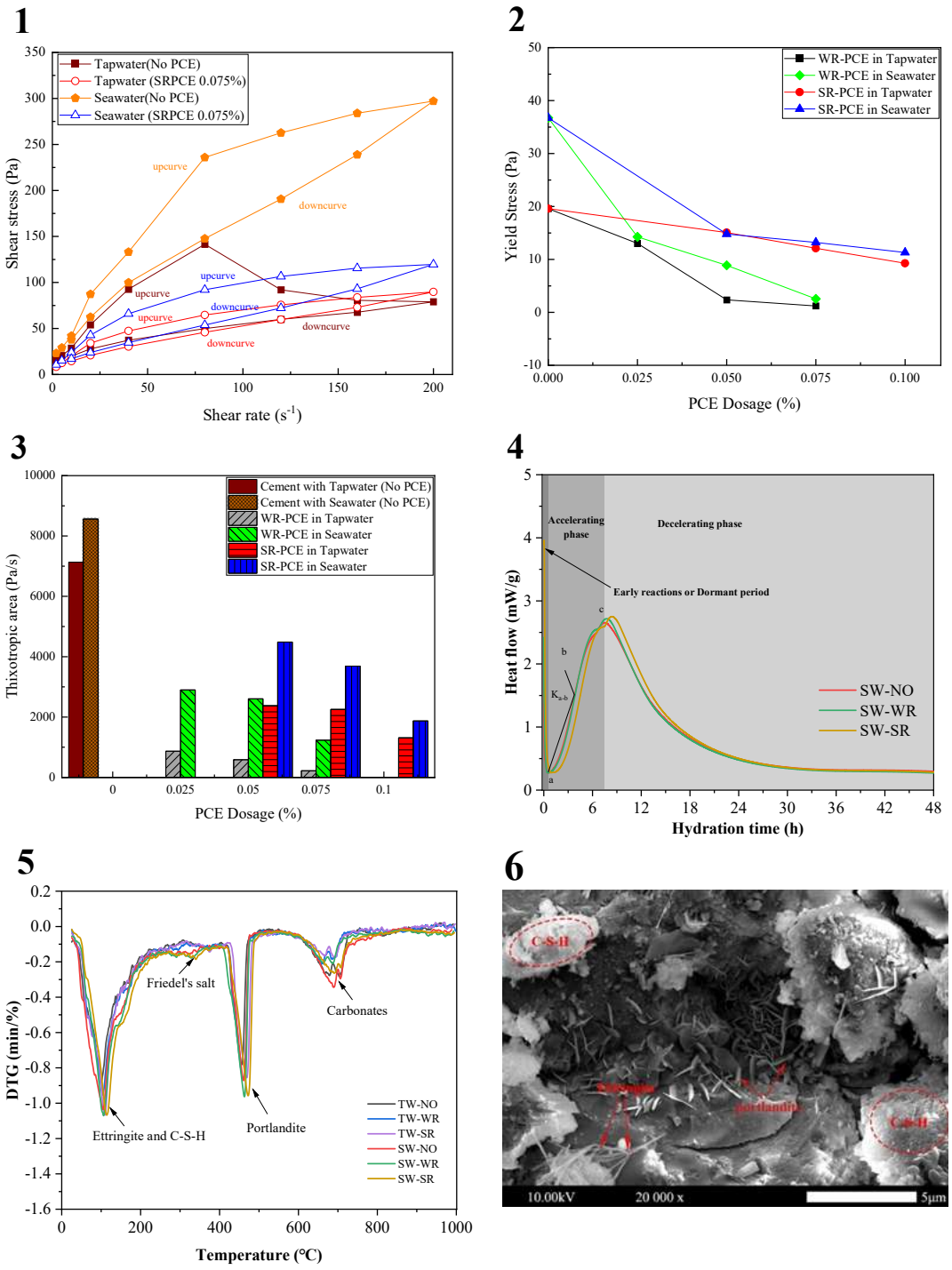

Fig. 1 Flow curve of cement with SR-PCE-0.075%; **Fig. 2** Effect of PCE dosage on the yield stress of cement paste fitted by the Modified Bingham model; **Fig. 3** Thixotropic area of cement; **Fig. 4** Hydration heat evolution of seawater cement pastes incorporated with different types of PCE; **Fig. 5** DTG curves of TW and SW blended cement pastes with different types of PCEs for three days; **Fig. 6** Microstructure of SW cement pastes without PCEs at the 28th day.

Effects of gypsum and premixed chlorides on hydration and binding mechanism for CSA cement

Jian-Sheng Huang[1*], Xue-Lei Jiang[1], Chen-Xi Su[1], Li-Li Sui[1,2,3], Wei-Wen Li[1,2,3], Yao-Cheng Wang[1,2,3#]

[1] College of Civil and Transportation Engineering, Shenzhen University, Shenzhen, Guangdong 518060, P. R. China
[2] Guangdong Province Key Laboratory of Durability for Marine Civil Engineering
[3] Key Laboratory for Resilient Infrastructure of Coastal Cities, Shenzhen University, Ministry of Education, Shenzhen 518060, P. R. China
[*]*Presenter:* jshuang_54@163.com, [#]*Corresponding author:* wangyc_szu@126.com

Abstract

Calcium sulfoaluminate cement (CSA) has been widely applied in marine civil engineering projects due to its high Cl^- binding capacity, which has been proved but not thoroughly explored. In-depth understanding on its hydration process and binding mechanism is the key step to guarantee its service durability. Up to date, most previous researches focused on hydration and binding mechanism on external ingress Cl^-, while only limited cases worked on those with premixed Cl^- introduced by raw materials. Within CSA mixes, gypsum plays an important role on its hydration and hardened properties. Therefore, it is greatly needed to reveal the effects of gypsum and premixed Cl^- on hydration and binding mechanism for CSA. In this paper, a series of experiments, including analysis on mineralogy quantification and testing indicators related to the binding properties, were carried out. Systematic results showed that the binding mechanism of premixed Cl^- was similar with that of the ingress Cl^-, i.e., the premixed Cl^- transformed into Friedel's salt by reacting with hydration products, such as Al-Fe-mono (AFm) (Fig.1). Besides, gypsum induced the formation of AFt at the early stage of hydration so that early compressive strength was improved (Fig. 2) but AFt did little contribution to binding Cl^-. On the other hand, premixed Cl^- in CSA shortened the setting time (Fig. 3), promoted the process of hydration heat, and effectively inhibited the generation of microcracks. More noteworthy, calcium aluminate hydrates (i.e., CAH_{10} and C_3AH_6) generated by CSA also made a significant contribution to Cl^- binding in addition to AFm.

The main product of samples with and without gypsum was Al-Fe-tri (AFt) and AFm, respectively. On the aspect of mechanical properties, compared to AFm, AFt contributed more on the compressive strength of pastes. On the aspect of Cl^- binding, samples with gypsum showed limited binding capacity than those without gypsum, because AFt, someone without binding ability, was the mainly product rather than AFm with excellent binding capacity (Fig. 4). In addition, gypsum in CSA consumed more water during the reaction, which resulted in a shorter setting time to some degree.

Premixed Cl^- promotes hydration of CSA cement, i.e., the acceleration of initial heat generation at first 5 hours, prevents formation of shrinkage cracks (Fig. 5) and results in a more densified microstructure, which benefited the compressive strength. On the other hand, the binding capacity of CSA on premixed Cl^- is closely related to the content of yielded AFm and the hydration degree of $C_4A_3\bar{S}$ clinker. Moreover, it is found that C_3AH_6, the stabilized form of yielded CAH_{10}, has the Cl^- binding capacity and displays a much higher binding ability on premixed Cl^- than AFm (Fig. 6).

Keywords: Calcium Sulfoaluminate Cement (CSA), Hydration, Chlorides, Binding Mechanism, Gypsum

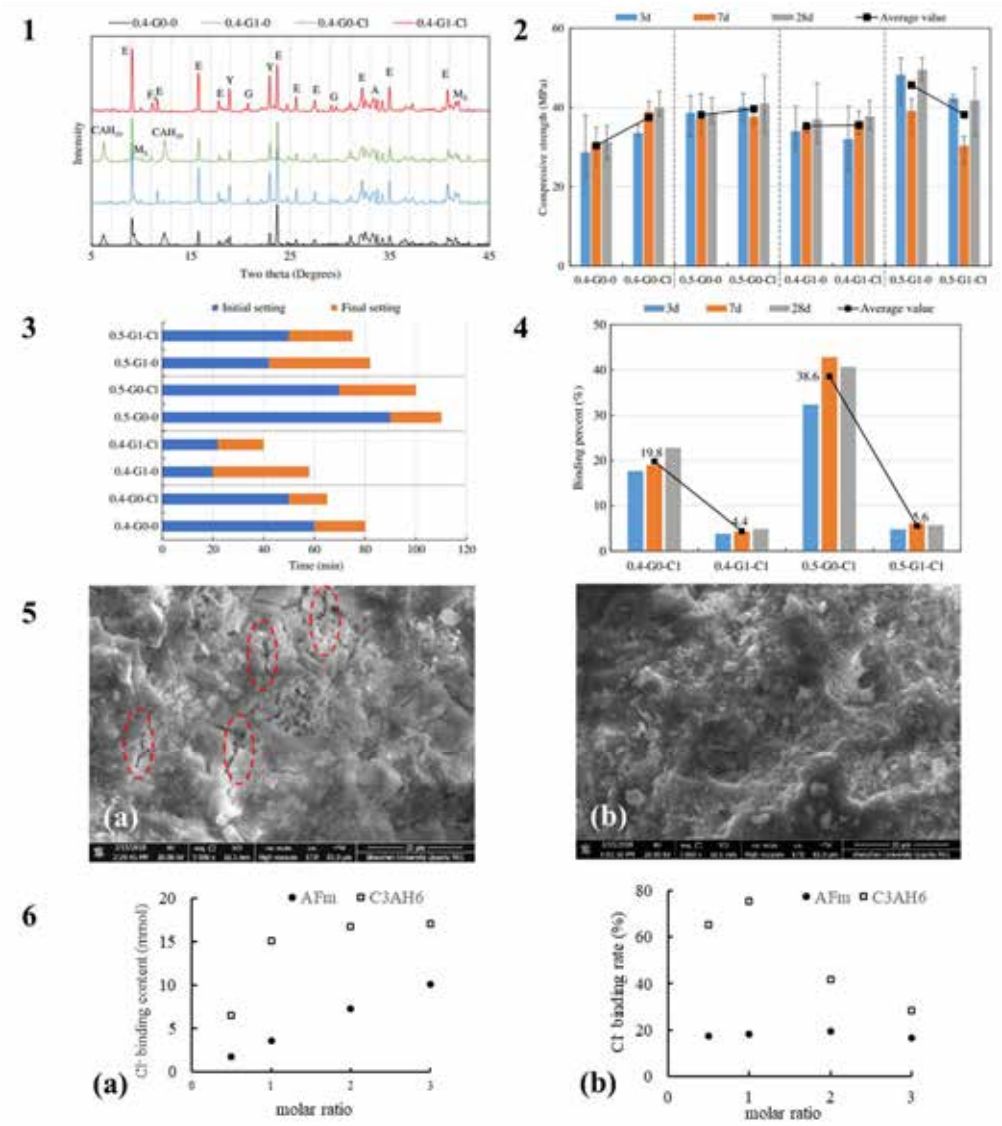

Fig. 1 XRD results of the samples; **Fig. 2** Compressive strength of CSA paste; **Fig. 3** Influence of Cl^- on setting time of CSA; **Fig. 4** Cl^- binding capacity of CSA mixes; **Fig. 5** SEM images of hydrated paste (×5000); **Fig. 6** Binding capacity of AFm and C_3AH_6 per unit.

Acknowledgment

The authors would like to appreciate the financial support provided by the National Natural Science Foundation of China (Nos. 52078301 and 51520105012) and the State Key Laboratory of Silicate Materials for Architectures (Wuhan University of Technology) (Project No. SYSJJ2019-13). Tangshan Polar Bear Building Materials Co. Ltd is also acknowledged for supplying raw materials used for this experiment work. Technical support is acknowledged from Guangdong Provincial Key Laboratory of Durability for Marine Civil Engineering (SZU), No. 2020B1212060074.

Parallel Sessions-10

Self-Healing/Self-Immune Concrete

Application of zeolitic imidazolate framework (ZIF-8) as high-efficient corrosion inhibitor for the reinforcement in cement extract

Yangyang Wang, Jie Hu*#, Haoliang Huang, Jiangxiong Wei, Qijun Yu

School of Materials Science and Engineering, South China University of Technology, Guangzhou 510640, People's Republic of China
*Presenter: msjiehu@scut.edu.cn, #Corresponding author: msjiehu@scut.edu.cn

Abstract

The deterioration of reinforced concrete structure caused by corrosion damage of the reinforcement is severe engineering problem, significantly shortening the service life of reinforced concrete. Admixing organic corrosion inhibitor is regarded as an efficient way to prevent the corrosion damage of the reinforcing steel. Metal-organic frameworks (MOFs) can be potentially applied as corrosion inhibitors for reinforced concrete due to their supramolecular structure.

In this study, the inhibition effect of the prepared zeolitic imidazolate framework (ZIF-8) corrosion inhibitor on the reinforcement in cement extract was extensively investigated by electrochemical measurements and surface analysis. It was found that the well-defined ZIF-8 with representative rhombic crystalline structure and uniform size distribution was successfully synthesized by solvent method (Fig. 1). ZIF-8 prepared in this study exhibited good chemical stability in alkaline and neutral solution; as a result, the concentration of the released 2-MeIm from ZIFG-8 was very low in alkaline and neutral solution, while ZIF-8 decomposed in acid solution (Fig. 2), leading to possible "self-repairing" effect after during pitting corrosion propagation of the reinforcement in cement extract.

In chloride-containing cement extract, ZIF-8 corrosion inhibitor was efficiently adsorbed on the reinforcement surface and mainly reduced the anodic reaction rate by halting the dissolution of the reinforcement, thus significantly increasing the charge transfer resistance of the reinforcement (Fig. 3) and exhibiting high inhibition efficiency during the initial 24 h. Meanwhile, the inhibition efficiency was still maintained at 87.8 % after 168 h with ZIF-8 concentration of 0.04 wt. % (Fig. 4) due to the pH drop caused by pitting propagation at the local corrosion sites resulted in the decomposition of ZIF-8 and Fe-N coordination bond formed between the released 2-MeIm ligands and reinforcement.

Based on SECM (Scanning Electrochemical Microscopy) mapping, no obvious current peaks occurred but relative homogeneous current distribution presented with a flat surface on the reinforcement surface in cement extract with ZIF-8 (Fig. 5), implying pitting corrosion was dramatically halted and uniform corrosion was aroused on the reinforcement surface in the presence of ZIF-8. The excellent corrosion inhibition performance of ZIF-8 was ascribed to the strong adsorption behaviors of ZIF-8 on steel surface. The adsorption of ZIF-8 on the reinforcement surface was finished during a very short period of 40 min in cement extract, including fast chemisorption stage within 20 s and film thickness increase stage resulting from the rearrangement process of ZIF-8 (Fig. 6). Therefore, ZIF-8 corrosion inhibitor proposed in this present study provides a promising way for the effective corrosion protection of reinforced concrete under chloride-contaminated environment.

Keywords: Metal-organic frameworks; Corrosion inhibitor; Adsorption; Steel reinforcement; Cement extract

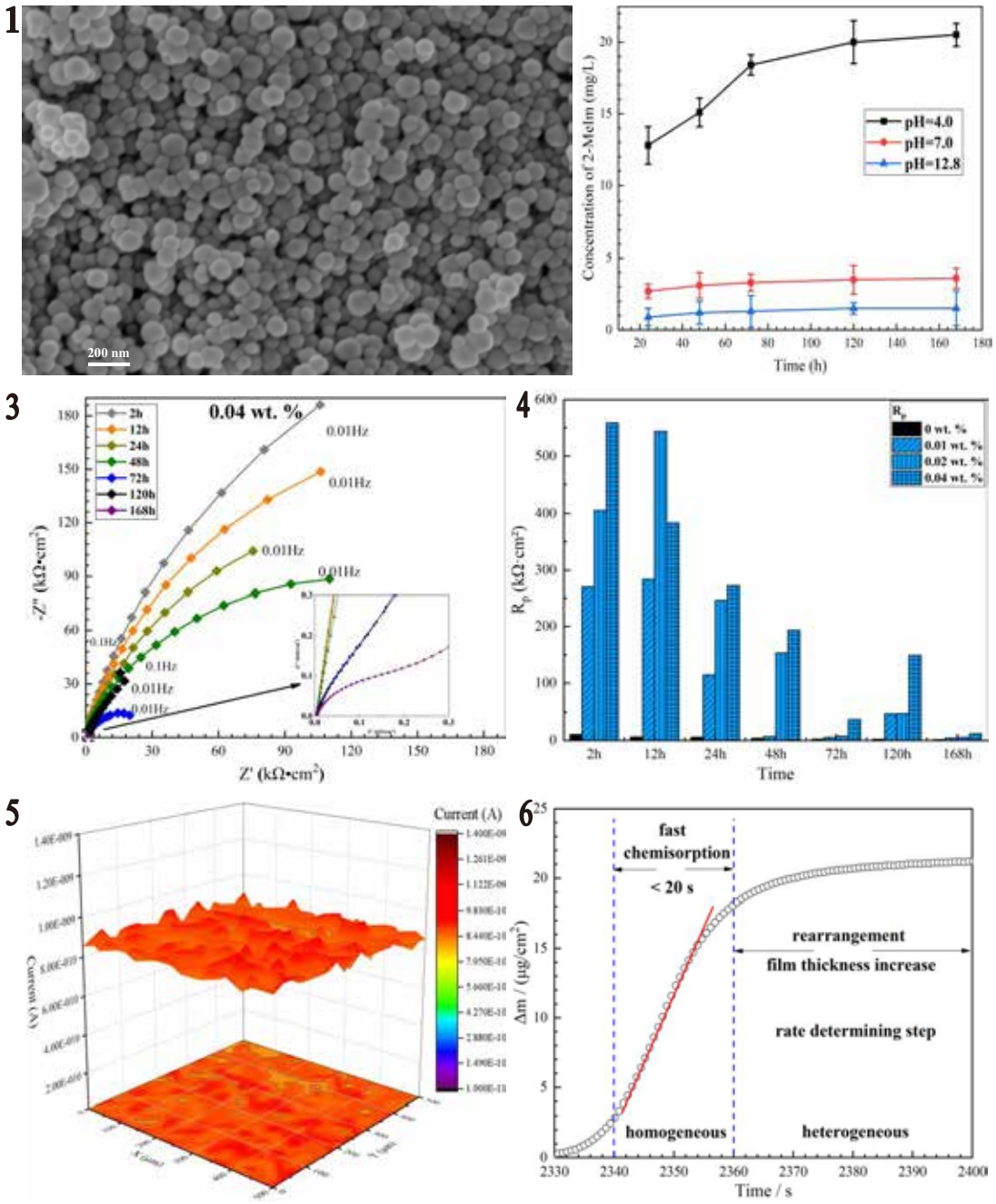

Fig. 1 SEM image of the prepared ZIF-8; **Fig. 2** Stability of the prepared ZIF-8 in deionized water with different pH values; **Fig. 3** EIS spectra of the reinforcement immersed in cement extract with ZIF-8; **Fig. 4** PD curves of the reinforcement immersed in cement extract; **Fig. 5** SECM images of the reinforcement at OCP in 3.5 % NaCl + ZIF-8 containing (0.04 wt.%) cement extract for 168 h; **Fig. 6** Real-time variations in frequency derived mass of iron deposited electrode during 2400 s immersion in cement extract with 0.04 wt.% ZIF-8.

Acknowledgment

The authors would like to acknowledge the National Natural Science Foundation of China (No. U2001225) and Guangdong International Science and Technology Project (No. 2020A0505100006).

Use of recycled concrete aggregates as carriers for concrete self-healing by high urease activity bacteria

Xianzhi Wang [a], Jing Xu [a, b*]

[a] School of Materials Science and Engineering, Tongji University, Shanghai 201804, PR China

[b] Key Laboratory of Advanced Civil Engineering Materials (Tongji University), Ministry of Education, Shanghai 201804, PR China

* Corresponding author. E-mail address: 09105@tongji.edu.cn (Jing Xu).

Abstract: Microbial induced carbonate precipitation (MICP) has become one of the most attractive strategies to achieve self-healing of concrete cracks in recent decades. In order to provide a moderate space for bacteria in the harsh environment of concrete, the incorporation of protective carriers is a necessity. In this study, the microbial urease activity at different generation of propagation in the selected culture medium was first investigated, followed by exploring the potential of using recycled concrete aggregates (RCAs) as microbial carriers, considering the porous nature of RCAs. The specific urease activity of bacteria at 48 h kept as high as 2.4×10^{-8} mM·min^{-1}·cells^{-1} even after 5 generations of propagation in the selected culturing medium. RCAs would not result in a loss of ureolytic activity after immobilization and were capable of retaining bacterial viability during concrete mixing. Compared with concrete without any healing agents or with only substrates and calcium source, the one with bio-agents loaded in RCAs completed most of the crack healing in the first week. When the initial crack widths were less than 0.6 mm, the average crack healing ratio and the crack area healing ratio were 71% and 84%, respectively, for microbial self-healing. The depth of crack healing was 17.8 mm as indicated by the microbial precipitates on the crack wall. After microbial self-healing, the compressive strength regain ratio achieved 99.7% while the water tightness regain ratio attained 99.2%, and the cracks were filled with densely packed irregular rhombohedral-shaped crystals consisting of calcite and a small amount of vaterite.

Keywords: concrete crack, self-healing, microbial induced carbonate precipitation, recycled concrete aggregate, water permeability

Self-healing of Cracks Based on Aggressive-ion-bonding Agent in Cement-based Materials in Sea Water

Haoliang Huang[a,b*], Xintong Wu[a], Jiachao Zheng[a], Hao Liu[a], Jie Hu[a,b], Suhong Yin[a,b], Jiangxiong Wei[a,b], Qijun Yu[a,b]

[a] School of Materials Science and Engineering, South China University of Technology, Guangzhou, China
[b] Guangdong Low Carbon Technologies Engineering Centre for Building Materials, Guangzhou, China
[*]*Presenter and corresponding author: huanghaoliang@scut.edu.cn*

Abstract

Concrete is a brittle material that easily cracks during construction and service processes. Cracks in concrete can accelerate invasion of aggressive ions in marine environments. As a result, cracks can extremely shorten the service life of concrete structures. It would be useful for concrete to have a self-healing capacity so that cracks can be healed autonomously once they appear. In order to significantly improve the durability of concrete structures in a marine environment by self-healing of cracks, it is necessary to promote the crack closure and simultaneously weaken the damage of aggressive ions in cracks from sea water. In this study, novel self-healing agents that can bind with aggressive ions in cracks and simultaneously form expanded reaction products to heal the cracks rapidly was developed via thermodynamic modeling and experimental study. The promotion and the mechanism of self-healing of cracks by the developed self-healing agents were explored.

It is found that the self-healing agent with CaO-metakaolin or CaO-$NaAlO_2$ as the main component can achieve the purpose of binding seawater erosion ions, and the amount of self-healing agent and the ratio of calcium to aluminum will affect the mineral phase composition of the reaction products. Besides, by adjusting the composition of self-healing agents, the volume expansion of self-healing agents can be optimized and the pH in crack solution can also increase to delay the destruction of passive film on steel bars.

The reaction kinetics of the developed self-healing agent with sea water was explored. It was found that $NaAlO_2$ can rapidly dissolve in water and release $Al(OH)_4^-$ and consequently, precipitates binding aggressive ions in synthetic water formed very fast. For the CaO-metakaolin agent, portlandite mainly formed within the first 1 day, while the reaction of metakaolin occurred mainly after 3 days, resulting in the formation of Friedel's salt, SO_4-CO_3-AFm salt, hydrotalcite and C-S-H. Therefore, reactions between CaO-$NaAlO_2$ agent and sea water, particularly the binding efficiency of Cl^-, is faster than that between CaO-metakaolin agent and sea water.

Crack closure tests showed that the self-healing agents developed in this study can promote the closure of cracks effectively. Moreover, the BSE/EDS results, the self-healing products tend to precipitate nearby the crack mouth and inside the broken artificial aggregates. Friedel's salt and hydrotalcite were found inside the broken artificial aggregates, which indicates the effective chemical binding of aggressive ions in sea water.

Keywords: Self-healing of cracks; Aggressive ions; Chemical binding; Thermodynamic modeling; Marine environment

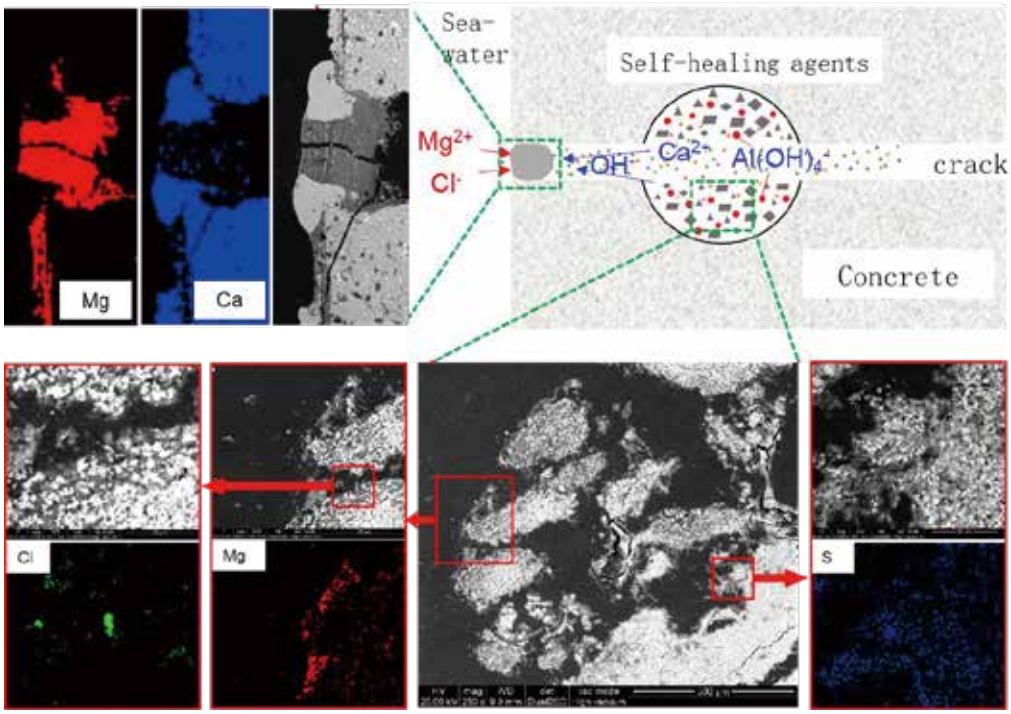

Fig.1 Characterization of reaction products of self-healing based on the aggressive-ion-bonding agent

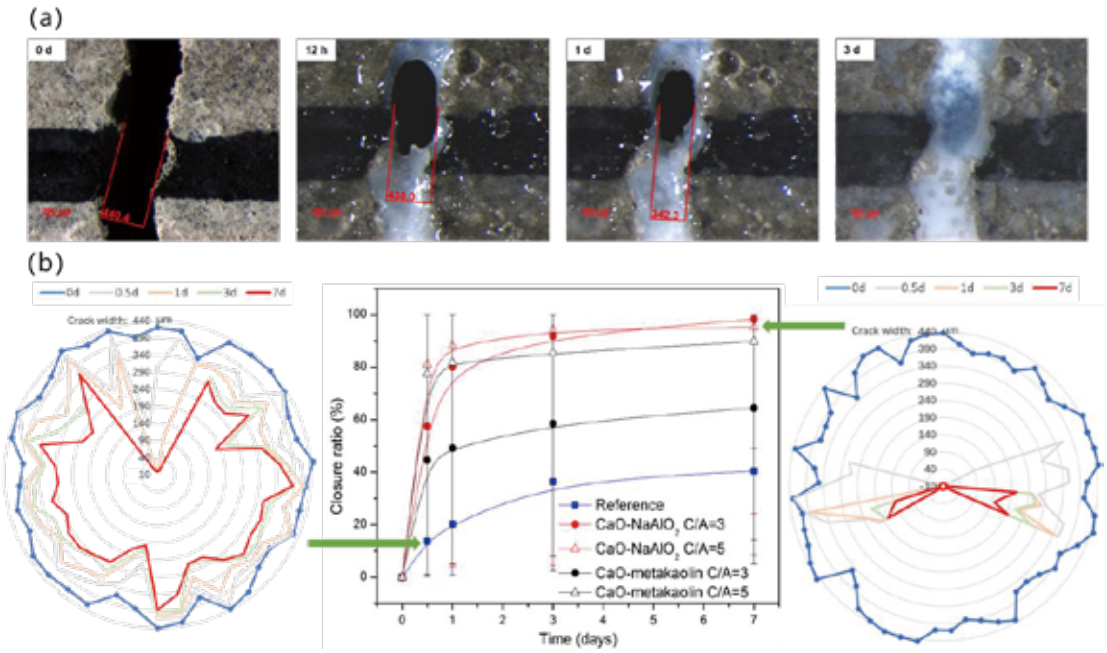

Fig.2 Kinetics of self-healing based on the aggressive-ion-bonding agent

Acknowledgment

The authors would like to acknowledge the funding support from the National Natural Science Foundation of China (No. 51602050 and No. 51872097), Open Fund Project of State Key Laboratory of Silicate Materials for Architectures (Wuhan University of Technology) (No.YSJJ2020-09) and Key Laboratory of Advanced Civil Engineering Materials of Ministry of Education (Tongji University) (No.202005).

Mechanical property and durability of mortar containing double-layers capsules

Chencong Li[1], Xiaolong Wang[1] and Honglei Chang[1*#]

[1] School of Qilu Transportation, Shandong University, Jinan, China
E-mail: lcc125@mail.sdu.edu.cn, wangxl923@mail.sdu.edu.cn, hlchang@sdu.edu.cn

Abstract

Microcapsule self-healing cement-based materials based on release control mechanism can timely sense and quickly repair the damage in the structure, curb the potential harm caused by cracks in the initial stage, and have great application potential in improving the service performance and durability of concrete structures. However, when the capsule is added into cement-based materials instead of a certain quality of sand, the strength of the poured concrete decreases significantly because the hardness of the existing microcapsule is much lower than that of sand. Therefore, in order to reduce the influence of microcapsule on the matrix, a new double-layer microcapsule was designed and prepared, and the influence of microcapsule on the mechanical properties and durability of mortar was studied. The results show that the compressive and flexural strength of the specimen with capsule is about 80% of that of the specimen without capsule. The addition of capsule is beneficial to improve the impermeability and frost resistance of mortar. The carbonation resistance does not change with the change of capsule content. The chloride ion erosion resistance decreases with the increase of the content of the capsule.

Keywords: Double layers, Durability, Mechanical properties, Microcapsule, Self-healing

*: Presenter; #: Corresponding author

Freeform embedded printing of vasculature in cementitious materials for healing-agent transport

Yuanyuan Zhang[1*], Guang Ming Zhu and Biqin Dong[#]

Guangdong Key Laboratory of Durability in Coastal Civil Engineering, College of Civil and Ttransportation Engineering, Shenzhen University, Shenzhen, Guangdong 518060, CHINA
E-mail: incise@szu.edu.cnx

Abstract

Vascular systems for mass recycling promise to endow cementitious materials with self-recovering abilities, which would prolong their durability. However, the CM opacity and hypercritical requirements on brittle vessels lead to the lack of a feasible approach to freeform construct vasculature with three-dimensional connectivity. To address this, we have developed a strategy for in-situ vasculature construction that involves the embedded writing of fugitive inks within a supporting CM matrix (Schematic). The fugitive ink is a two-phase emulsion gel, which is versatile in terms of printability, free-discharging ability, and channel-sealing ability, enabling the formation of freeform, isolated vascular networks. To support the development of embedded printing strategy, we also analyzed the relationships between vessel features, CM hydration, writing speed, and flow rate. The tested aqueous healing agent moved through the printed vasculature to reach and heal cracks, demonstrating the effectiveness of this internal structure in terms of mass transport. We conclude that embedded printing allows the creation of vascular structures in cementitious materials and, ultimately, of intelligent construction materials.

Keywords: Self-healing, Cement Paste, vascular network, Embedded 3D printing, Two-phase ink

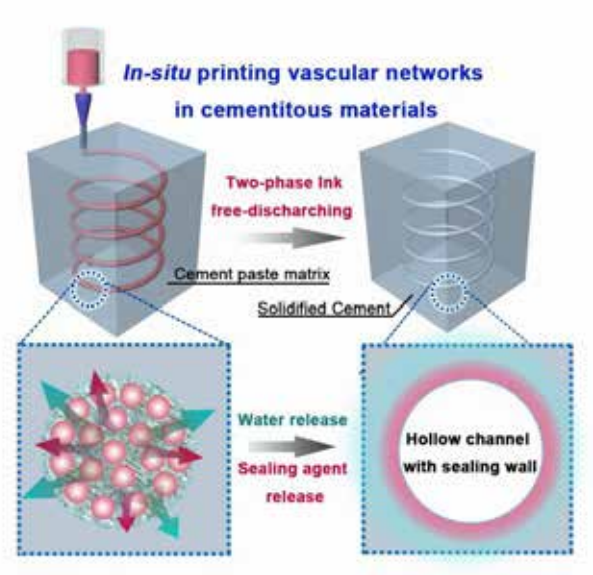

Schematic

*: Presenter; #: Corresponding author

Preparation and properties study of expansive mineral-based artificial aggregates for self-healing concrete

Jing-Lu Li[1,2*], Xin-Chun Guan[1,2#]

[1] Key Lab of Smart Prevention and Mitigation of Civil Engineering Disasters of the Ministry of Industry and Information Technology and Key Lab of Structures Dynamic Behavior and Control of the Ministry of Education,
[2] School of Civil Engineering, Harbin Institute of Technology, Harbin, Heilongjiang 150090, People's Republic of China
[*]*Presenter: lijinglu_ljl@163.com,* [#]*Corresponding author: guanxch@hit.edu.cn*

Abstract

Expansive minerals are commonly used to promote the self-healing capacity of cracked concrete. But they are gradually consumed with the progress of hydration, decreasing the self-healing efficiency of later cracks. In this paper, an expansive mineral-based artificial aggregate was prepared, and its basic properties were investigated. It was found that the expansive mineral could not react with water during the preparation process, ensuring its later healing potential. Meanwhile, the aggregates had a slightly negative effect on the mechanical property of mortar specimens, whereas the self-healing efficiency could be significantly improved.

The artificial aggregates were prepared by the disc granulation method, using magnesium oxide (MgO) expansive agent as the self-healing agent and geopolymer materials consisting of fly ash, sodium hydroxide and sodium silicate solution as the binder. Then the aggregates were coated with polyvinyl alcohol solution and fine sand to prevent MgO from reacting prematurely. After being sieved, the aggregates with a diameter of approximately 3.5 mm were obtained (Fig. 1).

The mineral components of artificial aggregates were identified by X-ray diffraction (XRD). For comparison, the compositions of the MgO expansive agent and the reacted MgO were also examined (Fig. 2). Results showed that the mineral composition of aggregates was mainly periclase rather than brucite, indicating that the aggregates had the potential to heal later cracks. In addition, with the increase of MgO content, the crushing load of aggregates showed a decreasing trend (Fig. 3). This revealed that there was an optimal content of MgO in terms of ensuring aggregates strength and self-healing efficiency.

Compared with natural aggregates, MgO-based artificial aggregates had lower strength. Therefore, they had a negative impact on the compressive strength of mortar specimens. With the increase of aggregates content, the compressive strength of mortar specimens decreased more and more (Fig. 4). In this study, the aggregates content of 10% was selected to investigate its effect on the self-healing properties of specimens, which were evaluated by the water absorption test (Fig. 5). After healing in wet-dry cycles for 20 days, the self-healing rate of the specimens mixed with artificial aggregate reached about 60%, which was three times higher than that of the control specimens. This research provides some guidance for the application of expansive mineral-based artificial aggregates in practical engineering.

Keywords: MgO Expansive Agent; Artificial Aggregates; Preparation; Cracks; Self-healing

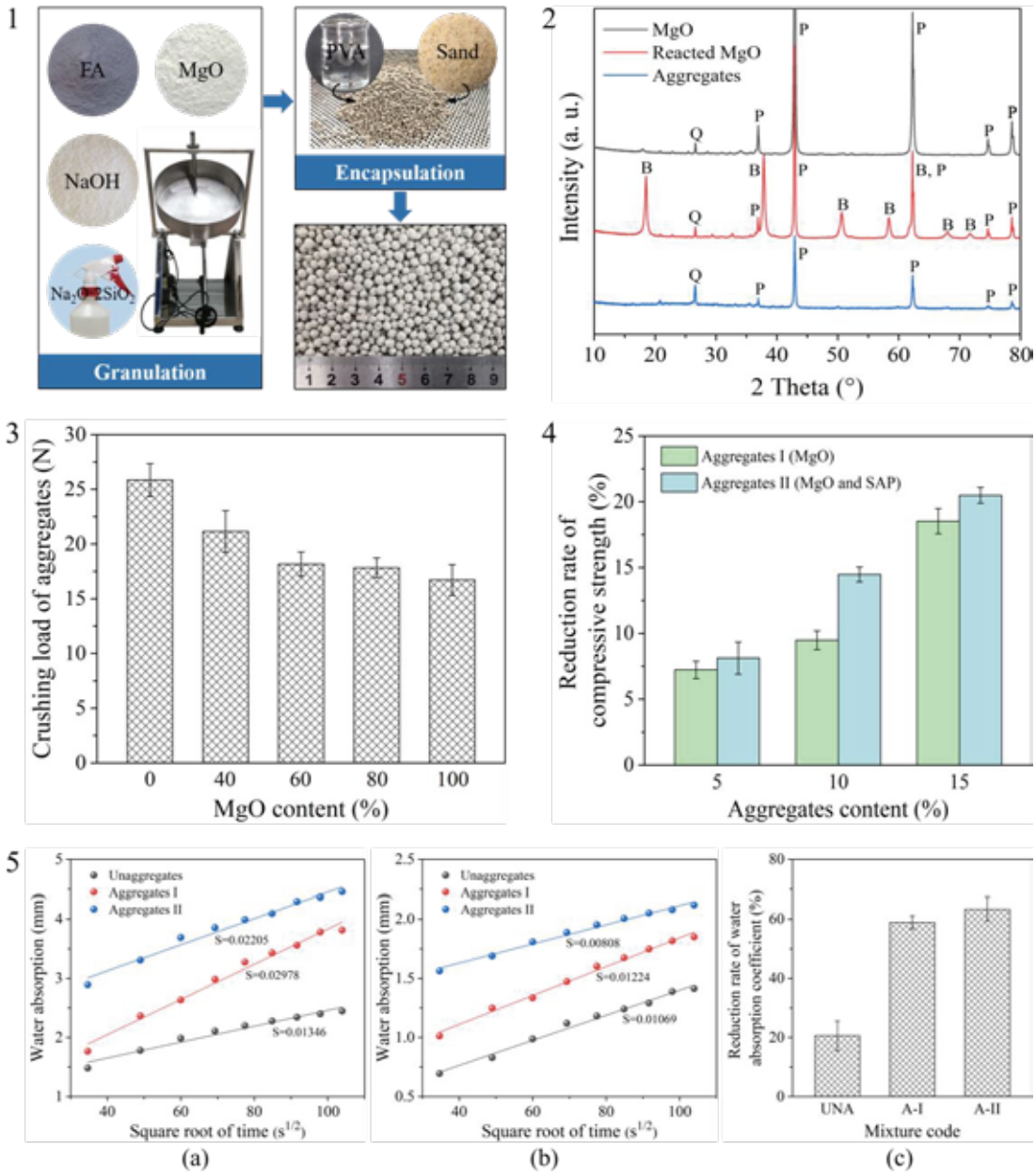

Fig. 1 Preparation process of expansive mineral-based artificial aggregates; **Fig. 2** XRD patterns of MgO, reacted MgO and aggregates (P: Periclase; B: Brucite; Q: Quartz); **Fig. 3** Effect of MgO content on the crushing load of aggregates; **Fig. 4** Effect of aggregates content on the compressive strength reduction rate of mortar specimens; **Fig. 5** Water absorption of cracked mortar specimens of (a) before and (b) after self-healing, and self-healing efficiency evaluated by (c) reduction rate of water absorption coefficient

Acknowledgment

The authors would like to acknowledge the funding support from the National Key Research and Development Program of China with Grant Number 2018YFC0705404 and the National Natural Science Foundation of China with Grant Number 51778189.

Experimental Study on the Repair Effect of Electrochemical Chloride Extraction for Corroded Reinforced Concrete

Kazuhide NAKAYAMA[1*#], Mika TAKAHASHI[1], Mitsuyasu IWANAMI[1], Takao UEDA[2]

[1] Department of Civil and Environmental Engineering, Tokyo Institute of Technology, Japan,
[2] Department of Civil and Environmental Engineering, Tokushima University, Japan.
[*]*Presenter: nakayama.k.au@m.titech.ac.jp,*
[#]*Corresponding author: nakayama.k.au@m.titech.ac.jp*

Abstract

Electrochemical chloride extraction (ECE) is an effective rehabilitation method for reinforced concrete (RC) structures against steel-corrosion due to chloride attack. The application cases of ECE in Japan have been increased gradually according to the publication of guideline for electrochemical corrosion control method (Concrete Library 157; JSCE 2020, in Japanese). However, there are few researches on the influence of the deterioration level of reinforced concrete on the repair effect of ECE. The repair effect might change due to the steel corrosion in concrete and cracks caused by the corrosion, since it changes the distribution of electrical current inside the concrete. To enhance the reliability of ECE, this study was conducted as an experimental investigation using RC specimens with different corrosion level for clarifying the influence of corrosion degree on chloride extraction efficiency and the property changes of cement paste and corrosion product.

In the experiment, ECE was carried out under the constant current condition (1344 A・h/m2) on specimens subjected to corrosion by the electrochemical corrosion acceleration. The steel corrosion degree in the specimen is shown in Table 1. Regarding the graph legends of Fig.3, Fig.4 and Fig.5, each number after the underscore indicates the current density and current application period of ECE.

The chloride extraction rate of specimen with slight corrosion or internal cracking caused by corrosion were comparable or higher than the rate of specimen with sound steel (Fig. 3). For specimens with corrosion cracks of about 0.2 mm with on the concrete surface, both pre-repaired and non-repaired specimens with crack injection material before applying ECE were examined. The chloride extraction rate in the area where the cracks were sealed by the crack injection material was similar to that of non-cracked specimen (Fig. 4). Within the scope of this study, pre-corrosion in reinforced concrete does not seem to have a negative effect on chloride extraction rate if the corrosion is not so progressed that cracks reach the surface of concrete. Even if surface cracks are observed, a certain level of chloride extraction effect can be expected if the cracks are filled by an appropriate pretreatment. Fig. 5 shows the maximum bond stress ratio from the pull-out test using round steel, indicating a decrease in bond stress due to ECE. It is also found that the effect of corrosion is not significant as long as cracks do not appear on the concrete surface even after applying ECE. The appearance of the specimen indicates that the corrosion products may have been passivated after applying ECE (Fig. 6), and it indicates that ECE may improve the protection effect against steel corrosion in concrete even if slight corrosion has progressed before applying ECE.

Keywords: Electrochemical chloride extraction, Steel corrosion, Chloride extraction rate, Bond performance between concrete and steel.

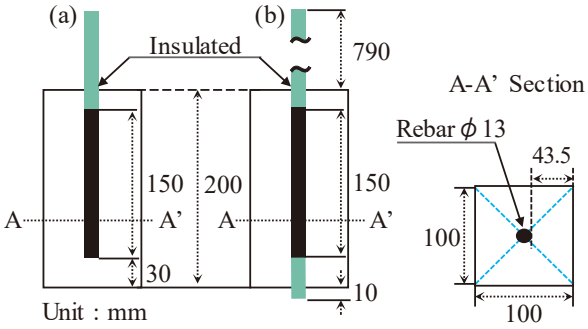

Fig. 1 Specimen Outline.

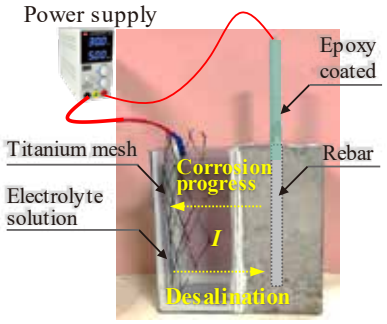

Fig. 2 Current application method.

Table. 1 Steel corrosion degree in specimen

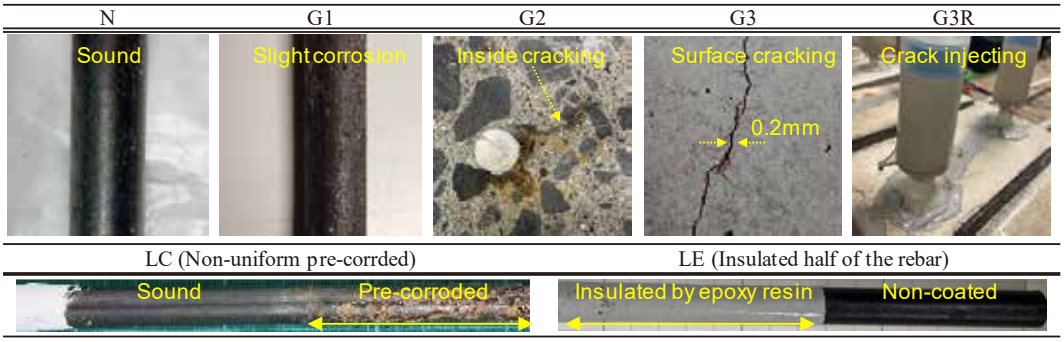

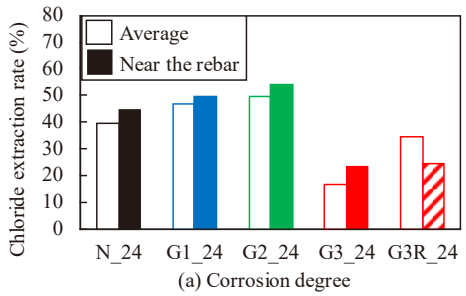

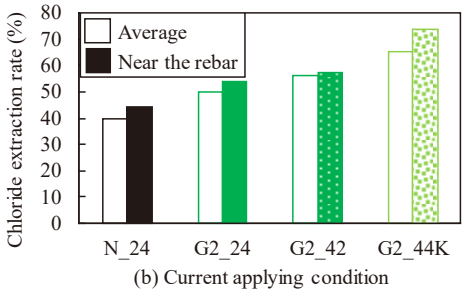

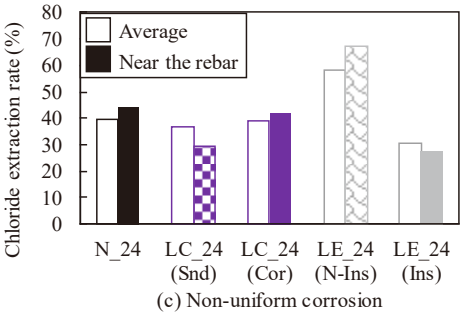

Fig. 3 Chloride extraction rate.

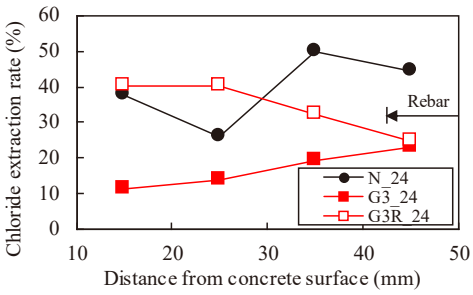

Fig. 4 Distribution of chloride extraction rate before and after crack injection.

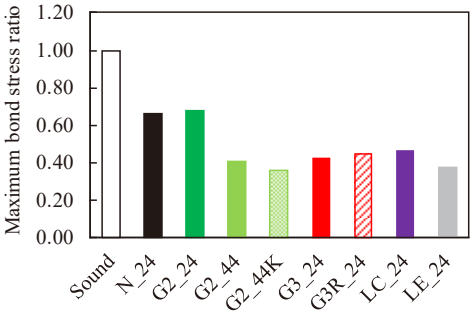

Fig. 5 Maximum bond stress ratio.

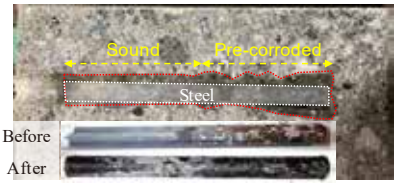

Fig. 6 Internal appearance of specimen after ECE.

Acknowledgment

This research was partially supported by JSPS KAKENHI Grant-in-Aid for Early-Career Scientists Number 19K15061.

Analytical models on the influence of crack geometrical pattern on capsule dosage

Huisu Chen[1*], Zhong Lv[2], Jianjun Lin[3]

[1.]Jiangsu Key Laboratory of Construction Materials, School of Materials Science and Engineering, Southeast University, Nanjing 211189, P.R. China

[2.]School of Architectural and Civil Engineering, Anhui University of Technology, Ma'anshan 243032, China

[3.] Key Laboratory of Green Construction and Intelligent Maintenance for Civil Engineering of Hebei Province, School of Civil Engineering & Mechanics, Yanshan University, Qinhuangdao 066004, China

*Corresponding author: chenhs@seu.edu.cn; +86-132 7089 0362

Abstract: Cracks at various scale levels are detrimental to the durability of concrete. Seal-healing technology is increasingly being used to extend the service life of structural materials. Numerous studies examined the efficiency of crack healing using experimental techniques, such as local morphological observation as well as mechanical or transport testing. Assuming that the crack geometrical pattern is known in advance, we wonder whether a theoretical model can be created to estimate the required dosage of the healing capsule. As a consequence, the complex geometrical pattern of an actual crack in materials is first reduced into a continuum or discrete crack network. Then, utilizing geometrical probability theory, analytical models of the capsule dosage are established for self-healing of cracks with various simplified geometrical patterns and varying capsule length to crack spacing ratios. Finally, the numerical simulation is performed to verify the reliability of the above analytical models.

Keywords: Self-healing; Crack geometrical pattern; Capsule dosage; Geometrical probability; Analytical model.

Quartz sand modified enamel coating for enhanced corrosion resistance of steel rebar

Fujian Tang[1,*#], Hao Cui[1], Hong-Nan Li[1]

[1] School of Civil Engineering, Dalian University of Technology, Dalian, Liaoning 116024, People's Republic of China
[*]*Presenter:* ftang@dlut.edu.cn, [#]*Corresponding author:* ftang@dlut.edu.cn

Abstract

Chloride-induced reinforcement steel corrosion is one of the main causes of premature deterioration of reinforced concrete (RC) structures in marine environment or in cold regions subjected to the use of deicing salts. Corrosion causes concrete cracking, bond loss between steel and concrete, mechanical degradation of reinforcement steel, reduction in carrying capacity of structural components, and even collapse of structures. Moreover, corrosion brings economic burden, and it is estimated that the annual direct corrosion cost for highway bridges was $13.6 billion in the US in 2013, and the corrosion cost for highway bridges, roads, ports was estimated to be 65 billion RMB in China in 2014. Therefore, it is of paramount importance to develop some methods to improve durability, reduce corrosion cost and extend service life of RC structures.

Protective coating is considered to be one of the most effective and economical methods to protect steel reinforcement from corrosion in RC structures, as it can establish a physical barrier between the steel rebar and the aggressive environment. Fusion bonded epoxy (FBE) is the most widely used coating material for steel reinforcement in RC structures. However, FBE coating reduces the bond strength with surrounding concrete, and leads to longer development length and consequently increased construction cost. Moreover, defect in the coating or damage induced during transportation or construction will cause localized corrosion and under-film corrosion. Galvanized zinc coating is also used to protect steel reinforcement from corrosion through sacrificially corroding before the underlying steel. However, zinc reacts in the alkaline environment of concrete pore solution to release hydrogen gas, which increases the steel-concrete interfacial porosity and results in a reduced bond strength between steel rebar and concrete.

Enamel coating is an inorganic coating which is made by fusing enamel powder to a metal substrate at temperature usually between 750 °C and 850 °C. Its properties are flexible and can be modified by adding different chemicals. For instance, the corrosion resistance in acidic environment can be increased by adding B_2O_3, the corrosion resistance in alkaline environment can be improved by introducing ZrO_2, and the bond strength with substrate steel can be enhanced by adding CoO and NiO. By adding cement in the enamel slurry, chemically reactive enamel coatings are proposed and applied on the surface of steel rebar for increased corrosion resistance and enhanced bond strength with concrete in previous studies. The microstructure, short-term and long-term corrosion resistance when applied on smooth steel rebar, deformed steel rebar and steel plates in 3.5 wt.% NaCl solution, simulated concrete pore solutions and mortar cylinders have been systematically investigated, and the bond strength has also been experimentally studied as well. Results show that cement modified enamel coatings increase both the corrosion resistance and bond strength of steel rebar. However, addition of cement introduces connected channels in the enamel coating, which provide potential passage for penetration of aggressive chemicals. River sand particle is also added in the enamel coating. However, appearance of micro-cracks around the river sand particles reduces the corrosion resistance of steel rebar.

In this study, quartz sand modified enamel coating is proposed and characterized for enhanced corrosion resistance of steel rebar. The enamel coating process is as follows: first of all, quartz sand particles with dimeter ranging from 0.38 mm to 0.83 mm~0.50 mm were mixed with the enamel powder, and tap water was added to form enamel slurry; next, the cleaned steel rebars were dipped in the enamel slurry to assure the entire surface is covered with a layer of wet enamel slurry; finally, the wet enamel coated steel rebars were moved into a furnace for firing 10 minutes at 840 °C, and cooled down to room temperature to form quartz sand modified enamel coated steel rebars. The microstructure of quartz sand modified enamel coating including the thickness and the porosity was examined with an optical microscopy. The corrosion performance of quartz sand modified enamel coated steel rebars was evaluated by immersing in 3.5 wt.% NaCl solution with open circuit potential (OCP), linear polarization resistance (LPR) and electrochemical impedance spectroscopy (EIS). Uncoated steel rebars were also prepared and tested for comparison.

Figure 1a shows the microstructure of quart sand modified enamel coating, and it can be observed that the enamel coating thickness is around 300 μm and a quartz sand particle is obviously embedded in the enamel coating layer. Some isolated small air bubbles are also present in the enamel coating which is generated due to the chemical reactions of oxides in the enamel powder with carbon in the steel rebar during the firing process. The open circuit potential (OCP) of uncoated steel rebar and enamel coated steel rebar is -589 mV/SCE and -539 mV/SCE, respectively, as shown in Fig. 1b. The polarization resistance R_p of enamel coated steel rebar is 798 kΩ cm^2, which is two order higher than the polarization resistance of uncoated steel rebar that is 3.73 kΩ cm^2. The impedance of quartz sand modified enamel coated steel rebar is also much higher than that of uncoated steel rebar as shown in Fig. 1c. Therefore, quartz sand particle modified enamel coating can effectively and significantly increase the corrosion resistance of steel rebar.

Keywords: Reinforcement steel corrosion, Enamel coating, Microstructural characterization, Electrochemical impedance spectroscopy, Linear polarization resistance.

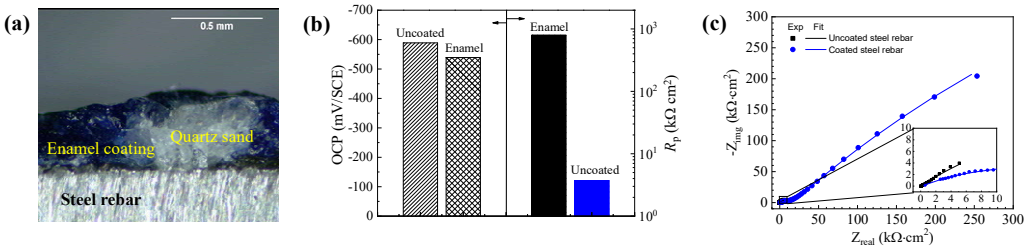

Fig. 1 (a) Microstructure of quartz sand modified enamel coating, (b) OCP & R_p and (c) EIS of uncoated and quartz sand modified enamel coated steel rebar.

Acknowledgment

The authors would like to acknowledge the funding support from the National Science Foundation of China (52078099).

Experimental and numerical study of crack behavior for capsule-based self-healing cementitious materials

Hongzhi Zhang[1*#], Le-Yang Lv[2]

[1] School of Qilu Transportation, Shandong University, Jinan, Shandong 250100, People's Republic of China
[2] College of Civil and Transportation Engineering, Shenzhen University, Shenzhen, Guangdong 518060, People's Republic of China
[*]*Presenter:* hzzhang@sdu.edu.cn, [#]*Corresponding author:* hzzhang@sdu.edu.cn

Abstract

Crack induced rupture behavior of microcapsules plays a decisive role in realizing the self-healing function. It is generally believed that the bonding strength, the size and the mechanical properties (e.g., elastic modulus, strength) of microcapsule are among the important factors greatly influencing the self-healing performance as well as the mechanical properties of cementitious composites. Thus, a proper selection and design of the microcapsules could offer a higher healing efficiency with lower degradation of mechanical properties of the cementitious systems.

In this work, a feasible approach was developed for simulating and evaluating the fracture and trigger behavior of capsule-based self-healing cementitious material. Micromechanical properties of the SIC zone were characterized by the nanoindentation mapping. 2D lattice fracture model with assigned micromechanical properties was built to simulate the fracture properties of SIC zone. The simulated tensile strength of SIC zone corresponds well with the experimental results. A 3D lattice model was constructed based on real microstructure obtained by XCT scanning of a capsule embedded cement paste specimen. This model was then used to simulate the crack behavior of microcapsule-based self-healing system. The parametric study of the constructed 3D model demonstrated the influence of mechanical properties of interlayer, shell and composite structure on the trigger efficiency of microcapsules. By combining the experimental results and numerical modelling, this study established a bridge between the local micromechanical properties of certain materials and its structural behavior. It provides a promising route for guiding the design of capsule-based self-healing cementitious composites and therefore obtaining an ideal self-healing performance.

Some improvements to the proposed study are still needed. Firstly, a better procedure for accurate measurement of bonding strength should be developed. The boundary conditions of the tensile test should be well controlled. A LVDT module can be used to record the displacement precisely. In addition, since the ratio between the measured hardness and the tensile strength of cement paste is only an assumed value in this study, further work will be carried out to establish an appropriate relationship between local hardness and the fracture strength of the cement paste.

Keywords: Crack behavior; Lattice model; Self-healing materials; X-ray microtomography

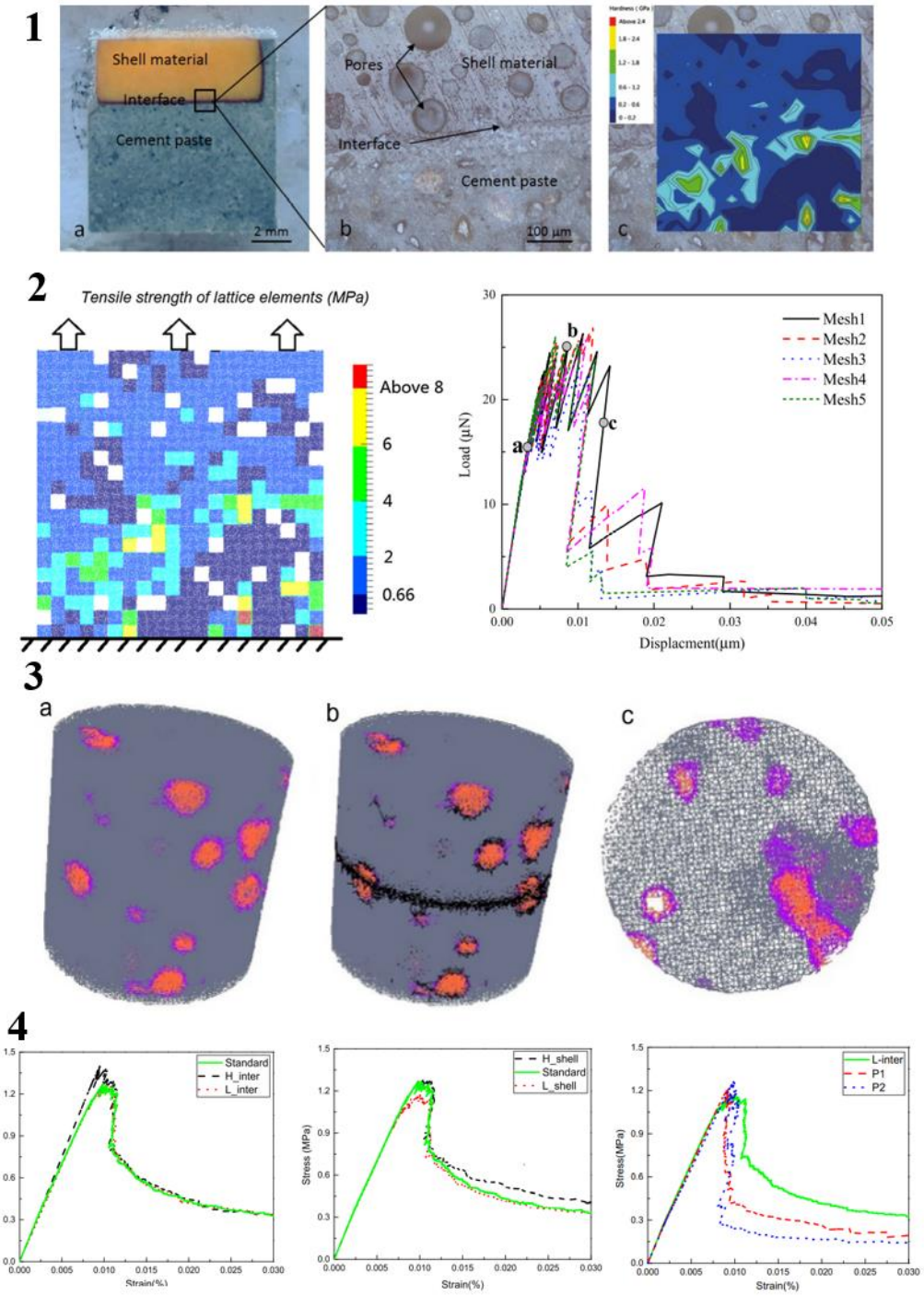

Fig. 1 Images of the (a) prepared SIC zone specimen, (b) test area of nanoindentation and (c) the corresponding hardness (right); **Fig. 2** The applied lattice mesh with assigned properties and boundary conditions(left) and the simulated load-displacement responses; **Fig. 3** The simulated crack pattern at different stage; **Fig. 4** Stress-strain diagram of the specimens with different strength of interlayer, shell material and different positions.

Acknowledgment

The author would like to acknowledge the financial support by the China Scholarship Council (201506120067), joint funds of the National Natural Science Foundation and Guangdong Province of China (U1301241), and the Collaborative Innovation Center for Advanced Civil Engineering Materials, Nanjing.

Mechanical properties of microcapsule-based self-healing concrete interface: a molecular dynamics study

Wei Xie [1#], Xianfeng Wang[2*], Xiaobo Ding[3*] and Jihua Zhu[4]

[1, 2,3,4] Guangdong Provincial Key Laboratory of Durability for Marine Civil Engineering, College of Civil and Transportation Engineering, Shenzhen University, Shenzhen 518060, CHINA

*#：talker; *: Correspondence.*

E-mail: xw13671400570@163.com, xfw@szu.edu.cn, dxxxxb@126.com, zhujh@szu.edu.cn

Abstract

As a new material, microcapsule-based self-healing concrete can effectively inhibit the propagation of cracks and improve the durability of concrete structures. In this study, the composite models of microcapsule core (epoxy) with C-S-H were established, and its interfacial behaviors were studied by molecular dynamics simulation, which is intended to analyze the mechanical properties of the microcapsule-based self-healing concrete and the interfacial behavior between the microcapsule and the cement matrix on the microscopic level. Three C-S-H/ epoxy models, in which the epoxy resins were uncured and cured with different curing agents (MC120D/TEPA), were established to study the effect of curing agents on the interfacial mechanical property. Through the analysis of interfacial binding energy, radial distribution function and stress-strain curve, it can be concluded that curing agent has a great influence on the bonding behavior of epoxy resin and cement matrix. The cured-epoxy resin can increase the interface binding energy by at least 50%, and can increase the strength of concrete, which is due to the interaction of N atoms and O atoms in TEPA and Ca atoms in C-S-H and the hydrogen-bond interaction.

Keywords: C-S-H, Microcapsule, Molecular dynamics, Self-healing concrete, Epoxy.

1

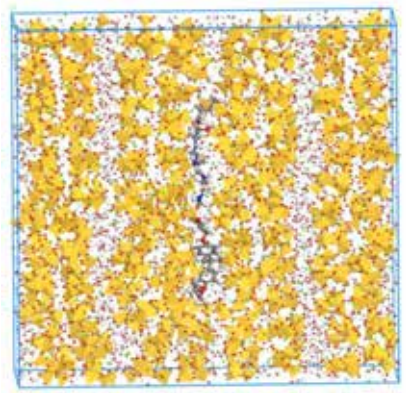

2

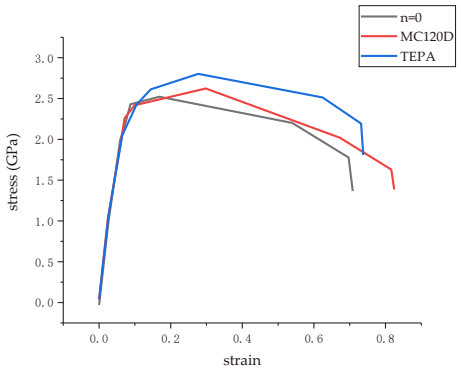

3

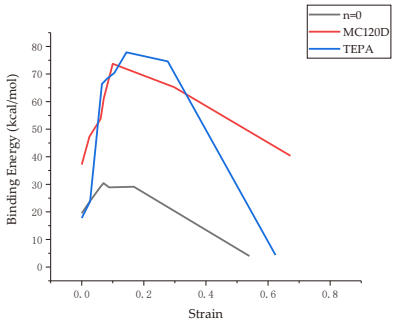

4

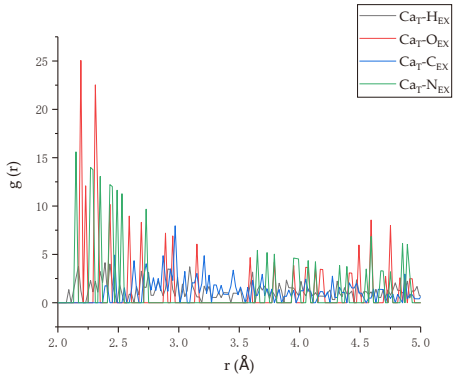

1

模型	Eb (kcal/mol)
n=0	19.50
MC120D	40.83
TEPA	50.53

FIG.1 The model of C-S-H/epoxy; **FIG.2** Comparison of tensile strength of different curing agents; **FIG.3** Variation trend of interface binding energy during tensile process; **FIG.4** Comparison of the interfacial strength of different atoms between C-S-H and epoxy resins; **TBL.1** Comparison of the interfacial binding energy through molecular dynamics simulation.

Acknowledgment

The authors would like to acknowledge the funding support from the Key-Area Research and Development Program of Guangdong Province (2019B111107002), the National Natural Science Foundation of China (51978409, 51908526), Guangdong Provincial Key Laboratory of Durability for Marine Civil Engineering (2020B1212060074), and Miss Lina Zhong from KZJ New Materials Group Co., Ltd is also gratefully acknowledged for her help in this work.

Effect of superabsorbent polymer on self-healing performance of fly ash-cement systems

Jing-Jing Lyu[1,2*], Xin-Chun Guan[1,2#]

[1] Key Lab of Smart Prevention and Mitigation of Civil Engineering Disasters of the Ministry of Industry and Information Technology and Key Lab of Structures Dynamic Behavior and Control of the Ministry of Education,
[2]College of Civil Engineering, Harbin Institute of Technology, Harbin, Heilongjiang 150001, People's Republic of China
[*]*Presenter:* lyujingjinghit@163.com , [#]*Corresponding author:* guanxch@hit.edu.cn

Abstract

To achieve practical autonomous healing in construction, an approach that uses superabsorbent polymer (SAP) has been proposed. SAP is a cost-effective, durable, and resilient material that can absorb large amounts of water and then expand into an impermeable gel. The application of supplementary cementitious represented by fly ash to the self-healing of concrete is a feature of many sustainable structures because it reduces maintenance costs and extends service life. The effect of SAP on the self-healing performance of fly ash-cement systems and its potential application in different environments is not well understood (Fig.1). The purpose of this study is to explore the possibility of SAP in the treatment of fly-ash cement systems (Fig.2).

Many self-healing studies have shown that concrete requires extensive exposure to water to promote crack sealing. This study was based on the good water absorption characteristics of SAP, which can absorb water from a certain humidity environment to promote the healing of cracks, the hygroscopicity of SAP was tested by self-made static water vapor adsorption apparatus (Fig.3). As SAP with different particle sizes has different water absorption capacities, the larger the particle size is, the more water it absorbs (Fig.4). Therefore, three different exposure conditions were considered in this study, such as curing in the air (33%RH), wet-dry cycling in water and saturated calcium hydroxide solution, 97%RH. SAP with three-particle sizes (Fig.5) was adopted as the research object.

Through fluidity test and compressive strength test, the feasible mix ratio design was studied, and the self-healing performance of concrete mixed with SAP and fly ash was analyzed and evaluated through physical properties, mainly including mechanical properties recovery experiment, crack closure experiment and capillary water absorption experiment (Fig.6). In addition to thermogravimetric analysis. The self-healing products were analyzed by XRD and FTIR, and the newly formed self-healing materials were analyzed by scanning electron microscopy (SEM) and energy dispersive spectroscopy (EDS).

The results showed that SAP can significantly improve the mid-term self-healing ability of the fly ash-cement system. With the increase of SAP particle size and content, the self-healing effect of SAP on fly ash-cement system was enhanced. The self-healing effects were sorted by saturated calcium hydroxide solution＞tap water ＞97%RH＞air. Crack closure was related to the development of self-healing products such as calcium carbonate C-S-H.

Keywords: Superabsorbent polymer; Fly ash-cement systems; Self-healing performance

1

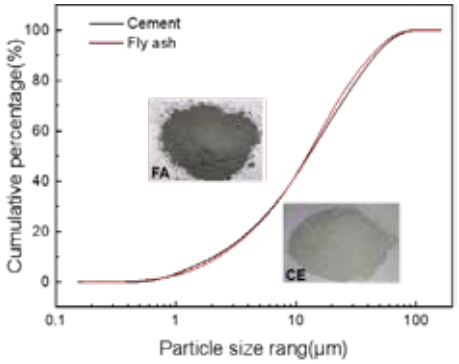

2

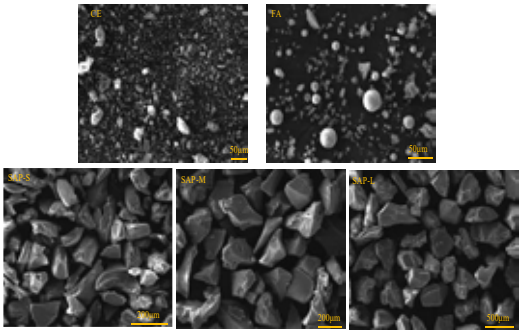

3

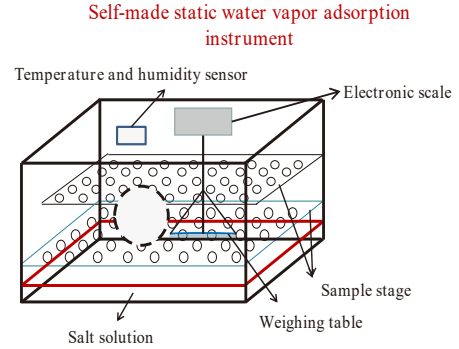

4

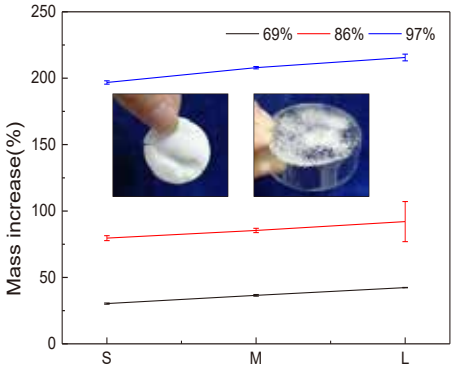

5

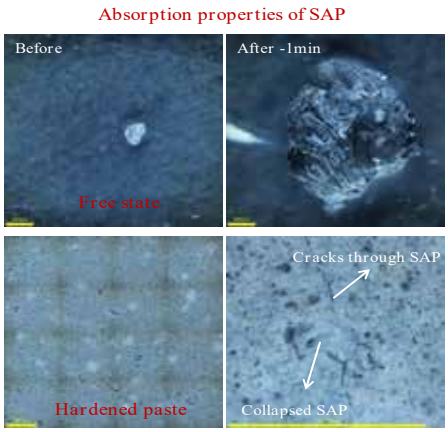

6

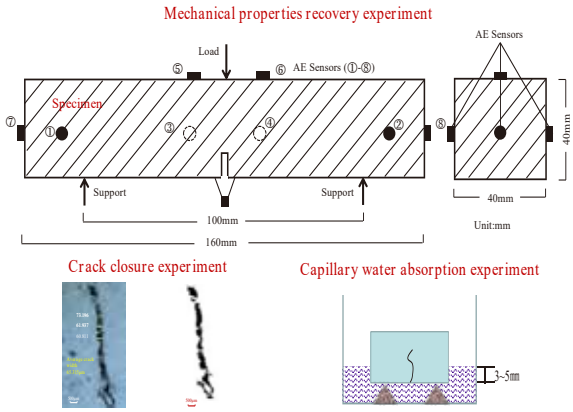

Fig. 1 Particle size distribution of cement and fly ash; **Fig. 2** SEM image of cement, fly ash, and SAP particles.; **Fig. 3** Self-made static water vapor adsorption instrument; **Fig. 4** Hygroscopicity of SAP under different humidity; **Fig. 5** Absorption properties of SAP in free state and hardened paste; **Fig. 6** Schematic diagram of mechanical properties recovery experiment, crack closure experiment and capillary water absorption experiment

Acknowledgment

This research is supported by the National Key Research and Development Program of China with Grant Number (2018YFC0705404) and the National Natural Science Foundation of China with Grant Number (51778189).

Calcium leaching from cement hydrates exposed to aggressive environments

Ming Zhang[1*], Shanshan Qin[2], Tiejun Liu[1], Dujian Zou[1#]

[1] School of Civil and Environmental Engineering, Harbin Institute of Technology, Shenzhen 518055, PR China,
[2] School of Construction Engineering, Shenzhen Polytechnic, Shenzhen 518055, PR China
[*]Presenter: hork.m.zhang@outlook.com, [#]Corresponding author: zoudujian@163.com

Abstract

Calcium leaching of cement hydrates increases the porosity and reduces the bonding strength of cementitious materials, compromising the durability of concrete elements exposed to aggressive environments. Previous studies have focused on investigating the leaching process in deionized water or ammonium nitrate solutions, neglecting the effects of aggressive ions concentrations, types, and environmental temperatures. In addition, the selection of critical parameters (x_1, x_2, and C_{satu}) of equilibrium curve in chemo-transport-damage models are empirical, with no specific equations or criteria. Reported here provide insights into the calcium leaching process of cement hydrates exposed to the sodium sulfate and sodium chloride solutions, respectively. This study was conducted experimentally to examine the effects of concentration and temperature of sulfate and chloride ions. The relationship of critical parameters of equilibrium curves with ions concentrations and temperatures was established quantitatively. The results show that, compared to deionized water, both sulfate and chloride ions accelerate the leaching process, but the latter has less impact than the former. Leaching can be accelerated by increasing the concentration of aggressive ions and decreasing the environmental temperature. The results allow to describe the calcium leaching in saline soil and marine environments, and can be used to calibrate a concrete deterioration model under aggressive ions attack.

Keywords: Calcium leaching; Aggressive ions; Equilibrium curve; Concrete durability

1

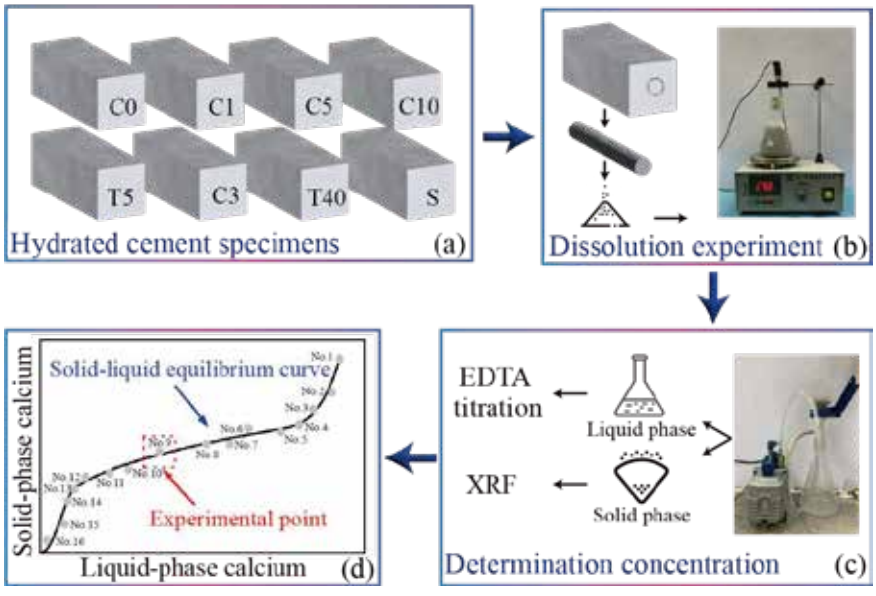

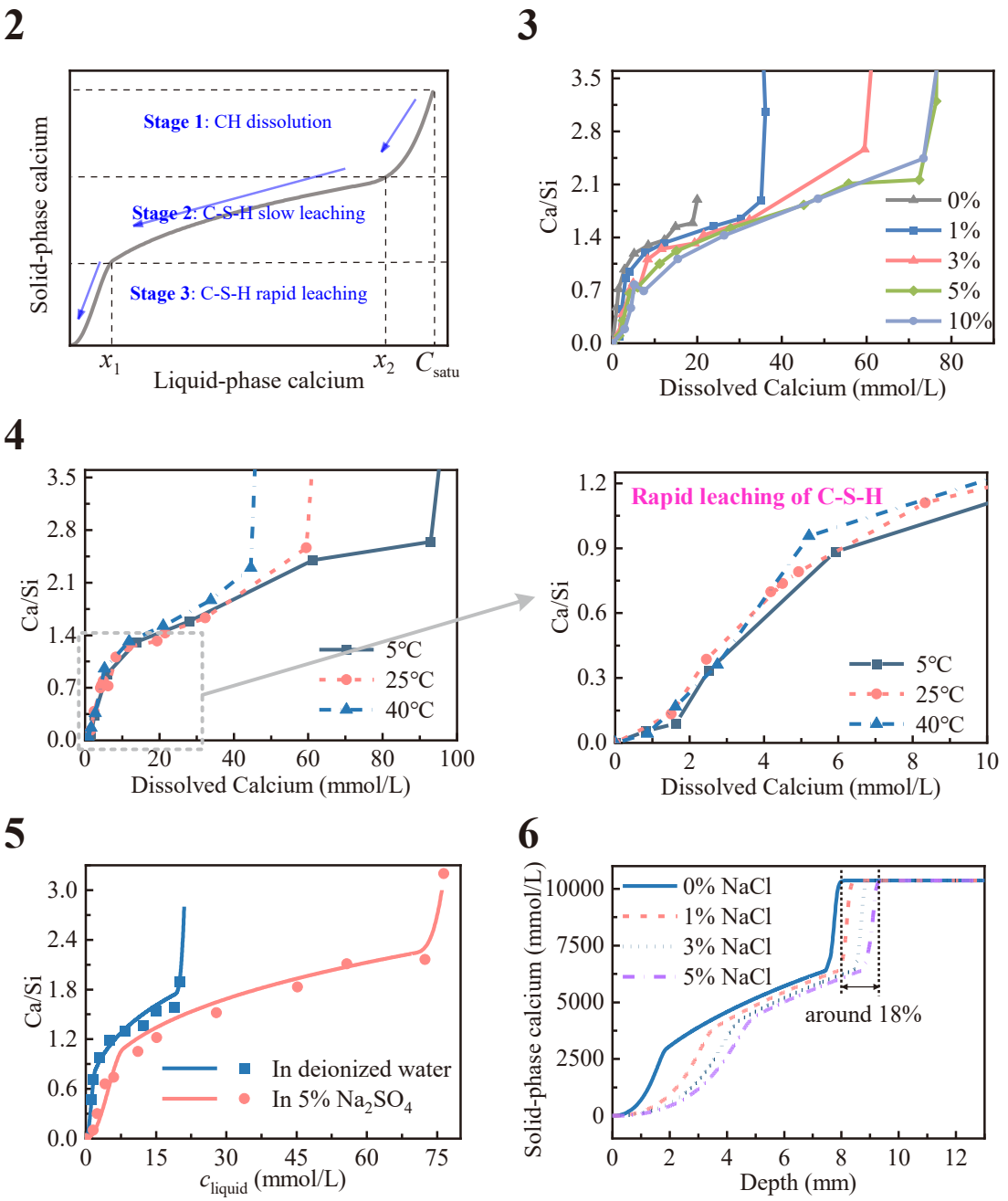

Fig. 1 The experimental process of determining the solid-liquid equilibrium curve; **Fig. 2** The diagram of the solid-liquid equilibrium curve; **Fig. 3** The calcium leaching curves at the different concentrations; **Fig. 4** The calcium leaching curves at the different temperatures; **Fig. 5** Accelerating effect of sulfate ions on calcium leaching compared to deionized water; **Fig. 6** Accelerating effect of chloride ions on calcium leaching compared to deionized water

Acknowledgment

This work was supported by the National key research and development program of China (Grant No. 2021YFF0500801), the National Science Fund for Distinguished Young Scholars (Grant No. 52025081), the National Natural Science Foundations of China (Grant Nos. 51978211, 52108234), the Shenzhen Science and Technology Program (Grant No. RCYX20200714114525013), and the Fundamental Research Fund for the Central Universities (Grant No. HIT.BRET.2021012).

Establishment of a prediction model of the failure thickness of concrete under sulfate attack

Shanshan Qin[1*], Chuyu Chen[2], Dujian Zou[2#], and Tiejun Liu [2]

[1,] School of Construction Engineering, Shenzhen Polytechnic, Shenzhen, CHINA
E-mail: qinshanshan@szpt.edu.cn
[2] School of Civil and Environmental Engineering, Harbin Institute of Technology, Shenzhen, Shenzhen, CHINA
E-mail: 20s154209@stu.hit.edu.cn, zoudujian@163.com, liutiejun@hit.edu.cn

Abstract

The durability of concrete under the sulfate attack environment is hard to predict as the deterioration performance is not described quantitatively. The indicators, such as strength, elastic modulus, mass, and length variations, are used widely to describe the effect of sulfate attack on concrete structures. However, these indicators do not provide sufficient information to assess the damage mechanisms. Moreover, they are difficult to obtain accurately in the actual engineering environment.

In the present work, sulfate attack experiments were carried out and the compressive strength, dynamic elastic modulus, and the concentration of sulfate ions with depth were measured. The durability failure index of concrete materials under sulfate attack was defined according to the mechanism of sulfate attack on concrete. The failure thickness was obtained by linear interpolation according to the calculated critical concentration of sulfate ions. Then the correlation analysis of the failure thickness and the change rate of the dynamic elastic modulus and compressive strength of concrete was carried out. The results indicate that the failure thickness can reflect the changing trend of the mechanical properties of concrete under sulfate attack. Then a prediction model for the failure thickness which is the square root of the attack time, was established. Furthermore, using the previously established chemical-diffusion-mechanical sulfate model, the influences of sulfate solution concentration, initial aluminate content of concrete, and diffusion coefficient on failure thickness were sensitivity analyzed. The results show that the failure thickness increases with the increase of the sulfate solution concentration and the diffusion coefficient, and the changing trend of the influence on the failure thickness presents a logarithmic curve. Whereas, the increase of aluminate concentration decreased the failure thickness to a certain extent, showing a negative linear correlation. The established model was verified by an experimental test, the results indicated that the prediction thickness was close to the test results and the error was acceptable.

In this research, a new durability failure index, failure thickness of concrete materials under sulfate attack was defined. And it's validated that it can reflect the changing trend of concrete macro-mechanical properties under sulfate attack. Furthermore, a prediction model for the failure thickness was established in relation to sulfate solution concentration, concrete initial aluminate content, and diffusion coefficient. These studies help to further develop the durability design and life prediction of concrete structures under sulfate attack environments.

Keywords: Concrete, Durability indicators, Prediction model, Sulfate attack.

[*]: Presenter; [#]: Corresponding author

Potential of nano-engineered concrete as a repair material for deteriorated concrete structures

Xinyue Wang[1], Sufen Dong[2] and Baoguo Han[3*]

[1] School of Civil Engineering, Dalian University of Technology, Dalian, CHINA
E-mail: xinyuewang@dlut.edu.cn
[2] School of Transportation & Logistics, Dalian University of Technology, Dalian, CHINA
E-mail: dongsufen@dlut.edu.cn
[3] School of Civil Engineering, Dalian University of Technology, Dalian, CHINA
E-mail: hithanbaoguo@163.com, hanbaoguo@dlut.edu.cn

Abstract

A large number of concrete structures cannot reach their design service life due to damage caused by the combined effects of mechanical loads and environmental actions including fatigue, shrinkage, creep, temperature change, freeze-thaw weathering, etc. To prolong their service life, deteriorated concrete structures are generally repaired with new concrete. However, it is estimated that about half of repairs failed, most of which can be attributed to debonding at the new-to-old concrete interfaces. This confirms the importance of reliable bonding between new and old concretes for repairing concrete structures. Thanks to their nano-core effect, nanofillers show great potential to improve the bond between new and old concrete.

Therefore, this study investigated the potential of nano-engineered concrete as a repair material for deteriorated concrete structures. For this purpose, the study characterized bond strength of nano-engineered concrete with old concrete, as well as explored the reinforcing mechanisms and established a prediction model for the bond strength between nano-engineered concrete with old concrete. The results indicated that bond strength between nano-engineered concrete and old concrete can reach 2.85 MPa, which is 0.8 MPa/39.0% higher than that between new concrete without nanofillers and old concrete. The reinforcing mechanisms can be attributed to the enrichment of nanofillers in the new-to-old concrete interface, compacting the interfacial microstructures and connecting hydration products in micropores of old concrete with that in new concrete. In addition, the prediction model proposed based on the above reinforcing mechanisms can accurately describe the relationship of the nanofiller content and the bond strength of nano-engineered concrete with old concrete.

This study demonstrates that nano-engineered concrete is a promising repair material for deteriorated concrete structures due to its strong bond with old concrete. Moreover, the mechanisms and model proposed in this study are beneficial for understanding and controlling the repair behavior of nano-engineered concrete.

Keywords: Nano-engineered concrete, Repair material, New-to-old concrete bond strength, Reinforcing mechanisms, Prediction model

Parallel Sessions-11

Valorization of Waste FRP Composites for Use in Civil Engineering

Performance Evaluation of Waste of Waste GFRP Powder/GGBS-Based Geopolymer Mortars for Rapid Repair of Concrete

Chuji Zheng[1], Jun Wang[2,*#]

[1, 2] College of Civil Engineering, Nanjing Tech University, Nanjing, People's Republic of China,
E-mail: zhengchuji97@163.com; wangjun3312@njtech.edu.cn

Abstract: A novel method is developed for reusing the waste glass fiber-reinforced polymer (GFRP) powder and ground granulated blast furnace slag (GGBS) as precursors in geopolymer mortars for rapid repair of concrete. The effects of GFRP powder content, activator concentration, liquid to solid (L/S) ratio, activator solution modulus, and sand to binder (S/B) ratio on the physico-mechanical properties of geopolymer mortars were evaluated. Based on the 1-day compressive strength, the optimal combination of the geopolymer mortars is determined to be 20 wt.% GFRP powder content, an activator concentration of 75%, an activator solution modulus of 1.2, L/S of 0.6, and S/B of 2.0. The highest compressive strength of GFRP powder/GGBS-based geopolymer mortar is 35.7 MPa at ages of 1 day, with initial setting time of 24 min and final setting time of 29 min. The bond strength between the geopolymer mortar and concrete is 10 times higher than the bond strength between cement mortar and concrete at ages of 1 day. Microstructural analysis indicates that incorporated GFRP powder into GGBS-based geopolymers could improve the pore structure. C-S-H gel and C-A-S-H gel are formed in the GFRP powder/GGBS-based geopolymer mortars. The developed GFRP powder/GGBS-based geopolymer mortars reduce the disadvantages of GGBS geopolymer mortars and cement mortars, and thus, offer high potential as a rapid-repair material.

Keywords: Glass fiber reinforced polymer powder; Ground granulated blast furnace slag; Geopolymer; Rapid repair; Concrete

* ***Presenter:*** *Jun Wang*

Corresponding Author: *Jun Wang*

Impact behavior of waste polyethylene terephthalate fiber reinforced concrete with recycled aggregate

Zhi-Wei Yan[1], Yu-Lei Bai[1,*#]

[1] Key Laboratory of Urban Security and Disaster Engineering of Ministry of Education, Faculty of Architecture, Civil and Transportation Engineering, Beijing University of Technology, Beijing 100124, People's Republic of China
Presenter: Yu-Lei Bai, #Corresponding author: baiyulei@bjut.edu.cn

Abstract
As one of green fiber materials, polyethylene terephthalate (PET) fibers are mainly produced from recycled plastic bottles. The composite material with PET fibers as reinforcement has a large tensile rupture strain of more than 5% and exhibits a bilinear stress-strain relationship. Meanwhile, the urbanization has led to the demolition of many existing reinforced concrete (RC) structures. The disposal of the waste concrete is posing threat to our environment. Crushing waste concrete, recycling the coarse aggregate and forming recycled aggregate concrete (RAC) will not only address environmental problems, but also save resources for new construction. Adding PET fibers into RAC can potentially mitigate damage and increase ductility. This study presents an experimental investigation on the effect of recycled coarse aggregate (RCA) replacement ratios, and fiber volume ratios on the dynamic compressive behaviors of PET fiber reinforced concrete under various strain rates. A split Hopkinson Pressure Bar (SHPB) device was used to carry out this study. The experimental results showed that the PET reinforced recycled aggregate concrete is a strain rate sensitive material. The compressive strength, critical strain and toughness increased with the growth of the strain rate. The addition of the RCAs increased the porosity of the specimen, which resulting in a reduction in the dynamic compressive strength and an increase in the critical strain. The inclusion of PET fibers into a concrete matrix improved the critical strain and substantially reduced the damage, owing to the bridging and cracking resistance of PET fibers. Nevertheless, the existence of fibers also enhanced the defects of the concrete, which decreased the dynamic compressive strength.

Keywords: Polyethylene terephthalate (PET) fiber; recycled aggregate concrete; Dynamic compressive behavior

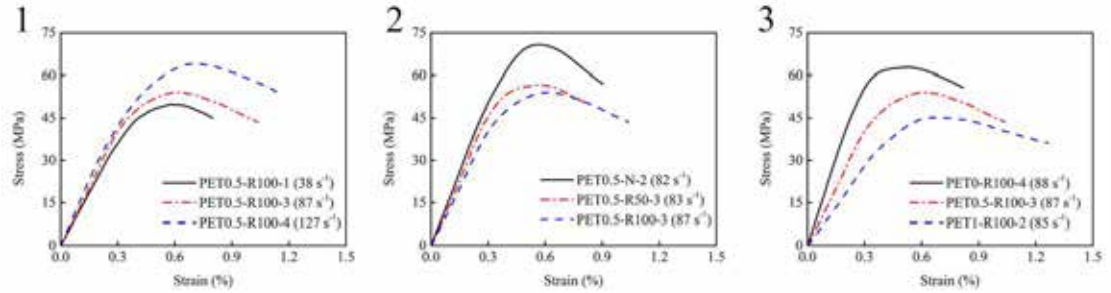

Fig. 1 Effect of strain rate on the stress-strain curve; **Fig. 2** Effect of RCA replacement ratio on the stress-strain curve; **Fig. 3** Effect of fiber volume ratio on the stress-strain curve

Acknowledgment
The authors would like to acknowledge the funding support from the Natural Science Fund of Beijing (No. 8212003), National Natural Science Fund of China (No. 51778019, 51978017), Beijing Nova Programme (No. Z201100006820095), Young Talents Cultivation Project of Beijing Municipal Institutions (No.CIT&TCD201904018).

Study on phase reconfiguration and alkali-aggregate reaction of regenerated glass fibers based on GFRP

GFRP has been widely used in various industrial fields because of its excellent properties such as high strength, high specific stiffness, corrosion resistance and temperature resistance, but in the process of recycling waste products that have expired in service, due to its refractory and difficult to process characteristics, the realization of high-value recycling and reuse of solid waste GFRP has always been a hot issue in the scientific and technological community and industry. The separation of glass fibers and resin matrix in solid waste GFRP and the preparation of recycled glass fibers in the geotechnical field is an effective consumption method with good promotion prospects, while the glass fiber sources used in waste GRFF Do not have homogeneity and stability, which is mainly manifested as the difference in alkali activity in glass fibers, resulting in alkali-aggregate reaction of glass fibers in the geotechnical field, affecting the large-scale promotion and application of recycled glass fibers. In view of the difficulties in the application of recycled glass fibers, this paper recrystallizes some of the active SiO2 with amorphous form and poor crystallinity in the waste glass fibers into a relatively stable crystal state by means of heat treatment regulation, so as to avoid alkali aggregate reaction with the alkali aggregate in cement matrix composites.

Key words: GFRP waste; Recycled glass fibers; Heat treatment; Alkali activity; Cement-based composite

Novel green concrete using plasma-treated recycled PET

Huali Hao[1]*

[1, 2] School of Civil Engineering, Wuhan University, Wuhan, China
E-mail: haohuali@whu.edu.cn

Abstract

Green concrete has great potential for application in construction to replace conventional concrete in order to minimize environmental impacts. For example, more than 10% of the manmade greenhouse gas emissions originate from cement manufacturing process in cement factories. It is estimated that more than 10 billion tonnes of concrete are manufactured globally every year. The traditional disposal of the large amounts of construction waste in landfills is no longer an acceptable option, due to the limited landfill capacity. The demand for green concrete in construction industry is spurred as it can reduce carbon footprint, limit greenhouse gas emission and extend the service life of landfills. The adoption of recycled waste plastics such as waste polyethylene terephthalate (PET) bottles can reduce environmental problems as well as solve problems of lack of aggregate on construction sites. However, the compressive strength, one of the most important properties of concrete, is reduced. Without solving the problem of reduction in compressive strength, the practical application of green concrete is limited. Plasma treatment has been widely used to modify the surface properties of polymer where the created favorable functional groups and the increased surface energy can increase the hydrophilicity and roughness of the surface. Plasma modification has been regarded as a flexible and eco-friendly approach to offer excellent compatibility with microfabrication process. The objective of this work is to study the effect of plasma treatment on the compressive strength of green concrete. The effect of surface modification on the interfacial behavior between motor and PET is studied at multiscale to figure out the underlying reason for the variation in strength. Our findings can provide a guideline for the control of plasma treatment enabling treated polymer with optimized properties.

Keywords: Green concrete, Plasma treatment, Compressive strength, Interfacial adhesion, Multiscale.

Mechanical properties of concrete containing macro fibers recycled from GFRP waste: Effects of fiber length and volume fraction

Qi-Qi Zou[1*], Bing Fu[2,3#], Jian-Fei Chen[1#], Jin-Guang Teng[4]

[1] Department of Ocean Science and Engineering, Southern University of Science and Technology, Shenzhen 518055, China
[2] School of Mechanics and Construction Engineering, Jinan University, Guangzhou 510632, China
[3] MOE Key Lab of Disaster Forecast and Control in Engineering, Jinan University, Guangzhou 510632, China
[4] Department of Civil and Environmental Engineering, The Hong Kong Polytechnic University, Hong Kong, China
[*]*Presenter:* 11849508@mail.sustech.edu.cn, [#]*Corresponding author:* fubing@jnu.edu.cn; chenjf3@sustech.edu.cn

Abstract

Fiber-reinforced polymer (FRP) composites have been widely used in many sectors such as the aerospace, wind energy, and construction industries due to their excellent mechanical performance, durability, and lightweightness. Inevitably, the increasing use of FRP composites led to an accumulation of FRP waste that needs to be disposed of. A new mechanical recycling method has recently been explored by the authors' group to process waste GFRP into "macro fibers" with their aspect ratios being close to those of steel fibers, which are then incorporated into concrete, resulting in what is referred to as macro fiber reinforced concrete (MFRC). This paper presents an experimental program on the mechanical properties of MFRC, in which the effects of fiber length and fiber volume fraction were examined through a series of compression, splitting, and bending tests. In particular, the load-deflection responses of the beam specimens obtained from the tests were used to derive the tensile constitutive law of the MFRC using a point-by-point double inverse analysis approach. The results indicate that the splitting tensile strength, flexural tensile strength, and toughness (i.e., Area under the load- net deflection curve 0 to L/150) of the concrete can be significantly enhanced through the incorporation of macro fibers.

The experimental compressive strengths of all MFRC cylinder specimens tested in the present study are shown in Fig. 1. The differences in compressive strength among the specimens are in the range of -5% to 4%, indicating that the fiber addition has a minor effect on the compressive strength. The incorporation of macro fibers has a significant effect on the splitting tensile strength of MFRC (Fig. 2), which is seen to be more significantly enhanced when a higher volume fraction or longer fibers are used. More specifically, the splitting tensile strength increased from 3.19 to 3.87, 4.12, and 4.86 MPa when the volume ratio of 90-mm long macro fibers increased from 0.5% to 1.0%, and 1.5%, representing an increase in splitting tensile strength of 21.3%, 29.3%, and 52.2% respectively.

The key results of bending tests are given in Figs. 3 and 4. Compared with the corresponding plain concrete, the incorporation of 90-mm long macro fibers into concrete led to significant increases in the flexural tensile strength and toughness: there are increased by 1.3 and 230 times respectively when macro fibers of 1.5% in volume fraction were added to the mix. The tensile stress-strain curves of MFRC were obtained from the bending test results through point-by-point double inverse analysis. All the tensile stress-strain curves exhibit a strain-softening phenomenon, and the slope of the descending portion reduces with an increase in the length and volume fraction of incorporated macro fibers.

In summary, the results from this study show that the incorporation of macro fibers significantly enhances the tensile properties of concrete. As a result, this new mechanical recycling method is expected to be both technically feasible and economically attractive.

Keywords: GFRP waste; Mechanical recycling; Macro fibers; Concrete; Mechanical properties

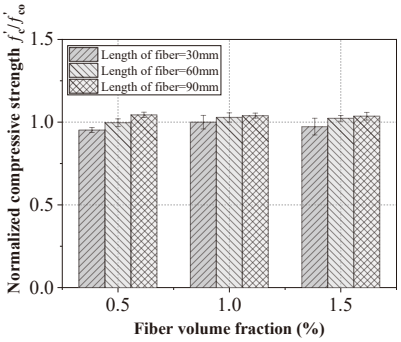

Fig. 1 Compressive strength

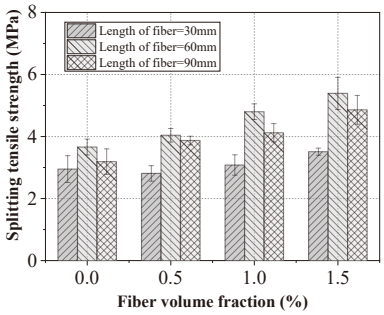

Fig. 2 Splitting tensile strength

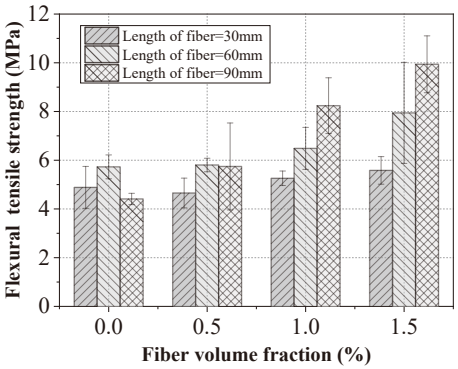

Fig. 3 Flexural tensile strength

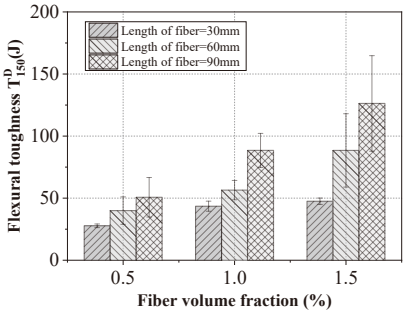

Fig. 4 Flexural toughness

Acknowledgment

The authors gratefully acknowledge the financial support provided by the National Natural Science Foundation of China (Project Nos: 52178212 and 51978176), and the Guangdong Basic and Applied Basic Research Foundation (Project No.: 2021A1515010414). The authors also wish to thank Mr. Huang Jun-Jian for his help in conducting some of the tests.

Ultra-high performance concrete reinforced with macro fibres recycled from a decommissioned turbine blade

X.M. YOU[1], L.B. LIN[1], Bing FU[1,2*] and Yu XIANG [3#]

[1] School of Mechanics and Construction Engineering, Jinan University, Guangzhou 510632, China
[2] MOE Key Lab of Disaster Forecast and Control in Engineering, Jinan University, Guangzhou 510632, China
[3] Department of Civil and Environmental Engineering, The Hong Kong Polytechnic University, Hong Kong, China

*Presenter: fubing@jnu.edu.cn, #Corresponding author: cee.yu.xiang@polyu.edu.hk

Abstract

Ultra-high-performance concrete (UHPC) is a class of cementitious composite exhibiting ultra-high compressive strength as well as excellent durability. Such characteristics make UHPC an idea candidate for constructing high performance, lightweight, and durable structures, which possibly have less carbon emission than constructing corresponding structures of other materials and therefore well satisfy the requirements for modern structures. UHPC has been used in an increasing number of highway infrastructure applications worldwide as field-cast connection material between prefabricated bridge components, thin overlays, as well as presstressed concrete girders. Relative high cost is one of major disadvantages of UHPC that impede its wider applications. The unit price of a 150 MPa-class UHPC per m^3 could be 20 times higher than that of conventional 50 MPa concrete; even when normalized by the strength class, the unit price of UHPC per MPa per m^3 could be still 8 times higher.

The steel fibres, whose cost roughly accounts for 50% the total cost of UHPC, are viewed as an essential constituent material, having two major effects on the properties of UHPC (1) reducing the workability of the fresh UHPC; (2) bridging cracks in the hardened UHPC. Despite the significant beneficial effect of the incorporation of steel fibres on enhancing the mechanical properties, balancing the material cost and property enhancement is a key issue to promote the practical applications of UHPC. Some attempts have been made on developing UHPC with non-metal fibres (e.g., synthetic fibres, inorganic fibres, and nature fibres) to partially or completely replace steel fibres. These studies have successfully demonstrated the feasibility of reinforcing UHPC with non-metal fibres, especially enhancing the strength and toughness of UHPC under tension, but these newly produced non-metal fibres still have a high unit cost, and cannot lower the price of fibre reinforced UHPC significantly.

Recycling and reusing fibres from solid waste is a cost efficient and environmentally-friendly routine to produce fibre reinforce cementitious composites. In recent studies, the authors' group has proposed an innovative routine to valorize waste GFRP by being processed into macro fibres as discrete reinforcement in concrete. The macro fibres recycled from waste GFRP have an aspect ratio close to that conventional macro steel fibres, and enhanced the compressive strength, tensile splitting strength, flexural strength and flexural toughness of concrete by up to 4.4%, 52%, 1.3 times and 230 times compared to those of plain concrete. The added value of GFRP waste can be further increased at the structural scale by an optimal use in structures. These studies indicate the ability of macro fibres recycled from waste GFRP to completely or partially replace steel fibres to produce cost efficient fibre reinforced cementitious composites.

Against the background above, a new concept is proposed in the present paper to produce UHPC reinforced with macro fibres processed from waste GFRP. With this concept, the cost of UHPC could be significantly reduced and the waste GFRP, which is difficult to dispose of, is recycled in

an economical and environmental way. A series of tests have been carried out to investigate the effect of adding macro fibres on the properties of UHPC. The test results show that the incorporation of macro fibres leads to a loss of the workability and a reduction of up to 21.8% in the compressive strength, but improves the its flexural strength and flexural toughness greatly by up to 27.9% and 46.9 times, respectively. The tensile constituting relationship has been converted from the results of the bending tests through their inverse analysis. The proposed concept of producing UHPC with recycled macro fibres and UHPC contributes to lowering the price of UHPC, whose properties are comparable to that of UHPC with steel fibres, and finding an effective routine to valorize the waste GFRP.

Keywords: Ultra-High Performance Concrete (UHPC); GFRP Waste; Mechanical Recycling; Fibre-Reinforced Concrete; Macro Fibres

1

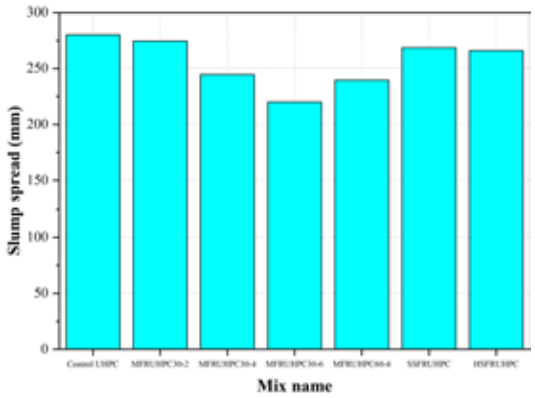

2

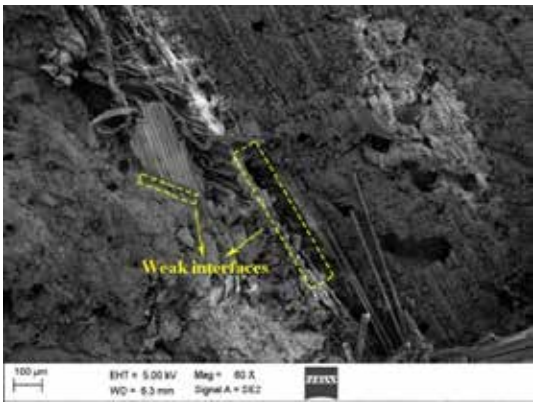

3

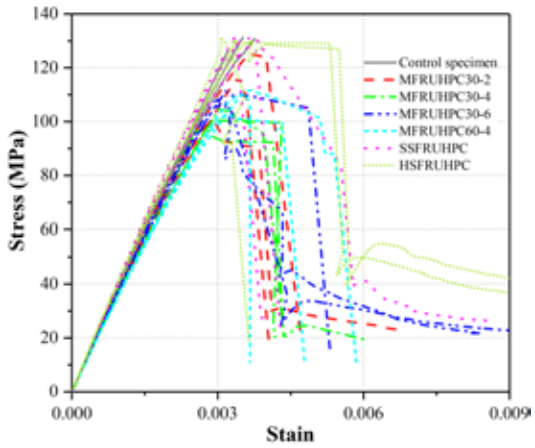

4

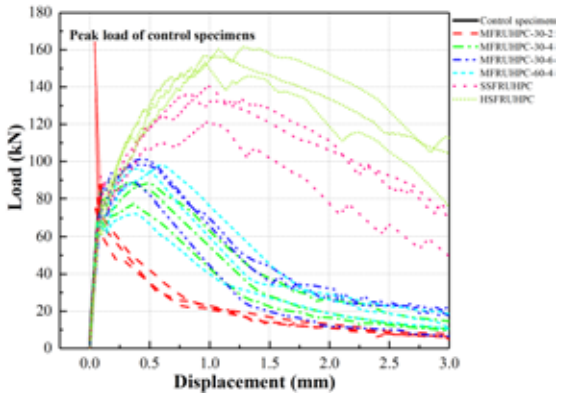

Fig. 1 Slumps of free mini-slump spread tests; **Fig. 2** Microscopic morphology on surface texture of macro fibres after tests; **Fig. 3** Compressive stress-strain curves of cylinder specimens; **Fig. 4** Load-deflection curves of beam specimens

Acknowledgment

The authors are grateful for the financial support provided by the National Natural Science Foundation of China (Project Nos.: 51978176 and 52178212) and the Guangdong Basic and Applied Basic Research Foundation (2021A1515010414).

Mechanical properties of recycled carbon fiber reinforced cementitious matrix composites

Pi-Yu Chen[1], Zhenxuan Liang[2], Ran Feng[3], Ying Xu[4] and Ji-Hua Zhu[5*]

[1,3,4] School of Civil and Environmental Engineering, Harbin Institute of Technology, Shenzhen, China
E-mail: 19B954012@stu.hit.edu.cn, fengran@hit.edu.cn, cexyx@hotmail.com
[2,5] Guangdong Provincial Key Laboratory of Durability for Marine Civil Engineering, College of Civil and Transportation Engineering, Shenzhen University, Shenzhen, China
E-mail: 1910472008@email.szu.edu.cn, zhujh@szu.edu.cn

Abstract

The extensive utilization of carbon fiber reinforced plastic (CFRP) has resulted in a significant accumulation of waste, posing significant environmental challenges. However, it is worth noting that the carbon fiber (CF) present in this waste still retains its exceptional material properties and exhibits a remarkably high level of utilization value. Consequently, considerable research efforts have been dedicated to exploring methods for recycling CF from CFRP waste. Nevertheless, the performance of recycled carbon fiber (rCF) is often considerably diminished compared to virgin carbon fiber (vCF), thereby limiting its potential applications to remanufacturing mixed resin-fiber products with subpar mechanical properties. Existing studies on the use of recycled carbon fiber reinforced cementitious matrices have yielded modest reinforcement effects due to the inclusion of resin in rCF and its slightly inferior performance. Furthermore, there is a dearth of comprehensive comparisons between rCF and vCF, further impeding the broader adoption of rCF.

In this study, we sought to address these limitations by employing rCF without resin and evaluating its non-destructive performance as a reinforcement material in cementitious matrices. Specifically, we examined the influence of rCF with varying contents and lengths on the mechanical properties of cementitious matrix composites through tests assessing fluidity, compressive strength, flexural strength, and splitting tensile strength. These findings were subsequently compared to those obtained using vCF.

Our results indicate that while the fluidity of recycled carbon fiber reinforced cementitious matrices experiences a slight reduction, their mechanical properties are significantly enhanced. Under optimal conditions, the compressive strength, flexural strength, and splitting tensile strength of recycled carbon fiber reinforced cementitious matrices were found to increase by 18.1%, 19.1%, and 44.3%, respectively. When compared to vCF, recycled carbon fiber generally exhibits slightly superior performance. Leveraging its excellent mechanical characteristics, rCF proves to be a viable reinforcement material for cementitious matrices. Furthermore, it offers distinct cost advantages, thereby facilitating the establishment of closed-loop recycling and the reuse of CFRP waste.

Keywords: Mechanical properties, Recycled carbon fiber, Recycled carbon fiber reinforced cementitious matrix, Virgin carbon fiber reinforced cementitious matrix

The observed improvements in the mechanical properties of cementitious matrices upon the inclusion of rCF can be attributed to several factors. First, the absence of resin in rCF eliminates the detrimental effects associated with its presence, leading to enhanced overall performance. Furthermore, the intrinsic properties of carbon fiber, such as its high strength-to-weight ratio and excellent corrosion resistance, contribute to the reinforcement effect. The interfacial bond between rCF and the cementitious matrix is strengthened due to the unique surface characteristics of carbon fiber, thereby improving the load transfer mechanism and overall structural integrity.

To delve further into the underlying mechanisms responsible for the observed enhancements, additional investigations can be conducted. For instance, microstructural analysis techniques such as scanning electron microscopy (SEM) and X-ray diffraction (XRD) can be employed to examine the interfacial properties and bonding characteristics of rCF-cementitious matrix composites. Furthermore, the long-term durability and sustainability of these composites could be evaluated through accelerated aging tests, environmental exposure experiments, and life cycle assessments. Such studies would provide valuable insights into the potential long-term performance and environmental implications of utilizing rCF as a reinforcement material.

In conclusion, this study demonstrates the significant potential of recycled carbon fiber without resin as a reinforcement material in cementitious matrices. By effectively enhancing the mechanical properties of the resulting composites, rCF offers a sustainable solution for the utilization of CFRP waste. Moreover, the cost advantages associated with rCF further strengthen its appeal for widespread adoption in construction applications. Future research endeavors should focus on exploring the interfacial characteristics and long-term performance of rCF-cementitious matrix composites, ultimately promoting the establishment of closed-loop recycling systems for CFRP waste.

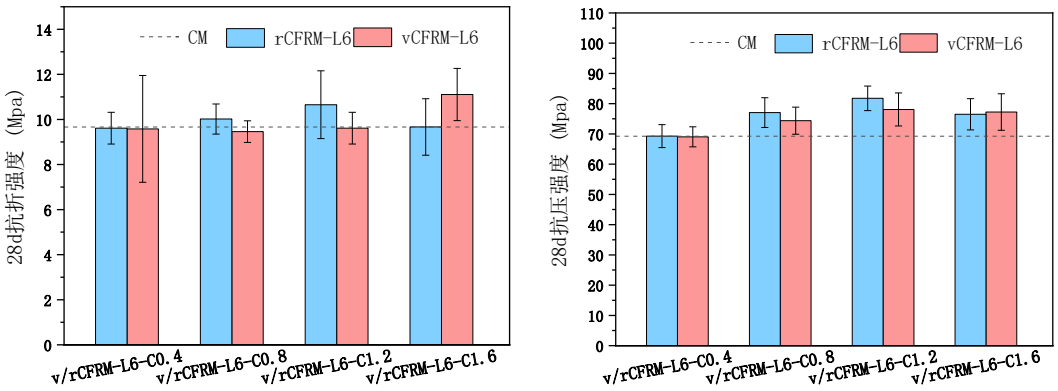

Fig. Mechanical properties of carbon fiber reinforced cementitious matrix

Acknowledgment

This work was supported by the National Key Research and Development Program of China (2018YFE0124900), the Key-Area Research and Development Program of Guangdong Province (2019B111107002), the National Natural Science Foundation of China (51538007/51778370/52108231), and the Shenzhen Science and Technology Project (GJHZ20180928155819738).

Mechanical properties of concrete containing macro fibers recycled from GFRP waste: Effects of fiber length and volume fraction

Zi-qi Li[1*], Chun Pei[2] and Ji-Hua Zhu[3#]
[1, 2, 3]Department of Civil Engineering, Shenzhen University, Shenzhen, China
E-mail: liziqi2017@email.szu.edu.cn, ccpei@szu.edu.cn, zhujh@szu.edu.cn

Abstract

Due to the exceptional mechanical properties and high durability of carbon fibers (CFs), they have gained widespread utilization in CF-reinforced cementitious composites. However, a major limitation of these composites is the inadequate interfacial strength between the hydrophobic CFs and cementitious matrix, which hinders the effective utilization of CFs' high tensile strength. To address this issue, the present study focuses on enhancing the interfacial strength by modifying the CFs' surface through electrophoretic deposition of nano-silica (NS). Various parameters, including voltage range, deposition time, electrolyte concentration, calcium salt concentration, and NS mass fraction, were examined to investigate their effects on the deposition outcomes. The modified CFs' microstructures and surface roughness were analyzed using scanning electron microscopy (SEM) and atomic force microscopy (AFM), respectively. The surface functional groups and elemental distribution of the modified CFs were characterized by X-ray photoelectron spectroscopy (XPS). Additionally, the CFs single bundle pull-out test and microcharacterization of the interface between cement and CFs were conducted. The influence of modified CFs on the interface properties between cement under different parameters was studied using orthogonal analysis.

The results demonstrate the successful deposition of NS on the surface of CFs, which led to an increased fiber surface roughness compared to untreated fibers. Orthogonal analysis revealed that the deposition voltage was the most crucial factor influencing the outcomes. The single bundle pull-out test indicated a significant enhancement in the interfacial strength between the cementitious matrix and CFs, particularly at higher NS concentrations. The pullout strength was enhanced by up to 139%, which can be attributed to the deposition of NS on the CFs' surface. This deposition process not only increased the surface roughness, thereby enhancing the physical anchoring effect, but also improved the chemical bonding between the fiber and the matrix through the silica pozzolanic reaction.

The deposition of NS on CFs' surface plays a vital role in strengthening the interface between CFs and cementitious composites. The modified CFs exhibited improved adhesion to the cementitious matrix, which can be attributed to the roughened surface facilitating mechanical interlocking and the chemical reaction between the silica nanoparticles and cementitious constituents. SEM analysis revealed the presence of a uniform NS layer on the CFs' surface, confirming the successful electrophoretic deposition process. AFM images further demonstrated the increased surface roughness of the modified CFs compared to untreated fibers, validating the efficacy of the NS deposition method.

Keywords: Carbon fiber, Cement-based composites, Electrophoretic modification, Nanosilica, Interfacial strength

XPS analysis provided valuable insights into the surface chemistry of the modified CFs. The presence of characteristic peaks corresponding to silica confirmed the successful deposition of NS. Furthermore, the elemental mapping revealed a uniform distribution of silica nanoparticles on the CFs' surface, indicating a homogeneous modification. These findings collectively support the effectiveness of the electrophoretic deposition technique in enhancing the interfacial strength between CFs and the cementitious matrix.

The orthogonal analysis elucidated the significance of various parameters in the deposition process. Among these parameters, the voltage range exerted the most substantial influence on the outcomes. Higher deposition voltages resulted in a more pronounced increase in interfacial strength. However, other factors such as deposition time, electrolyte concentration, calcium salt concentration, and NS mass fraction also played important roles in determining the effectiveness of the modification process.

In conclusion, the present study successfully improved the interfacial strength between CFs and cementitious composites by modifying the CFs' surface through electrophoretic deposition of nano-silica. The deposition process enhanced the physical anchoring effect by increasing the surface roughness of CFs and improved the chemical bonding between the fiber and the matrix through the silica pozzolanic reaction. The findings emphasize the importance of optimizing parameters such as voltage range, deposition time, electrolyte concentration, calcium salt concentration, and NS mass fraction to achieve the desired interfacial strength. Further investigations in this area may involve exploring alternative surface modification techniques and assessing the long-term durability and performance of CF-reinforced cementitious composites.

Acknowledgment

This work was supported by the National Key Research and Development Program of China (2018YFE0124900), the Key-Area Research and Development Program of Guangdong Province (2019B111107002), the National Natural Science Foundation of China (51538007/51778370/52108231), and the Shenzhen Science and Technology Project (GJHZ20180928155819738).

Parallel Sessions-12

Low-Carbon and Sustainable Concrete

Green and low-carbon cement with sintered sludge: Microstructure and performance

Abstract: To achieve carbon peaking and carbon neutrality goals and the diversified utilization of resources, it is necessary to speed up the process of combining the improvement of the ecological environment governance system with the industrial upgrading of all walks of life, which is a top priority for the cement industry with huge carbon emission pressure and insufficient raw material reserves. Considering the current situation that river and lake sludge reserves are huge and cannot be treated in an environmentally friendly way, its utilization in building materials to replace cement provides a new idea for solving the above problems. Therefore, a green and low-carbon cement with sintered sludge is innovatively proposed in this report. The process of "grinded-calcined at 750℃-grinded" is the primary treatment for application and activation of the dried sludge. Subsequently, the cement with different sintered sludge contents is systematically studied from the aspects of macroscopic properties and microstructural characteristics. With the enlargement of sintered sludge content, the water absorption, shrinkage resistance and durability are enhanced, and the mechanical properties show a trend of first increase and then decrease, with the maximum value at 10% sintered sludge. Due to high specific surface area, the incorporation of 10% sintered sludge plays the role of micro-filling in early hydration stage, leading to the densification of the microstructure and the addition of potential nucleation sites. In later hydration stage, numerous amorphous silica in the sintered sludge undergoes secondary hydration based on pozzolanic activity and generates massive C-S-H and C-A-H, which is marked the formation of a stronger cement matrix. The improvement in long-term mechanical properties and durability is the combined result of the pozzolanic activity and internal curing properties of the sintered sludge. In the future, considering the shortage of fresh water and river sand caused by concrete mixing and the abundance of seawater and sea sand, research will focus on the combination of seawater, sea sand and cement with sintered sludge.

A general approach to exfoliate and disperse 2D nanomaterials for improving cement hydration and chloride binding

Wu-Jian Long[1,2*], Peng Xu[1,2], Gan-Lin Feng[1,2], Chuang He[1,2]

[1] Guangdong Province Key Laboratory of Durability for Marine Civil Engineering,
[2] College of Civil and Transportation Engineering, Shenzhen University, Shenzhen, Guangdong 518060, People's Republic of China
Presenter: longwj@szu.edu.cn, #Corresponding author: longwj@szu.edu.cn

Abstract

Tremendous progress has been made in the employment of two-dimensional (2D) nanomaterials in cement composites. However, poor dispersion of 2D nanomaterials immensely hinder their extensive use. To address these issues, in this work, a simple and general method for exfoliating 2D nanomaterials (GO, CLDH, CN) which use graphene quantum dots (GQDs) and low-power ultrasonic treatment was elaborately designed to efficiently delaminate and disperse 2D nanomaterials, and investigate the effects of 2D nanomaterial dispersion on cement hydration and chloride binding properties in depth (Fig. 1). The addition of GQDs significantly improves the material's dispersibility, as evidenced by its morphological and structural characteristics, compared to 2D nanomaterials without GQDs-assisted exfoliating. The exfoliation mechanism of GQDs acting on 2D nanomaterials is reasonably proposed based on their properties and the dispersion results of three 2D nanomaterials. Furthermore, the effect of the dispersion method on cement hydration was investigated, and a correlation was established between the dispersion parameters of 2D nanomaterials, cement mechanical properties, and cement hydration degree. More importantly, highly dispersed 2D nanomaterials (G-GO、G-CLDH and G-CN) was more propitious to accelerate cement hydration and refine microstructure, thereby dramatically boosting the compressive strength of cement paste at 7-day curing by 43% , 52% and 46% compared with that of GO、CLDH and CN, respectively. And the 2D nanomaterials assisted by GQDs exfoliation can generally increase the chloride ion curing capacity of cement-based materials by 50%, compared with the control group. This research shows that GQDs have a great deal of potential for dispersing 2D nanomaterials, that they can significantly enhance the poor dispersibility of 2D nanomaterials currently used to reinforce cement-based materials, and that they can pave the way for the effective application of 2D nanomaterials to cement-based materials.

Keywords: 2D nanomaterials; Graphene quantum dots; Dispersion; Hydration; Chloride binding.

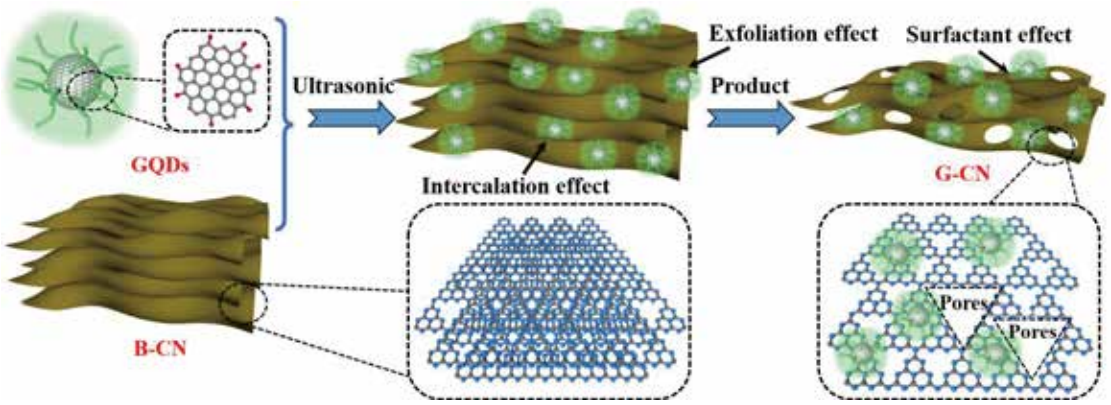

Fig. 1 Schematic illustration of GQDs-assisted exfoliation mechanism for CN

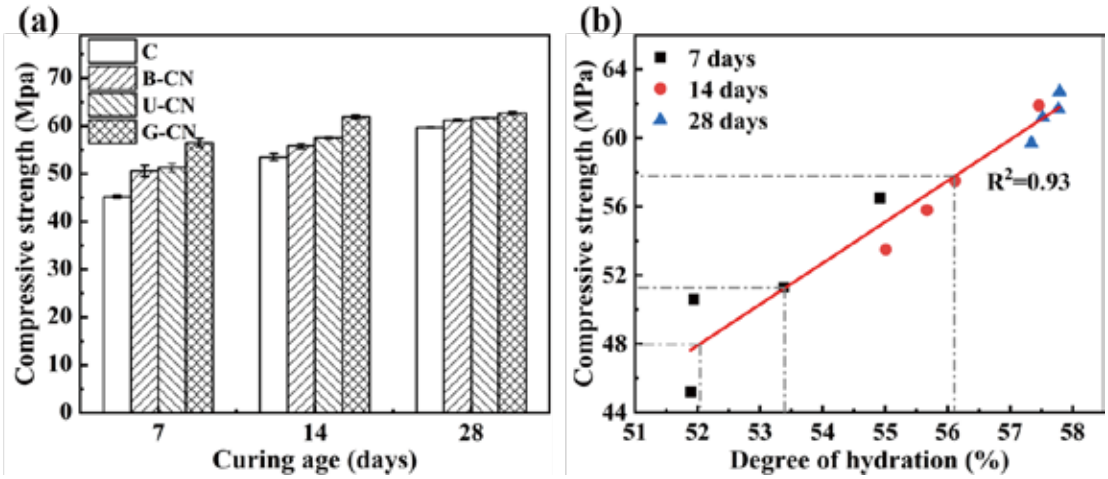

Fig.2 (a) Compressive strength of different paste specimens, and (b) its correlation with hydration degree.

Acknowledgment

The authors would like to acknowledge the National Natural Science Foundations of China, NSFC-Shandong Joint Fund (No. U2006223), the Science and Technology Project of Shenzhen, China (No. JCYJ20190808151011502, No. JCYJ20180305124844894), the Guangdong Provincial Key Laboratory of Marine Civil Engineering (SZU) (No. 2020B1212060074).

Effect of Carya Cathayensis Peels Biochar on Basic Properties of Cementitious Material

XUE Wen*, ZHOU Wenjian# and LI Zhu

Department of Civil Engineering, Zhejiang University of Science and Technology, Hangzhou, China
E-mail: xuewen@zust.edu.cn

Abstract

Producing biochar by consuming biomass was an effective way to reduce the environmental impact from biomass waste. However, there is limited exploration on its positive effects for improving the mechanical and durability properties of cementitious material. This study investigates the influence of biochar particles, which are made of Carya cathayensis peels biomass waste, on the mechanical properties (including compressive strength and split-tensile strength), thermal insulation and chloride ions prevention of cementitious materials at 28days age. The biochar was grinded into two different sizes of particles and added at 1%, 2%, 3%, 4% and 5% by weight of cement. The strength, thermal insulation and chloride resistance performance of biochar-cementitious composite were compared with plain ones. The results show that, addition of 2wt% of biochar increase the compressive and split-tensile strength of the composite by 3.5% and 33% respectively compared to the control set. The addition of biochar led to an increasing of thermal insulation by about 4% to 17%. The chloride ions penetration was stuck significantly in biochar mortar. The findings suggest that biochar from Carya cathayensis peels can be applied as a sustainable admixture in order to improve the basic properties of cementitious material. Meanwhile, this offers an interdisciplinary attempt of valorizing biomass waste in producing green building and construction materials.

Keywords: Biochar, cementitious material, strength, thermal isolation, chloride prevention

*: *Presenter*; #: *Corresponding author*

Self-healing of inorganic porous aggregate in concrete: Methods, Characterization and Application

He-Ming Sun[1*], Ao-Xuan Wang[1], Yuan Fang[1#], Xian-Feng Wang[1]

[1] College of Civil and Transportation Engineering, Shenzhen University, Shenzhen, Guangdong 518060, People's Republic of China

[*]Presenter: sunheming2022@email.szu.edu.cn, [#]Corresponding author: yuanfang@szu.edu.cn

Abstract

In engineering practice, concrete cracks under the compound stress field will significantly accelerate the deterioration rate of concrete durability. However, the efficiency of traditional concrete crack repair methods is low, so concrete self-healing technology, an efficient and convenient crack repair method, has attracted more and more attention. In this paper, self-healing concrete is prepared by using self-healing aggregate instead of traditional crushed stone aggregate. When the self-healing concrete is cracked by external damage, the aggregate is triggered by physical action to break and release the repair agent. Then the repair agent reacts with the cement material in the crack to generate the repaired product to repair the crack. Firstly, the performance of self-healing concrete was tested through the mix's working and mechanical properties tests. It was found that the self-healing aggregate completely replacing the traditional aggregate had no significant impact on the impermeability of concrete and the functional performance of the mix, and the mechanical properties of the concrete matrix were improved. After that, the image method, microscope observation method and backscattering scanning electron microscope (BSE) were used to study the repair effect of the fracture. The results show that when the crack width is less than 300 μm, the crack repair effect within 15 mm depth is good, the flexural strength recovers to 40.8% at seven days of age, and the area repair rate reaches 100%. At the age of 28 days, the flexural strength recovery rate reached 83.1%, and the impermeable pressure value recovered by 45 %. Using self-repairing aggregate can achieve the purpose of self-repairing concrete cracks, and the repaired product has a good interface with the concrete matrix. The results of this study provide a new idea for concrete self-healing technology.

Keywords: Concrete; Inorganic materials; Self-healing materials; Aggregate; Crack;

Enhancing recycled fine concrete aggregate by a two-step wet carbonation process

Xiaoliang Fang[1,*#], Wenwen Lian[1], Danni Qu[1], Renjie Zhou[2]

[1] School of Civil & Environmental Engineering and Geography Science, Ningbo University, Ningbo, Zhejiang, China,
[2] School of Material Science and Chemical Engineering, Ningbo University, Ningbo, Zhejiang, China
Presenter: fangxiaoliang@nbu.edu.cn, #Corresponding author: fangxiaoliang@nbu.edu.cn

Abstract

The construction industry is eager to develop upcycling techniques for transforming secondary by-products derived from concrete waste into value-added new products due to the shortage of practical and economical solutions. Currently, recycled concrete aggregates (RCA) were mainly used in low-graded applications, especially the fine portion of the RCA due to a higher mortar content.

This paper presents a study aiming to enhance the quality of recycled fine aggregate (FRCA) by utilizing a wet carbonation process developed by the authors previously. The fine recycled concrete aggregate (FRCA) ranging from 0.15-5 mm was prepared through demolishing a concrete with a known mixture design. The FRCA was treated by a Na2CO3 solution. The particle size, water absorption, and density of the FRCA were tested and compared. The chemical characteristics of the RFA after wet carbonation were analyzed by a series of experiments. The results showed that the density and the water absorption properties of the FRCA improved significantly

The chemical compositions of the FRCA were analyzed by XRF, XRD, and TGA before and after the wet carbonation. The results revealed an increase in carbonation production and a significant reduction in cement hydration products. The microscopic observation of the FRCA showed a densified surface layer with carbonation products after wet carbonation. The by-product of calcite and silica-rich gel were also collected and analyzed.

A rough estimation of the environmental and economic impact of wet carbonation on FRCA was conducted. The proposed approach was expected to avoid millions of disposal charges and provide FRCA with solid properties. Meanwhile, the calcite-rich residue and silica-rich gel showed high potential industrial values. Moreover, the material and energy consumption of the wet carbonation process were environmentally friendly.

Keywords: wet carbonation; recycled fine concrete aggregate; upcycling; chemical treatment

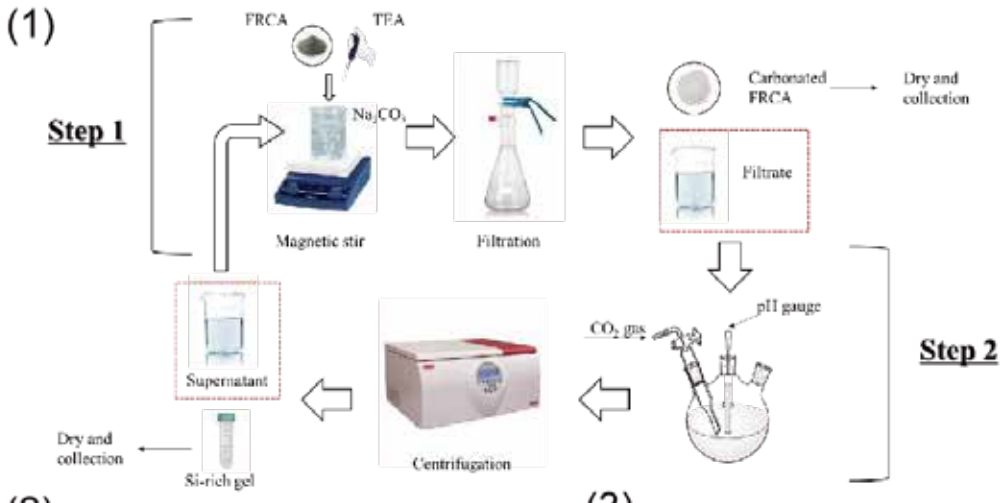

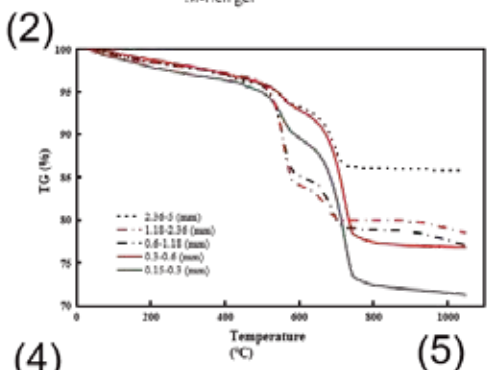

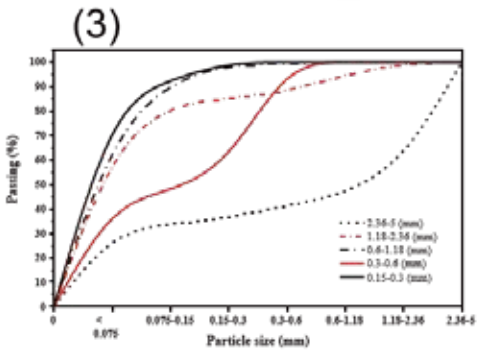

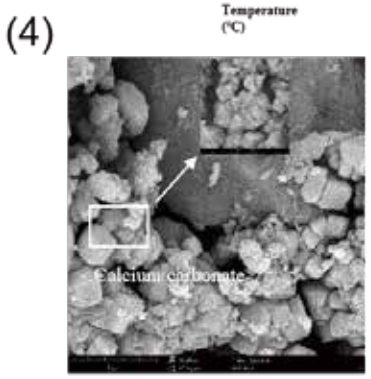

(5)

Particle size (mm)	CH (wt%)		CC (wt%)	
	before	after	before	after
0.15-0.3	24.49	3.87	9.28	46.16
0.3-0.6	20.40	4.29	7.31	39.64
0.6-1.18	19.02	3.61	6.49	28.11
1.18-2.36	17.55	3.49	6.04	15.82
2.36-5	17.24	5.13	6.04	19.69

Fig. 1 Illustration of the wet carbonation process; **Fig. 2** TG of carbonated FRCA; **Fig. 3** article size distribution of carbonated FRCA; **Fig. 4** SEM images of FRCA (1.18-2.36 mm); **Table. 5** Content of CH and CC by TGA

Acknowledgment

This work was supported by Ningbo University (NBU 42221823) and Ningbo Natural Science Foundation (2022J082)

Investigation on the effect of reinforcement confinement on the mechanical property of ASR damaged concrete by 3D RBSM

Luo J[1*], Wang Y[2], Asamoto S[3] and Nagai K[4#]

[1] Department of Civil Engineering, The University of Tokyo, Tokyo, Japan,
[2] School of Civil Engineering, Central South University, Changsha, People's Republic of China
[3] Department of Civil & Environmental Engineering, Saitama University, Saitama, Japan
[4] Institute of Industrial Science, The University of Tokyo, Tokyo, Japan

[*]*Presenter: luojie@iis.u-tokyo.sc.jp,* [#]*Corresponding author: nagai325@iis.u-tokyo.ac.jp*

Abstract

Alkali-silica reaction (ASR) is a major durability issue that would induce the deterioration of concrete structures. It causes expansion and cracking in concrete, which would degrade the material properties of concrete. In reinforced concrete structures, the reinforcements could restrain the ASR-induced concrete expansion and change the direction of crack development, which may further affect the material properties of concrete. Studying the effect of reinforcement confinement on the degradation of mechanical properties of concrete suffers from ASR damage is important for further estimating the residual capacity of a structure. In this study, a discrete numerical method, 3-dimensional rigid-body-spring-model (3D RBSM) (Fig. 1 and Fig. 2) is used to study the deterioration of the mechanical properties of concrete and the effect of reinforcement confinement. Four cases: compression loading for concrete model without ASR damage and reinforcement confinement (NC-NA), for concrete model without ASR damage but with reinforcement confinement (C-NA), for concrete model with ASR damage and reinforcement confinement (C-A), and for concrete model with ASR damage but without reinforcement confinement (NC-A) are simulated. The macroscopic ASR expansion before compressive loading is around 13000 μ.

The internal stress condition and crack development after ASR expansion is visualized through 3D RBSM (Fig. 3), large lateral cracks occur at the height where stirrups are placed due to the confinement of stirrups against the ASR expansion. The stress-strain curves are plotted in Fig. 4. It was found that the reinforcement confinement could delay the degradation of the material properties of concrete. When ASR expansion exists before compressive loading, the initial stiffness in the case with stirrup confinement decreases due to the lateral cracks induced by ASR expansion. The strain development on the middle stirrup in each model is shown in Fig.5. For case C-NA, there is no ASR expansion before compression, the strain on middle stirrup increases during the loading process. The strain on the inner bent parts increases rapidly and stress concentration may occur. The maximum strain on the stirrup is around 4000 μ when peak load is reached, indicating the yielding of the stirrup. As for model with serious ASR expansion before compressive loading (C-A), the maximum strain on stirrup already exceeds 5000 μ after expansion, and it increases very fast during the compressive loading stage. The maximum strain occurs at the inner bent parts of the stirrup and increases to over 15000 μ when the load is 80% of the peak load. Thereafter, the strain on the stirrup keeps increasing and rupture may happen during the loading stage. This result implies when real structures suffer from ASR damage are under external loading, the reinforcement inside may rupture and the safety of the structure would be threatened.

Keywords: alkali-silica reaction; mechanical properties degradation; reinforcement confinement; Strain on stirrups; 3D RBSM

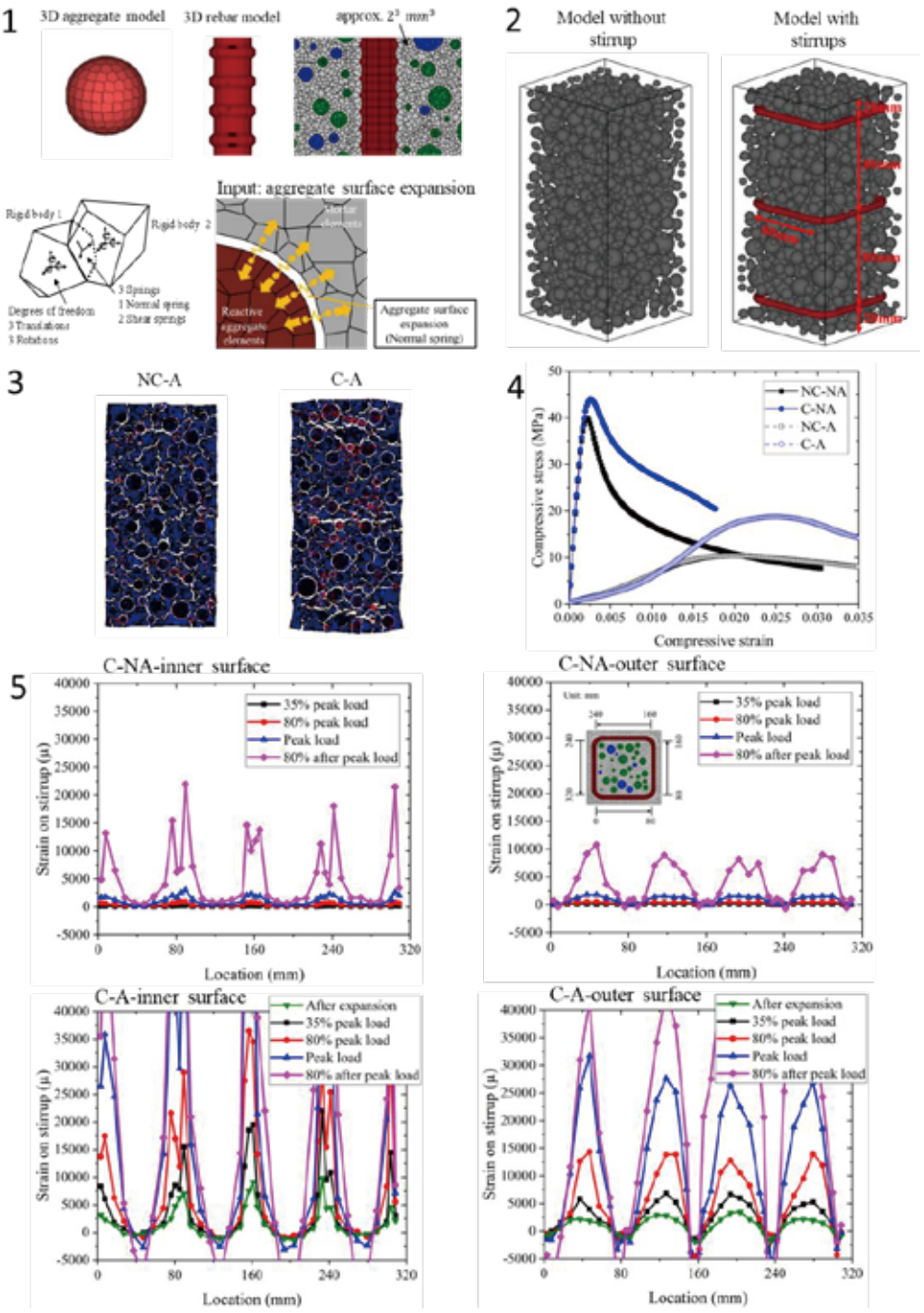

Fig. 1 3D RBSM model; **Fig. 2** Model size; **Fig. 3** Stress condition after ASR expansion; **Fig. 4** Stress-strain curves; **Fig. 5** Strain development on stirrup

Acknowledgment

The authors would like to acknowledge the funding support from JSPS KAKENHI Grant Numbers JP22H00224.

An Experimental Study on Flexural Performance of One-Way RC Slab Strengthened by FRCM

Yujae Seo[1*], Undram Naidanjav[1], Munkhtuvshin Ochirbud[1], Gyeongchan Hong[1], Hyunjin Ju[2#], Donguk Choi[3]

[1] Department of Architecture and Architectural Engineering, Hankyong National University, Anseong 17579, Republic of Korea
[2] School of Architecture and Design Convergence, Hankyong National University, Anseong 17579, Republic of Korea
[3] Industry-Academic Cooperation Foundation, Hankyong National University, Anseong 17579, Republic of Korea

Presenter: tjdbwo@hknu.ac.kr, #Corresponding author: hju@hknu.ac.kr

Abstract

The performance of reinforced concrete (RC) structures is deteriorating internally and externally due to artificial and environmental factors over time. Therefore, the RC structures are required to be repaired and strengthened. Fiber reinforced polymer (FRP) systems, one of the externally strengthened methods, have advantages of low weight ratio to high strength, corrosion resistance, and convenience of construction. However, FRP systems have a disadvantage that the fibers are vulnerable to high temperature such as fire. Recently, to overcome the drawbacks of FRP systems, many researchers have been studying fabric reinforced cementitious matrix (FRCM). The big difference from FRP systems is that the FRCM system have several layers of fabrics embedded in cementitious matrix, thus fabrics can be protected by the cementitious matrix from high temperature and any harmful environment. In this study, five one-way RC slabs strengthened by FRCM including the control slab were tested to investigate their flexural performance.

FRCM used to strengthen RC slab consists of carbon fabric and alkali resistant (AR) glass fabric, and Table 1 shows their material properties. The tensile strength of the carbon fabric and AR glass fabric embedded in FRCM are 1,753MPa and 941 MPa, respectively, and their moduli of elasticity are 139,000 MPa and 42,000 MPa, respectively. The design compressive strength of RC slabs is 31.5 MPa at 28 days after casting. As illustrated in Fig. 1, five specimens have a cross-section with width of 600mm, height of 210mm, and length of 2,300mm. Key variables for four specimens are fabric type, the layer number and spacing of fabrics. The name of the specimens follows SCnGn in which n is the number of fabric layers, C and G refer to carbon and glass fabrics, respectively. SRC means the control specimens. The flexural test was conducted under two-point loading until the concrete is crushed.

Fig. 2 shows load-deflection curves of five specimens, and Table 2 presents experimental results including load, deflection, and strengthening effect at cracking, yielding, and maximum load. The initial stiffness before and after cracking of specimens strengthened by C-FRCM were larger than that of the control specimen. The cracking load of SC1G6, SC3G0, SC4G0, and SC6G0 were 61%, 55%, 100%, and 181% greater than that of SRC. Also, their maximum loads were 9%, 21%, 23%, and 44% greater than that of SRC.

It appeared that not only the maximum load but also the initial stiffness tends to increase as the number of layers of fabric increases. The strengthened specimens showed superior flexural performance compared to the control specimen after cracking load. The one-way slabs strengthened by FRCM showed similar plastic behavior after sudden load decrease due

to fracture of fabric at maximum load and the test was terminated by concrete crushing in the maximum moment section.

Keywords: Carbon Fabric; AR Glass Fabric; Fabric Reinforced Cementitious Matrix; Flexural Performance; Strengthening

Table 1

Fiber Type	Tensile strength (MPa)	Ultimate tensile strain	Elastic modulus (GPa)
Carbon	1,753	0.0126	139
AR glass	941	0.0227	42

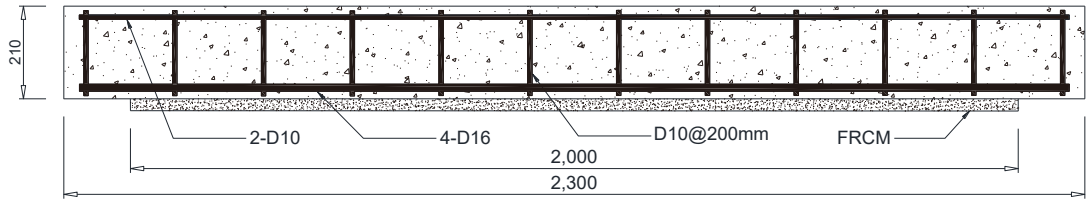

Figure 1

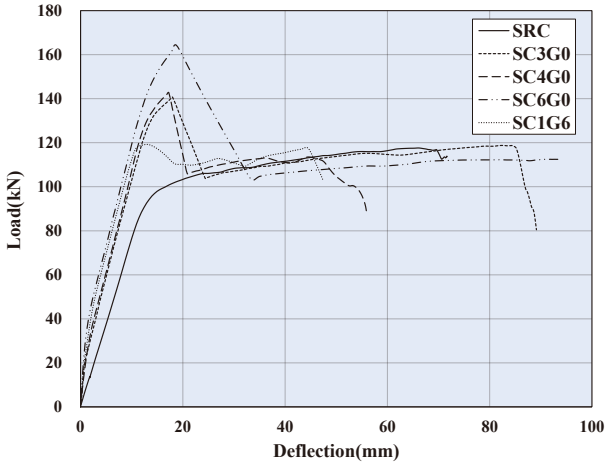

Figure 2

Table 2

Specimen	Load			Moment			Note
	P_{cr}	P_y	P_{max}	M_{cr}	M_y	M_{max}	Strength effect
	kN	kN	kN	kN·m	kN·m	kN·m	%
SRC	13.74	101.18	117.66	8.93	65.77	76.48	-
SC1G6	22.16	111.64	127.92	14.40	72.57	83.15	1.09
SC3G0	21.32	121.80	142.22	13.86	79.17	92.44	1.21
SC4G0	27.44	119.09	144.93	17.84	77.41	94.21	1.23
SC6G0	38.57	137.94	169.66	25.07	89.67	110.28	1.44

Note. P_{cr}: cracking load, P_{cr}: cracking load, P_y: yielding load, P_{max}: maximum load, δ_{cr}: cracking deflection at mid-span, δ_y: yielding deflection at mid-span, δ_{max}: deflection at maximum load at mid-span

Table 1 Material properties of fabrics; **Table 2** Test results; **Fig. 1** Details of specimens; **Fig. 2** Load-deflection curves of experimental specimens

Acknowledgment
This research was supported by Global Infrastructure Program through the National Research Foundation of Korea (NRF) funded by the Ministry of Science and ICT (grant number: 2021K1A3A1A20001722 and 2021R1C1C2093437)

Basic Properties of Cement Mortar used Carbonated Water as Mixing Water

Sang-Chul SHIN[1*], In-Gyu KANG[1], Geon-Woo KIM[1], Jin-Man KIM[1#]

[1] Kongju National University, Cheonan, Korea

[*]Presenter: hiykhj@kongju.ac.kr, [#]Corresponding author: jmkim@kongju.ac.kr

Abstract

This study was conducted to investigate the properties of cement paste and mortar using carbonated water as mixing water for the development of CCUS(Carbon Capture Utilization and Storage) technology in the cement industry. As a result of the experiment, it was found that using carbonated water has a hydration delay effect at the early age and can secure a equivalent strength compared to the control cement composites. Therefore, the use of carbonated water confirmed the applicability in the cement-concrete industry.

Keywords: Carbon neutrality; Cement mortar; Carbonated water; CCUS technology; Hydration delay; Strength

1. Introduction

Global climate change is a global issue that has been criticized for a long time. Many climate-related reports have suggested that the global mean temperature has already risen by approximately 1°C compared to the global temperature in the latter half of the 19th century. They also predict that it will rise further rapidly due to rapid industrialization. Due to such climate change, natural disasters due to abnormal climate (e.g., heat waves, heavy snowfalls, typhoons, tsunamis, and forest fires) have occurred frequently around the world. Some scientists have argued for a long time that this situation is a "climate crisis" threatening the basis of survival for all living things including humanity, no longer just "climate change".

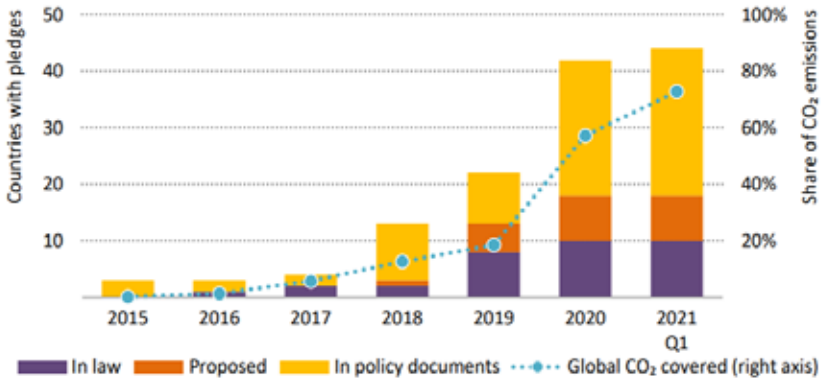

Figure 1. The number of countries that have declared carbon neutrality and their shares of CO_2 emissions.[1)]

Carbon neutrality refers to the concept of lower the actual greenhouse gas emissions to zero, equivalent to the level before industrial activity, by reducing greenhouse gas emissions due to human activities as much as possible, absorbing emitted greenhouse gases through forests and vegetation, or removing them using carbon capture, utilization, and storage (CCUS) technology. In other words, it means to equalize the amount of carbon emission and absorption, and it is sometimes called "Net Zero". The EU announced the European Green Deal in December 2019 and is taking the lead in carbon neutrality policies through a carbon neutral declaration and legislation with the announcement of the Carbon Reduction Legislative Package (Fit for 55) in July 2021. In addition, as of June 2021, 137 countries have declared carbon neutrality, and some countries have completed legislation. The number of countries that have declared to reach carbon neutrality is rapidly increasing (Figure 1). The International Energy Agency (IEA) reported that the sum of carbon emissions of countries that had pledged to achieve carbon neutrality accounted for approximately 70% of global carbon emissions[1)].

The calcination process of limestone is the basic process for cement. Therefore, it inevitably generates CO_2. In South Korea, it emits 830kg of CO_2 to manufacture 1 ton of Portland cement. As of 2019, South Korea emitted approximately 39 million tons of CO_2 per year to produce cement. As shown, the cement industry is a major carbon-emitting industry, along with the steel and power generation industries. Therefore, it is under strong pressure to reduce carbon emissions. The "2050 Carbon Neutrality Scenario" published by the South Korean government suggested conversion of fuel and raw materials, development of new additives, use of eco-friendly heat sources, development of CO_2 reaction hardening technology, and development of CCUS technology as key reduction measures for the cement industry. Among them, CCUS technology is a core technology for achieving carbon neutrality and Net Zero. The IEA expects that it will account for a meaningful portion of the carbon-neutral market[2)]. Many experts have indicated that carbon neutrality, a major challenge in the world, may end in failure without the commercialization of this technology[3)].

Currently, CCUS technology in cement and concrete fields has been tried in many countries, and some products have been commercialized. However, most of them are secondary concrete products based on CO_2 curing or mineral carbonation technology[4)]. Therefore, it is necessary to develop technologies for construction while utilizing and storing CO_2 by expanding the CCUS technology to a larger domain such as applying it to ready-mixed concrete manufacturing. The following factors can be considered for the technology of directly injecting and immobilizing CO_2 in the concrete manufacturing step.

a) State of injected CO_2 – liquid or gaseous form
b) CO_2 pressure
c) When and how to input CO_2

This is a basic study for developing carbonation technology that captures and stores carbon dioxide in the cement and concrete industries. This study aimed to confirm the possibility of developing CO_2 utilization technology in ready-mixed concrete BP by examining the basic characteristics of cement paste and cement mortar made by using carbonated water in the H_2CO_3 state, produced by injecting CO_2 into the water, as mixing water.

2. Experimental degisn

2.1 Experiment outline

The basic carbonation reactions of this study are shown in Eqs. 1 and 2. When CO_2 dissolves in water, it becomes H_2CO_3, which first dissociates into hydrogen and bicarbonate, and then dissociates secondarily into hydrogen and carbonate. This carbonate creates calcium carbonate through electrostatic bonding with calcium ions eluted from the hydration reaction of cement. As such, the basic concept of using carbonated water as mixing water is that the hydrate and the carbonate form the microstructure of the cement matrix together as the hydration and carbonation reactions of the cement occur simultaneously.

$$CO_2 + H_2O \leftrightarrow H_2CO_3 \leftrightarrow H^+ + HCO_3^- \leftrightarrow 2H^+ + CO_3^{2-} \quad \text{(Eq. 1)}$$

$$Ca^{2+} + CO_3^{2-} = CaCO_3 \quad \text{(Eq. 2)}$$

Table 1 shows the mixture and measurement items of this experiment. The experiment was conducted on cement paste and cement mortar, and the water-cement ratio was set to 40 and 50%, respectively. As the cement, domestic commercial Ordinary Portland Cement was used. The mixing water was tested using general constants and randomly prepared carbonated water as variables. pH, temperature, flow, hydration heat, and setting were measured in a fresh state, and compressive strength and flexural strength were measured in a hardened state.

Table 1 Experiment design

Types		W/C(%)	C(g)	W1(g)	W2(g)	S(g)	Test items
Cement paste	Plain	40	5,000	2,000	-	-	- flow, pH, temp. - hydration heat - setting time - Comp. strength - Flexural strength*
	Carbonated water			-	2,000	-	
Cement mortar	Plain	50	6,087	3,044	-	18,262	
	Carbonated water			-	3,044		

C : Cement, W1 : Plain water, W2 : Carbonated water, S : sand
* Flexural strength : Only cement mortar experiment

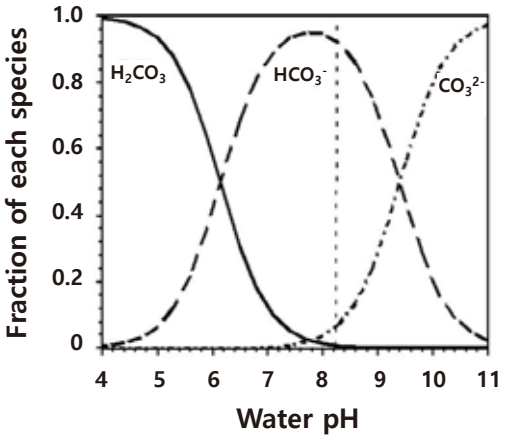

Figure 2 Forms of CO2 in water

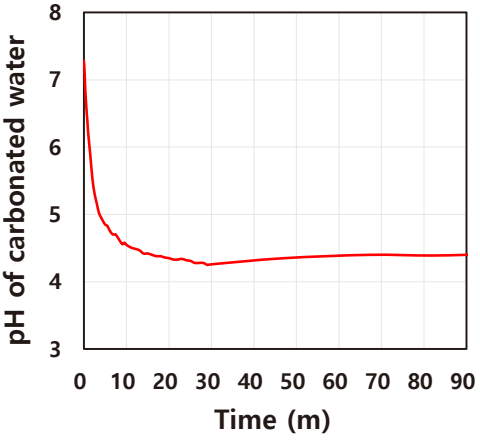

Figure 3 pH change by CO_2 injection time

2.2 Carbonated water

Figure 1 shows the fraction of each carbonated species by pH. In this experiment, carbonated water (pH ≈ 4.0) was prepared by directly injecting CO_2 into 4 liters of water to make carbonated water in the form of H_2CO_3. Figure 2 shows the pH change of carbonated water according to the CO_2 injection time. It was confirmed that the pH dropped abruptly from 7.26 to 5.0 after 5 minutes, and then decreased gradually. After 30 minutes from the injection of carbon dioxide, pH was around 4.2, and carbonated water in this state was used for the experiment.

2.3 Test items and method

The flow, pH, and temperature of cement paste and cement mortar were measured immediately after mixing. The cement paste was measured according to KS L ISO 9597 (Determination of setting time and soundness of cements) [5], and the cement mortar was measured according to KS F 2436 (Standard test method for setting times of concrete mixture by penetration resistance) [6] to examine the setting properties. Compressive strength and flexural strength were measured according to KS L ISO 679 (Methods of testing cements - Determination of strength)[7]. A Styrofoam insulation box (300×300×300 mm) was made to measure the hydration heat. In the center of it (100×100×100 mm), a sample was placed, and a thermocouple was installed. Moreover, the outer surface of the insulation box was sealed with aluminum tape to block it from the outside air and minimize heat loss during the experiment. Figure 4 shows the schematic diagram of the insulation box for measuring the hydration heat and the installation of the T-type thermocouple in it.

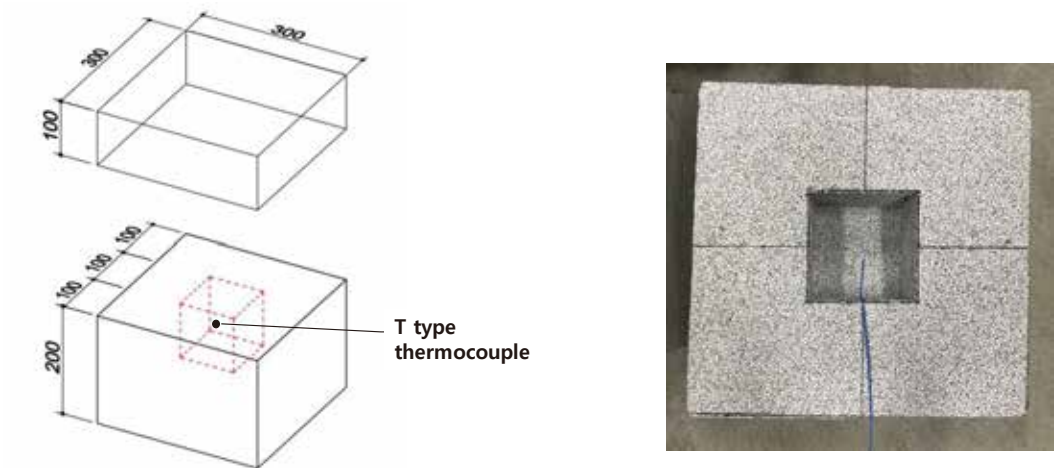

Figure 4. The insulation box for measuring hydration heat.

3. Discussion

3.1 Properties of fresh concrete

Table 2 shows the characteristics of cement paste and cement mortar in the fresh state. It was found that the mixtures using carbonated water had a higher flow, approximately 10cm, in both the paste experiment and the mortar experiment. The pH of the used carbonated water was acidic

(pH of 4.14 and 4.37), but it increased to a pH of 11 to 12 by contacting the cement, a strong alkali material. However, although the paste experiment showed similar values, the pH of the carbonated water condition was approximately 1.1 lower than that of the plain condition in the mortar experiment. The temperature was similar regardless of the type of mixing water. In summary, the flow slightly increased when carbonated water was used as the mixing water, and the pH and temperature of the slurry and mortar states was no significantly change.

Table 2. Properties of fresh state

Types		Flow (mm)	pH		Temperature (°C)
			Water	Paste/Mortar	
Cement paste	Plain	145	7.17	12.82	24.2
	Carbonated water	155	4.14	12.76	23.2
Cement mortar	Plain	190	7.26	12.62	19.5
	Carbonated water	198	4.37	11.48	18.5

3.2 Hydrarion heat

Figure 5 shows the measurement result of hydration heat by using the simple insulation test. It was found that the hydration rate of the cement paste using carbonated water as the mixing water was approximately an hour slower than that of the general mixture. The temperature difference for the same elapsed time was between 15 and 20 °C, and the maximum temperature was approximately 103°C. It was not significantly affected by the type of mixing water. The maximum temperature of the mortar was similar to each other: the mortar of the general mixture was 41.4°C and that of the carbonated water was 41.8°C. The time to reach the maximum temperature of the mortar of carbonated water mixture took 2 hours more. The results of the experiment confirmed that using carbonated water as mixing water for cement paste and cement mortar delayed hydration by about 1 to 2 hours.

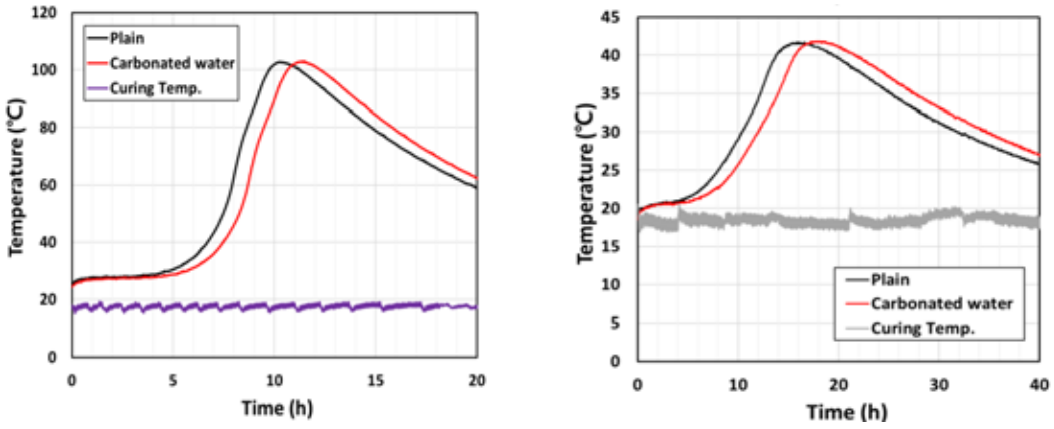

(a) Cement paste (b) Cement mortar

Figure 5 Results of hydration heat

3.3 Setting time

Figure 6 shows the results of the setting test. The experimental results indicated that the initial and final sets of the cement paste using carbonated water were delayed by 90 and 60 minutes, respectively. It is believed that it was due to the above-described hydration heat characteristics. Although the mortar experiment showed similar setting characteristics until the initial set regardless of the type of mixing water, setting after the initial set was slightly delayed in the mixture using carbonated water. The final setting time was delayed about one hour or more, indicating that using carbonated water could delay hydration even at the mortar level. It was confirmed from these experimental results that using carbonated water as mixing water delayed hydration by about one hour as the hydration rate was delayed.

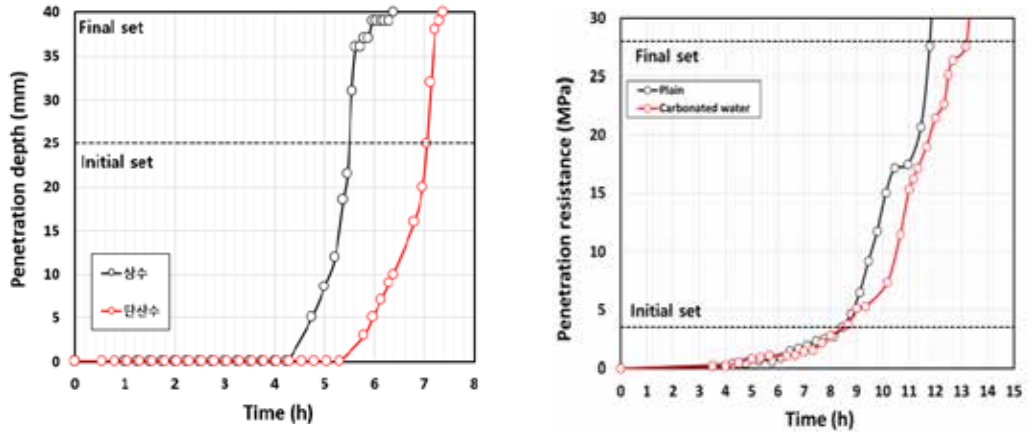

(a) Cement paste **(b) Cement mortar**

Figure 6 Results of setting time

3.4 Compressive strength

Figure 7 shows the measured compressive strength of cement paste and mortar. In the paste experiment, the compressive strength was generally similar regardless of the type of mixing water. Particularly, at 28 days of age, the strength of the specimen using carbonated water was 34.1 MPa, which was about 2.3 to 4 MPa higher than that of the general specimen. This result confirmed the possibility of a technology that fixes CO_2 by using carbonated water as mixing water. The mortar specimen was cured in two ways: air-dry curing and water curing. Regardless of the curing conditions, the strength of the mortar using carbonated water was slightly lower than that of the general specimen at all ages. In addition, while the increase in the compressive strength of dry curing specimens decreased after 7 days of age, that of water curing specimens continued to increase until 28 days of age.

These results revealed that, when carbonated water was used as the mixing water, the cement paste showed the same strength as the general mixture. However, its compressive strength was slightly lower than that of the general mixture in the mortar experiment. It will be necessary to review the hardening mechanism of CO-absorbing concrete and the mechanical properties and durability at long-term age through further studies.

Figure 8 shows flexural strength results. It was confirmed that the results were similar to the compressive strength measurements. Therefore, it was found that using carbonated as mixing water did not decrease flexural strength much.

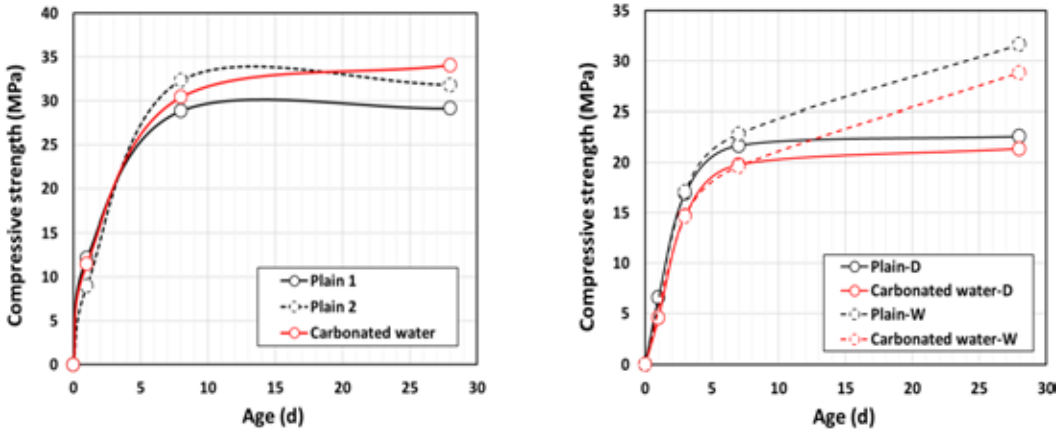

(a) Cement paste **(b) Cement mortar**

Figure 7 Results of compressive strength

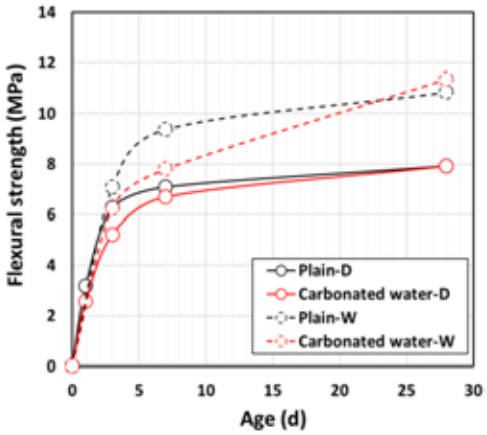

Figure 8 Results of flexural strength of cement mortar

4. Conclusions

This study was conducted to evaluate the basic properties of cement paste and mortar used carbonated water as mixing water and obtained the following results.

1) When carbonated water was used as mixing water, its fluidity became slightly higher than that of mixtures using common constants, while pH and temperature showed similar results.

2) Cement composites using carbonated water as mixing water delayed hydration because it took longer to rise hydration temperature and it affected the setting properties.

3) When carbonated water was used, the paste and compressive strength were almost equal to those of the general mixtures.

4) The results of this study confirmed that using carbonated water as the mixing water for cement composites delayed hydration while securing an equivalent strength level. It is expected that further developing these results would produce baseline results for the commercialization of CCUS technology in the South Korean cement-concrete field. Furthermore, it will ultimately contribute to carbon neutrality in the cement industry by using CO.

Acknowledgment

This work was supported by the National Research Foundation of Korea(NRF) grant funded by the Korea government(MSIT) (No. 2020R1C1C2010362)

References

1) IEA, Net Zero by 2050 – A Roadmap for the Global Energy Sector, 2021. 05
2) CEMBUREAU, Cementing the European Green Deal - RREACHING CLIMATE NEUTRALITY ALONG THE CEMENT AND CONCRETE VALUE CHAIN BY 2050, 2018
3) IEA, Technology Roadmap, Low-Carbon Transition in the Cement Industry, 2018
4) Jacek Kwasny et al., CO2 Sequestration in Cement-Based Materials During Mixing Process Using Carbonated Water and Gaseous CO2, 4th International Conference on the Durability of Concrete Structures, pp. 72-79, 2014
5) KS L ISO 9597 Determination of setting time and soundness of cements, 2019
6) KS F 2436 Standard test method for setting times of concrete mixture by penetration resistance, 2017
7) KS L ISO 679 Methods of testing cements - Determination of strength, 2018

Parallel Sessions-13

Novel & High-Performance Materials for Sensing and Improving the Serviceability of Transportation Infrastructure

A TFM method for the detection of internal defects in concrete using ultrasound array

Rong Lifan , Hu Jinlin, Zhao Weigang, Tian Xiushu, Yang yong

(1. *Collaborative Innovation Center for Performance and Security of Large-scale Infrastructure, Shijiazhuang Tiedao University, Shijiazhuang 050043, China;* 2. *School of safety engineering and emergency management, Shijiazhuang Tiedao University, Shijiazhuang 050043, China;*)

Total focusing method(TFM)based ultrasound array is considered as the “gold standard” for the detection of internal defects, such as voids, impurities and cracks in solid. And the TFM method is also potential for high-precision imaging of internal void defects in concrete. However, the fact that concrete structure contains aggregates, gravel and steel bars, results in the significant structural noise when ultrasound propagates in concrete, and brings about the reduction of internal void defects image quality. A numerical concrete model based on random aggregate model is established, and ultrasound propagation in concrete is simulate in order to research the relation between the aggregates distribution and structural noise. A process of convolution filtering for the received signal is carried out to suppress the structural noise in advance. Then the full matrix capture ultrasound data are processed for imaging according to the total focusing algorithm, and the model detection result is displayed as color map. Finally, the quantitative relation between the values in color map and the internal defect location is discussed. The results show that the imaging signal to noise ratio can be effectively improved, and the image regions with higher value indicate more accurate internal defect locations.

Keywords: Ultrasound test, Concrete internal defects, TFM, Structural noise

Preparation and mechanism of high early strength sulphoaluminate cement-based UHPC

Haijun Zhou[1,2,3], Xuan Qi[2], Cong Ma[1*], Zefeng Fang[2], Jianing Lou[2], Haoyang Chen[2], Xiang Guo[2]

[1] Institute of Urban Smart Transportation & Safety Maintenance,
[2] Guangdong Province Key Laboratory of Durability for Marine Civil Engineering,
[3] Key Laboratory for Resilient Infrastructures of Coastal Cities, Ministry of Education,
Shenzhen University, Shenzhen, Guangdong Province, 518061, China
Presenter: 574681948@qq.com, #Corresponding author: macong@szu.edu.cn

Abstract

Some major construction projects require materials that can quickly and easily obtain high mechanical properties. Incorporating early-strength agents is an efficient method to improve the performances of cement with low cost. The authors chose to study Ultra-High Performance Concrete (UHPC) materials based on SulfoAluminate Cement (SAC) at a low water-cement ratio in order to improve the early performance. Set out from this, the author introduced common early-strength agents into SAC to prepare and study the mechanism. Experimental results indicate $Ca(HCOO)_2$ had the best effects on reducing the setting time (Fig.1) and improving the early strength (Fig.2) at the low water-cement ratio. The compressive strength after 4 h reached 41.2 MPa, which was 86.4% higher than that of the blank. The reason was found that $Ca(HCOO)_2$ promoted the hydration ratio in the early stage. Most importantly, unlike other early-strength agents, a new exothermic peak appeared (Fig.3) in the deceleration phase stage after mixing with $Ca(HCOO)_2$. Besides, $Ca(HCOO)_2$ did not change the type of hydration products (Fig.4), but it significantly increased the AFt content (Fig.5, Fig.6) at an early stage.

Keywords: sulfoaluminate cement; early strength agent; high early strength; hydration process;

1

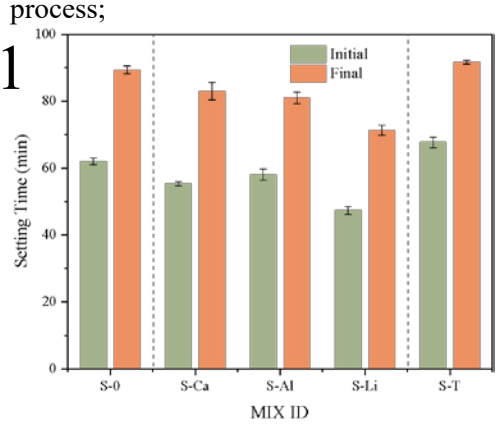

2

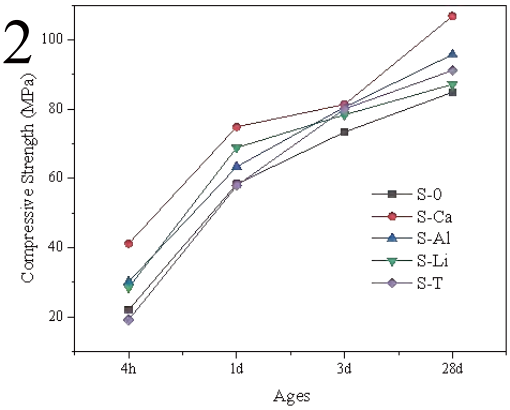

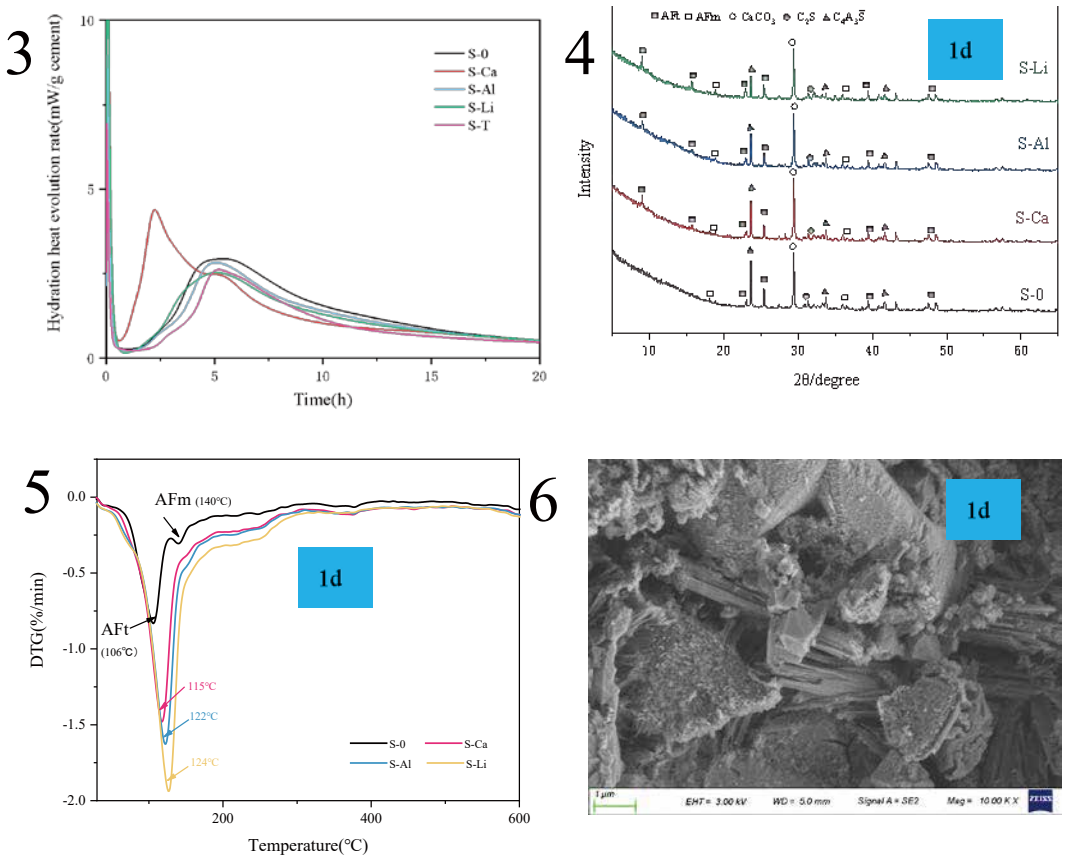

Fig. 1 Setting time of specimens; **Fig. 2** Compressive strength of specimens; **Fig. 3** Hydration heat exothermic rate of specimens; **Fig. 4** XRD patterns for 1d-aged specimens; **Fig. 5** DTG curves of the 1d-aged specimens; **Fig. 6** SEM images for 1d-aged specimens

Acknowledgment

The work described in this paper was financially supported by the Ministry of Science and Technology of China (No. 2019YFB2102701), the National Natural Science Foundation of China (No. 51378313), the Department of Science and Technology of Guangdong Province (No. 2019B111106002 & No. 2018B020207015), to whom the writers are grateful.

Theoretical and experimental studies on accurate cable tension identification of short cables

Changzhao Li[1,2*], Yichao Xu[1,2], Yiren Li[1,2], Yufeng Zhang[1,2#]

[1] State Key Laboratory of Safety and Health for In-service Long Span Bridge,Nanjing 211112,China,
[2] JSTI Group Co.,Ltd.,Nanjing 211112，China
Presenter: lzz275@jsti.com, #Corresponding author: kolya@jsti.com

Abstract

Cables as the force transmission components are widely used in large-span bridges, such as the cable-stayed bridge, the suspension bridge and the bottom-through arch bridge. The damage of the cable will reduce the safety and durability of the bridges. Thus, the change of cable force is an important indicator to judge the service status of bridge. However, practice indicates that the existing methods have inevitable errors in the identification of short cable force, which are difficult to satisfy the needs of engineering. Therefore, This paper proposed an improved cable force identification method based on the mode shape method. This paper proposed an improved cable force identification method based on the mode shape. The method established the equivalent string model of the cable-bar system. Then, the Galerkin was adopted to convert the structural parameters. Finally, the equivalent parameters are used to obtain the cable force according to the string theory. The cable force test is carried out by taking a short cable of about 8.11m in the three-span arch bridge. The experimental results show that the proposed method has high accuracy for the identification of short cable force, and the identification error is within 3%.

Keywords: Cable Tension Identification; Galerkin Method;String Theory;Short Cables

1 2 3

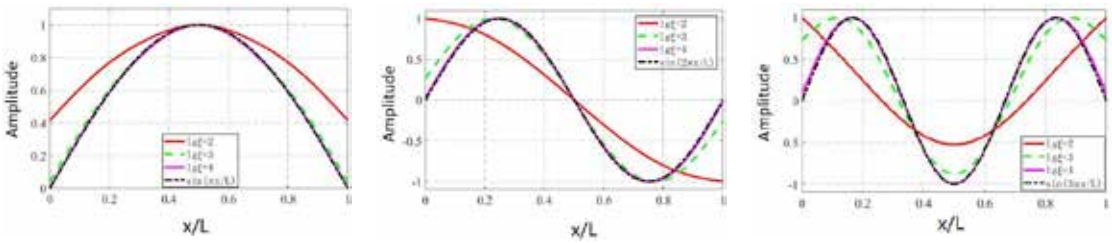

4 5 6

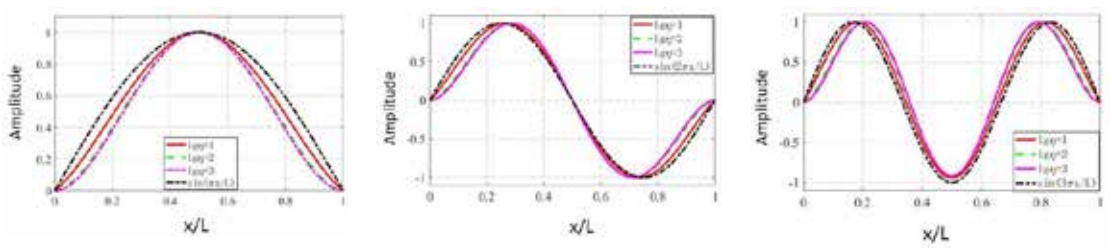

7 8 9

10

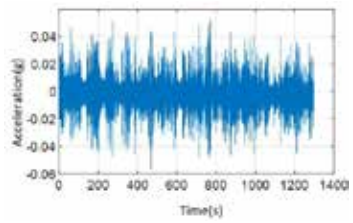

11

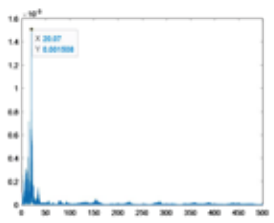

12

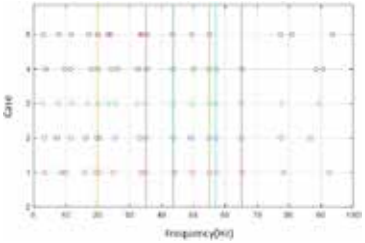

13

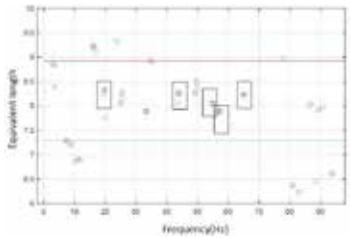

Fig. 1~Fig. 6 The influence of boundary conditions on mode shapes; **Fig. 7** Scene of a three-span arch bridge and target cable; **Fig. 8~Fig. 9** Sensors and acquisition equipment; **Fig. 10** Acceleration time history of 1# sensor; **Fig. 11** Spectrum map by FFT; **Fig. 12~Fig. 13** Results of frequency and equivalen length in five cases.

Acknowledgment

The authors would like to acknowledge the funding support from The National Key Research and Development Program of China (No.: 2021YFB2601000).

Comparative study of different molecular structures of diluents on the curing of epoxy adhesives and the bonding properties with concrete

Hao Yao[1,2*], Zan Wang[1,2], Qiang Yuan[1,2]

[1]School of Civil Engineering, Central South University, Changsha, Hunan 410075, People's Republic of China
[2] National Engineering Research Center of High-Speed Railway Construction Technology, Changsha, Hunan 410075, People's Republic of China
[*]*Presenter:* yaohao@csu.edu.cn

Abstract

Epoxy adhesives own various advantages of high strength, fast curing speed and good chemical corrosion resistance, hence become one of the most extensively organic repair materials. Aim to satisfy the different needs of various engineering, it is necessary to develop various epoxy resin materials with different properties by tailoring their molecular structure. In this paper, a precursor (PPM) reacted by 1,4-butanediol and trimethylolpropane triglycidyl ether was firstly synthesized. Then, PPM and three commercial reactive diluents, namely alkyl C12-C14 glycidyl ether, butyl glycidyl ether, 1,4-butanediol diglycidyl ether were separately used to prepare epoxy adhesives, the effects of various types and contents of reactive diluents on the viscosity, exothermic temperature, mechanical properties and bonding strength with concrete of epoxy adhesives were comparatively studied. The results indicated that all reactive diluents can drastically reduce the viscosity of epoxy adhesives while increasing the ductility of cured products. The molecular structure of the diluents within epoxy adhesives has a significant impact on the exothermic peak temperature and bonding strength with concrete. The samples with monofunctional or lower epoxy value diluents exhibit lower bonding strength at the epoxy-concrete interface. In addition, high epoxy value of reactive diluents causes the increase of the peak exothermic temperature. More interestingly, the synthetic PPM with the introduction of a certain amount of polar hydroxyl groups and partial consumption of epoxy groups, which makes the PPM-based epoxy adhesives simultaneously show excellent interfacial bonding properties and reducing the peak exothermic temperature. This study implies that the molecular structure design of epoxy adhesives has great potential to meet the various requirements in improving the serviceability of transportation infrastructure.

Keywords: Repair materials; Concrete crack repair; Epoxy resin; Adhesives; Molecular structure.

Acknowledgment

The authors would like to acknowledge the funding support from the Science and Technology Research and Development Program Project of China railway group limited (Major Special Project, No. 2020-Special-02) and National Natural Science Foundation of China (contract No. 52108261).

Bond performance and mechanisms of sulphoaluminate cement-based UHPC for reinforcing old concrete substrate

Haijun Zhou[1,2,3], Yeting Li[1,2], Cong Ma[1*], Zonglong Zhou[1,2], Zefeng Fang[1,2], Jianing Lou[1,2], Yu Liu[1,2]

[*]Presenter: haijun@szu.edu.cn, [#]Corresponding author: macong@szu.edu.cn

[1] Institute of Urban Smart Transportation & Safety Maintenance, Shenzhen University, Shenzhen, Guangdong Province, 518061, PR China

[2] Guangdong Province Key Laboratory of Durability for Marine Civil Engineering, Shenzhen University, Shenzhen, Guangdong Province, 518061, PR China

[3] Key Laboratory for Resilient Infrastructures of Coastal Cities (Shenzhen University), Ministry of Education, Shenzhen University, Shenzhen, 518060, China

Abstract

One of the major problems facing reinforced concrete structures nowadays is their repair and reinforcement. Sulphoaluminate cement (SAC)-based material is an effective repair material. This paper examined the bond performance between SAC-based UHPC with low water to cement ratio and old OPC concrete substrate using the bond strength test and SEM analysis. It was found that SAC-based UHPC has beneficial mechanical properties, including compressive and flexural strength, at an early age (Fig. 1). This paper provided a reference for the reinforcement of reinforced concrete structures that are exposed to the marine environment.

SAC-based UHPC mixture could rapidly bond the old OPC substrate, and the bond strength of all the cylinder and prism specimens at 1 day reached over 8MPa (Fig. 2). The bond strength of the cylinder and prism increased greatly significantly with more curing time and achieved more than 10 and 12 MPa at 28 days, respectively，which can be attributed to the early strength properties of SAC. Comparing the cylinder and prism specimens, the bond strength of the latter is higher than that of the former.

The bond strength when using the cylinder specimen was lower than that of the prism. A linear trend was obviously demonstrated between the bond strength of the cylinder and prism specimen (Fig. 3). The findings indicated that it was feasible to measure bond performance using the cylinder specimen when the shrinkage around the interface of old concrete needed to be considered and that SAC-based UHPC could be applied in repair work that required high-early strength repair material.

For both cylinder and prism specimens, the prepared bonded specimens whose interface was covered without any agents had higher bond strength than that of samples using different bonding agents, including waterborne epoxy resin and modified epoxy resin in different recipes (Fig. 4).

The SEM diagrams of interfacial microstructure showed that there were some small fiber-like AFt crystals that were produced by the hydration of SAC in the interface of the specimen with no agents when magnified to 20,000 times (Fig. 5). For the specimens with different kinds of agents, visible cracks at the interface were observed. The observations were consistent with the evaluated bond strength of the specimens applied with different interfacial agents.

Keywords: repair materials; bond strength; bond performance; interfacial microstructure; interfacial agents; assessment;

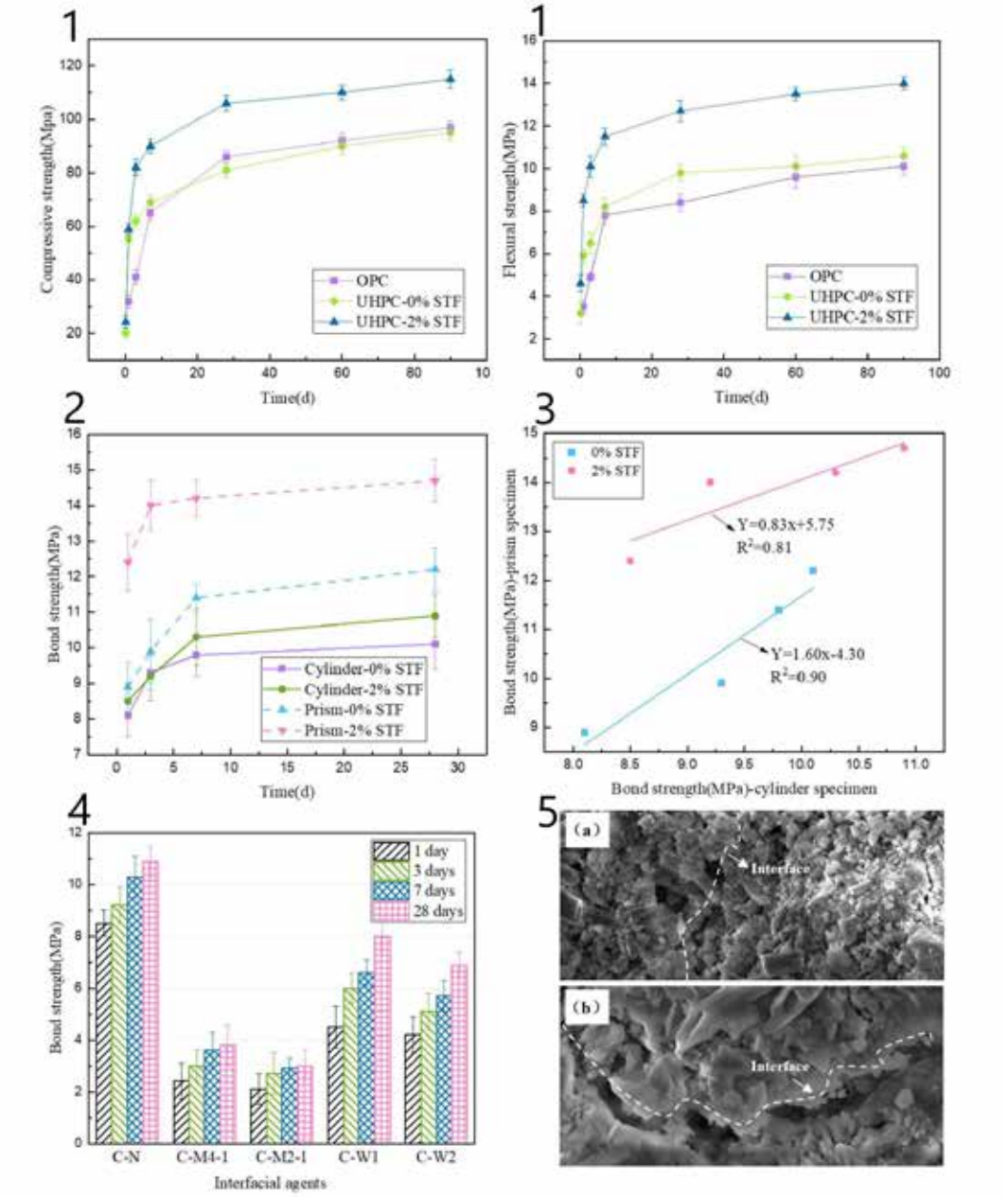

Fig. 1. Compressive strength and flexural strength of OPC and SAC-based UHPC specimens. **Fig. 2.** Comparison of bonding strength with no agents between cylinder and prism specimens. **Fig. 3.** Correlation of bonding strength with no agents between cylinder and prism specimens. **Fig. 4.** Bonding strength of different interfacial agents for cylinder specimens with 2% steel fiber. **Fig. 5.** SEM micrograph of microstructure of the interface between old OPC substrate and SAC-based UHPC with some different interfacial agents. (a) C-N for 1 day; (b) C-W1 for 1 day

Acknowledgment

The authors would like to acknowledge the funding support from the Ministry of Science and Technology of China (Grant No. 2019YFB2102701), the National Natural Science Foundation of China (Grants No. U2005216 & 51778372), and the Department of Science and Technology of Guangdong Province (Grant No. 2019B111106002 & 2018B020207015)

Application of Deflection Dynamic Load Allowance Test Method of Simply Supported Girder Bridge Based on Suspension Hammer System

XUE Yu-xin[1], ZHOU Yong-jun[1,2], ZHAO Yu[1]

(1. School of Highway，Chang'an University, Xi'an 710064, Shaanxi, China;

2.Research Center of Highway Large Structure Engineering on Safety, Ministry of Education, Xi'an 710064, Shaanxi, China)

Abstract：In order to explore the application of hammer system in bridge dynamic test, standard span simply supported T-girder bridge, box girder bridge and hollow slab bridge were selected as the research objects, and the research on deflection dynamic load allowance (DLA) test of simply supported girder bridge were undertaken, adopting numerical simulation and experimental verification. The vehicle-bridge-hammer coupling vibration analysis program was compiled based on ANSYS software, combining with numerical calculation and response surface analysis, deflection DLA test results of suspension hammer method and scaffolding method were compared to explore influence of suspension length, wire tensile stiffness and suspension hammer mass on the accuracy of the DLA tested by suspension hammer method. Furthermore, the suggested value of suspension hammer system parameters was proposed. Finally, a 30m simply supported box girder bridge was tested under dynamic load. Dynamic deflection of the bridge was tested by scaffolding method and suspension hammer method to verify the proposed parameter suggested value. Results show that in order to meet requirement, difference between deflection DLA measured by suspension hammer method and scaffolding method is less than 5%, the optimal values of wire tensile stiffness and suspension hammer mass increase with wire length. The research results can provide theoretical basis for DLA test of bridge load test.

Keywords：bridge engineering; simply supported girder bridge; dynamic load allowance; dynamic deflection; suspension hammer system

Temperature effects of CRTS II slab track under various field meteorological conditions

Rui Zhou[1*], Yinggang Tao[1], Haijun Zhou[1]

[1] College of Civil and Transportation Engineering, Shenzhen University, Shenzhen, Guangdong 518060, People's Republic of China
[*]*Presenter: zhourui@szu.edu.cn,*

Abstract

Temperature effects of ballastless track in high-speed railway under complicated environment conditions become increasingly important, which are governed by a number of meteorological factors, including solar radiation, ambient temperature, wind speed and direction, humidity, and many others. Since these meteorological factors are highly depending on the site-specific conditions, the routes of ballastless track in China has huge spread of territory and their meteorological condition variation could have the significant effect on the mechanical behavior of the track-bridge system. China Railway Track System type II (CRTS II) slab track is one of typical ballastless track in high-speed railway. In order to guarantee the good structural performance of CRTS II track in long-term operation, it is necessary to study the influence of meteorological conditions on the thermal transfer effects of CRTS II track.

The meteorological parameters and the internal temperature in the track structure were collected for six months in Beijing-Shanghai high-speed railway as a case study,. The relationship between ambient temperature and temperature at the midspan and end of bridge are analyzed, and the relationship among four meteorological parameters (*e.g.* temperature, solar radiation, wind speed, humidity) were also investigated. The change of temperature within the track structure could obviously lags behind the change ambient temperature and their temperature variation are smaller than that of the ambient temperature. Furthermore, Pearson correlation analysis show that there is a strong positive correlation between the ambient temperature and the solar radiation with a Pearson correlation coefficient of 0.85, while the correlation coefficient between the ambient temperature and air humidity of 0.22 is the smallest.

the heat transfer models of CRTS II track were established based on finite element software of Comsol. The total dimensions of five track slabs are 32 m length × 13.4 m width × 3.35m height, and the track slab, the CAM layer, and base plate are simulated by the solid elements. Two ends of the track slabs are constrained and the thermal responses of the track structure under the above four meteorological parameters were compared. The internal temperature and vertical displacement at the mid-span of the track slab become larger with the increase of the wind speed or solar radiation, especial for the wind speed exceed 6m/s or the solar radiation exceed 750 W/m^2. According to the 3D temperature field, the increase of the solar radiation or ambient temperature could lead to the rapid heat transfer process from the track slab to the base plate. The role of wind speed on the heat transfer effect in track structure is limited.

Keywords: CRTS II slab track; Temperature effects; meteorological factors; heat transfer

Fig.1

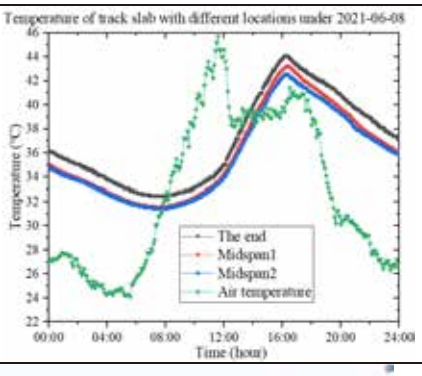

Fig.2

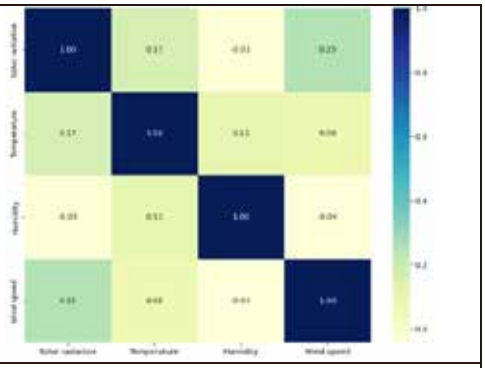

Fig.3

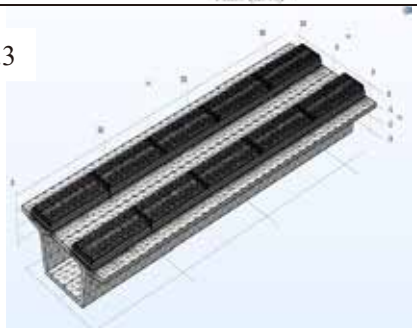

Fig.4

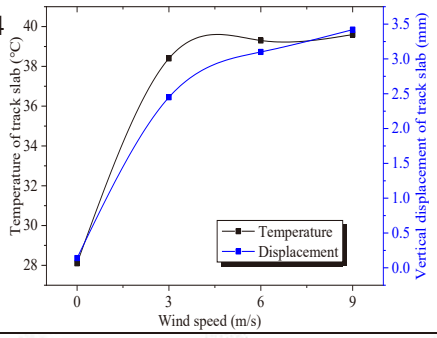

Fig.5

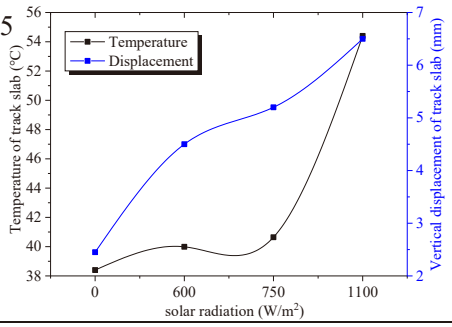

Fig.6

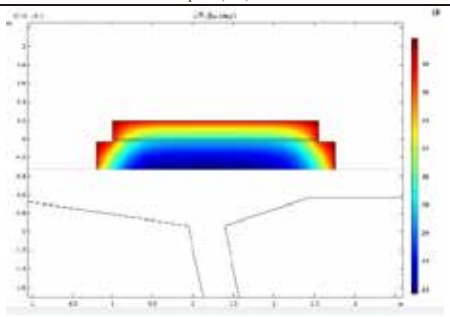

Fig. 1 Internal temperature characteristics; **Fig. 2** Relationship among four meteorological parameters; **Fig. 3** finite element model of CRTS II track-bridge structure; **Fig. 4**-5 Temperature and displacement responses under various wind speeds and solar radiations; **Fig.6** Temperature field of the mid-span section

Acknowledgment

The authors would like to acknowledge the funding support from the National Natural Science Foundation of China (No. 52278311) and Guangdong Province Natural Science Foundation (No. 2022A1515010665).

Moisture diffusion behavior in cementitious materials with carboxylic acid hydrophobic agent

Hao Zhang [a,b,#], Song Mu [a,b], Jingshun Cai [a,b], Qi Ma [a,b,c], Jianzhong Liu [a,b]c, Jinxiang Hong [a,b,c]

a State Key Laboratory of High Performance Civil Engineering Materials, Nanjing 210008, China;

b Sobute New Materials Co. LTD, Nanjing 210008, China;

c Jiangsu Research Institute of Building Science, Nanjing 210008, China.

Presenter：zhanghao@cnjsjk.cn. # Corresponding author: zhanghao@cnjsjk.cn.

Abstract

One of the most effective methods to improve durability of cementious materials is to resist the intrusion of water with aggressive ions by mixing with hydrophobic agent. In this study, the mechanism of carboxylic acid ammonium salt hydrophobic agent addition on hydrophobicity of cementitious materials is analyzed. The impact of hydrophobic agent on water adsorption, moisture diffusion and hydration products is investigated by experimental method. It is shown that carboxylic acid ammonium salt hydrophobic agent performs the excellent water repellence. The results of water vapor sorption isotherm show that the addition of carboxylic acid ammonium salt increases the pore volume. The simplified analytical hydrodynamic model of cone type pore and Young's relationship is proposed to analyze the relation between characteristic parameters of pore and the permeability of cementitious materials. It can be concluded that the hydrophobicity results from the change of pore structure and the hydrophobic surface of cone region. These results provide the guidance to design the durability and develop the new hydrophobic agent used in cementitious material.

Key words: Hydrophobicity; Permeability; Pore structure; Hydrodynamic effects.

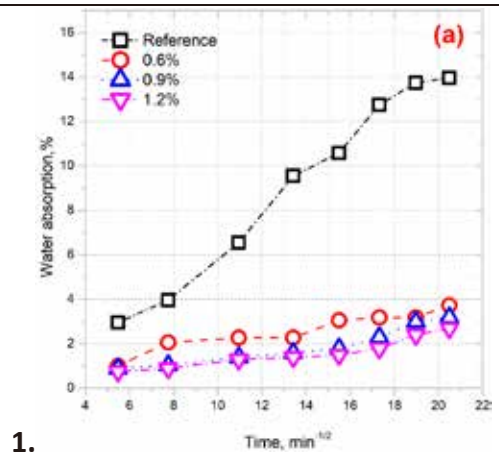

1.

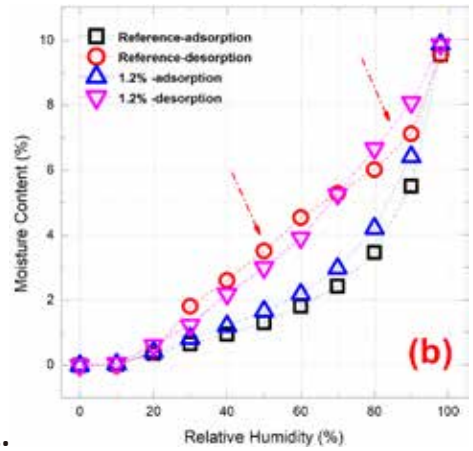

2.

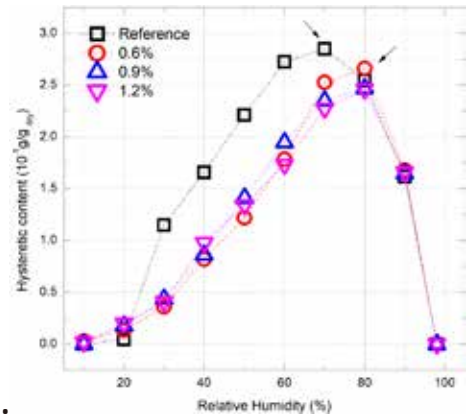

3.

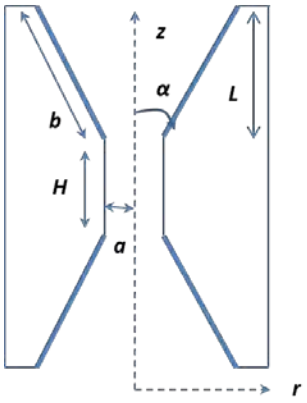

4.

Fig.1 Water adsorption properties of mortars containing various amounts of hydrophobic agents. Fig.2.Moisture sorption isotherms for cement pastes containing different amount of hydrophobic agent acquired across a range of relative humidity. Fig.3. The hysteretic curve with respect to pastes mass acquired across moisture sorption isotherms for cement pastes containing different amount of hydrophobic agent. Fig.4 An illustration of pore structure of cement paste in presence and in absence of hydrophobic agent including cylinder type pore and cone type pore, the thick solid line represents the hydrophobic surface.

Acknowledgment

We wish to acknowledge financial supports from National Key R&D Program of China (No. 2021YFB2601000), National Natural Science Foundation of China (No. 5210081817, 51908254, 52078240), Natural Science Foundation of Jiangsu Province (BK20210954), Key R&D Program of Guangdong Province (No.2019B111106002) and Opening Project of State Key Laboratory of Green Building Materials (NO. 2021GBM04).

The role of supplementary materials on micro/macro properties and water stability of magnesium phosphate cement

Chaofan Wang[1,2*], Bing Chen[1,2#]

[1] State Key Laboratory of Ocean Engineering, Shanghai Jiao Tong University, Shanghai, 200240, PR China
[2] Shanghai Key Laboratory for Digital Maintenance of Buildings and Infrastructure, Department of Civil Engineering, Shanghai Jiao Tong University, Shanghai, 200240, PR China
*Presenter: chaofanw@sjtu.edu.cn, #Corresponding author: hntchen@sjtu.edu.cn

Abstract

Magnesium phosphate cement (MPC) is broadly known as one of ideal repair materials for its high early strength, rapid setting time and good adhesion. However, the existing amorphous phase of MPC could react with water when immersing in water, resulting in large internal stress and cracking in the MPC, thus limiting its application. In this paper, supplementary materials (SMs) including fly ash (FA), silica fume (SF), aluminum silicate (AS) and bauxite (BX) were used to improve both mechanical properties and water stability of MPC. Besides, the hydration mechanism and the microstructural progress were studied. It was found that the addition of SMs to MPC decreased the hydration heat release (Fig. 1) and retarded the final setting time (Fig. 2) compared with pure MPC mixture. Moreover, significant improvement in mechanical strength (including early strength) and sorptivity properties were observed with 5%, 3% and 12% contents of SF, AS and BX mixed in the MPC and FA amalgams.

For water stability, the mass loss behavior, pH characteristics of curing water and mechanical strength of specimens cured in water were studied in this paper. The results showed that with the addition of SF, AS and BX to the MPC-FA composites, the mass loss reduced to 1.56%, 0.93% and 0.92%, respectively as compared to the 6% mass loss of the pure MPC mortar at 28d. Besides, the strength retention coefficients for pure MPC mortar, MPC+FA+5%SF, MPC+FA+3%AS, MPC+FA+12%BX at 28d were 0.87, 0.98, 0.90 and 0.98, respectively for compressive strength and 0.81, 0.94, 0.93 and 0.95, respectively for flexural strength. Furthermore, it was found that the variations of pH behavior of MPC specimens blended with SMs were relatively lower than those of pure MPC mortars, indicating that the penetration of curing water was occurred low amount into the microstructure and dissociated a little amount of materials from insides in curing water. Based on the obtained results, it was revealed that the water stability of MPC was improved by the addition of SMs.

The reason for the improvement of water stability of MPC-SMs was further explained via the investigation of microstructural progress and hydration mechanism. Huge cavities were found in the pure MPC specimen (Fig. 3) due to the high temperature release and water evaporation, leading to high permeability, low mechanical strength and water resistance. However, by investigating the microstructure of MPC-SMs, it was revealed that unreacted FA particles and the formation of intermediate crystals reduced the void spaces and increased the structural compactness, resulting in the enhancement of mechanical strength and water stability of MPC composites. Moreover, it was found that amorphous contents were reduced with the increase in hydration ages. Overall, this research provided reliable theoretical basis and technical support for the subsequent studies and engineering application of MPC blended with SMs.

Keywords: Magnesium phosphate cement; Supplementary materials; Mechanical properties; Water stability; Microstructural progress

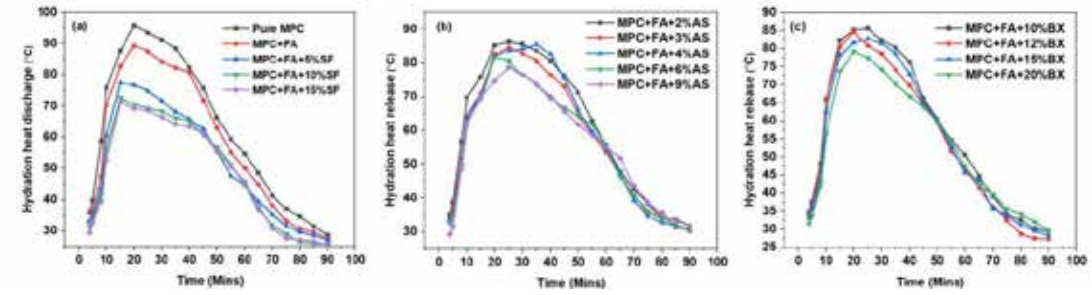

Fig. 1. Hydration heat release profiles of MPC fresh mixtures blended with SMs: (a) SF, (b) AS, and (c) BX

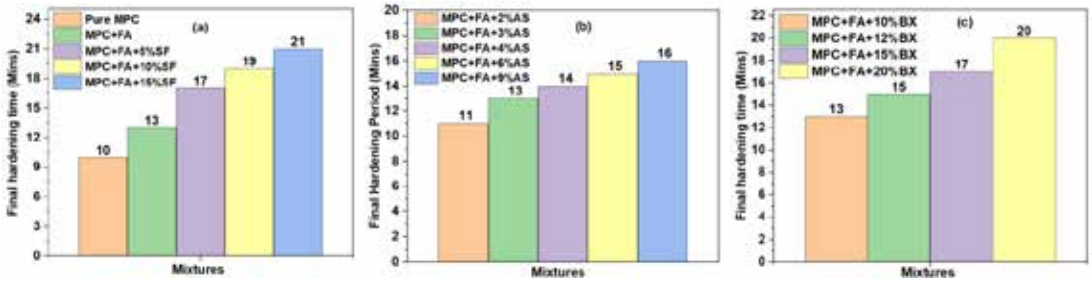

Fig. 2. Final hardening periods of MPC fresh mixtures blended with SMs: (a) SF, (b) AS, and (c) BX

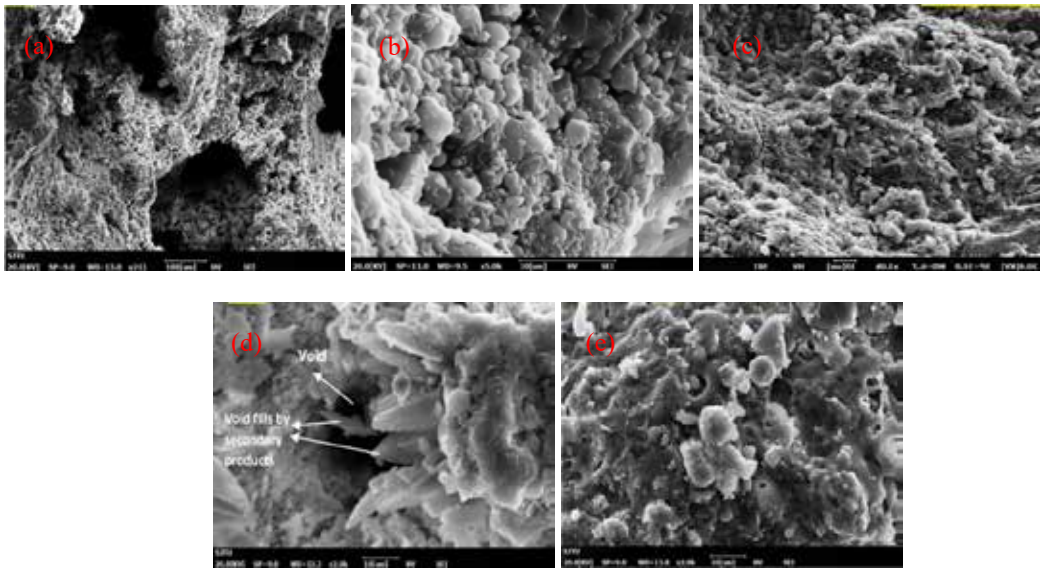

Fig. 3. SEM observations of (a) pure MPC, (b) MPC+FA, (c) MPC+FA+5%SF, (d) MPC+FA+3%AS, and (e) MPC+FA+12%BX

Acknowledgment

The authors would like to acknowledge the funding support from the National Natural Science Foundation of China, Grant No. 51778363 and 51972209.

Rheological Properties of Ultra High Performance Concrete and its Viscosity Control for Application

Jian-Zhong Liu[1,2*#], Fang-Yu Han[1,2], Wei-Lin[1,2], Qian-Qian zhang[1,2], Xin Zhen[1,2], Xin Shu[1,2], Xiao-Bo zhen[1,2],

[1] Jiangsu Sobute New Materials Co., Ltd, Nanjing 211103, China
[2] State Key Laboratory of High Performance Civil Engineering Materials, Nanjing 211103, China
[*]*Presenter: ljz@cnjsjk.cn*, [#]*Corresponding author: ljz@cnjsjk.cn*

Abstract

Ultra high performance concrete (UHPC) is a pioneer concrete, which occupies remarkably mechanical properties, especially a tensile strength above 7 MPa with significant remaining post-cracking bearing capacity. However, the introduction of an extremely low W/B and high content of varying ultrafine powders, superplasticizer and steel fiber makes UHPC have higher viscosity and longer mixing time, compared to ordinary concrete. Both exert difficulties in on-site pouring of UHPC. In this paper, the effects of superplasticizer and ultra-fine powders on rheological properties of UHPC are investigated and analyzed. The packing density and viscosity of interstitial solution between particles are found to be the two important parameters.

At a low W/B ratio of paste of bellowing 0.16, it is found that packing density and the water film thickness cannot be improved by further increasing superplasticizer dosage above a certain value of 0.4% (**Fig.1** and **Fig. 2**). This will result in a very small interparticle spacing of particles in paste. Besides, a large dosage of residual superplasticizer is found to be existed in paste solutions and entangled within the small interparticle spacing (about 35~40nm) (**Fig.3**). Both make UHPC increase viscosity rapidly. Moreover, ultrafine powder with a rounder shape and a suitable diameter can reduce the pulping time of paste more significantly (**Fig.4**). Meanwhile, to improve particle dense packing and releases entrapped water in agglomeration by selecting the satisfied shape and size of ultrafine powders, a low viscosity and high flow rate of paste can be obtained (**Fig. 5** and **Fig. 6**).

Basically, two solutions are proposed for tailoring the rheological of UHPC. One is the mix optimization design to optimize particle packing and release entrapped water in agglomeration, by introducing satisfied ultrafine powder combination. The other is the specialized SP design, with features of longer side chain, enhanced adsorption capacity and excellent compatibility with various surfaces, to disperse particles better with a lower dosage, which should be beneficial for enhancing the particle separation and lowering the viscosity of interstitial solution.

With the help of the proposed solutions, two excellent applications are employed. One is the Fifth Nanjing Yangtze River Bridge, a cable-stayed bridge of three towers with a streamlined steel-UHPC composite beam, where the UHPC is prepared with a slump flow of 420 mm and the ingredients are regulated to be distributed uniformly by adjusting a satisfied viscosity and yield stress (**Fig. 7**). The other is the UHPC pavement of two steel bridges on the Ning-Hang Highway, where the UHPC is successfully tailored with a good self-consolidating property during pumping and a highly thixotropic property after pumping (**Fig. 8**).

Keywords: UHPC, rheological properties, superplasticizer, ultrafine powders, engineering applications

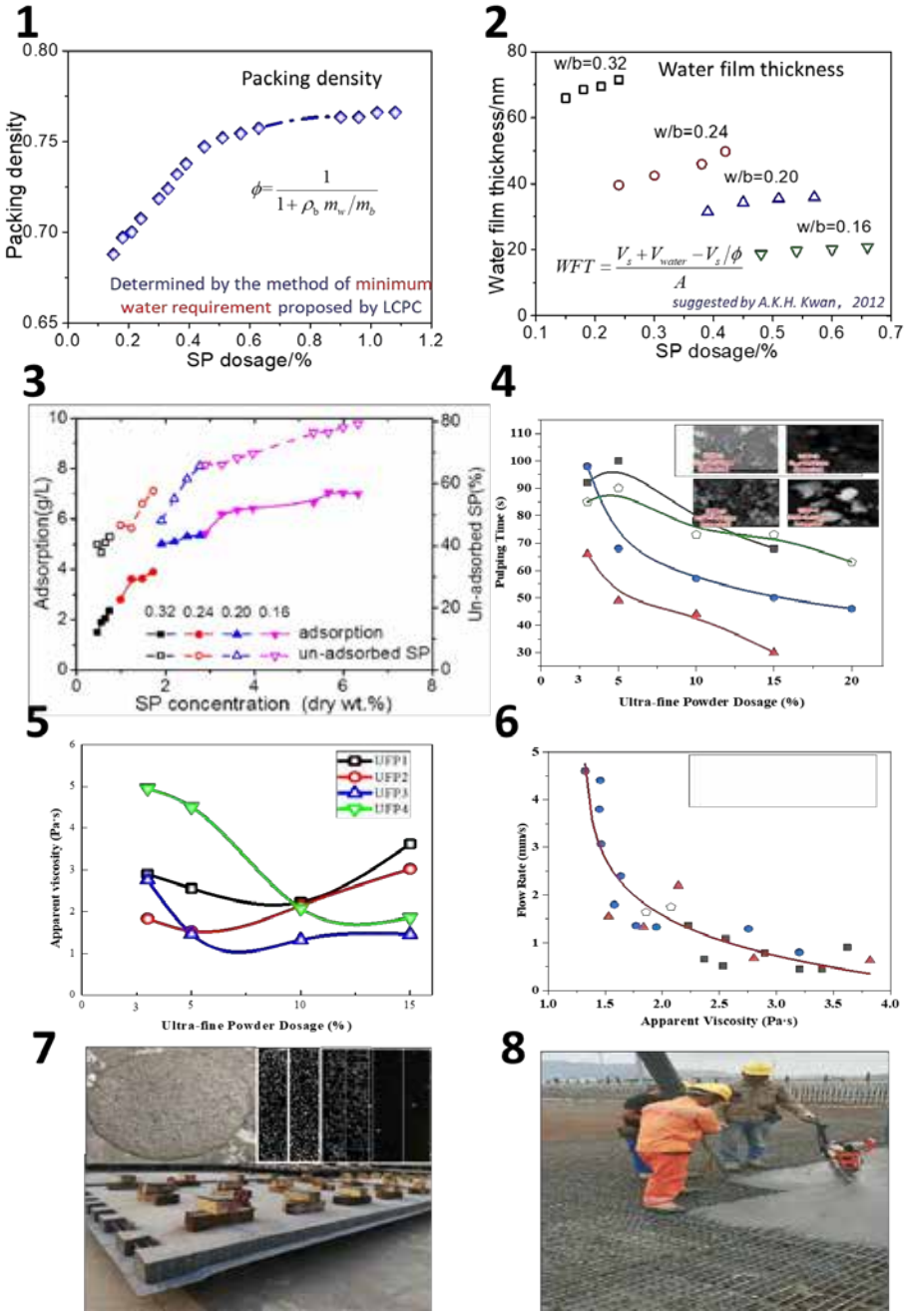

Fig. 1 Dependence of packing density of paste on superplasticizer dosage. **Fig. 2** Dependence of calculated water film thickness of particles on superplasticizer dosage. **Fig. 3** Dependence of superplasticizer adsorption on its concertation. **Fig. 4** Dependence of pulping time of paste on varying ultrafine powders with different dosage. **Fig. 5** Dependence of apparent viscosity of paste on varying ultrafine powders with different dosage. **Fig. 6** Dependence of flow rate of paste on apparent viscosity. **Fig. 7** The UHPC with well-distributed phases applies for precast slab of the Fifth Nanjing Yangtze River Bridge. **Fig. 8** The UHPC with satisfied pumping and thixotropic property applies for steel bridges on the Ning-Hang Highway.

Acknowledgment

The authors would like to acknowledge the funding support from the National Natural Science Foundation of China (No. 51578269 and No.52008191).

Parallel Sessions-14

Issues And Measure for Concrete Structures in Hot Weather Conditions

Activity of ACF Technical Committee 2 (TC2): Concrete practices and feasible measures for construction and design in hot weather conditions based on material characteristics

Shingo Asamoto[1]

[1] Department of civil and environmental engineering, Saitama university, Saitama, Japan
[**]*Presenter: asamoto@mail.saitama-u.ac.jp, Corresponding author: asamoto@mail.saitama-u.ac.jp*

Abstract

In Asia, most of tropical countries have used design codes developed by other countries such ACI, BS and Euro-code, which categorize hot weather concreting as a special concreting. The high ambient temperature over 30 °C in all seasons, strong sun radiation and frequent rainfall would cause the unexpected initial defects even though the design or construction requirement is satisfied. In addition, the time-dependent behavior of concrete related to the durability such as shrinkage, creep, ion transfer and others is difficult to be reasonably predicted under hot weather conditions using the empirical models in the codes, which are generally based on laboratory experiment under extratropical conditions. Since the material properties and qualities of cement and aggregate are also different in each country, development of design and construction specification for concrete in tropical countries based on the climate and materials is necessary.

ACF Technical Committee 2 (TC2), "Concrete practices and feasible measures for construction and design in hot weather conditions based on material characteristics", was established in 2020 including members in Japan, Thailand, Vietnam, Sri Lanka, Hong Kong, Indonesia, India and Russia. This TC aims to survey the problems of concrete practices in Asian hot climate countries to comprehend the common practical issues and characteristics of initial defects and deterioration due to hot climate and then to find out the possible measures according to the technical level, cost and local materials in each country. Finally, it is expected that the TC activity would lead to the development of Asian Concrete Model Code.

First kick off meeting was carried out in February 2020 in person as well as internet participation and then only web meetings have been conducted due to COVID-19. Against difficultly to have a physical meeting, a survey on problems of concrete standards and specifications for concrete practicing in hot climate countries/regions has been in progress to collect the information in member countries. The survey results will be summarized as ACF report soon and the analysis on the survey would be submitted to an international journal as a technical report. In the symposium, the activity of TC will be introduced.

Keywords: Hot Weather Conditions; Concrete Practices; Material Characteristics; Measures; Asian Concrete Model Code

Acknowledgment

The TC activity is based on the project "Collaborative research network on standardization of design and construction for hot weather concreting based on Asian climate and materials", which was accepted as a JSPS (Japan Society for the Promotion of Science) Core-to-core program (Asia-Africa Science Platforms) from FY2017 to FY2019 (Project coordinator: Dr. Shingo Asamoto). The author appreciates for contribution of TC members to the presentation.

Risk of thermal cracking in mass concrete footing construction under hot weather condition

T. Prasanthan[1*], Shingo Asamoto[1], S.M.A Nanayakkara[2]

[1] Department of Civil & Environmental Engineering, Saitama University, Saitama, Japan
[2] Department of Civil Engineering, University of Moratuwa, Katubedda, Sri Lanka
[*]*Presenter:* Prasanthan1301@gmail.com
[#]*Corresponding author:* Prasanthan1301@gmail.com

Abstract

At the present stage, many large-scale construction activities are taking place in developing countries. Designers are paying a special attention of temperature to design of massive foundations which are necessary to accommodate design loads. While designing these massive foundations, the use of medium strength reinforced concrete such as grades C30, C35, and C40 is becoming a common practice. In case of South Asian countries, fly ash is currently used as the main cement substitute to control thermal cracking while designing medium-grade concrete by considering its benefits in engineering and economic nature. Even though the grade of the concrete and percentage of fly ash replacement are differed from project to project, a common temperature differential value of 20^0C based on American or European design codes is often used as a capping value to control early age thermal cracking. In this study, the influence of temperature differential on early-age thermal cracking risk, possible cracking location, the influence of supporting structure on the risk of cracking in mass footing construction are studied through numerical analysis for the rational design under hot weather conditions.

A suitable geometry model for the numerical analysis was selected as an initial step based on the preliminary analysis and literature studies. JCMAC3 FEA software for the thermal cracking analysis developed by Japan Concrete Institute (JCI) was utilized for the analysis. Concrete mix design details and environmental conditions were extracted from past project reports in hot weather countries, and relevant thermal and structural properties of concrete were found through test reports and model codes. Table -01, Figure 01 and Figure 02 show the results of two example analysis cases.

The findings of this study show that the risk is mainly due to the internal restraint when the structure is supported on soft/ordinary ground. Also, the minimum crack index was observed at less temperature differential than the maximum temperature differential observed at the same location in later time step (see Figure 1 &2). This illustrates that the strength development of concrete is the most sensitive to cause cracking comparing to thermal stress development. Also, analytical results show that the temperature differential that had the highest cracking probability in the concretes varied from one concrete mix to another. This is because of different strength development in each concrete mix selected for the design. In estimating cracking risk, early age tensile strength development of the concrete is more dominant than developed tensile stress due to internal restraint. Moreover, results show that early age cracking risk is significantly higher at very early age of fly ash mixed concrete, because its strength development is slower than OPC mixed concrete. Also, analytical results indicate that widely use allowable temperature differential limit 20^0C is conservative for hot climate countries. Early age surface cracking begins at the edges of the concrete structures, and the chances of crack occurrence in surfaces are comparatively less. The occurrence of surface cracks due to internal restraint only remains in shallow surfaces. Moreover, crack width and crack spacing are controlled by surface reinforcement in footing structures. Hence, internal restraint effect would not affect both structural and durability performance of concrete.

To ascertain the effect of supporting ground condition on thermal cracking risk, different supporting conditions were considered and developed thermal stress was evaluated as shown in Figure 3. The results show that footing supported on the ordinary ground/soft ground does not significantly influence the cause of thermal cracking due to the edge restraint effect. Structure supported on bedrock/hardened concrete restrained the deformation during the cooling period, and this led to increase of restrained stress along the joint, thus cracking risk is higher near the bottom surface of the structure as shown in Figure 4. The minimum crack index was observed at the bottom surface of the structure, and crack index observed at the core of the structure is greater than 1.85 and the probability of cracking is less than 5%. Hence, there is very small possibility to cause internal cracking, because the mature concrete at the core of the structure has been gained sufficient strength at the later ages. However, considering the durability aspects, the effect of external confinement by bedrock or hardened concrete is much more significant than internal confinement.

Table 1: Numerical analysis results of crack index and relevant temperature differential

Analysis case	Minimum crack index	Probability of cracking	Temperature differential during minimum crack index	Time at minimum crack index
Case – 01 (C40 fly ash blended cement mixed concrete)	0.92	63.2%	18.2	33 hours
Case - 02 (C40 OPC mixed concrete)	0.98	53.35%	33.2	27 hours

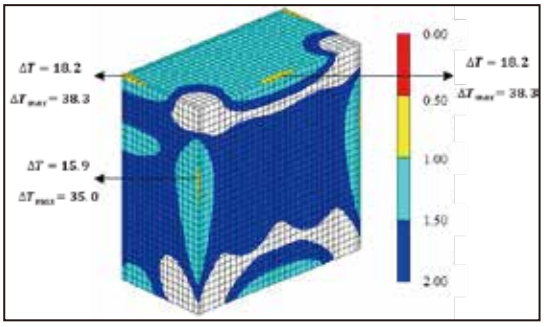

Figure 1: Location and temperature differential at minimum crack index (case -01)

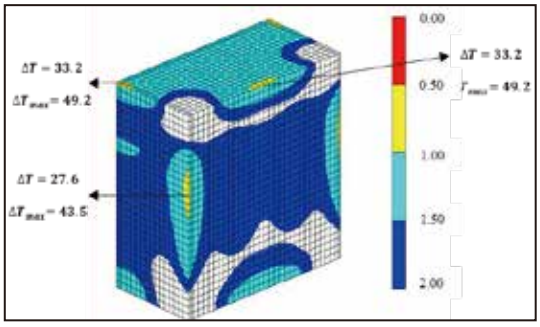

Figure 2: Location and temperature differential at minimum crack index (case -02)

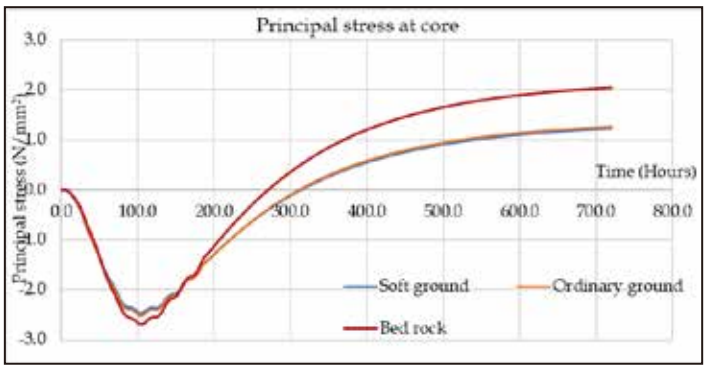

Figure 3: Principal stress variation with time at core of the structure for different supporting condition

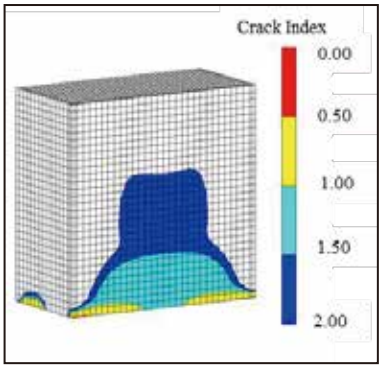

Figure 4: Visual representation of minimum crack index for structure supported on hardened concrete

Acknowledgment

The authors would like to acknowledge JCI for providing the JCMAC3 finite element modeling software package for this study.

Study on chloride binding property of slag blended cement considering different slag blending ratios

Yao Luan[1*#], Fahmida Parvin[2]

[1] Department of Civil and Environmental Engineering, Saitama University, Saitama 338-8570, Japan
[2] Health Engineering Department, Government of the People's Republic of Bangladesh
[*]*Presenter and* [#]*Corresponding author:* luanyao@mail.saitama-u.ac.jp

Abstract

Chloride ingress through pore solution to embedded steel is the reason for corrosion induction in reinforced concrete structures exposed to seawater environment. As chloride ion ingress, some are bound physically by hydration products, and some bound chemically that are mainly in the form of Friedel's salt, leading to the immobilization of those ions. The more chlorides are bound, the less free chlorides are available to cause corrosion. The use of ground granulated blast furnaced slag (BFS) as a supplementary cementitious material has been known beneficial for chloride resistance because of their high alumina content and the refinement of pore structure. Slag blended in Portland cement may exhibit different reactivity and characteristics of hydration product depending on chemical compositions, slag ratio, water-to-binder ratio (w/b), and curing temperature, which may lead to different chloride binding property. In the present study, experimental study on chemical and physical binding were performed for slag blended cement with different slag blending ratios.

Slag was blended in OPC with four ratios (0, 20, 50, and 70%), two w/b ratios (0.3 and 0.5) and cured in two temperatures (20 and 40°C), respectively. The cement paste was cured to 186 days. The equilibrium method developed by Luping and Nilsson (1993) was applied for chloride binding test. After curing, the hardened cement paste was crushed into small pieces and dried for three days to eliminate most of the excess water. Subsequently, the samples were stored for 14 days while maintaining a relative humidity of 11% using saturated lithium chloride. The samples were then ground and sieved to obtain particles with sizes in the range of 150–300 μm. Distilled water pre-saturated with $Ca(OH)_2$ was used to prepare NaCl solutions with concentrations of 0.1, 0.3, 0.5, 0.7, 1, 2, and 3 mol/L. The samples were soaked in the NaCl solutions. The temperature of the solutions was maintained at 20°C and 40°C, corresponding to the curing temperatures. Potentiometric titration against silver nitrate was performed to determine the concentration change of chloride ions. When the equilibrium of binding was reached, bound chloride was determined by the reduction in chloride concentration from its initial value. After the chloride binding test, the samples in the NaCl solution were reclaimed. They were ground again using a mortar and pestle to obtain finer powder for thermogravimetric analysis (TGA). The ground sample was analyzed by TGA, heated to 950°C. According to Shi et al. (2017), the decomposition of Friedel's salt occurred in two temperature ranges due to the loss of four interlayer water molecules and six main layer water molecules, respectively. The amount of Friedel's salt was quantified for six main layers of water in the temperature range of approximately 230–410°C.

The isotherms of total chloride binding are shown in Fig. 1. It can be found that the addition of slag was beneficial in chloride binding than OPC and 50% slag ratio provided the highest values. In slag blended cement, more alumina than OPC reacts with available SO_4^{2-} to form AFm that was converted to more Friedel's salt by combining Cl^-. Meanwhile, C-S-H from slag reaction adsorbed more Cl^- physically due to higher surface area and charge density. In addition, past studies have reported that the reaction degree of slag in blended cement

generally decreased with increasing slag ratio. Therefore, low values at 70% slag ratio and lower w/b ratio correlated to the less hydration products, denser pore structure and the different properties of C-S-H. At high slag ratio, C-S-H become less positive, which cause the reduction of Cl^- adsorption. Meanwhile, less SO_4^{2-} is available from OPC, so the amount of AFm available for Friedel's salt formation decreased. Fig. 2 shows a result of DTG for samples with the w/b of 0.5 and the temperature of 20°C after chloride binding in 3.0 mol/L NaCl. Friedel's salt peak increased up to 50% slag ratio and around 1/3 chloride were bound chemically due to formation of Friedel's salt (Fig. 3). Effectively all slag ratios provided high values than OPC. Physically bound chloride was determined by subtracting chemically bound from total bound chloride (Fig. 4). It can be seen that physically bound chloride increased up to 50% slag ratio, while 70% slag ratio exhibited lower values than 50% but still higher than OPC, which was similar with chemically binding chloride in trend.

Keywords: Blast Furnace Slag; Slag Blended Cement; Chloride Binding; Friedel's salt

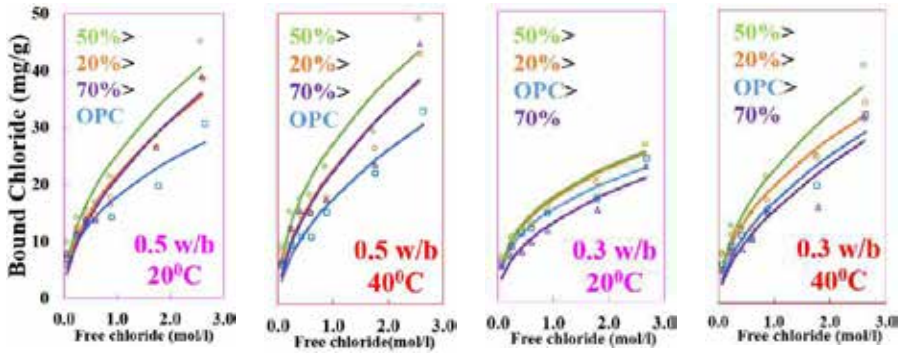

Fig. 1 Chloride binding isotherms

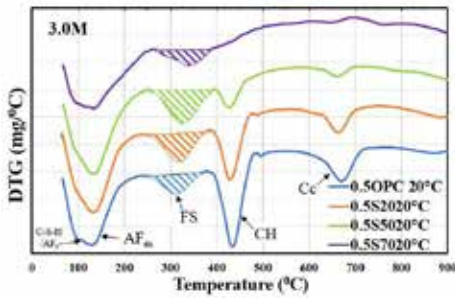

Fig. 2 Friedel's salt decomposition in DTG

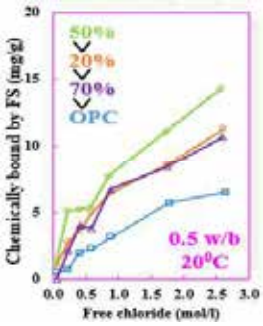

Fig. 3 Bound chloride by Friedel's salt

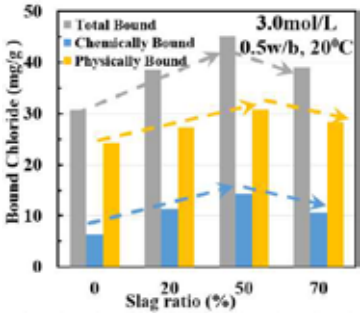

Fig. 4 Total, chemically and physically bound chloride

Acknowledgment

The authors would like to acknowledge the funding support from JSPS KAKENHI Grant Number 19K04547.

References

Luping, T. and Nilsson, L. O.: Chloride binding capacity and binding isotherms of OPC pastes and mortars, Cement and Concrete Research, 1993, Vol.23, pp.247-253
Shi, Z. et al.: Friedel's salt profiles from thermogravimetric analysis and thermodynamic modelling of Portland cement-based mortars exposed to sodium chloride solution, Cement and Concrete Composites, 2017, Vol. 78, pp. 73-83

The application of newly developed test methods to prevent the damages caused by oxidation of iron sulfide in aggregates

Thuraisingam Jeyakaran[1*], Niraporn Pornsiri[1], Warangkana Saengsoy[2#], Somnuk Tangtermsirikul[1]

[1] School of Civil Engineering and Technology, Sirindhorn International Institute of Technology, Thammasat University, Pathum Thani, Thailand.
[2] Construction and Maintenance Technology Research Center (CONTEC), School of Civil Engineering and Technology, Sirindhorn International Institute of Technology, Thammasat University, Pathum Thani, Thailand.
[*]*Presenter:* d6222300250@g.siit.tu.ac.th, [#]*Corresponding author:* warangkana@siit.tu.ac.th

Abstract

Iron sulfide-bearing aggregates can undergo oxidation reactions that can cause an internal sulfide attack in concrete, leading to severe damage on concrete surfaces by the formation of rust, gypsum, ettringite, and pop-outs. Solving these issues is extremely important in the modern construction industry. Currently, several approaches such as screening, alternative mix design, and protection techniques are being investigated to achieve the desired goal, and this paper mainly focuses on the protection measures. Systematic performance-based evaluation methods are required for formulating guidelines to solve these issues. Nevertheless, appropriate test methods are not available in the state of the art standards. Therefore, this research made an effort to establish a complete set of test methods to evaluate the performance of concrete containing iron sulfide-bearing aggregates. These methods include evaluating expansion, quantitative evaluation of rusting, and quantitative determination of pop-out parameters. An accelerated mortar bar test was developed to assess the expansion by modifying the test method available in ASTM C1260 (accelerated mortar bar test for ASR). Accordingly, a storing temperature of 60°C, 80% RH, and wetting and drying cycles of 7 cycles per two weeks (6% NaOCl or H_2O with oxygen added through the pump while submerging) were found to be very effective in accelerating the oxidation process in the laboratory (Fig. 1). The digital image processing method based on the 'Otsu technique' was used to evaluate the rusting quantitatively (Fig. 2). Moreover, the pop-out frequency (n) and the average chord length (l) were used to characterize the pop-out, and these parameters were evaluated based on the image-processing algorithm (Fig. 3).

The developed test methods were used to evaluate the effectiveness of different surface treatments, such as water repellent, crystalline waterproof system, and epoxy coating, in controlling the oxidation. The cast samples were oxidized and measured to obtain the expansion variation, as shown in Fig. 4. The samples treated with water repellent showed higher expansion, while the epoxy coating and crystalline waterproof system showed lower expansion than the control samples, as shown in Fig. 4. The microstructural examination was also carried out using SEM with EDS to understand the mechanisms that led to the significant expansion of the samples. Fig. 5 illustrates the SEM image of the damages that occurred in the controlled samples due to the presence of iron sulfide-bearing aggregates, where the micro-cracks and ettringite were detected. The efficacy of surface treatments in lowering the level of rusting caused by the presence of iron sulfide-bearing aggregates was also examined. The obtained results for rusting and expansion showed a similar trend, as shown in Fig. 4 and Fig. 6. Furthermore, pop-outs have been observed in the control samples and the samples treated with water repellent. Accordingly, the control sample's pop-out frequency and average chord length were found to be 280 pop-outs per m^2 and 0.01 m, respectively. Severe pop-outs have been observed in the samples that are treated with hydrophobic surface treatment compared to control samples, and the pop-out frequency and average chord length of these specimens were

520 pop-outs per m^2 and 0.015 m, respectively. The Epoxy and crystalline waterproof system were highly effective in reducing the oxidation rate of iron sulfide-bearing aggregates, as evidenced by the expansion, rusting, and pop-out evaluations. Further research is being conducted to propose a comprehensive set of guidelines to prevent the damages caused by the iron sulfide-bearing aggregates, which will be documented in the near future.

Keywords: Iron Sulfide-Bearing Aggregates; Internal Sulfide Attack; Expansion; Rusting; Pop-out.

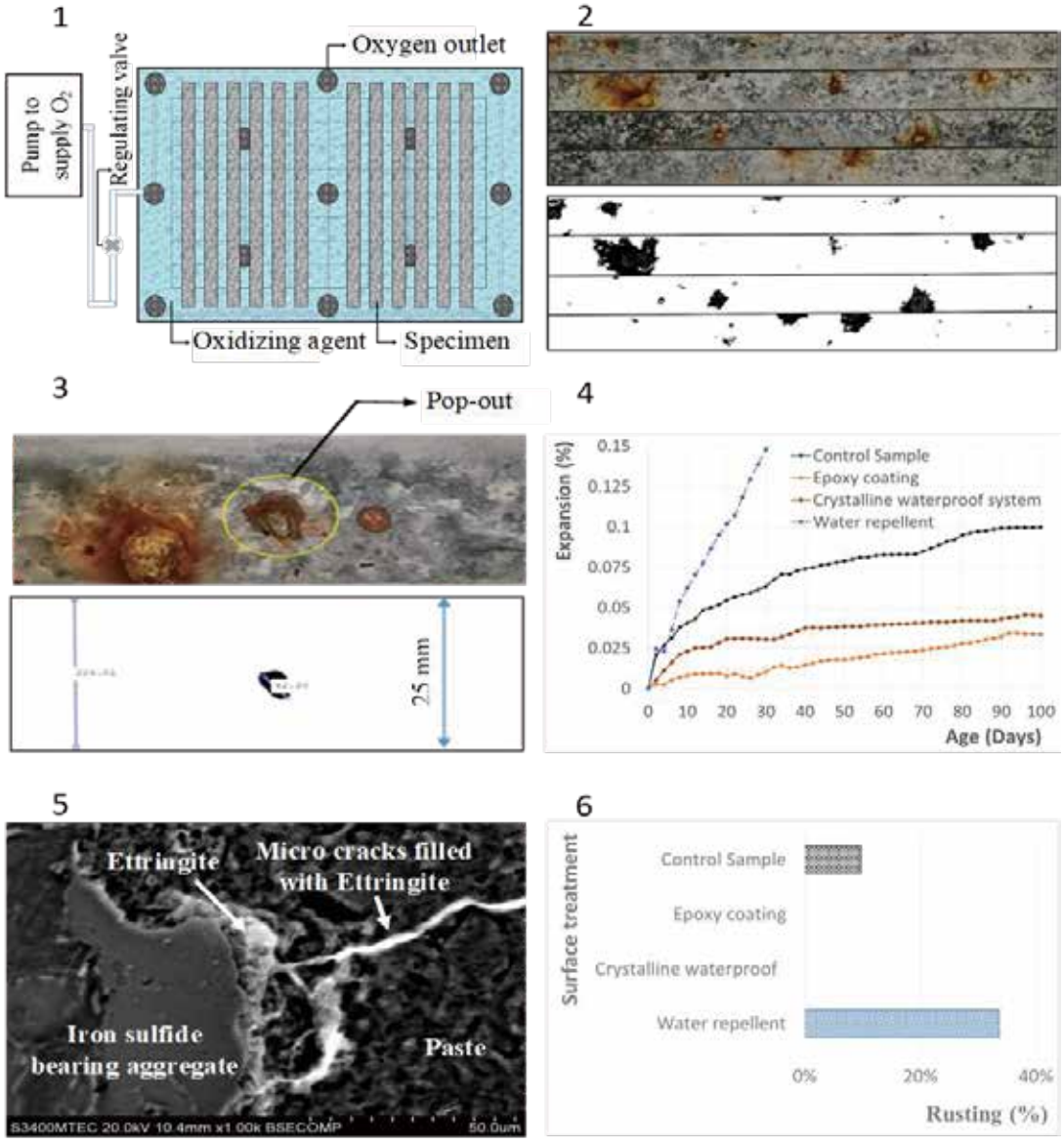

Fig. 1 Experimental setup to accelerate the oxidation of iron sulfide-bearing aggregates; **Fig. 2** Actual and processed images of rusting; **Fig. 3** Evaluation of pop-out parameters; **Fig. 4** Evaluation of Expansion; **Fig. 5** SEM image of the formed ettringite and micro-cracks filled with ettringite found in the control sample; **Fig. 6** Level of rusting observed in the samples.

Acknowledgment

The authors would like to acknowledge the research supports provided by the Chair Professor Program (P-19-52302), the National Science and Technology Development Agency (NSTDA), Thailand, the Center of Excellence in Material Science, Construction, and Maintenance Technology, Thammasat University.

Study on effect of internal swelling reaction in concrete on structural performance of prestressed concrete beams

Shingo Asamoto[1*], Ayumu Matsumoto[1]

[1] Department of civil and environmental engineering, Saitama university, Saitama, Japan
[*]*Presenter: asamoto@mail.saitama-u.ac.jp, Corresponding author: asamoto@mail.saitama-u.ac.jp*

Abstract

The internal chemical reactions of concrete such as alkali silica reaction (ASR) and delayed ettringite formation (DEF) can cause expansion in concrete leading to map cracking on the surface of concrete structures. DEF can occur when the concrete is exposed to high temperature over 70 C at early ages and then continuous water supply while the occurrence of ASR is dependent on the reactive aggregate in concrete. DEF has been focused on in hot weather conditions due to large hydration heat under high ambient temperature and strong sun radiation. In Japan, the cracking certainly related to DEF has not been found in concrete structures with on-site casting even though the internal temperature exceeds 70 C while ASR map cracking has been observed in many structures, especially in Hokuriku area. Considering future risk of DEF expansion, the effect on the structural performance should be consistently examined but few studies on the structural performance have been reported while DEF expansion mechanism from a chemical viewpoint has been widely studied.

This study investigated the effect of DEF and combined ASR and DEF in concrete on the structural performance of Prestressed Concrete (PC) beams (150 mm in width, 200 mm in the depth, and 1800 mm in length as shown in Fig. 1). The PC beam with the expansion by combined DEF and ASR or DEF in the concrete had many split cracks in the axial direction due to the concrete swelling (Fig. 2). Although the flexural rigidity in the deflection direction decreased to some extent with increase of concrete swelling, it did not decrease significantly in the subsequent continuous expansion as shown in Fig. 3. It was observed that the combination of ASR and DEF (ASR-DEF) expansion in the test specimen leads to a slight decrease in the load flexural loading capacity of the PC beam (Fig. 4) even though compressive strength of cylinder specimen was less than 5 MPa. Although the small compressive strength indicates flexural compression failure at low load of around 20 kN, the beams with large internal swelling finally failed at much higher load due to the flexural tension failure with concrete compressive crushing at top after the reinforcing bars yielded (Fig. 5). The cracking pattern of DEF or ASR-DEF affected beams arising from the loading was the similar that of beam without expansion as given in Fig. 6. Hence, it was identified that even large ASR-DEF or DEF expansion in concrete has a slight effect on structural performance in PC structures.

Keywords: Delayed Ettringite Formation; Alkali Silica Reaction; Concrete Expansion; Prestressed Concrete Beam; High Temperature at early ages

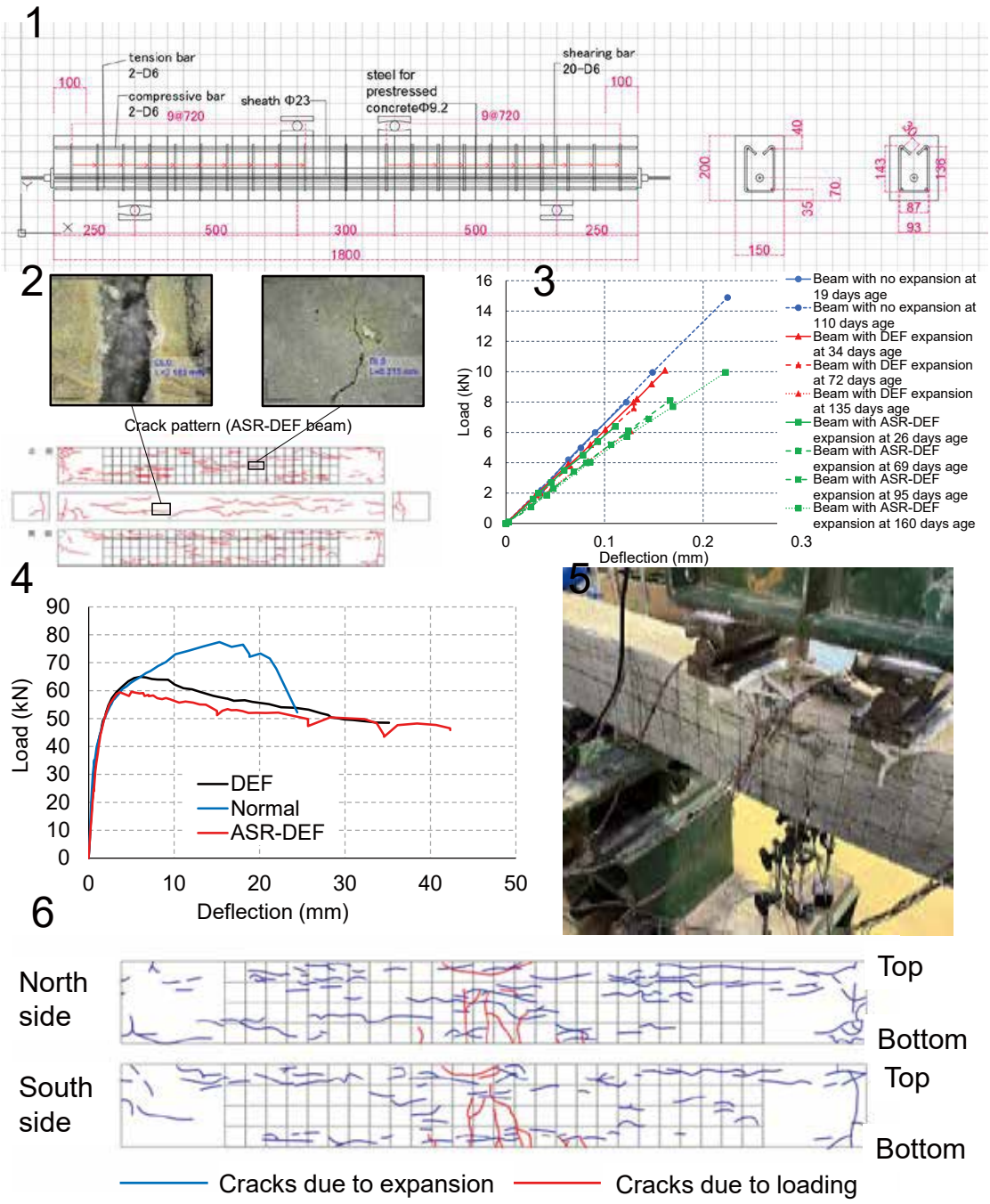

Fig. 1 Overview of prestressed concrete beam (unit: mm); **Fig. 2** Cracking in beam with ASR-DEF expansion; **Fig. 3** Load and deflection relationship variation of prestressed concrete bam under low loading with internal swelling reaction progress; **Fig. 4** Load and deflection relationships of prestressed concrete beams to failure; **Fig. 5** Photo at flexural tensile failure of prestressed concrete beam with DEF expansion; **Fig. 6** Cracking pattern due to ASR-DEF expansion and loading

Acknowledgment

This research was financially supported by JSPS Grants for Scientific Research Kiban B (grant numbers 20H02219).

3D Finite Element Analysis of Steel Fiber Reinforced Ultra-High Strength Concrete Beam-Column Joints

Hiroto Takatsu[1*]

[1] Research and Development Institute, TAKENAKA CORPORATION, JAPAN
[*] *Presenter:* takatsu.hiroto@takenaka.co.jp

Abstract

When steel fibers are added into a concrete mix, the tension stiffening effect of the resulting concrete, especially after cracking, is thought to be different from the one of normal concrete, as fibers between cracks can bear tensile forces. To investigate this effect on structural elements, pull-out tests of reinforcing bars from steel fiber (SF) reinforced and normal concretes were carried out to examine the tension stiffening properties at first. Silica fume-cement was used for the ultra-high strength concrete with a water-binder ratio of 18%. For the specimen with SF, a volumetric ratio of 0.5% SF were added to the concrete. The added SF were of 30mm length and 0.6mm diameter, and hooked at their both ends. They had a tensile strength exceeding 1000 MPa. 3D finite element (FE) analyses were carried out to reproduce the pull-out test results and identify the parameter characterizing the post-cracking softening behavior (Fig. 1). Eight-node isoparametric solid elements were used for concrete elements, and two-node truss elements were used for reinforcement bars. The reinforcing bar was assumed to be perfectly bonded to the concrete. In the tension region of concrete, a linear ascending model was used before the tensile strength, and Izumo equation (Eq. (1)), which takes into account the tension stiffening effect by coefficient "c", was used to define the descending section. Fig. 2 is the comparison between experimental test results and analytical results with varied coefficient c. The mean squared error between the experimental result of SF concrete used in this program and analytical result became the smallest when c=0.2 (c=1.0 for normal concrete).

$$\sigma_t / f_t = (\varepsilon_{cr} / \varepsilon_t)^c \quad (1)$$

(σ_t: average tensile stress of concrete, f_t: concrete tensile strength, ε_{cr}: average tensile strain at tensile cracking, ε_t: average tensile strain orthogonal to cracks)

And then, a 3D FE analysis of the tested beam-column joints made of steel fiber reinforced (J120-05) and normal ultra-high strength concretes (J120-0) was conducted using a material model deduced from the previous FE analysis. The outline of the FE model and boundary conditions used in this study is shown in Fig. 3. Only half of each specimen was modelled, taking advantage of specimens' symmetry to reduce the analysis time. In addition to the symmetry condition, the boundary conditions of the experimental test were properly simulated in the model.

The equivalent compressive and tensile stress-strain relationships and cyclic behavior of concrete are presented in Fig. 4. Core concrete and cover concrete were modelled separately in this analysis. In the tension region, a linear ascending model was used before the tensile strength, and Izumo equation was adopted to define the descending section. The difference in the analysis of the models J120-0 without SF and J120-05 with SF was only in the tension stiffening slope.

The analytical results, in terms of the story shear force-story drift angle relationships and maximum story shear force, agreed well with the experimental data (Fig. 5). The minimum principal stress distribution obtained from the 3D FE analysis (Fig. 6) also showed an expansion of the effective section of the diagonal compression strut in the joint of the steel fiber reinforced concrete specimen, in comparison to the specimen of normal concrete, which might explain the increase of the maximum strength when steel fibers were used.

Keywords: FE Analysis; Steel Fibers; Tension Stiffening; Ultra-High Strength Concrete

Fig. 1 FE model of pull-out test
(Axial strain contours)

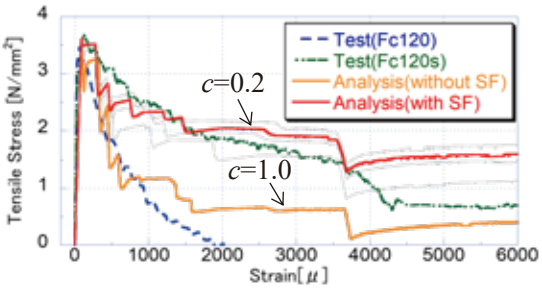

Fig. 2 Test and analysis results of stress-strain relationships of concrete (Fc120: without SF, Fc120s: with 0.5 %vol. SF)

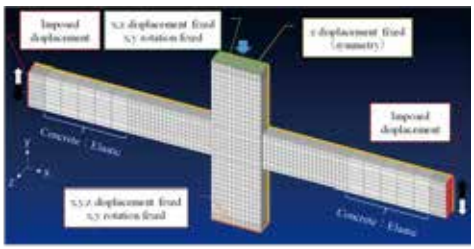

(a) Solid elements and boundary conditions

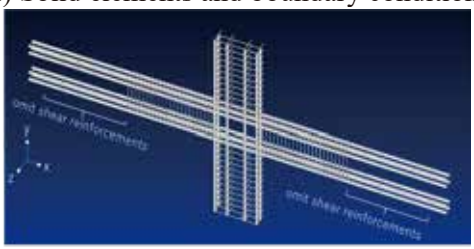

(b) Truss elements

Fig. 3 Outline of the FE model

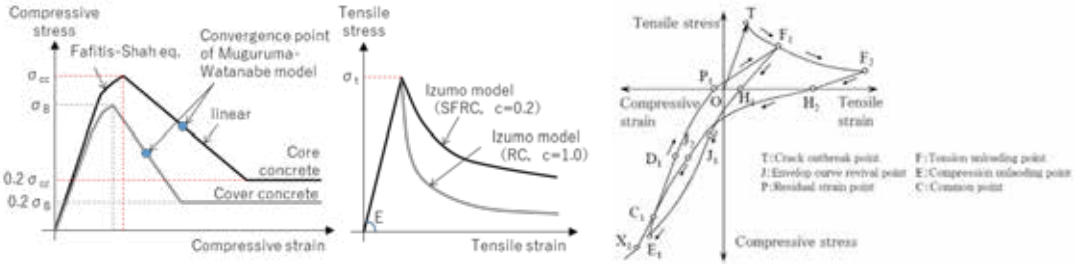

(a) Compression side (b) Tension side (c) Behavior between compression and tension

Fig. 4 Skeleton curves and cyclic behavior of concrete

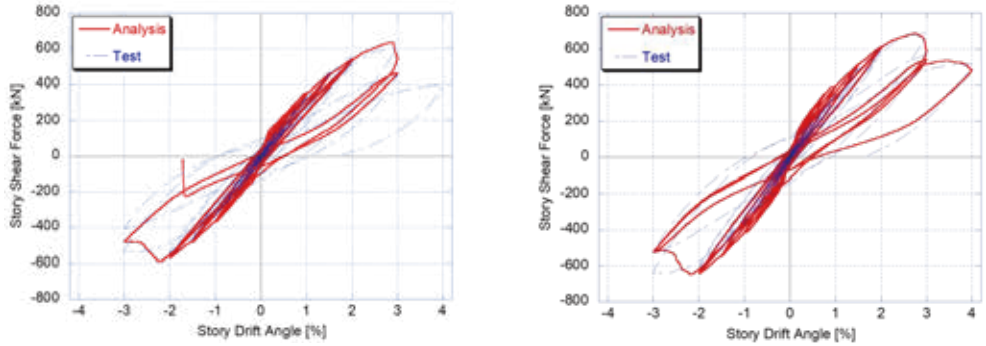

(a) J120-0 (without SF) (b) J120-05 (with SF)

Fig. 5 Story-shear force drift angle relationships: Comparison of test and analysis

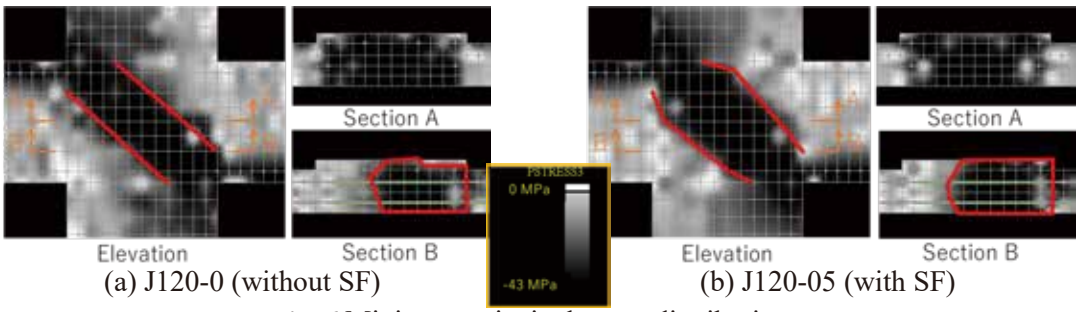

(a) J120-0 (without SF) (b) J120-05 (with SF)

Fig. 6 Minimum principal stress distributions

Influence of Cover depth and mortar quality on Rebar corrosion under aggressive chloride environment

Khalid Muhammad Afaq[1], Shinichi Miyazato[2], Norihiro Sugawara[3]

[1] Ph.D. Scholar, Kanazawa Institute of Technology, 7-1 Ohgigaoka, Nonoichi, Ishikawa Japan.
[2] Professor, Kanazawa Institute of Technology, 7-1 Ohgigaoka, Nonoichi, Ishikawa Japan.
[3]Kanazawa Institute of Technology, Graduate School, 3-1 Yatsukaho, Hakusan, Ishikawa 924-0833 Japan.

Presenter: engrafaq@gmail.com*Corresponding author:* miyazato@neptune.kanazawa-it.ac.jp

Abstract

With the recent developments in industrial revolution and the ever-increasing demand of reinforced concrete in the construction, it is imperative to investigate the factors that influence the durability, safety and sustainability of concrete structures in coastal regions and aggressive Chloride induced environments. In this study, the influence of cover depth and mortar quality on rebar corrosion in aggressive marine environment was investigated.

The mortar was prepared for two different water-cement (W/C) ratios of 0.30 and 0.70, with Zero (0) kg/m^3 and 15kg/m^3 of chloride ion. The chloride ion was added by mixing sodium chloride (NaCl) solution to the mortar prepared by using Ordinary Portland Cement (OPC). A 10mm dia, deformed rebar was divided into six (06) equal segments of 25mm in length, intended for the measurement of microcell and microcell corrosion currents. Lead wires were soldered at both the ends of single segment. They were joined together with epoxy resin of high insulating capacity and strength to enable fabrication of 180mm long rebar having a minimum and maximum cover depth of 7.5mm and 20mm. The rebar was divided into small segments in order to investigate the influence on corrosion due to change in strength of mortar and cover depth.

The bottom half part of sample was casted first and the next half on the following day due the difference in water-cement ratio, cover depth and chloride ion content. The samples were then cured at very high Relative humidity (Rh) ≥ 90 % and at room temperature of around 20℃. The specimens were exposed to wet environment for 27 days and were tested on the 28th day. The Twenty-Four (24) specimens were each tested for Macrocell and Microcell current densities and the additional twelve (12) specimens were tested for Compressive strength and Mortar Resistivity. The findings of this research study can prove to be a milestone for the researchers who intend to explore the impacts of cover depth and mortar quality on the mechanical performance of mortar subjected to aggressive chloride environment.

Keywords: Rebar corrosion; cover depth; Macrocell and Microcell; Water-Cement ratio; Chloride ion content

Ultimate strength determination of reinforced concrete dapped end beams based on a physical model

Takeru Kanazawa[1*]

[1] Department of Civil and Environmental Engineering, Hokkai Gakuen University, 0640926 Minami 26, Nishi 11, Chuo-ku, Sapporo, Japan
[*] *Presenter and corresponding author: t-kanazawa@hgu.jp*

Abstract

Dapped-end connections (Fig. 1) are used widely to lengthen bridge spans. Most reported studies have been experimental and analytical investigations of dapped-end failure resulting from inclined cracks at the re-entrant corner (Fig. 2), whereas failure at the full-depth section has received limited attention despite the fact that it was observed in the catastrophic collapse of Concorde overpass. We therefore developed a rigorous physical model that accommodates unified treatment of both the dapped-end failure and the full-depth section failure.

To derive the ultimate strength based on the lower bound theorem within the framework of limit analysis, the following assumptions were made.
(a) The analyzed beams are in an in-plane stress state.
(b) Concrete and steel reinforcement are idealized respectively as a rigid – perfectly plastic material and as an elastic – perfectly plastic material.
(c) The concrete and steel reinforcement are perfectly bonded: proper anchorage is provided.
The free-body diagram presented in Fig. 3 suggests equilibrium equations of the vertical direction, horizontal direction, and moment. Under these equations, we treat the ultimate strength derivation as an optimization problem. Specifically, the vertical equilibrium gives the objective function. Maximizing it under the equality constraints of the horizontal and moment equilibrium, one obtains an analytical solution of dimensionless ultimate strength $v_{ana.}$ The expression of critical crack, $f(x)$ in Fig. 3, allows unified treatment of the two failure patterns.

To validate the accuracy of this analysis, nine test results of reinforced concrete dapped-end beams were collected from the available literature as presented in Table 1. Few available results of specimens exist to show the full-depth section failure when excluding those with improper arrangement of reinforcement. v_{exp} and v_{STM} respectively represent the experimentally obtained strengths and predicted values using a strut–tie model, the latter of which is conventionally used for strength prediction. The present model shows better agreement with the test results than the strut-and-tie-based predictions do.

From the present analysis, one obtains the magnitude of each internal force component because of the explicit formulation of equilibrium equations. Table 1 presents the internal force contributions as a ratio of the analytically obtained strength (%). Results demonstrate that hanger reinforcement provides the most resistance, irrespective of the failure mode. It has at least 77% of the total internal force. The second largest component is given by either the dowel action of main reinforcement or the concrete in compression zone. The aggregate interlock action does not participate in resisting the external force, except for the specimen 2B.

It is noteworthy that the conclusion above is limited to nine specimens because of the text length limitation. However, the generality of this model is useful to elucidate the internal force system and to provide accurate ultimate strength prediction.
Keywords: dapped-end failure; full-depth section failure; ultimate strength; physical model; reinforced concrete dapped-end beams

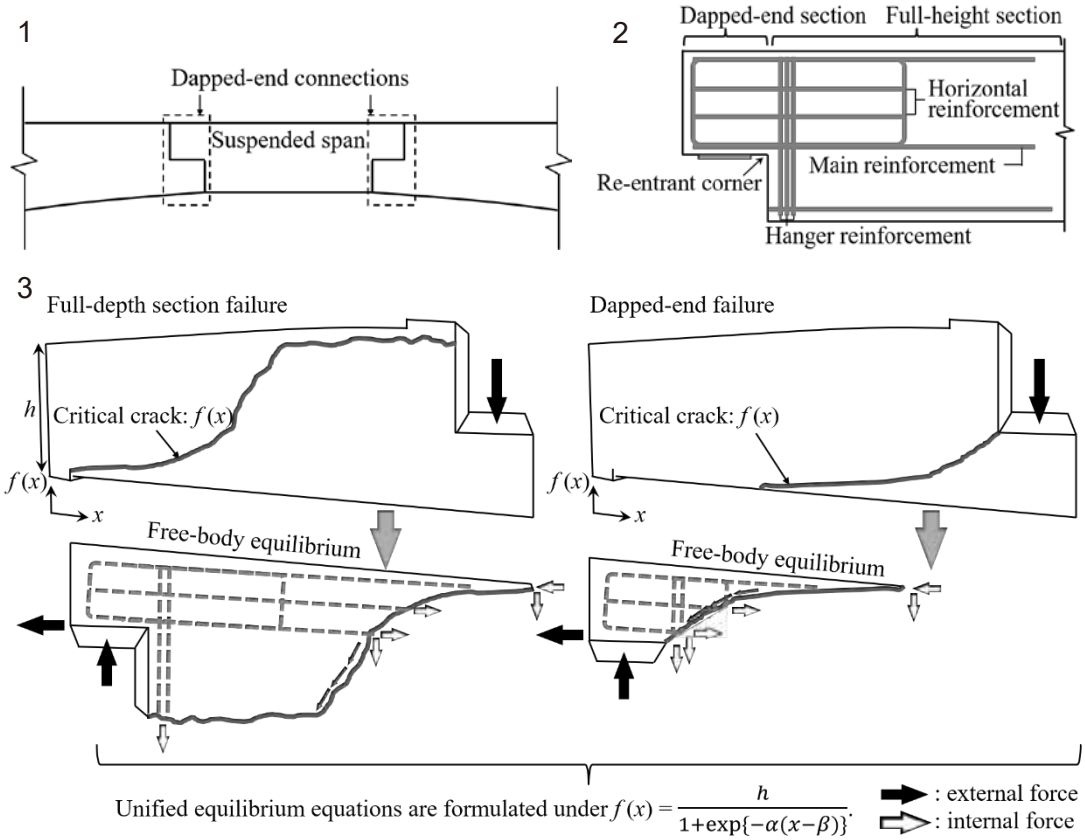

Specimens	Failure mode	CC (%)	AG (%)	DW (%)	HG (%)	v_{exp}/v_{ana}	v_{exp}/v_{STM}
1A	dapped	0.00	0.00	2.30	97.7	1.19	1.53
1B	dapped	0.00	0.00	6.50	93.5	1.10	4.81
2A	dapped	13.1	0.00	0.80	86.1	1.18	2.31
2B	dapped	2.90	6.20	13.7	77.2	0.97	11.9
3A	dapped	4.10	0.00	0.70	95.2	1.26	2.24
3B	dapped	5.20	0.00	2.10	92.7	0.96	6.27
4A	dapped	2.00	0.00	0.70	96.5	1.08	1.52
4B	dapped	2.80	0.00	2.40	94.8	1.05	2.12
DB1-N	full-depth	6.00	0.00	1.30	92.7	0.84	–
					Mean	1.07	4.09
					Coefficient of variation	0.10	0.82

CC, concrete in compression zone; AG, interlocking action of aggregates; DW, dowel action of main reinforcement; HG, hanger reinforcement contribution

Fig. 1 Schematic representation of a structural form with dapped-end connections. **Fig. 2** Reinforcement layout of RC dapped-end beams. **Fig. 3** Free-body equilibrium of the full-depth section failure (left) and dapped-end failure (right). **Table 1** Contributions of internal force components and comparison of prediction accuracy

Acknowledgment

The authors would like to acknowledge funding support from the Grant-in-Aid for Scientific Research from the Japan Society of Promotion of Science (22K14310).

深圳大學
SHENZHEN UNIVERSITY

THE HONG KONG
POLYTECHNIC UNIVERSITY
香港理工大學